

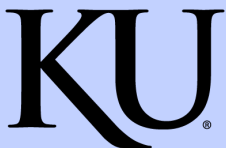
ANCHORAGE OF HIGH-STRENGTH REINFORCING BARS IN CONCRETE

By
Luay Ali Nazzal
David Darwin
Matthew O'Reilly

A Report on Research Sponsored by

Charles Pankow Foundation, ACI Foundation,
BarSplice Products, Headed Reinforcement Corporation,
nVENT Lenton, CRSI Education and Research Foundation,
Precast/Prestressed Concrete Institute,
Commercial Metals Company, Nucor Corporation

Structural Engineering and Engineering Materials
SM Report No. 150
January 2023



THE UNIVERSITY OF KANSAS CENTER FOR RESEARCH, INC.
2385 Irving Hill Road, Lawrence, Kansas 66045-7563

ANCHORAGE OF HIGH-STRENGTH REINFORCING BARS IN CONCRETE

By
Luay Ali Nazzal
David Darwin
Matt O'Reilly

A Report on Research Sponsored by

**Charles Pankow Foundation, ACI Foundation,
BarSplice Products, Headed Reinforcement Corporation,
nVENT Lenton,
CRSI Education and Research Foundation,
Precast/Prestressed Concrete Institute,
Commercial Metals Company, Nucor Corporation**

Structural Engineering and Engineering Materials

SM Report No. 150

THE UNIVERSITY OF KANSAS CENTER FOR RESEARCH, INC.

LAWRENCE, KANSAS

January 2023

ABSTRACT

Hooked and headed reinforcing bars are commonly used as a means of shortening development length of reinforcing bars, but a limited amount of previous research has resulted in restrictions on their use in practice. This study included two phases: In the first phase, 31 tests of simulated column-foundation joints were conducted to investigate the anchorage strength and behavior of large and high-strength headed bars as functions of the distance between the anchored headed bar and the compression reaction, number of headed bars tested simultaneously (1 or 2), size of the headed bars (No. 11 or No. 14), center-to-center spacing between headed bars loaded simultaneously (3.2 or $8.2d_b$), amount of confining reinforcement within the joint region (zero to six No. 4 closed stirrups), and concrete compressive strength (5,060 to 14,470 psi). The embedment length of the headed bars ranged from $12\frac{5}{8}$ to 14 in., and the stresses in the headed bars at failure ranged from 41,800 to 144,400 psi. The test results are compared with anchorage strengths based on the descriptive equations for headed bars developed at the University of Kansas, ACI 318-19 Code provisions, and proposed Code provisions. Recommended changes to Chapters 17 and 25 of ACI 318-19 are presented. In the second phase of the study, descriptive equations for beam-column joints tested under monotonic loading are investigated their applicability to predict the anchorage strength of hooked bars anchored in members subjected to reversed cyclic loading. Comparisons are made with test results from 24 studies of 146 exterior beam-column joint specimens subjected to reversed cyclic loading in which the beam bars are anchored by hooks. Key variables include embedment lengths of the hooked bars (6 to 21 in.), concrete compressive strength (3,140 to 13,700 psi), center-to-center spacing between the hooked bars (1.75 to 6.5 in.), bar size (No. 3 to No. 9), and confining reinforcement within the joint region parallel to the straight portion of the hooked bars (none to nine hoops spaced at 1.25 to 6.0 in.). The yield strength of the hooked bars ranged from 42,900 to 103,000 psi. Proposed changes to Chapters 18 of ACI 318-19 are presented.

The results of the experimental study show that the anchorage strength of headed bars anchored in column-foundation joints is improved by parallel tie reinforcement located on all sides of the headed bars, a contribution that is not included in the provisions of ACI 318-19. Similar to observations for beam-column joints, the anchorage strength of headed bars anchored in simulated

column-foundation joints decreases as the center-to-center spacing decreases below $8d_b$. The descriptive equations developed based on tests of beam-column joints are suitable for predicting the anchorage strength of headed bars anchored in column-foundation joints. Chapter 17 of ACI 318-19 does not accurately predict the anchorage strength of headed bars tested when parallel tie/anchor reinforcement is used and should be modified to combine the contributions of concrete strength and parallel tie reinforcement. The descriptive equations developed for beam-column joints apply to column-foundation joints and could serve as a basis for the anchorage provisions in Chapter 17 of ACI 318. The provisions in Chapter 25 of ACI 318-19 should be updated to include the effect of parallel tie reinforcement in connections other than beam-column joints. The descriptive equations for the anchorage strength of hooked bars in beam-column joints tested under monotonic loading are suitable for predicting the anchorage strength of hooked bars anchored in members subjected to reversed cyclic loading. The ACI Code provisions for the development length of hooked bars in tension in beam-column joints in special moment frames (Section 18.8.5.1 of ACI 318-19), derived from the development length provisions for non-seismic loading in earlier Codes, permit development lengths that are shorter needed for gravity load by Chapter 25. Changes in Chapter 18 of ACI 318-19 are proposed that require the use of the provisions in Chapter 25 to establish the minimum development length for hooked bars anchored in joints for frames subjected to seismic loading.

Keywords: anchorage, beam-column joint, column-foundation joint, development length, headed bar, high-strength concrete, high-strength steel, hooked bar, reversed cyclic loading

ACKNOWLEDGEMENTS

This report is based on a thesis presented by Luay Ali Nazzal in partial fulfillment of the requirements for the Ph.D. degree from the University of Kansas. Support for the study was provided by the Charles Pankow Foundation, the ACI Foundation, BarSplice Products, Headed Reinforcement Corporation, nVENT Lenton, the CRSI Education and Research Foundation, the Precast/Prestressed Concrete Institute, Commercial Metals Company, and Nucor Corporation. Additional support was provided by Dayton Superior, Midwest Concrete Materials, and Grace Construction Products. Thanks are due to Jack Moehle, Amy Trygstad, Javeed Munshi, and Andrew Taylor who served on the advisory panel.

TABLE OF CONTENTS

ABSTRACT.....	i
ACKNOWLEDGEMENTS.....	iii
LIST OF FIGURES.....	ix
LIST OF TABLES.....	xv
CHAPTER 1: INTRODUCTION.....	1
1.1 GENERAL.....	1
1.2 HOOKED AND HEADED REINFORCING BARS.....	4
1.2.1 Hooked reinforcing bars.....	4
1.2.2 Headed reinforcing bars.....	5
1.3 PREVIOUS WORK.....	6
1.3.1 Early studies on hooked and headed bars.....	6
1.3.1.1 Hooked bars.....	6
1.3.1.2 Headed studs and bars.....	10
1.3.2 Simulated beam-column joints with hooked bars subjected to monotonic loading.....	11
1.3.3 Beam-column joints with hooked bars subjected to reversed cyclic loading.....	20
1.3.4 Simulated beam-column joints with headed bars subjected to monotonic loading.....	21
1.3.5 Headed bars in slab specimens.....	27
1.4 CONCRETE CAPACITY DESIGN METHOD.....	30
1.5 UNIVERSITY OF KANSAS - SIMULATED COLUMN-FOUNDATION JOINTS.....	36
1.6 UNIVERSITY OF CALIFORNIA, BERKELEY – STEEL COLUMN-CONCRETE FOUNDATION JOINTS.....	39
1.7 CODE PROVISIONS.....	43
1.7.1 Anchorage provisions.....	43
1.7.2 Design provisions for hooked and headed bars.....	46
1.7.3 Design provisions for hooked bars in earthquake resistant structures.....	48
1.8 OBJECTIVE AND SCOPE.....	49

CHAPTER 2: EXPERIMENTAL WORK.....	52
2.1 MATERIAL PROPERTIES	52
2.1.1 Concrete Properties	52
2.1.2 Steel Properties	53
2.2 SLAB SPECIMEN DESIGN.....	54
2.3 TEST PARAMETERS.....	66
2.4 SPECIMEN DESIGNATION.....	67
2.5 SPECIMEN FABRICATION.....	68
2.6 TEST PROCEDURE	69
2.7 SPECIMEN INSTRUMENTATION.....	72
CHAPTER 3: TEST RESULTS AND ANALYSIS OF SIMULATED COLUMN- FOUNDATION JOINT SPECIMENS TESTED IN THE CURRENT AND PREVIOUS STUDIES AND COMPARISON BETWEEN THE PROPOSED EQUATIONS AND ACI 318-19 CODE PROVISIONS.....	74
3.1 TESTS OF HEADED BARS ANCHORED IN SIMULATED COLUMN-FOUNDATION JOINT SPECIMENS WITH SHALLOW EMBEDMENT	74
3.1.1 Failure and Failure Modes	81
3.1.2 Effect of Strut Angle.....	90
3.1.3 Effect of Concrete Compressive Strength.....	93
3.1.4 Effect of Grouped Anchors and Headed Bar Spacing	97
3.1.5 Effect of Parallel Tie Reinforcement	101
3.1.6 Examination of Value of Effective Parallel Tie Reinforcement A_{tt} used in Descriptive Equation, Eq. (1.8).....	115
3.2 ANALYSIS OF TEST RESULTS FROM OTHER STUDIES AND COMPARISONS WITH THE CURRENT STUDY	117
3.2.1 Headed Bars Tested in Slab Specimens.....	122
3.2.1.1 Analysis Based on Descriptive Equations, ACI 318-19 Code Provisions, and Proposed Version of Code Provisions	128
3.2.1.2 Comparison Between the Descriptive Equations, ACI 318-19 Code Provisions, and Proposed Code Provisions	140
3.3 RECOMMENDED CHANGES TO CHAPTERS 17 AND 25 OF ACI 318-19	144

3.3.1 Proposed Changes in Chapter 25 of ACI 318-19.....	145
CHAPTER 4: ANALYSIS OF BEAM-COLUMN JOINT SPECIMENS WITH BEAM BARS ANCHORED WITH HOOKS SUBJECTED TO REVERSED CYCLIC LOADING	151
4.1 INTRODUCTION	151
4.2 ANALYSIS BASED ON PROPOSED DESCRIPTIVE AND DESIGN EQUATIONS..	151
4.2.1 Descriptive Equations and Design Provisions Proposed by Ajaam et al. (2017)	151
4.2.2 Exterior Beam-Column Joints.....	154
4.2.2.1 Specimens with $d/\ell_{eh} \leq 1.5$ and $\ell_{eh}/\ell_{ehy} < 1.0$	169
4.2.2.2 Specimens with $d/\ell_{eh} \leq 1.5$ and $\ell_{eh}/\ell_{ehy} \geq 1.0$	171
4.2.2.3 Specimens with $d/\ell_{eh} > 1.5$	174
4.2.2.4 Applicability of Descriptive Equations to Predict Anchorage Strength of Hooked Bars Anchored in Members Subjected to Reversed Cyclic Loading.....	185
4.3 GUIDELINES AND RECOMMENDATIONS FOR CHAPTER 18 OF ACI 318-19	198
4.3.1 Comparison Between the Development Lengths of Hooked Bars Required for Seismic and Non-Seismic (Gravity) Loading (Chapter 18 vs. 25 of ACI 318-19)	198
4.3.2 Proposed Changes in Chapter 18 of ACI 318-19.....	200
CHAPTER 5: SUMMARY AND CONCLUSIONS	202
5.1 SUMMARY	202
5.2 CONCLUSION	203
5.3 FUTURE WORK.....	205
REFERENCES.....	206
APPENDIX A: NOTATION.....	213
APPENDIX B: DETAILS OF SLAB SPECIMENS TESTED IN THE CURRENT STUDY	217
B.1 STRESS-STRAIN CURVES FOR HEADED BARS	217
B.2 SCHEMATICS OF SLAB SPECIMENS	219
B.3 TEST RESULTS AND SPECIMENS CONSTRUCTED AND TESTED IN THE CURRENT STUDY	223

APPENDIX C: TEST RESULTS AND SPECIMENS FROM OTHER STUDIES INCLUDED IN THE CURRENT STUDY	229
C.1 SLAB SPECIMENS TESTED BY DEVRIES ET AL. (1999) AND CHOI ET AL. (2002) 229	
C.2 SLAB SPECIMENS TESTED AT THE UNIVERSITY OF KANSAS	233
C.3 SLAB SPECIMENS TESTED AT THE UNIVERSITY OF CALIFORNIA, BERKELEY 236	
C.4 EXTERIOR BEAM-COLUMN JOINT SPECIMENS	237
APPENDIX D: SUMMARY OF STUDIES ON BEAM-COLUMN JOINT SPECIMENS TESTED UNDER REVERSED CYCLIC LOADING	279

LIST OF FIGURES

Figure 1.1 Force transfer on a hooked bar (Minor and Jirsa 1975)	4
Figure 1.2 Standard hook details (ACI 318-11).....	5
Figure 1.3 Force transfer on a headed bar (Bashandy 1996)	5
Figure 1.4 Maximum dimensions of obstructions or interruptions for headed bars (ASTM A970/A970M-17)	6
Figure 1.5 Small concrete blocks (a) specimen for 90° hooked bars, (b) specimen for 180° hooked bars (Hribar and Vasko 1969).....	7
Figure 1.6 Loading apparatus (Hribar and Vasko 1969)	8
Figure 1.7 Test specimen (Minor and Jirsa 1975)	9
Figure 1.8 Details of push-out specimens (Viest 1956).....	10
Figure 1.9 Test specimen (Marques and Jirsa 1975)	12
Figure 1.10 Specimen and test setup (Hamad et al. 1993).....	14
Figure 1.11 Test setup (Ramirez and Russell 2008)	15
Figure 1.12 Test setup (Sperry et al. 2015a).....	16
Figure 1.13 Test Setup (Bashandy 1996).....	22
Figure 1.14 Test setup (Chun et al. 2009).....	24
Figure 1.15 Failure modes: (a) concrete breakout, (b) and (c) joint shear failure (Chun et al. 2009)	24
Figure 1.16 Test Frame (Shao et al. 2016).....	25
Figure 1.17 Test setup (DeVries et al. 1999)	28
Figure 1.18 Headed reinforcing bars (a) unbonded and (b) bonded embedment length (DeVries et al. 1999)	28
Figure 1.19 Transverse reinforcement configuration (DeVries et al. 1999).....	28
Figure 1.20 Slab specimens (Choi et al. 2002)	30
Figure 1.21 CCD idealized concrete cone for an individual anchor (Fuchs et al. 1995).....	31

Figure 1.22 Projected area of an individual anchor according to the CCD method (Fuchs et al. 1995)	32
Figure 1.23 Calculation of the projected area, A_N , according to the CCD method (Fuchs et al. 1995)	34
Figure 1.24 Test setup (Nilforoush et al. 2017)	35
Figure 1.25 Test setup of the first group (a) front view, (b) side view (Ghimire et al. 2018)	37
Figure 1.26 Test setup of the final group (a) front view, (b) side view (Ghimire et al. 2018)	38
Figure 1.27 Steel-column-to-concrete-foundation joint specimen M01 (Worsfold et al. 2022) .	40
Figure 1.28 Steel-column-to-concrete-foundation joint specimen M02 (Worsfold et al. 2022) .	41
Figure 1.29 Plan view of specimen M02 (Worsfold et al. 2022).....	41
Figure 1.30 Idealized cone geometry shown in elevation and observed cone geometry intersecting top surface in plan view for specimen M01 (Worsfold et al. 2022).....	42
Figure 1.31 Cross section and plan view highlighting crack patterns and breakout cone geometry for Specimen M02 (Worsfold et al. 2022)	43
Figure 1.32 Calculation of A_{Nco} for a single anchor (ACI 318-19).....	45
Figure 1.33 Calculation of A_{Nc} for a single anchor and group of anchors (ACI 318-19)	46
Figure 1.34 Strut angle between anchored headed bar and nearest support reaction	51
Figure 2.1 Headed bars (a) No. 11 S5.5 bar (b) No. 11 S9.2 bar (c) No. 14 B4.2 headed bar	54
Figure 2.2 Location of headed bars and reinforcement for Slab 1 (a) side view, (b) end view...	58
Figure 2.3 Location of headed bars and reinforcement for Slab 2 (a) side view, (b) end view...	59
Figure 2.4 Location of headed bars and reinforcement for Slab 3 (a) side view, (b) end view...	60
Figure 2.5 Location of headed bars and reinforcement for Slab 4 (a) side view, (b) end view...	61
Figure 2.6 Location of headed bars and reinforcement for Slab 5 (a) side view, (b) end view...	62
Figure 2.7 Location of headed bars and reinforcement for Slabs 6,7, and 10 (a) side view, (b) end view	63
Figure 2.8 Location of headed bars and reinforcement for Slabs 8, 9, and 11 (a) side view, (b) end view	64

Figure 2.9 Location of headed bars and reinforcement for Slabs 12 and 14 (a) side view, (b) end view.....	65
Figure 2.10 Location of headed bars and reinforcement for Slabs 13 and 15 (a) side view, (b) end view	66
Figure 2.11 Example specimen designation	68
Figure 2.12 Slab specimen formwork	69
Figure 2.13 Test frame – first configuration	70
Figure 2.14 Test frame – second configuration	71
Figure 2.15 LVDTs clamped to the top flange of the spreader beams	72
Figure 2.16 LVDT plates attached to test bars.....	72
Figure 2.17 Location of the strain gauges on parallel ties	73
Figure 3.1 Concrete surface failure (crack propagation top and side views).....	84
Figure 3.2 Concrete cone-shaped breakout failure (a) schematic drawing (b) Slab Specimen 5 (test 2, 11-5-S5.5-6#6-2#4-12.75) after removal of breakout region	85
Figure 3.3 Concrete breakout failure. Slab Specimen 5 (test 1, 11-5-S5.5-6#6-2#4-12.75) with both support reactions just outside anticipated failure region (test had one headed bar with parallel tie reinforcement on both sides of headed bar).....	86
Figure 3.4 Concrete breakout failure of Slab Specimen 6 (test 1, (2@8.2)11-5-S5.5-7#11-0-12.75) with one of the support reactions placed within anticipated failure region (test had two headed bars without parallel tie reinforcement) (a) concrete surface failure (b) cone-shaped failure after removal of breakout region	87
Figure 3.5 Concrete breakout failure of Slab Specimen 8 (test 1, (2@8.2)11-5-S9.2-7#11-3#4-12.75) with one of the support reactions placed within anticipated failure region (test had two headed bars with parallel tie reinforcement only on one side of headed bars) (a) concrete surface failure (b) cone-shaped failure after removal of breakout region	88
Figure 3.6 Concrete breakout failure of Slab Specimen 8 (test 2, (2@8.2)11-5-S9.2-7#11-6#4-12.75) with one of the support reactions placed within anticipated failure region (test had two headed bars with parallel tie reinforcement on both sides of headed bars) (a) concrete surface failure (b) cone-shaped failure after removal of breakout region	89

Figure 3.7 Concrete breakout failure of Slab Specimen 3 (11-5-S5.5-6#11-0-12.75) with both support reactions placed far away from anticipated failure region (test had one headed bars without parallel tie reinforcement).....	90
Figure 3.8 Strut angle between anchored headed bar and nearest support reaction (Krishna et al. 2018)	91
Figure 3.9 Bar force at failure normalized with respect to a concrete compressive strength of 5,000 psi, and an embedment length of 12.75 in., T_N , versus the ratio h_{cl}/ℓ_{eh} (defined in Figure 3.8). Tests with No. 8 headed bars are from Ghimire et al. (2018), and tests with No. 11 headed bars are from the current study	92
Figure 3.10 Normalized bar force at failure T_N [using Eq. (3.2)] versus concrete compressive strength f_{cm} for specimens presented in Table 3.3.....	95
Figure 3.11 Ratio of test-to-calculated failure load T/T_h versus concrete compressive strength f_{cm} for all the current study tests that contained two headed bars load simultaneously with the presence of the parallel tie reinforcement within the joint region presented in Table 3.1.....	96
Figure 3.12 Bar force at failure normalized with respect to a concrete compressive strength of 5,000 psi and an embedment length of 12.75 in. T_N versus the number of headed bars being developed in tests (a) with individual and closely spaced headed bars loaded simultaneously (b) with individual and widely spaced headed bars loaded simultaneously. Results for individual bars are the same in figures (a) and (b).....	99
Figure 3.13 Bar force at failure normalized with respect to a concrete compressive strength of 5,000 psi and an embedment length of 12.75 in. T_N versus center-to-center spacing between headed bars with respect to the bar diameter (d_b)	100
Figure 3.14 Parallel tie reinforcement for Slab Specimen 5 (11-5-S5.5-6#6-2#4-12.75) (a) front view, (b) side view, (c) load versus strain curves for Test 1, (d) load versus strain curves for Test 2, (e) load versus strain curves for Test 3	104
Figure 3.15 Average load per headed bar versus strain in parallel tie reinforcement for Slab Specimen 8 (a) location of the parallel tie reinforcement and the strain gauge locations (b) load versus strain curves for hoops in test included hoops only on one side of the bars Group A [(2@8.2)11-5-S9.2-7#11-3#4-12.75] (c) load versus strain curves for hoops in the test included hoops on both sides of the bars Group B [(2@8.2)11-5-S9.2-7#11-6#4-12.75]	106
Figure 3.16 Average load per headed bar versus strain in parallel tie reinforcement for Slab Specimen 9 (a) load versus strain curves for hoops in test included hoops only on one side of the bars Group A [(2@8.2)11-5-S9.2-7#11-3#4-12.75] (b) load versus strain curves for hoops in the test included hoops on both sides of the bars Group B [(2@8.2)11-5-S9.2-7#11-6#4-12.75] ...	110

Figure 3.17 Normalized bar force at failure T_N [using Eq. (3.1)] versus normalized parallel tie reinforcement A_{t1}/A_{hs} , within a $10d_b$ radial distance from the centerline of the headed bars, for specimens with and without parallel tie reinforcement	113
Figure 3.18 Headed reinforcing bars (a) unbonded and (b) bonded embedment length (DeVries et al. 1999)	123
Figure 3.19 Slab specimens (Choi et al. 2002)	124
Figure 3.20 Steel-column-to-concrete-foundation joint specimen M01 (Worsfold et al. 2022)	126
Figure 3.21 Steel-column-to-concrete-foundation joint specimen M02 (Worsfold et al. 2022)	127
Figure 3.22 Plan view of specimen M02 (Worsfold et al. 2022).....	127
Figure 3.23 Measured force at failure T versus anchorage strength T_h calculated using Eq. (3.3) and (3.4) for slab specimens tested by DeVries et al. (1999), Choi et al. (2002), Ghimire et al. (2018), Worsfold et al. (2022), and in the current study; a reduction factor of 0.8 is applied to T_h for headed bars with concrete cover less than $8d_b$	130
Figure 3.24 Measured force at failure T versus the anchorage strength T_{anc} calculated using Eq. (3.6), incorporating the modification factor ψ_{mean} , for slab specimens tested by DeVries et al. (1999), Choi et al. (2002), Ghimire et al. (2018), Worsfold et al. (2022), and in the current study	133
Figure 3.25 Measured force at failure T versus the anchorage strength T_{ACI318} calculated using Eq. (3.11) for slab specimens tested by DeVries et al. (1999), Choi et al. (2002), Ghimire et al. (2018), Worsfold et al. (2022), and in the current study.....	136
Figure 3.26 Measured force at failure T versus the anchorage strength T_{calc} calculated using Eq. (3.14) for slab specimens tested by DeVries et al. (1999), Choi et al. (2002), Ghimire et al. (2018), Worsfold et al. (2022), and in the current study.....	139
Figure 3.27 Average values of T/T_h , T/T_{anc} , T/T_{ACI318} , and T/T_{calc} for tests involving two headed bars without and with parallel tie reinforcement, Slab Specimens 6, 7 and 10 [(2@8.2)11-5-S5.5-7#11-0-12.75], Slab Specimens 12 and 14 [(2@6.8)14-5-B4.2-7#11-0-12.75], Slab Specimens 8, 9 and 11 [(2@8.2)11-5-S9.2-7#11-6#4-12.75], and Slab Specimens 13 and 15 [(2@6.8)14-5-B4.2-7#11-6#4-12.75].....	142
Figure 4.1 Effective confining reinforcement for hooked bars within the joint region of beam-column joints suggested by Ajaam et al. (2017).....	152
Figure 4.2 M_{peak}/M_n versus ℓ_{eh}/ℓ_{ehy} for specimens with $d/\ell_{eh} \leq 1.5$ and $V_p/V_n \leq 1.0$. M_{peak}/M_n is the ratio of peak moment to nominal flexural strength, and ℓ_{eh}/ℓ_{ehy} is the ratio of embedment length	

to the embedment length required to yield the hooked bar calculated using the descriptive equations developed by Ajaam et al. (2017), Eq. (4.1) and (4.2)	168
Figure 4.3 M_{peak}/M_n versus ℓ_{eh}/ℓ_{ehy} for specimens with $d/\ell_{eh} \leq 1.5$ and $V_p/V_n > 1.0$. M_{peak}/M_n is the ratio of peak moment to nominal flexural strength, and ℓ_{eh}/ℓ_{ehy} is the ratio of embedment length to the embedment length required to yield the hooked bar calculated using the descriptive equations developed by Ajaam et al. (2017), Eq. (4.1) and (4.2)	169
Figure 4.4 V_p/V_n versus ℓ_{eh}/ℓ_{ehy} for specimens with $d/\ell_{eh} \leq 1.5$. V_p/V_n is the ratio of peak joint shear to nominal joint shear strength, and ℓ_{eh}/ℓ_{ehy} is the ratio of embedment length to the embedment length required to yield the hooked bar calculated using the descriptive equations developed by Ajaam et al. (2017), Eq. (4.1) and (4.2)	173
Figure 4.5 M_{peak}/M_n versus V_p/V_n for specimens with $d/\ell_{eh} \leq 1.5$ and $\ell_{eh}/\ell_{ehy} \geq 1.0$. M_{peak}/M_n is the ratio of peak moment to nominal flexural strength, and V_p/V_n is the ratio of peak joint shear to nominal joint shear strength.....	174
Figure 4.6 Ratio of test-to-calculated bar force at failure T/T_h versus ratio of effective beam depth to embedment length d/ℓ_{eh} for specimens without confining reinforcement [T_h is calculated using Eq. (4.1)] (Ajaam et al. 2017)	175
Figure 4.7 Ratio of test-to-calculated bar force at failure T/T_h versus ratio of effective beam depth to embedment length d/ℓ_{eh} for specimens with confining reinforcement [T_h is calculated using Eq. (4.2)] (Ajaam et al. 2017)	176
Figure 4.8 Load transfer within the beam-column joint based on the strut-and-tie mechanism (column longitudinal reinforcement and beam compression reinforcement are not shown for clarity)	180
Figure 4.9 M_{peak}/M_n versus ℓ_{eh}/ℓ_{ehy} for specimens with $d/\ell_{eh} > 1.5$. M_{peak}/M_n is the ratio of peak moment to nominal flexural strength, and ℓ_{eh}/ℓ_{ehy} is the ratio of embedment length to the embedment length required to yield the hooked bar calculated using the descriptive equations developed by Ajaam et al. (2017), Eq. (4.1) and (4.2)	184
Figure 4.10 M_{peak}/M_n versus ℓ_{eh}/ℓ_{ehy} for beam-column joint specimens with $\ell_{eh}/\ell_{ehy} \geq 1.0$. The value of M_{peak}/M_n for one specimen is projected on the line $\ell_{eh}/\ell_{ehy} = 1.0$ line by extending a line parallel to the trend line for specimens with $\ell_{eh}/\ell_{ehy} \geq 1.0$	192
Figure 4.11 Estimated hooked bar force at failure T'_{mod} versus hooked bar force T_h [based on the descriptive equations, Eq. (4.1) and (4.2)] for specimens with $d/\ell_{eh} \leq 1.5$, $V_p/V_n \leq 1.0$, and $\ell_{eh}/\ell_{ehy} \geq 1.0$	197

LIST OF TABLES

Table 1.1 Modification factor ψ_{cs} for confining reinforcement and spacing	19
Table 1.2 Modification factor ψ_{cs} for confining reinforcement and spacing	26
Table 2.1 Concrete mixture proportions	53
Table 2.2 Properties of headed bars and parallel tie reinforcement	53
Table 2.3 Head dimensions	54
Table 2.4 Detail of slab specimens	55
Table 2.4 Cont. Detail of slab specimens	56
Table 3.1 Summary of key parameters of slab specimens	76
Table 3.1 Cont. Summary of key parameters of slab specimens	76
Table 3.1 Cont. Summary of key parameters of slab specimens.....	77
Table 3.1 Cont. Summary of key parameters of slab specimens.....	78
Table 3.2 Summary of key parameters of slab specimens (Ghimire et al. 2018)	79
Table 3.2 Cont. Summary of key parameters of slab specimens (Ghimire et al. 2018).....	80
Table 3.3 Test results for specimens containing No. 11 and No. 14 headed bars tested with different concrete strength	94
Table 3.4 Statistical parameters of T/T_h values for tests containing two headed bars with parallel tie reinforcement within the joint region	96
Table 3.5 Test results for specimens containing individual and two closely-spaced or widely-spaced grouped headed bars.....	98
Table 3.6 Test results for specimens containing No. 11 and No. 14 headed bars with and without parallel tie reinforcement	112
Table 3.6 Cont. Test results for specimens containing No. 11 and No. 14 headed bars with and without parallel tie reinforcement.....	113
Table 3.7 Effective parallel tie reinforcement (A_{tt}) and T/T_h values for tests containing two headed bars loaded simultaneously with parallel tie reinforcement within the joint region, the cap $0.3A_b$ is not applied to the descriptive equation (Eq. 1.8).....	116

Table 3.8 Effective parallel tie reinforcement (A_{tt}) and T/T_h values for tests containing two headed bars loaded simultaneously with parallel tie reinforcement within the joint region, the cap $0.3A_b$ is applied to the descriptive equation (Eq. 1.8).....	117
Table 3.9 Test results for headed bars anchored in slab specimens tested by DeVries et al. (1999), Choi et al. (2002), and Worsfold et al. (2022) and comparisons with anchorage provisions of Chapter 17 of ACI 318-19 [Eq. (3.9)], descriptive equations [Eq. (3.3) and (3.4)], design provisions of Chapter 25 of ACI 318-19 [Eq. (3.11)], and proposed Code provisions [Eq. (3.14)], (a reduction factor of 0.8 is applied to T_h as appropriate).....	129
Table 3.10 Statistical parameters of T/T_h values for slab specimens tested by DeVries et al. (1999), Choi et al. (2002), Ghimire et al. (2018), Worsfold et al. (2022), and in the current study	132
Table 3.11 Statistical parameters of T/T_{anc} values for slab specimens for which T_{anc} is governed by concrete breakout tested by DeVries et al. (1999), Choi et al. (2002), Ghimire et al. (2018), Worsfold et al. (2022), and in the current study	135
Table 3.12 Statistical parameters of $T/T_{ACI 318}$ values for slab specimens tested by DeVries et al. (1999), Choi et al. (2002), Ghimire et al. (2018), Worsfold et al. (2022), and in the current study	138
Table 3.13 Statistical parameters of T/T_{calc} values for slab specimens tested by DeVries et al. (1999), Choi et al. (2002), Ghimire et al. (2018), Worsfold et al. (2022), and in the current study	140
Table 4.1 Modification factor ψ_{cs} for confining reinforcement, expressed as ratio of area of confining reinforcement, A_{th} , to area of hooked bars, A_{hs} , and center-to center bar spacing, $c_{ch}^{[1]}$	154
Table 4.2 Detail of exterior beam-column joint specimens tested under reversed cyclic loading	156
Table 4.2 Cont. Detail of exterior beam-column joint specimens tested under reversed cyclic loading.....	157
Table 4.2 Cont. Detail of exterior beam-column joint specimens tested under reversed cyclic loading.....	158
Table 4.2 Cont. Detail of exterior beam-column joint specimens tested under reversed cyclic loading.....	159
Table 4.2 Cont. Detail of exterior beam-column joint specimens tested under reversed cyclic loading.....	160

Table 4.2 Cont. Detail of exterior beam-column joint specimens tested under reversed cyclic loading.....	161
Table 4.2 Cont. Detail of exterior beam-column joint specimens tested under reversed cyclic loading.....	162
Table 4.2 Cont. Detail of exterior beam-column joint specimens tested under reversed cyclic loading.....	163
Table 4.2 Cont. Detail of exterior beam-column joint specimens tested under reversed cyclic loading.....	164
Table 4.2 Cont. Detail of exterior beam-column joint specimens tested under reversed cyclic loading.....	165
Table 4.3 Detail of exterior beam-column joint specimens tested under reversed cyclic loading with $d/\ell_{eh} > 1.5$	178
Table 4.3 Cont. Detail of exterior beam-column joint specimens tested under reversed cyclic loading with $d/\ell_{eh} > 1.5$	179
Table 4.4 Test parameters for exterior beam-column joint specimens containing hooked bars with $d/\ell_{eh} > 1.5$ and tested under reversed cyclic loading	181
Table 4.4 Cont. Test parameters for exterior beam-column joint specimens containing hooked bars with $d/\ell_{eh} > 1.5$ and tested under reversed cyclic loading.....	183
Table 4.5 Detail of exterior beam-column joint specimens tested under reversed cyclic loading with $d/\ell_{eh} \leq 1.5$ and $V_p/V_n \leq 1.0$ used in this evaluation and comparisons with descriptive equations, Eq. (4.1) and (4.2).....	186
Table 4.5 Cont. Detail of exterior beam-column joint specimens tested under reversed cyclic loading with $d/\ell_{eh} \leq 1.5$ and $V_p/V_n \leq 1.0$ used in this evaluation and comparisons with descriptive equations, Eq. (4.1) and (4.2).....	187
Table 4.5 Cont. Detail of exterior beam-column joint specimens tested under reversed cyclic loading with $d/\ell_{eh} \leq 1.5$ and $V_p/V_n \leq 1.0$ used in this evaluation and comparisons with descriptive equations, Eq. (4.1) and (4.2).....	188
Table 4.6 Statistical parameters for test-to-calculated ratio in beam-column joint specimens with $\ell_{eh}/\ell_{ehy} < 1.0$ tested under reversed cyclic loading and in beam-column joint specimens tested under monotonic loading and used by Ajaam et al. (2017) to develop the descriptive equations, Eq. (4.1) and (4.2).....	190

Table 4.7 Statistical parameters for T'_{mod}/T_h in beam-column joint specimens with $\ell_{eh}/\ell_{ehy} \geq 1.0$ tested under reversed cyclic loading 193

Table 4.8 Detail of exterior beam-column joint specimens tested under reversed cyclic loading with $d/\ell_{eh} \leq 1.5$, $V_p/V_n \leq 1.0$, and $\ell_{eh}/\ell_{ehy} \geq 1.0$ used in this evaluation and comparisons with descriptive equations, Eq. (4.1) and (4.2) 194

Table 4.8 Cont. Detail of exterior beam-column joint specimens tested under reversed cyclic loading with $d/\ell_{eh} \leq 1.5$, $V_p/V_n \leq 1.0$, and $\ell_{eh}/\ell_{ehy} \geq 1.0$ used in this evaluation and comparisons with descriptive equations, Eq. (4.1) and (4.2) 195

Table 4.8 Cont. Detail of exterior beam-column joint specimens tested under reversed cyclic loading with $d/\ell_{eh} \leq 1.5$, $V_p/V_n \leq 1.0$, and $\ell_{eh}/\ell_{ehy} \geq 1.0$ used in this evaluation and comparisons with descriptive equations, Eq. (4.1) and (4.2) 196

CHAPTER 1: INTRODUCTION

1.1 GENERAL

In reinforced concrete structures, the reinforcing steel and the surrounding concrete must be sufficiently bonded to each other to transfer internal stresses, allowing the structure to behave as a composite and resist external forces. When smooth bar reinforcement was used, the mechanism of the bond involved only adhesion and friction between the reinforcing steel and the surrounding concrete. For deformed bar reinforcement, an additional (and principal) bond mechanism results from physical interlocking between the reinforcing steel and the surrounding concrete, along with the frictional and adhesive forces.

Reinforcing steel must be embedded in the concrete for a certain length to fully develop the required stress, usually the yield strength, at critical sections where stresses in reinforcement are maximum. In cases such as external beam-column joints, however, the length required for a bar to develop its yield strength may be greater than the column dimensions. In such cases, hooks or heads can provide the required anchorage strength with a much shorter embedment length than is possible with straight reinforcing bars. The required embedment length is referred to as the development length in the ACI Building Code (ACI Committee 318 2019). Sections 25.4.3.1 and 25.4.4.2 of ACI 318-19 Building Code Requirements for Structural Concrete contain equations to calculate the development length of hooked and headed deformed bars in tension.

Prior to ACI 318-19, the development length provisions for hooked and headed bars were based on studies of limited scope. As a result, significant limitations were placed on the application of hooked and headed bars, such as limiting the yield strength of the bar to 60,000 psi for headed bars and 80,000 psi for hooked bars and limiting the concrete compressive strength to 6,000 psi for headed bars and 10,000 psi for hooked bars. Higher-strength materials (reinforcing steel with yield strengths up to 120,000 psi and concrete strengths above 16,000 psi), however, are now available for use in reinforced concrete construction. To gain a better understanding of the behavior of hooked and headed bars and to allow the use of higher strength materials, researchers at the University of Kansas (KU) initiated a comprehensive study to investigate the anchorage strength of both methods of anchorage for bars in tension (Sperry et al. 2015a,b, 2017a,b, 2018, Ajaam et al. 2017, 2018, Yasso et al. 2017, 2021, Shao et al. 2016, Ghimire et al. 2018, 2019a,b) that

included a range in values of concrete cover, bar spacing, and embedment length, and high-strength materials. Based on these studies, the development length provisions in ACI 318 were updated in 2019. In spite of this comprehensive effort, however, a number of key questions remain. Two of those questions are specifically addressed in this study.

Headed reinforcing bars serve as a viable alternative to hooked bars for anchorage in concrete due to their ability to reduce congestion and development length. Very limited research, however, has been performed on the behavior of headed bars anchored in members other than beam-column joints, with none available regarding the effect of parallel reinforcement (stirrups or hoops oriented parallel to the headed bars). As a result, Section R25.4.4.5 of ACI 318-19 prohibits consideration of parallel reinforcement in the anchorage strength in members other than beam-column joints. Shao et al. (2016) and Ghimire et al. (2018, 2019a,b) have shown that the presence of parallel tie reinforcement (the term used for parallel reinforcement when used with headed bars) within the joint region increases the anchorage strength of headed bars. Taking full advantage of headed reinforcing bars requires a better understanding of the behavior of headed reinforcing bars in a wider range of member configurations, including, but not limited to, column-foundations joints.

The design provisions for calculating the development lengths of hooked and headed bars, ℓ_{dh} and ℓ_{dt} , respectively, are presented in Sections 25.4.3 and 25.4.4 of ACI 318-19 (described in greater detail in Section 1.6.2). In ACI 318-19, ℓ_{dh} and ℓ_{dt} are functions of the specified yield strength of the bar (f_y), the square root of concrete compressive strength (f'_c), bar diameter (d_b) to the power of 1.5, bar location (inside or outside of a column core) and spacing, quantity of confining reinforcement for hooks and parallel tie reinforcement for heads, and if used, epoxy coating on the bar and lightweight concrete.

The design provisions in Section 25.4.4.2 of ACI 318-19 for calculating the development length of headed bars can be used if the headed bars satisfy specific requirements, described in Section 25.4.4.1 of ACI 318-19. For cases where the development length of headed bars cannot be designed in accordance with 25.4.4.2 and for cases where concrete breakout (a mass of concrete being pulled out of the specimen along with the headed bar, forming a cone-shaped failure surface) is expected, use of the anchorage provisions in Chapter 17 of ACI 318-19 should be considered.

Current ACI anchorage provisions, particularly for concrete breakout strength, given in Section 17.6.2.1 of ACI 318-19 and described in Section 1.6.1 of this report, were developed for headed studs and headed anchor bolts that are generally smooth. Therefore, the effect of deformations on reinforcing bars, which contribute significantly to bond in straight reinforcing bars, are not considered. Moreover, Section 17.6.2.1 of ACI 318-19 does not take into account the effect of the parallel tie reinforcement on anchorage capacity. Because the ACI anchorage provisions may be overly conservative when applied to headed reinforcing bars, it is important to evaluate the accuracy of those provisions for predicting the anchorage strength in parallel with consideration of the development length provisions in the Code.

The current Code design provisions (ACI 318 Building Code and ACI 349 Code Requirements for Nuclear Safety-Related Concrete Structures) for the development length of hooked bars in tension under reversed cyclic loading (Section 18.8.5.1 of ACI 318-19) were derived directly from the development length provisions for non-seismic (monotonic) loading (Section 25.4.3.1) that existed in ACI 318 Building Codes prior to 2019. Even though the development length provisions (Section 25.4.3.1) were updated in ACI 318-19 due to the comprehensive study conducted at KU using specimens tested under monotonic loading (Sperry et al. 2015a,b, 2017a,b, 2018, Ajaam et al. 2017, 2018, Yasso et al. 2017), the code design provisions for the development length of hooked bars in tension under cyclic loading did not change. This has resulted in provisions that permit hooked bar development lengths designed under the provisions of Chapter 18 to be *shorter* than those required for gravity load by Chapter 25. This rather strange situation justifies an evaluation of the current code provisions in Section 18.8.5.1 and the appropriateness of applying the development length requirements of 25.4.3 to the design of hooked bars subjected to reversed cyclic loading. Such an evaluation has already been performed for beam-column joints under reversed cyclic loading in which the beam bars are anchored with heads (Ghimire et al. 2018, 2021), resulting in a modification of Section 18.8.5.2 of ACI 318-19 to require that the development length of headed bars in such cases satisfy the requirements of Section 25.4.4 of Chapter 25 of the Code.

This study addresses two areas: The first focuses on an experimental investigation of the anchorage strength of headed bars anchored in members other than beam-column joints, such as

column-foundation joints, using larger bar sizes (No. 11 and No. 14) and high-strength materials, both with and without parallel tie reinforcement. The second involves the analysis of test data for exterior beam-column joints subjected to reversed cyclic loading in which the beam bars are anchored with hooks. The goal of this second area is to determine the applicability of the development length provisions for hooked bars in tension to hooked bars under reversed cyclic loading.

This chapter introduces previous research relevant to the current study, provides a detailed explanation of the code anchorage provisions, and describes the objective and the scope of the research effort.

1.2 HOOKED AND HEADED REINFORCING BARS

1.2.1 Hooked reinforcing bars

Hooked reinforcing bars provide anchorage strength by a combination of the direct bearing of the hook on the concrete and the bond along the straight portion of the bars. The force transfer on a hooked bar is shown in Figure 1.1.

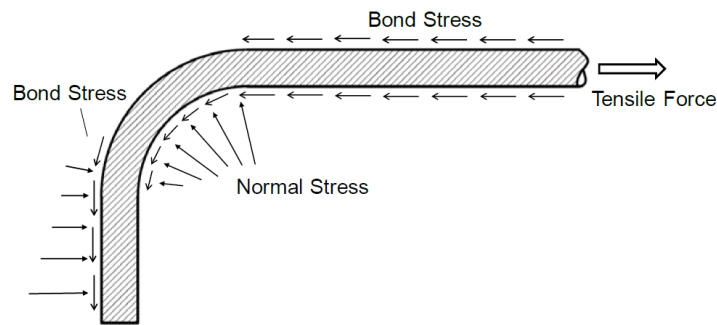


Figure 1.1 Force transfer on a hooked bar (Minor and Jirsa 1975)

Hooked bars are referred to as “standard hooks” if the geometry of the hooked bars meets the requirement specified in ACI 318-19 Section 25.3.1. Figure 1.2 shows the details of standard hooks with 90° and 180° bend angles.

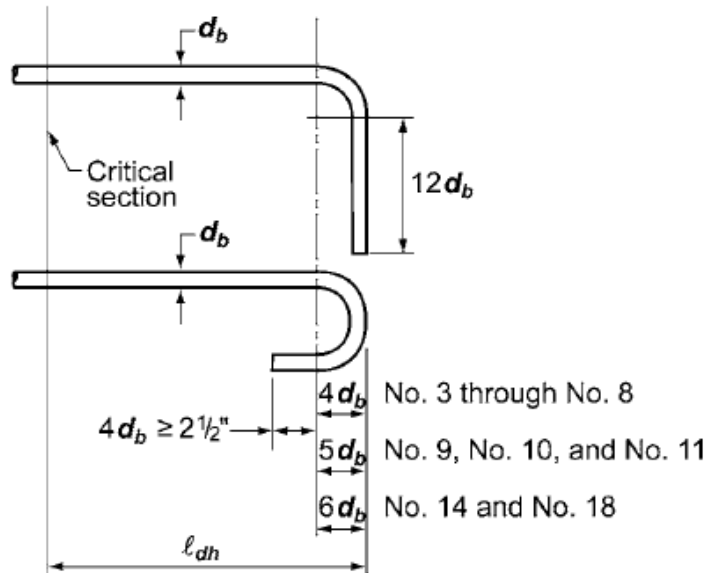


Figure 1.2 Standard hook details (ACI 318-11)

1.2.2 Headed reinforcing bars

A headed reinforcing bar is a type of deformed bar with a round, elliptical, or rectangular shape attached to one or both ends (ASTM A970). Headed reinforcing bars provide anchorage strength by a combination of direct bearing of the head on the concrete and the bond along the straight portion of the bars. The force transfer on a headed bar is shown in Figure 1.3.

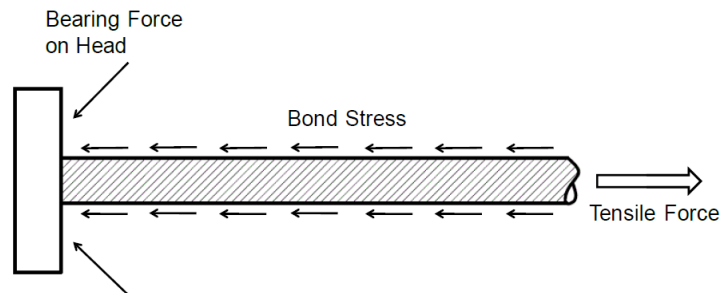


Figure 1.3 Force transfer on a headed bar (Bashandy 1996)

Headed reinforcing bars do not have a bend or tail extension length as with hooked reinforcing bars, so they have the ability to reduce congestion and ease construction. Heads may vary in size, shape, and manufacturing process, but only those comply with the Class HA requirements in ASTM A970 are allowed for use in reinforced concrete structures by ACI 318-19. According to Annex A1.2.1 of ASTM A970/A970M – 17, Class HA headed bars must develop the minimum specified tensile strength of the reinforcing bars. According to Annex A1.1.1.3 of

ASTM A970/A970M – 17, the net bearing area of a head (A_{brg}) shall be equal to or greater than four times the nominal cross-sectional area of the bar ($4A_b$). The net bearing area of a head (A_{brg}) is the gross area of the head minus the nominal area of the deformed reinforcing bar (A_b).

In addition to the head size, the obstructions or interruptions produced from the manufacturing process also must comply with certain dimensional requirements in order for the headed bars to meet Class HA requirements. According to Annex A1 of ASTM A970/A970M – 17, the maximum dimensions of the obstructions or interruptions is shown in Figure 1.4. Headed bars not meeting the requirements of Class HA heads may be used in concrete structures if tests showing the adequacy of these devices are approved by the building official.

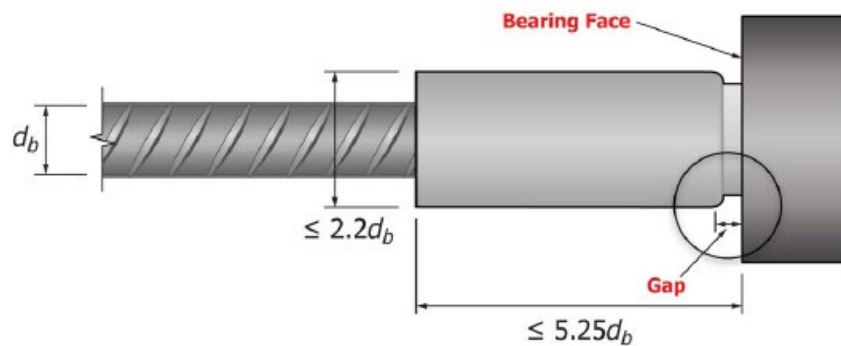


Figure 1.4 Maximum dimensions of obstructions or interruptions for headed bars (ASTM A970/A970M-17)

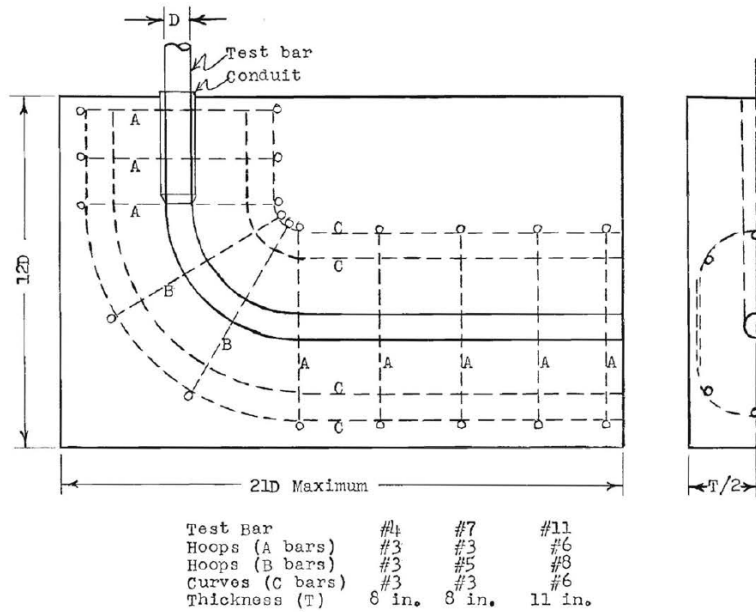
1.3 PREVIOUS WORK

1.3.1 Early studies on hooked and headed bars

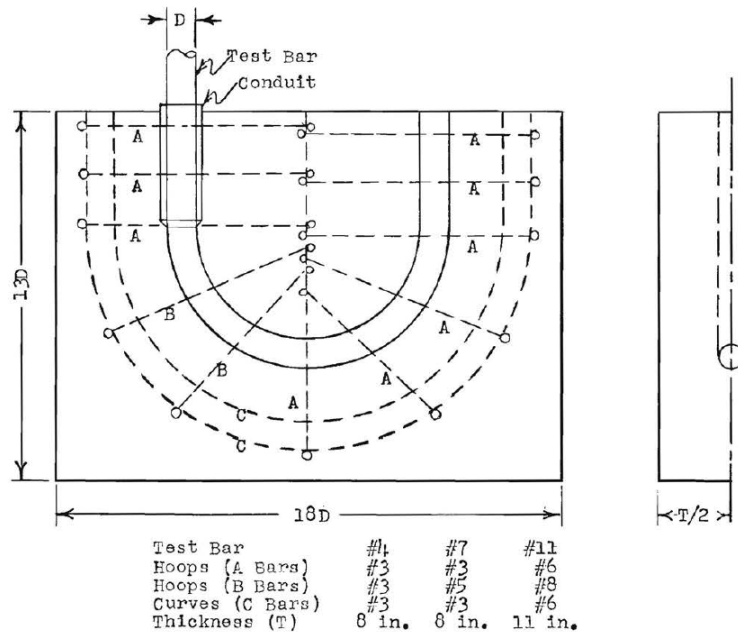
1.3.1.1 Hooked bars

Hribar and Vasko (1969) conducted 96 pull-out tests on straight and hooked bars to evaluate the end anchorage of the test bars. Three test series were performed in the study. The first series included 35 test bars, of which 18 were embedded individually, and the remaining 17 were embedded in a $16 \times 16 \times 5$ ft concrete block. In the second series, 44 test bars were embedded in a $16 \times 16 \times 5.5$ ft concrete block, and the third series included 17 bars embedded in a $10 \times 12 \times 5$ ft concrete block. Test bars embedded in large concrete blocks were embedded far apart (center-to-center 2 to 4 ft) so that a test failure of one bar did not interfere with the failure of the others. The main variables included in the study were the bar size (No. 4, No. 7, and No. 11), type of hook

(straight, 90° bend angle hooked bars, and 180° bend angle hooked bars), and bend diameter (5 to 12 d_b). The smaller concrete blocks were heavily reinforced, as shown in Figure 1.5, to prevent splitting, while the larger concrete blocks were unreinforced. Concrete compressive strengths ranged from 3,700 to 4,750 psi. The loading apparatus is shown in Figure 1.6.



(a)



(b)

Figure 1.5 Small concrete blocks (a) specimen for 90° hooked bars, (b) specimen for 180° hooked bars (Hribar and Vasko 1969)

As shown in Figure 1.5, the dimensions of the specimens are given in bar diameters. Therefore, the size of the small concrete blocks varied with the size of the test bar. The dashed lines shown in Figure 1.5 represent supplementary steel reinforcement. A thin-wall conduit was used to debond the straight portion of the bar preceding the hook, as shown in Figure 1.5.

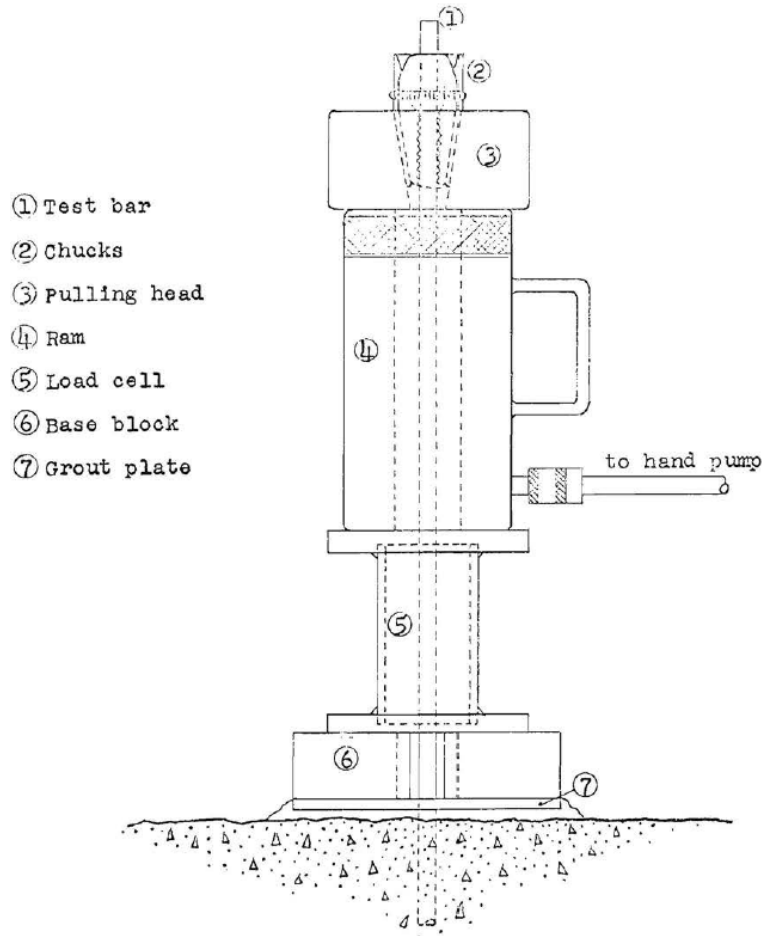


Figure 1.6 Loading apparatus (Hribar and Vasko 1969)

Hribar and Vasko found that the anchorage capacity of the test bars increased as the bend angle increased for an equivalent embedment length. Hribar and Vasko observed that the anchorage capacity of the test bars and the average bond stress at a given displacement increased with the square root of the concrete compressive strength (f'_c). Hribar and Vasko also found that the bar failure load increased as the embedment length and the bar diameter increased.

Minor and Jirsa (1975) conducted pullout tests on 80 deformed straight and hooked bars embedded in concrete blocks to examine some of the parameters that affect the anchorage capacity

of bent deformed reinforcing bars. The dimensions of the concrete block were chosen to be large enough to provide adequate cover for the hooked bars and to prevent the concrete block from splitting. Each concrete block contained one test bar without confining reinforcement. For specimens with a hooked bar, the straight portion of the bars was covered with a loose-fitting plastic tube so that bond was provided only by the hooked portion and the tail extension, as shown in Figure 1.7. The main variables included in the study were the bonded length measured from the beginning of the bend (1.6 to 8.5 in.), the bend angle (0° to 180° in 45° increments), the inside radius of bend (1.15 to $4.6d_b$), and bar diameter (No. 5, No. 7, and No. 9). The average concrete compressive strengths were 4,500, 5,500, and 3,300 psi for specimens containing No. 5, No. 7, and No. 9 test bars, respectively.

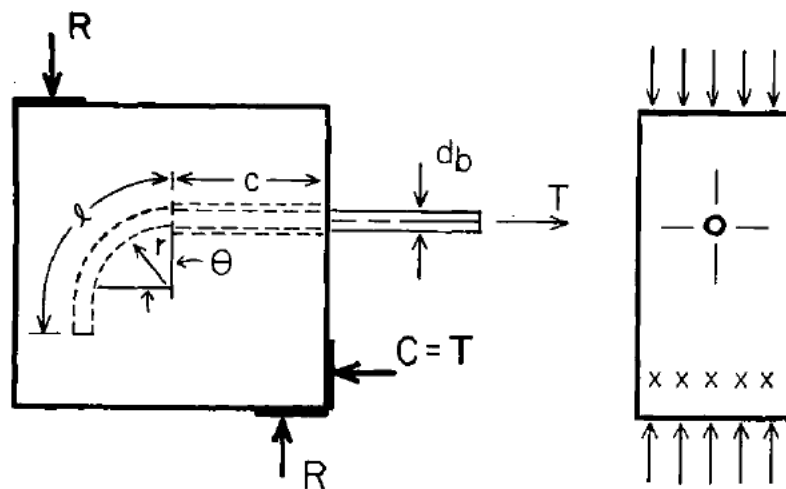


Figure 1.7 Test specimen (Minor and Jirsa 1975)

Minor and Jirsa observed that for test bars with both bent and straight sections (tail extension), most of the slip occurred in the bent portion of the bars. They also found that there was little difference in strength between the straight and bent bars for an equal bonded length, which is the length of the bar in contact with the concrete (see l in Figure 1.7). It is important to note that the bonded length as defined by Minor and Jirsa is different than the development length defined by ACI 318 and ACI 408. Minor and Jirsa found that for equal bonded length to bar diameter ratios, bar slip increased as the bend angle increased and as the ratio of bend radius to bar diameter decreased. Therefore, they stated that in joint details where hooked or bent bars are required,

hooked bars with 90° bend angles were preferable to those with 180° bend angles, and the bend radius should be as large as practical to reduce the slip of the hooked bar.

1.3.1.2 Headed studs and bars

Viest (1956) tested 12 push-out specimens to study the behavior and the load-carrying capacity of stud shear connectors (headed steel studs). Each specimen (Figure 1.8) consisted of two rectangular concrete slabs (30 × 24 × 7 in.) connected to a wide flange steel beam by four or eight headed steel studs, which were welded to the steel beam. Viest found that headed steel studs could be used as shear connectors in composite concrete and steel construction. He proposed empirical equations for calculating the shear capacity of the stud shear connectors.

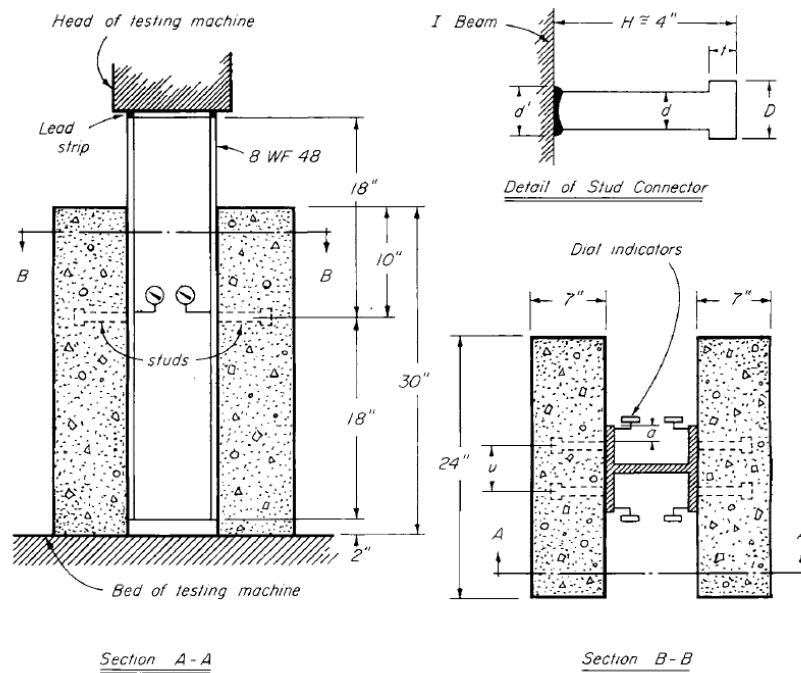


Figure 1.8 Details of push-out specimens (Viest 1956)

McMackin et al. (1973) tested 60 headed steel anchor studs embedded in twelve concrete blocks to study their behavior and strength under a variety of loading conditions. They conducted pure tension loading tests on 22 anchor studs, pure shear loading tests on 12 anchor studs, and combined shear and tension loading tests on the remaining 26 anchor studs. The main variables involved in this study were the type of concrete (normalweight or lightweight), anchor stud length (4 to 8 in.), angle of loading (0°, 30°, and 60°), and free edge distance, distance from the center of

the anchor to the edge of the concrete block, (2 to 12 in.). McMackin et al. concluded that an edge distance of at least 4 in. was required to develop the capacity of anchors with 7 in. embedment lengths loaded in pure tension.

Stoker et al. (1974) conducted pullout tests on 19 concrete blocks with 1-in. thick steel plates attached to the end of No. 11, No. 14, or No. 18 test bars to evaluate their anchorage strength. The 1-in. thick steel plates were 5 in. square, 6 in. square, and 7.5 in. square for the No. 11, No. 14, and No. 18 bars, respectively. The net bearing areas (gross area of the plate minus the nominal area of the test bar, A_b) were $15A_b$ for No. 11 and No. 14 test bars and $13A_b$ for No. 18 test bars. Stoker et al. found that an anchorage device consisting of a 1-in. thick steel plate attached to the bar allowed for the use of shorter embedment lengths than required for straight bars.

1.3.2 Simulated beam-column joints with hooked bars subjected to monotonic loading

Marques and Jirsa (1975) tested 22 exterior beam-column joint specimens to investigate the anchorage strength of hooked bars. The main variables were column axial load (135 to 540 kips), concrete side cover (1.5 to 2.875 in.), location of the hooked bars (inside or outside the column core, the region of the column cross-section confined by the column longitudinal reinforcement), and confining reinforcement within the joint (none or No. 3 hoops spaced at 2.5 or 5 in.). The tests were performed using either No. 7 or No. 11 hooked bars with 90° or 180° bends. Each specimen contained two hooked bars. The nominal concrete compressive strength was 4,500 psi. Figure 1.9 shows the type of test specimen used in this study. Marques and Jirsa found that the effect of the column axial load on the anchorage strength of hooked bars was negligible. They observed that the specimens with 90° hooked bars showed similar behavior to those with 180° hooked bars. They also found that the location of the hooked bars, inside or outside the column core, had very little influence on the anchorage strength of hooked bars. All of the specimens with hooked bars outside the column core, however, had confining reinforcement. Marques and Jirsa found that the effect of closely spaced confining reinforcement within the joints was higher in the case of large anchored hooked bars and that the reduction of the concrete side cover from 2.875 in. to 1.5 in. reduced anchorage strength.

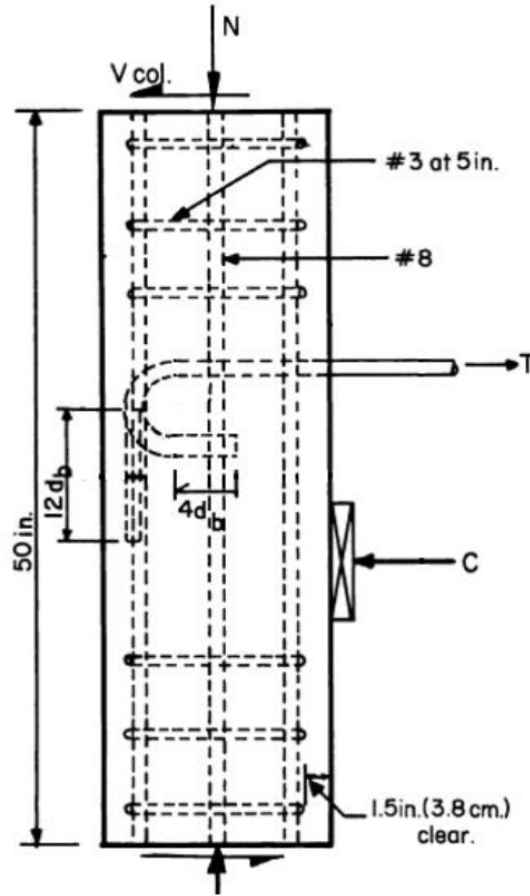


Figure 1.9 Test specimen (Marques and Jirsa 1975)

Based on the test results, Marques and Jirsa developed a design equation to calculate the anchorage strength of standard hooked bars:

$$f_h = 700(1 - 0.3d_b)\psi\sqrt{f'_c} \leq f_y \quad (1.1)$$

where f_h is the tensile stress of a hooked bar (psi); d_b is the hooked bar diameter (in.); f'_c is the concrete compressive strength (psi). ψ is equal to 1.4 if the hooked bar is No. 11 or smaller, the lead straight embedment length (the length of the straight portion of the hooked bar between the hook and the column face) is at least the greater of $4d_b$ or 4 in., the concrete side cover to the hooked bar is at least 2.5 in., and the concrete cover on the tail extension is at least 2 in; ψ equals 1.8 if there is confining reinforcement spaced at $3d_b$ or less within the joint region and the joint meets the requirements for $\psi = 1.4$.

Soroshian et al. (1988) tested seven exterior beam-column joint specimens to determine the anchorage strength and behavior of hooked bars. The main variables were hooked bar diameter

(No. 6, No. 8, and No. 10), confining reinforcement within the joint region (No. 3 hoops spaced at 3 in. or 4 in., and No. 4 hoops spaced at 3 in.), and concrete compressive strength (3,780 to 6,050 psi). Each specimen contained two 90° hooked bars; the straight embedment lengths were covered with a plastic tube to eliminate the bond of the straight portion of the bar. No axial load was applied to the specimens in this study. Soroushian et al. found that the anchorage strength (force at failure) of hooked bars increased as bar diameter increased and as the confining reinforcement within the joint region increased. Soroushian et al. also found that within the range of test variables, concrete compressive strength did not significantly affect the anchorage strength of hooked bars.

Hamad et al. (1993) tested 25 simulated exterior beam-column joint specimens to determine anchorage characteristics of uncoated and epoxy-coated hooked bars. The test setup (Figure 1.10) was similar to that used by Marques and Jirsa (1975) but without horizontal support at the top and no axial load applied to the concrete columns. Each specimen contained two hooked bars. The main variables were bar size (No. 7 and No. 11), hooked bar geometry (90° and 180° bend angles), concrete compressive strength (2,570 to 7,200 psi), concrete side cover (1.75 to 3 in.), confining reinforcement within the joint (none, No. 3 hoops spaced at 4 in. or 6 in.), and hooked bar surface condition (uncoated or epoxy-coated hooked bar).

Hamad et al. found that No. 11 hooked bars (coated and uncoated) showed more slip than No. 7 hooked bars at a given stress level. They also found that the anchorage capacity of hooked bars increased as the concrete compressive strength increased, and using the square root of concrete compressive strength was appropriate for modeling the effect of concrete strength on bond strength. The anchorage capacity of hooked bars increased as the confining reinforcement within the joint region increased. At load levels prior to failure, hooked bars with 90° bend angles were stiffer than hooked bars with 180° bend angles. Hamad et al. observed that the anchorage strength of hooked bars decreased about 8% when the concrete side cover was reduced from 3 to 1.75 in. Specimens with epoxy-coated hooked bars consistently showed lower anchorage strength than specimens with uncoated hooked bars. Hamad et al. recommended a 20 percent increase in the basic development length of an uncoated hooked bar for epoxy-coated hooked bars.

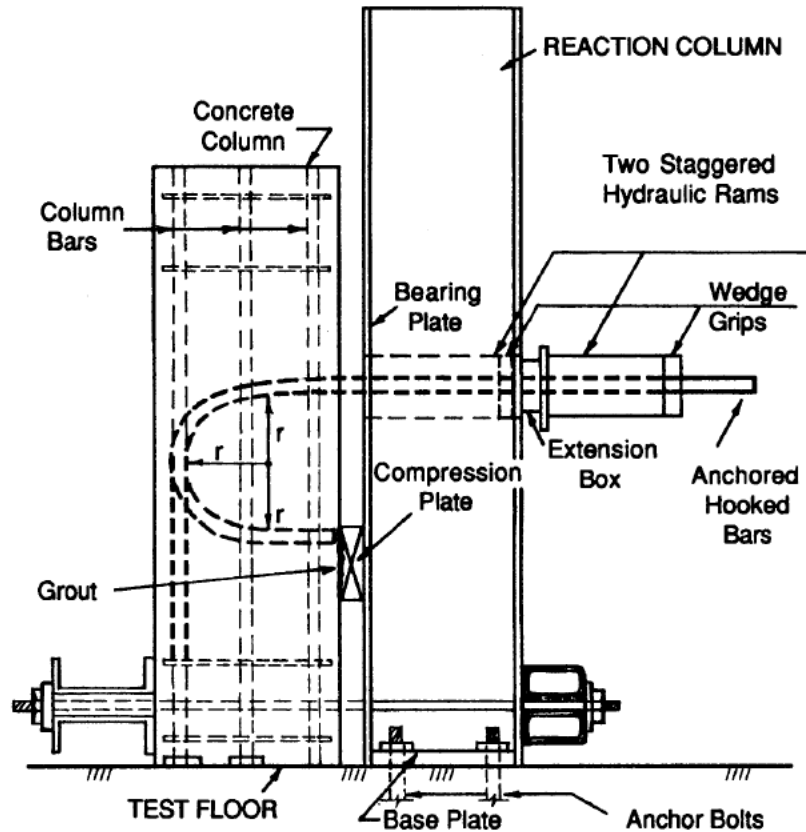


Figure 1.10 Specimen and test setup (Hamad et al. 1993)

Ramirez and Russell (2008) tested 21 exterior beam-column joint specimens to evaluate the anchorage strength of uncoated and epoxy-coated hooked bars anchored in high-strength concrete specimens. The main variables were bar size (No. 6 and No. 11), concrete compressive strength (8,910 to 16,500 psi), confining reinforcement within the joint region (none and ties spaced at $3d_b$), and tail cover (0.75 to 2.5 in.). Each specimen contained two 90° bend angle hooked bars. The test setup (Figure 1.11) was similar to that used by Marques and Jirsa (1975) and Hamad et al. 1993, except that the columns had no horizontal support at the top. No axial load was applied to these specimens.

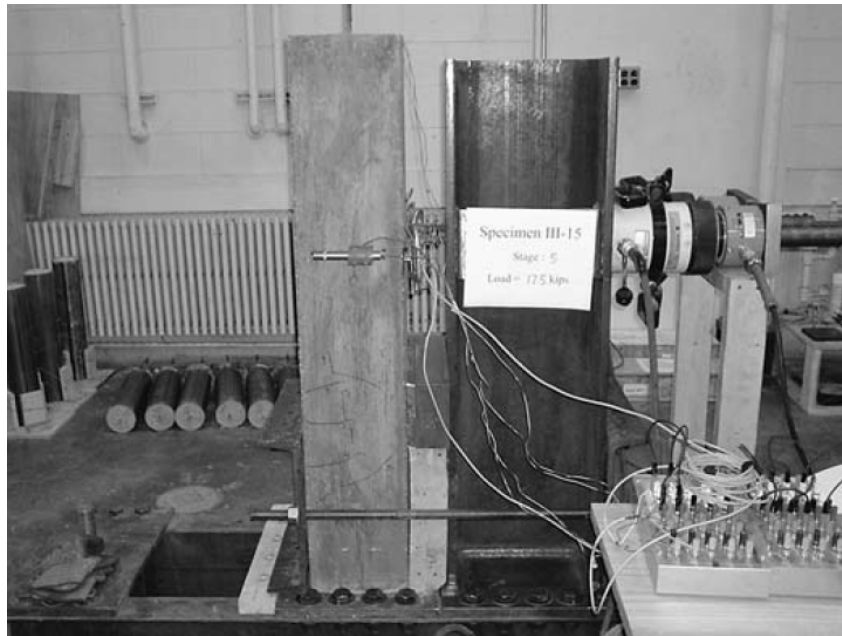
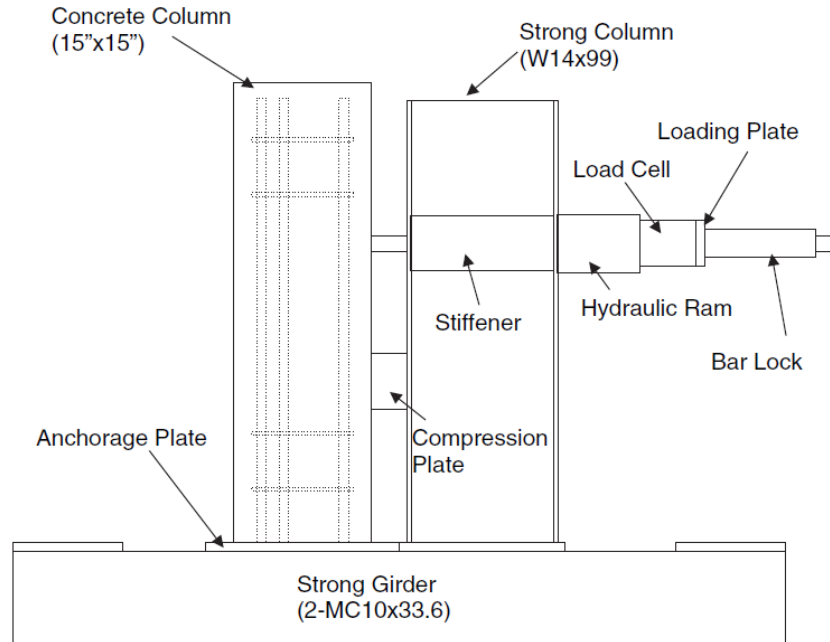


Figure 1.11 Test setup (Ramirez and Russell 2008)

Ramirez and Russell found that specimens with epoxy-coated hooked bar had lower anchorage strength than specimens with uncoated hooked bars. The presence of confining reinforcement within the joint region increased the anchorage strength of both coated and uncoated hooked bars. Ramirez and Russell concluded that the limit on the concrete compressive strength in the ACI 318-05 provisions for the anchorage of standard hooked bars could be extended up to

15,000 psi. However, they also recommended that minimum confining reinforcement spaced at $3d_b$ should be provided in high-strength concrete. Ramirez and Russell proposed that the minimum tail concrete cover of 2.5 in. be reduced to d_b if confining reinforcement is provided.

Sperry et al. (2015a, 2015b, 2017a, 2017b, 2018) tested 337 simulated exterior beam-column joint specimens to investigate the factors that affect the anchorage strength of hooked bars and to develop design guidelines for the development length of hooked bars. The main variables were the number of hooked bars in a specimen (2, 3, or 4), concrete compressive strength (4,300 to 16,510 psi), hooked bar stress at failure (22,800 to 141,600 psi), test bar size (No. 5, No. 8, and No. 11), concrete side cover (1.5 to 4 in.), confining reinforcement within the joint region (none, two No. 3 hoops, or No. 3 hoops spaced at $3d_b$), center-to-center spacing between the test bars (3 to $11d_b$), hook bend angle (90° or 180°), location of hooked bars (inside or outside the column core), and embedment length. Of the 337 beam-column joint specimens, 276 specimens contained two hooked bars, and 61 specimens included three or four hooked bars. The test setup was a modified version of the test setup used by Marques and Jirsa (1975).

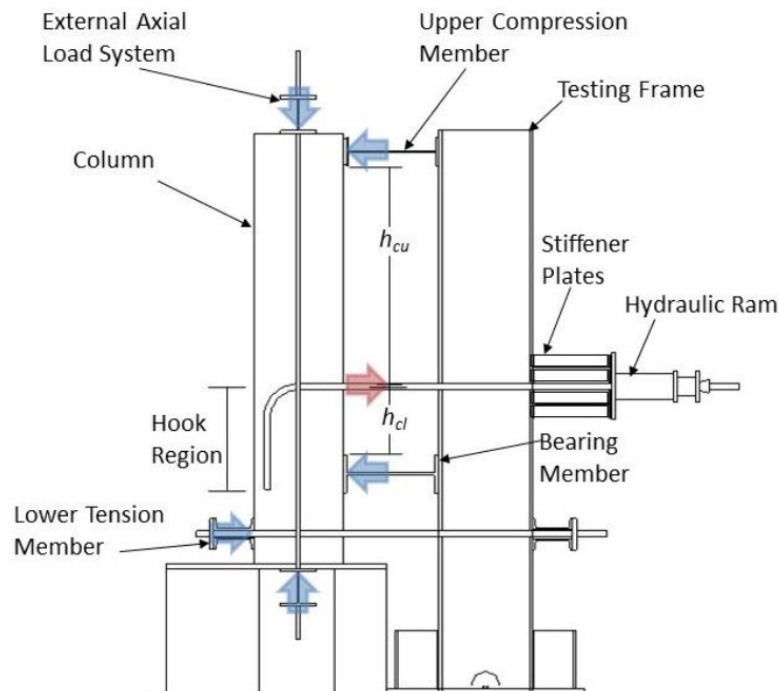


Figure 1.12 Test setup (Sperry et al. 2015a)

Sperry et al. found that the concrete contribution to the anchorage strength of hooked bars can be represented by the concrete compressive strength to the 0.29 power, instead of the square root of concrete compressive strength used in the ACI 318 provisions. Sperry et al. further found that for a given embedment length, the anchorage strength of hooked bars, expressed as a force, increases as the test bar diameter increases. The anchorage strength of hooked bars with a 90° bend was similar to that of hooks with a 180° bend. There was no effect on anchorage strength when the concrete side cover was increased from 2.5 to 3.5 in. Based on the test results, Sperry et al. (2015 a,b) developed descriptive equations, Eqs. (1.2) and (1.3), to characterize the anchorage strength of hooked bars in beam-column joints without and with confining reinforcement, respectively.

$$T_c = 332 f_{cm}^{0.29} \ell_{eh}^{1.06} d_b^{0.54} \quad (1.2)$$

$$T_h = 332 f_{cm}^{0.29} \ell_{eh}^{1.06} d_b^{0.54} + 54,250 \left(\frac{N A_{tr}}{n} \right)^{1.06} d_b^{0.59} \quad (1.3)$$

where T_c is the anchorage strength of a hooked bar without confining reinforcement (lb); T_h is the anchorage strength of a hooked bar with confining reinforcement (lb); f_{cm} is the measured concrete compressive strength (psi); ℓ_{eh} is the embedment length of hooked bar (in.); d_b is the diameter of the hooked bar (in.); N is the number of legs of effective confining reinforcement parallel to the hooked bars being developed; A_{tr} is the area of a single leg of the confining reinforcement (in²); n is the number of hooked bars. Sperry et al. (2015b) found that only confining reinforcement placed within $8d_b$ of the straight portion of the hooked bar for No. 3 through No. 8 test bars or within $10d_b$ of the straight portion of the hooked bar for No. 9 through No. 11 test bars was effective in beam-column joints.

Ajaam et al. (2017, 2018) tested 67 simulated beam-column joint specimens to expand the understanding of the behavior of hooked bars and to develop design guidelines allowing for the use of high-strength materials with special emphasis on the effects of spacing between hooked bars. The main variables were bar size (No. 5, No. 8, and No. 11), hook bend angle (90° and 180°), embedment length (5.5 to 23.5 in.), confining reinforcement within the joint region (none to nine No. 3 hoops), maximum stress in the hooked bar (22,800 to 138,800 psi), concrete compressive strength (4,490 to 14,050 psi), center-to-center spacing between the hooked bars (2 to $11.8d_b$), number of hooked bars in a specimen (2 to 6 bars), and one layer or two layers of test bars in a

specimen. The test frame was the same as that used by Sperry et al. (2015a, 2015b). Ajaam et al. analyzed their results, along with 214 test results from previous studies, and found that the contribution of concrete compressive strength to the anchorage strength of hooked bars can be represented by the concrete compressive strength to the 0.295 power, and that the anchorage strength of hooked bars increases as the amount of confining reinforcement within the joint region increases and is lower for individual closely-spaced (less than or equal to $6d_b$) hooked bars than it is for individual widely-spaced bars. Specimens with a ratio of beam effective depth to embedment length (d/ℓ_{eh}) greater than 1.5 exhibited lower anchorage strengths than those with a (d/ℓ_{eh}) ratio of less than 1.5. Based on the results of this and previous studies, Ajaam et al. developed descriptive equations, Eq. (1.4) and (1.5), to characterize the anchorage strength of hooked bars in beam-column joints for concrete compressive strengths up to 16,000 psi and hooked bar stresses up to 120,000 psi, respectively, without and with confining reinforcement:

$$T_c = \left(294 f_{cm}^{0.295} \ell_{eh}^{1.0845} d_b^{0.47} \right) \left(0.0974 \frac{c_{ch}}{d_b} + 0.3911 \right) \quad (1.4)$$

$$\text{with } \left(0.0974 \frac{c_{ch}}{d_b} + 0.3911 \right) \leq 1.0$$

$$T_h = \left(294 f_{cm}^{0.295} \ell_{eh}^{1.0845} d_b^{0.47} + 55050 \left(\frac{A_{th}}{n} \right)^{1.0175} d_b^{0.73} \right) \left(0.0516 \frac{c_{ch}}{d_b} + 0.6572 \right) \quad (1.5)$$

$$\text{with } \left(0.0516 \frac{c_{ch}}{d_b} + 0.6572 \right) \leq 1.0$$

where T_c is the anchorage strength of a hooked bar without confining reinforcement (lb); T_h is the anchorage strength of a hooked bar with confining reinforcement (lb); f_{cm} is the measured concrete compressive strength (psi); ℓ_{eh} is the embedment length of hooked bar (in.); d_b is the diameter of the hooked bar (in.); c_{ch} is the center-to-center spacing between hooked bars (in.); A_{th} is the total cross-sectional area of all parallel confining reinforcement located within $8d_b$ of the top or bottom of the test bars for No. 3 through No. 8 hooked bars or within $10d_b$ for No. 9 through No. 11 hooked bars (in.²); and n is the number of hooked bars.

Based on their study, Ajaam et al. (2017) recommended design provisions for hooked bars, with ℓ_{dh} (incorporating a strength reduction, ϕ , factor of 0.81) based on the bar diameter d_b to the 1.5 power and the concrete compressive strength f'_c to the 0.25 power.

$$\ell_{dh} = 0.003 \frac{f_y \Psi_e \Psi_{cs} \Psi_o}{\lambda f_c^{1.25}} d_b^{1.5} \quad (1.6)$$

where Ψ_e is the epoxy coating factor, equal to 1.2 for epoxy-coated or zinc and epoxy dual-coated reinforcement and 1.0 for uncoated or zinc-coated (galvanized) reinforcement; Ψ_o equals 1.0 for hooked bars terminating inside a column core with clear side cover to the bar ≥ 2.5 in., or terminating in a supporting member with side cover to the bar $\geq 6d_b$; in other cases, Ψ_o is taken as 1.25. Ψ_{cs} is confining reinforcement and spacing factor, calculated using Table 1.1.

Table 1.1 Modification factor Ψ_{cs} for confining reinforcement and spacing ^[1]

Confinement level	f_y	C_{ch}	
		$2d_b$	$\geq 6d_b$
$\frac{A_{th}}{A_{hs}} \geq 0.2$ ^[2] or $\frac{A_{th}}{A_{hs}} \geq 0.4$ ^[3]	60,000	0.6	0.5
	120,000	0.66	0.55
No confining reinforcement	all	1.0	0.6

^[1] Ψ_{cs} may be linearly interpolated for spacing or yield strengths not listed

^[2] Confining reinforcement parallel to straight portion of bar

^[3] Confining reinforcement perpendicular to straight portion of bar

Yasso et al. (2017, 2021) examined a subset of 195 specimens from those reported by Sperry et al. (2015a, 2015b) to investigate the effects of concrete tail cover and tail kickout on the anchorage strength of 90-degree hooked bars. The main variables were concrete tail cover (0.75 to 3.625 in.), concrete compressive strength (4,490 to 16,180 psi), hooked bar stresses at failure (33,000 to 141,000 psi), test bar size (No. 5, No. 8, and No. 11), confining reinforcement within the joint region (none to six No. 3 hoops), and location of hooked bars (inside or outside the column core). All specimens contained two hooked bars. Of the 195 beam-column joint specimens, 167 had hooked bars placed inside the column core, 113 with confining reinforcement within the joint region and 54 without. Twenty-eight specimens had the hooked bars placed outside the column core, 14 with confining reinforcement within the joint region and 14 without. Yasso et al. observed that tail kickout occurred for approximately 7% of the specimens used in the analysis and was only observed in conjunction with other failure modes, with the likelihood of tail kickout increasing as

confining reinforcement within the joint region decreased, as the hooked bar size increased, and for hooked bars placed outside the column core. The anchorage strength of hooked bars was not affected by hook tail covers as low as 0.75 in. or by tail kickout at failure.

1.3.3 Beam-column joints with hooked bars subjected to reversed cyclic loading

This study includes an analysis of the results of 146 exterior beam-column joint specimens containing hooked bars tested under reversed cyclic loading by Hanson and Connor (1967), Hanson (1971), Megget (1974), Uzumeri (1977), Lee et al. (1977), Scribner (1978), Paulay and Scarpas (1981), Ehsani and Wight (1982), Kanada et al. (1984), Zerbe and Durrani (1985), Ehsani et al. (1987), Ehsani and Alameddine (1991), Kaku and Asakusa (1991), Tsonos et al. (1992), Pantelides et al. (2002), Chutarat and Aboutaha (2003), Hwang et al. (2005), Lee and Ko (2007), Chun et al. (2007), Tsonos (2007), Kang et al. (2010), Chun and Shin (2014), Hwang et al. (2014), and Choi and Bae (2019). A summary of these studies is presented in this section, and complete details are presented in Appendix D.

The main variables used in these studies were embedment length (6 to 21 in.), concrete compressive strength (3,140 to 13,700 psi), center-to-center spacing between the hooked bars (1.75 to 6.5 in.), bar size (No. 3 to No. 9), and confining reinforcement within the joint region. In addition, Hanson (1971), Uzumeri (1977), and Zerbe and Durrani (1985) studied the effect of transverse beams (beams perpendicular to the test beam at the joint) and slabs on the performance of beam-column joints. Of the 146 beam-column joint specimens, 3 contained transverse beams and slabs, and 6 had only transverse beams. The yield strength of the hooked bars ranged from 42,900 to 103,000 psi. Concrete side cover ranged from 0.7 to 8.6 in. Deformed confining reinforcement within the joint region, parallel to the straight portion of the hooked bars, ranged from none to 8 hoops, and the area of a single leg of a hoop ranged from 0.078 to 0.31 in.², with the exception of two studies (Kaku and Asakusa 1991, Tsonos 2007), which used plain round steel bars as confining reinforcement within the joint region with an area of a single leg ranging from 0.011 to 0.044 in.². Of the 146 specimens, 14 had no confining reinforcement within the joint region. Column axial compressive load applied during the test ranged from zero to $0.25A_g f'_c$, where A_g is the column cross-sectional area (in.²) and f'_c is the nominal concrete compressive

strength (psi). Of the 146 specimens, 11 specimens had $M_R \leq 1.2$, and 135 specimens had $M_R \geq 1.2$, where M_R is a ratio of the flexural strength of the column to the flexural strength of the beam. In accordance with Section 4.4.2 of ACI 352R-02 for connections that are subjected to reversed cyclic loading, the flexural strength of the column should be at least 20 percent greater than the flexural strength of the beam to produce flexural hinging in the beams rather than in the columns. Therefore, only specimens with $M_R \geq 1.2$ were used in this analysis.

The test results showed that 120 out of the 135 beam-column joint specimens with $M_R \geq 1.2$ performed satisfactorily under reversed cyclic loading, attaining a peak moment 1 to 45% greater than the nominal flexural strength of the beam anchored at the joint using hooked bars. Of the 120 specimens, 108 exhibited less than a 20% reduction in peak load at 3.5% drift, indicating a satisfactory level of performance, and the remaining specimens exhibited less than a 20% reduction in peak load at a drift less than 3.5% (1.1 to 3.0%). The peak moment of the remaining 15 specimens was less than the nominal flexural strength. A detailed description of the performance of these specimens is presented in Appendix D.

1.3.4 Simulated beam-column joints with headed bars subjected to monotonic loading

Bashandy (1996) tested 32 simulated exterior beam-column joint specimens to evaluate the effects of head size (ranging from 2 to $7.1A_b$), head aspect ratio and orientation (the ratio between the vertical and horizontal dimensions of the head based on orientation relative to the concrete surface), anchored bar size (No. 8 and No. 11), embedment length (8.5 to 17 in.), side cover to the headed bar (1.5 and 3 in.), and confining reinforcement within the joint region (no ties or No. 3 ties spaced at 2 in. or 4 in.) on the anchorage strength of headed bars. The column width was 12 in., while the depth depended on the embedment length of the headed bars. Each specimen contained two headed bars with a spacing that depended on the concrete side cover. The concrete compressive strength ranged from 3,200 to 5,800 psi. Figure 1.13 shows the test setup used by Bashandy.

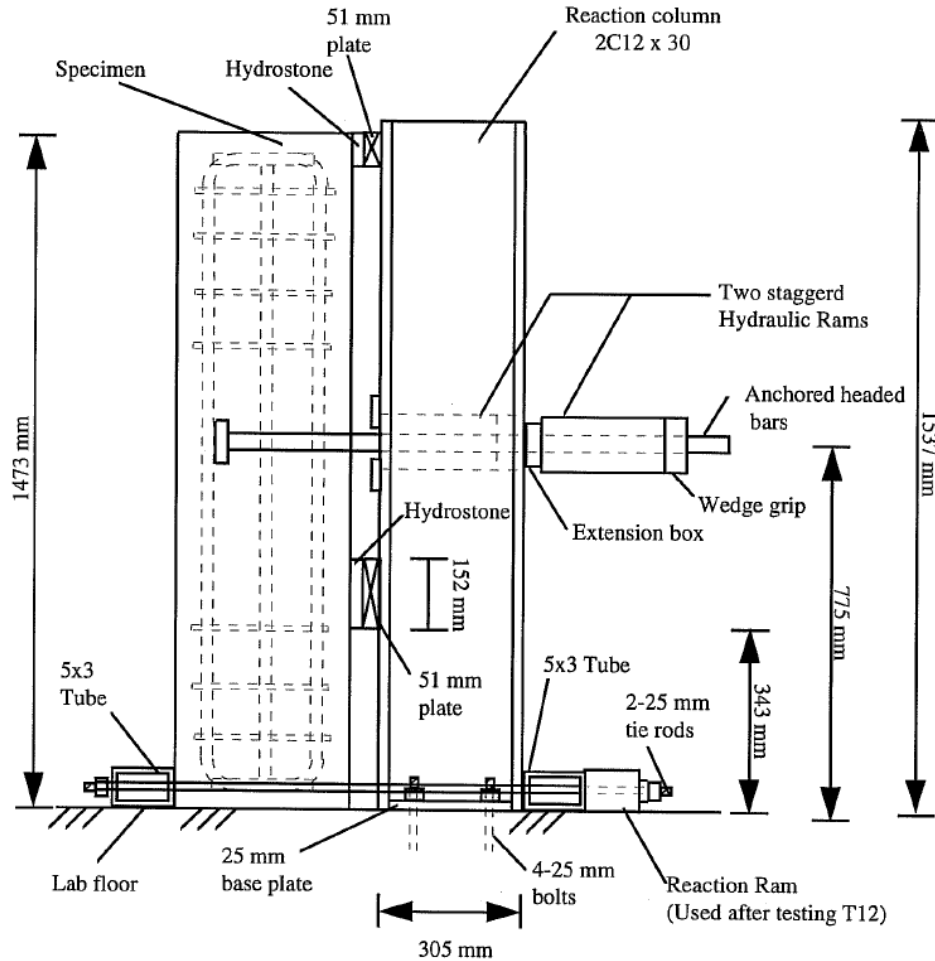


Figure 1.13 Test Setup (Bashandy 1996)

Bashandy divided the test specimens into two major groups depending on the mode of failure. Eighteen specimens failed in a mode referred to as side blowout, characterized by spalling of concrete side cover. This failure mode was a function of embedment length, head dimensions, confining reinforcement, and concrete side cover. The remaining fourteen specimens failed in shear. This failure mode was a function of the embedment depth and shear reinforcement. Bashandy found that the anchorage capacity of the headed bars increased as embedment length, head size, and confining reinforcement within the joint region increased. The effects of aspect ratio, head orientation, and bar diameter on the anchorage capacity of headed bars were insignificant.

Chun et al. (2009) tested 30 exterior beam-column joint specimens to measure the anchorage strength of hooked and headed bars. The main variables were the anchorage configuration (headed bar or 90-degree hooked bar), bar size (No. 8, No. 11, or No. 18), and

embedment length (6.3 to 35.7 in.). The specimens were tested in a horizontal position, as shown in Figure 1.14. No axial load was applied to the columns during the test. Each specimen contained a single hooked or headed bar without confining reinforcement in the joint region. The column depth was fixed for each bar size, and the ratio of the embedment length to column depth was 0.5, 0.7, and 0.9 for No. 8, No. 11, and No. 18 bars, respectively. Two types of failure, concrete breakout and joint shear, were observed in this study. In a concrete breakout failure, diagonal cracks radiating from both sides of the head and a concrete cone was formed and pulled out with the bar, as shown in Figure 1.15a. In a joint shear failure, a diagonal crack formed within the joint and extended to the other column side, as shown in Figures 1.15b and c. Chun et al. compared the test results of headed bar specimens with the models proposed by Thompson et al. (2006), Bashandy (1996), and DeVries (1996). Chun et al. found that the existing models were not suitable for predicting the contribution of the concrete to the anchorage strength of a single headed bar. Therefore, based on the experimental results of this study, Chun et al. developed a new model to predict the anchorage strength of headed bars in exterior beam-column joints. Chun et al. concluded that the anchorage strength of a headed bar results from a combination of bearing on the head and bond along the bar. Chun et al. also found that the anchorage strength of headed bars increased as the embedment length increased.

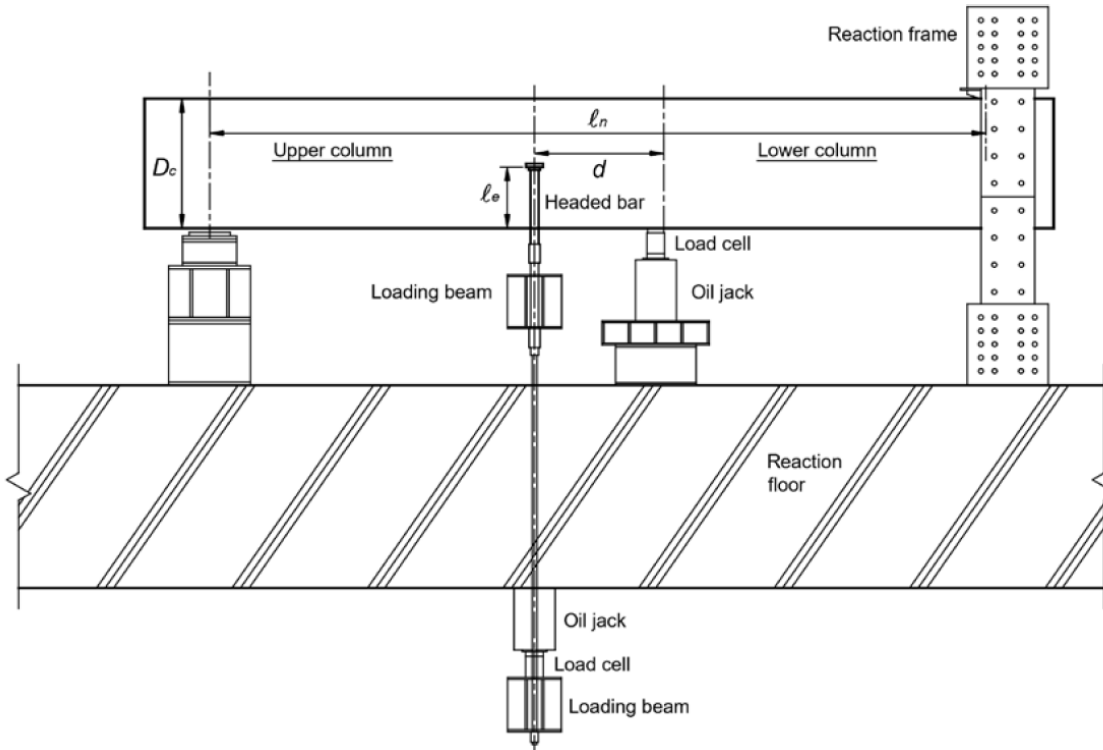


Figure 1.14 Test setup (Chun et al. 2009)

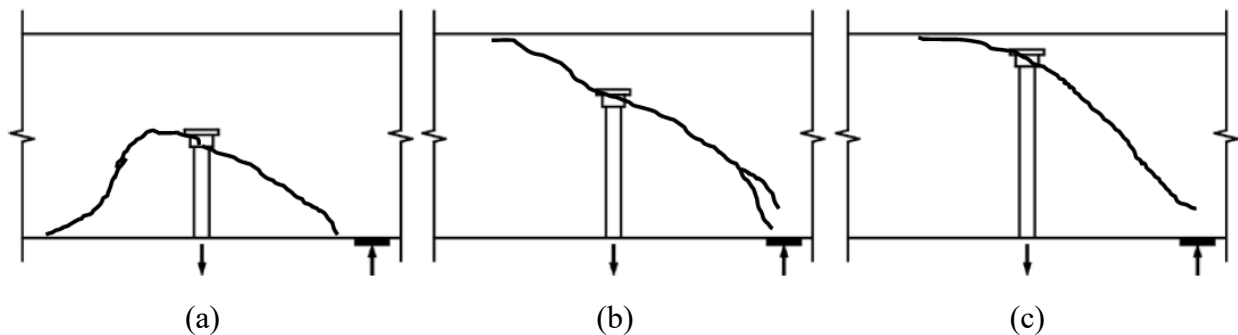


Figure 1.15 Failure modes: (a) concrete breakout, (b) and (c) joint shear failure (Chun et al. 2009)

Shao et al. (2016) and Ghimire et al. (2019a, 2019b) tested 202 simulated exterior beam-column joint specimens to investigate the anchorage strength of headed bars. The main variables were embedment length (4 to 19.25 in.), confining reinforcement within the joint region (no confining reinforcement, two No. 3 hoops, or No. 3 hoops spaced at $3d_b$, where d_b is the bar diameter), concrete compressive strength (3,960 to 16,030 psi), bar size (No. 5, No. 8, and No. 11), head size (the net bearing area from 3.8 to $14.9A_b$, where A_b is bar area), test bar stresses at failure (26,100 to 153,200 psi), number of test bars in a specimen (2, 3, or 4 bars), center-to-center spacing between the test bars (3 to $11.8d_b$), and concrete side cover to the test bar (2.5 to 4 in.).

The test frame (Figure 1.16) was the same as that used by Sperry et al. (2015a, 2015b) and Ajaam et al. (2017).

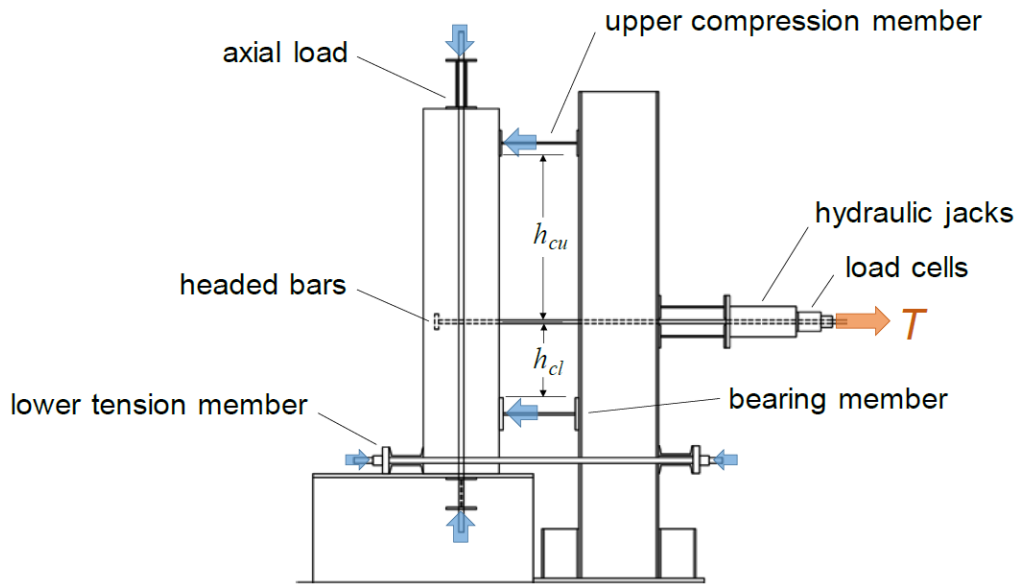


Figure 1.16 Test Frame (Shao et al. 2016)

Shao et al. (2016) and Ghimire et al. (2019 a, 2019b) found that the contribution of concrete to the anchorage strength of a headed bar is more accurately represented by the compressive strength of the concrete to the 0.24 power, instead of the square root of the compressive strength, as used in ACI 318. Shao et al. (2016) and Ghimire et al. (2019a, 2019b) observed that the anchorage strength of headed bars increased as the confining reinforcement parallel to the bars increased and that the strength increase was proportional to the amount of confining reinforcement per headed bar. They also found that the headed bars with bearing areas between 12.9 and $14.9A_b$ provided higher anchorage strengths than those with bearing areas between 3.8 and $9.5A_b$. Based on the results of the study, Shao et al. developed descriptive equations for concrete compressive strengths up to 16,000 psi and headed bar stresses up to 120,000 psi for headed bars without and with confining reinforcement shown, respectively, in Eq. (1.7) and (1.8).

$$T_c = \left(781 f_{cm}^{0.24} \ell_{eh}^{1.03} d_b^{0.35} \right) \left(0.0836 \frac{s}{d_b} + 0.3444 \right) \quad (1.7)$$

with $0.0836 \frac{s}{d_b} + 0.3444 \leq 1.0$, and

$$T_h = \left(781 f_{cm}^{0.24} \ell_{eh}^{1.03} d_b^{0.35} + 48,800 \frac{A_{tr}}{n} d_b^{0.88} \right) \left(0.0622 \frac{s}{d_b} + 0.5428 \right) \quad (1.8)$$

with $0.0622 \frac{s}{d_b} + 0.5428 \leq 1.0$ and $\frac{A_{tr}}{n} \leq 0.3 A_b$

where T_c is the anchorage strength of a headed bar without confining reinforcement (lb); T_h is the anchorage strength of a headed bar with confining reinforcement (lb); f_{cm} is the measured concrete compressive strength (psi); ℓ_{eh} is the embedment length (in.); d_b is the diameter of the headed bar (in.); s is the center-to-center spacing between the bars (in.); A_{tr} is the total cross-sectional area of effective confining reinforcement (NA_{tr}) parallel to the headed bars being developed (in.²); N is the number of legs of effective confining reinforcement parallel to the headed bars being developed; A_{tr} is the area of a single leg of the confining reinforcement (in.²); n is the number of headed bars in tension; A_b is the area of the headed bar (in.²).

Based on their study, Shao et al. (2016) recommended design provisions for headed bars, with ℓ_{dt} (incorporating a strength reduction, ϕ , factor of 0.833) based on the bar diameter d_b to the 1.5 power and the concrete compressive strength f'_c to the 0.25 power.

$$\ell_{dt} = \left(0.0024 \frac{f_y \psi_e \psi_{cs} \psi_o}{f_c'^{0.25}} \right) d_b^{1.5} \quad (1.9)$$

where ψ_e is the epoxy coating factor, equal to 1.2 for epoxy-coated or zinc and epoxy dual-coated reinforcement and 1.0 for uncoated or zinc-coated (galvanized) reinforcement; ψ_o equals 1.0 for headed bars terminating inside a column core with clear side cover to the bar ≥ 2.5 in., or terminating in a supporting member with side cover to the bar $\geq 8d_b$; in other cases, ψ_o is taken as 1.25. ψ_{cs} is confining reinforcement and spacing factor, calculated using Table 1.2.

Table 1.2 Modification factor ψ_{cs} for confining reinforcement and spacing ^[1]

Confinement level	f_y	s	
		$2d_b$	$\geq 8d_b$
$\frac{A_{tr}}{A_{hs}} \geq 0.3$	$\leq 60,000$	0.6	0.4
	120,000	0.7	0.45
No confining reinforcement	all	1.0	0.5

^[1] ψ_{cs} is permitted to be linearly interpolated for values of A_{tr}/A_{hs} between 0 and 0.3 and for spacing s or yield strength of headed bar f_y intermediate to those in the table

1.3.5 Headed bars in slab specimens

DeVries et al. (1999) tested three concrete slab specimens containing three to 11 headed reinforcing bars each (for a total of 18 test bars) embedded in concrete slabs to investigate the effects of several variables on the anchorage capacity and behavior of headed bars. The slabs (Figure 1.17) had dimensions of $5 \times 9 \times 1.75$ ft. The test bars were spaced at a center-to-center distance of at least three times the embedment length of the headed bars to avoid an overlap of the anticipated failure region. The bars were tested individually in tension until failure. The main variables were embedment length (1.375 to 9 in.), bonded length (length along the deformed bar in contact with concrete as shown in Figure 1.18, ranging from 0 to 9 in.), concrete cover to the bar (1.6 to 17.6 in.), bar size (No. 6, No. 8, and No. 11), head size (net bearing area 4.7 to $7.4A_b$), head aspect ratio (the ratio of the largest to the smallest dimension of the head, ranging from 1 to 2), concrete compressive strength (3,920 to 12,040 psi), and transverse reinforcement (of the 18 tests, four had two No. 3 bars as transverse reinforcement perpendicular to the headed bar, distributed evenly along the embedment length, as shown in Figure 1.19, and the other 14 had none). The nominal yield strength of the headed bars was 72,000 psi. Fourteen of the headed bars were unbonded along the embedment length using a PVC pipe, as shown in Figure 1.18a. Four headed bars with embedment lengths equal to 9 in. were bonded, as shown in Figure 1.18b. During the test, the bearing reactions (support plates) were placed at least two times the embedment length away from the headed bars, outside the anticipated failure region, as shown in Figure 1.17, to limit the effect of the bearing reaction on the anchorage strength of the bars.

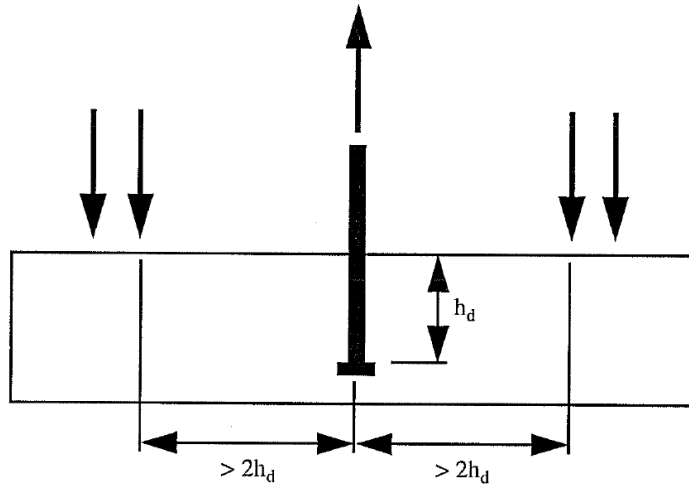


Figure 1.17 Test setup (DeVries et al. 1999)

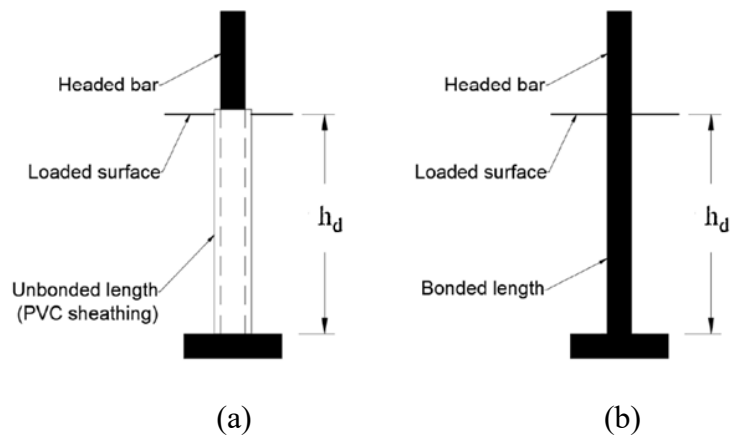


Figure 1.18 Headed reinforcing bars (a) unbonded and (b) bonded embedment length (DeVries et al. 1999)

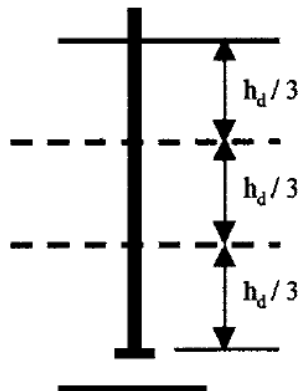


Figure 1.19 Transverse reinforcement configuration (DeVries et al. 1999)

DeVries et al. observed two types of failure – concrete breakout and fracture of the test bar. The three bars that fractured before a concrete breakout occurred were excluded from their analysis. Concrete breakout failures were sudden, and the load carried by the test bar dropped to zero instantly; no cracking was observed before failure – even for the bonded specimens. DeVries et al. observed that the size of the pullout cone (concrete breaking out with headed bar) increased as the edge distance, head size, and embedment length increased. DeVries et al. found that the anchorage strength of headed bars increased and the slip of the head prior to failure decreased as the embedment length and the edge distance were increased. They also found that transverse reinforcement placed perpendicular to the headed bar did not affect the anchorage strength of the headed bar. Lastly, they observed that the anchorage strength of headed bars was not affected by changing the aspect ratio of the head.

Choi et al. (2002) conducted 16 tests on headed bars anchored in slabs (Figure 1.20) to investigate the anchorage strength and behavior of headed bars. The main variables were concrete compressive strength (3,930 to 5,270 psi), bar size (No. 5 to No. 9), embedment length (4.4 to 13.7 in.), and concrete cover to the bar (1.6 to 35 in.). Two test configurations were used for slab specimens. In the first configuration, the headed bar was anchored in the middle of the concrete slab so that the concrete breakout failure region was not affected by the test support reactions. In this configuration, the distance measured from the surface of the headed bar to the edge of the slab was greater than two times the embedment length of the bar, as shown in Figure 1.20. In the second configuration, the headed bar was anchored close to the slab boundaries to study the effect of edge distance on the anchorage strength of headed bars. In this configuration, the concrete cover to the bar ranged from 1.6 to 4.9 in. Headed bars anchored in slab specimens were tested one at a time. Choi et al. (2002) found that the anchorage strength of headed bars decreased as the edge distance decreased.

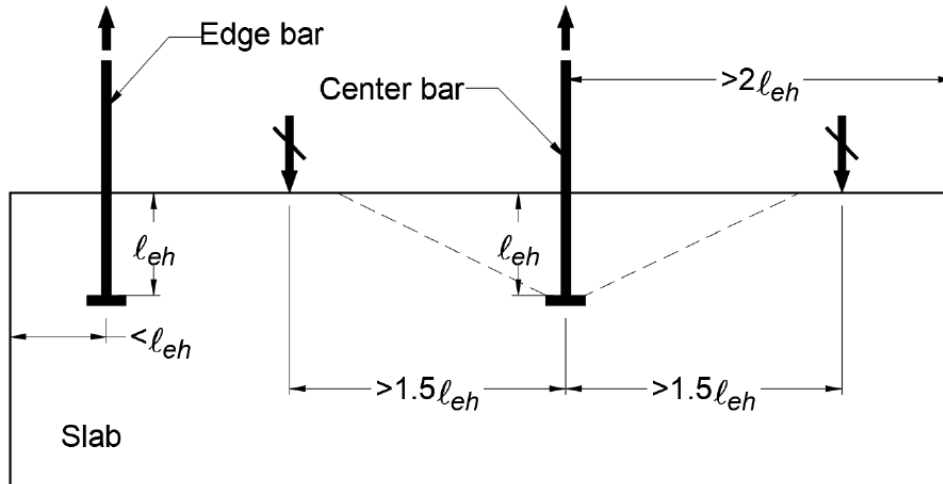


Figure 1.20 Slab specimens (Choi et al. 2002)

1.4 CONCRETE CAPACITY DESIGN METHOD

Fuchs et al. (1995) presented a new method, Concrete Capacity Design (CCD), to predict the concrete failure load of anchor bolts and headed studs embedded in uncracked concrete. The CCD method is the basis for the equations in Sections 17.6.2.1 through 17.6.2.4 of ACI 318-19, calculating the concrete breakout strength of a single anchor or an anchor group. The main variables included the use of single anchors away from and close to the edge of the concrete, anchor groups, and tension loading. The CCD method is an adapted version of the so-called Kappa Method (K-method), which was developed at the University of Stuttgart (Eligehausen et al. 1987), with an assumed breakout failure surface angle of approximately 35 degrees. The CCD method is based on a physical model in which the tension force on an anchor bolt or headed stud is resisted by the stress distributed in the concrete over a failure area. Fuchs et al. assumed that the concrete failure surface of an individual anchor is a pyramid with a base length equal to three times the embedment length and a height equal to the embedment length, as shown in Figure 1.21.

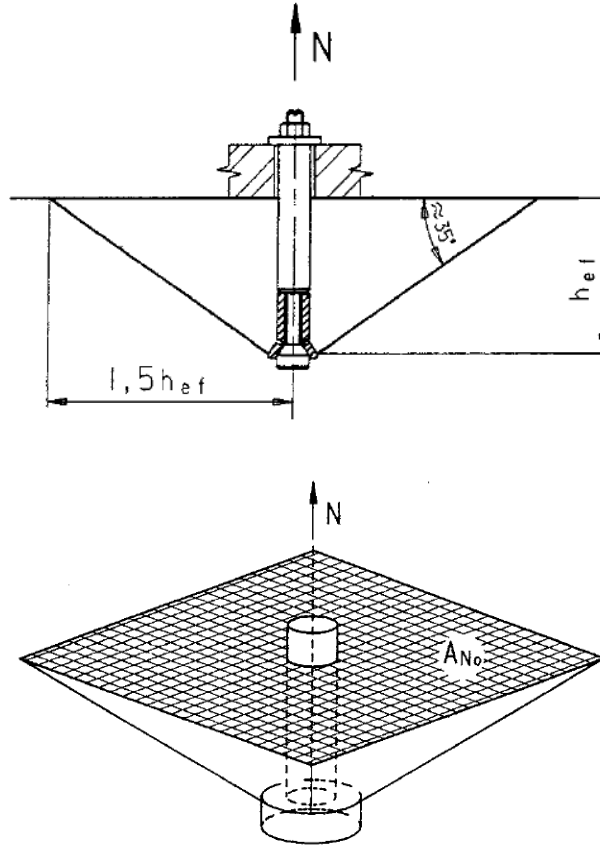


Figure 1.21 CCD idealized concrete cone for an individual anchor (Fuchs et al. 1995)

The concrete cone failure load of a single anchor bolt or headed stud in uncracked concrete unaffected by close spacing of adjacent anchors or edge influences can be represented by a best fit equation:

$$N_{no} = k_{nc} \cdot \sqrt{f'_c} \cdot h_{ef}^{1.5} \quad (1.10)$$

where N_{no} is the concrete cone failure load of a single anchor (lb), k_{nc} is a calibration factor equal to 40 for cast-in headed studs and headed anchor bolts in uncracked concrete, f'_c is the concrete compressive strength (psi), and h_{ef} is the embedment length (in.).

When an anchor bolt is placed close to an edge or corner, the concrete failure area is less than the area assumed for Eq. (1.10), and the anchor's resulting failure load is also reduced. This scenario is also true for anchor groups spaced so closely that the concrete breakout cones overlap. To take into account the reduction in the concrete failure area, N_{no} [Eq. (1.10)] is multiplied by the ratio of the available concrete failure area and the concrete failure area for an individual anchor placed away from an edge and a modification factor Ψ_1 , as shown in Eq. (1.11).

$$N_n = \frac{A_N}{A_{No}} \cdot \psi_1 \cdot N_{no} \quad (1.11)$$

where A_N is the actual projected area at the concrete surface (in.²); A_{No} is the assumed projected area of an individual anchor uninfluenced by edge effects (Figure 1.22), equal to $9h_{ef}^2$; ψ_1 is a modification factor for edge effects for single or anchor groups, equal to 1.0 if the smallest side cover distance is at least $1.5h_{ef}$; otherwise, ψ_1 is equal to $0.7 + 0.3(c_1/1.5h_{ef})$, where c_1 is the smallest distance between the center of an anchor and the edge of the concrete (in.).

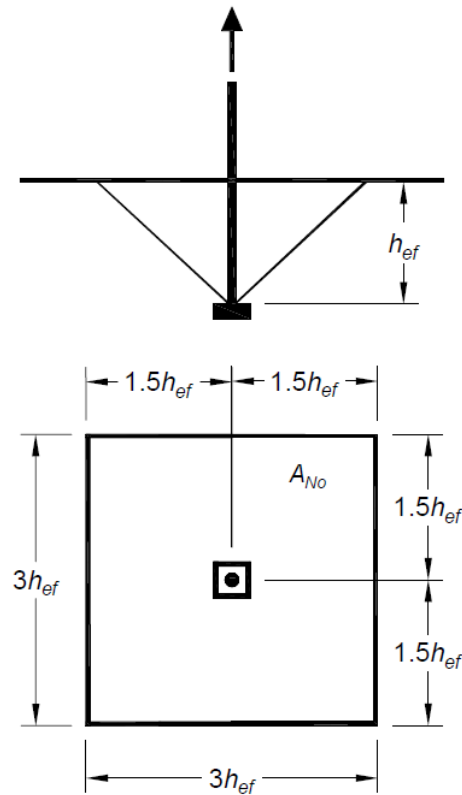
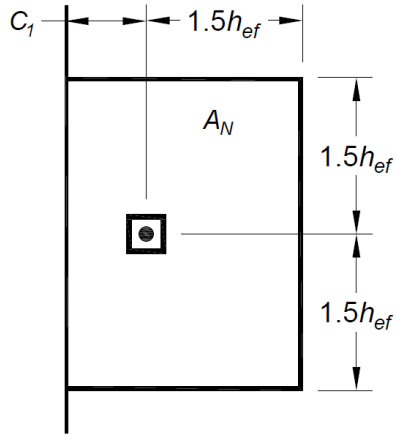


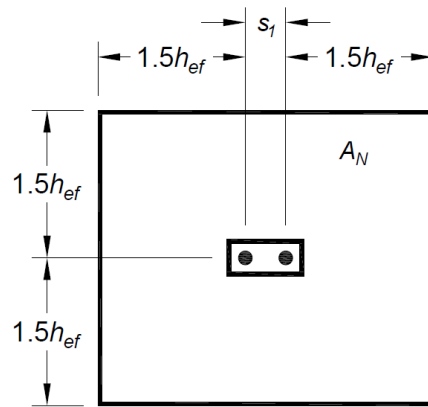
Figure 1.22 Projected area of an individual anchor according to the CCD method (Fuchs et al. 1995)

Fuchs et al. proposed examples for calculating the projected areas, A_N , in accordance with the CCD method shown in Figure 1.23.



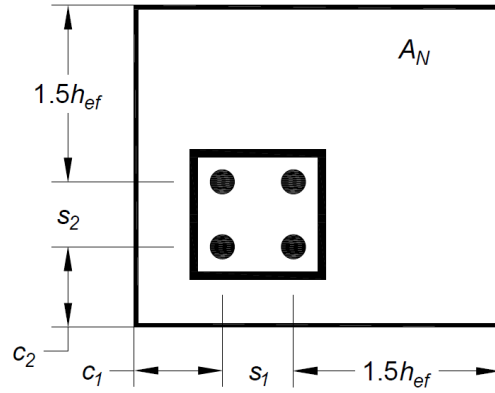
$$A_N = (c_1 + 1.5h_{ef}) \times (2 \times 1.5h_{ef})$$

$$c_1 < 1.5h_{ef}$$



$$A_N = (2 \times 1.5h_{ef} + s_1) \times (2 \times 1.5h_{ef})$$

$$s_1 < 3h_{ef}$$



$$A_N = (c_1 + s_1 + 1.5h_{ef}) \times (c_2 + s_2 + 1.5h_{ef})$$

$$c_1, c_2 < 1.5h_{ef}$$

$$s_1, s_2 < 3h_{ef}$$

Figure 1.23 Calculation of the projected area, A_N , according to the CCD method (Fuchs et al. 1995)

Fuchs et al. developed Eq. (1.11) based on the assumption that the anchor groups are loaded concentrically in tension. However, if the anchor group is loaded eccentrically in tension, the applied resultant tensile load is not shared equally by the anchors. Fuchs et al. added another modification factor to Eq. (1.11) to consider the eccentricity of the applied resultant tensile load, as shown in Eq. (1.12).

$$N_n = \frac{A_N}{A_{No}} \cdot \Psi_1 \cdot \Psi_2 \cdot N_{no} \quad (1.12)$$

where Ψ_2 is a modification factor for anchor groups loaded eccentrically in tension, equal to $\frac{1}{1 + 2e_N' / (3h_{ef})} \leq 1$, where e_N' is the distance between the resultant tensile load on a group of anchors loaded in tension and the centroid of the group of anchors loaded in tension (in.).

The CCD method does not take into account the effect of the parallel tie reinforcement on the concrete failure load of the anchor bolts. The CCD method also applies to expansion anchors embedded in plain concrete, as well as anchor bolts and headed studs.

Nilforoush et al. (2017) tested 19 single cast-in-place headed anchors in plain and steel fiber-reinforced normal- and high-strength concrete specimens to investigate anchorage capacity

and behavior of headed anchors and to evaluate the Concrete Capacity Design (CCD) method. The main variables were concrete compressive strength, use of steel fibers, and concrete member thickness. The concrete slabs had plan dimensions of 51×51 in. and depths ranging from 13 to 26 in. The yield strength of the anchors was 130 ksi, and concrete compressive strengths ranged from 5,650 to 11,890 psi. Each specimen contained a single anchor placed at the center of the slab with an embedment length of 8.5 in. The test setup used is shown in Figure 1.24.

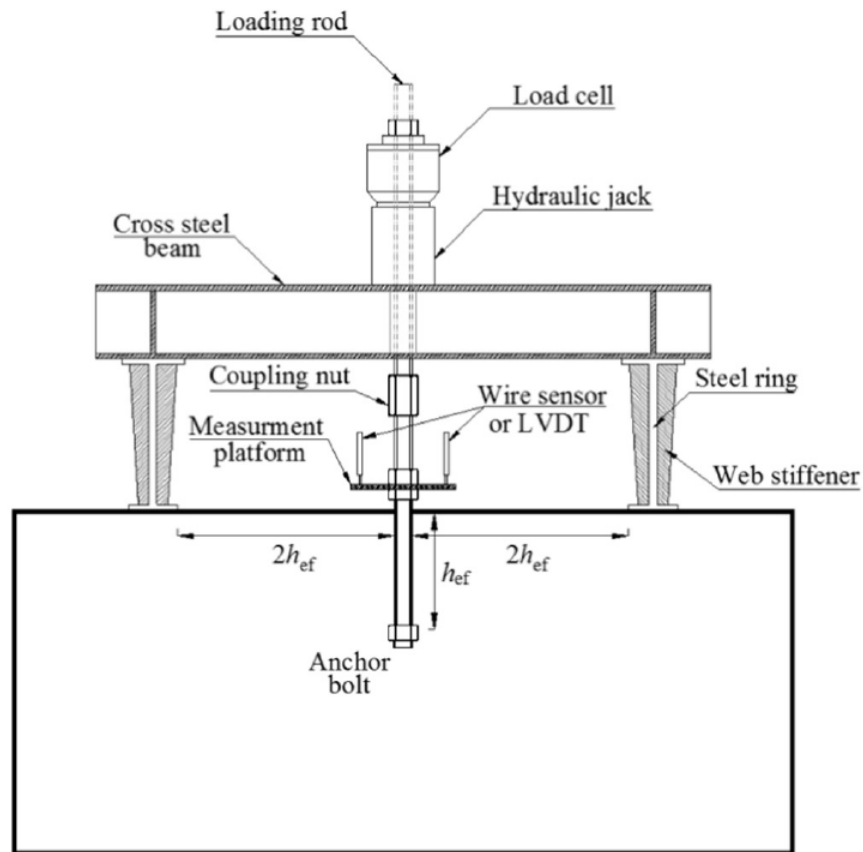
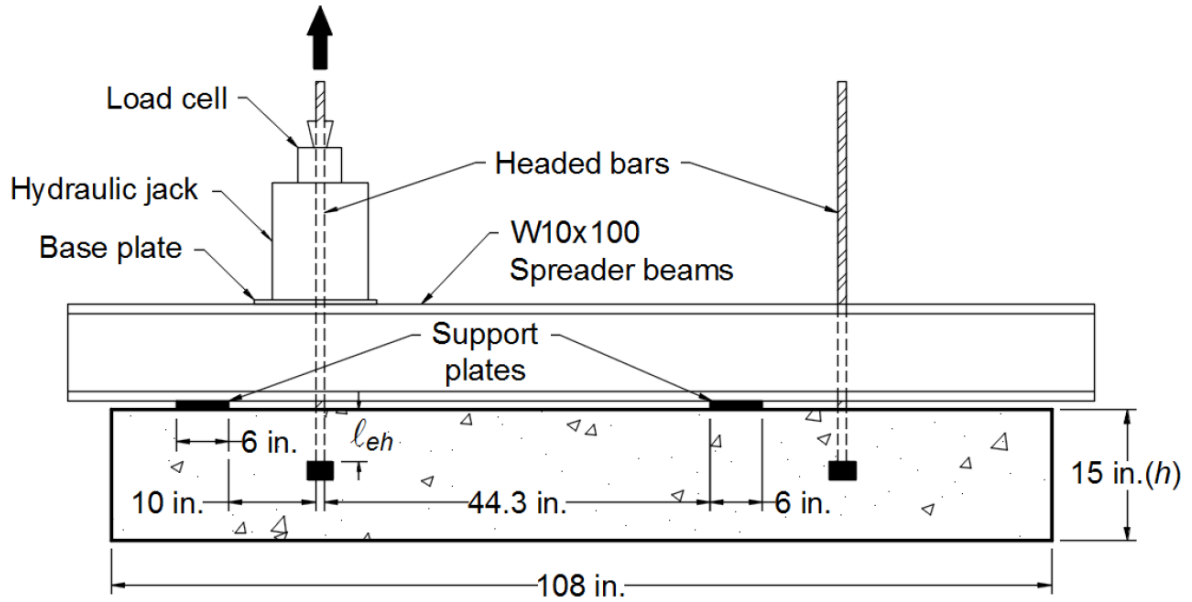


Figure 1.24 Test setup (Nilforoush et al. 2017)

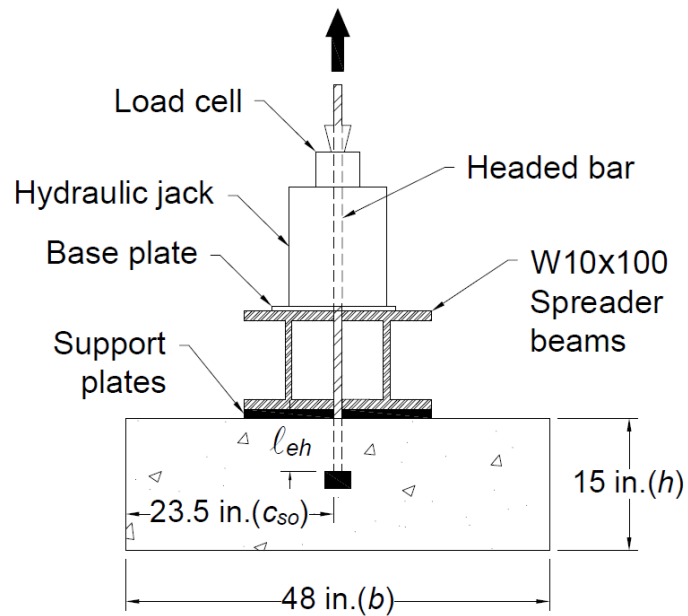
Nilforoush et al. found that the capacity of the headed anchors increased as the concrete member thickness and concrete compressive strength increased. They also found that the anchorage capacity of headed anchors significantly increased when steel fibers were used in the concrete mixture. Nilforoush et al. concluded that the CCD method underestimates the anchorage capacity of headed anchors in steel-fiber reinforced concrete.

1.5 UNIVERSITY OF KANSAS - SIMULATED COLUMN-FOUNDATION JOINTS

Ghimire et al. (2018) tested 32 headed bars anchored in simulated column-foundation joints (represented by headed bars anchored in slab specimens) to study the anchorage capacity and behavior of headed bars in tension. The test bars were embedded in a concrete slab simulating column foundation reinforcement, as shown in Figures 1.26 and 1.27. The main variables were the head size (net bearing area 4 to 15 times the bar area), embedment length (6 to 8.5 in.) ℓ_{eh} , reinforcement in a plane perpendicular to the test bars, and concrete compressive strength (4,200 to 8,620 psi). Stresses in the headed bars at failure ranged from 49,500 to 117,000 psi. The concrete slab specimens contained 2 or 3 test bars, which were tested one at a time. The slab specimens were tested in two groups, each with a different test configuration; the first group had one of the support plates located close to the test bar, while the other support plate was located far away from the test bar, as shown in Figure 1.25. This test configuration was intended to simulate loading conditions of a column subjected to an overturning moment, with the reaction support plate nearest to the test bar representing the compression zone of the column and the test bar representing anchored tension reinforcement. The other reaction support plate was placed far away from the test bar to avoid interference with the concrete breakout failure surface. In the second group, both support plates were located outside the anticipated failure region, as shown in Figure 1.26. The anticipated failure region was equal to $1.5\ell_{eh}$ from the center of the headed bar according to Section 17.6.2.1 of ACI 318-19.



(a)



(b)

Figure 1.25 Test setup of the first group (a) front view, (b) side view (Ghimire et al. 2018)

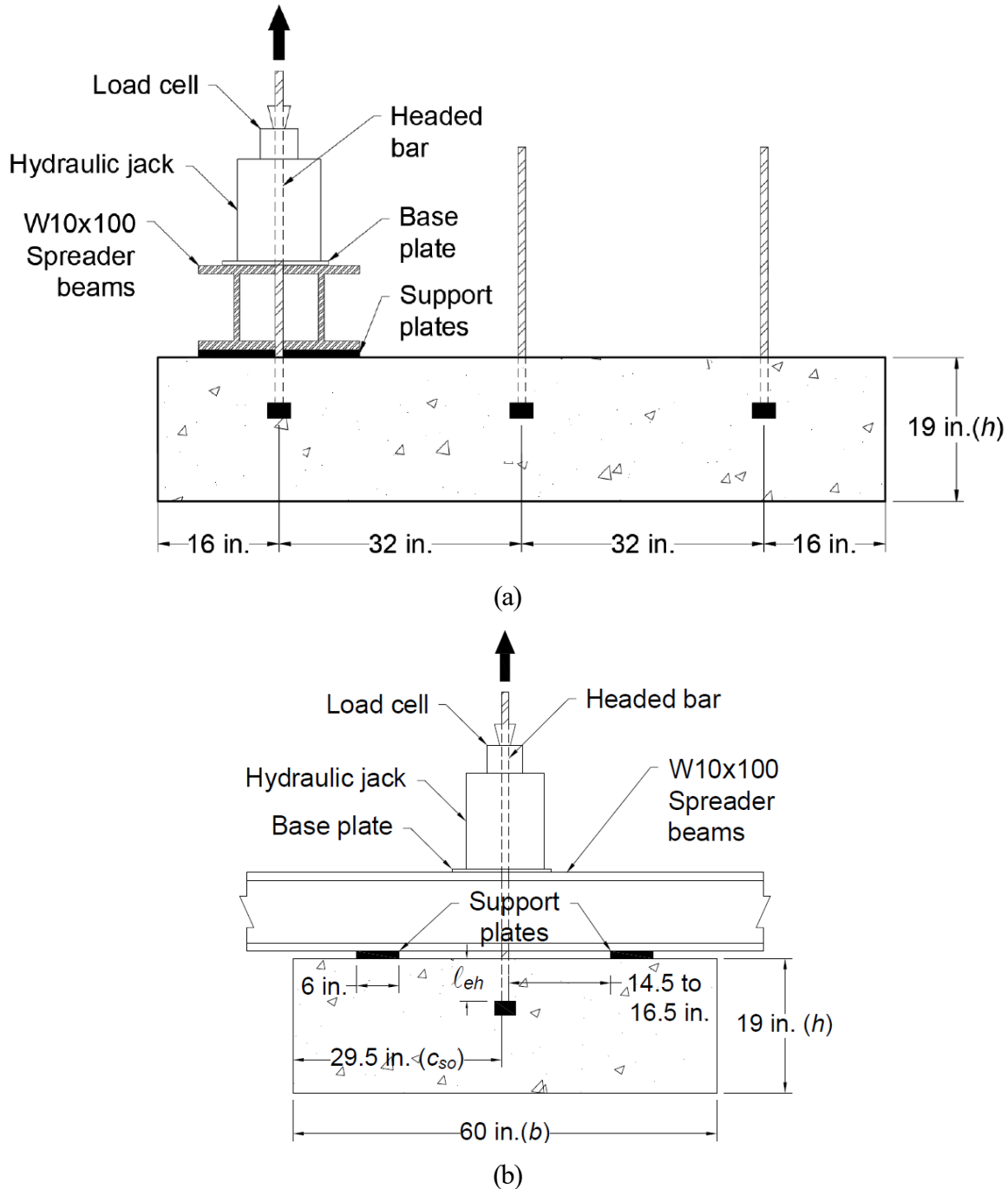


Figure 1.26 Test setup of the final group (a) front view, (b) side view (Ghimire et al. 2018)

All specimens tested by Ghimire et al. exhibited breakout failure (a cone shape of concrete pulled out of the slab along with the test bar). Like Choi et al. (2002), Ghimire et al. found that the presence of reinforcement perpendicular to headed bars did not increase the anchorage strength of headed bars. They also found that increasing the net bearing area of the head from 4 to $9.5A_b$ did not increase the anchorage strength of headed bars; however, the anchorage strength of headed

bars increased about 15% for heads with a net bearing area ranging from 13 to $15A_b$. Ghimire et al. observed that the anchorage strength of headed bars increased about 37% as the concrete compressive strength increased from 4,200 to 8,600 psi.

1.6 UNIVERSITY OF CALIFORNIA, BERKELEY – STEEL COLUMN-CONCRETE FOUNDATION JOINTS

Worsfold et al. (2022) tested two steel-column-to-concrete-foundation joints located away from foundation edges under reversed cyclic loading with and without parallel tie reinforcement in the foundation to study the failure mechanisms and design requirements. As depicted in Figures (1.27) and (1.28), the test specimens consisted of a steel column (W12x106 ASTM A992 Grade 50) connected to a foundation slab by cast-in-place anchor bolts. The column was subjected to reversed cyclic lateral loads with no axial load other than column self-weight. Four 1.5 in. diameter anchor bolts with heavy hex nuts as heads in the first specimen M01 and with steel plate washers in the second specimen M02, as shown in Figures (1.27) and (1.28), respectively, were cast into the 18 in. thick foundation on each side of the column with an effective embedment length from the top of the slab to the bearing surface equal to 14.3 in. The head net bearing areas A_{brg} in specimens M01 and M02 were $1.5A_b$ and $5.5A_b$, respectively. The concrete compressive strengths were 3700 and 3930 psi on test day in specimens M01 and M02, respectively. The nominal yield strength of the anchor bolts was 105,000 psi. Specimen M01 had five perpendicular No. 4 hoops in the joint region, as shown in Figure (1.27), whereas specimen M02 contained No.4 parallel tie reinforcement shaped as 180-degree hooks on the top and heads on the bottom, as shown in Figure (1.28). The parallel tie reinforcement in specimen M02 extended two rows farther on the west side than on the east side of the slab (Figure 1.29), with no hoops placed around the anchors. A load cell was placed on each anchor bolt to measure the anchorage strength.

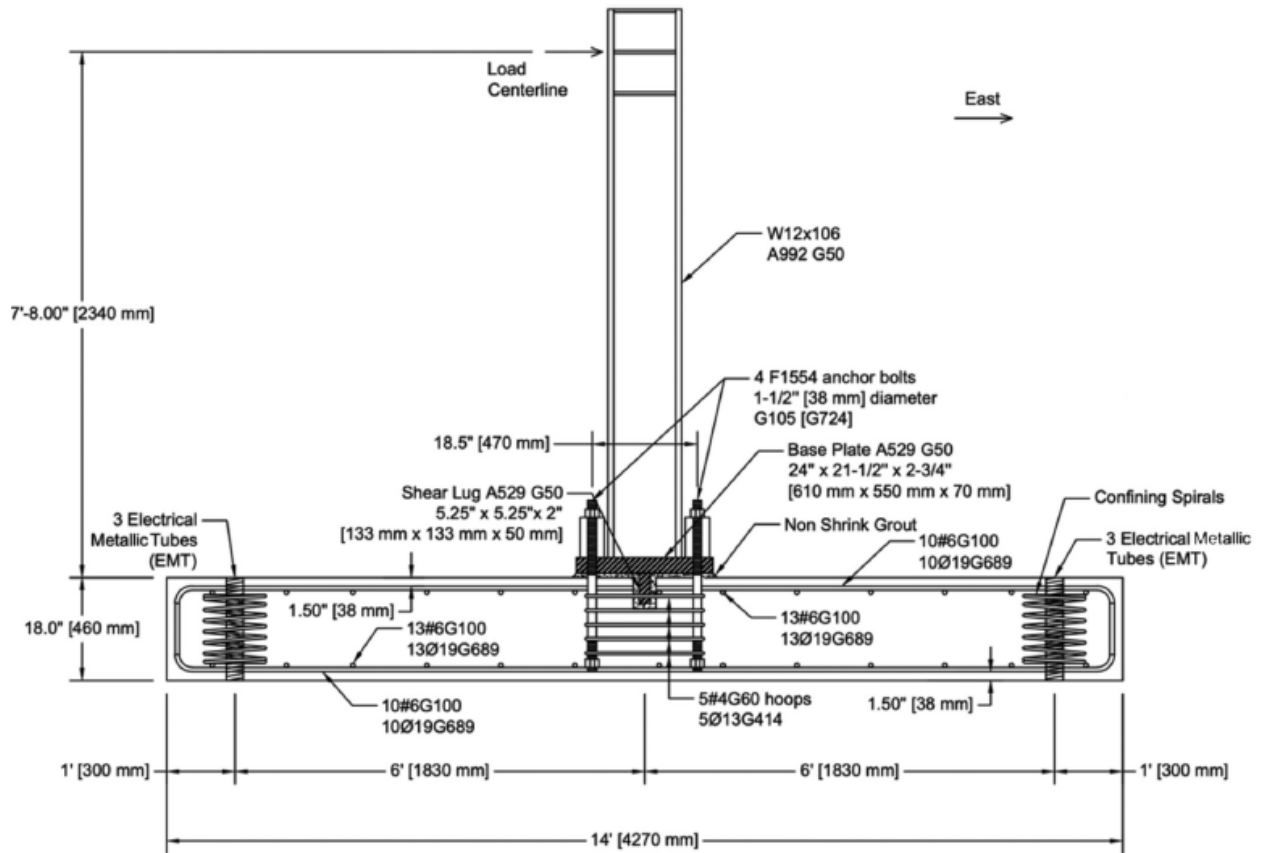


Figure 1.27 Steel-column-to-concrete-foundation joint specimen M01 (Worsfold et al. 2022)

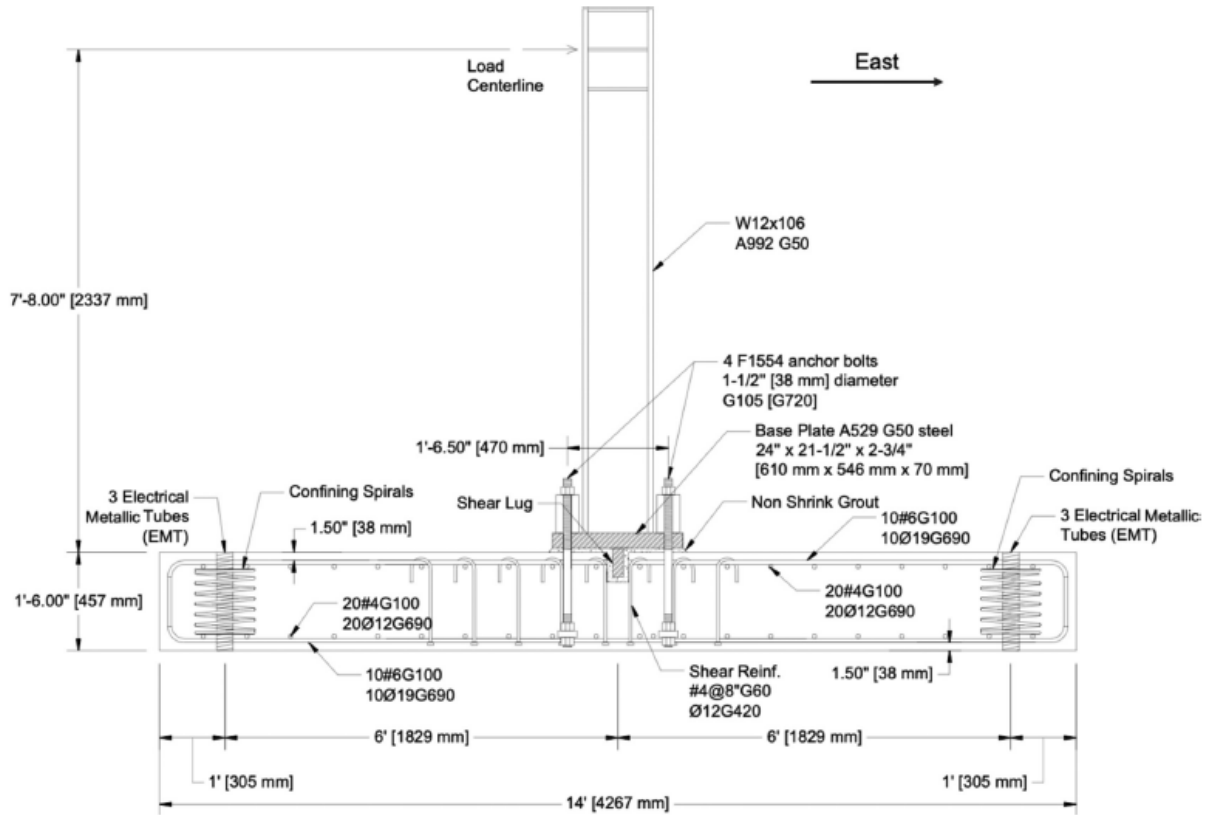


Figure 1.28 Steel-column-to-concrete-foundation joint specimen M02 (Worsfold et al. 2022)

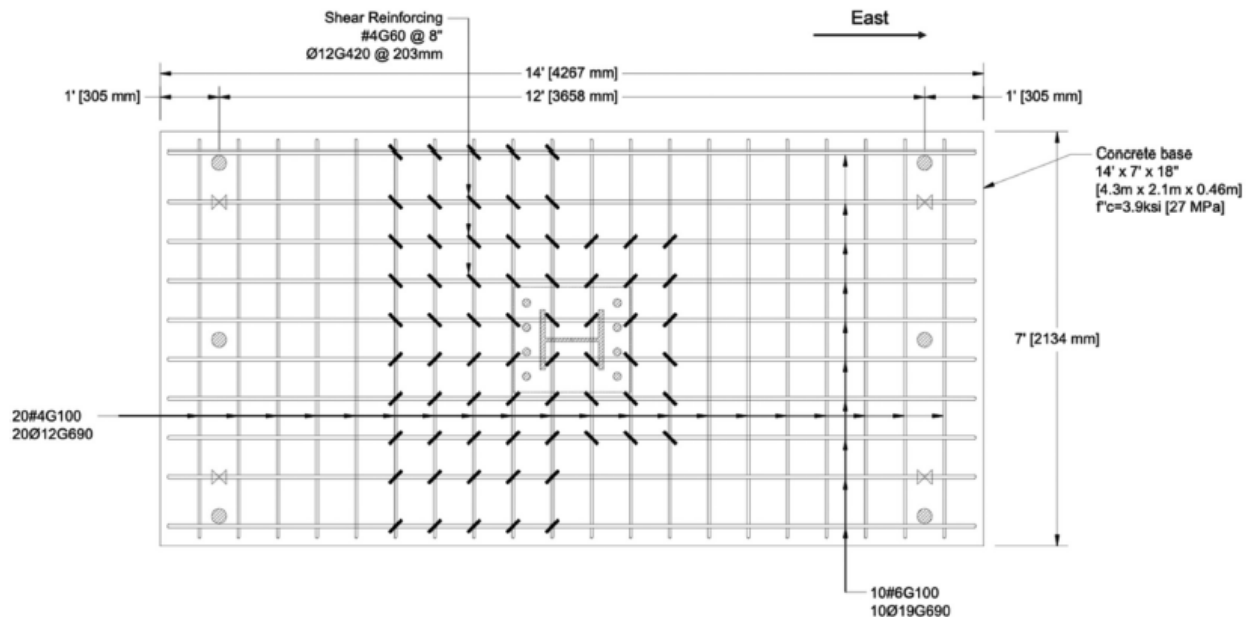


Figure 1.29 Plan view of specimen M02 (Worsfold et al. 2022)

Both specimens M01 and M02 tested by Worsfold et al. exhibited breakout failure (a cone shape of concrete pulled out of the slab along with the anchor bolts). Based on the surface cracks,

Worsfold et al. observed that the breakout failure cones were asymmetric with a steeper slope toward the interior of the joint, as shown in Figures (1.30) and (1.31) for specimens M01 and M02, respectively. Like Choi et al. (2002) and Ghimire et al. (2018), Worsfold et al. found, based on the strain gauge data, that the perpendicular No. 4 hoops in the joint region of specimen M01 were not effective in increasing the anchorage strength of anchor bolts. Worsfold et al. discovered that adding parallel tie reinforcement to Specimen M02 increased the breakout force by 72% and displacement capacity by a factor of three on average compared to Specimen M01. Worsfold et al. suggested that ACI 318 should consider including provisions that combine concrete strength and shear reinforcement (parallel tie reinforcement) for the concrete breakout failure mode.

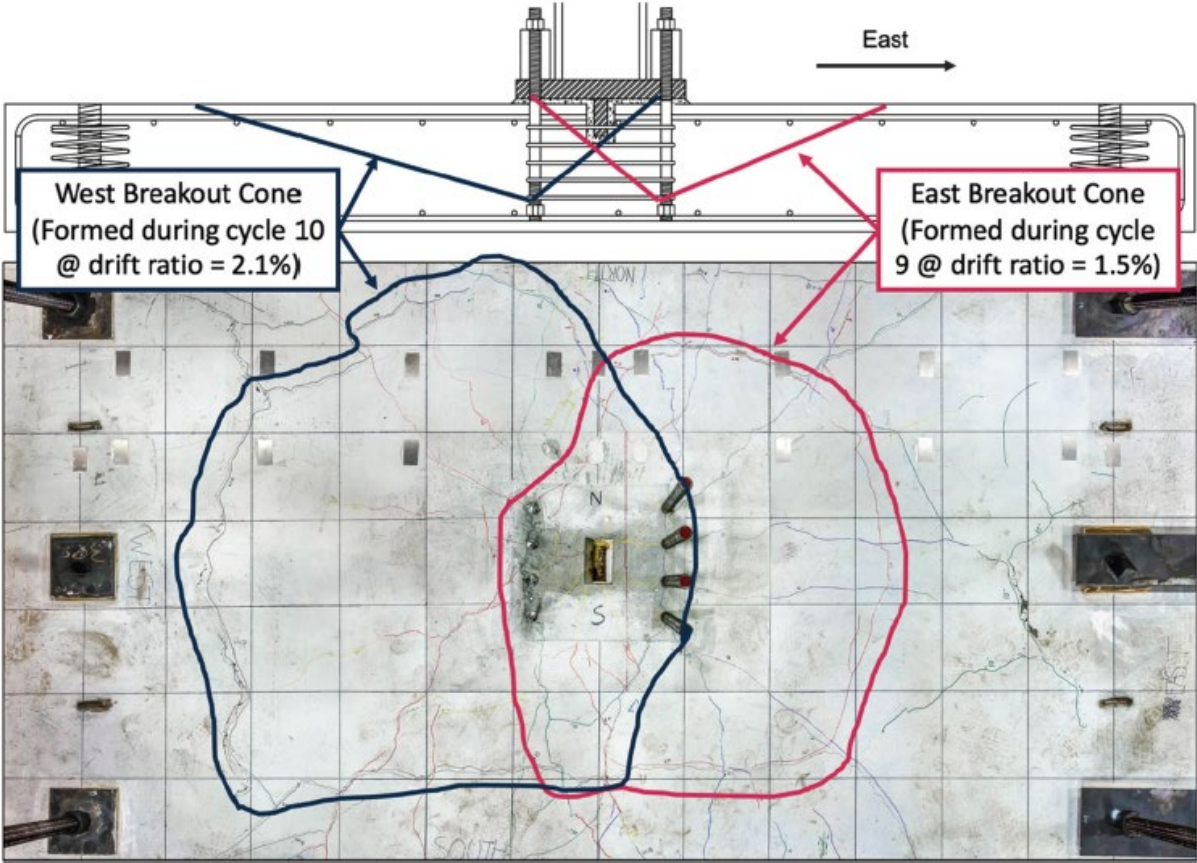


Figure 1.30 Idealized cone geometry shown in elevation and observed cone geometry intersecting top surface in plan view for specimen M01 (Worsfold et al. 2022)



Figure 1.31 Cross section and plan view highlighting crack patterns and breakout cone geometry for Specimen M02 (Worsfold et al. 2022)

1.7 CODE PROVISIONS

1.7.1 Anchorage provisions

The provisions for calculating the concrete breakout strength of the anchors first appeared in ACI 318-02 Appendix D, with no significant changes through the current ACI 318-19 provisions. These provisions are based on the CCD method. In accordance with Section 17.6.2.1 of ACI 318-19, the nominal concrete breakout strength of a single anchor (N_{cb}) or group of anchors (N_{cbg}) in tension is given by Eq. (1.13) and (1.14).

$$N_{cb} = \frac{A_{Nc}}{A_{Nco}} \Psi_{ed,N} \Psi_{c,N} \Psi_{cp,N} N_b \tag{1.13}$$

$$N_{cbg} = \frac{A_{Nc}}{A_{Nco}} \Psi_{ec,N} \Psi_{ed,N} \Psi_{c,N} \Psi_{cp,N} N_b \tag{1.14}$$

where A_{Nco} is the projected concrete failure area of a single anchor with an edge distance of at least $1.5h_{ef}$ and is equal to $9h_{ef}^2$ (in.²), as shown in Figure 1.32, where h_{ef} is the embedment length of

headed bars (in.); A_{Nc} is the projected concrete failure area of a single anchor or group of anchors (in.²), as shown in Figure 1.33; N_b is the basic concrete breakout strength of a single anchor loaded in tension, calculated as

$$N_b = k_c \cdot \lambda_a \cdot \sqrt{f'_c} \cdot h_{ef}^{1.5} \quad (1.15)$$

where k_c is a calibration factor equal to 24 for cast-in anchors in cracked concrete based on the 5 percent fractile; λ_a is a modification factor for lightweight concrete equal to 1.0λ for cast-in and undercut anchors and 0.8λ for expansion, screw, and adhesive anchors, λ is equal to 0.75 for lightweight concrete and 1.0 for normalweight concrete; f'_c is the concrete compressive strength (limited to a maximum 10,000 psi). $\Psi_{ec,N}$ is a modification factor for a group of anchors loaded

eccentrically in tension, equal to $\frac{1}{1 + e'_N / (1.5h_{ef})} \leq 1$, where e'_N is the distance between resultant

tensile load on a group of anchors loaded in tension and the centroid of the group of anchors loaded in tension (in.). $\Psi_{ed,N}$ is a modification factor for edge effects for a single anchor or group of anchors loaded in tension, equal to 1.0 if the smallest side concrete cover distance from the center of an anchor is at least $1.5h_{ef}$; otherwise, $\Psi_{ed,N}$ is equal to $0.7 + 0.3(c_{a,min} / 1.5h_{ef})$, where $c_{a,min}$ is the minimum distance from the center of an anchor to the edge of concrete (in.). $\Psi_{c,N}$ is a modification factor for the influence of cracking in anchor regions at service load levels, equal to 1.25 if anchors are located in a region of a concrete member where analysis indicates no cracking at service load levels; otherwise, $\Psi_{c,N}$ is equal to 1.0. $\Psi_{cp,N}$ is a modification factor for post-installed anchors, and is equal to 1.0 for cast-in anchors.

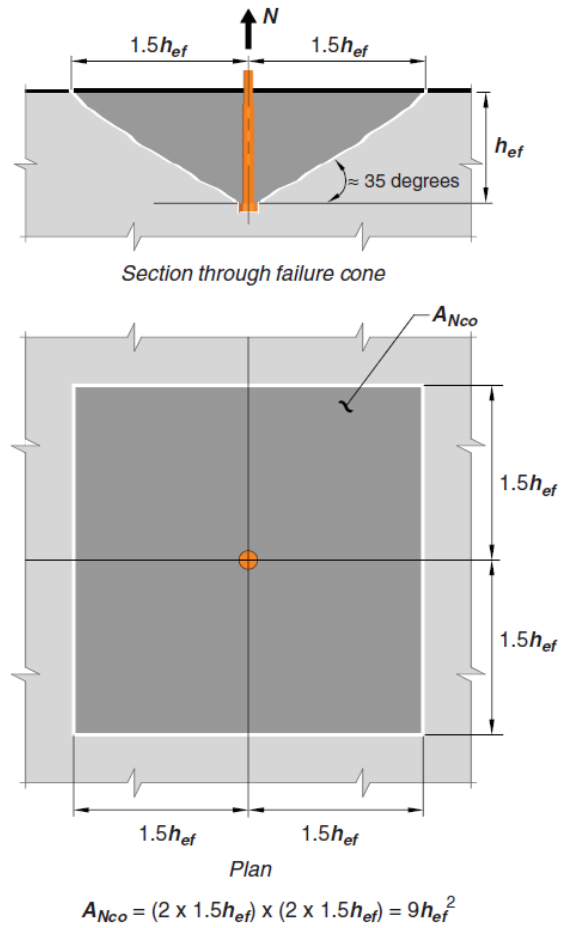
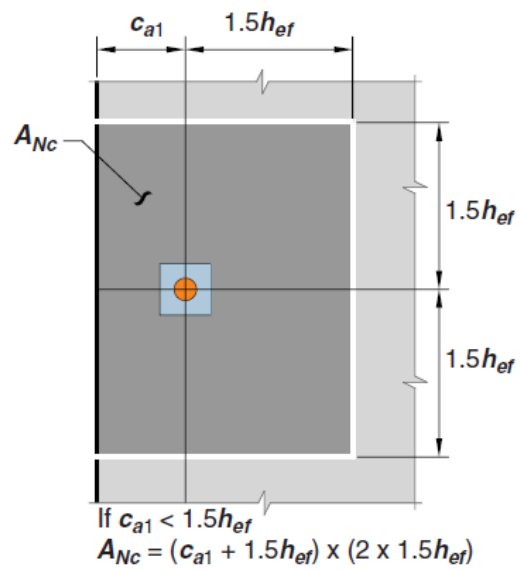


Figure 1.32 Calculation of A_{Nco} for a single anchor (ACI 318-19)



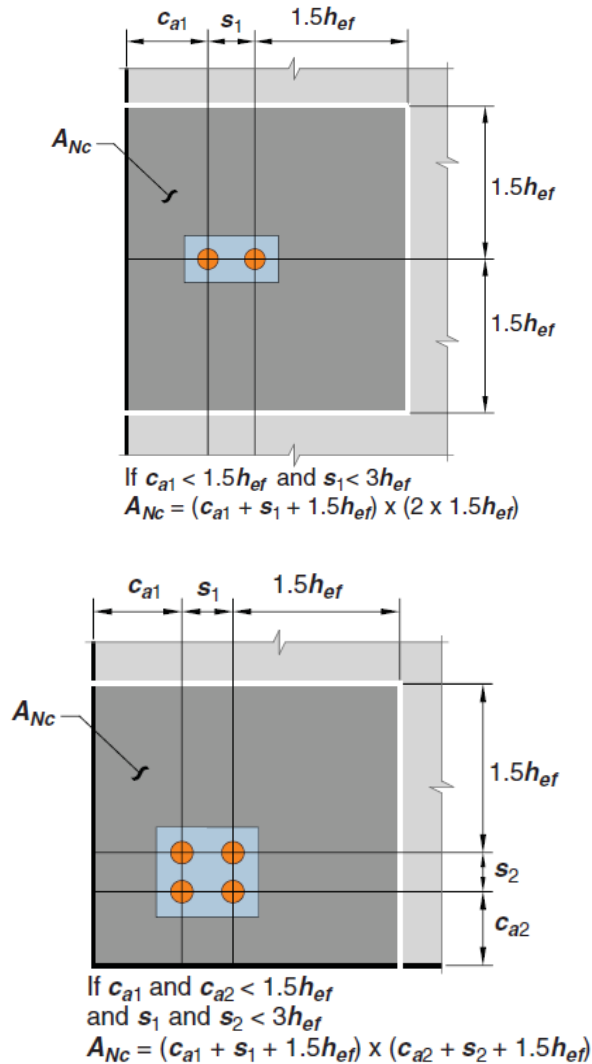


Figure 1.33 Calculation of A_{Nc} for a single anchor and group of anchors (ACI 318-19)

Anchorage provisions in Section 17.6.2.1 of ACI 318 do not take into account the effect of the parallel tie reinforcement on the concrete breakout strength of the anchor(s). Moreover, the anchorage provisions in Chapter 17 of ACI 318 are based on the CCD method, which was developed for anchor bolt types such as studs, bolts, and expansion anchors embedded in plain concrete. Anchor bolts are generally smooth, and thus the CCD method does not take into account contributions of deformed reinforcing bars on anchorage strength.

1.7.2 Design provisions for hooked and headed bars

The equations in ACI 318-19 for calculating the development lengths of hooked and headed bars are presented in Sections 25.4.3 and 25.4.4 and shown in Eq. (1.16) and (1.17),

respectively. The development lengths are functions of the yield strength of the bar (f_y); the square root of concrete compressive strength (f'_c), not to exceed maximum of 10,000 psi for use in the equation; and the bar diameter (d_b) to the power of 1.5.

$$\ell_{dh} = \left(\frac{f_y \Psi_e \Psi_r \Psi_o \Psi_c}{55 \lambda \sqrt{f'_c}} \right) d_b^{1.5} \quad (1.16)$$

$$\ell_{dt} = \left(\frac{f_y \Psi_e \Psi_p \Psi_o \Psi_c}{75 \sqrt{f'_c}} \right) d_b^{1.5} \quad (1.17)$$

where ℓ_{dh} is the development length of a hooked bar in tension (in.); ℓ_{dt} is the development length of a headed bar in tension (in.); ψ_e is a factor based on the presence or absence of a coating on the bars, equal to 1.2 for epoxy-coated or zinc and epoxy dual-coated reinforcement and 1.0 for uncoated or zinc-coated (galvanized) reinforcement; ψ_r is a confining reinforcement factor equal to 1.0 for No. 11 and smaller hooked bars spaced at a center-to-center distance not less than $6d_b$ and for hooked bars with A_{th}/A_{hs} not less than 0.4, where A_{th} is the total cross-sectional area of ties or stirrups confining hooked bars (in.²) and A_{hs} is the total cross-sectional area of hooked bars being developed at a critical section (in.²); otherwise, ψ_r is equal to 1.6; ψ_o is the bar location factor equal to 1.0 for No. 11 and smaller hooked or headed bars anchored within a column core with side cover not less than 2.5 in. or in other members with side cover not less than $6d_b$; otherwise, ψ_o is equal to 1.25; ψ_c is the concrete strength factor equal to $f'_c/15,000 + 0.6$ if f'_c is less than 6000 psi and equal to 1.0 if f'_c is greater than or equal to 6000 psi; ψ_p is the parallel tie reinforcement factor equal to 1.0 for No. 11 and smaller headed bars spaced at a center-to-center distance not less than $6d_b$ and with A_{tt}/A_{hs} not less than 0.3, where A_{tt} is the total cross-sectional area of ties or stirrups acting as parallel tie reinforcement (in.²) and A_{hs} is the total cross-sectional area of headed bars being developed at a critical section (in.²); otherwise, ψ_p is equal to 1.6; λ is a lightweight concrete factor equal to 0.75 for lightweight concrete and 1.0 for normalweight concrete. The modification factors in Eq. (1.16) and (1.17) are defined in Table 25.4.3.2 and Table 25.4.4.3 of ACI 318-19, respectively.

The development lengths, ℓ_{dh} and ℓ_{dt} , may not be less than either $8d_b$ or 6 in.

The design provisions in Section 25.4.4.2 of ACI 318-19 for headed bars can be used if the headed bars satisfy specific requirements, described in Section 25.4.4.1 of ACI 318-19.

The key differences in the ACI 318-19 provisions and those proposed by Ajaam et al. (2017) and Shao et al. (2016) for hooked and headed bars, respectively, are:

1. Use of the $\sqrt{f'_c}$ combined with ψ_c in ACI 318-19 in place of $f_c^{0.25}$ to represent the role of concrete strength.
2. An effective upper limit on f'_c of 10,000 psi in ACI 318-19, rather than an upper limit of 16,000 psi.
3. Use of the step functions ψ_r and ψ_p in ACI 318-19 to represent the effect of anchored bar spacing and confining reinforcement or parallel ties (in the case of headed bars) in place of the variable values permitted for ψ_{cs} .

1.7.3 Design provisions for hooked bars in earthquake resistant structures

The current code design provisions (ACI 318 Building Code and ACI 349 Code Requirements for Nuclear Safety-Related Concrete Structures) for the development length of hooked bars in tension under reversed cyclic loading in earthquake resistant structures (Section 18.8.5.1 of ACI 318-19) were derived directly from the development length provisions for non-seismic loading (Section 25.4.3.1) that existed in ACI 318 Building Codes before 2019. These provisions were based on studies of limited scope conducted in the 1970s (Marques and Jirsa 1975, 1977, Pinc et al. 1977) that included reinforcing steel with yield strengths of 64,000 and 68,000 psi and concrete compressive strengths between 3,750 and 5,100 psi. However, high-strength materials (reinforcing steel with yield strengths up to 120,000 psi and concrete strengths up to 16,000 psi) are now in use. The development length provisions for monotonic loading (Section 25.4.3.1) were modified in the 2019 Code based on the comprehensive study conducted at KU of high-strength hooked bars anchored in beam-column joints tested under monotonic loading (Sperry et al. 2015a,b, 2017a,b, 2018, Ajaam et al. 2017, 2018, Yasso et al. 2017). However, the code design provisions for the development length of hooked bars in tension under cyclic loading did not change in the new ACI Building Code. Therefore, it is important to evaluate the current code provisions for monotonic loading to determine if they can be applied under cyclic loading.

The design provisions for the development of standard hooked bars for beam-column joints under reversed cyclic loading first appeared in the ACI 318-83 Building Code, with no changes in the current ACI 318-19 provisions. In accordance with Section 18.8.5.1 of ACI 318-19, the development length of a standard hooked bar in tension, ℓ_{dh} , for No. 11 and smaller bars embedded in beam-column joints under reversed cyclic loading is given in Eq. (1.18), with ℓ_{dh} should not be less than the maximum of $8d_b$ and 6 in. for normalweight concrete and $10d_b$ and 7.5 in. for lightweight concrete.

$$\ell_{dh} = \frac{f_y d_b}{65\lambda\sqrt{f'_c}} \quad (1.18)$$

where f_y is the specified yield strength of the hooked bar (psi); d_b is the hooked bar diameter (in.); λ is the lightweight modification factor, equal to 0.75 for lightweight concrete and 1.0 for normalweight concrete; f'_c is the concrete compressive strength (psi).

1.8 OBJECTIVE AND SCOPE

In 2013, the University of Kansas started a comprehensive study of the anchorage strength of hooked and headed bars, primarily in exterior beam-column joints. Sperry et al. (2015a,b, 2017a,b, 2018), Ajaam et al. (2017, 2018), Yasso et al. (2017, 2021), Shao et al. (2016), and Ghimire et al. (2018, 2019a,b) developed descriptive equations, presented in Sections 1.3.2 and 1.3.4, and proposed design equations to allow for the use of hooked and headed reinforcing bars with yield strengths up to 120,000 psi and concrete compressive strengths up to 16,000 psi. These equations were developed based on the results of testing 394 simulated beam-column joint specimens using hooked bars and 202 simulated beam-column joint specimens using headed bars. It is worth noting that the proposed design equations were modified in the process of development the provisions in ACI 318-19. The current study is an extension of the earlier comprehensive research program.

The objectives of this study are as follows:

First, expand KU's study on the behavior of large, high-strength headed bars anchored in members other than beam-column joints, such as column-foundation joints;

Second, use data from previous studies and from the current study to evaluate the accuracy of the anchorage provisions in Chapter 17 of ACI 318-19 for predicting the anchorage strength of headed bars; third, use data from the current study to evaluate the applicability of the equations developed by Shao et al. (2016) for predicting the anchorage strength of headed bars anchored in members other than beam-column joints, such as column-foundation joints; and

Third, use and analyze test results of 146 exterior beam-column joint specimens subjected to reversed cyclic loading tested by researchers from outside of KU [Hanson and Connor (1967), Hanson (1971), Megget (1974), Uzumeri (1977), Lee et al. (1977), Scribner (1978), Paulay and Scarpas (1981), Ehsani and Wight (1982), Kanada et al. (1984), Zerbe and Durrani (1985), Ehsani et al. (1987), Ehsani and Alameddine (1991), Kaku and Asakusa (1991), Tsonos et al. (1992), Pantelides et al. (2002), Chutarat and Aboutaha (2003), Hwang et al. (2005), Lee and Ko (2007), Chun et al. (2007), Tsonos (2007), Kang et al. (2010), Chun and Shin (2014), Hwang et al. (2014), and Choi and Bae (2019)] to investigate the applicability of the descriptive equations developed at KU for beam-column joints tested under monotonic loading to predict the anchorage strength of hooked bars anchored in members subjected to reversed cyclic loading.

This study includes two phases:

The first phase involves 31 tests of simulated column-foundation joints to investigate the anchorage strength and behavior of large and high-strength headed bars. The work involved 15 specimens, each with one to three simulated column-foundation joints. The main variables were strut angle between the anchored headed bar and the nearest support reaction (Figure 1.34), number of headed bars tested simultaneously (1 or 2), size of the headed bars (No. 11 or No. 14), spacing between headed bars loaded simultaneously (3.2 or $8.2d_b$), amount of parallel tie reinforcement within the joint region (zero to six No. 4 closed stirrups), and concrete compressive strength (5,060 to 14,470 psi). The embedment length of the headed bars ranged from 12.625 to 14 in. The stresses in the headed bars at failure ranged from 41,800 to 144,400 psi. The net bearing area of the headed bars ranged from 4.2 to $9.2A_b$. This study also includes an evaluation of tests on headed bars tested in simulated column-foundation joints by DeVries et al. (1999), Choi et al. (2002), and Ghimire et al. (2018), and on anchor bolts tested in steel column-concrete foundation joints by Worsfold et al. (2022), described earlier in this chapter. The test results of this study and other studies are

compared with anchorage strengths based on the anchorage provisions in Section 17.6.2 of ACI 318-19 with a strength reduction, ϕ , factor equal to 1.0, and the descriptive equations for headed bars developed by Shao et al. (2016).

The second phase of the study involves the analysis of the test results of 146 exterior beam-column joint specimens subjected to reversed cyclic loading. The summary of these tests is presented in Section 1.2.4. The data from these tests are analyzed using the equations developed by Ajaam et al. (2017) to investigate their applicability to calculate the anchorage strength of hooked bars anchored in beam-column joints subjected to reversed cyclic loading. This analysis is used, in turn, to propose a change in Section 18.8.5.1 of ACI 318 to require the use of Section 25.4.3 of ACI 318 to establish the minimum development length ℓ_{dh} for hooked bars anchored in joints for frames subjected to seismic loading.

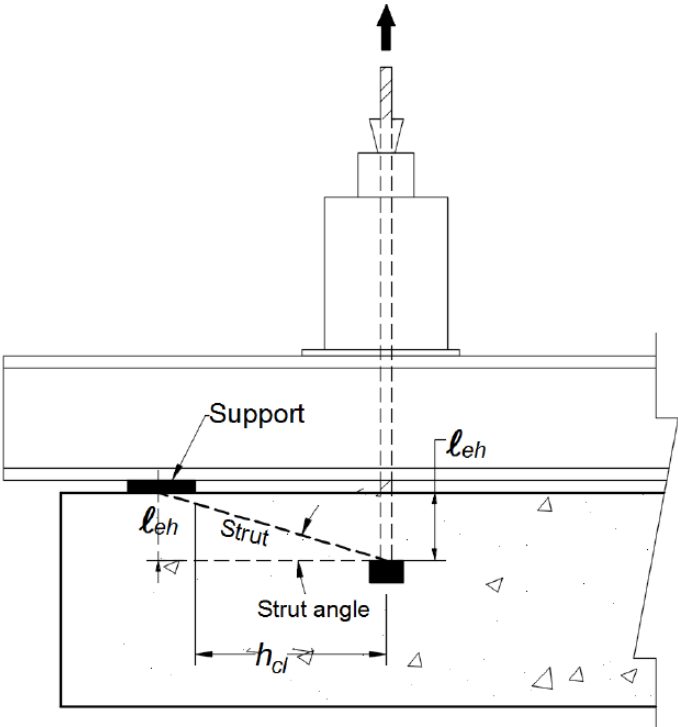


Figure 1.34 Strut angle between anchored headed bar and nearest support reaction

CHAPTER 2: EXPERIMENTAL WORK

Thirty-one tests were performed on headed reinforcing bars in slab specimens to investigate the anchorage strength and behavior of No. 11 and No. 14 headed bars used as column longitudinal reinforcing bars in column-foundation joints. The details of the slab specimens, including material properties, specimen design, test parameters, specimen designations, specimen fabrication and test procedures, and specimen instrumentation, are presented in this chapter.

2.1 MATERIAL PROPERTIES

2.1.1 Concrete Properties

Non-air entrained ready-mix concrete with nominal compressive strengths of 5,000 and 15,000 psi was used in this study. Type I/II portland cement and Kansas River sand were used for both 5,000 and 15,000 psi concrete mixtures. In the 5,000 psi concrete mixture, a mid-to-high-range polycarboxylate-based water reducer (ADVA 140 or ADVA 195) was used as the water reducing agent, while in the 15,000 psi concrete mixture, a high-range polycarboxylate-based water reducer (ADVA 575) was used as the water reducing agent. Crushed limestone with a maximum aggregate size of $\frac{3}{4}$ in. was used in the 5,000 psi concrete mixture, while crushed granite with a maximum aggregate size of $\frac{3}{4}$ in. was used in the 15,000 psi concrete mixture. Class C fly ash and a viscosity modifier (V-MAR) were also used in the 15,000 psi concrete mixtures to increase the workability, strength, and viscosity of the concrete. The mixture proportions of the concrete are given in Table 2.1.

Table 2.1 Concrete mixture proportions

Material	Quantity (SSD)	
	5,000 psi w/cm ^[1] = 0.44	15,000 psi w/cm = 0.21
Type I/II Cement (lb/yd ³)	600	800
Water (lb/yd ³)	263	210
Fly Ash Type C (lb/yd ³)	-	200
Crushed Limestone (lb/yd ³)	1735	-
Granite (lb/yd ³)	-	1430
Kansas River Sand (lb/yd ³)	1396	1430
Mid-to-High Range Water Reducer, ADVA 140 or 195 (oz.) (US)	40	-
High Range Water Reducer, ADVA 575 (oz.) (US)	-	147
Viscosity Modifier (V-MAR) (oz.) (US)	-	20

^[1] w/cm = Water-to-cementitious material ratio

2.1.2 Steel Properties

The No. 11 and No. 14 headed bars used in this study were fabricated from ASTM A1035 Grade 120 steel to ensure that anchorage failure was not governed by the tensile strength of the headed bars. The No. 6 and No. 11 flexural reinforcement placed perpendicular to the headed bars and the No. 4 parallel tie reinforcement were all made of ASTM A615 Grade 60 steel. The properties of the headed bars and parallel tie reinforcement are shown in Table 2.2. Head types used in this study are shown in Figure 2.1, and the head dimensions are given in Table 2.3.

Table 2.2 Properties of headed bars and parallel tie reinforcement

Bar Size	Head Designation	Yield Strength (ksi)	Nominal Diameter (in.)	Average Rib Spacing (in.)	Average Rib Height (in.)		Average Gap Width (in.)	Relative Rib Area ^[2]
					A ^[1]	B ^[2]		
11	S5.5, S9.2	135	1.41	0.917	0.092	0.087	0.424	0.086
14	B4.2	127	1.69	0.992	0.085	0.078	0.523	0.070
4	-	63	0.50	0.350	0.026	0.025	0.220	0.062

^[1] Per ASTM A615, A706; ^[2] Per ACI 408-3

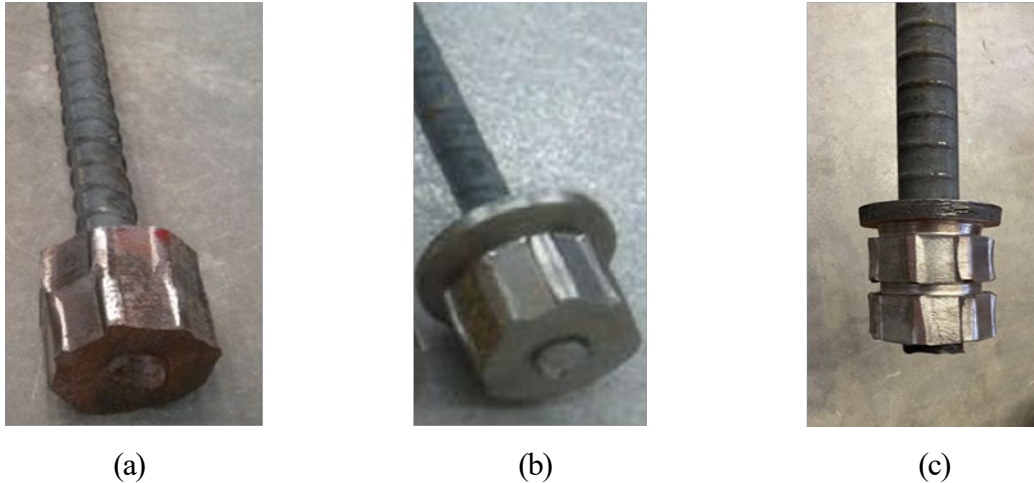





Figure 2.1 Headed bars (a) No. 11 S5.5 bar (b) No. 11 S9.2 bar (c) No. 14 B4.2 headed bar

Table 2.3 Head dimensions

Headed bars	Designation	Bar Size	d (in.)	t (in.)	Net Bearing Area ^[1]
	S5.5 ^[2]	No. 11	3.5	2.75	$5.5A_b$
	S9.2	No. 11	4.5	3.75	$9.2A_b$
	B4.2	No. 14	3.875	4.375	$4.2A_b$

^[1] Net bearing area calculated as gross head area minus bar area

^[2] Octagonal-shape head

2.2 SLAB SPECIMEN DESIGN

Fifteen slab specimens were designed to simulate column-foundation joints: A total of 31 tests, summarized in Table 2.4, were conducted on headed bars anchored with a nominal embedment length $\ell_{eh} = 12\frac{3}{4}$ in. to study the effects of support location (distance between the headed bars and the compression reaction), the number of headed bars (group effects), the spacing between headed bars in a group, bar size (No. 11 and No. 14), the quantity of parallel tie

reinforcement (stirrups or ties placed parallel to the headed bars), and the concrete compressive strength on the anchorage strength of headed bars. The specimens are shown in Figures 2.2 through 2.10.

Table 2.4 Detail of slab specimens ^[1]

Specimens ^[2]			ℓ_{eh} (in.)	f_{cm} (psi)	A_{tt} (in. ²)	$\frac{h_{cl}}{\ell_{eh}}$	$\frac{A_{brg}}{A_b}$	$\frac{A_{tt}}{A_{hs}}$
SN	Description	Head						
1	11-5-S5.5-6#6-0-12.75	A	13.375	5060	0.0	1.85	5.5	0.00
	11-5-S5.5-6#6-0-12.75	B	13.125		0.0	1.88	5.5	0.00
	11-5-S5.5-6#6-0-12.75	C	13.375		0.0	1.85	5.5	0.00
2	11-5-S5.5-10#6-0-12.75	A	13.375	5490	0.0	1.47	5.5	0.00
	11-5-S5.5-10#6-0-12.75	B	12.75		0.0	1.55	5.5	0.00
3	11-5-S5.5-6#11-0-12.75 ^[3]	A	13.625	5740	0.0	5.24	5.5	0.00
4	(2@3.2)11-5-S5.5-6#11-0-12.75	A1	13.50	5550	0.0	1.46	5.5	0.00
		A2	13.50		0.0	1.46	5.5	0.00
	(2@3.2)11-5-S5.5-6#11-0-12.75	B1	13.375	6190	0.0	1.47	5.5	0.00
		B2	13.375		0.0	1.47	5.5	0.00
5	11-5-S5.5-6#6-2#4-12.75	A	13.00	5810	0.8	1.90	5.5	0.51
	11-5-S5.5-6#6-2#4-12.75	B	12.875		0.8	1.92	5.5	0.51
	11-5-S5.5-6#6-2#4-12.75	C	13.125		0.8	1.88	5.5	0.51
6	(2@8.2)11-5-S5.5-7#11-0-12.75	A1	13.50	5370	0.0	1.46	5.5	0.00
		A2	13.50		0.0	1.46	5.5	0.00
	(2@8.2)11-5-S5.5-7#11-0-12.75	B1	14.0625		0.0	1.40	5.5	0.00
		B2	14.0625		0.0	1.40	5.5	0.00
7	(2@8.2)11-5-S5.5-7#11-0-12.75	A1	13.25	5110	0.0	1.49	5.5	0.00
		A2	13.25		0.0	1.49	5.5	0.00
	(2@8.2)11-5-S5.5-7#11-0-12.75	B1	13.3125		0.0	1.48	5.5	0.00
		B2	13.3125		0.0	1.48	5.5	0.00
8	(2@8.2)11-5-S9.2-7#11-3#4-12.75	A1	13.125	7950	0.8	1.50	9.2	0.26
		A2	13.125		0.8	1.50	9.2	0.26
	(2@8.2)11-5-S9.2-7#11-6#4-12.75	B1	13.00		1.6	1.52	9.2	0.51
		B2	13.00		1.6	1.52	9.2	0.51
9	(2@8.2)11-5-S9.2-7#11-3#4-12.75	A1	13.25	7680	0.8	1.49	9.2	0.26
		A2	13.25		0.8	1.49	9.2	0.26
	(2@8.2)11-5-S9.2-7#11-6#4-12.75	B1	13.375		1.6	1.47	9.2	0.51
		B2	13.375		1.6	1.47	9.2	0.51

^[1] SN = specimen number; ℓ_{eh} = measured embedment length; f_{cm} = measured concrete compressive strength; A_{tt} = total cross-sectional area of effective confining reinforcement parallel to the headed bars being developed; h_{cl} = distance between the center of headed bar to the inner face of the nearest support plate; A_{brg} = net bearing area of the head (Table 2.3); A_b = area of the headed bar; A_{hs} = total cross-sectional area of headed bars being developed (nA_b), where n is the number of headed bars being developed.

^[2] Multiple headed bars in a single specimen tested individually are denoted by letters A, B, and C, and grouped headed bars tested simultaneously are denoted with a number after a common letter (A1, A2).

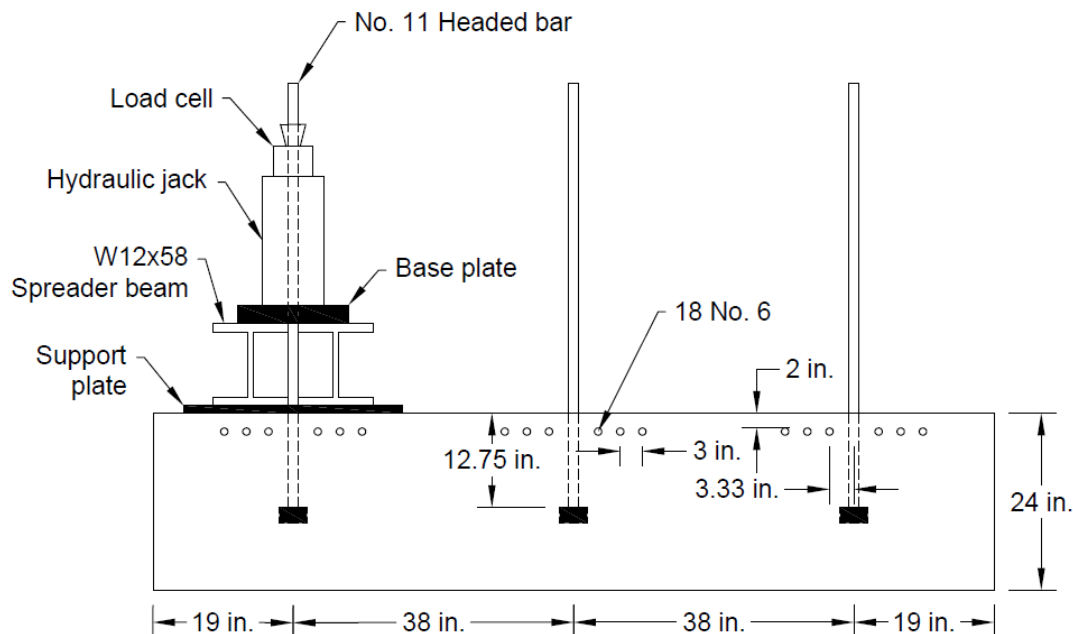
^[3] Specimen contained a single centrally placed headed bar.

Table 2.4 Cont. Detail of slab specimens

Specimens			ℓ_{eh} (in.)	f_{cm} (psi)	A_{tt} (in. ²)	$\frac{h_{cl}}{\ell_{eh}}$	$\frac{A_{brg}}{A_b}$	$\frac{A_{tt}}{A_{hs}}$
SN	Description	Head						
10	(2@8.2)11-15-S9.2-7#11-0-12.75	A1	12.6875	14470	0.0	1.55	9.2	0.00
		A2	12.6875		0.0	1.55	9.2	0.00
	(2@8.2)11-15-S9.2-7#11-0-12.75	B1	12.75		0.0	1.55	9.2	0.00
		B2	12.75		0.0	1.55	9.2	0.00
11	(2@8.2)11-15-S9.2-7#11-3#4-12.75	A1	12.75	14140	0.8	1.55	9.2	0.26
		A2	12.75		0.8	1.55	9.2	0.26
	(2@8.2)11-15-S9.2-7#11-6#4-12.75	B1	12.625	14080	1.6	1.56	9.2	0.51
		B2	12.625		1.6	1.56	9.2	0.51
12	(2@6.8)14-5-B4.2-7#11-0-12.75	A1	13.00	6040	0.0	1.53	4.2	0.00
		A2	13.00		0.0	1.53	4.2	0.00
	(2@6.8)14-5-B4.2-7#11-0-12.75	B1	13.125	6180	0.0	1.51	4.2	0.00
		B2	13.125		0.0	1.51	4.2	0.00
13	(2@6.8)14-5-B4.2-7#11-3#4-12.75	A1	13.00	5440	0.8	1.53	4.2	0.18
		A2	13.00		0.8	1.53	4.2	0.18
	(2@6.8)14-5-B4.2-7#11-6#4-12.75	B1	12.75	5480	1.6	1.56	4.2	0.36
		B2	12.75		1.6	1.56	4.2	0.36
14	(2@6.8)14-15-B4.2-7#11-0-12.75	A1	13.125	14030	0.0	1.51	4.2	0.00
		A2	13.125		0.0	1.51	4.2	0.00
	(2@6.8)14-15-B4.2-7#11-0-12.75	B1	13.125	14050	0.0	1.51	4.2	0.00
		B2	13.125		0.0	1.51	4.2	0.00
15	(2@6.8)14-15-B4.2-7#11-3#4-12.75	A1	13.375	13190	0.8	1.48	4.2	0.18
		A2	13.375		0.8	1.48	4.2	0.18
	(2@6.8)14-15-B4.2-7#11-6#4-12.75	B1	12.875	13020	1.6	1.54	4.2	0.36
		B2	12.875		1.6	1.54	4.2	0.36

The slab specimens were designed as simply-supported beams (neglecting self-weight) to resist bending and shear at the maximum expected failure stress on the anchored bars. Of the 15 slab specimens, four contained one, two, or three headed bars, which were loaded one at a time, as shown in Figures 2.2 through 2.4, and eleven contained two groups of two headed bars loaded simultaneously, as shown in Figures 2.5 through 2.10. The individual or groups of headed bars were embedded sufficiently far apart so that an anchorage failure in one test did not interfere with the anchorage failure of the other test or tests in the slab. The width of the slabs was chosen so that it was greater than the diameter of the anticipated concrete breakout failure region, which is equal to $3\ell_{eh}$ according to Section 17.6.2.1 of ACI 318-19, where ℓ_{eh} is the embedment length of the headed bars. The depth of the slab specimens was sufficient to provide flexural and shear strength;

the specimens included flexural reinforcement in the vicinity of the head, as shown in Figures 2.2 through 2.10; Ghimire et al. (2018) showed that the presence of reinforcement perpendicular to headed bars does not affect anchorage strength. In the test of Slabs 1 and 5, both support reactions were placed just outside the anticipated failure region; the clear distance between the support reactions and the headed bar was 24 in., as shown in Figures 2.2 and 2.6. In the test of Slab 3, both support reactions were located far away from the anticipated failure region, as shown in Figure 2.4, to avoid interference with the concrete breakout failure surface. In the tests of the remaining slabs, the test headed bars involved a shallow compressive strut on one side of the bars, indicative of loading conditions of a column or wall subjected to an overturning moment; the clear distance between the nearest support reaction representing the compression zone of the column and the headed bars representing anchored tension reinforcement was 19 in.; the clear distance between the other support reaction, which was placed far away from the anticipated failure region to avoid interference with the concrete breakout failure surface, and the headed bars was 83 in., as shown in Figure 2.3. Six slab specimens contained parallel tie reinforcement; in one specimen, the parallel ties were located on both sides of the headed bars, as shown in Figure 2.6, and in the remaining specimens, one pair of headed bars had parallel ties on both sides of the headed bars, and the other pair had parallel ties only on one side, as shown in Figures 2.8 and 2.10.



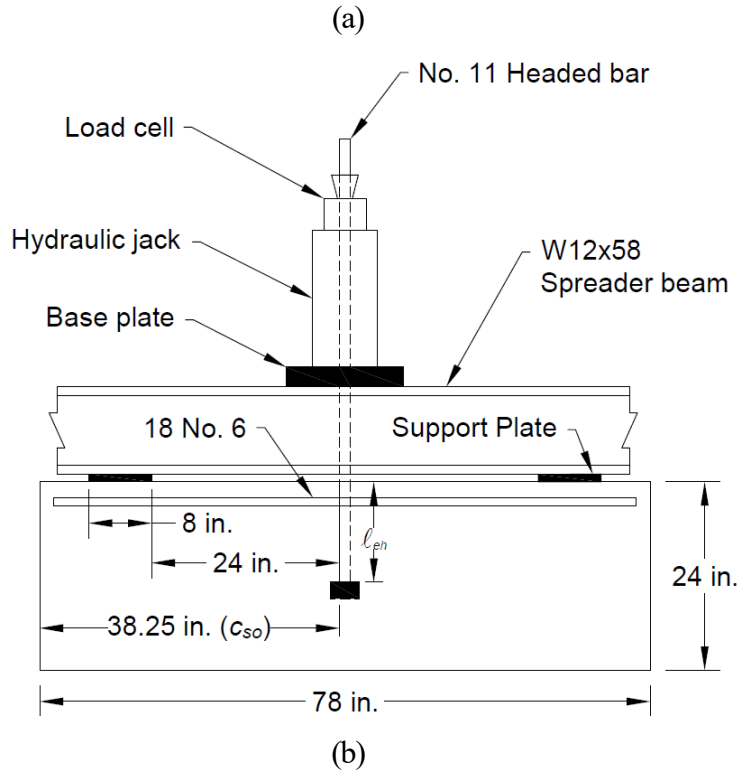
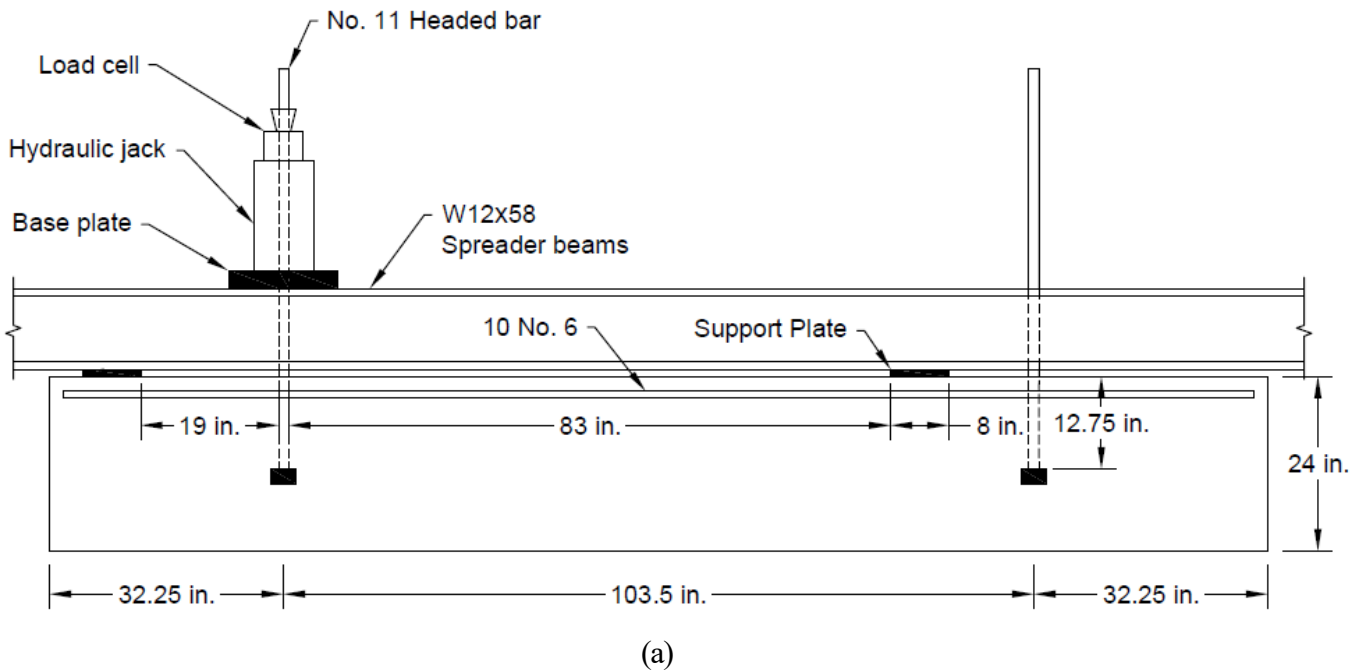
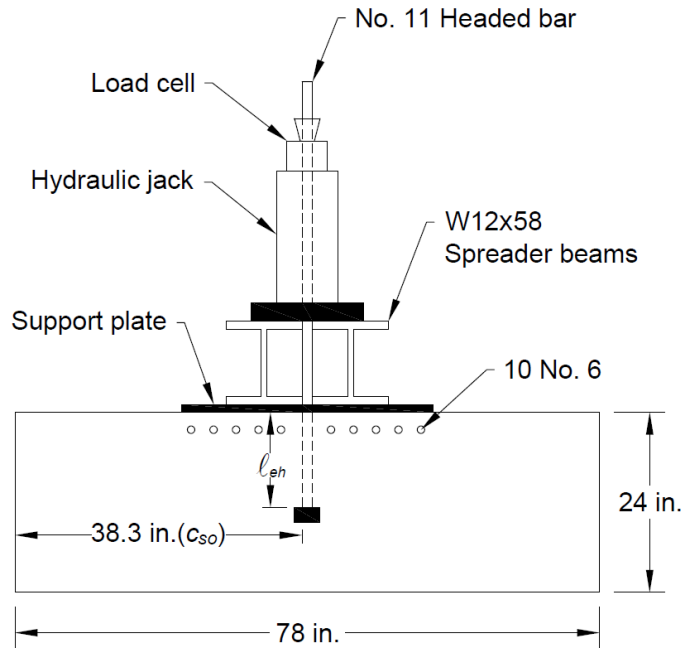


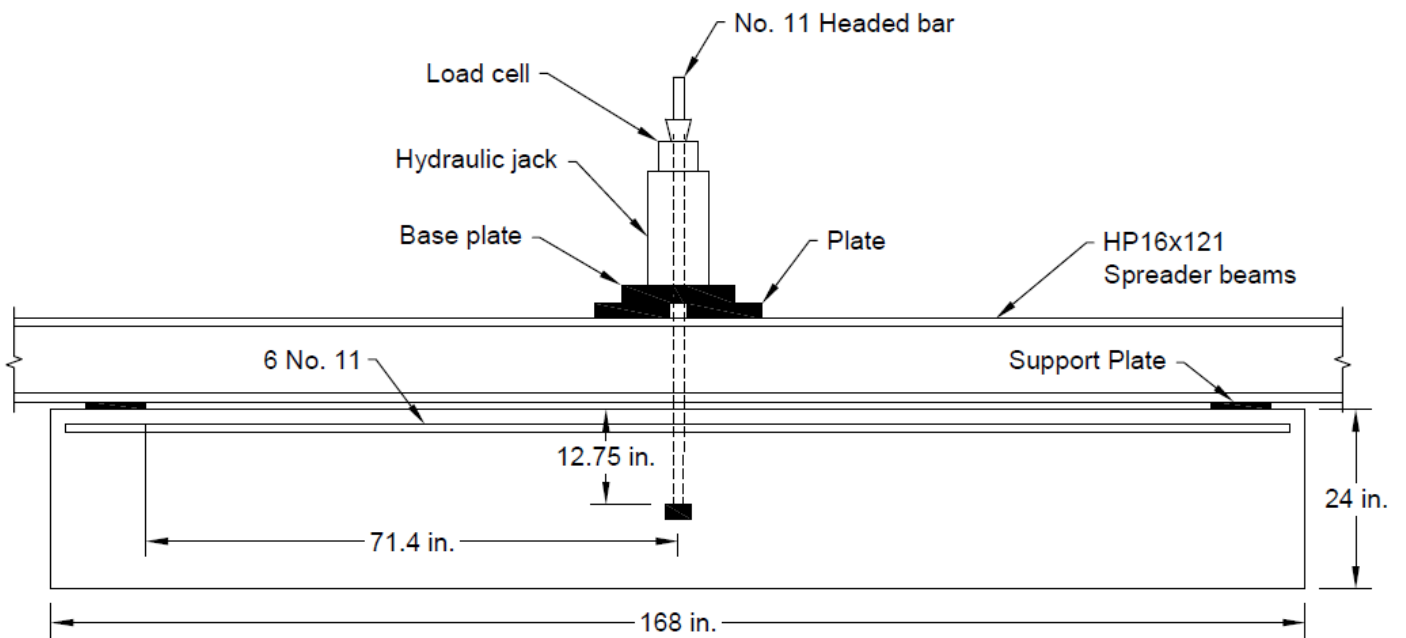
Figure 2.2 Location of headed bars and reinforcement for Slab 1 (a) side view, (b) end view



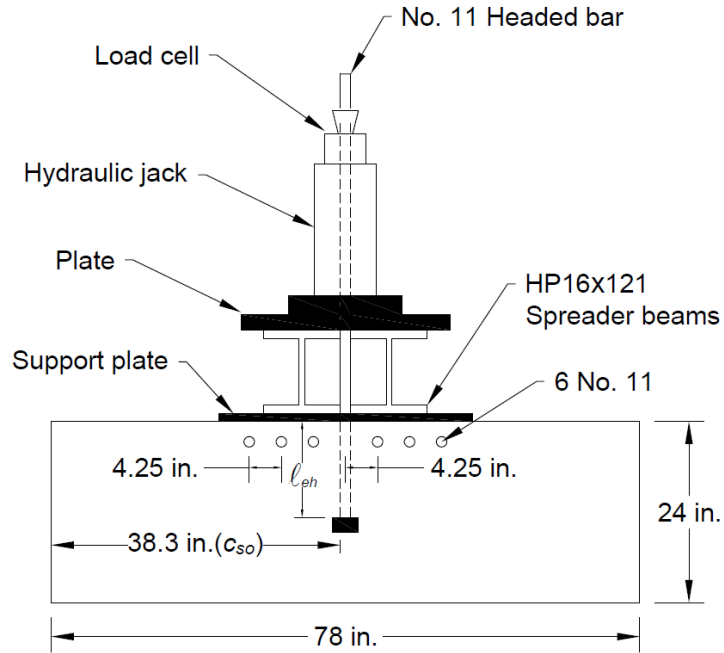


(b)

Figure 2.3 Location of headed bars and reinforcement for Slab 2 (a) side view, (b) end view

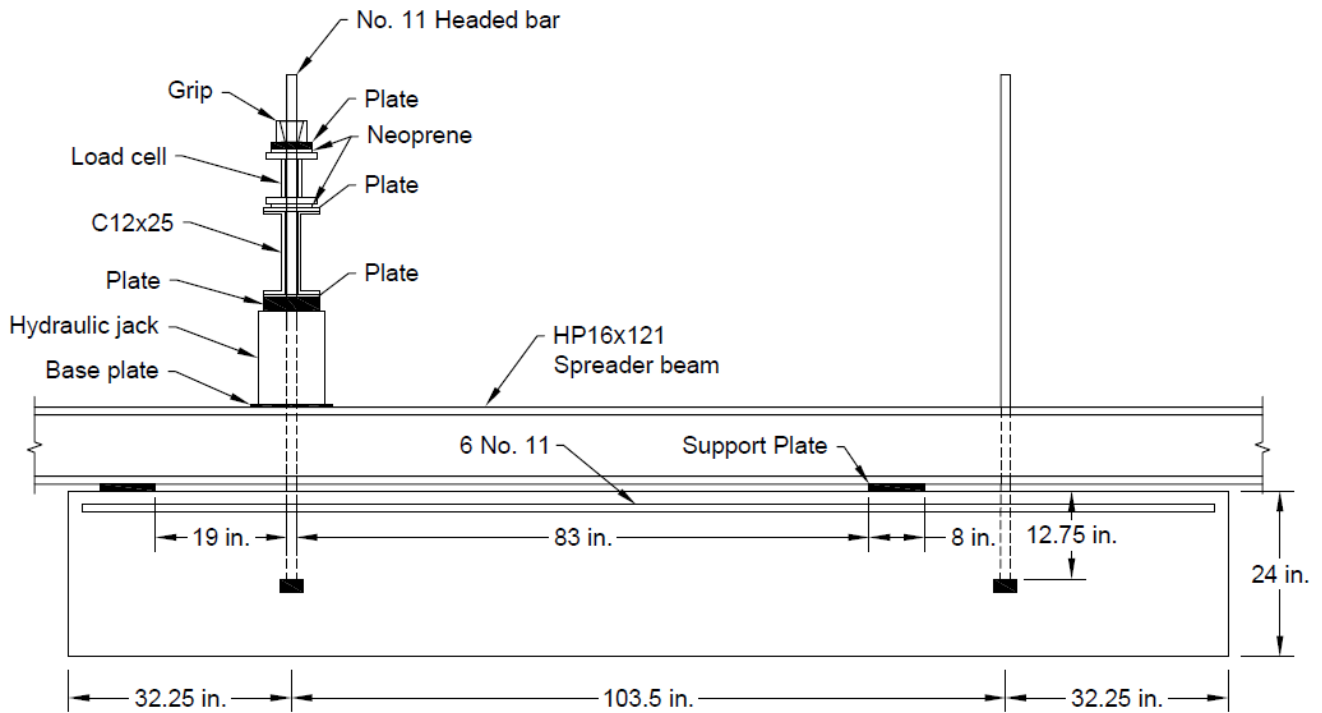


(a)

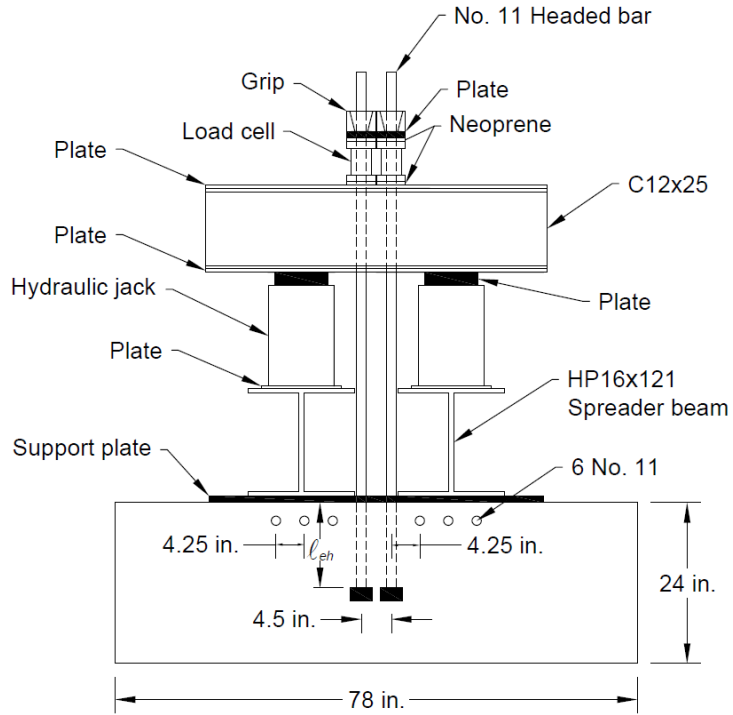


(b)

Figure 2.4 Location of headed bars and reinforcement for Slab 3 (a) side view, (b) end view

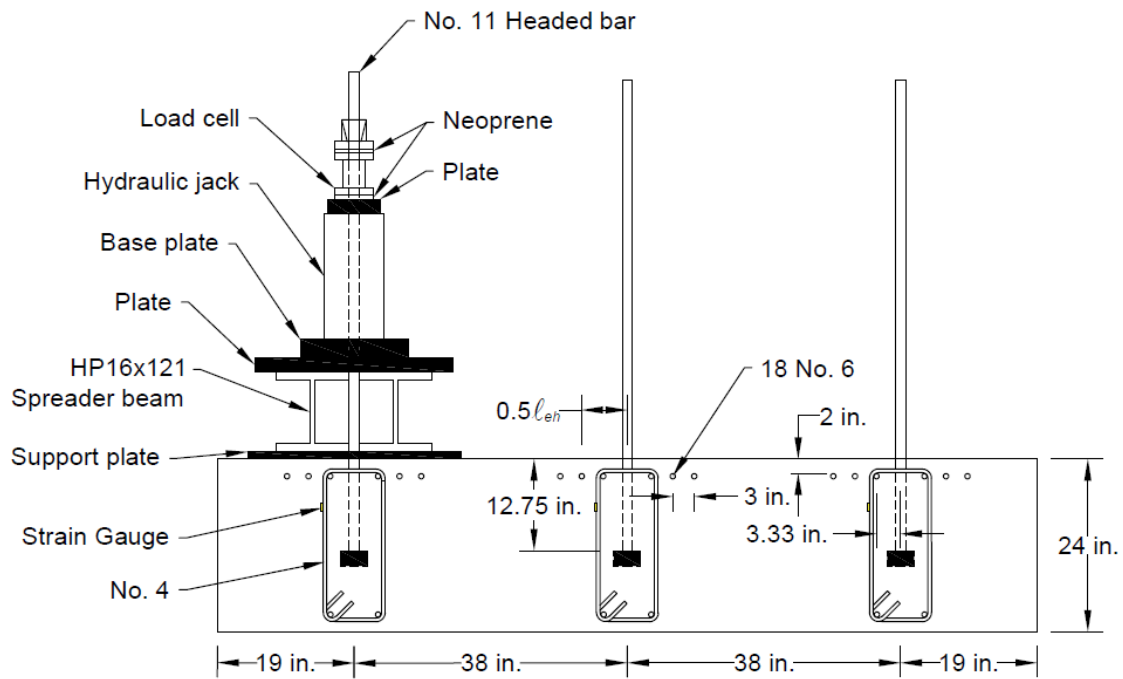


(a)

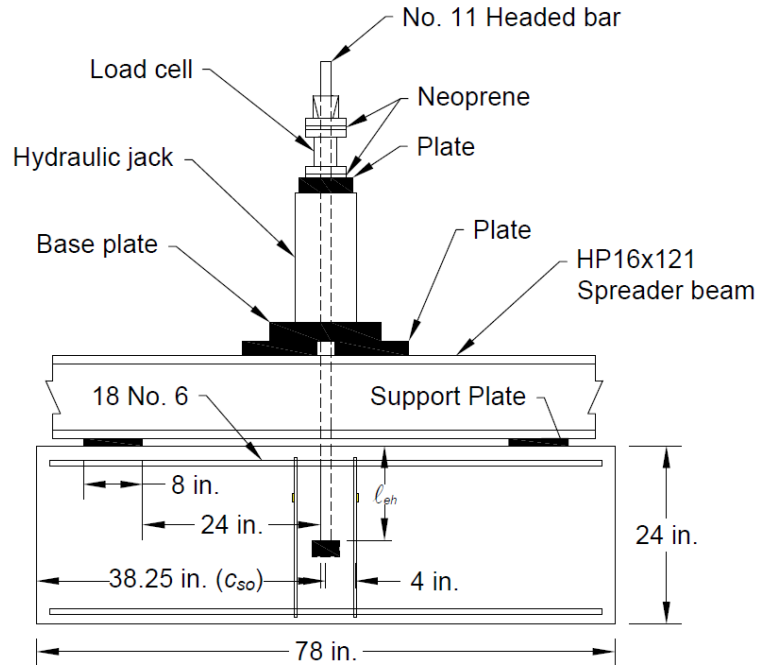


(b)

Figure 2.5 Location of headed bars and reinforcement for Slab 4 (a) side view, (b) end view

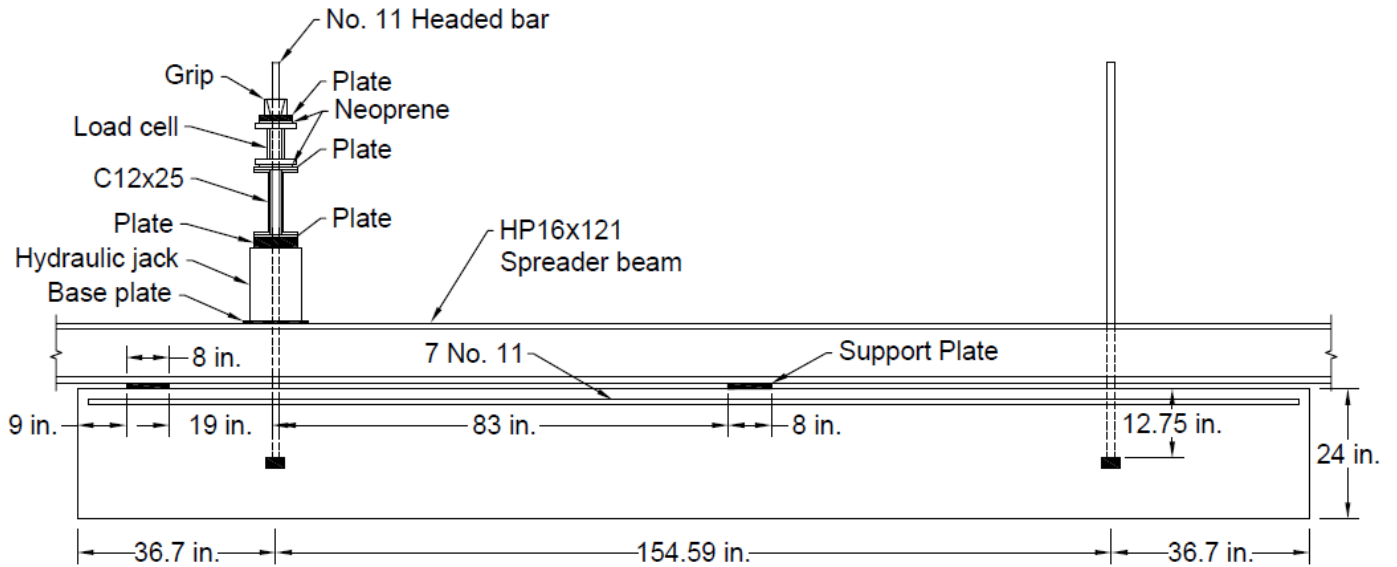


(a)

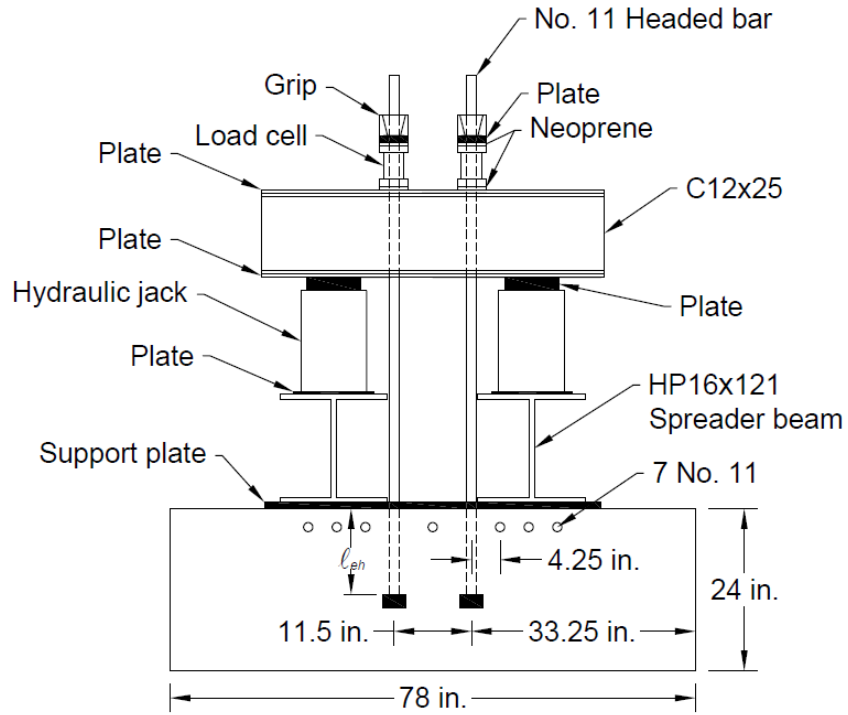


(b)

Figure 2.6 Location of headed bars and reinforcement for Slab 5 (a) side view, (b) end view

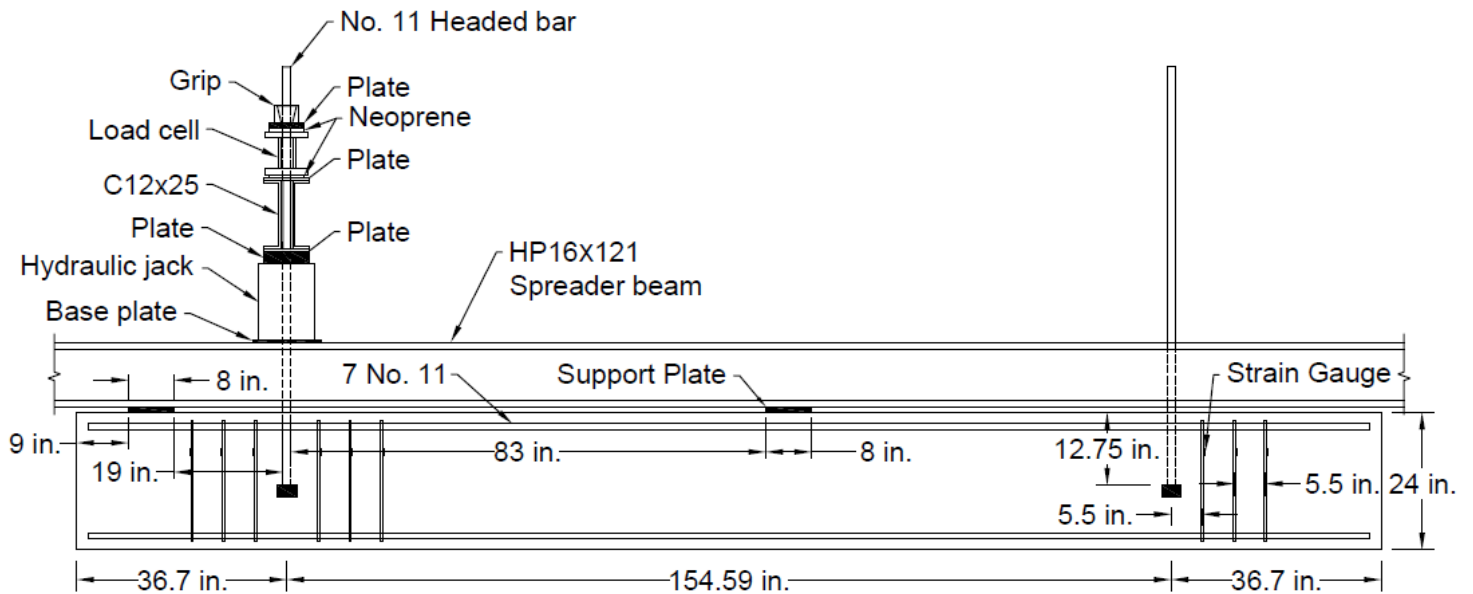


(a)

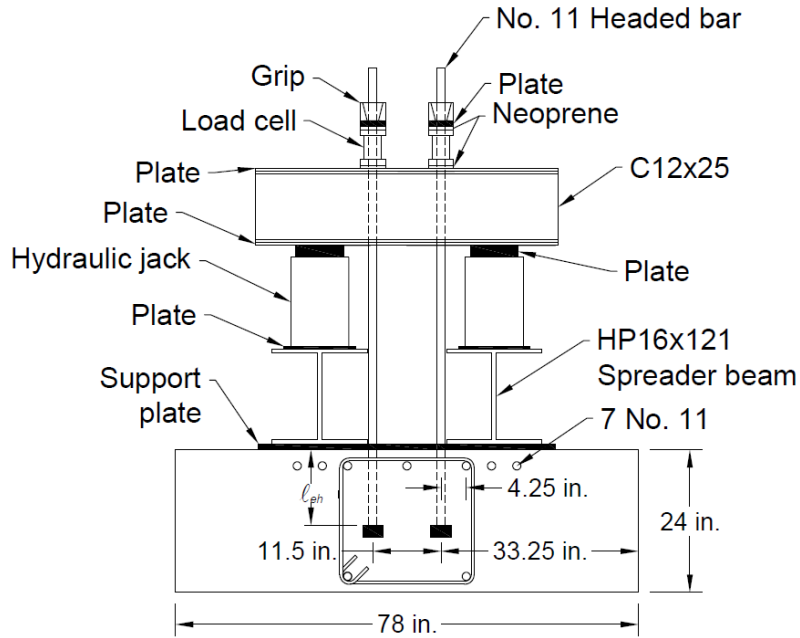


(b)

Figure 2.7 Location of headed bars and reinforcement for Slabs 6,7, and 10 (a) side view, (b) end view

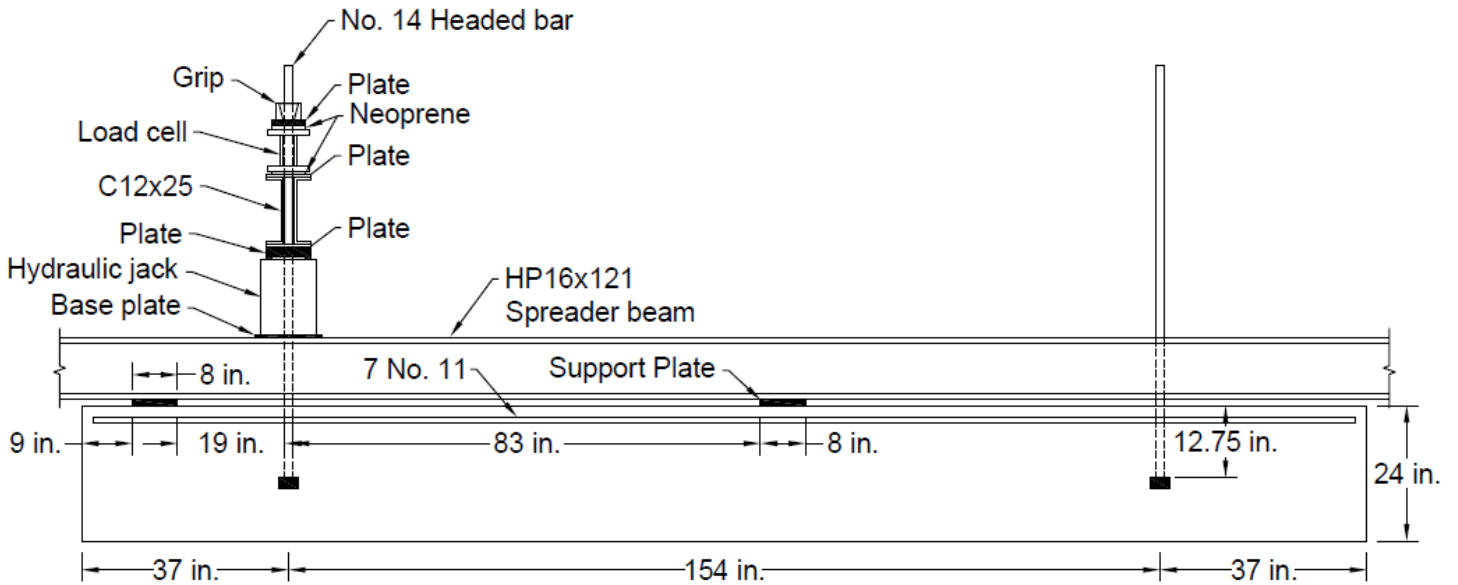


(a)

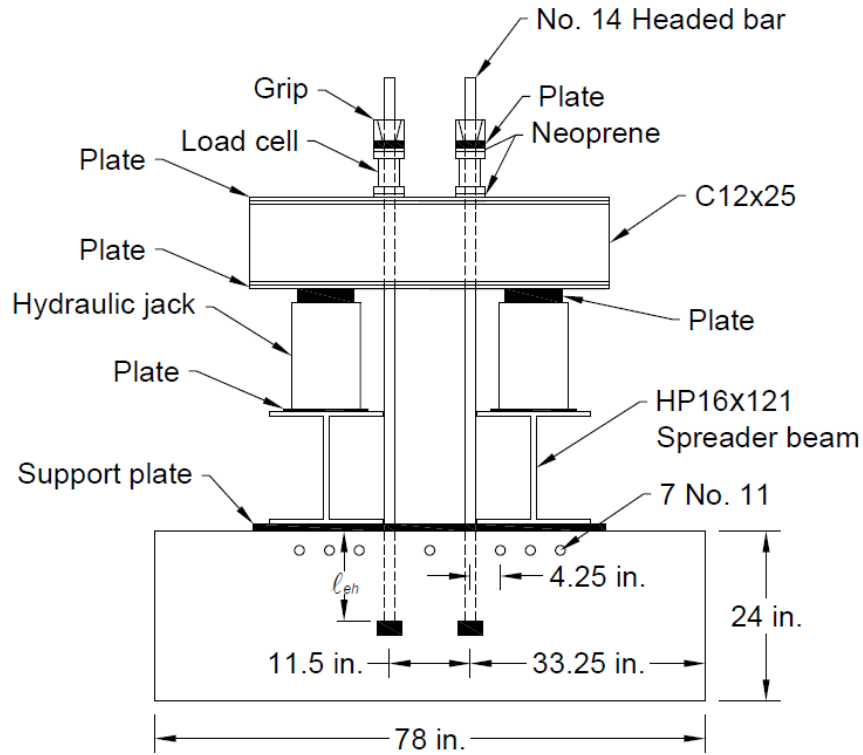


(b)

Figure 2.8 Location of headed bars and reinforcement for Slabs 8, 9, and 11 (a) side view, (b) end view

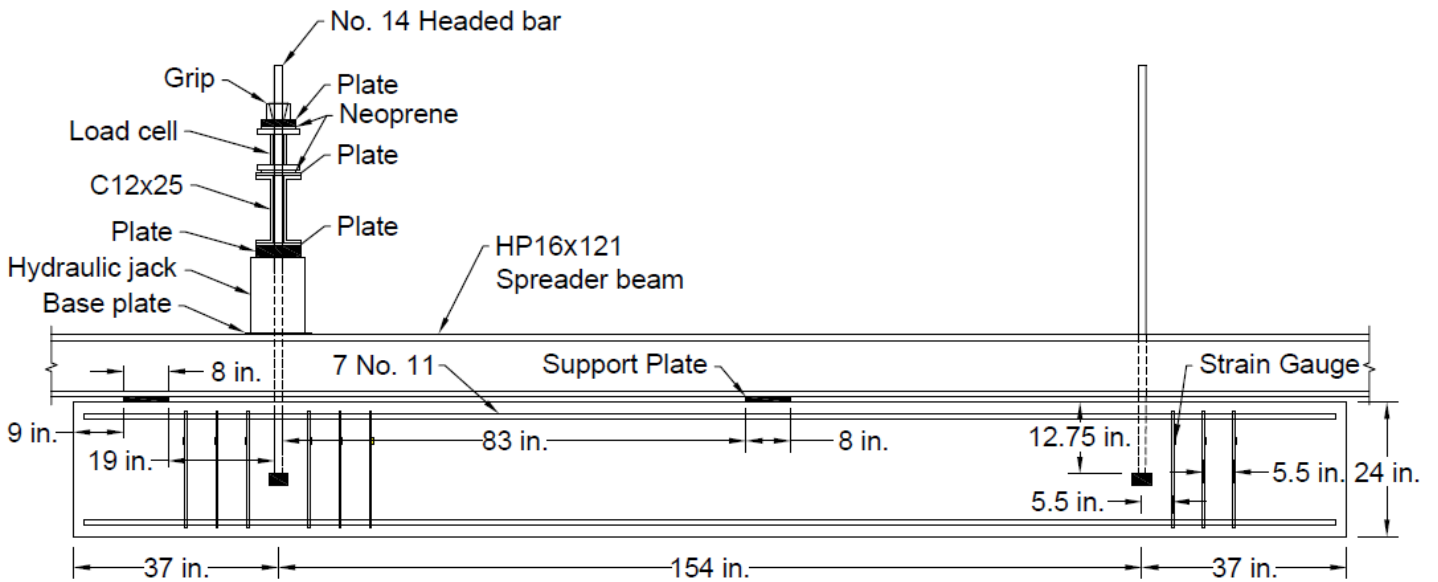


(a)

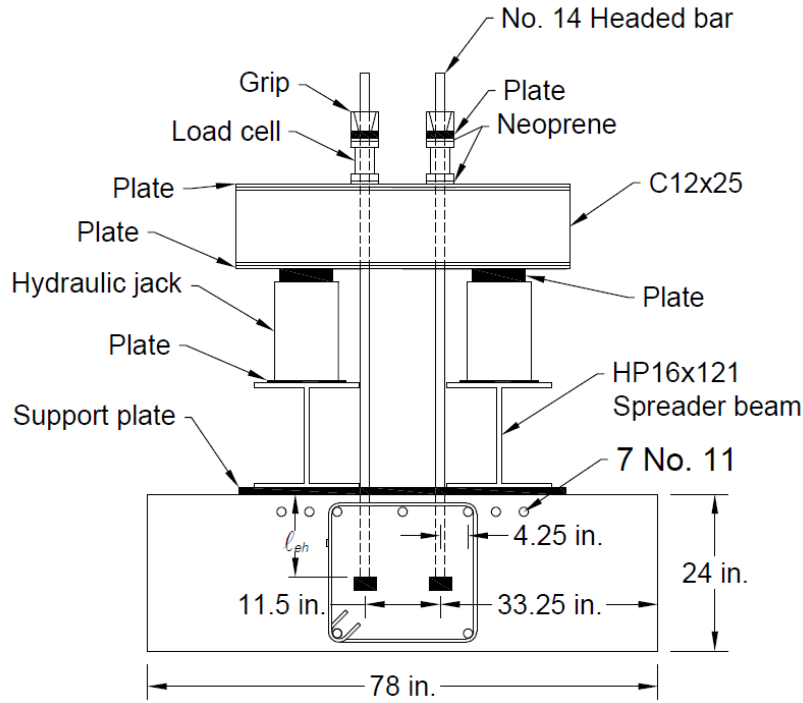


(b)

Figure 2.9 Location of headed bars and reinforcement for Slabs 12 and 14 (a) side view, (b) end view



(a)



(b)

Figure 2.10 Location of headed bars and reinforcement for Slabs 13 and 15 (a) side view, (b) end view

2.3 TEST PARAMETERS

The test parameters in this study were bar size, concrete compressive strength, number of headed bars, the spacing between the headed bars, embedment length, support reaction placement, and parallel tie reinforcement. The ranges of these variables are described below:

Bar size: Two headed bar sizes were used – No. 11 and No. 14. The net bearing areas A_{brg} of the headed bars were $5.5A_b$ and $9.2A_b$ for No. 11 headed bars and $4.2A_b$ for No. 14 headed bars, where A_b is the bar area. Shao et al. (2016) and Ghimire et al. (2018) found that the anchorage strength of headed bars was not sensitive to bearing area for bars with net bearing areas A_{brg} between $3.8A_b$ and $9.5A_b$.

Concrete compressive strength: The target concrete compressive strengths were 5,000 and 15,000 psi. Measured concrete compressive strengths ranged from 5,060 to 14,470 psi. Concrete mixture proportions are given in Section 2.1.1.

Number and spacing of headed bars: Of the 31 tests, nine tests contained one headed bar, and twenty-two tests included two headed bars loaded simultaneously. For the tests with two headed bars, the nominal center-to-center spacing between the bars was either $3.2d_b$ or $8.2d_b$ (where d_b is the bar diameter). The spacing between the bars ($3.2d_b$ and $8.2d_b$) is considered closely and widely spaced, respectively, according to Shao et al. (2016).

Embedment length: Nominal embedment length was $12^{3/4}$ in., and measured embedment lengths ranged from $12^{5/8}$ to $14^{1/16}$ in.

Support reaction placement: The distance from the center of the headed bar to the center of the closest support reaction plate ranged from $23^{3/4}$ to $75^{3/8}$ in.

Parallel tie reinforcement: Parallel tie reinforcement within the joint region ranged from no parallel tie reinforcement to 6 No. 4 hoops, each with two legs. Of the 31 tests, 18 had no parallel tie reinforcement, three had two No. 4 hoops placed on both sides of the headed bar, spaced at $3d_b$ from the center of the headed bar; five had three No. 4 hoops placed only on one side of the headed bars, spaced at $4d_b$ from the center of the headed bar (with one hoop placed outside $10d_b$), and five had six No. 4 hoops placed on both sides of the bars, spaced at $4d_b$ from the center of the headed bar (with two hoops located outside $10d_b$). Details of the three levels of parallel tie reinforcement are shown in Figures 2.6 and 2.8.

2.4 SPECIMEN DESIGNATION

The test variables are denoted in the specimen designation. An example is shown in Figure 2.11. In this example, the first term [(2@8.2)11] indicates that the test had two No. 11 headed bars spaced at 8.2 times the bar diameter (center-to-center); the second term (5) is the nominal concrete compressive strength (ksi); the third term (S9.2) represents the head type (refer to Table 2.3); the fourth term (7#11) denotes the amount of flexural reinforcement placed perpendicular to the headed bars; the fifth term (6#4) represents the number and size of the parallel tie used within the joint region (six hoops, with three on each side of the headed bars); and the final term ($12^{3/4}$) represents the nominal value of the embedment length (in.).

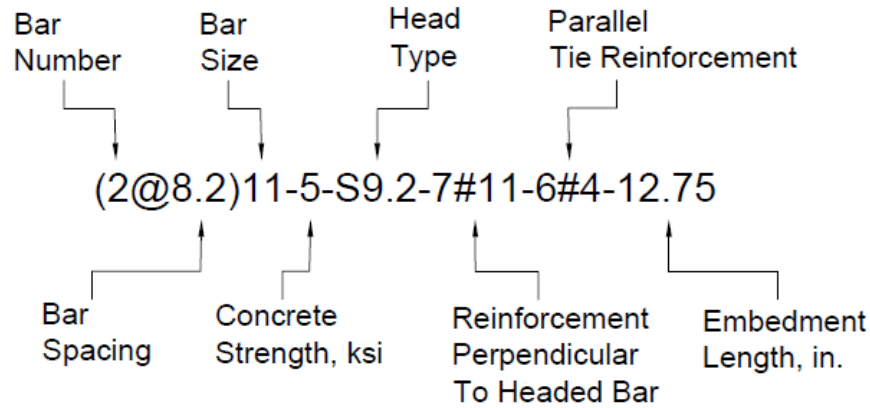


Figure 2.11 Example specimen designation

2.5 SPECIMEN FABRICATION

Formwork of the slab specimens was constructed using $\frac{3}{4}$ -in. thick plywood and 2×4 dimension lumber, as shown in Figure 2.12. The reinforcing steel and headed bars were then placed in the formwork with the support provided for headed bars from the bottom by chairs made of wood and from the top with a wooden truss to hold the headed bar(s) upright until the concrete had set. The specimens were cast in two layers, and each layer was consolidated using a spud vibrator. In accordance with ASTM C172, during casting, two samples of fresh concrete were obtained from the middle portion of the batch and combined to measure slump, temperature, and unit weight. Concrete cylinders (4×8 in. and 6×12 in.) were prepared in accordance with ASTM C31 and stored with the specimens until they were tested. The 4×8 in. concrete cylinders were used to track of concrete compressive strength gain, and the 6×12 in. concrete cylinders were used to measure the concrete compressive strength on the day of testing. For 5,000 psi concrete, the test specimens were wet-cured with saturated burlap and plastic sheeting until the concrete compressive strength reached 3,000 psi; the formwork was then removed, and the specimens were allowed to dry until they reached the desired strength before testing. For high-strength concrete (15,000 psi concrete), the specimens were continuously wet-cured after removing the formwork at a strength of 3,000 psi to allow the concrete to continue to gain strength. When the concrete reached the desired strength, the burlap and the plastic sheeting were removed and the specimens were prepared for testing.



Figure 2.12 Slab specimen formwork

2.6 TEST PROCEDURE

The test frame systems were a modified version of the test system used by Ghimire et al. (2018). Two test frame configurations were used in this study. The first configuration was used for tests with a single headed bar, while the second configuration was used for tests with two bars. In the first configuration (Figures 2.2 to 2.4 and Figure 2.13), two $1 \times 8 \times 50$ in. support reaction plates were first placed on the slab using high-strength gypsum cement paste (Hydrostone) between the concrete and the plates to ensure uniform contact. Two $W12 \times 58$ spreader beams were then placed on the support plates on either side of the anchored headed bar(s) to transfer loads from the hydraulic cylinder to the reaction support plates, as shown in Figures 2.2 to 2.4. A $15 \times 15 \times 2.5$ in. steel plate with a center hole (lower steel plate in Figure 2.13) was placed on the two spreader beams with the test bar passing through the hole in the plate. A 150-ton capacity hydraulic cylinder was then placed on the steel plate. A $6 \times 6 \times 1$ in. steel plate with a center hole (middle steel plate in Figure 2.13) was placed on the hydraulic cylinder. Then, a load cell with a $6 \times 6 \times 1$

in. steel plate (upper steel plate in Figure 2.13) was installed. The headed bar was locked in place using a collar and wedges.

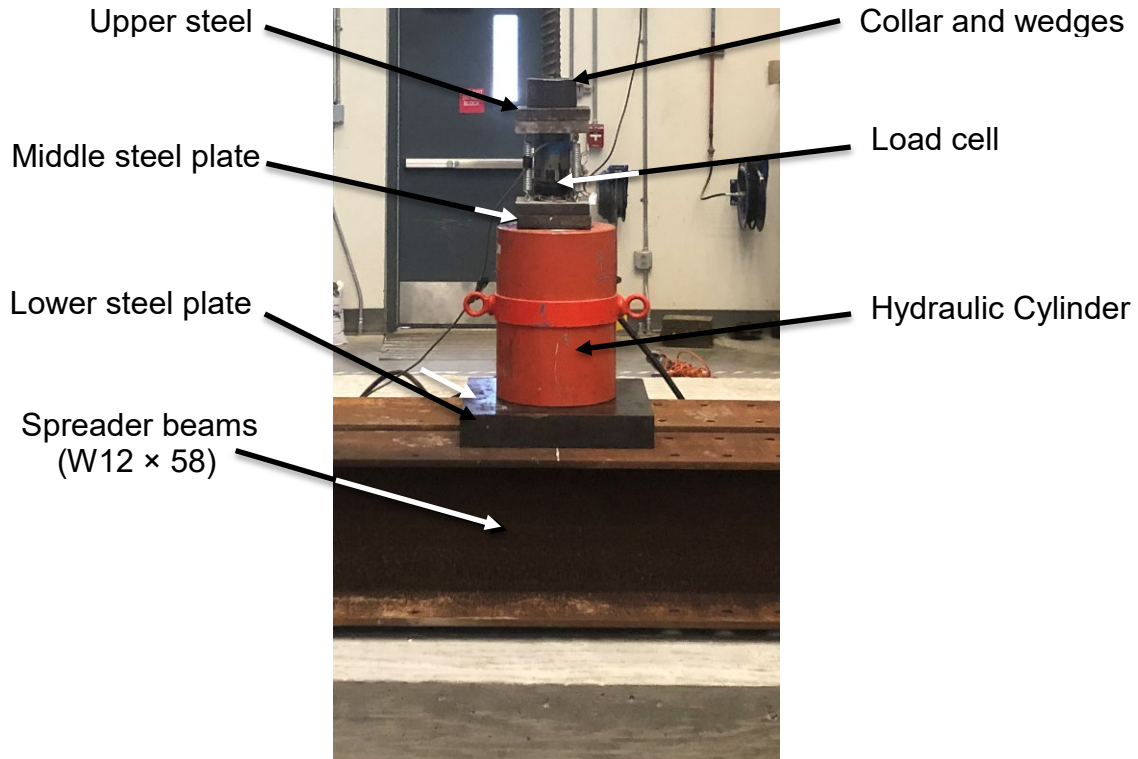


Figure 2.13 Test frame – first configuration

The second configuration (Figures 2.5 to 2.10 and Figure 2.14) was assembled with two $1 \times 8 \times 50$ in. support reaction plates placed on the slab using gypsum cement paste between the concrete and the plates to ensure uniform contact. Two HP16 \times 121 spreader beams were then placed on the support plates on either side of the headed bars to transfer loads from the hydraulic cylinders to the reaction support plates, as shown in Figures 2.5 to 2.10. Two 150-ton hydraulic cylinders were then placed on the spreader beams. An $8 \times 8 \times 2$ in. steel plate was placed on each hydraulic cylinder (the steel plate between the built-up section and the hydraulic cylinder in Figure 2.14). A built-up section, which consists of two steel channels (C12 \times 25) and two 1 in. thick steel plates welded on top and bottom of the steel channels, was then placed on top of the plates and hydraulic cylinders; the built-up section has holes on the top and the bottom plates that allow the test headed bars to pass through. Load cells, with $8 \times 8 \times 2$ in. steel plates (upper and lower steel

plates in Figure 2.14) and neoprene pads above and below each load cell, were placed on each test bar. The test bars were locked in place using collars and wedges. The complete test frame set up for this configuration is shown in Figure 2.14.



Figure 2.14 Test frame – second configuration

During testing, tensile load was applied monotonically to the headed bar(s) at intervals of 10 kips or 20 kips, depending on the anticipated failure load. Loading was paused after each interval to allow cracks to be marked. When the applied tensile load reached about 80% of the expected failure load, the specimen was loaded continuously until failure. The tensile load applied to each headed bar was measured using a load cell. After failure, cracks were marked, and photos were taken. The test frame was then disassembled, and the specimen dissected to examine internal cracks.

2.7 SPECIMEN INSTRUMENTATION

In addition to using the load cells to measure the applied tensile loads, LVDTs (linear variable differential transformers) and strain gauges were used in slab specimens that contained parallel tie reinforcement. LVDTs were used in specimens 8 through 15 to measure the slip of the headed bars. The LVDTs were clamped to the top flange of the spreader beams, as shown in Figure 2.15. A flat 1/8-in. thick plate welded to a steel ring was attached to each test bar and tightened in place using bolts to give the LVDTs a point of contact during the test, as shown in Figure 2.16.



Figure 2.15 LVDTs clamped to the top flange of the spreader beams

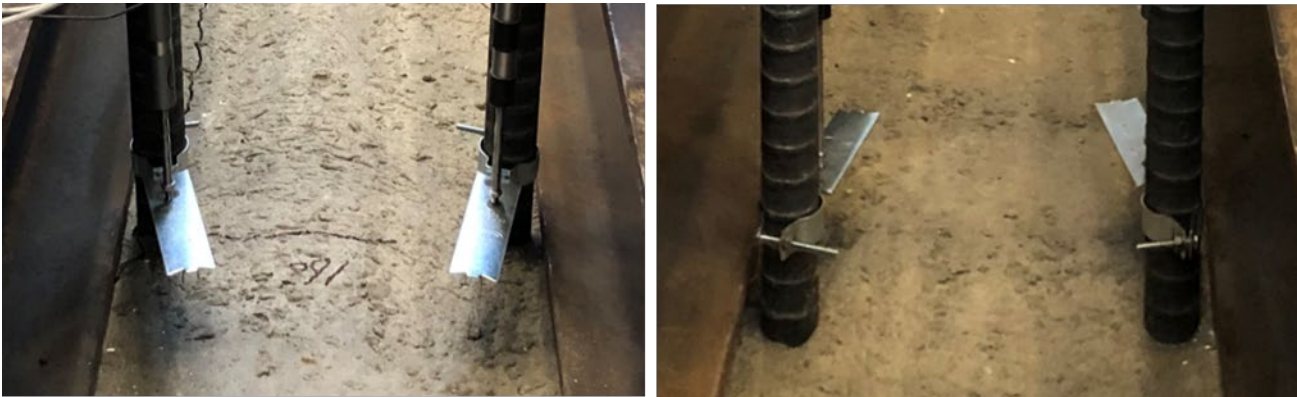


Figure 2.16 LVDT plates attached to test bars

Strain gauges were used on the parallel ties of slab specimens to measure the change in strain in the tie reinforcement at varying distances from the headed bar(s). One strain gauge was attached to a single leg of each hoop in the top quarter of the leg, as shown in Figure 2.17.

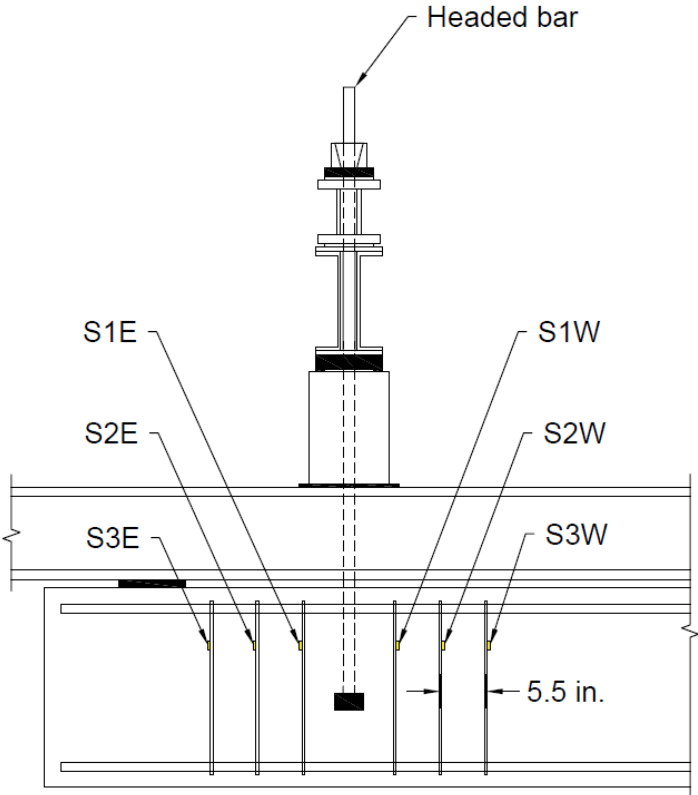


Figure 2.17 Location of the strain gauges on parallel ties

CHAPTER 3: TEST RESULTS AND ANALYSIS OF SIMULATED COLUMN-FOUNDATION JOINT SPECIMENS TESTED IN THE CURRENT AND PREVIOUS STUDIES AND COMPARISON BETWEEN THE PROPOSED EQUATIONS AND ACI 318-19 CODE PROVISIONS

In this chapter, the test results for the simulated column-foundation joint specimens using headed bars are presented. Failure mode, effects of test parameters on the anchorage strength of headed bars, and an analysis of test results from other studies and comparisons with the current study are presented. A comparison between descriptive equations developed by Shao et al. (2016) and the ACI 318-19 Code provisions is conducted. Finally, this chapter ends with recommended changes to Chapters 17 and 25 of ACI 318-19.

Student's t-test, is used throughout the chapter to determine if differences between two sets of data for a particular test parameter (such as the difference in failure load for test bars anchored in slab specimens with different concrete compressive strengths) are statistically significant. In the current study, a significance level of $\alpha = 0.05$ is used as the threshold, which means that there is at most a 5% probability that the difference between the two sets of data is due to random variation and not a difference in behavior. Smaller values of α indicate a greater probability of statistical significance.

3.1 TESTS OF HEADED BARS ANCHORED IN SIMULATED COLUMN-FOUNDATION JOINT SPECIMENS WITH SHALLOW EMBEDMENT

Headed bars, representing column longitudinal reinforcing bars, anchored in slab specimens were tested to investigate the anchorage strength and behavior of headed bars in column-foundation joints with the columns subjected to bending. Fifteen slab specimens, described in detail in Chapter 2, were tested to study the effects of support location, grouping of headed bars, spacing between the bars, bar size, parallel tie reinforcement, and concrete compressive strength on the anchorage strength of headed bars. Of the fifteen slab specimens, 11 contained two groups of two headed bars with the two bars in a group loaded simultaneously, two specimens had three headed bars loaded individually, one specimen contained two headed bars, each loaded individually, and one specimen had only one headed bar anchored in the center of the slab, for a total of 31 tests. The individual and grouped headed bars were embedded sufficiently far apart so that the anchorage failure of one headed bar or group did not interfere with anchorage

of the others. Of the 31 tests, 13 had parallel tie reinforcement within the joint region, while the remaining 18 had none. In the tests with parallel tie reinforcement, three tests included one No. 11 headed bar with one No. 4 bar hoop on both sides of the headed bar spaced at $2.8d_b$ (4 in.) from the centerline of the headed bar, as shown in Figure 2.6; three tests included two No. 11 headed bars loaded simultaneously with three No. 4 bar hoops placed on one side of the headed bars and spaced at $3.9d_b$ (5.5 in.), as shown in Figure 2.8; three tests involved two No. 11 headed bars loaded simultaneously with three No. 4 bar hoops placed on both sides of the headed bars and spaced at $3.9d_b$ (5.5 in.), as shown in Figure 2.8; two tests included two No. 14 headed bars loaded simultaneously with three No. 4 bar hoops placed on one side of the headed bars and spaced at $3.2d_b$ (5.5 in.), as shown in Figure 2.10; and two tests involved two No. 14 headed bars loaded simultaneously with three No. 4 bar hoops placed on both sides of the headed bars and spaced at $3.2d_b$ (5.5 in.), as shown in Figure 2.10. Embedment lengths ranged from $12\frac{5}{8}$ to 14 in., and parallel tie reinforcement within the joint region ranged between zero and six No. 4 stirrups, in the latter case with three on both sides of the headed bar. Concrete compressive strengths ranged from 5,060 to 14,470 psi, and stresses in the headed bars at failure ranged from 41,800 to 144,400 psi. The net bearing area of the headed bars ranged from 4.2 to $9.2A_b$.

A summary of 31 tests performed on the fifteen slab specimens, including the measured embedment length ℓ_{eh} , the measured concrete compressive strength f_{cm} , the total cross-sectional area of effective confining reinforcement parallel to the headed bars being developed A_{tt} (see Section 3.1.5), the distance between the center of the headed bars and the inner face of the nearest support reaction h_{cl} divided by the measured embedment length ℓ_{eh} , the net bearing area of the head A_{brg} divided by the headed bar area A_b , the ratio A_{tt}/A_{hs} (A_{hs} is the total cross-sectional area of headed bars being developed), the peak load on the headed bar at failure T_{peak} , the total peak load applied on the specimen T_{total} , the average peak load (total peak load applied on the specimen divided by the number of headed bars being developed) T , the anchorage strength calculated based on anchorage provisions in Chapter 17 of ACI 318-19 T_{anc} , the anchorage strength of a headed bar calculated based on descriptive equations (Shao et al. 2016) T_h , and the anchorage strength calculated based on Chapter 25 of ACI 318-19 $T_{ACI 318}$, is provided in Table 3.1, with the full details in Table B.1 of Appendix B. In addition to these specimens, the results of 32 tests conducted

on simulated column-foundation joints and reported by Ghimire et al. 2018 are shown in Table 3.2, with the full details in Table C.2 of Appendix C.

Table 3.1 Summary of key parameters of slab specimens^[1]

Specimens ^[2]			ℓ_{eh} (in.)	f_{cm} (psi)	A_{tt} (in. ²)	$\frac{h_{cl}}{\ell_{eh}}$	$\frac{A_{brg}}{A_b}$	$\frac{A_{tt}}{A_{hs}}$	T_{peak} (kips)	T_{total} (kips)	T (kips)
SN	Description	Group/ Head									
1	11-5-S5.5-6#6-0-12.75	A	13.38	5060	0.0	1.85	5.5	0.0	147.1	-	147.1
	11-5-S5.5-6#6-0-12.75	B	13.13		0.0	1.88	5.5	0.0	137.8	-	137.8
	11-5-S5.5-6#6-0-12.75	C	13.38		0.0	1.85	5.5	0.0	136.3	-	136.3
2	11-5-S5.5-10#6-0-12.75	A	13.38	5490	0.0	1.47	5.5	0.0	161.0	-	161.0
	11-5-S5.5-10#6-0-12.75	B	12.75		0.0	1.55	5.5	0.0	143.7	-	143.7
3	11-5-S5.5-6#11-0-12.75 ^[3]	A	13.63	5740	0.0	5.24	5.5	0.0	119.2	-	119.2
4	(2@3.2)11-5-S5.5-6#11-0-12.75	A1	13.50	5550	0.0	1.46	5.5	0.0	84.6	180.5	90.3
		A2	13.50		0.0	1.46	5.5	0.0	95.9		
	(2@3.2)11-5-S5.5-6#11-0-12.75	B1	13.38	6190	0.0	1.47	5.5	0.0	65.3	154.3	77.2
		B2	13.38		0.0	1.47	5.5	0.0	89.0		
5	11-5-S5.5-6#6-2#4-12.75	A	13.00	5810	0.8	1.90	5.5	0.51	203.7	-	203.7
	11-5-S5.5-6#6-2#4-12.75	B	12.88		0.8	1.92	5.5	0.51	220.9	-	220.9
	11-5-S5.5-6#6-2#4-12.75	C	13.13		0.8	1.88	5.5	0.51	225.2	-	225.2
6	(2@8.2)11-5-S5.5-7#11-0-12.75	A1	13.50	5370	0.0	1.46	5.5	0.0	91.3	199.0	99.5
		A2	13.50		0.0	1.46	5.5	0.0	107.7		
	(2@8.2)11-5-S5.5-7#11-0-12.75	B1	14.06		0.0	1.40	5.5	0.0	89.8	213.0	106.5
		B2	14.06		0.0	1.40	5.5	0.0	123.2		
7	(2@8.2)11-5-S5.5-7#11-0-12.75	A1	13.25	5110	0.0	1.49	5.5	0.0	84.7	176.2	88.1
		A2	13.25		0.0	1.49	5.5	0.0	91.5		
	(2@8.2)11-5-S5.5-7#11-0-12.75	B1	13.31		0.0	1.48	5.5	0.0	93.7	175.3	87.7
		B2	13.31		0.0	1.48	5.5	0.0	81.6		
8	(2@8.2)11-5-S9.2-7#11-3#4-12.75	A1	13.13	7950	0.8	1.50	9.2	0.26	130.4	267.0	133.5
		A2	13.13		0.8	1.50	9.2	0.26	136.5		
	(2@8.2)11-5-S9.2-7#11-6#4-12.75	B1	13.00		1.6	1.52	9.2	0.51	190.4	370.0	185.0
		B2	13.00		1.6	1.52	9.2	0.51	179.6		

^[1] SN = specimen number; ℓ_{eh} = measured embedment length; f_{cm} = measured concrete compressive strength; A_{tt} = total cross-sectional area of effective confining reinforcement (NA_{tr}) parallel to the headed bars being developed (in.²), N = total number of legs of effective confining reinforcement parallel to the headed bars being developed, A_{tr} = area of a single leg of confining reinforcement (in.²); h_{cl} = distance between the center of headed bar to the inner face of the nearest support plate; A_{brg} = net bearing area of the head (Table 2.3); A_b = area of the headed bar; A_{hs} = total cross-sectional area of headed bars being developed (nA_b), where n is the number of headed bars being developed; T_{peak} = peak load on the headed bar at failure; T_{total} = total peak load applied on the specimen; T = average peak load (total peak load applied on the specimen divided by the number of headed bars being developed)

^[2] Multiple headed bars in a single specimen loaded individually are denoted by letters A, B, and C, and grouped headed bars loaded simultaneously are denoted with a number after a common letter (A1, A2)

^[3] Specimen contained a single centrally placed headed bar

Table 3.1 Cont. Summary of key parameters of slab specimens^[1]

Specimens			T_{anc}	T_h	$T_{ACI\ 318}$	T_{calc}	$\frac{T}{T_{anc}}$	$\frac{T}{T_h}$	$\frac{T}{T_{ACI\ 318}}$	$\frac{T}{T_{calc}}$
SN	Description	Group/ Head	(kips)	(kips)	(kips)	(kips)				
1	11-5-S5.5-6#6-0-12.75	A	142.3	98.6	70.9	84.1	1.03	1.49	2.07	1.75
	11-5-S5.5-6#6-0-12.75	B	137.9	96.7	69.6	82.5	1.00	1.42	1.98	1.67
	11-5-S5.5-6#6-0-12.75	C	142.3	98.6	70.9	84.1	0.96	1.38	1.92	1.62
2	11-5-S5.5-10#6-0-12.75	A	148.3	100.6	71.7	85.8	1.09	1.60	2.25	1.88
	11-5-S5.5-10#6-0-12.75	B	136.9	95.7	68.3	81.8	1.05	1.50	2.10	1.76
3	11-5-S5.5-6#11-0-12.75	A	156.4	103.6	73.4	88.4	0.76	1.15	1.62	1.35
4	(2@3.2)11-5-S5.5-6#11-0-12.75	A1	84.1	62.3	45.3	48.3	1.07	1.45	1.99	1.87
		A2								
	(2@3.2)11-5-S5.5-6#11-0-12.75	B1	87.5	63.3	46.0	49.1	0.88	1.22	1.68	1.57
		B2								
5	11-5-S5.5-6#6-2#4-12.75	A	145.5	129.9	70.1	105.8	1.40	1.57	2.90	1.93
	11-5-S5.5-6#6-2#4-12.75	B	143.1	128.9	69.5	104.7	1.54	1.71	3.18	2.11
	11-5-S5.5-6#6-2#4-12.75	C	147.8	130.9	70.8	106.8	1.52	1.72	3.18	2.11
6	(2@8.2)11-5-S5.5-6#11-0-12.75	A1	95.6	101.0	72.2	86.1	1.04	0.99	1.38	1.16
		A2								
	(2@8.2)11-5-S5.5-6#11-0-12.75	B1	101.4	105.3	75.2	89.7	1.05	1.01	1.42	1.19
		B2								
7	(2@8.2)11-5-S5.5-6#11-0-12.75	A1	90.8	97.9	70.4	83.5	0.97	0.90	1.25	1.06
		A2								
	(2@8.2)11-5-S5.5-6#11-0-12.75	B1	91.4	98.4	70.7	83.9	0.96	0.89	1.24	1.04
		B2								
8	(2@8.2)11-5-S9.2-7#11-3#4-12.75	A1	111.7	134.2	81.8	111.4	1.19	0.99	1.63	1.20
		A2								
	(2@8.2)11-5-S9.2-7#11-6#4-12.75	B1	110.2	137.6	81.0	114.4	1.68	1.34	2.28	1.62
		B2								

^[1] SN = specimen number; T = average peak load (total peak load applied on the specimen divided by the number of headed bars being developed); T_{anc} = anchorage strength calculated based on anchorage provisions in Chapter 17 of ACI 318-19 divided by the number of headed bars being developed (in all cases concrete breakout failure governed the anchorage strength); T_h = anchorage strength of a headed bar calculated based on descriptive equations (Shao et al. 2016); $T_{ACI\ 318}$ = anchorage strength calculated based on Chapter 25 of ACI 318-19; T_{calc} = anchorage strength calculated based on the proposed Code provisions

Table 3.1 Cont. Summary of key parameters of slab specimens

Specimens			ℓ_{eh} (in.)	f_{cm} (psi)	A_{tt} (in. ²)	$\frac{h_{cl}}{\ell_{eh}}$	$\frac{A_{brg}}{A_b}$	$\frac{A_{tt}}{A_{hs}}$	T_{peak} (kips)	T_{total} (kips)	T (kips)
SN	Description	Group/ Head									
9	(2@8.2)11-5-S9.2- 7#11-3#4-12.75	A1	13.25	7680	0.8	1.49	9.2	0.26	138.6	281.3	140.7
		A2	13.25		0.8	1.49	9.2	0.26	142.7		
	(2@8.2)11-5-S9.2- 7#11-6#4-12.75	B1	13.38		1.6	1.47	9.2	0.51	179.3	354.2	177.1
		B2	13.38		1.6	1.47	9.2	0.51	174.9		
10	(2@8.2)11-15-S9.2- 7#11-0-12.75	A1	12.69	14470	0.0	1.55	9.2	0.00	124.3	249.6	124.8
		A2	12.69		0.0	1.55	9.2	0.00	125.3		
	(2@8.2)11-15-S9.2- 7#11-0-12.75	B1	12.75		0.0	1.55	9.2	0.00	134.5	261.9	131.0
		B2	12.75		0.0	1.55	9.2	0.00	127.4		
11	(2@8.2)11-15-S9.2- 7#11-3#4-12.75	A1	12.75	14140	0.8	1.55	9.2	0.26	156.6	314.5	157.3
		A2	12.75		0.8	1.55	9.2	0.26	157.9		
	(2@8.2)11-15-S9.2- 7#11-6#4-12.75	B1	12.63	14080	1.6	1.56	9.2	0.51	168.4	335.5	167.8
		B2	12.63		1.6	1.56	9.2	0.51	167.1		
12	(2@6.8)14-5-B4.2- 7#11-0-12.75	A1	13.00	6040	0.0	1.53	4.2	0.00	121.5	239.0	119.5
		A2	13.00		0.0	1.53	4.2	0.00	117.5		
	(2@6.8)14-5-B4.2- 7#11-0-12.75	B1	13.13	6180	0.0	1.51	4.2	0.00	129.1	259.0	129.5
		B2	13.13		0.0	1.51	4.2	0.00	129.9		
13	(2@6.8)14-5-B4.2- 7#11-3#4-12.75	A1	13.00	5440	1.2	1.53	4.2	0.27	139.0	274.6	137.3
		A2	13.00		1.2	1.53	4.2	0.27	135.6		
	(2@6.8)14-5-B4.2- 7#11-6#4-12.75	B1	12.75	5480	2.4	1.56	4.2	0.53	164.0	319.8	159.9
		B2	12.75		2.4	1.56	4.2	0.53	155.8		
14	(2@6.8)14-15-B4.2- 7#11-0-12.75	A1	13.13	14030	0.0	1.51	4.2	0.00	171.2	346.0	173.0
		A2	13.13		0.0	1.51	4.2	0.00	174.8		
	(2@6.8)14-15-B4.2- 7#11-0-12.75	B1	13.13	14050	0.0	1.51	4.2	0.00	160.5	323.8	161.9
		B2	13.13		0.0	1.51	4.2	0.00	163.3		
15	(2@6.8)14-15-B4.2- 7#11-3#4-12.75	A1	13.38	13190	1.2	1.48	4.2	0.27	182.6	370.1	185.1
		A2	13.38		1.2	1.48	4.2	0.27	187.5		
	(2@6.8)14-15-B4.2- 7#11-6#4-12.75	B1	12.88	13020	2.4	1.54	4.2	0.53	195.0	388.8	194.4
		B2	12.88		2.4	1.54	4.2	0.53	193.8		

Table 3.1 Cont. Summary of key parameters of slab specimens

Specimens			T_{anc}	T_h	T_{ACI318}	T_{calc}	$\frac{T}{T_{anc}}$	$\frac{T}{T_h}$	$\frac{T}{T_{ACI318}}$	$\frac{T}{T_{calc}}$
SN	Description	Group/ Head	(kips)	(kips)	(kips)	(kips)				
9	(2@8.2)11-5-S9.2-7#11-3#4-12.75	A1	111.3	134.4	81.1	111.5	1.26	1.05	1.73	1.26
		A2								
	(2@8.2)11-5-S9.2-7#11-6#4-12.75	B1	112.8	139.9	81.9	116.7	1.57	1.27	2.16	1.52
		B2								
10	(2@8.2)11-15-S9.2-7#11-0-12.75	A1	143.5	120.2	106.7	103.7	0.87	1.04	1.17	1.20
		A2								
	(2@8.2)11-15-S9.2-7#11-0-12.75	B1	144.5	120.8	107.2	104.2	0.91	1.08	1.22	1.26
		B2								
11	(2@8.2)11-15-S9.2-7#11-3#4-12.75	A1	142.9	146.5	105.9	125.0	1.10	1.07	1.48	1.26
		A2								
	(2@8.2)11-15-S9.2-7#11-6#4-12.75	B1	140.6	149.7	104.7	128.1	1.19	1.12	1.60	1.31
		B2								
12	(2@6.8)14-5-B4.2-7#11-0-12.75	A1	96.0	97.2	77.4	77.9	1.24	1.23	1.54	1.53
		A2								
	(2@6.8)14-5-B4.2-7#11-0-12.75	B1	98.5	98.7	79.0	79.1	1.32	1.31	1.64	1.64
		B2								
13	(2@6.8)14-5-B4.2-7#11-3#4-12.75	A1	91.1	145.2	76.3	99.6	1.51	0.95	1.80	1.38
		A2								
	(2@6.8)14-5-B4.2-7#11-6#4-12.75	B1	88.9	149.0	74.9	101.8	1.80	1.07	2.13	1.57
		B2								
14	(2@6.8)14-15-B4.2-7#11-0-12.75	A1	148.4	120.1	119.1	97.1	1.17	1.44	1.45	1.78
		A2								
	(2@6.8)14-15-B4.2-7#11-0-12.75	B1	148.5	120.2	119.2	97.2	1.09	1.35	1.36	1.67
		B2								
15	(2@6.8)14-15-B4.2-7#11-3#4-12.75	A1	147.8	172.6	117.7	127.8	1.25	1.07	1.57	1.45
		A2								
	(2@6.8)14-15-B4.2-7#11-6#4-12.75	B1	139.0	172.9	112.5	127.6	1.40	1.12	1.73	1.52
		B2								

Table 3.2 Summary of key parameters of slab specimens (Ghimire et al. 2018) ^[1]

Specimens			ℓ_{eh} (in.)	f_{cm} (psi)	h_{cl} (in.)	$\frac{h_{cl}}{\ell_{eh}}$	$\frac{A_{brg}}{A_b}$	$\frac{A_{st}}{A_b}$ [2]	T (kips)
SN	Description	Group/ Head							
1	8-5-T9.5-8#5-6 ^[3]	A	8.00	7040	10.5	1.31	9.5	1.29	65.6
	8-5-T9.5-8#5-6 ^[3]	B	8.25		10.5	1.27	9.5	1.29	67.8
2	8-5-T4.0-8#5-6	A	8.50	7040	10.5	1.24	4	0.00	61.8
	8-5-T4.0-8#5-6	B	7.50		10.5	1.40	4	0.00	56.3
3	8-5-F4.1-8#5-6 ^[3]	A	7.44	5220	10.5	1.41	4.1	1.29	68.9
	8-5-F4.1-8#5-6 ^[3]	B	7.38		10.5	1.42	4.1	1.29	64.4
4	8-5-F9.1-8#5-6 ^[3]	A	7.13	5220	10.5	1.47	9.1	1.29	69.9
	8-5-F9.1-8#5-6 ^[3]	B	7.00		10.5	1.50	9.1	1.29	54.9
5	8-5-F4.1-2#8-6	A	6.00	7390	10.5	1.75	4.1	0.00	64.4
	8-5-F9.1-2#8-6	B	6.00		10.5	1.75	9.1	0.00	65.0
6	8-5-T4.0-2#8-6	A	6.06	7390	10.5	1.73	4	0.00	60.5
	8-5-T9.5-2#8-6	B	6.13		10.5	1.71	9.5	0.00	57.7
7	8-8-O12.9-6#5-6	A	6.25	8620	9.8	1.57	13	0.00	79.0
	8-8-O9.1-6#5-6	B	6.25		10.5	1.68	9.1	0.00	70.9
8	8-8-S6.5-6#5-6	A	6.38	8620	10	1.57	6.5	0.00	73.0
	8-8-O4.5-6#5-6	B	6.50		10.8	1.66	4.5	0.00	74.0
9	8-5-S14.9-6#5-6	A	6.50	4200	10.3	1.58	15	0.00	61.8
	8-5-S6.5-6#5-6	B	6.50		10	1.54	6.5	0.00	49.2
10	8-5-O12.9-6#5-6	A	6.63	4200	10	1.51	13	0.00	52.4
	8-5-O4.5-6#5-6	B	6.50		10.1	1.55	4.5	0.00	50.1
11	8-5-S9.5-6#5-6	A	6.50	4200	10.3	1.58	9.5	0.00	48.9
	8-5-S9.5-6#5-6	B	6.38		10.1	1.58	9.5	0.00	54.5
12	8-5-F4.1-6#5-6 ^[4]	-	8.44	4200	47.3	5.60	4.1	0.00	39.1
13	8-5-F4.1-0-6	A	6.50	5180	15	2.31	4.1	0.00	50.5
	8-5-F4.1-0-6	B	6.25		17	2.72	4.1	0.00	48.9
	8-5-F4.1-2#5-6	C	6.75		17	2.52	4.1	0.78	61.5
14	8-5-F4.1-4#5-6	A	6.00	5180	16.8	2.80	4.1	1.57	53.4
	8-5-F4.1-4#5-6	B	6.13		17	2.77	4.1	1.57	52.4
	8-5-F4.1-4#5-6	C	6.75	5460	17	2.52	4.1	1.57	53.5
15	8-5-F4.1-6#5-6	A	6.25	5460	17	2.72	4.1	2.35	47.3
	8-5-F4.1-6#5-6	B	6.63		16.8	2.53	4.1	2.35	55.9
	8-5-F4.1-6#5-6	C	6.88		17	2.47	4.1	2.35	52.6

^[1] All tests had individual headed bar; T = peak load on the headed bar at failure

^[2] A_{st} = area of reinforcement in a plane perpendicular to the headed bar within a $1.5\ell_{eh}$ radial distance from the center of the bar (in.²)

^[3] In addition to 8 No. 5 bars as reinforcement perpendicular to the headed bar, specimens contained No. 4 bars spaced at 12 in. in a direction perpendicular to the No. 5 bars

^[4] Specimen contained a single centrally placed headed bar

Table 3.2 Cont. Summary of key parameters of slab specimens (Ghimire et al. 2018)

Specimens			T_{anc}	T_h	T_{ACI318}	T_{calc}	$\frac{T}{T_{anc}}$	$\frac{T}{T_h}$	$\frac{T}{T_{ACI318}}$	$\frac{T}{T_{calc}}$
SN	Description	Group/ Head	(kips)	(kips)	(kips)	(kips)				
1	8-5-T9.5-8#5-6	A	75.6	55.8	39.8	46.3	0.87	1.18	1.65	1.42
	8-5-T9.5-8#5-6	B	79.2	57.5	41.0	47.8	0.86	1.18	1.65	1.42
2	8-5-T4.0-8#5-6	A	82.8	59.3	42.3	49.2	0.75	1.04	1.46	1.26
	8-5-T4.0-8#5-6	B	68.6	52.2	37.3	43.4	0.82	1.08	1.51	1.30
3	8-5-F4.1-8#5-6	A	58.4	48.2	33.6	40.0	1.18	1.43	2.05	1.72
	8-5-F4.1-8#5-6	B	57.7	47.8	33.3	39.6	1.12	1.35	1.93	1.62
4	8-5-F9.1-8#5-6	A	54.8	46.1	32.2	38.3	1.28	1.52	2.17	1.82
	8-5-F9.1-8#5-6	B	53.3	45.2	31.6	37.6	1.03	1.21	1.74	1.46
5	8-5-F4.1-2#8-6	A	50.3	41.9	30.6	35.2	1.28	1.54	2.11	1.83
	8-5-F9.1-2#8-6	B	50.3	41.9	30.6	35.2	1.29	1.55	2.13	1.85
6	8-5-T4.0-2#8-6	A	51.1	42.4	30.9	35.5	1.18	1.43	1.96	1.70
	8-5-T9.5-2#8-6	B	52.0	42.9	31.2	35.9	1.11	1.35	1.85	1.61
7	8-8-O12.9-6#5-6	A	57.8	45.4	34.4	38.1	1.37	1.74	2.30	2.08
	8-8-O9.1-6#5-6	B	57.8	45.4	34.4	38.1	1.23	1.56	2.06	1.86
8	8-8-S6.5-6#5-6	A	59.6	46.4	35.1	38.9	1.23	1.57	2.08	1.88
	8-8-O4.5-6#5-6	B	61.3	47.3	35.8	39.6	1.21	1.57	2.07	1.87
9	8-5-S14.9-6#5-6	A	42.8	39.8	28.4	33.1	1.44	1.55	2.18	1.87
	8-5-S6.5-6#5-6	B	42.8	39.8	28.4	33.1	1.15	1.24	1.73	1.49
10	8-5-O12.9-6#5-6	A	44.1	40.6	28.9	33.7	1.19	1.29	1.81	1.55
	8-5-O4.5-6#5-6	B	42.8	39.8	28.4	33.1	1.17	1.26	1.77	1.51
11	8-5-S9.5-6#5-6	A	42.8	39.8	28.4	33.1	1.14	1.23	1.72	1.48
	8-5-S9.5-6#5-6	B	41.6	39.0	27.8	32.5	1.31	1.40	1.96	1.68
12	8-5-F4.1-6#5-6	-	63.3	52.0	36.8	42.9	0.62	0.75	1.06	0.91
13	8-5-F4.1-0-6	A	47.5	41.8	29.3	34.9	1.06	1.21	1.72	1.45
	8-5-F4.1-0-6	B	44.8	40.2	28.2	33.5	1.09	1.22	1.73	1.46
	8-5-F4.1-2#5-6	C	50.3	43.5	30.4	36.2	1.22	1.41	2.02	1.70
14	8-5-F4.1-4#5-6	A	42.1	38.5	27.1	32.2	1.27	1.39	1.97	1.66
	8-5-F4.1-4#5-6	B	43.5	39.4	27.7	32.9	1.20	1.33	1.89	1.59
	8-5-F4.1-4#5-6	C	51.6	44.0	30.7	36.7	1.04	1.22	1.75	1.46
15	8-5-F4.1-6#5-6	A	46.0	40.7	28.4	34.0	1.03	1.16	1.67	1.39
	8-5-F4.1-6#5-6	B	50.2	43.2	30.1	36.0	1.11	1.29	1.86	1.55
	8-5-F4.1-6#5-6	C	53.1	44.9	31.2	37.4	0.99	1.17	1.68	1.41

3.1.1 Failure and Failure Modes

The anchorage failures observed during the tests are described in this section. Anchorage failure is defined as the failure of the concrete around the test bar(s) accompanied by the loss of load carrying capacity of the bars. Figure 3.1 depicts the typical concrete surface failure and crack progression observed on the top and sides of the specimens. Although the quantity and shape of

cracking varied between specimens, overall crack propagation followed similar patterns. Cracking almost always started with a horizontal crack on the top face of the specimen at the level of the headed bars, extending slightly on both sides of the bars, as shown in Figure 3.1a. This cracking pattern is similar to that found in reinforced concrete beams with bond failures for straight bar reinforcement, and it is most likely caused by slip of the straight portion of the bar. As the load increased, the horizontal cracks on both sides of the bars connected and extended toward the sides of the specimen, accompanied by radial cracks extending from the bars, as shown in Figure 3.1b. As the load further increased, the horizontal and the radial cracks continued to grow toward the sides of the specimen and the test frame support reactions. In the meantime, vertical and diagonal cracks branching from the horizontal and the radial cracks towards the sides of the specimen and the test frame support reactions. At this level, as shown in Figure 3.1c, the cracks on the top face of the specimen had reached the nearest test frame support reaction, which served as the compression region of the virtual column in a column-foundation joint; at this point, no cracks had formed on the sides of the specimen. Near failure, new cracks branching from the existing cracks on the top face of the specimen extended along with the horizontal and radial cracks toward the sides of the specimen and the test frame support reactions. Cracks around the headed bars grew toward the farthest test frame support reaction and the sides of the specimen, forming diagonal cracks on the side face of the specimen extending from the headed bar toward the nearest and farthest test frame support reactions, as shown in Figure 3.1d. The presence of parallel tie reinforcement within the joint region was found to have a direct correlation with the amount of cracking: specimens that contained parallel tie reinforcement, in general, exhibited a greater amount of cracking prior to failure than those that did not contain parallel tie reinforcement. All specimens exhibited a concrete breakout failure, as defined by Section R17.5.1.2 of ACI 318-19. Concrete breakout failures are characterized by a mass of concrete being pulled out of the slab along with the headed bar, forming a cone-shaped failure surface, as shown in Figure 3.2. The cone-shaped pattern region formed during concrete breakout suggests that the head attached to the test bar provides the primary anchorage after slip has occurred along the straight portion of the headed bar. The specific failure pattern was dependent on the location of the test frame support reactions, as shown in Figures 3.3 through 3.7. Figure 3.3 shows the failure pattern of specimens

that have both of the test frame support reactions placed at a clear distance of 24 in. from the headed bar to the inner face of the support reaction plate, just outside the anticipated failure region; this test included one headed bar with parallel tie reinforcement on both sides of the headed bar (Figure 2.6). Figures 3.4 through 3.6 show the failure patterns of specimens that have one of the test frame support reactions placed at a clear distance of 19 in. from the headed bar to the inner face of the support reaction plate (within the anticipated failure region) and the other support reaction placed at a clear distance of 83 in. from the headed bar to the inner face of the support reaction plate (outside the anticipated failure region); a configuration representing the compression zone of a column anchored in a foundation subjected to an overturning moment. Figure 3.4 shows the failure pattern of slab specimens containing two headed bars loaded simultaneously without parallel tie reinforcement, while Figures 3.5 and 3.6 show the failure patterns of slab specimens containing two headed bars loaded simultaneously with parallel tie reinforcement only on one side and on both sides of the headed bars, respectively. Figure 3.7 shows the failure pattern of the slab specimen containing only one headed bar anchored at the middle of the slab without parallel tie reinforcement, with both of the test frame support reactions located at a clear distance of 74 in. from the headed bar to the inner face of the support reaction plate, outside of the anticipated failure region to avoid interference with the concrete breakout failure surface. The effect of the test frame support reactions on the anchorage strength of headed bar(s) is described in Section 3.1.2.

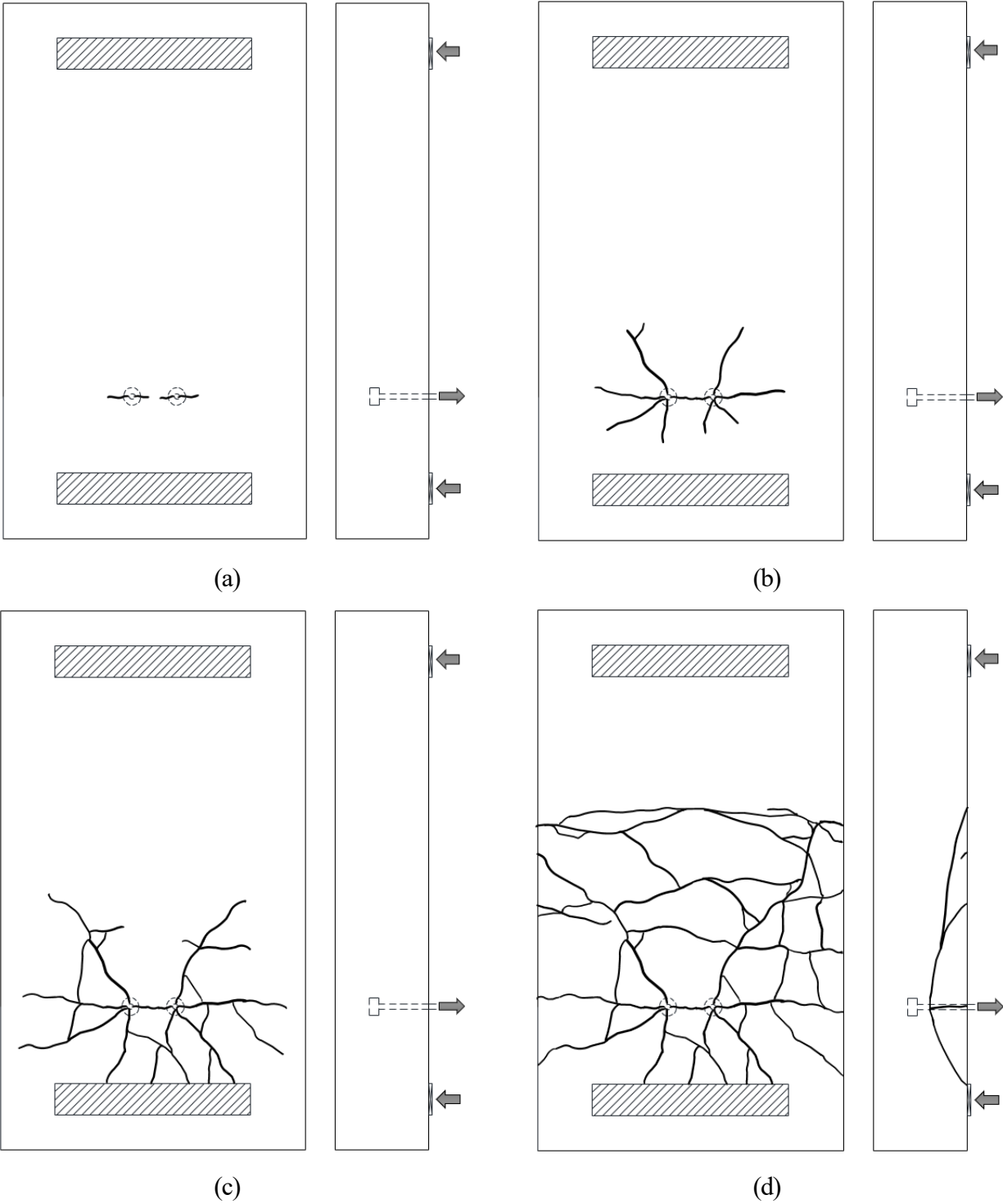
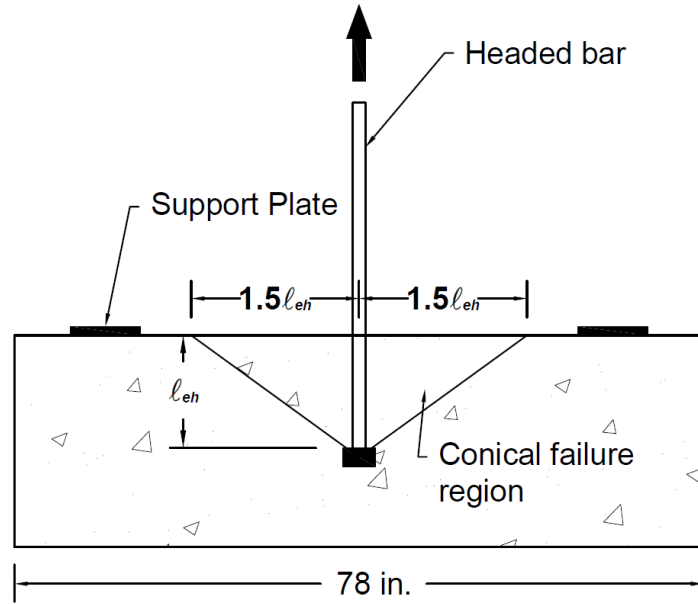
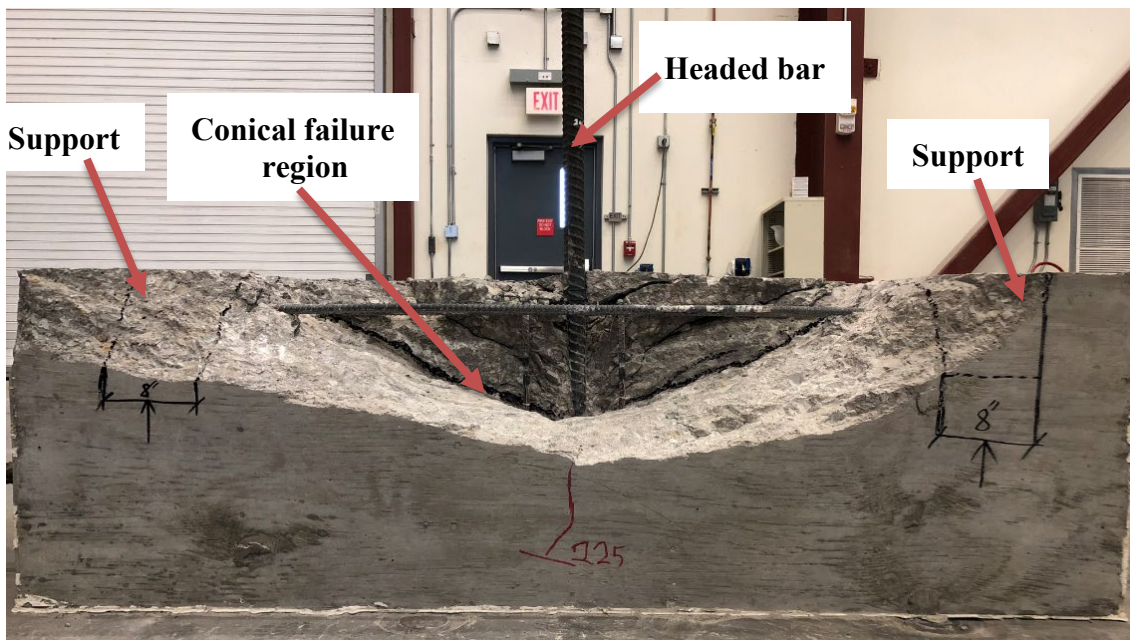


Figure 3.1 Concrete surface failure (crack propagation top and side views)



(a)



(b)

Figure 3.2 Concrete cone-shaped breakout failure (a) schematic drawing (b) Slab Specimen 5 (test 2, 11-5-S5.5-6#6-2#4-12.75) after removal of breakout region

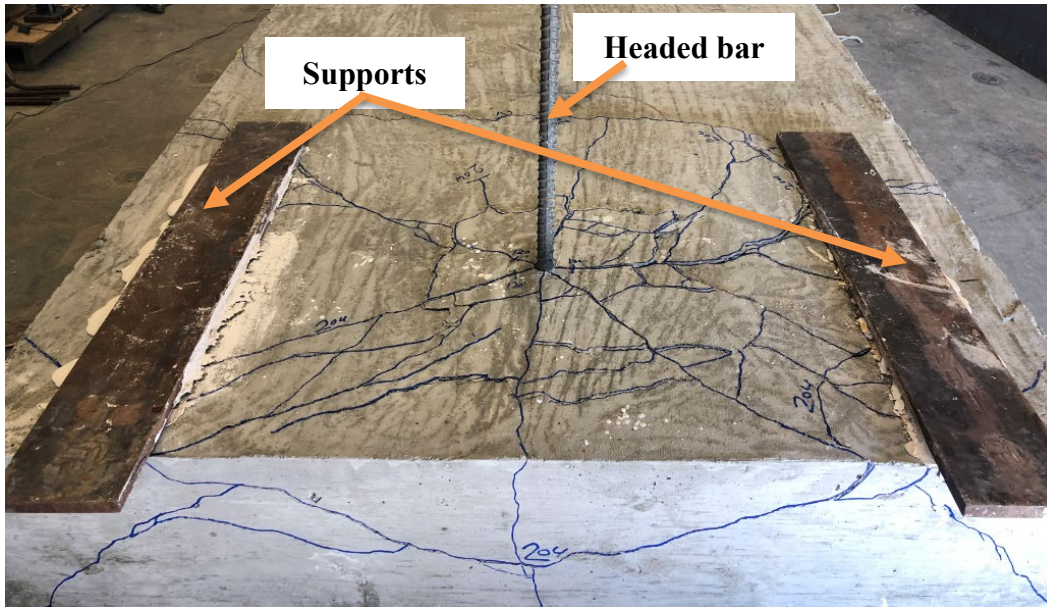
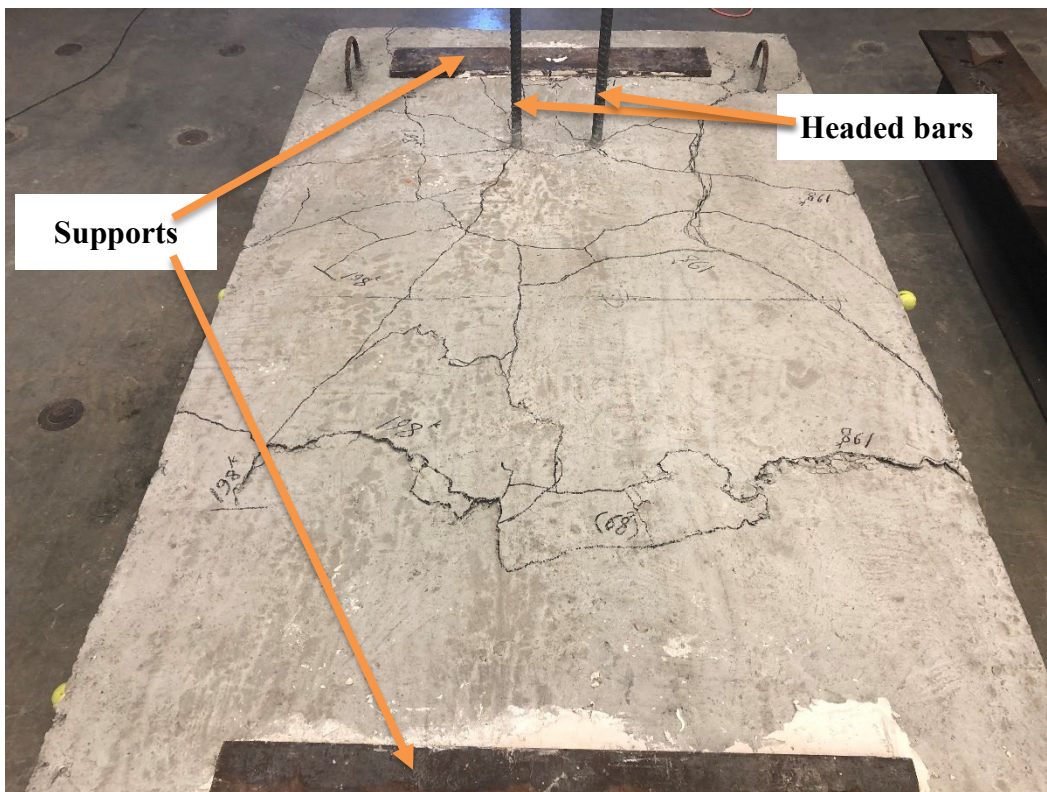
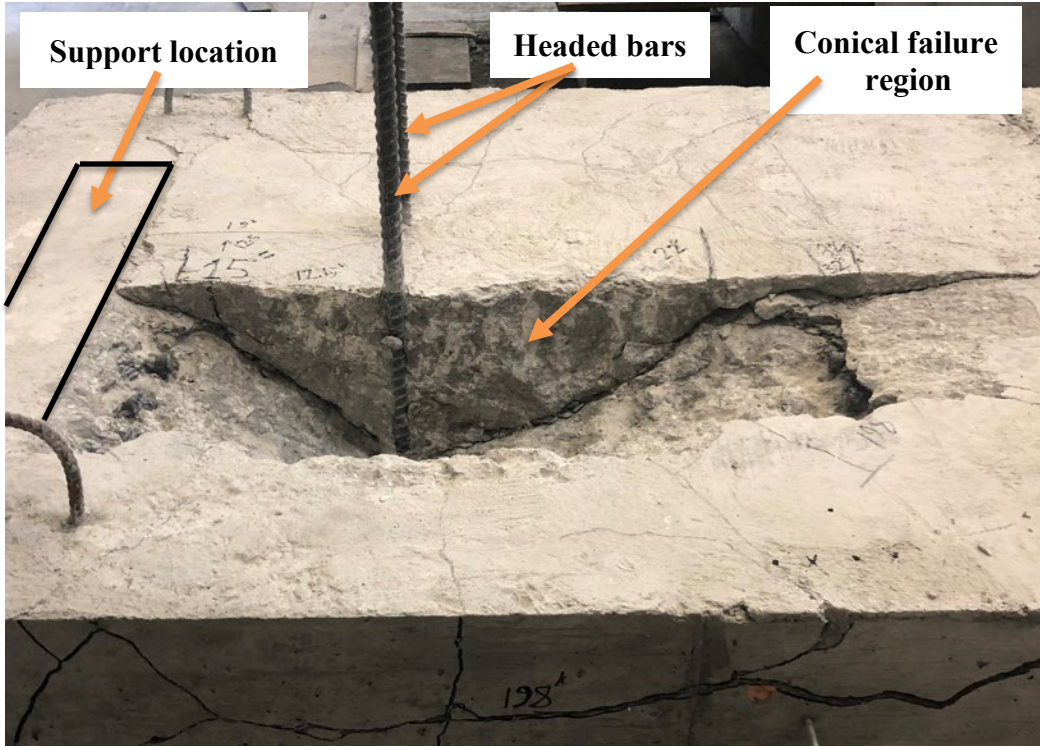


Figure 3.3 Concrete breakout failure. Slab Specimen 5 (test 1, 11-5-S5.5-6#6-2#4-12.75) with both support reactions just outside anticipated failure region (test had one headed bar with parallel tie reinforcement on both sides of headed bar)

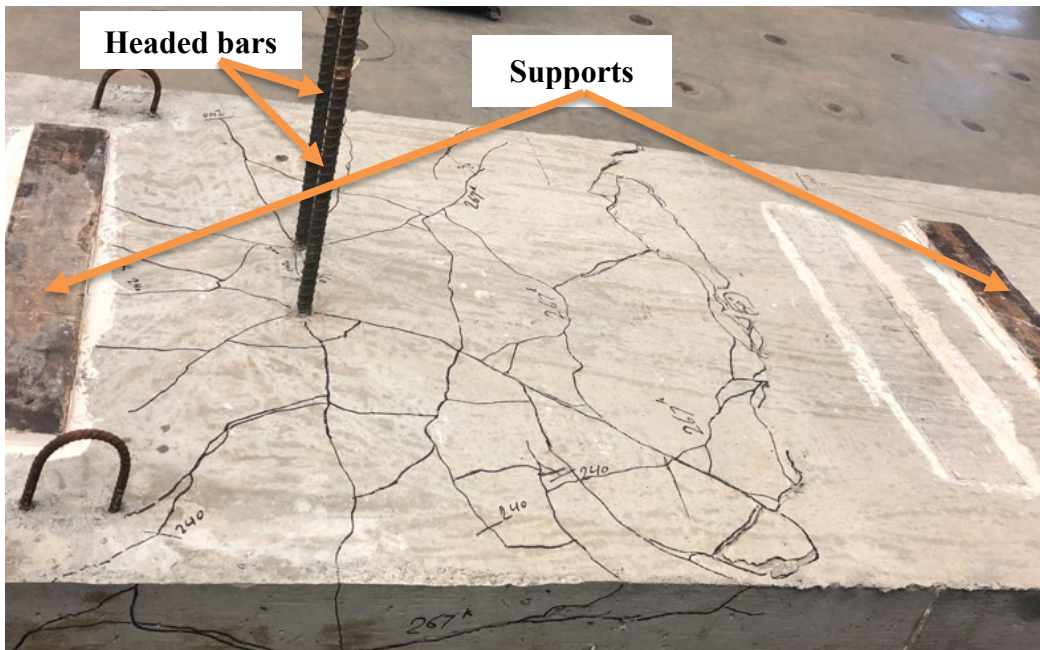


(a)

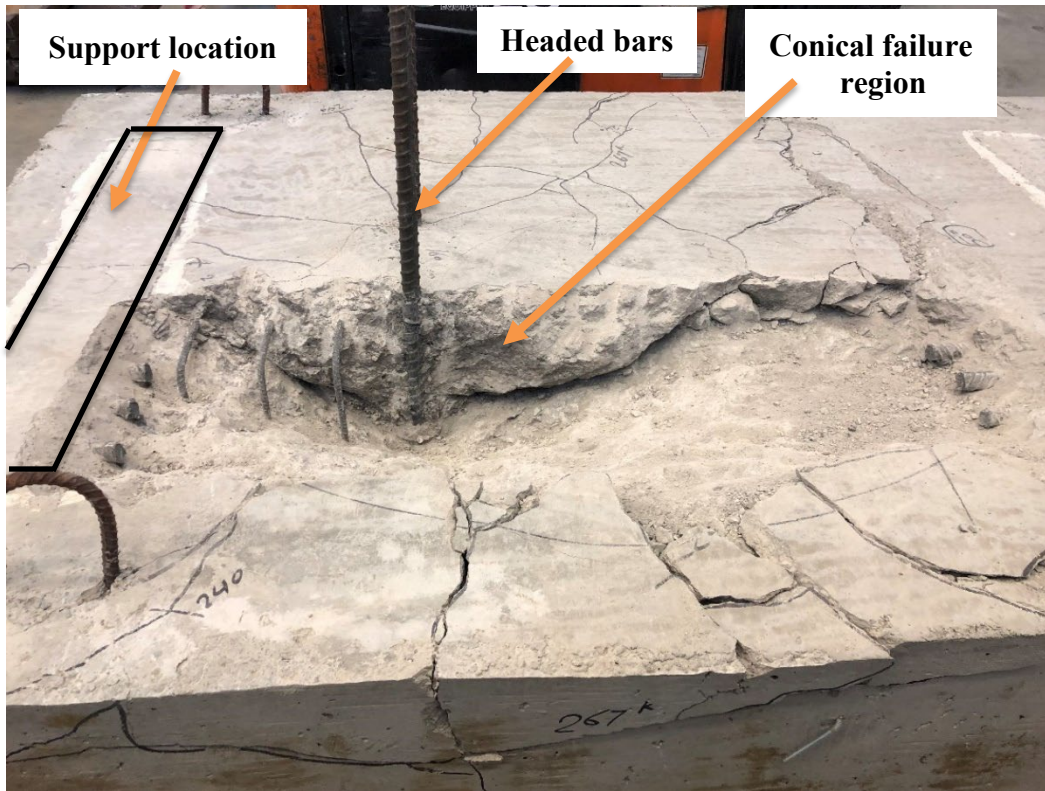


(b)

Figure 3.4 Concrete breakout failure of Slab Specimen 6 (test 1, (2@8.2)11-5-S5.5-7#11-0-12.75) with one of the support reactions placed within anticipated failure region (test had two headed bars without parallel tie reinforcement) (a) concrete surface failure (b) cone-shaped failure after removal of breakout region

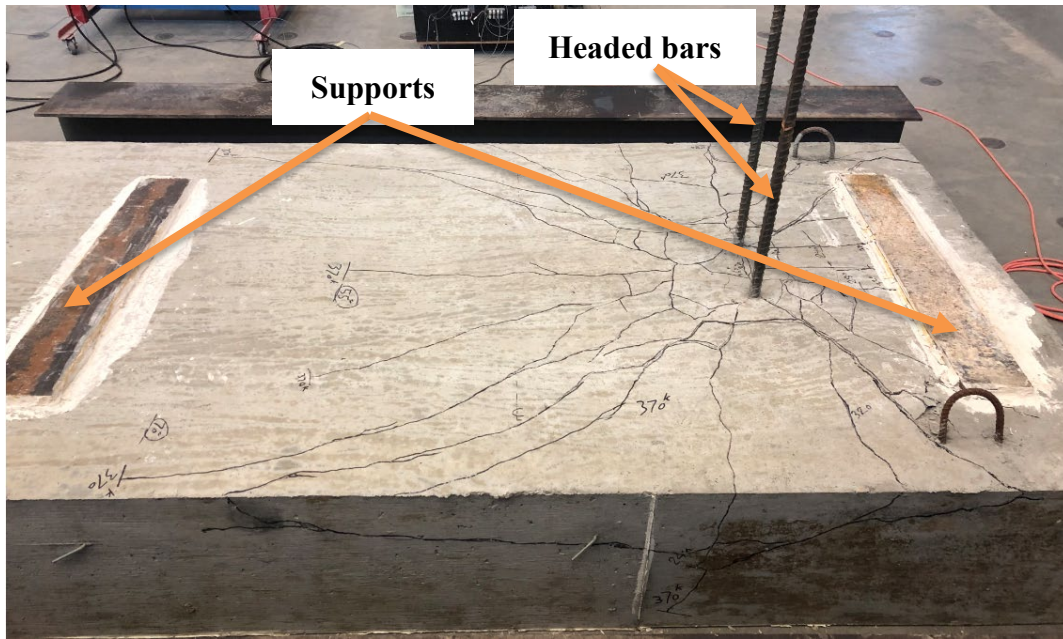


(a)

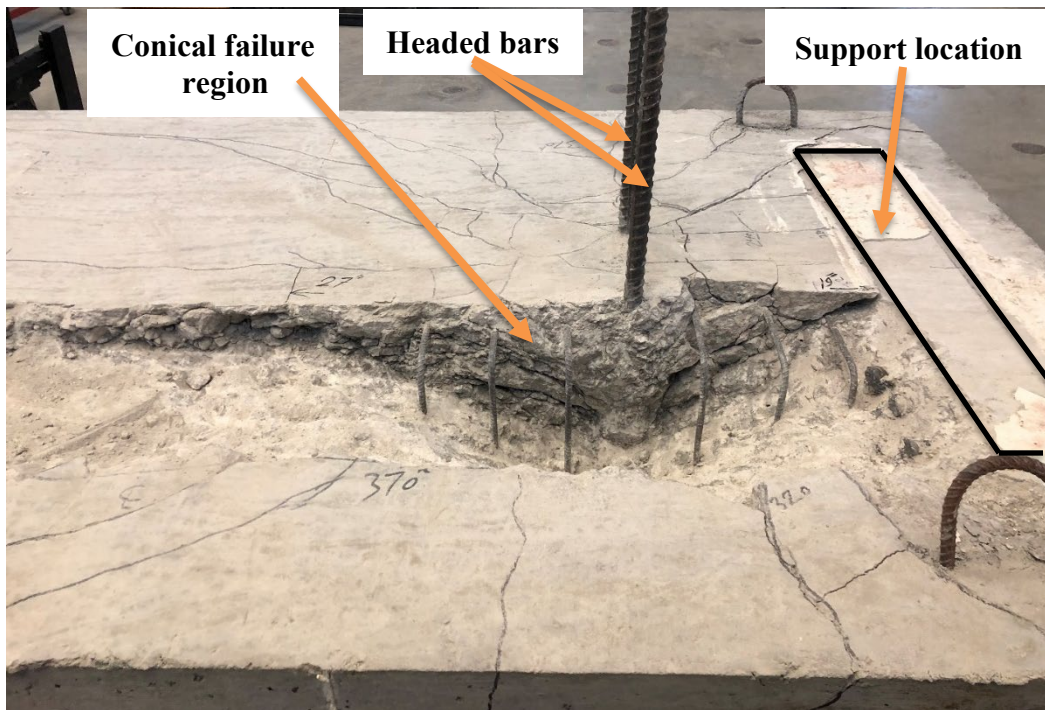


(b)

Figure 3.5 Concrete breakout failure of Slab Specimen 8 (test 1, (2@8.2)11-5-S9.2-7#11-3#4-12.75) with one of the support reactions placed within anticipated failure region (test had two headed bars with parallel tie reinforcement only on one side of headed bars) (a) concrete surface failure (b) cone-shaped failure after removal of breakout region



(a)



(b)

Figure 3.6 Concrete breakout failure of Slab Specimen 8 (test 2, (2@8.2)11-5-S9.2-7#11-6#4-12.75) with one of the support reactions placed within anticipated failure region (test had two headed bars with parallel tie reinforcement on both sides of headed bars) (a) concrete surface failure (b) cone-shaped failure after removal of breakout region

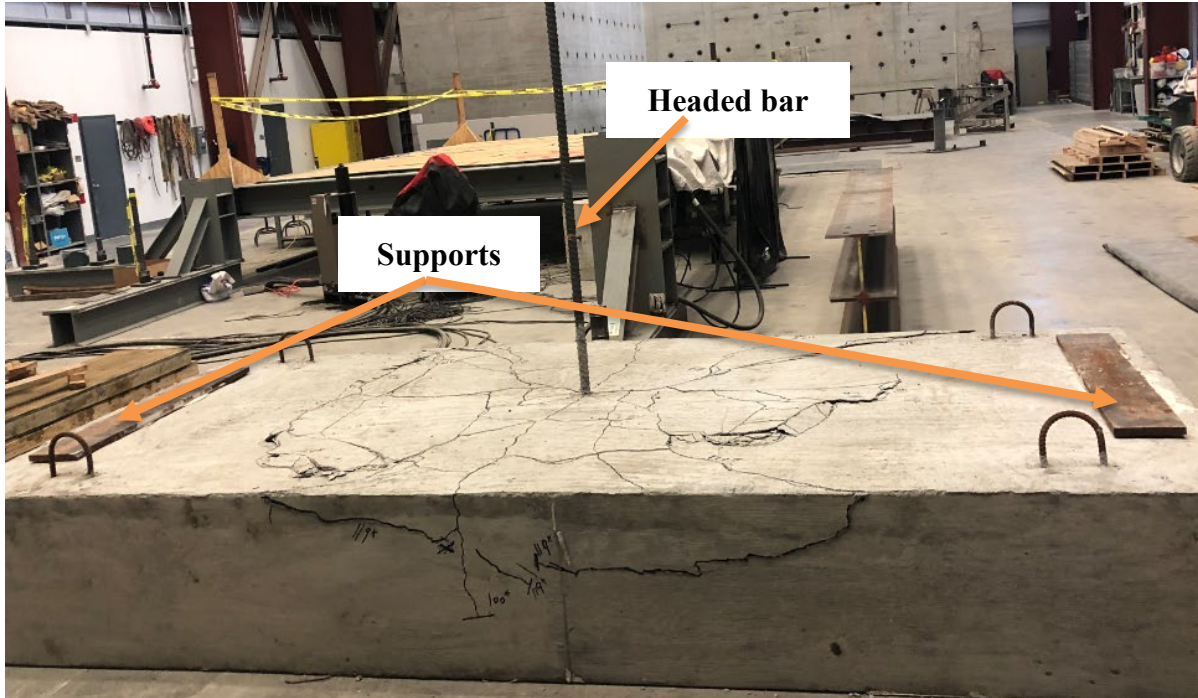


Figure 3.7 Concrete breakout failure of Slab Specimen 3 (11-5-S5.5-6#11-0-12.75) with both support reactions placed far away from anticipated failure region (test had one headed bars without parallel tie reinforcement)

3.1.2 Effect of Strut Angle

The anchorage strength of headed bars is affected by the strut angle (Figure 3.8) between the head and the compressive reaction (Eligehausen et al. 2006b). In general, the flatter the strut angle, the lower the anchorage strength. Shao et al. (2016) found that headed bars in beam-column joints exhibited low anchorage strengths when the ratio of the effective depth of the beam d to the embedment length ℓ_{eh} increased above 1.5, equivalent to a strut angle of 35 degrees. Shao et al.'s (2016) observations match the recommendations in Commentary Section R25.4.4.2 of ACI 318-19, which states that “anchorage strengths will be generally higher if the anchorage length is equal to or greater than $d/1.5$.” To determine if this behavior is observable in column-foundation joints as well, the effect of the strut angle on the anchorage strength of headed bars was investigated. The anchorage strength of headed bars in the slab specimens is plotted versus the ratio h_{cl}/ℓ_{eh} in Figure 3.9, where h_{cl} is the horizontal distance from the center of the headed bar to the face of the nearest support reaction plate, as shown in Figure 3.8. The effect of the strut angle on the anchorage

strength of headed bars was examined using the test results of Slab Specimens 1, 2, and 3 (Table 3.1) and the results from the tests conducted by Ghimire et al. (2018) (Table 3.2).

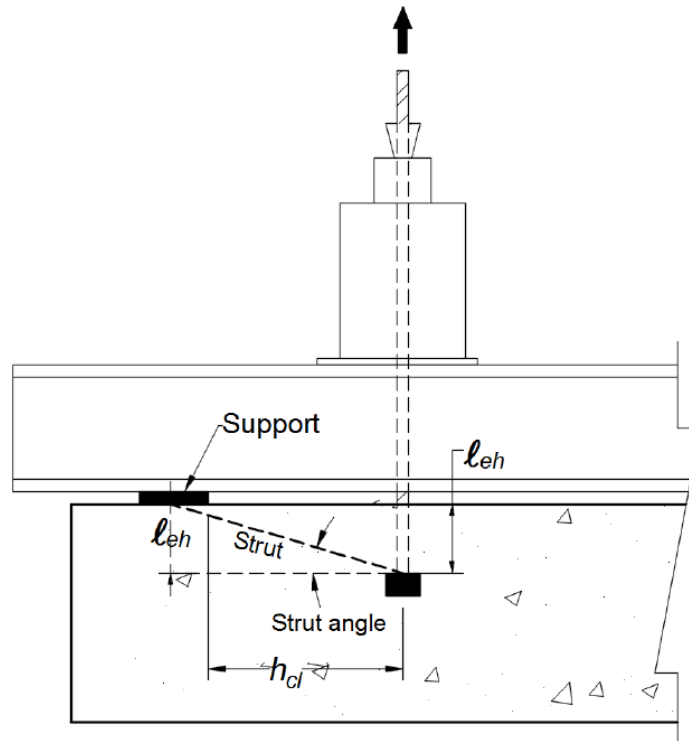


Figure 3.8 Strut angle between anchored headed bar and nearest support reaction (Krishna et al. 2018)

Shao et al. (2016) observed from tests of exterior beam-column joints that headed bars with a net bearing area, A_{brg} , ranging from 3.8 to $9.5A_b$ had similar anchorage strengths; in contrast, A_{brg} greater than $9.5A_b$ ($A_{brg} = 13$ to $15A_b$) tended to increase the anchorage strength of headed bars by about 15%. Therefore, only tests with A_{brg} less than or equal to $9.5A_b$ are included in Figure 3.9. Specimens included in Figure 3.9 have different concrete compressive strengths and embedment lengths. Thus, the peak load on the headed bar at failure (T) is normalized with respect to a concrete compressive strength of 5,000 psi and an embedment length of 12.75 in. using Eq. (3.1). The powers of 0.24 and 1.03 in Eq. (3.1) are those for f_{cm} and l_{eh} , respectively, in the descriptive equations developed by Shao et al. (2016), Eq. (1.7) and (1.8).

$$T_N = T \left(\frac{5000 \text{ psi}}{f_{cm}} \right)^{0.24} \left(\frac{12.75 \text{ in.}}{l_{eh}} \right)^{1.03} \quad (3.1)$$

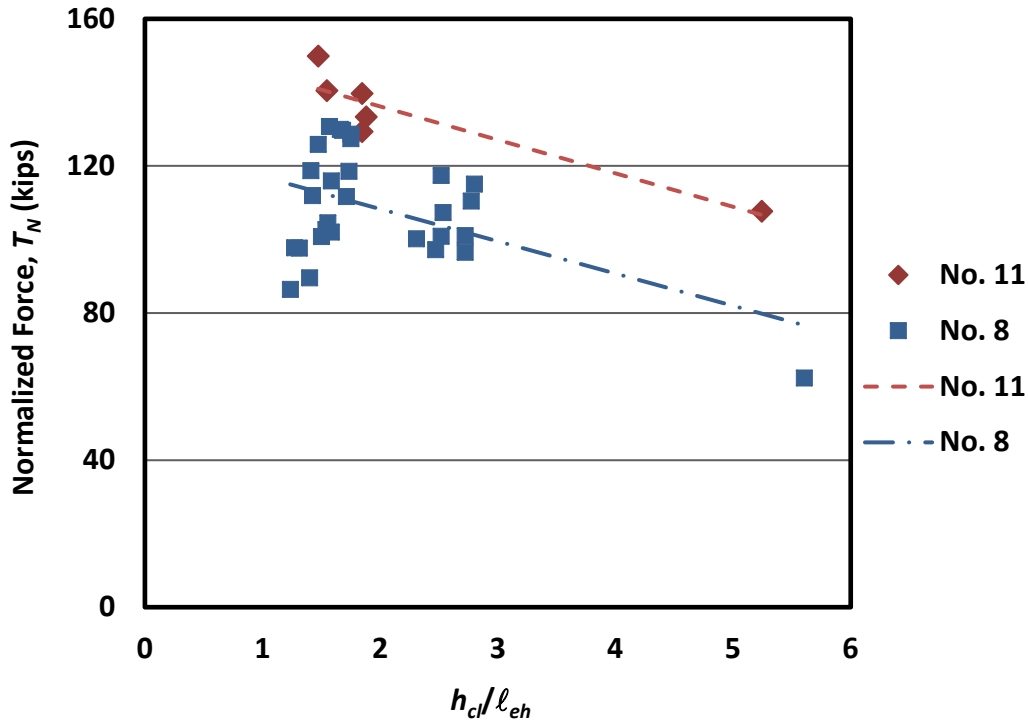


Figure 3.9 Bar force at failure normalized with respect to a concrete compressive strength of 5,000 psi, and an embedment length of 12.75 in., T_N , versus the ratio h_{cl}/ℓ_{eh} (defined in Figure 3.8). Tests with No. 8 headed bars are from Ghimire et al. (2018), and tests with No. 11 headed bars are from the current study

As shown in Figure 3.9, the specimens containing No. 11 headed bars showed a slight drop in anchorage strength T_N as the ratio h_{cl}/ℓ_{eh} increased from 1.47 to 1.88 and a much greater drop as the ratio h_{cl}/ℓ_{eh} increased to 5.24. This observation matches that of Ghimire et al. (2018) for specimens containing No. 8 headed bars. Ghimire et al. (2018) concluded that the anchorage strength of headed bars did not significantly change as the value of the ratio h_{cl}/ℓ_{eh} increased from 1.24 to 2.79, while T_N decreased when the ratio h_{cl}/ℓ_{eh} increased to 5.6, as shown in Figure 3.9. In light of the plot shown in Figure 3.9, it may be appropriate to observe Ghimire et al. also had a slight drop in T_N as the ratio h_{cl}/ℓ_{eh} increased from 1.24 to 2.79. The anchorage strength of specimens with a ratio h_{cl}/ℓ_{eh} of 5.24 and 5.6 are only about 80% and 60% of the average anchorage strength of the other specimens, respectively. Since there is only one specimen with a ratio h_{cl}/ℓ_{eh} of 5.24 and 5.6 for tests with No. 11 and No. 8 headed bars, respectively, the statistical significance of these differences cannot be evaluated. The ratios of h_{cl}/ℓ_{eh} of these specimens, however, are

much higher than the maximum ratio of 1.5 suggested in Commentary Section R25.4.4.2 of ACI 318-19, which explains the reduction of the anchorage strength of the headed bars.

3.1.3 Effect of Concrete Compressive Strength

The effect of concrete compressive strength on the anchorage strength of headed bars anchored in a simulated column-foundation joint is presented in this section. Ten tests were conducted on headed bars anchored in slab specimens to investigate the effect of concrete compressive strength on the anchorage strength. Only specimens with $A_{brg} \leq 9.5A_b$ are included in this evaluation. Of the ten tests, six included two No. 11 headed bars spaced at $8.2d_b$ (widely-spaced) and loaded simultaneously, and four involved two No. 14 headed bars spaced at $6.8d_b$ (closely-spaced) and loaded simultaneously. “Widely-spaced” and “closely-spaced” are defined in accordance with Shao et al. (2016) for beam-column joint specimens as bars with a center-to-center bar spacing greater than or equal to $8d_b$ and with a center-to-center bar spacing less than $8d_b$, respectively. The concrete compressive strength ranged from 5,110 to 14,470 psi. The test results for the specimens used in this analysis are presented in Table 3.3. Since the embedment length of headed bars varied, the average peak load on the headed bar at failure (total peak load applied on the specimen divided by the number of headed bars loaded simultaneously) is normalized with respect to an embedment length of 12.75 in. using Eq. (3.2).

$$T_N = T \left(\frac{12.75 \text{ in.}}{\ell_{eh}} \right)^{1.03} \quad (3.2)$$

where T is the average peak load on the headed bar at failure (kips), and ℓ_{eh} is the measured embedment length of the headed bar (in.). The power 1.03 in Eq. (3.2) is that for ℓ_{eh} in the descriptive equations developed by Shao et al. (2016), Eq. (1.7) and (1.8).

The slab specimen properties, including the measured embedment length ℓ_{eh} , the measured concrete compressive strength f_{cm} , the distance between the center of the headed bars and the inner face of the nearest support reaction h_{cl} , the ratio h_{cl}/ℓ_{eh} , the net bearing area of the head A_{brg} divided by the headed bar area A_b , the average peak load on the headed bar at failure T , and the normalized average peak load on the headed bar at failure T_N , are presented in Table 3.3. T_N is plotted versus the concrete compressive strength in Figure 3.10.

Table 3.3 Test results for specimens containing No. 11 and No. 14 headed bars tested with different concrete strength

Specimens			ℓ_{eh}	f_{cm}	h_{cl}	$\frac{h_{cl}}{\ell_{eh}}$	$\frac{A_{brg}}{A_b}$	$T^{[1]}$	$T_N^{[2]}$
SN	Description	Head	(in.)	(psi)	(in.)			(kips)	(kip)
6	(2@8.2)11-5-S5.5-7#11-0-12.75	A1	13.50	5370	19.7	1.46	5.5	99.5	93.8
		A2	13.50		19.7	1.46	5.5		
	(2@8.2)11-5-S5.5-7#11-0-12.75	B1	14.06		19.7	1.40	5.5	106.5	96.4
		B2	14.06		19.7	1.40	5.5		
7	(2@8.2)11-5-S5.5-7#11-0-12.75	A1	13.25	5110	19.7	1.49	5.5	88.1	84.7
		A2	13.25		19.7	1.49	5.5		
	(2@8.2)11-5-S5.5-7#11-0-12.75	B1	13.31		19.7	1.48	5.5	87.7	83.8
		B2	13.31		19.7	1.48	5.5		
10	(2@8.2)11-15-S9.2-7#11-0-12.75	A1	12.69	14470	19.7	1.55	9.2	124.8	125.4
		A2	12.68		19.7	1.55	9.2		
	(2@8.2)11-15-S9.2-7#11-0-12.75	B1	12.75		19.7	1.55	9.2	131.0	131.0
		B2	12.75		19.7	1.55	9.2		
12	(2@6.8)14-5-B4.2-7#11-0-12.75	A1	13.00	6040	19.8	1.53	4.2	119.5	117.1
		A2	13.00		19.8	1.53	4.2		
	(2@6.8)14-5-B4.2-7#11-0-12.75	B1	13.13	6180	19.8	1.51	4.2	129.5	125.7
		B2	13.13		19.8	1.51	4.2		
14	(2@6.8)14-15-B4.2-7#11-0-12.75	A1	13.13	14030	19.8	1.51	4.2	173.0	167.9
		A2	13.13		19.8	1.51	4.2		
	(2@6.8)14-15-B4.2-7#11-0-12.75	B1	13.13	14050	19.8	1.51	4.2	161.9	157.1
		B2	13.13		19.8	1.51	4.2		

^[1] Average peak load (total peak load applied on the specimen divided by the number of headed bars being developed)

^[2] Normalized force on the headed bar at failure using Eq. (3.2)

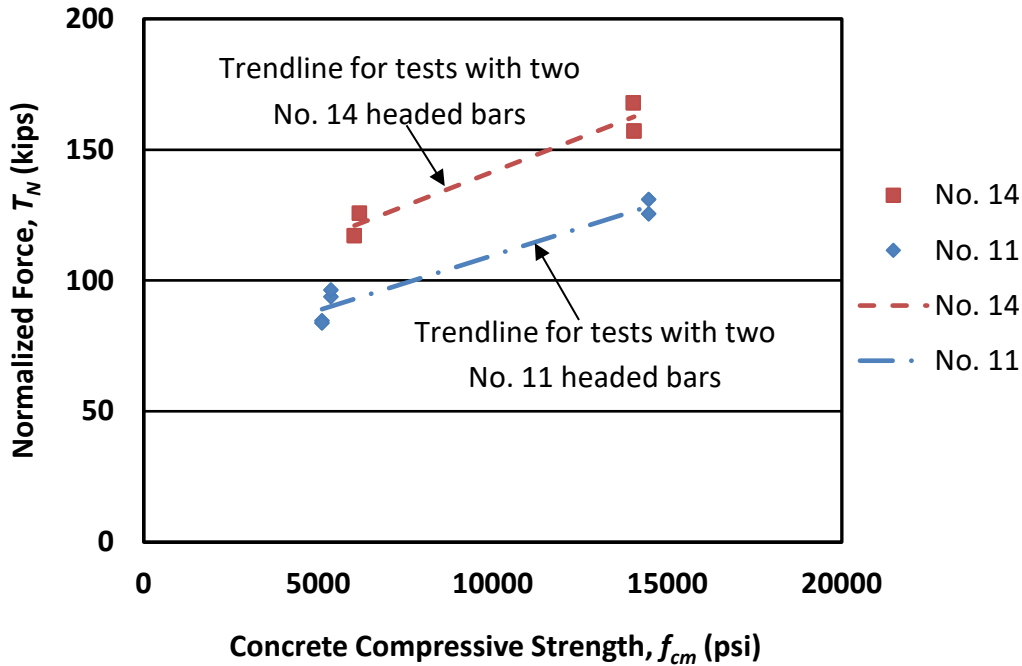


Figure 3.10 Normalized bar force at failure T_N [using Eq. (3.2)] versus concrete compressive strength f_{cm} for specimens presented in Table 3.3.

Figure 3.10 shows that, on average, the anchorage strength of No. 11 headed bars increased about 42% (from 90 to 128 kips) as the concrete compressive strength increased from 5,240 to 14,470 psi, while the anchorage strength of No. 14 headed bars increased about 34% (from 122 to 163 kips) as the concrete compressive strength increased from 6,110 to 14,040 psi. Student's t-test shows that these differences are statistically significant, with $p = 0.0016$ for No. 11 headed bars and $p = 0.0269$ for No. 14 headed bars.

Figure 3.11 compares the ratio T/T_h to the concrete compressive strength f_{cm} for all tests that contained two headed bars load simultaneously with parallel tie reinforcement within the joint region from the current study. T is the average peak load on the headed bar at failure, and T_h is the calculated anchorage strength based on the descriptive equations developed by Shao et al. (2016), Eq. (1.7) and (1.8).

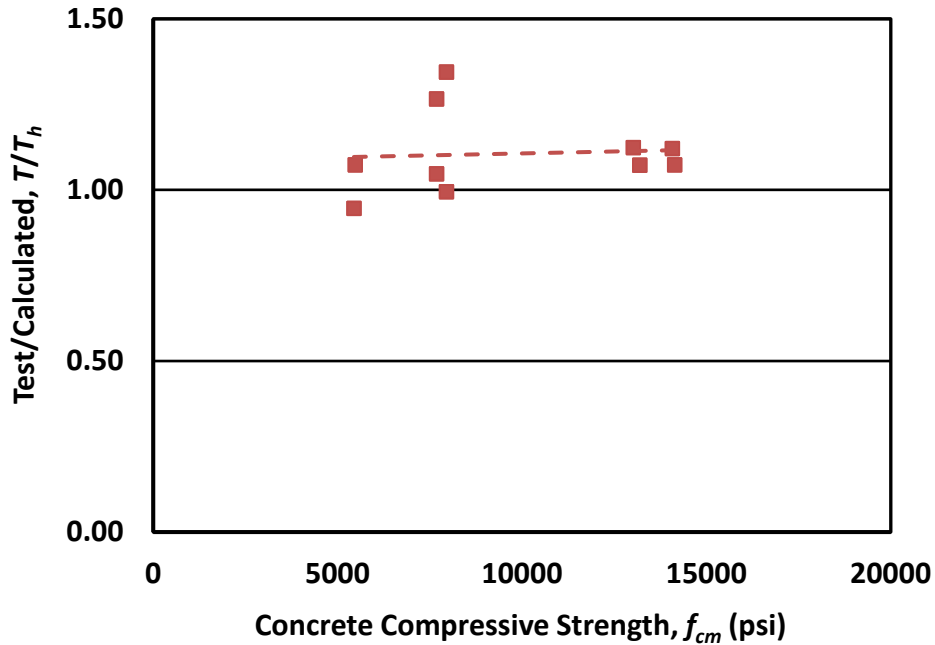


Figure 3.11 Ratio of test-to-calculated failure load T/T_h versus concrete compressive strength f_{cm} for all the current study tests that contained two headed bars load simultaneously with the presence of the parallel tie reinforcement within the joint region presented in Table 3.1.

The trend line in Figure 3.11 is almost horizontal, indicating that the effect of concrete compressive strength is accurately captured by the 0.24 power in the descriptive equation, Eq.(1.8). The values of T/T_h range from 0.95 to 1.34, with a coefficient of variation of 0.105. The maximum, minimum, mean, standard deviation (STD), and coefficients of variation (COV) of T/T_h for the results shown in Figure 3.11 are presented in Table 3.4.

Table 3.4 Statistical parameters of T/T_h values for tests containing two headed bars with parallel tie reinforcement within the joint region

Number of tests	All (10)	No. 11 (6)	No. 14 (4)
Max	1.34	1.34	1.12
Min	0.95	0.99	0.95
Mean	1.11	1.14	1.05
STD	0.116	0.130	0.070
COV	0.105	0.114	0.067

3.1.4 Effect of Grouped Anchors and Headed Bar Spacing

The effects of grouped anchors–headed bars placed closely or widely and loaded simultaneously–and headed bar spacing on the anchorage strength of a headed bar embedded in simulated column–foundation joints are discussed in this section. Thirteen tests were conducted on individual and grouped headed bars anchored in slab specimens to investigate the effect of grouped anchors and the spacing between the headed bars on the anchorage strength (Table 3.5). Of the thirteen tests, five included only one headed bar, two included two headed bars loaded simultaneously with a center-to-center spacing of $3.2d_b$ (closely-spaced), and six included two headed bars with a center-to-center spacing of $8.2d_b$ (widely-spaced). The slab specimen properties, including the measured embedment length ℓ_{eh} , the measured concrete compressive strength f_{cm} , the distance between the center of the headed bars and the inner face of the nearest support reaction h_{cl} , the ratio h_{cl}/ℓ_{eh} , the net bearing area of the head A_{brg} divided by the headed bar area A_b , the average peak load T (total peak load applied on the specimen divided by the number of headed bars loaded simultaneously), and the normalized anchorage strength of headed bars T_N , which is calculated using Eq. (3.1), are presented in Table 3.5.

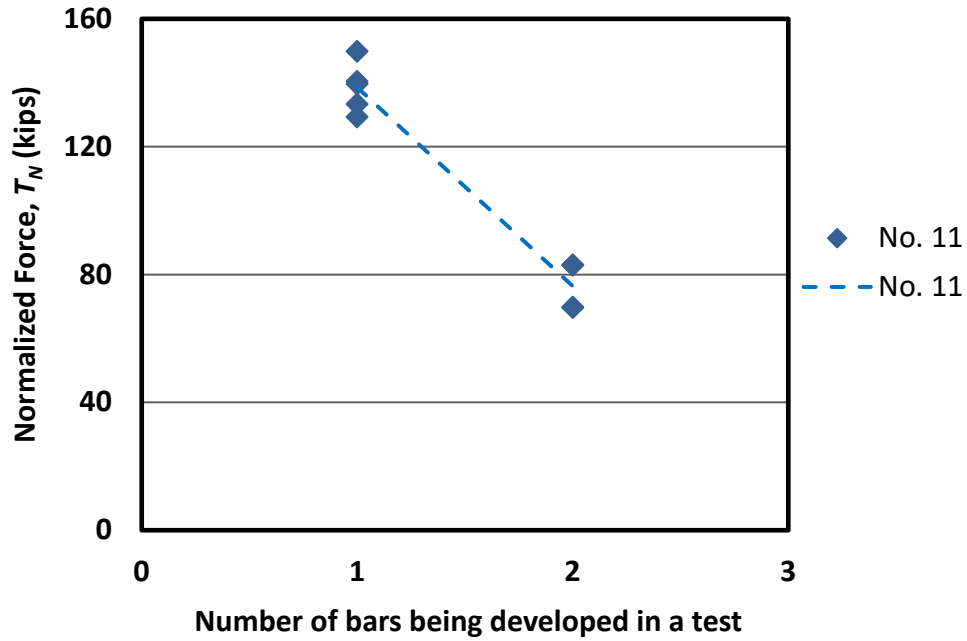
For comparison between the anchorage strength of headed bars tested individually and in a group of headed bars loaded simultaneously, the anchorage strength of headed bars in the slab specimens, normalized with respect to the concrete compressive strength f_{cm} and the embedment length of the headed bar ℓ_{eh} using Eq. (3.1), is plotted versus the number of headed bars being developed in a test in Figures 3.12a (closely-spaced bars) and 3.12b (widely-spaced bars). Since Ghimire et al. (2018) found that the anchorage strength of headed bars did not significantly change with the presence of reinforcement oriented perpendicular to the headed bars, Figures 3.12a and 3.12b include specimens with reinforcement placed perpendicular to the headed bars. The figures include specimens containing headed bars with a net bearing area of the head (A_{brg}) ranging from 3.8 to $9.5A_b$ based on the observation by Shao et al. (2016) that headed bars with bearing area A_{brg} between 3.8 to $9.5A_b$ had similar anchorage strengths. The figures include specimens with h_{cl}/ℓ_{eh} 1.24 to 2.79 based on the observation, discussed in relation to Fig 3.9 showing results presented by Ghimire et al. (2018), that there was drop in T_N as h_{cl}/ℓ_{eh} increased from 1.24 to 2.79 , but that the drop was small.

Table 3.5 Test results for specimens containing individual and two closely-spaced or widely-spaced grouped headed bars

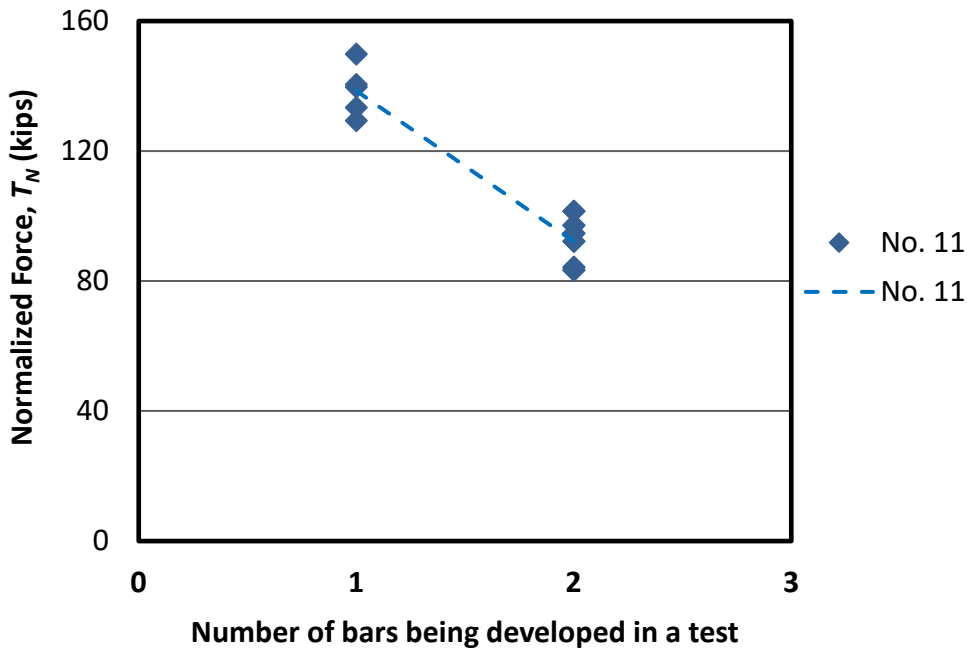
Specimens			l_{eh}	f_{cm}	h_{cl}	$\frac{h_{cl}}{l_{eh}}$	$\frac{A_{brg}}{A_b}$	$T^{[1]}$	$T_N^{[2]}$
SN	Description	Head	(in.)	(psi)	(in.)			(kips)	(kips)
1	11-5-S5.5-6#6-0-12.75	A	13.38	5060	24.7	1.85	5.5	147.1	139.7
	11-5-S5.5-6#6-0-12.75	B	13.13		24.7	1.88	5.5	137.8	133.4
	11-5-S5.5-6#6-0-12.75	C	13.38		24.7	1.85	5.5	136.3	129.3
2	11-5-S5.5-10#6-0-12.75	A	13.38	5490	19.7	1.47	5.5	161.0	149.9
	11-5-S5.5-10#6-0-12.75	B	12.75		19.7	1.55	5.5	143.7	140.5
4	(2@3.2)11-5-S5.5-6#11-0-12.75	A1	13.50	5550	19.7	1.46	5.5	90.3	82.9
		A2	13.50		19.7	1.46	5.5		
	(2@3.2)11-5-S5.5-6#11-0-12.75	B1	13.38	6190	19.7	1.47	5.5	77.2	69.7
		B2	13.38		19.7	1.47	5.5		
6	(2@8.2)11-5-S5.5-7#11-0-12.75	A1	13.50	5370	19.7	1.46	5.5	99.5	92.2
		A2	13.50		19.7	1.46	5.5		
	(2@8.2)11-5-S5.5-7#11-0-12.75	B1	14.06		19.7	1.40	5.5	106.5	94.7
		B2	14.06		19.7	1.40	5.5		
7	(2@8.2)11-5-S5.5-7#11-0-12.75	A1	13.25	5110	19.7	1.49	5.5	88.1	84.2
		A2	13.25		19.7	1.49	5.5		
	(2@8.2)11-5-S5.5-7#11-0-12.75	B1	13.31		19.7	1.48	5.5	87.7	83.4
		B2	13.31		19.7	1.48	5.5		
10	(2@8.2)11-15-S9.2-7#11-0-12.75	A1	12.69	14470	19.7	1.55	9.2	124.8	97.2
		A2	12.69		19.7	1.55	9.2		
	(2@8.2)11-15-S9.2-7#11-0-12.75	B1	12.75		19.7	1.55	9.2	131.0	101.5
		B2	12.75		19.7	1.55	9.2		

^[1] Average peak load (total peak load applied on the specimen divided by the number of headed bars being developed)

^[2] Normalized force on the headed bar at failure using Eq. (3.1)



(a)



(b)

Figure 3.12 Bar force at failure normalized with respect to a concrete compressive strength of 5,000 psi and an embedment length of 12.75 in. T_N versus the number of headed bars being developed in tests (a) with individual and closely spaced headed bars loaded simultaneously (b) with individual and widely spaced headed bars loaded simultaneously. Results for individual bars are the same in figures (a) and (b)

Based on the test results shown in Figures 3.12a and 3.12b for these tests of No. 11 bars, the average anchorage strength of headed bars loaded individually was 139 kips, compared to values of 76 and 92 kips for two headed bars loaded simultaneously when closely and widely spaced, respectively. In these cases, on average, loading two closely or widely spaced headed bars simultaneously resulted in an anchorage strength of about 55% and 66%, respectively, of the anchorage strength of headed bars tested individually. Student's t-test indicates that these differences are statistically significant, with $p = 0.0003$ and 0.000003 , respectively. The reduction in the anchorage strength of grouped headed bars is likely due to the limited amount of concrete available between the bars to resist the applied forces.

Figure 3.13 compares the normalized anchorage strengths of two headed bars as a function of the center-to-center spacing divided by the bar diameter d_b for headed bars with a net bearing area of the head A_{brg} ranging from 3.8 to $9.5A_b$ and specimens with ratios h_{cl}/ℓ_{eh} ranging from 1.24 to 2.79.

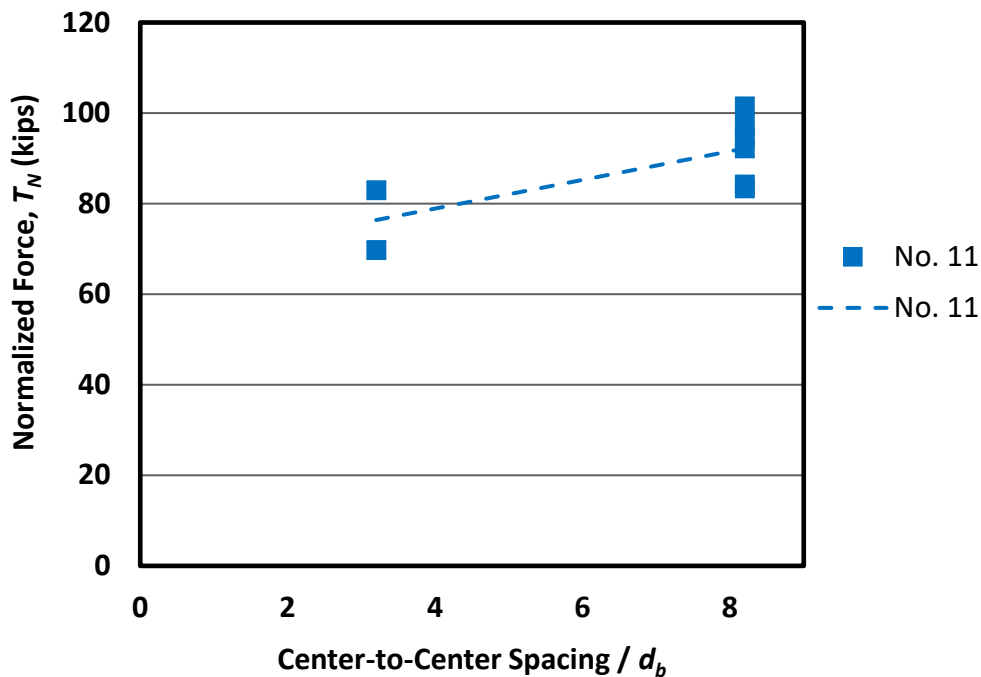


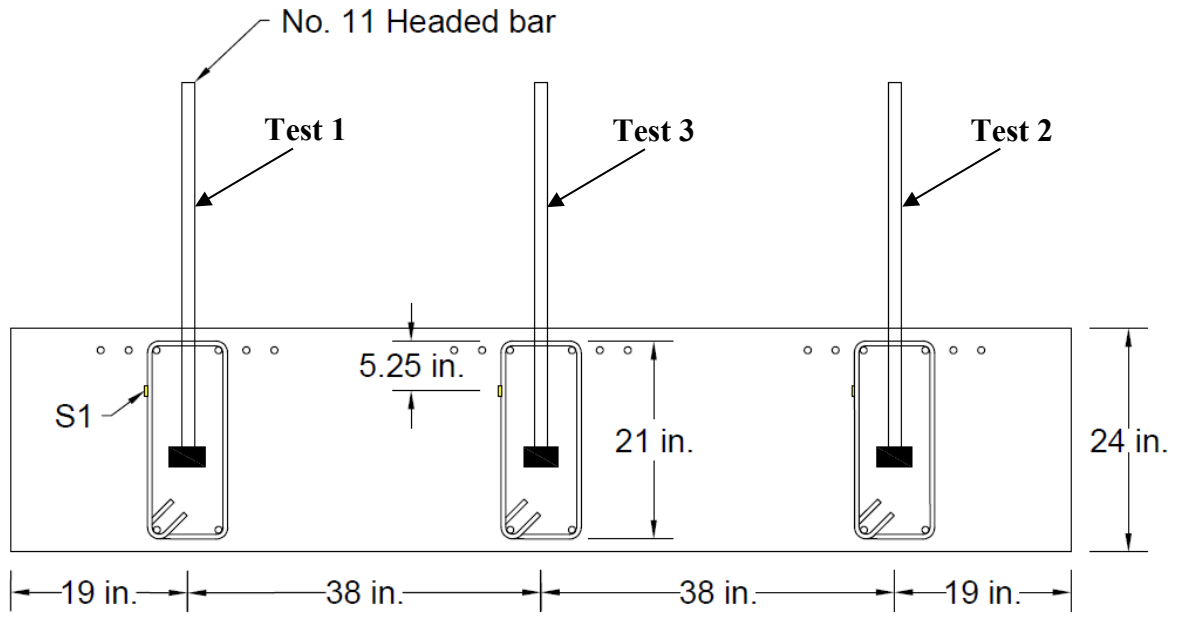
Figure 3.13 Bar force at failure normalized with respect to a concrete compressive strength of 5,000 psi and an embedment length of 12.75 in. T_N versus center-to-center spacing between headed bars with respect to the bar diameter (d_b)

For these tests, the average anchorage strength of headed bars with a center-to-center spacing of $3.2d_b$ is 76.4 kips, while the average anchorage strength of headed bars with a center-to-center spacing of $8.2d_b$ is 92.2 kips, a 21% increase. This difference is statistically significant, with $p = 0.043$. This observation indicates that headed bar spacing has an effect on anchorage strength that the ACI 318-19 Chapter 17 anchorage provisions do not account for. This observation matches the findings by Shao et al. (2016) for beam-column joints who observed that the anchorage strength of headed bars decreases with center-to-center as the center-to-center spacing decreases below $8d_b$.

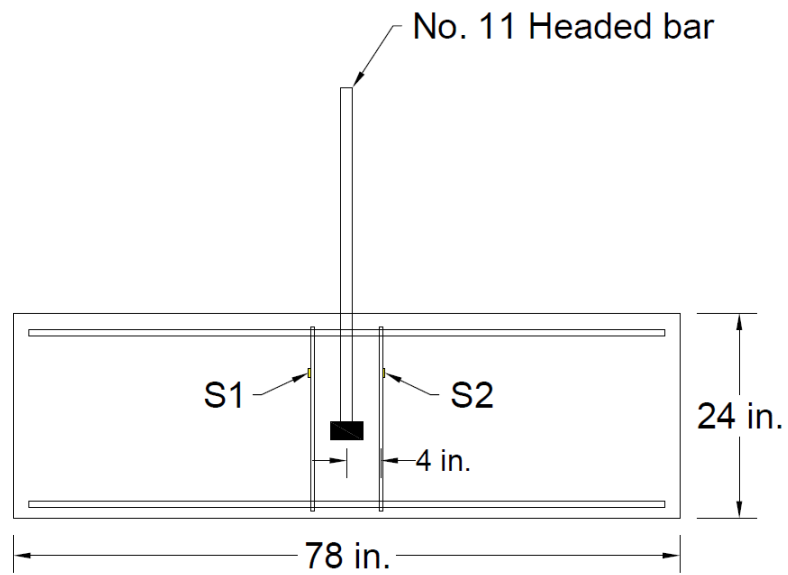
3.1.5 Effect of Parallel Tie Reinforcement

The contribution of parallel tie reinforcement—ties or hoops placed parallel to the headed bars within the joint region—to the anchorage strength of headed bars is discussed in this section. In beam-column joints, Sperry et al. (2015b) and Shao et al. (2016) found that only hoops within $8d_b$ of the top of the hooked or headed bars for No. 3 through No. 8 bars or within $10d_b$ for No. 9 through No. 11 bars were effective in increasing the anchorage strength of hooked or headed bars. To investigate the contribution of parallel tie reinforcement to the anchorage strength of headed bars anchored in simulated column-foundation joints, 26 tests were conducted on headed bars anchored in specimens with and without parallel tie reinforcement within the joint region.

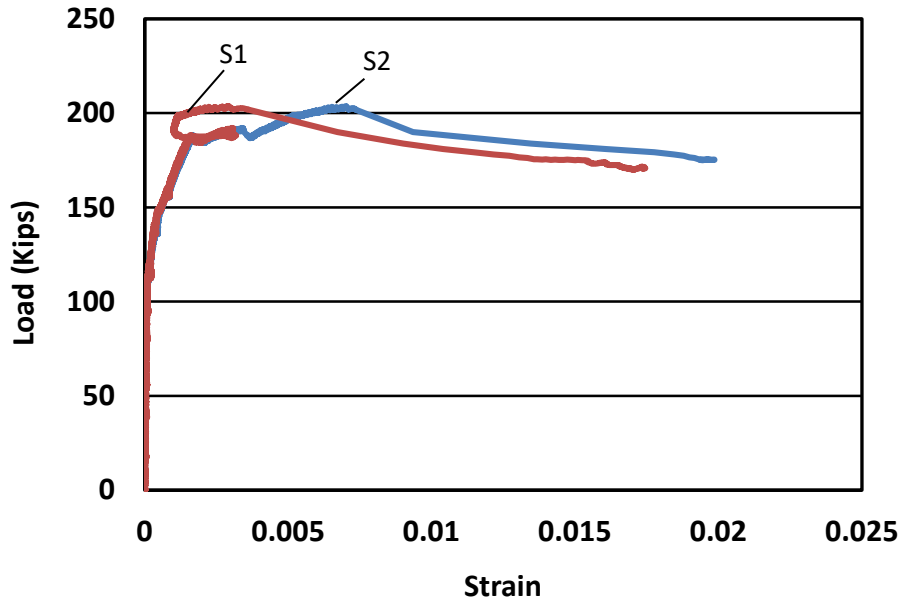
To support this investigation, described in Section 2.7, strain gages were used to measure the strain in parallel tie reinforcement (in the form of hoops) at different distances from the headed bars. One strain gauge was mounted to each hoop mounted in the top quarter of the leg, oriented parallel to the headed bars, as shown in Figures 3.14a and b for Slab Specimen 5 (11-5-S5.5-6#6-2#4-12.75), which contained three headed bars loaded individually and had No. 4 bar hoops placed within the joint region on both sides of the headed bars. Figures 3.14c, d, and e show the load-strain curves for the parallel ties in each of the three tests. A summary of the key parameters of Slab Specimen 5 is presented in Table 3.1. As shown in Figure 3.14b, one No. 4 bar hoop was placed on both sides of the headed bar spaced at $2.8d_b$ (4 in.) from the centerline of the headed bar.



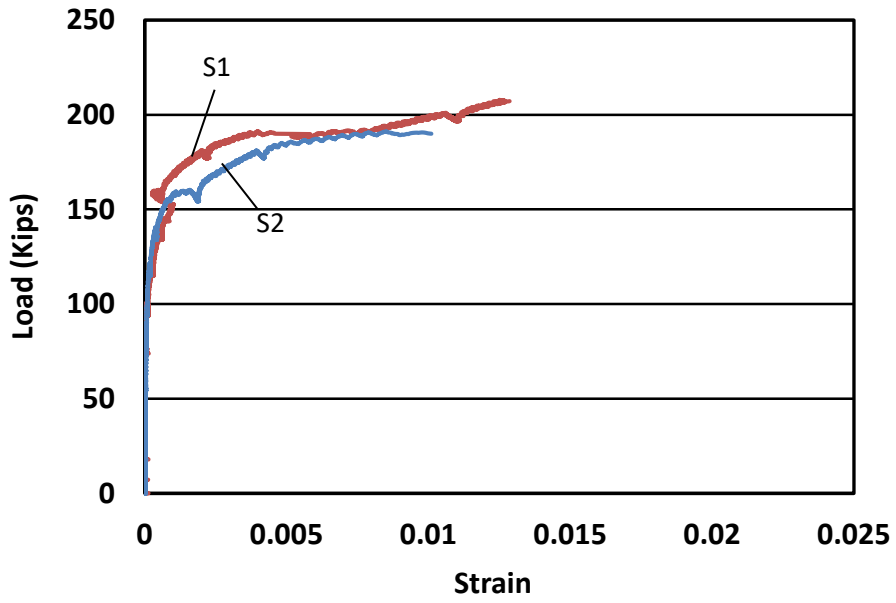
(a)



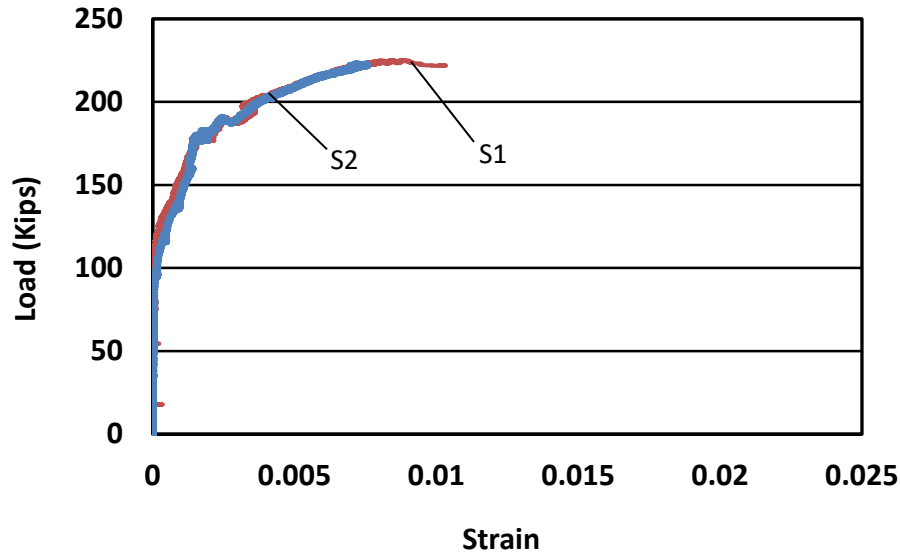
(b)



(c)



(d)



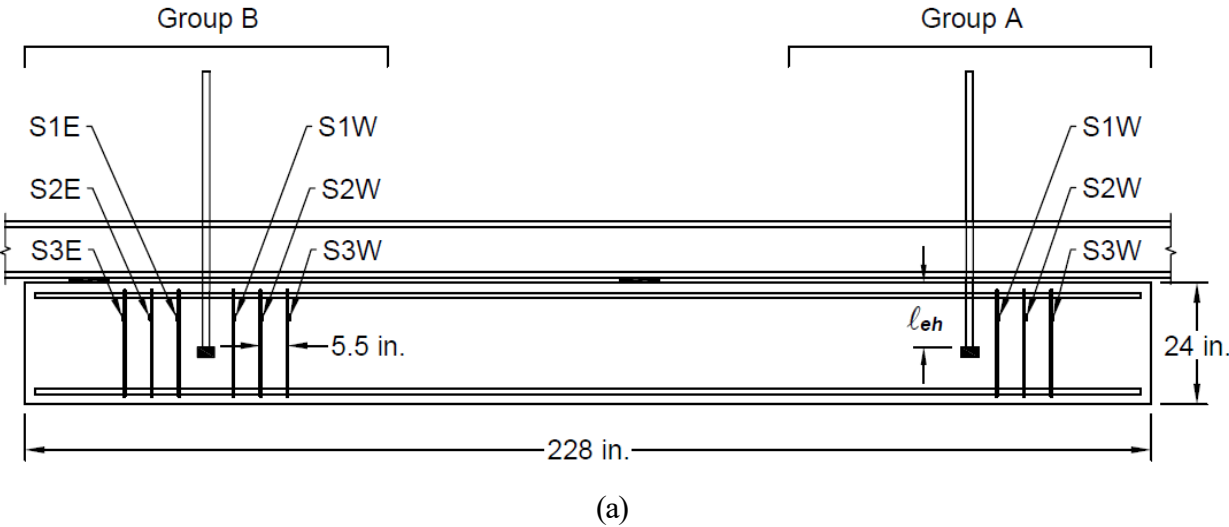
(e)

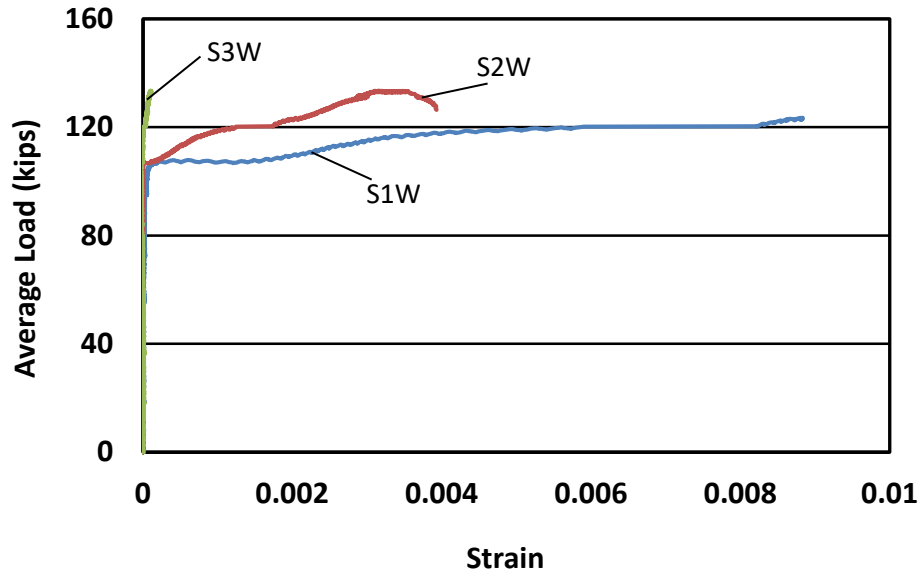
Figure 3.14 Parallel tie reinforcement for Slab Specimen 5 (11-5-S5.5-6#6-2#4-12.75) (a) front view, (b) side view, (c) load versus strain curves for Test 1, (d) load versus strain curves for Test 2, (e) load versus strain curves for Test 3

Figure 3.14c shows the load-strain curves for Test 1 of Slab Specimen 5 (11-5-S5.5-6#6-2#4-12.75). As shown in the figure, the strain in both hoops (S1 and S2) began to increase once the load reached about 120 kips (59% of the peak load) when the first crack in the concrete appeared. The strain in the hoops increased slowly at loads above 120 kips. S1 and S2 reached a strain of 0.001 at about 170 kips (83% of the peak load), and increased more rapidly at loads above 170 kips, reaching 0.003 and 0.006 for S1 and S2, respectively, at the peak load, indicating that both hoops yielded. The load-strain curve for Test 2 of Slab Specimen 5 (11-5-S5.5-6#6-2#4-12.75) is shown in Figure 3.14d. The strain in hoops began to increase at an applied load of about 110 kips (49% of the peak load) when the first crack in the concrete formed. The strain in the hoops increased slowly at loads below 150 kips (67% of the peak load), increasing more rapidly above 150 kips, reaching a strain of 0.01 for both S1 and S2 at the peak load, indicating that both hoops yielded. Figure 3.14e shows the load-strain curve for Test 3. The strain in the hoops started to increase at an applied load of 120 kips (54% of the peak load) when the first crack in the concrete formed. The strain increase for S1 and S2 continued with the applied load and reached as much as 0.007 at the peak load, again indicating that both hoops had yielded. Overall, the strain in the hoops

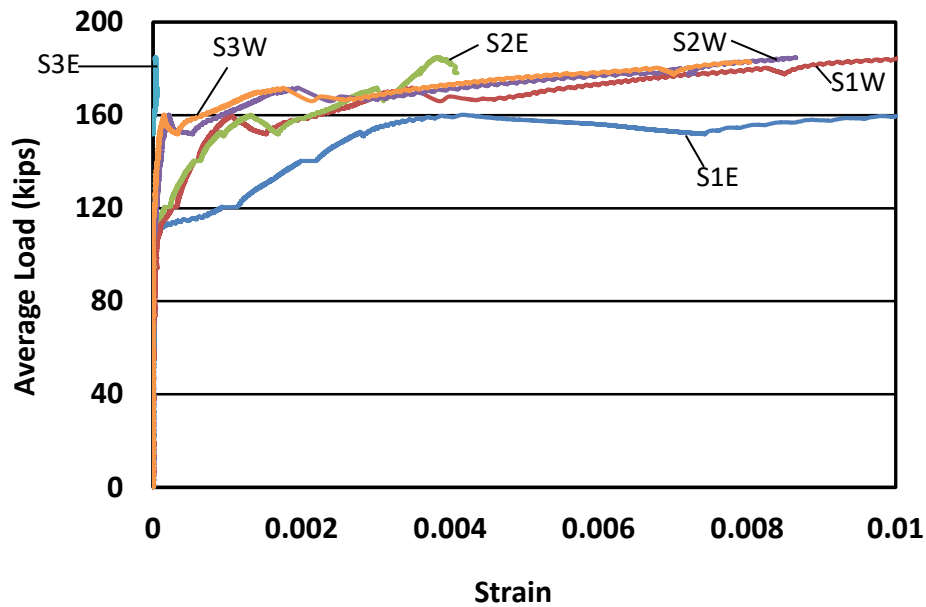
in these tests, located at a distance equal to $2.8d_b$ from the centerline of the headed bar, began to increase once the first crack formed in the concrete and exceeded the yield point before the peak load was reached.

Figure 3.15 shows the strain gauge locations and the load-strain curves for Slab Specimen 8. This specimen contained two groups of two headed bars loaded simultaneously with parallel tie reinforcement (hoops) in the joint region. Group A [(2@8.2)11-5-S9.2-7#11-3#4-12.75] contained three No. 4 bar hoops on one side of the headed bars spaced at $3.9d_b$ (5.5 in.) and Group B [(2@8.2)11-5-S9.2-7#11-6#4-12.75] included three No. 4 bar hoops on two sides of the headed bars spaced at $3.9d_b$ (5.5 in.), as shown in Figure 3.15a. The key parameters of Slab Specimen 8 are presented in Table 3.1. The strain gauge locations are shown in Figure 3.15a. Figures 3.15b and 3.14c show the average load (total load applied during the test divided by the number of headed bars being developed) versus the strain in the hoops used in Group A [(2@8.2)11-5-S9.2-7#11-3#4-12.75] and Group B [(2@8.2)11-5-S9.2-7#11-6#4-12.75], respectively.





(b)



(c)

Figure 3.15 Average load per headed bar versus strain in parallel tie reinforcement for Slab Specimen 8 (a) location of the parallel tie reinforcement and the strain gauge locations (b) load versus strain curves for hoops in test included hoops only on one side of the bars Group A [(2@8.2)11-5-S9.2-7#11-3#4-12.75] (c) load versus strain curves for hoops in the test included hoops on both sides of the bars Group B [(2@8.2)11-5-S9.2-7#11-6#4-12.75]

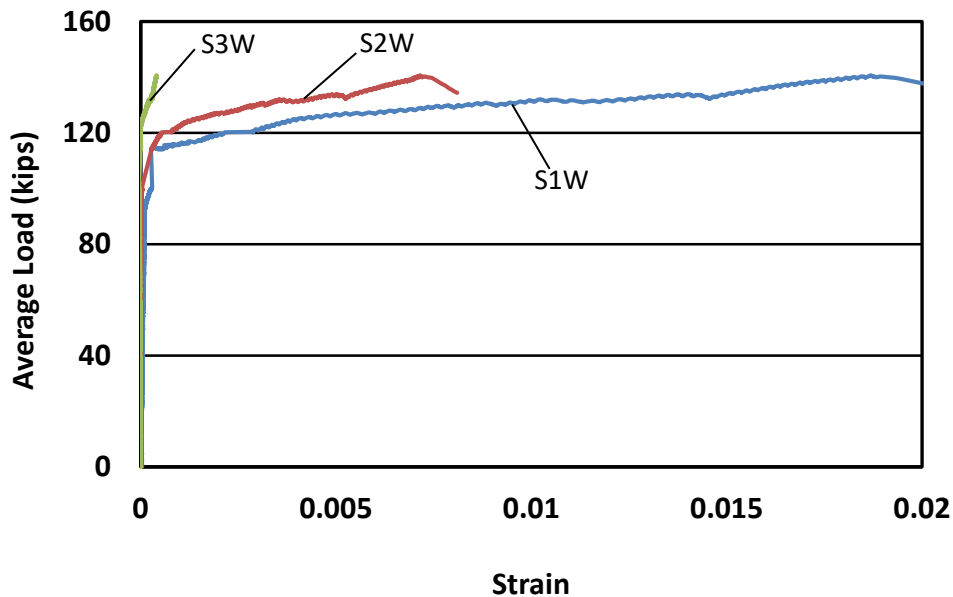
Figure 3.15b shows the hoop load-strain curves for the test conducted on the Group A headed bars anchored in Slab Specimen 8 [(2@8.2)11-5-S9.2-7#11-3#4-12.75], which had two No. 11 headed bars loaded simultaneously with three No. 4 bar hoops placed on one side of the headed bars between the nearest support reaction and the headed bars and spaced at $3.9d_b$ (5.5 in.), as shown in Figure 3.15a. The hoop closest to the headed bars (S1W), $3.9d_b$ (5.5 in.) from the centerline of the headed bars, showed an increase in the strain at lower loads than the hoops placed further from the headed bars (S2W and S3W), as shown in the figure. The strain in hoop S1W began to increase at an applied load of about 106 kips (80% of the average peak load) and exceeded the yield strain at a load of about 111 kips (83% of the average peak load), while the strain in the hoop S2W, located $7.8d_b$ (11 in.) from the centerline of the headed bars, started to increase at 82% of the average peak load and exceeded the yield strain at 98% of the peak load. Hoop S3W, located close to the nearest support reaction and $11.7d_b$ (16.5 in.) from the centerline of the headed bars, exhibited minimal strain throughout the test, reaching a strain of just 0.0001 at the peak load, demonstrating, as shown for beam-column joints tests (Sperry et al. (2015b) and Shao et al. (2016)), that the effectiveness of hoops is directly related to their location from the headed bars and the angle of the concrete crack, as shown in Figure 3.5b; the flatter the concrete crack, the greater the chance that the crack will intercept a hoop.

Figure 3.15c shows the hoop load-strain curves for the test conducted on the Group B headed bars in Slab Specimen 8 [(2@8.2)11-5-S9.2-7#11-6#4-12.75]. This test included two No. 11 headed bars loaded simultaneously with No. 4 bar hoops placed on both sides of the headed bars and spaced at $3.9d_b$ (5.5 in.). As shown in Figure 3.15c, the load-strain curves for the hoops differ depending on the location of hoops from the headed bars. Hoops S1E, S2E, and S3E were located at $3.9d_b$ (5.5 in.), $7.8d_b$ (11 in.), and $11.7d_b$ (16.5 in.), respectively, from the centerline of the headed bars, while hoops S1W, S2W, and S3W were located on the other side of the headed bars at $3.9d_b$ (5.5 in.), $7.8d_b$ (11 in.), and $11.7d_b$ (16.5 in.), respectively, from the centerline of the headed bars. The hoops close to the headed bars (S1E, S1W, S2E, and S2W) showed increases in the strain at lower loads than the hoops placed further from the headed bars (S3W and S3E). Hoop S1E, the closest to the headed bars in the region between anchored headed bars and the nearest support reaction, exhibited an increase in strain at an applied load of about 110 kips (59% of the

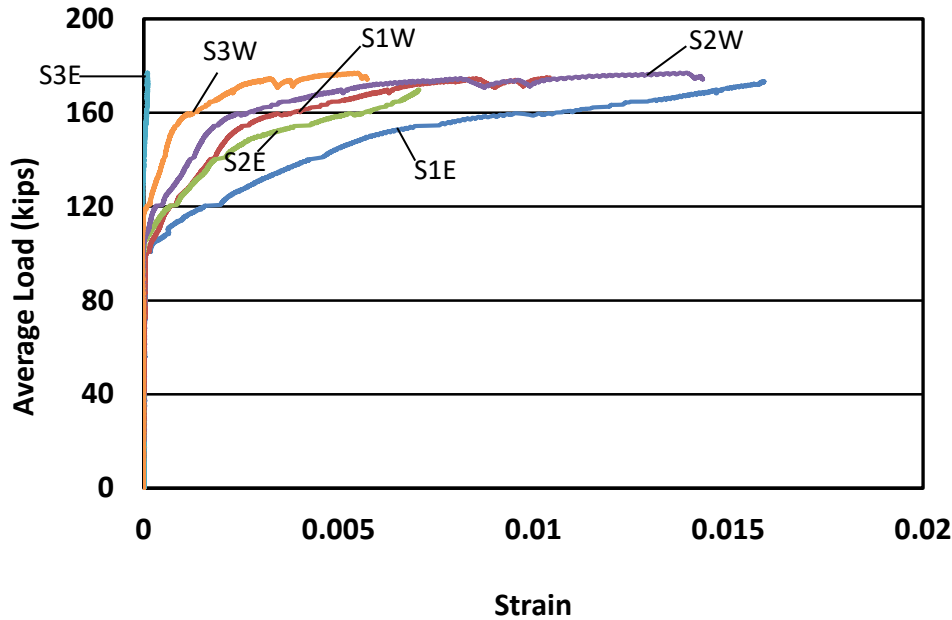
average peak load), with a steady increase in strain up to 0.004 (beyond the yield strain) at an applied load of about 160 kips (86% of the average peak load) and reached a strain of 0.01 at the peak load. The strain in hoops S1W and S2E began to increase at an applied load of about 117 kips (63% of the average peak load), and both hoops reached a strain value of 0.001 at a load of 160 kips (86% of the average peak load). The strain increase for S1W and S2E continued with the applied load, and reached strains of 0.01 and 0.004, respectively, at the peak load, indicating that both hoops had yielded. The strain in hoops S2W and S3W started to increase at an applied load of about 140 kips (76% of the average peak load) and reached a value of 0.0008 at an applied load of about 160 kips (86% of the average peak load). The strain in hoops S2W and S3W continued increasing with applied load and reached a strain of 0.006 at the peak load, indicating that both hoops (S2W and S3W) yielded. Hoop S3E, located close to the nearest support reaction, exhibited minimal strain throughout the test, reaching a strain of just 0.00004 at the peak load. These observations indicate that hoops placed close to the headed bars are more effective in improving the anchorage strength of headed bars than those located further from the bars. Moreover, in this test conducted, two of the three hoops located between the headed bars and the nearest support reaction yielded, while all three hoops located on the other side of the headed bars between the headed bars and the furthest support reaction yielded. These results support the observation for the Group A test that the effectiveness of hoops is directly related to their distance from the headed bars *and* the angle of the concrete failure cracks. The effect of concrete crack angle on the effectiveness of hoops is shown in Figure 3.6b.

Figure 3.16 shows the load-strain curves for Slab Specimen 9. This specimen contained two groups of two headed bars loaded simultaneously with the presence of No. 4 bar hoops in the joint region. Group A [(2@8.2)11-5-S9.2-7#11-3#4-12.75] contained three No. 4 bar hoops spaced at $3.9d_b$ (5.5 in.) on one side of the headed bars while Group B [(2@8.2)11-5-S9.2-7#11-6#4-12.75] contained three No. 4 bar hoops spaced at $3.9d_b$ (5.5 in.) on both sides of the headed bars. The location of the hoops and the strain gauges are the same as shown in Figure 3.15a for Slab Specimen 8. The key parameters of Slab Specimen 9 are presented in Table 3.1. Figures 3.16a and 3.16b show the average load versus strain in hoops used in Group A [(2@8.2)11-5-S9.2-7#11-3#4-12.75] and Group B [(2@8.2)11-5-S9.2-7#11-6#4-12.75], respectively.

Figure 3.16a shows the load-strain curves for the test conducted on the first group of headed bars anchored in Slab Specimen 9 Group A [(2@8.2)11-5-S9.2-7#11-3#4-12.75]. This test contained two No. 11 headed bars loaded simultaneously with three No. 4 bar hoops spaced at $3.9d_b$ (5.5 in.) on one side of the headed bars between the nearest support reaction and the headed bars, as shown in Figure 3.15a for Slab Specimen 8. The strain in hoop S1W, located $3.9d_b$ (5.5 in.) from the centerline of the headed bars, began to increase at an applied load of about 92 kips (66% of the average peak load) and exceeded the yield strain at a load of 120 kips (86% of the average peak load), while the strain in hoop S2W, located $7.8d_b$ (11 in.) from the centerline of the headed bars, started to increase at a load of about 114 kips (81% of the average peak load) and passed the yield strain at a load of about 130 kips (93% of the average peak load). Hoop S3W, located close to the nearest support reaction and $11.7d_b$ (16.5 in.) from the centerline of the headed bars, exhibited minimal strain throughout the test, reaching a strain of just 0.0003 at the peak load. These findings again support the earlier observations that the effectiveness of hoops depends on where they are placed with respect to headed bars and the direction of concrete cracks, as illustrated in figure 3.5b.



(a)



(b)

Figure 3.16 Average load per headed bar versus strain in parallel tie reinforcement for Slab Specimen 9 (a) load versus strain curves for hoops in test included hoops only on one side of the bars Group A [(2@8.2)11-5-S9.2-7#11-3#4-12.75] (b) load versus strain curves for hoops in the test included hoops on both sides of the bars Group B [(2@8.2)11-5-S9.2-7#11-6#4-12.75]

Figure 3.16b shows the load-strain curves for the test conducted on the second group of headed bars anchored in Slab Specimen 9 [(2@8.2)11-5-S9.2-7#11-6#4-12.75]. This test contained two No. 11 headed bars loaded simultaneously with three No. 4 bar hoops spaced at $3.9d_b$ (5.5 in.) and placed on both sides of the headed bars. As shown in Figure 3.16b, the load-strain curves for the hoops are a function of the hoop locations from the headed bars. The strain in hoop S1W, located $3.9d_b$ (5.5 in.) from the centerline of the headed bars, exhibited an increase at a load of 100 kips (56% of the average peak load) and passed the yield strain at a load of 152 kips (86% of the average peak load), while hoop S2W, located $7.8d_b$ (11 in.) from the centerline of the headed bars, showed an increase in strain at a load of 110 kips and exceeded the yield strain at a load of 160 kips (91% of the average peak load). The strain in hoop S3W, located $11.7d_b$ (16.5 in.) from the centerline of the headed bars, began to increase at a load of 120 kips (68% of the average peak load) and reached the yield strain at 170 kips (96% of the peak load). The strain in hoop S1E, located $3.9d_b$ (5.5 in.) from the centerline of the headed bars, began to increase at a load of 100 kips (56% of the average peak load) and passed the yield strain at a load of 125 kips (70% of the

average peak load), while hoop S2E, located $7.8d_b$ (11 in.) from the centerline of the headed bars, exhibited an increase in strain at a load of 107 kips (60% of the average peak load) and exceeded the yield strain at a load of 144 kips (81% of the average peak load). Hoop S3E, the furthest from the headed bars at $11.7d_b$ (16.5 in.) from the centerline of the headed bars and located close to the nearest support reaction, exhibited minimal strain increase throughout the test, reaching a strain of just 0.0001 at the peak load. Once again, these findings suggest that the effectiveness of hoops is directly proportional to their distance from the headed bars and the angle of the concrete cracks. The illustration in Figure 3.6b supports these conclusions.

A summary of test results of the 26 tests with No. 11 and No. 14 headed bars is given in Table 3.1 and repeated in Table 3.6. The specimen properties, including the measured embedment length ℓ_{eh} , the measured concrete compressive strength f_{cm} , h_{cl} , the ratio h_{cl}/ℓ_{eh} , the net bearing area of the head A_{brg} divided by the headed bar area A_b , the average peak load T (the total peak load applied on the specimen divided by the number of headed bars loaded simultaneously), and the normalized anchorage strength of headed bars T_N , which is calculated using Eq. (3.1), are presented in Table 3.6. Based on the strain gauge results, the hoops located within the region of $8d_b$ from the centerline of the headed bars experienced a significant increase in strain at failure. In contrast, the hoops located outside this region ($8d_b$) on the side of the headed bars between the nearest support reaction and the headed bars did not yield, but on the other side, between the furthest support reaction and the headed bars, they did yield because the concrete crack has a flatter angle and thus intercepted the hoop, as described in Section 3.1.1. For comparison, the normalized anchorage strengths of headed bars at failure T_N based on Eq. (3.1) are plotted versus A_{tl}/A_{hs} in Figure 3.17, where A_{tl} is the total cross-sectional area of parallel tie reinforcement within a $10d_b$ radial distance from the centerline of the headed bars (in.²) and A_{hs} is the total cross-sectional area of the headed bars being developed (in.²). As described earlier, these specimens had $A_{brg} \leq 9.5A_b$ and h_{cl}/ℓ_{eh} ranging from 1.46 to 1.92. As described in Section 2.2, the slab specimens contained flexural reinforcement in the vicinity of the head.

Table 3.6 Test results for specimens containing No. 11 and No. 14 headed bars with and without parallel tie reinforcement

Specimens			ℓ_{eh} (in.)	f_{cm} (psi)	h_{cl} (in.)	$\frac{h_{cl}}{\ell_{eh}}$	$\frac{A_{brg}}{A_b}$	$\frac{A_{tt}}{A_{hs}}$	$T^{[1]}$ (kips)	$T_N^{[2]}$ (kip)
SN	Description	Head								
1	11-5-S5.5-6#6-0-12.75	A	13.38	5060	24.70	1.85	5.5	0.00	147.1	139.7
	11-5-S5.5-6#6-0-12.75	B	13.13		24.70	1.88	5.5	0.00	137.8	133.4
	11-5-S5.5-6#6-0-12.75	C	13.38		24.70	1.85	5.5	0.00	136.3	129.3
5	11-5-S5.5-6#6-2#4-12.75	A	13.00	5810	24.70	1.90	5.5	0.51	203.7	192.6
	11-5-S5.5-6#6-2#4-12.75	B	12.88		24.70	1.92	5.5	0.51	220.9	210.9
	11-5-S5.5-6#6-2#4-12.75	C	13.13		24.70	1.88	5.5	0.51	225.2	210.8
6	(2@8.2)11-5-S5.5-7#11-0-12.75	A1	13.50	5370	19.70	1.46	5.5	0.00	99.5	92.2
		A2	13.50		19.70	1.46	5.5	0.00		
	(2@8.2)11-5-S5.5-7#11-0-12.75	B1	14.06		19.70	1.40	5.5	0.00	106.5	94.7
		B2	14.06		19.70	1.40	5.5	0.00		
7	(2@8.2)11-5-S5.5-7#11-0-12.75	A1	13.25	5110	19.70	1.49	5.5	0.00	88.1	84.2
		A2	13.25		19.70	1.49	5.5	0.00		
	(2@8.2)11-5-S5.5-7#11-0-12.75	B1	13.31		19.70	1.48	5.5	0.00	87.7	83.4
		B2	13.31		19.70	1.48	5.5	0.00		
8	(2@8.2)11-5-S9.2-7#11-3#4-12.75	A1	13.13	7950	19.70	1.50	9.2	0.26	133.5	115.9
		A2	13.13		19.70	1.50	9.2	0.26		
	(2@8.2)11-5-S9.2-7#11-6#4-12.75	B1	13.00		19.70	1.52	9.2	0.51	185.0	162.2
		B2	13.00		19.70	1.52	9.2	0.51		
9	(2@8.2)11-5-S9.2-7#11-3#4-12.75	A1	13.25	7680	19.70	1.49	9.2	0.26	140.7	121.9
		A2	13.25		19.70	1.49	9.2	0.26		
	(2@8.2)11-5-S9.2-7#11-6#4-12.75	B1	13.38		19.70	1.47	9.2	0.51	177.1	152.1
		B2	13.38		19.70	1.47	9.2	0.51		
10	(2@8.2)11-15-S9.2-7#11-0-12.75	A1	12.69	14470	19.70	1.55	9.2	0.00	124.8	97.2
		A2	12.69		19.70	1.55	9.2	0.00		
	(2@8.2)11-15-S9.2-7#11-0-12.75	B1	12.75		19.70	1.55	9.2	0.00	131.0	101.5
		B2	12.75		19.70	1.55	9.2	0.00		
11	(2@8.2)11-15-S9.2-7#11-3#4-12.75	A1	12.75	14140	19.70	1.55	9.2	0.26	157.3	122.5
		A2	12.75		19.70	1.55	9.2	0.26		
	(2@8.2)11-15-S9.2-7#11-6#4-12.75	B1	12.63	14080	19.70	1.56	9.2	0.51	167.8	132.2
		B2	12.63		19.70	1.56	9.2	0.51		
12	(2@6.8)14-5-B4.2-7#11-0-12.75	A1	13.00	6040	19.85	1.53	4.2	0.00	119.5	111.9
		A2	13.00		19.85	1.53	4.2	0.00		
	(2@6.8)14-5-B4.2-7#11-0-12.75	B1	13.13	6180	19.85	1.51	4.2	0.00	129.5	119.5
		B2	13.13		19.85	1.51	4.2	0.00		

^[1] Average peak load (total peak load applied on the specimen divided by the number of headed bars being developed)

^[2] Normalized force on the headed bar at failure using Eq. (3.1)

Table 3.6 Cont. Test results for specimens containing No. 11 and No. 14 headed bars with and without parallel tie reinforcement

Specimens			l_{eh} (in.)	f_{cm} (psi)	h_{cl} (in.)	$\frac{h_{cl}}{l_{eh}}$	$\frac{A_{brg}}{A_b}$	$\frac{A_{tt}}{A_{hs}}$	$T^{[1]}$ (kips)	$T_N^{[2]}$ (kip)
SN	Description	Head								
13	(2@6.8)14-5-B4.2-7#11-3#4-12.75	A1	13.00	5440	19.85	1.53	4.2	0.27	137.3	131.9
		A2	13.00		19.85	1.53	4.2	0.27		
	(2@6.8)14-5-B4.2-7#11-6#4-12.75	B1	12.75	5480	19.85	1.56	4.2	0.53	160.0	156.4
		B2	12.75		19.85	1.56	4.2	0.53		
14	(2@6.8)14-15-B4.2-7#11-0-12.75	A1	13.13	14030	19.85	1.51	4.2	0.00	173.0	131.1
		A2	13.13		19.85	1.51	4.2	0.00		
	(2@6.8)14-15-B4.2-7#11-0-12.75	B1	13.13	14050	19.85	1.51	4.2	0.00	161.9	122.6
		B2	13.13		19.85	1.51	4.2	0.00		
15	(2@6.8)14-15-B4.2-7#11-3#4-12.75	A1	13.38	13190	19.85	1.48	4.2	0.27	185.1	139.6
		A2	13.38		19.85	1.48	4.2	0.27		
	(2@6.8)14-15-B4.2-7#11-6#4-12.75	B1	12.88	13020	19.85	1.54	4.2	0.53	194.4	153.0
		B2	12.88		19.85	1.54	4.2	0.53		

^[1] Average peak load (total peak load applied on the specimen divided by the number of headed bars being developed)

^[2] Normalized force on the headed bar at failure using Eq. (3.1)

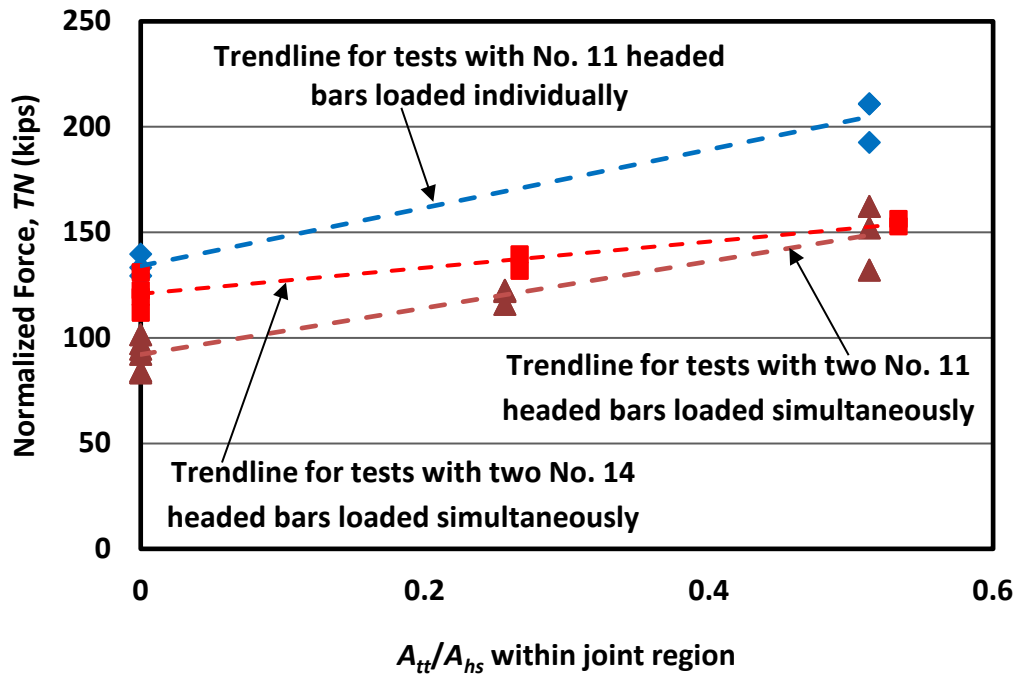


Figure 3.17 Normalized bar force at failure T_N [using Eq. (3.1)] versus normalized parallel tie reinforcement A_{tt}/A_{hs} , within a $10d_b$ radial distance from the centerline of the headed bars, for specimens with and without parallel tie reinforcement

As shown in Figure 3.17, the presence of parallel tie reinforcement within the joint region increases the anchorage strength of headed bars. The average anchorage strength for No. 11 headed bars loaded individually without parallel tie reinforcement in the form of hoops within the joint region is 134 kips, while the average strength for similar specimens with parallel tie reinforcement located on both sides of the headed bars $2.8d_b$ (4 in.) from the centerline of the headed bars with $A_{tl}/A_{hs} = 0.51$ is 205 kips (53% greater). Student's t-test shows that this difference in anchorage strength is statistically significant, with $p = 0.0005$. The average anchorage strength for two widely-spaced ($8.2d_b$) No. 11 headed bars loaded simultaneously without parallel tie reinforcement within the joint region is 92 kips, while the average strength for similar specimens with parallel tie reinforcement on both sides of the headed bars and spaced at $3.9d_b$ (5.5 in.) with $A_{tl}/A_{hs} = 0.51$ is 148 kips (61% greater). Student's t-test also shows that this difference is statistically significant, with $p = 0.0001$. The average strength for tests that included two widely-spaced ($8.2d_b$) No. 11 headed bars loaded simultaneously with parallel tie reinforcement placed only on one side of the headed bars and spaced at $3.9d_b$ (5.5 in.) with $A_{tl}/A_{hs} = 0.26$ is 120 kips (about 30% greater than those that did not include parallel tie reinforcement ($p = 0.0005$) and about 23% less than those that contained parallel tie reinforcement on both sides of the headed bars ($p = 0.034$)).

The average anchorage strength for two No. 14 headed bars spaced at $6.8d_b$ and loaded simultaneously without parallel tie reinforcement within the joint region is 121 kips, while the average strength for similar specimens with parallel tie reinforcement on both sides of the headed bars and spaced at $3.2d_b$ (5.5 in.) with $A_{tl}/A_{hs} = 0.53$ is 155 kips (28% greater). Student's t-test shows that this difference is statistically significant, with $p = 0.005$. The average strength for tests that included two No. 14 headed bars spaced at $6.8d_b$ and loaded simultaneously with parallel tie reinforcement placed only on one side of the headed bars and spaced at $3.2d_b$ (5.5 in.) with $A_{tl}/A_{hs} = 0.27$ is 136 kips (about 12% greater than those that did not include parallel tie reinforcement ($p = 0.086$) and about 14% less than those that contained parallel tie reinforcement on both sides of the headed bars ($p = 0.046$)). These observations indicate that the parallel tie reinforcement within column-foundation joint is effective in improving the anchorage strength of headed bars—behavior that is not accounted for in ACI 318-19. Moreover, these results show that parallel tie reinforcement increases the anchorage strength of widely-spaced bars. This observation matches

the findings by Shao et al. (2016) for beam-column joints, who observed that even for widely-spaced headed bars, the addition of parallel tie reinforcement increases the anchorage strength. The contribution of parallel tie reinforcement to the anchorage strength of widely-spaced bars is not taken into account by the development length provisions of the ACI 318-19 Code.

3.1.6 Examination of Value of Effective Parallel Tie Reinforcement A_{tt} used in Descriptive Equation, Eq. (1.8)

As mentioned earlier, Sperry et al. (2015b) and Shao et al. (2016) found that confining reinforcement within $8d_b$ of the top of the hooked or headed bars for No. 3 through No. 8 bars or within $10d_b$ for No. 9 through No. 11 bars were effective in increasing the anchorage strength of hooked or headed bars in beam-column joints. Shao et al. (2016) found that, based on their analysis, the total area of the effective parallel tie reinforcement per headed bar A_{tt}/n in the descriptive equation (Eq. 1.8) must be less than or equal to $0.3A_b$, where A_{tt} is the total area of the effective parallel tie reinforcement in the joint region, n is the number of headed bars being developed and A_b is the area of the headed bar. Shao et al. (2016) concluded that the values above $0.3A_b$ did not contribute to the anchorage strength of headed bars in beam-column joints. The value of A_{tt}/n versus the $0.3A_b$ for column-foundation joint specimens is explained next.

For the specimens with two widely-spaced No. 11 headed bars with parallel tie reinforcement only on one side of the headed bars, A_{tt}/n within $10d_b$ equals 0.40 in.^2 (area of four legs of No. 4 ties), which is less than the value of $0.3A_b$ (0.47 in.^2). For tests conducted on similar specimens but with parallel tie reinforcement on both sides of the headed bars, A_{tt}/n within $10d_b$ has an area of 0.80 in.^2 (area of eight No. 4 ties), which is greater than the $0.3A_b$. The ratio of the measured anchorage strength T to that calculated using the descriptive equation (Eq. 1.8) T_h ranges from 0.98 to 1.16 when the cap of $0.3A_b$ is not applied and from 0.99 to 1.34 when the cap is applied, as shown in Tables 3.7 and 3.8, respectively. For tests of the specimens with No. 14 headed bars with parallel tie reinforcement only on one side of the headed bars, the value of A_{tt}/n for the hoops within $10d_b$ equals 0.60 in.^2 (area of six legs of No. 4 ties), which is less than $0.3A_b$ (0.68 in.^2). However, for similar specimens with parallel tie reinforcement on both sides of the headed bars, A_{tt}/n within $10d_b$ has an area of 1.2 in.^2 (area of twelve No. 4 ties), which is greater

than the value of $0.3A_b$. The ratio of the measured anchorage strength T to that calculated using the descriptive equation (Eq. 1.8) T_h ranges from 0.85 to 1.07 when the cap of $0.3A_b$ is not applied and from 0.95 to 1.12 when the cap is applied, as shown in Tables 3.7 and 3.8, respectively.

Table 3.7 Effective parallel tie reinforcement (A_{tt}) and T/T_h values for tests containing two headed bars loaded simultaneously with parallel tie reinforcement within the joint region, the cap $0.3A_b$ is not applied to the descriptive equation (Eq. 1.8)

Specimens			$N_{legs}^{[1]}$	$N_{layers}^{[2]}$	A_{tt} (in. ²)	$\frac{A_{tt}}{n}$	$0.3A_b$ (in. ²)	$T^{[3]}$ (kips)	T_h (kips)	$\frac{T}{T_h}$
SN	Description	Head								
8	(2@8.2)11-5-S9.2-7#11-3#4-12.75	A1	2	2	0.80	0.40	0.47	133.5	134.2	0.99
		A2								
	(2@8.2)11-5-S9.2-7#11-6#4-12.75	B1	2	4	1.60	0.80	0.47	185.0	159.6	1.16
		B2								
9	(2@8.2)11-5-S9.2-7#11-3#4-12.75	A1	2	2	0.80	0.40	0.47	140.7	134.4	1.05
		A2								
	(2@8.2)11-5-S9.2-7#11-6#4-12.75	B1	2	4	1.60	0.80	0.47	177.1	161.8	1.09
		B2								
11	(2@8.2)11-15-S9.2-7#11-3#4-12.75	A1	2	2	0.80	0.40	0.47	157.3	146.5	1.07
		A2								
	(2@8.2)11-15-S9.2-7#11-6#4-12.75	B1	2	4	1.60	0.80	0.47	167.8	171.6	0.98
		B2								
13	(2@6.8)14-5-B4.2-7#11-3#4-12.75	A1	2	3	1.20	0.60	0.68	137.3	145.2	0.95
		A2								
	(2@6.8)14-5-B4.2-7#11-6#4-12.75	B1	2	6	2.40	1.20	0.68	160.0	188.3	0.85
		B2								
15	(2@6.8)14-15-B4.2-7#11-3#4-12.75	A1	2	3	1.20	0.60	0.68	185.1	172.6	1.07
		A2								
	(2@6.8)14-15-B4.2-7#11-6#4-12.75	B1	2	6	2.40	1.20	0.68	194.4	212.2	0.92
		B2								

^[1] Number of legs in one layer

^[2] Number of layers included in the calculation of A_{tt}

^[3] T = average peak load (total peak load applied on the specimen divided by the number of headed bars being developed)

Table 3.8 Effective parallel tie reinforcement (A_{tt}) and T/T_h values for tests containing two headed bars loaded simultaneously with parallel tie reinforcement within the joint region, the cap $0.3A_b$ is applied to the descriptive equation (Eq. 1.8)

Specimens			$N_{legs}^{[1]}$	$N_{layers}^{[2]}$	A_{tt} (in. ²)	$\frac{A_{tt}}{n}$	$0.3A_b$ (in. ²)	$T^{[3]}$ (kips)	T_h (kips)	$\frac{T}{T_h}$
SN	Description	Head								
8	(2@8.2)11-5-S9.2-7#11-3#4-12.75	A1	2	2	0.80	0.40	0.47	133.5	134.2	0.99
		A2								
	(2@8.2)11-5-S9.2-7#11-6#4-12.75	B1	2	4	1.60	0.80	0.47	185.0	137.6	1.34
		B2								
9	(2@8.2)11-5-S9.2-7#11-3#4-12.75	A1	2	2	0.80	0.40	0.47	140.7	134.4	1.05
		A2								
	(2@8.2)11-5-S9.2-7#11-6#4-12.75	B1	2	4	1.60	0.80	0.47	177.1	139.9	1.27
		B2								
11	(2@8.2)11-15-S9.2-7#11-3#4-12.75	A1	2	2	0.80	0.40	0.47	157.3	146.5	1.07
		A2								
	(2@8.2)11-15-S9.2-7#11-6#4-12.75	B1	2	4	1.60	0.80	0.47	167.8	149.7	1.12
		B2								
13	(2@6.8)14-5-B4.2-7#11-3#4-12.75	A1	2	3	1.20	0.60	0.68	137.3	145.2	0.95
		A2								
	(2@6.8)14-5-B4.2-7#11-6#4-12.75	B1	2	6	2.40	1.20	0.68	160.0	149.0	1.07
		B2								
15	(2@6.8)14-15-B4.2-7#11-3#4-12.75	A1	2	3	1.20	0.60	0.68	185.1	172.6	1.07
		A2								
	(2@6.8)14-15-B4.2-7#11-6#4-12.75	B1	2	6	2.40	1.20	0.68	194.4	172.9	1.12
		B2								

^[1] Number of legs in one layer

^[2] Number of layers included in the calculation of A_{tt}

^[3] T = average peak load (total peak load applied on the specimen divided by the number of headed bars being developed)

3.2 ANALYSIS OF TEST RESULTS FROM OTHER STUDIES AND COMPARISONS WITH THE CURRENT STUDY

The descriptive equations developed by Shao et al. (2016) are based on beam-column joint specimens. In this section, test results from current and previous studies are compared with the anchorage strengths predicted by the descriptive equations developed by Shao et al. (2016) to evaluate their applicability to predict the anchorage strength of headed bars anchored in members other than beam-column joints. The test results are also compared with the anchorage strengths predicted by the ACI code provisions in Chapter 17 and Chapter 25 of ACI 318-19 and proposed Code provisions to evaluate their accuracy for predicting the anchorage strength of headed bars

anchored in members other than beam-column joints. Equations (3.3) and (3.4) are the descriptive equations developed by Shao et al. (2016) for the anchorage of headed bars without and with confining reinforcement, respectively. The descriptive equations were developed as a best fit of the test results with an *average* ratio of test-to-calculated failure load equal to 1.0.

$$T_h = \left(781 f_{cm}^{0.24} \ell_{eh}^{1.03} d_b^{0.35} \right) \left(0.0836 \frac{s}{d_b} + 0.3444 \right) \quad (3.3)$$

with $0.0836 \frac{s}{d_b} + 0.3444 \leq 1.0$, and

$$T_h = \left(781 f_{cm}^{0.24} \ell_{eh}^{1.03} d_b^{0.35} + 48,800 \frac{A_{tr}}{n} d_b^{0.88} \right) \left(0.0622 \frac{s}{d_b} + 0.5428 \right) \quad (3.4)$$

with $0.0622 \frac{s}{d_b} + 0.5428 \leq 1.0$ and $\frac{A_{tr}}{n} \leq 0.3 A_b$

where T_h is the anchorage strength of a headed bar (lb); f_{cm} is the measured concrete compressive strength (psi); ℓ_{eh} is the embedment length (in.); d_b is the diameter of the headed bar (in.); s is the center-to-center spacing between the bars (in.); A_{tr} is the total cross-sectional area of effective confining reinforcement (NA_{tr}) parallel to the headed bars being developed (in.²); N is the number of legs of the effective confining reinforcement parallel to the headed bars being developed; A_{tr} is the area of a single leg of the confining reinforcement (in.²); n is the number of headed bars in tension; A_b is the nominal area of the headed bar (in.²).

A modification factor of 0.8 is applied to the anchorage strength T_h for headed bars terminating outside a column core (a region of column cross-section confined by the column longitudinal reinforcement) with side cover to the bar < 2.5 in., or terminating in a member other than beam-column joints with side cover to the bar < $8d_b$.

The test results are also compared with the anchorage strengths predicted by the anchorage provisions in Chapter 17 of ACI 318-19. The anchorage provisions for different failure modes, such as concrete breakout strength (Section 17.6.2 of ACI 318-19) and the anchorage strength provided by anchor reinforcement (Section 17.5.2.1 of ACI 318-19), are presented below. Anchor reinforcement is defined in accordance with Section 17.5.2.1 of ACI 318-19 as stirrups, ties, or hairpins parallel to the headed bars and placed within $0.5\ell_{eh}$ from the centerline of the headed bars.

According to Section 17.6.2.1 of ACI 318-19, the nominal concrete breakout strength of a

single anchor (N_{cb}) or group of anchors (N_{cbg}) in tension is given by Eq. (3.5) and (3.6), respectively. The nominal concrete breakout strength equations are based on the 5% fractile of the test results used to develop the breakout equations. Therefore, the anchorage strength calculated based on the concrete breakout strength equations must be converted to a mean value to have a fair comparison with other design equations. A modification factor (ψ_{mean}) of 1.33 can be applied to the concrete breakout strength equations in ACI 318-19 to convert the 5% fractile value to a mean value. The 1.33 modification factor is calculated using Eq. (3.7), which is based on the standard normal distribution n -value = -1.645 for a 5% fractile (ACI 318-19) and the coefficient of variation (COV = 0.15) of the data used to develop the concrete breakout equations (Fuchs et al. 1995).

$$N_{cb} = \frac{A_{Nc}}{A_{Nco}} \psi_{ed,N} \psi_{c,N} \psi_{cp,N} N_b \quad (3.5)$$

$$N_{cbg} = \frac{A_{Nc}}{A_{Nco}} \psi_{ec,N} \psi_{ed,N} \psi_{c,N} \psi_{cp,N} N_b \quad (3.6)$$

$$\psi_{mean} = \frac{1}{1 + n \cdot COV} \quad (3.7)$$

where A_{Nc} is the projected concrete failure area of a single anchor or group of anchors (in.²); A_{Nco} is the projected concrete failure area of a single anchor with an edge distance of at least $1.5\ell_{eh}$ and is equal to $9\ell_{eh}^2$ (in.²), where ℓ_{eh} is the embedment length of headed anchors (in.); N_b is the basic concrete breakout strength of a single anchor loaded in tension, calculated as $N_b = k_c \cdot \lambda_a \cdot \sqrt{f'_c} \cdot \ell_{eh}^{1.5}$ if the embedment length of the headed bar $\ell_{eh} < 11$ in. and as $N_b = 16 \cdot \lambda_a \cdot \sqrt{f'_c} \cdot \ell_{eh}^{5/3}$ if $11 \text{ in.} \leq \ell_{eh} \leq 25 \text{ in.}$, where k_c is a calibration factor equal to 24 for cast-in anchors in cracked concrete; λ_a is a modification factor for lightweight concrete equal to 1.0λ for cast-in and undercut anchors and 0.8λ for expansion, screw, and adhesive anchors, λ is equal to 0.75 for lightweight concrete and 1.0 for normalweight concrete; f'_c is the concrete compressive strength (limited to 10,000 psi). $\psi_{ec,N}$ is a modification factor for a group of anchors loaded eccentrically in tension equal to $1/\left[1 + e'_N/(1.5\ell_{eh})\right] \leq 1$, where e'_N is the distance between resultant tensile load on a group of anchors loaded in tension and the centroid of the group of anchors loaded in tension (in.). $\psi_{ed,N}$ is a modification factor for edge effects for a single anchor or group of anchors loaded in tension equal to 1.0 if the smallest side concrete cover distance from the center

of an anchor is at least $1.5\ell_{eh}$; otherwise, $\psi_{ed,N}$ is equal to $0.7 + 0.3(c_{a,\min} / 1.5\ell_{eh})$, where $c_{a,\min}$ is the minimum distance from the center of an anchor to the edge of concrete (in.). $\Psi_{c,N}$ is a modification factor for the influence of cracking in anchor regions at service load levels, equal to 1.25 if anchors are located in a region of a concrete member where analysis indicates no cracking at service load levels; otherwise, $\Psi_{c,N}$ is equal to 1.0. $\psi_{cp,N}$ is a modification factor for post-installed anchors and is equal to 1.0 for cast-in anchors.

The nominal anchorage strength of headed bars provided by anchor reinforcement N_{arg} (Section 17.5.2.1 of ACI 318-19) is given by Eq. (3.8).

$$N_{arg} = NA_{tr}f_y \quad (3.8)$$

where N is the total number of legs of anchor reinforcement parallel to the headed bars within a $0.5\ell_{eh}$ radial distance from the centerline of the headed bars; A_{tr} is the area of a single leg of the anchor reinforcement (in.²); f_y is the yield strength of the anchor reinforcement (psi).

The nominal anchorage strength of a headed bar in tension T_{anc} , governed by anchor reinforcement N_{arg} or concrete breakout N_{cbg} (incorporating the modification factor ψ_{mean}), is calculated using Eq. (3.9).

$$T_{anc} = \max\left(\frac{N_{cbg}}{n}, \frac{N_{arg}}{n}\right) \quad (3.9)$$

where n is the number of headed bars tested simultaneously in tension.

The test results are also compared with the anchorage strength of headed bars predicted by the design provisions in Chapter 25 of ACI 318-19 Section 25.4.4. The design provision is shown in Eq. (3.10).

$$\ell_{dt} = \left(\frac{f_y \Psi_e \Psi_p \Psi_o \Psi_c}{75\sqrt{f'_c}}\right) d_b^{1.5} \quad (3.10)$$

where ℓ_{dt} is the development length of a headed bar in tension (in.) not less than either $8d_b$ or 6 in.; Ψ_e is a factor based on the presence or absence of a coating on the bars, equal to 1.2 for epoxy-coated or zinc and epoxy dual-coated reinforcement and 1.0 for uncoated or zinc-coated (galvanized) reinforcement; Ψ_o is the bar location factor equal to 1.0 for No. 11 and smaller headed bars anchored within a column core with side cover not less than 2.5 in. or in other members with

side cover not less than $6d_b$; otherwise, ψ_o is equal to 1.25; ψ_c is the concrete strength factor equal to $f'_c/15,000 + 0.6$ if f'_c is less than 6000 psi and equal to 1.0 if f'_c is greater than or equal to 6000 psi; ψ_p is the parallel tie reinforcement factor equal to 1.0 for No. 11 and smaller headed bars spaced at a center-to-center distance not less than $6d_b$ or with A_{tt}/A_{hs} not less than 0.3, where A_{tt} is the total cross-sectional area of ties or stirrups acting as parallel tie reinforcement (in.²) and A_{hs} is the total cross-sectional area of headed bars being developed at a critical section (in.²); otherwise, ψ_p is equal to 1.6. It is worth noting that the value of ψ_p for column-foundation joint specimens is taken as 1.0 in this analysis only when the center-to-center spacing between headed bars $\geq 6d_b$ because parallel tie reinforcement, A_{tt} , is not considered for members other than beam-column joints, as mentioned in Section 25.4.4.5 of ACI 318-19. The modification factors in Eq. (3.10) are defined in Table 25.4.4.3 of ACI 318-19.

The design provisions in Chapter 25 of ACI 318-19 are a modified version of the descriptive equations, Eq. (3.3) and (3.4), with a strength reduction factor, ϕ , of 0.83 built-in, the square root of concrete compressive strength f'_c and ψ_c (defined above) rather than f_{cm} to the 0.24 power as in the descriptive equations, and use the modification factor ψ_p equal to 1 or 1.6 (intermediate values are not permitted) to represent the effect of anchored bar spacing and parallel ties instead of factors that varied as a function of bar spacing and the level of parallel tie reinforcement. Therefore, the anchorage strength calculated based on this design provision is expected to be conservative.

Equation (3.10) is solved for anchorage strength $T_{ACI\ 318}$ and replacing ℓ_{dt} and f'_c with ℓ_{eh} and f_{cm} , respectively, as shown in Eq. (3.11).

$$T_{ACI\ 318} = \left(\frac{75\sqrt{f_{cm}}\ell_{eh}}{\Psi_e\Psi_p\Psi_o\Psi_c d_b^{1.5}} \right) A_b \quad (3.11)$$

The test results are also compared with the anchorage strength of headed bars calculated using a proposed version of the design provisions based on a smoothed version of the descriptive equations that incorporates the effects headed bar spacing and parallel ties. The expression for development length in the proposed provisions is shown in Eq. (3.12). This expression is a modified version of the descriptive equations, Eq. (3.3) and (3.4), with a built-in strength reduction

factor, ϕ , of 0.83. Thus, the anchorage strength calculated based on Eq. (3.12) is expected to be conservative.

$$\ell_{dt} = \left(\frac{f_y \Psi_e \Psi_p \Psi_o}{600 f_c'^{0.25}} \right) d_b^{1.5} \quad (3.12)$$

where ℓ_{dt} is the development length of a headed bar in tension (in.) not less than either $8d_b$ or 6 in.; Ψ_e is a factor based on the presence or absence of a coating on the bars, equal to 1.2 for epoxy-coated or zinc and epoxy dual-coated reinforcement and 1.0 for uncoated or zinc-coated (galvanized) reinforcement; Ψ_o is the bar location factor equal to 1.0 for headed bars anchored within a column core with side cover not less than 2.5 in. or in other members with side cover not less than $6d_b$; otherwise, Ψ_o is equal to 1.25; Ψ_p is the parallel tie reinforcement factor calculated using Eq. (3.13).

$$\Psi_p = \frac{1}{4} \left(7 - 10 \frac{A_{tt}}{A_{hs}} - 0.5 \frac{s}{d_b} + \frac{A_{tt}}{A_{hs}} \frac{s}{d_b} \right) \quad (3.13)$$

where A_{tt} is the total cross-sectional area of ties or stirrups acting as parallel tie reinforcement (in.²), A_{hs} is the total cross-sectional area of headed bars being developed at a critical section (in.²), s is the minimum center-to-center spacing of headed bars, d_b is the nominal diameter of headed bars, A_{tt}/A_{hs} shall not exceed 0.3, and s/d_b shall not exceed 8 when calculating Ψ_p .

Equation (3.12) is solved for anchorage strength T_{calc} and replacing ℓ_{dt} and f_c' with ℓ_{eh} and f_{cm} , respectively, as shown in Eq. (3.14).

$$T_{calc} = \left(\frac{600 f_{cm}^{0.25} \ell_{eh}}{\Psi_e \Psi_p \Psi_o d_b^{1.5}} \right) A_b \quad (3.14)$$

3.2.1 Headed Bars Tested in Slab Specimens

DeVries et al. (1999) tested 18 headed bars with net bearing areas A_{brg} ranging from 4.7 to $7.4A_b$ in three concrete slab specimens with embedment lengths ranging from 1.375 to 9 in. The concrete compressive strength ranged from 3,920 to 12,040 psi, and the nominal yield strength of the headed bars was 72,000 psi. The headed bars anchored in slabs were spaced at a center-to-

center distance of at least three times the embedment length of the headed bars to avoid an overlap of the anticipated failure region. Of the 18 headed bars, eight bars were anchored at the center of the slab with a clear cover to the bars not less than two times the embedment length of the headed bars, five bars were anchored at the edge of the slab with a clear cover of 1.6 in. on one side and 17.6 in. on the adjacent side, and five bars were anchored at the corner of the slab with a clear cover of 1.6 in. on both side faces. These headed bars were tested individually in tension. During the tests, the support reaction plates were placed away from the headed bars at a distance equal to at least two times the embedment length with the goal of preventing the support reactions from influencing the anchorage strength. Of the 18 headed bars, 14 were unbonded along the total embedment length using a PVC pipe, as shown in Figure 3.18a, and four, all with an embedment length equal to 9 in., were bonded, as shown in Figure 3.18b. Results of the tests with unbonded headed bars are not included in the analysis because the behavior of unbonded bars is expected to be different from that of fully bonded bars. The center-to-center spacing between the headed bars s required in the descriptive equations [Eq. (3.3) and (3.4)] to calculate anchorage strength of headed bars is taken as twice of the minimum concrete cover to the center of the headed bar.

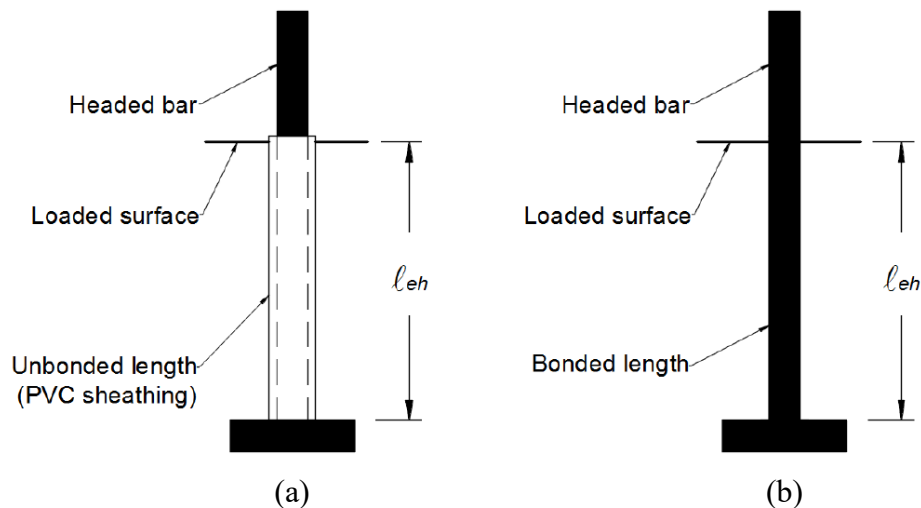


Figure 3.18 Headed reinforcing bars (a) unbonded and (b) bonded embedment length (DeVries et al. 1999)

Choi et al. (2002) conducted 16 tests on headed bars anchored in slabs (Figure 3.19), with embedment lengths ranging from 6.9 to $12.1d_b$. The concrete compressive strength ranged from 3,930 to 5,270 psi. The slab specimens contained headed bars anchored in the middle of the slab

with a clear cover to the bar of 35 in., as well as headed bars anchored close to the slab boundaries with a clear cover to the bar ranging from 1.6 to 4.9 in., as shown in Figure 3.19. The headed bars in the slab specimens were tested individually. During the tests, the support reaction plates were placed away from the headed bars at a distance equal to at least $1.5\ell_{eh}$ from the headed bars, as shown in Figure 3.19. For tests involving individual headed bars, the center-to-center spacing between the bars s required in the descriptive equations [Eq. (3.3) and (3.4)] to calculate anchorage strength is taken as twice of the minimum concrete cover to the center of the headed bar. Headed bars tested by Choi et al. (2002) had net bearing areas A_{brg} ranging from 2.6 to $3.2A_b$, which is less than the minimum net bearing area of $4A_b$ required in ACI 318-19.

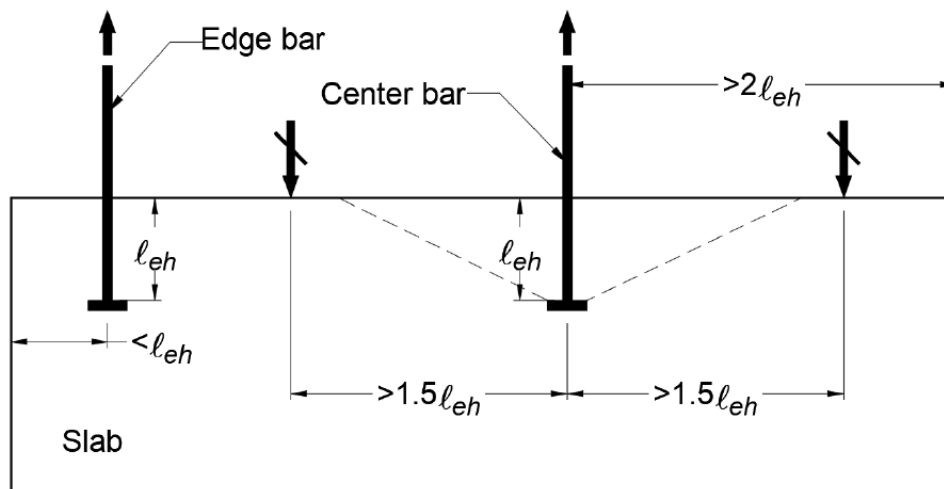


Figure 3.19 Slab specimens (Choi et al. 2002)

Ghimire et al. (2018) tested 32 headed bars anchored in slab specimens with embedment lengths ranging from 6 to 8.5 in. Concrete compressive strength ranged from 4,200 to 8,620 psi. The slab specimens contained two or three headed bars, with the exception of one slab that contained one headed bar anchored in the center of the slab. All headed bars were tested individually. The center-to-center spacing between the bars was at least three times the embedment length of the headed bars to avoid an overlap of the anticipated concrete failure region. Of the 32 tests, 22 had one of the support reaction plates located close to the headed bar at a distance of 10 in. ($1.2\ell_{eh}$ to $1.7\ell_{eh}$), and the other support plate was located far away from the headed bar at a distance of 44.3 in. ($5.2\ell_{eh}$ to $7.4\ell_{eh}$), nine tests had both support plates located outside the

anticipated concrete failure region at a distance ranging from 14.5 to 16.5 in. ($2.3\ell_{eh}$ to $2.8\ell_{eh}$), and one test had both support plates located far away from the headed bars at a distance of 47.5 in. ($5.6\ell_{eh}$). In accordance with Section 17.6.2.1.1 of ACI 318-19, the anticipated concrete failure region is measured as $1.5\ell_{eh}$ radial distance from the centerline of the headed anchors. Headed bars with net bearing areas A_{brg} ranging from 4 to $15A_b$ were tested. Shao et al. (2016) and Ghimire et al. (2018) found that increasing the net bearing area of the head from 3.8 to $9.5A_b$ did not increase the anchorage strength of headed bars; however, the anchorage strength of headed bars increased about 15% for heads with a net bearing area ranging from 13 to $15A_b$. Therefore, the results of the tests with headed bars with net bearing areas ranging from 13 to $15A_b$ are not included in this analysis.

Worsfold et al. (2022) and Worsfold and Moehle (2019, 2022) tested two steel-column-to-concrete-foundation joints located away from foundation edges under reversed cyclic loading with and without parallel tie reinforcement in the foundation to study the failure mechanisms and design requirements. As depicted in Figures (3.20) and (3.21), the test specimens consisted of a steel column (W12x106 ASTM A992 Grade 50) connected to a foundation slab by cast-in-place anchor bolts. The column was subjected to reversed cyclic lateral loads with no axial load other than column self-weight. Four 1.5 in. diameter anchor bolts with heavy hex nuts as heads in the first specimen M01 and with steel plate washers in the second specimen M02, as shown in Figures (3.20) and (3.21), respectively, were cast into the 18 in. thick foundation on each side of the column. The anchor bolts had an effective embedment length from the top of the slab to the bearing surface equal to 14.3 in. The net head bearing areas A_{brg} in specimens M01 and M02 were $1.5A_b$ and $5.5A_b$, respectively. The concrete compressive strengths were 3700 and 3930 psi for specimens M01 and M02, respectively. The nominal yield strength of the anchor bolts was 105,000 psi. Specimen M01 had five perpendicular No. 4 hoops in the joint region, as shown in Figure (3.20), while specimen M02 had No.4 bar parallel ties shaped as 180-degree hooks on the top and heads on the bottom, as shown in Figure (3.21). The parallel tie reinforcement in specimen M02 extended two rows farther on the west side than on the east side of the slab (Figure 3.22), and had no perpendicular hoops around the anchor bolts. A load cell was placed on each anchor bolt to measure the anchorage strength.

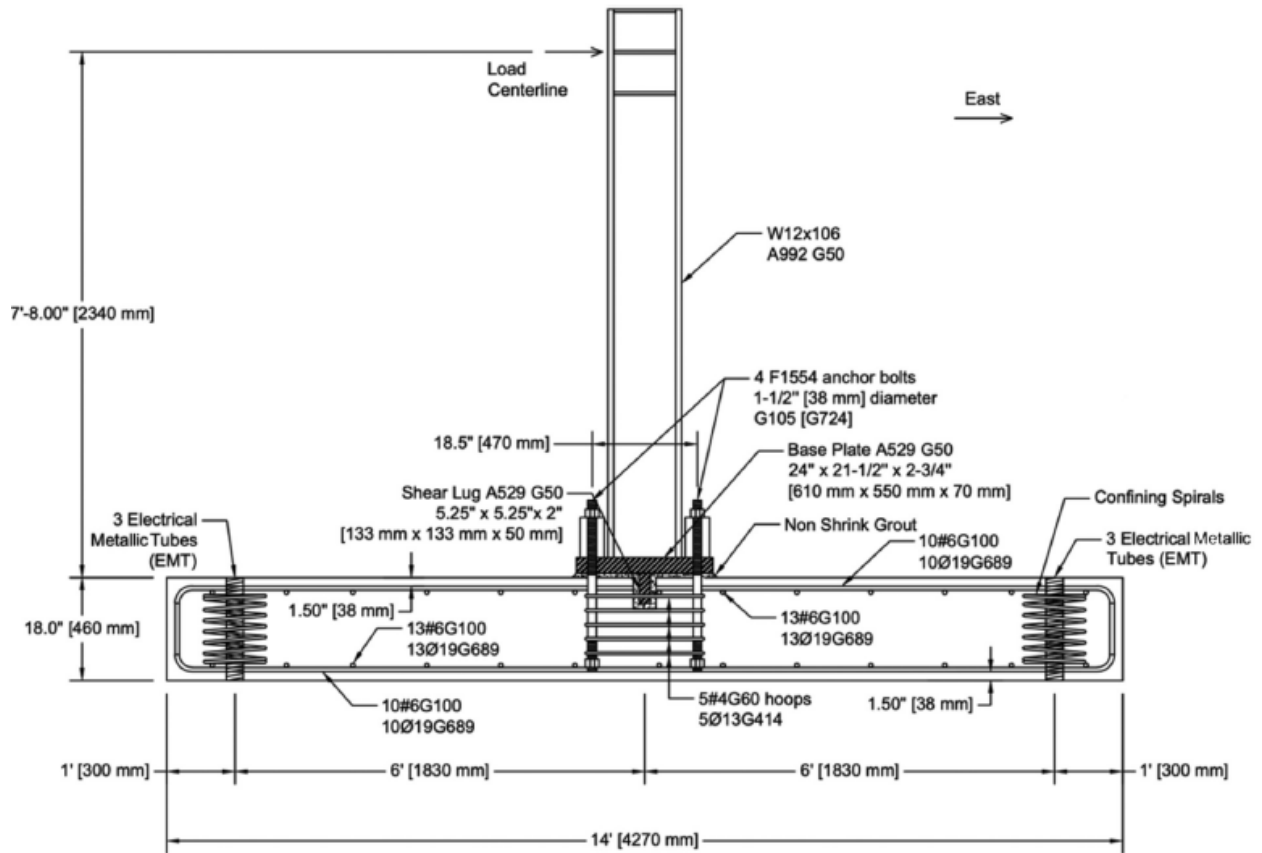


Figure 3.20 Steel-column-to-concrete-foundation joint specimen M01 (Worsfold et al. 2022)

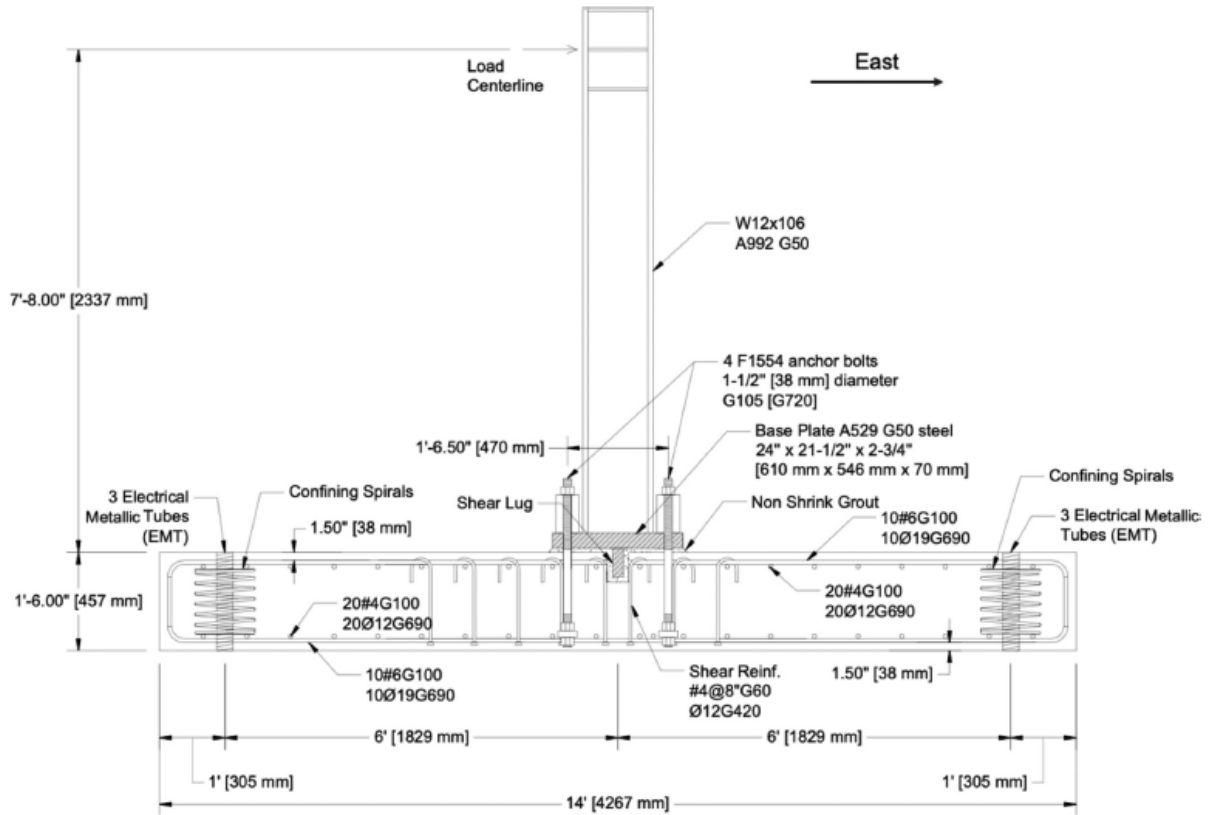


Figure 3.21 Steel-column-to-concrete-foundation joint specimen M02 (Worsfold et al. 2022)

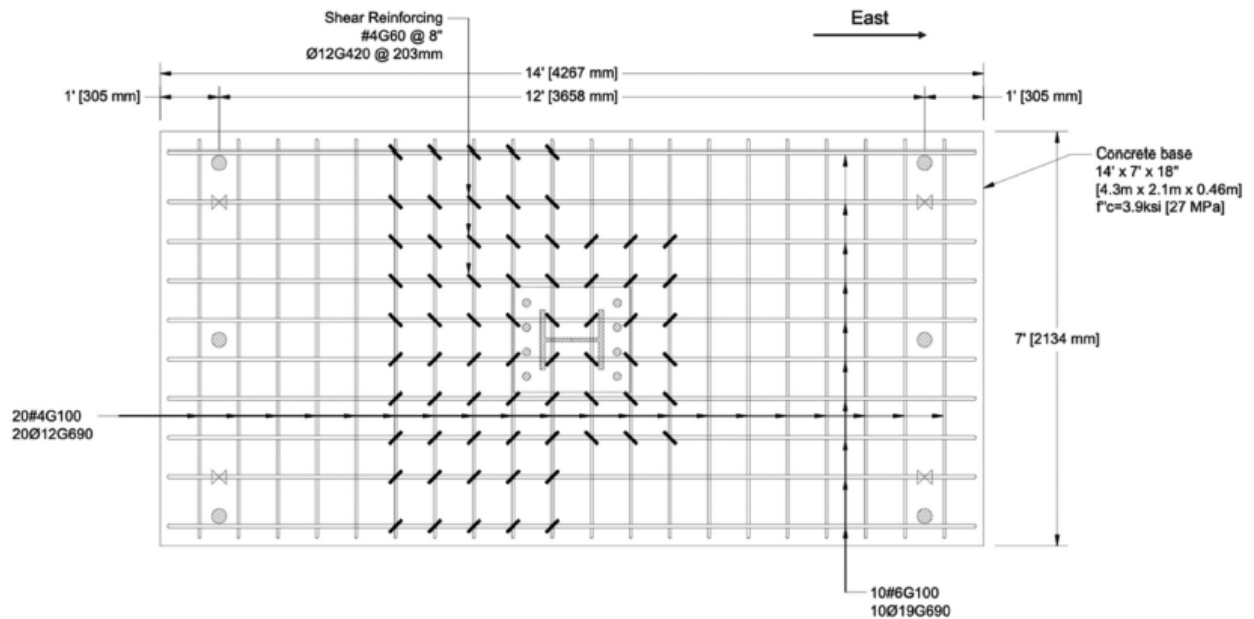


Figure 3.22 Plan view of specimen M02 (Worsfold et al. 2022)

3.2.1.1 Analysis Based on Descriptive Equations, ACI 318-19 Code Provisions, and Proposed Version of Code Provisions

The measured failure loads T on the headed bars tested by DeVries et al. (1999), Choi et al. (2002), Ghimire et al. (2018), Worsfold et al. (2022), and in the current study are compared with the calculated failure loads T_h [based on the descriptive equations, Eq. (3.3) and (3.4)], T_{anc} [based on the anchorage provisions of Chapter 17 of ACI 318-19, Eq. (3.9)], $T_{ACI\ 318}$ [based on the design provisions of Chapter 25 of ACI 318-19, Eq. (3.11)], and T_{calc} [based on the proposed version of the design provisions, as shown in Eq. (3.14)]. A 0.8 reduction factor is applied to the calculated failure load T_h from Eq. (3.3) and (3.4) for headed bars with side cover c_{so} less than $8d_b$ in slab specimens. The effective parallel tie reinforcement A_{tt} used in the descriptive equation, Eq. (3.4), is taken as the total parallel tie reinforcement on all sides of the headed bar(s) within $8d_b$ distance from the center of the headed bar for No. 3 through No. 8 bars or within $10d_b$ for No. 9 through No. 14 bars applying the $0.3A_b$ limit. The measured failure loads T and the calculated failure loads T_h , T_{anc} , $T_{ACI\ 318}$, and T_{calc} , along with the values of the embedment length ℓ_{eh} for specimens tested by DeVries et al. (1999), Choi et al. (2002), and Worsfold et al. (2022) are presented in Table 3.9, with full details provided in Tables C.1 and C.3 of Appendix C. Only headed bars that did not reach the yield strength are included in the analysis. The measured failure loads T and the calculated failure loads T_h , T_{anc} , $T_{ACI\ 318}$, and T_{calc} , along with the specimen properties for headed bars tested in the current study and by Ghimire et al. (2018), are presented in Table 3.1 and 3.2, respectively, with complete details provided in Table B.1 of Appendix B and Table C.2 of Appendix C, respectively.

Table 3.9 Test results for headed bars anchored in slab specimens tested by DeVries et al. (1999), Choi et al. (2002), and Worsfold et al. (2022) and comparisons with anchorage provisions of Chapter 17 of ACI 318-19 [Eq. (3.9)], descriptive equations [Eq. (3.3) and (3.4)], design provisions of Chapter 25 of ACI 318-19 [Eq. (3.11)], and proposed Code provisions [Eq. (3.14)], (a reduction factor of 0.8 is applied to T_h as appropriate ^[1])

Study	Specimen	ℓ_{eh} ^[2] (in.)	T ^{[2][3]} (kips)	T_{anc} (kips)	T_h (kips)	$T_{ACI 318}$ (kips)	T_{calc} (kips)	$\frac{T}{T_{anc}}$	$\frac{T}{T_h}$	$\frac{T}{T_{ACI318}}$	$\frac{T}{T_{calc}}$	Remarks
DeVries et al. (1999)	T2B2 ^[1]	9.0	33.3	31.9	32.6	17.7	22.6	1.04	1.02	1.88	1.48	Edge bars in slab specimens
	T2B4 ^[1]	9.0	38.7	31.9	32.6	17.7	22.6	1.21	1.19	2.18	1.71	
	T2B6 ^[1]	9.0	27.4	18.3	32.6	17.7	22.6	1.50	0.84	1.55	1.22	Corner bars in slab specimens
	T2B8 ^[1]	9.0	28.1	18.3	32.6	17.7	22.6	1.53	0.86	1.58	1.25	
Choi et al. (2002)	S16-7db.1	4.4	16.4	26.8	23.9	15.8	18.9	0.61	0.69	1.04	0.87	Center bars in slab specimens
	S16-7db.2	4.4	18.0	26.8	23.9	15.8	18.9	0.67	0.75	1.14	0.95	
	S25-7db.1	6.9	36.0	52.3	44.6	31.2	37.1	0.69	0.81	1.15	0.97	
	S25-7db.2	6.9	33.9	52.3	44.6	31.2	37.1	0.65	0.76	1.09	0.91	
	E16-7db.1 ^[1]	4.4	10.6	13.5	16.2	12.7	11.4	0.78	0.65	0.83	0.93	Edge bars in slab specimens
	E16-7db.2 ^[1]	4.4	10.6	13.5	16.2	12.7	11.4	0.78	0.65	0.83	0.93	
	E19-7db.1 ^[1]	5.2	11.7	16.0	21.1	15.5	15.5	0.73	0.55	0.76	0.76	
	E19-7db.2 ^[1]	5.2	10.8	16.0	21.1	15.5	15.5	0.67	0.51	0.70	0.70	
	E19-7db.3 ^[1]	5.2	17.5	22.4	22.7	15.5	17.9	0.78	0.77	1.13	0.98	
	E19-7db.4 ^[1]	5.2	16.9	22.4	22.7	15.5	17.9	0.75	0.74	1.09	0.94	
	E25-7db.1 ^[1]	6.9	19.6	26.4	29.9	15.6	22.0	0.74	0.65	1.26	0.89	
E25-7db.2 ^[1]	6.9	20.7	26.4	29.9	15.6	22.0	0.78	0.69	1.33	0.94		
Worsfold et al. (2022)	M01	14.3	66.5	45.9	62.4	46.3	48.3	1.45	1.07	1.44	1.38	Steel column-concrete foundation
	M02	14.3	113.0	47.3	103.9	46.9	78.4	2.39	1.09	2.41	1.44	

^[1] A 0.8 reduction factor is applied when calculating T_h for headed bars with side cover c_{so} less than $8d_b$ in slab specimens

^[2] Values are converted from the SI unit (1 in. = 25.4 mm; 1 psi = 1/145 MPa; and 1 kip = 4.4484 kN)

^[3] T = average peak load (total peak load applied on the specimen divided by the number of headed bars being developed)

Descriptive Equations

The measured failure loads T of the headed bars in slab specimens tested by DeVries et al. (1999), Choi et al. (2002), Ghimire et al. (2018), Worsfold et al. (2022), and in the current study are plotted versus the calculated failure loads T_h [based on the descriptive equations, Eq. (3.3) and (3.4)] in Figure 3.23. The slab specimens tested by DeVries et al. (1999) and Choi et al. (2002)

had a ratio of distance between the center of the headed bars and the inner face of the nearest support reaction to the embedded length, h_{cl}/ℓ_{eh} , greater than 2 and 1.5, respectively (exact values were not reported), while h_{cl}/ℓ_{eh} in specimens tested by Ghimire et al. (2018), Worsfold et al. (2022), and in the current study ranged from 1.24 to 5.6.

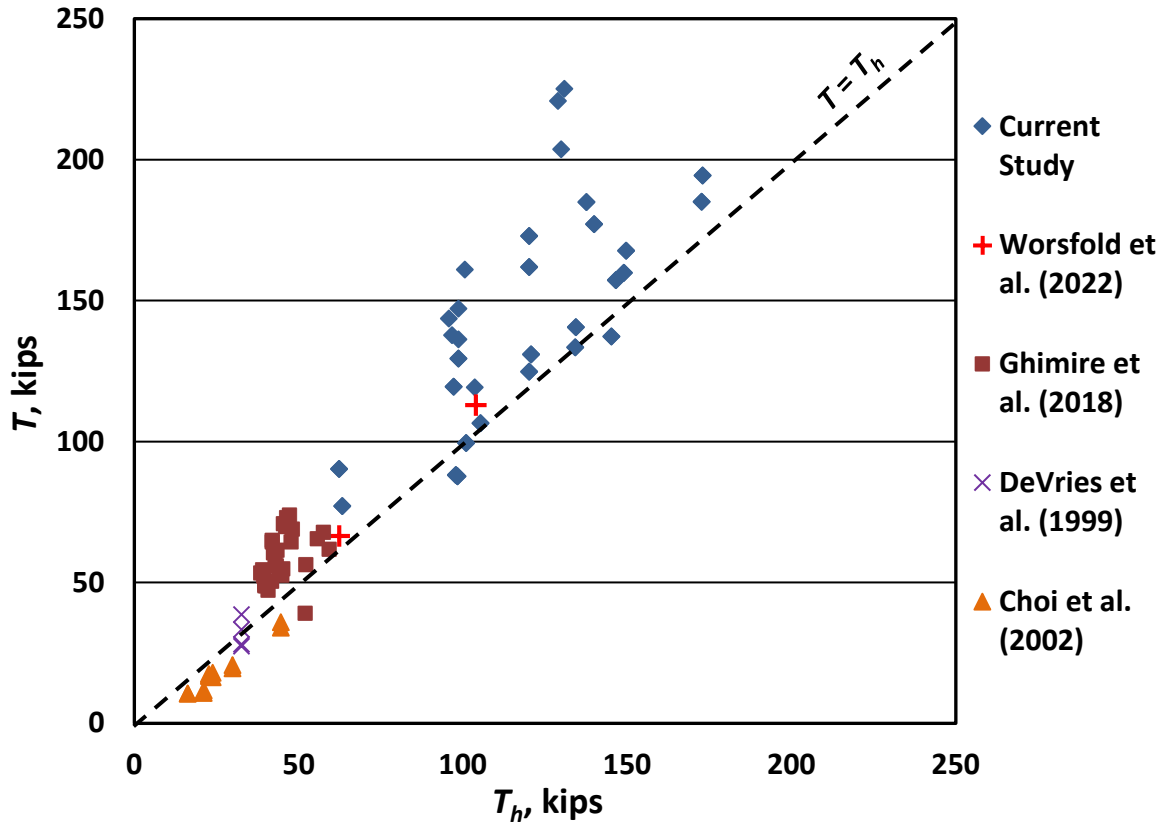


Figure 3.23 Measured force at failure T versus anchorage strength T_h calculated using Eq. (3.3) and (3.4) for slab specimens tested by DeVries et al. (1999), Choi et al. (2002), Ghimire et al. (2018), Worsfold et al. (2022), and in the current study; a reduction factor of 0.8 is applied to T_h for headed bars with concrete cover less than $8d_b$

For the specimens shown in Figure 3.23, the reduction factor of 0.8 for clear cover c_{so} less than $8d_b$ is applied to the four specimens tested by DeVries et al. (1999) and 8 out of 12 specimens tested by Choi et al. (2002). All specimens tested by Ghimire et al. (2018), Worsfold et al. (2022), and in the current study had $c_{so} > 8d_b$. The maximum, minimum, mean, standard deviation (STD), and coefficients of variation (COV) of T/T_h for the headed bars tested by DeVries et al. (1999), Choi et al. (2002), Ghimire et al. (2018), Worsfold et al. (2022) and in the current study are presented in Table 3.10. As shown in the table, all specimens tested by Choi et al. (2002) exhibited

lower anchorage strengths than those calculated by the descriptive equations with T/T_h between 0.51 and 0.81 and an average of 0.69. The values of T/T_h for the four edge and corner bars tested by DeVries et al. (1999) ranged from 0.84 to 1.19; the average for the four specimens is 0.98. The values of T/T_h for the headed bars tested by Ghimire et al. (2018) ranged from 0.75 to 1.57, with an average of 1.30. For the tests by Ghimire et al., only one specimen, which contained a single centrally placed headed bar with h_{cl}/ℓ_{eh} equal to 5.6, had a value of T/T_h less than 1.0. The values of T/T_h for the two specimens tested by Worsfold et al. (2022) are 1.07 and 1.09, with an average of 1.08. For the specimens in the current study, the values of T/T_h ranged from 0.89 to 1.72, with an average of 1.20. The ratio of test to calculated failure load of headed bars T/T_h in beam-column joint specimens tested and used by Shao et al. (2016) to develop the descriptive equations Eq. (3.3) and (3.4) ranged, respectively, from 0.68 to 1.27 with a mean, STD, and COV of 1.00, 0.111, and 0.111 for headed bar specimens without parallel ties and from 0.81 to 1.24 with a mean, STD, and COV of 1.00, 0.095, and 0.095 for headed bar specimens with parallel ties. Overall, the headed bars anchored in the column-foundation joint specimens shown in Tables 3.1, 3.2, 3.9, and the statistical parameters shown in Table 3.10 had values of T/T_h within or above the range of T/T_h for the beam-column joint specimens used to develop the descriptive equations Eq. (3.3) and (3.4), except for five of the edge bar specimens tested by Choi et al. (2002) (shown in Table 3.9). These results indicate that the descriptive equations based on tests of beam-column joints [Eq. (3.3) and (3.4)] are suitable for predicting the anchorage strength of headed bars anchored in slab specimens and, by extension, column-foundation joints. As previously stated, the net bearing areas A_{brg} of the headed bars tested by Choi et al. (2002) ranged from 2.6 to $3.2A_b$, which is less than the minimum net bearing area of $4A_b$ required by ACI 318-19. The low strengths of the specimens tested by Choi et al. (2002) may have been due to the small net bearing area, but specimen M01 tested under reversed cyclic loading by Worsfold et al. (2022) had anchor bolts with a net head bearing area A_{brg} of $1.5A_b$, and had a value of T/T_h equal to 1.07.

Table 3.10 Statistical parameters of T/T_h values for slab specimens tested by DeVries et al. (1999), Choi et al. (2002), Ghimire et al. (2018), Worsfold et al. (2022), and in the current study

Test/Calculated T/T_h ^[1] (a reduction factor of 0.8 is applied to the calculated strength as appropriate ^[2])											
Study [tests]	All	Current Study				Worsfold et al. (2022)	Ghimire et al. (2018)	Choi et al. (2002)		DeVries et al. (1999)	
		Individual headed bars		Multiple headed bars				Center bars	Edge bars	Edge bars	Corner bars
		without parallel tie ^[3]	with parallel tie ^[4]	without parallel tie ^[5]	with parallel tie ^[6]						
Number of specimens	81	6	3	12	10	2	32	4	8	2	2
Max	1.72	1.60	1.72	1.45	1.34	1.09	1.57	0.81	0.77	1.19	0.86
Min	0.51	1.15	1.57	0.89	0.95	1.07	0.75	0.69	0.51	1.02	0.84
Mean	1.16	1.43	1.67	1.16	1.11	1.08	1.30	0.75	0.65	1.10	0.85
STD	0.268	0.154	0.086	0.196	0.116	0.015	0.186	0.049	0.088	0.117	0.015
COV	0.232	0.108	0.052	0.169	0.105	0.014	0.143	0.066	0.135	0.106	0.017
Number of specimens with $T/T_h < 1.0$	20	0	0	3	2	0	1	4	8	0	2

^[1] T_h is calculated based on Eq. (3.3) and (3.4) for specimens without and with parallel tie reinforcement, respectively

^[2] A reduction factor of 0.8 is applied to T_h for headed bars terminating in slab specimens with side cover to the bar $< 8d_b$

^[3] Tests involved individual headed bars without parallel tie reinforcement in the joint region

^[4] Tests involved individual headed bars with parallel tie reinforcement in the joint region

^[5] Tests involved two headed bars loaded simultaneously without parallel tie reinforcement in the joint region

^[6] Tests involved two headed bars loaded simultaneously with parallel tie reinforcement in the joint region

Anchorage Provisions – Chapter 17 of ACI 318-19

To determine the applicability of the anchorage provisions in Chapter 17 of ACI 318-19, the failure loads T on the headed bars in the specimens tested by DeVries et al. (1999), Choi et al. (2002), Ghimire et al. (2018), Worsfold et al. (2022), and in the current study are compared with the calculated failure loads T_{anc} based on the anchorage provisions in Chapter 17 of ACI 318-19, Eq. (3.9). The calculated failure loads T_{anc} , governed by concrete breakout strength N_{cbg} [Eq. (3.6)] or anchorage strength of headed bars provided by anchor reinforcement N_{arg} [Eq. (3.8)].

Figure 3.24 presents the measured failure loads T on the headed bars in slab specimens tested by DeVries et al. (1999), Choi et al. (2002), Ghimire et al. (2018), Worsfold et al. (2022), and in the current study versus the calculated failure loads T_{anc} [based on the anchorage provisions

of Chapter 17 of ACI 318-19, Eq. (3.9)]. The calculated failure load T_{anc} values for the headed bars tested by DeVries et al. (1999), Choi et al. (2002), and Worsfold et al. (2022) are presented in Table 3.9, and for the headed bars tested in the current study and by Ghimire et al. (2018) in Tables 3.1 and 3.2, respectively. The calculated anchorage strengths of these headed bars were governed by the concrete breakout strength [Eq. (3.6), incorporating the modification factor ψ_{mean}] for all specimens.

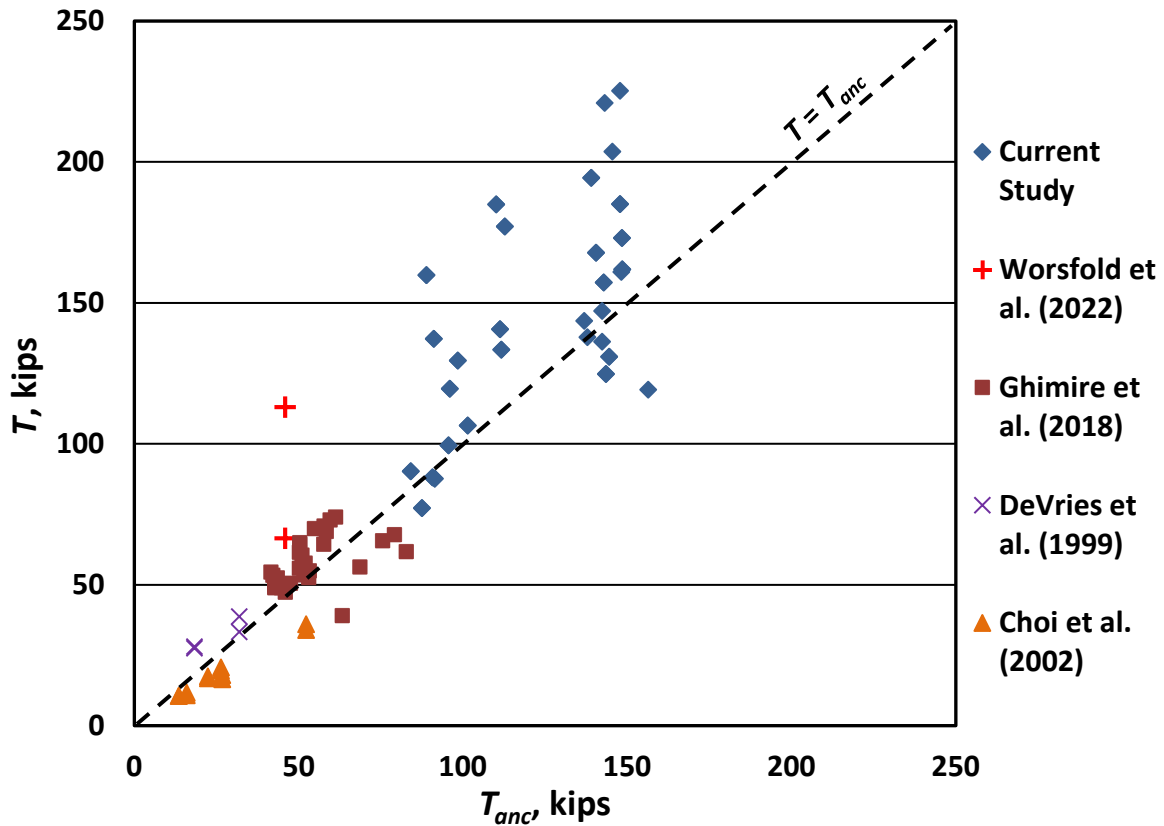


Figure 3.24 Measured force at failure T versus the anchorage strength T_{anc} calculated using Eq. (3.6), incorporating the modification factor ψ_{mean} , for slab specimens tested by DeVries et al. (1999), Choi et al. (2002), Ghimire et al. (2018), Worsfold et al. (2022), and in the current study

As shown in Figure 3.24, the specimens tested by DeVries et al. (1999) and Worsfold et al. (2022) and the majority of the specimens tested by Ghimire et al. (2018) and in the current study exhibited higher anchorage strengths than those calculated based on the concrete breakout strength. In contrast, the specimens tested by Choi et al. (2002) exhibited lower anchorage strengths than calculated by Eq. (3.6). The maximum, minimum, mean, standard deviation (STD),

and coefficients of variation (COV) of T/T_{anc} for the headed bars tested by DeVries et al. (1999), Choi et al. (2002), Ghimire et al. (2018), Worsfold et al. (2022), and in the current study are presented in Table 3.11. As shown in the table, the values of T/T_{anc} for the center bars in slab specimens tested by Choi et al. (2002) ranged from 0.61 to 0.69, with an average of 0.66, and the values of T/T_{anc} for the edge bars tested by Choi et al. (2002) ranged from 0.67 to 0.78, with an average of 0.75. The values of T/T_{anc} for the four edge and corner bars tested by DeVries et al. (1999) ranged from 1.04 to 1.53; the average for the four specimens was 1.32. The headed bars tested by Ghimire et al. (2018) had T/T_{anc} ranging from 0.62 to 1.31, with an average of 1.10; six out of the 32 specimens tested by Ghimire et al. (2018) had values of T/T_{anc} below 1.00 (with values ranging from 0.62 to 0.99). The values of T/T_{anc} for the two specimens tested by Worsfold et al. (2022) are 1.45 and 2.46, with an average of 1.95. For specimens tested in the current study, the values of T/T_{anc} ranged from 0.76 to 1.80, with an average value of 1.20; seven out of the 31 specimens tested in the current study had values of T/T_{anc} below 1.00 (with values ranging from 0.76 to 0.97). As previously mentioned, the net bearing area A_{brg} of the headed bars tested by Choi et al. (2002) ranged from 2.6 to $3.2A_b$, which is less than the minimum net bearing area of $4A_b$ required in ACI 318-19.

Table 3.11 Statistical parameters of T/T_{anc} values for slab specimens for which T_{anc} is governed by concrete breakout tested by DeVries et al. (1999), Choi et al. (2002), Ghimire et al. (2018), Worsfold et al. (2022), and in the current study

Test/Calculated T/T_{anc} ^[1]											
Study [tests]	All	Current Study				Worsfold et al. (2022)	Ghimire et al. (2018)	Choi et al. (2002)		DeVries et al. (1999)	
		Individual headed bars		Multiple headed bars				Center bars	Edge bars	Edge bars	Corner bars
		without parallel tie ^[2]	with parallel tie ^[3]	without parallel tie ^[4]	with parallel tie ^[5]						
Number of specimens	81	6	3	12	10	2	32	4	8	2	2
Max	2.39	1.09	1.54	1.32	1.80	2.39	1.31	0.69	0.78	1.21	1.53
Min	0.61	0.76	1.40	0.87	1.10	1.45	0.62	0.61	0.67	1.04	1.50
Mean	1.13	0.98	1.49	1.05	1.40	1.92	1.10	0.66	0.75	1.13	1.52
STD	0.293	0.116	0.077	0.138	0.227	0.664	0.173	0.032	0.038	0.120	0.026
COV	0.260	0.118	0.052	0.132	0.163	0.346	0.158	0.050	0.051	0.106	0.017
Number of specimens with $T/T_{anc} < 1.0$	25	2	0	5	0	0	6	4	8	0	0

^[1] T_{anc} is calculated using Eq. (3.6), incorporating the modification factor ψ_{mean}

^[2] Tests involved individual headed bars without parallel tie reinforcement in the joint region

^[3] Tests involved individual headed bars with parallel tie reinforcement in the joint region

^[4] Tests involved two headed bars loaded simultaneously without parallel tie reinforcement in the joint region

^[5] Tests involved two headed bars loaded simultaneously with parallel tie reinforcement in the joint region

Design Provisions – Chapter 25 of ACI 318-19

The measured failure load T on the headed bars in slab specimens tested by DeVries et al. (1999), Choi et al. (2002), Ghimire et al. (2018), Worsfold et al. (2022), and in the current study are plotted versus the calculated failure loads $T_{ACI 318}$ [based on the design provisions in Chapter 25 of ACI 318-19, Eq. (3.11)] in Figure 3.25. The values of $T_{ACI 318}$ for the headed bars tested by DeVries et al. (1999), Choi et al. (2002), and Worsfold et al. (2022) are presented in Table 3.9, and for the headed bars tested in the current study and by Ghimire et al. (2018) are presented in Tables 3.1 and 3.2, respectively.

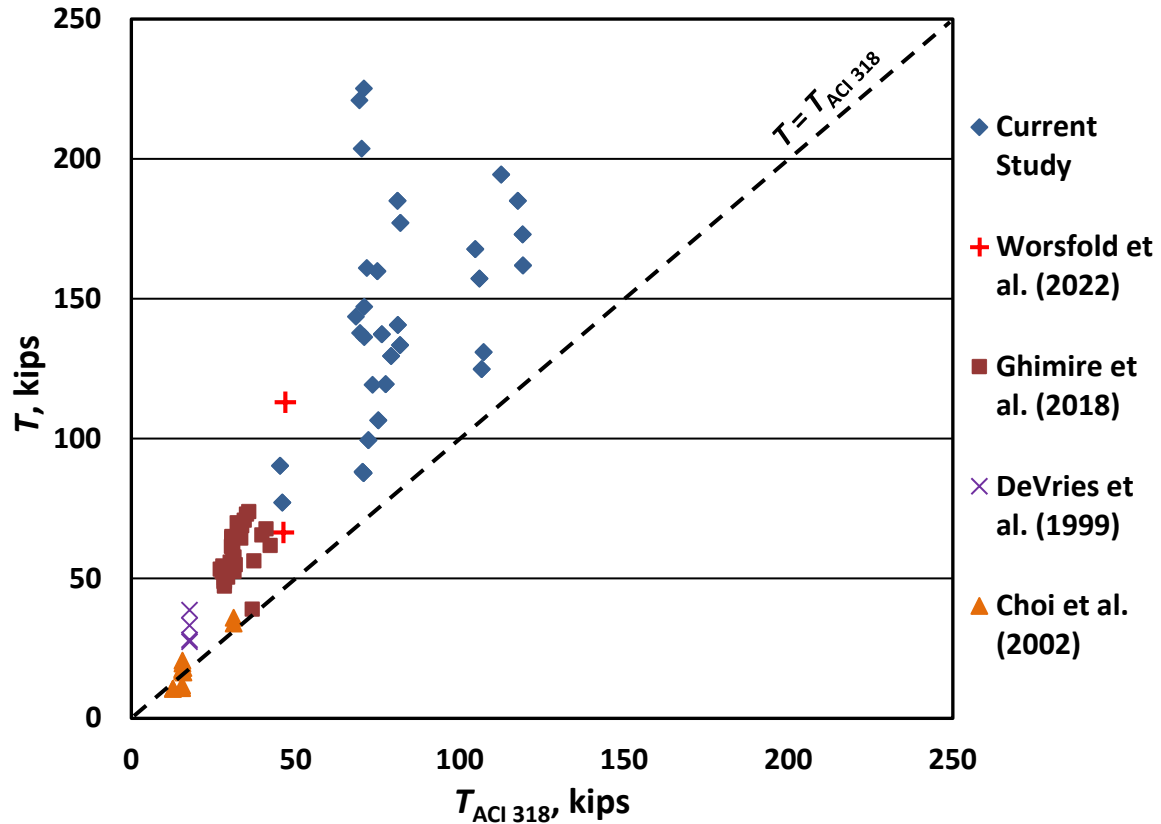


Figure 3.25 Measured force at failure T versus the anchorage strength $T_{ACI\ 318}$ calculated using Eq. (3.11) for slab specimens tested by DeVries et al. (1999), Choi et al. (2002), Ghimire et al. (2018), Worsfold et al. (2022), and in the current study

As shown in Figure 3.25, the specimens tested by DeVries et al. (1999), Ghimire et al. (2018), Worsfold et al. (2022), and in the current study, as well as 8 out of 12 specimens tested by Choi et al. (2002), exhibited higher anchorage strengths than those calculated by the design provisions Eq. (3.11), $T/T_{ACI\ 318} > 1.0$. The maximum, minimum, mean, standard deviation (STD), and coefficient of variation (COV) of $T/T_{ACI\ 318}$ for the headed bars tested by DeVries et al. (1999), Choi et al. (2002), Ghimire et al. (2018), Worsfold et al. (2022) and in the current study are presented in Table 3.12. The values of $T/T_{ACI\ 318}$ for the center bars in slab specimens tested by Choi et al. (2002) ranged from 1.04 to 1.15, with an average of 1.10, and the values of $T/T_{ACI\ 318}$ for the edge bars tested by Choi et al. (2002) ranged from 0.70 to 1.33, with an average of 0.99. The values of $T/T_{ACI\ 318}$ for the four edge and corner bars tested by DeVries et al. (1999) ranged from 1.55 to 2.18; the average for the four specimens was 1.80. The headed bars tested by Ghimire

et al. (2018) had T/T_{ACI318} ranging from 1.06 to 2.17, with an average of 1.83. The values of T/T_{ACI318} for the two specimens tested by Worsfold et al. (2022) are 1.44 and 2.41, with an average of 1.92. For specimens tested in the current study, the values of T/T_{ACI318} ranged from 1.17 to 3.18, with an average value of 1.74. These results indicate that the design provisions in Chapter 25 of ACI 318-19, Eq. (3.11), are conservative, and in most cases very conservative, in predicting the anchorage strength of headed bars anchored in column-foundation joints as expected. The design provisions in Chapter 25 of ACI 318-19, as previously stated, is a modified version of the descriptive equations, Eq. (3.3) and (3.4), with a strength reduction factor of 0.83 built-in, the square root of concrete compressive strength f'_c and ψ_c (defined in Section 3.2) rather than f_{cm} to the 0.24 power as in the descriptive equations, and use the modification factor ψ_p equal to 1 or 1.6 (intermediate values are not permitted) to represent the effect of anchored bar spacing and parallel ties instead of factors that varied as a function of bar spacing and the level of parallel tie reinforcement.

Table 3.12 Statistical parameters of T/T_{ACI318} values for slab specimens tested by DeVries et al. (1999), Choi et al. (2002), Ghimire et al. (2018), Worsfold et al. (2022), and in the current study

Test/Calculated T/T_{ACI318} ^[1]											
Study [tests]	All	Current Study				Worsfold et al. (2018)	Ghimire et al. (2018)	Choi et al. (2002)		DeVries et al. (1999)	
		Individual headed bars		Multiple headed bars				Center bars	Edge bars	Edge bars	Corner bars
		without parallel tie ^[2]	with parallel tie ^[3]	without parallel tie ^[4]	with parallel tie ^[5]						
Number of specimens	81	6	3	12	10	2	32	4	8	2	2
Max	3.18	2.25	3.18	1.99	2.28	2.41	2.17	1.15	1.33	2.18	1.58
Min	0.70	1.62	2.90	1.17	1.48	1.44	1.06	1.04	0.70	1.88	1.55
Mean	1.69	1.99	3.09	1.45	1.81	1.92	1.83	1.10	0.99	2.03	1.57
STD	0.447	0.212	0.159	0.232	0.272	0.689	0.240	0.053	0.240	0.215	0.027
COV	0.265	0.106	0.052	0.161	0.150	0.358	0.131	0.048	0.243	0.106	0.017
Number of specimens with $T/T_{ACI318} < 1.0$	4	0	0	0	0	0	0	0	4	0	0

^[1] T_{ACI318} is calculated using Eq. (3.11)

^[2] Tests involved individual headed bars without parallel tie reinforcement in the joint region

^[3] Tests involved individual headed bars with parallel tie reinforcement in the joint region

^[4] Tests involved two headed bars loaded simultaneously without parallel tie reinforcement in the joint region

^[5] Tests involved two headed bars loaded simultaneously with parallel tie reinforcement in the joint region

Proposed Code Provisions

The measured failure load T on the headed bars in slab specimens tested by DeVries et al. (1999), Choi et al. (2002), Ghimire et al. (2018), Worsfold et al. (2022), and in the current study are plotted versus the calculated failure loads T_{calc} [based on the proposed development length provisions, Eq. (3.14)] in Figure 3.26. The values of T_{calc} for the headed bars tested by DeVries et al. (1999), Choi et al. (2002), and Worsfold et al. (2022) are presented in Table 3.9, and for the headed bars tested in the current study and by Ghimire et al. (2018) are presented in Tables 3.1 and 3.2, respectively.

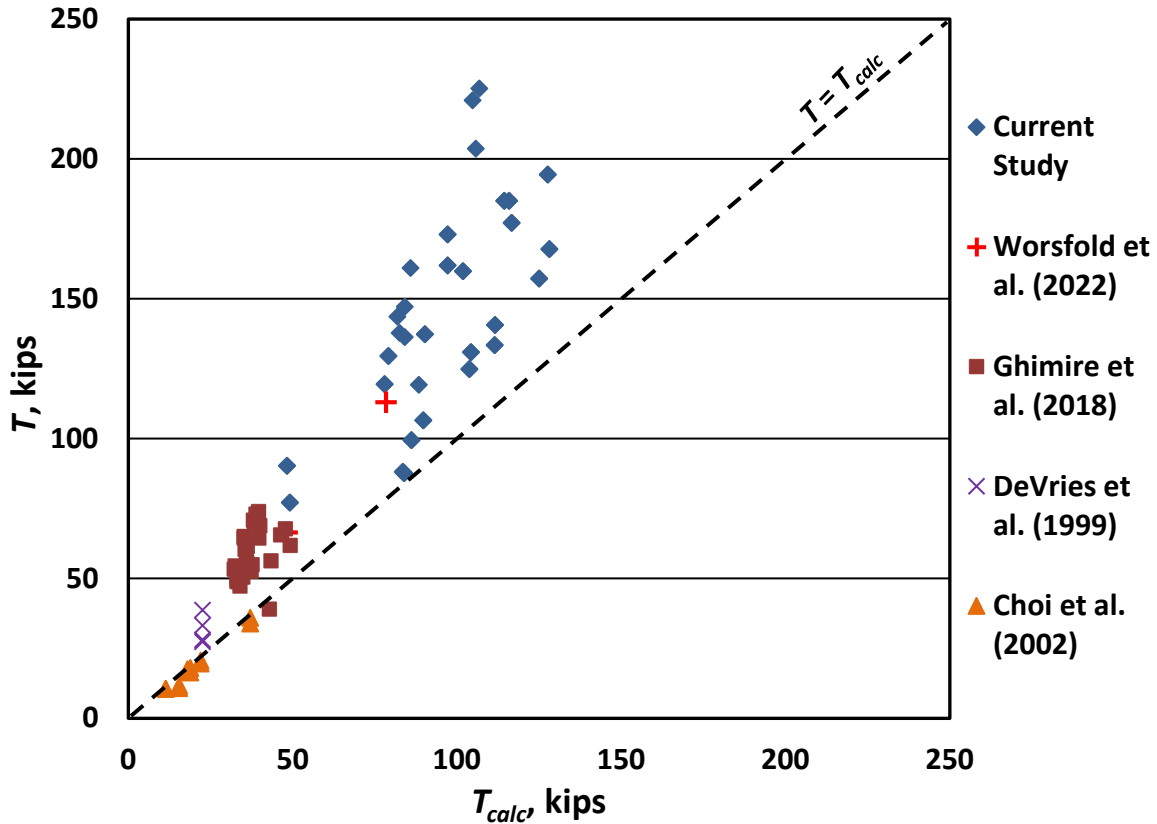


Figure 3.26 Measured force at failure T versus the anchorage strength T_{calc} calculated using Eq. (3.14) for slab specimens tested by DeVries et al. (1999), Choi et al. (2002), Ghimire et al. (2018), Worsfold et al. (2022), and in the current study

As shown in Figure 3.26, the specimens tested by DeVries et al. (1999), Ghimire et al. (2018) [except one specimen with h_{cl}/ℓ_{eh} equal to 5.6], Worsfold et al. (2022), and in the current study had higher anchorage strengths than those calculated using Eq. (3.14). In contrast, the specimens tested by Choi et al. (2002) had lower anchorage strengths than those calculated using Eq. (3.14). The maximum, minimum, mean, standard deviation (STD), and coefficient of variation (COV) of T/T_{calc} for the headed bars tested by DeVries et al. (1999), Choi et al. (2002), Ghimire et al. (2018), Worsfold et al. (2022) and in the current study are presented in Table 3.13. The values of T/T_{calc} for the center bars in slab specimens tested by Choi et al. (2002) ranged from 0.87 to 0.97, with an average of 0.93, and the values of T/T_{calc} for the edge bars tested by Choi et al. (2002) ranged from 0.70 to 0.98, with an average of 0.88. The values of T/T_{calc} for the four edge and corner bars tested by DeVries et al. (1999) ranged from 1.22 to 1.71; the average for the four

specimens is 1.41. The headed bars tested by Ghimire et al. (2018) had T/T_{calc} ranging from 0.91 to 1.88, with an average of 1.56. For the tests by Ghimire et al., only one specimen, which contained a single centrally placed headed bar with h_{cl}/ℓ_{eh} equal to 5.6, had a value of T/T_{calc} less than 1.0. The values of T/T_{calc} for the two specimens tested by Worsfold et al. (2022) are 1.38 and 1.44, with an average of 1.41. For specimens tested in the current study, the values of T/T_{calc} ranged from 1.04 to 2.11, with an average value of 1.48.

Table 3.13 Statistical parameters of T/T_{calc} values for slab specimens tested by DeVries et al. (1999), Choi et al. (2002), Ghimire et al. (2018), Worsfold et al. (2022), and in the current study

Test/Calculated T/T_{calc} ^[1]											
Study [tests]	All	Current Study				Worsfold et al. (2022)	Ghimire et al. (2018)	Choi et al. (2002)		DeVries et al. (1999)	
		Individual headed bars		Multiple headed bars				Center bars	Edge bars	Edge bars	Corner bars
		without parallel tie ^[2]	with parallel tie ^[3]	without parallel tie ^[4]	with parallel tie ^[5]						
Number of specimens	81	6	3	12	10	2	32	4	8	2	2
Max	2.11	1.88	2.11	1.87	1.62	1.44	1.88	0.97	0.98	1.71	1.25
Min	0.70	1.35	1.93	1.04	1.20	1.38	0.91	0.87	0.70	1.48	1.22
Mean	1.43	1.67	2.05	1.41	1.41	1.41	1.56	0.93	0.88	1.59	1.23
STD	0.310	0.180	0.106	0.287	0.144	0.045	0.219	0.044	0.100	0.169	0.021
COV	0.217	0.108	0.052	0.203	0.102	0.032	0.140	0.048	0.113	0.106	0.017
Number of specimens with $T/T_{calc} < 1.0$	13	0	0	0	0	0	1	4	8	0	0

^[1] T_{calc} is calculated using Eq. (3.14)

^[2] Tests involved individual headed bars without parallel tie reinforcement in the joint region

^[3] Tests involved individual headed bars with parallel tie reinforcement in the joint region

^[4] Tests involved two headed bars loaded simultaneously without parallel tie reinforcement in the joint region

^[5] Tests involved two headed bars loaded simultaneously with parallel tie reinforcement in the joint region

3.2.1.2 Comparison Between the Descriptive Equations, ACI 318-19 Code Provisions, and Proposed Code Provisions

The comparisons between the descriptive equations developed by Shao et al. (2016) Eq. (3.3) and (3.4), the provisions in Chapters 17 and 25 of ACI 318-19. Eq. (3.9) and (3.11),

respectively, and the proposed Code provisions. Eq. (3.14) are presented in this section. The four methods to predict the failure load of the headed bars anchored in a simulated column-foundation joint are compared. As previously stated, the descriptive equations were developed to give an average ratio of test-to-calculated failure load equal to 1.0 for beam-column joint specimens. In this analysis, the effective parallel tie reinforcement A_{tt} used in the descriptive equation, Eq. (3.4), is defined as the total parallel tie reinforcement within $8d_b$ radial distance from the center of the headed bar for No. 3 through No. 8 bars or within $10d_b$ for No. 9 through No. 14 bars and is not limited to a single side, as is the case in beam-column joints, as is the case in Chapter 25 of ACI 318-19. The anchorage provisions in Chapter 17 of ACI 318-19 are based on the 5% fractile. In this case, a modification factor (ψ_{mean}), 1.33, is used to convert the 5% fractile value to a mean value. The design provisions in Chapter 25 of ACI 318-19 are a modified version of the descriptive equations, Eq. (3.3) and (3.4), with a strength reduction factor, ϕ , of 0.83 built-in, the square root of concrete compressive strength f'_c and ψ_c (defined in Section 3.2) rather than f_{cm} to the 0.24 power as in the descriptive equations, and use the modification factor ψ_p equal to 1 or 1.6 (intermediate values are not permitted) to represent the effect of anchored bar spacing and parallel ties instead of factors that varied as a function of bar spacing and the level of parallel tie reinforcement. Therefore, anchorage strengths calculated based on these design provisions are expected to be conservative. Finally, the proposed Code provisions are also based on the descriptive equations, Eq. (3.3) and (3.4), with a strength reduction factor, ϕ , of 0.83 built-in, but with a more accurate representation of the effect of the concrete strength, confining reinforcement, and the center-to-center spacing between the headed bars. Therefore, the anchorage strength calculated based on proposed Code provisions is expected to be conservative as well, but not as conservative as the provisions in ACI 318-19. The results for the headed bars tested in the current study (Table 3.1) are used in this comparison.

Figure 3.27 shows the average values of T/T_h , T/T_{anc} , T/T_{ACI318} , and T/T_{calc} for tests with two headed bars loaded simultaneously without and with parallel tie reinforcement [Slab Specimens 6, 7 and 10 [(2@8.2)11-5-S5.5-7#11-0-12.75], Slab Specimens 12 and 14 [(2@6.8)14-5-B4.2-7#11-0-12.75], Slab Specimens 8, 9 and 11 [(2@8.2)11-5-S9.2-7#11-6#4-12.75], and Slab Specimens 13 and 15 [(2@6.8)14-5-B4.2-7#11-6#4-12.75], where T is the measured anchorage

strength on the headed bar at failure, T_h is the calculated anchorage strength of the headed bar [based on the descriptive equations, Eq. (3.3) and (3.4)], T_{anc} is the calculated anchorage strength of the headed bar [based on the anchorage provisions of Chapter 17 of ACI 318-19, Eq. (3.9)], $T_{ACI 318}$ is the calculated anchorage strength of the headed bar [based on the design provision in Chapter 25 of ACI 318-19, Eq. (3.11)], and T_{calc} is the calculated anchorage strength of the headed bar [based on the proposed Code provisions, Eq. (3.14)]. The specimen details and test results of the twenty tests used in this comparison are presented in Table 3.1. As shown in Figure 3.27, the average values of T/T_h for tests with two headed bars loaded simultaneously without and with parallel tie reinforcement are nearly identical at 1.12 and 1.11, respectively, indicating that the descriptive equations [Eq. (3.3) and (3.4)] provide a consistent and somewhat conservative representation of headed bars anchored in a region that is larger than a beam-column connection.

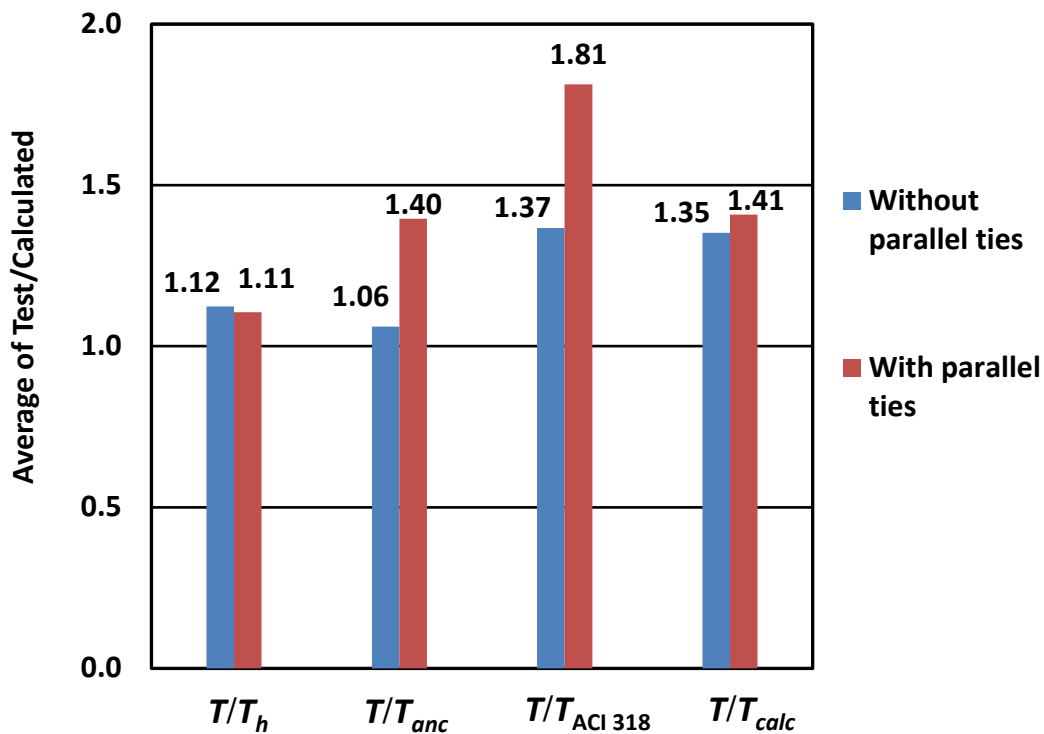


Figure 3.27 Average values of T/T_h , T/T_{anc} , $T/T_{ACI 318}$, and T/T_{calc} for tests involving two headed bars without and with parallel tie reinforcement, Slab Specimens 6, 7 and 10 [(2@8.2)11-5-S5.5-7#11-0-12.75], Slab Specimens 12 and 14 [(2@6.8)14-5-B4.2-7#11-0-12.75], Slab Specimens 8, 9 and 11 [(2@8.2)11-5-S9.2-7#11-6#4-12.75], and Slab Specimens 13 and 15 [(2@6.8)14-5-B4.2-7#11-6#4-12.75]

The average values of T/T_{anc} for tests involving two headed bars loaded simultaneously without and with parallel tie reinforcement in the joint region are 1.06 and 1.40, respectively. Student's t-test shows that the difference in the average values of T/T_{anc} for two headed bars tested simultaneously without and with parallel tie reinforcement in the joint region is statistically significant, with $p = 0.0012$. Because the anchorage provisions of Chapter 17 of ACI 318-19, [Eq. (3.9)] T_{anc} account for the contribution of concrete and parallel tie reinforcement (anchor reinforcement) separately, with only the stronger of the two controlling the strength. On the other hand, the descriptive equations (T_h) account for the contribution of both parallel tie reinforcement and concrete compressive strength on the anchorage strength of headed bars, and because T_{anc} for these specimens is governed by concrete breakout and does not include the contribution of the parallel tie reinforcement within the joint region in these tests, this difference is expected.

The average values of T/T_{ACI318} for tests including two headed bars loaded simultaneously without and with parallel tie reinforcement in the joint region are 1.37 and 1.81, respectively, a difference that is statistically significant, with $p = 0.00032$. The higher values of 1.81 results at least in part to the fact that the ACI design provisions take into account the contribution of parallel tie reinforcement for beam-column joints, but not for column-foundation joints.

The average values of T/T_{calc} for tests involving two headed bars loaded simultaneously without and with parallel tie reinforcement in the joint region are 1.35 and 1.41, respectively. Student's t-test shows that the difference in the average values of T/T_{calc} for two headed bars tested simultaneously without and with parallel tie reinforcement in the joint region is not statistically significant, with $p = 0.574$. These results indicate that proposed Code provisions [Eq. (3.14)] are conservative and consistent for this case if the contribution of parallel ties can be counted.

Summary

The anchorage provisions in Chapter 17 and the design provisions in Chapter 25 of ACI 318-19 Equations (3.9) and (3.11), respectively, do not accurately capture the effect of parallel tie reinforcement on the anchorage strength of headed bars tested with parallel tie reinforcement within the joint region. On the other hand, the descriptive equations [Eq. (3.3) and (3.4)] and the proposed Code provisions [Eq. (3.14)] accurately capture the effect of parallel tie reinforcement on the anchorage strength. In these tests, T_{anc} is governed by the concrete breakout strength N_{cbg}

[Eq. (3.6), incorporating the modification factor ψ_{mean}], which does not account for the contribution of anchor reinforcement to anchorage strength. That is, the anchorage provisions in Chapter 17 of ACI 318-19 [Eq. (3.9)] T_{anc} account for the contribution of concrete and parallel tie reinforcement (anchor reinforcement) separately, with only the stronger of the two controlling the strength. In contrast, the descriptive equations [Eq. (3.3) and (3.4)] T_h account for the contribution of both parallel tie reinforcement and concrete to anchorage strength. The design provisions in Chapter 25 of ACI 318-19 [Eq. (3.11)] T_{ACI318} do not consider the effect of parallel tie reinforcement for other than beam-column joints or the spacing between headed bars when the headed bars are spaced at a center-to-center distance less than $6d_b$. On the other hand, the Code provisions as proposed here [Eq. (3.14)] account for the contribution of parallel tie reinforcement and the effect of the center-to-center spacing between the headed bars on the anchorage strength.

3.3 RECOMMENDED CHANGES TO CHAPTERS 17 AND 25 OF ACI 318-19

Based on the analysis of the data presented in this chapter and the observations described in Sections 3.2.1.1 and 3.2.1.2, the following changes are recommended for ACI 318.

- 1- The anchorage provisions in Chapter 17 of ACI 318-19 do not accurately predict the anchorage strength of headed bars tested when parallel tie/anchor reinforcement is used. The anchorage provisions account for the contribution of concrete and parallel tie reinforcement (anchor reinforcement) separately, with only the stronger of the two controlling the strength. Therefore, the ACI 318 Code should consider including provisions that combine the contributions of concrete strength and parallel tie reinforcement.
- 2- The contributions of concrete strength and parallel tie reinforcement are combined in the descriptive equations [Eq. (3.3) and (3.4)]. Based on the analysis presented in this chapter, the descriptive equations [Eq. (3.3) and (3.4)] accurately capture the effect of parallel tie reinforcement and the contribution of concrete strength to the anchorage strength of headed bars. Therefore, a version of the descriptive equations [Eq. (3.3) and (3.4)] could be used within the anchorage provisions in Chapter 17 of the ACI 318 Code.

- 3- The design provisions in Chapter 25 of ACI 318-19 [Eq. (3.10)] do not consider the contribution of parallel tie reinforcement to the development of headed bars anchored in members other than beam-column joints. Furthermore, the design provisions in Chapter 25 of ACI 318-19 ignore the contribution of parallel tie reinforcement when headed bars are spaced at a center-to-center distance equal to or greater than $6d_b$. However, the analysis presented by Shao et al. (2016) for beam-column joints and in this chapter for column-foundation joints shows that the effect of parallel tie reinforcement is real even for widely-spaced headed bars. Therefore, the design provisions in Chapter 25 of ACI 318-19 should be further modified to accurately represent the effect of parallel tie reinforcement, headed bar spacing, and concrete strength.
- 4- Based on the analysis presented in Sections 3.2.1.1 and 3.2.1.2, the proposed Code provisions [Eq. (3.12) and (3.13)] accurately capture the effect of parallel tie reinforcement on the anchorage strength of headed bars. Therefore, the ACI 318 Code should consider including proposed Code provisions [Eq. (3.12) and (3.13)] in the next version. Section 3.3.1 addresses the proposed changes in Chapter 25 of ACI 318-19.

3.3.1 Proposed Changes in Chapter 25 of ACI 318-19

Based on the analysis presented in this chapter and the summary presented in Sections 3.2.1.2 and 3.3, proposed changes to Chapter 25 of ACI 318-19 are provided in this section. The original text of the Code is presented in black, while proposed code and commentary changes are shown in **red underlined** or **strikeout**.

25.4.4 *Development of headed deformed bars in tension*

25.4.4.1 Use of a head to develop a deformed bar in tension shall be permitted if conditions (a) through (f) are satisfied:

- (a) Bar shall conform to 20.2.1.6
- (b) Bar size shall not exceed No. 11
- (c) Net bearing area of head A_{brg} shall be at least $4A_b$
- (d) Concrete shall be normalweight

- (e) Clear cover for bar shall be at least $2d_b$
- (f) Center-to-center spacing between bars shall be at least $3d_b$

R25.4.4 Development of headed deformed bars in tension

R25.4.4.1 As used in this section, development describes cases in which the force in the bar is transferred to the concrete through a combination of a bearing force at the head and bond forces along the bar. In contrast, Chapter 17 anchorage provisions describe cases in which the force in the bar is transferred through bearing to the concrete at the head alone. Headed bars are limited to those types that meet the criteria in 20.2.1.6 for Class HA heads.

The provisions for headed deformed bars were formulated with due consideration of the provisions for anchorage in Chapter 17 (Shao et al. 2016). Chapter 17 contains provisions for headed anchors related to the individual failure modes of concrete breakout, side-face blowout, and pullout. These failure modes were considered in the formulation of 25.4.4.2. The restrictions to maximum bar size of No. 11 and normalweight concrete are based on a lack of data for larger bars or lightweight concrete (Thompson et al. 2005, 2006a,b; Shao et al. 2016). ~~The upper limit of 60,000 psi on f_y that appeared prior to the 2019 Code has been removed.~~

For bars in tension, heads allow the bars to be developed in a shorter length than required for standard hooks, but otherwise perform in a similar manner (Thompson et al. 2005, 2006a,b; Shao et al. 2016). The head is considered to be part of the bar for the purposes of satisfying the specified cover requirements in 20.5.1.3 and aggregate size requirements of 26.4.2.1(a)(5).

Headed bars with $A_{brg} < 4A_b$ have been used in practice, but their performance is not accurately represented by the provisions in 25.4.4.2, and they should be used only with designs that are supported by test results under 25.4.5. These provisions do not address the design of studs or headed stud assemblies used for shear reinforcement.

25.4.4.2 Development length ℓ_{dt} for headed deformed bars in tension shall be the longest of (a) through (c):

$$(a) \frac{\left(\frac{f_y \Psi_e \Psi_p \Psi_o \Psi_c}{75 \sqrt{f'_c}} \right) d_b^{1.5}}{\left(\frac{f_y \Psi_e \Psi_p \Psi_o}{600 f'_c{}^{0.25}} \right) d_b^{1.5}} \text{ with } \Psi_e, \Psi_p, \text{ and } \Psi_o, \text{ and } \Psi_c \text{ given in 25.4.4.3}$$

and where the value of f'_c used to calculate ℓ_{dt} shall not exceed 16,000 psi

(b) $8d_b$

(c) 6 in.

R25.4.4.2 The provisions for developing headed deformed bars give the length of bar, ℓ_{dt} , measured from the critical section to the bearing face of the head, as shown in Fig. R25.4.4.2a. The provisions are primarily based on tests of simulated beam-column joints and have been verified up to concrete compressive strengths of 16,000 psi and bar stresses at failure up to 150,000 psi (Shao et al. 2016, Ghimire et al. 2019).

If longitudinal headed deformed bars from a beam, slab, or corbel terminate in a supporting member, such as the column shown in Fig. R25.4.4.2b, the bars should extend through the joint to the far face of the confined core of the supporting member, allowing for cover and avoidance of interference with column reinforcement, even though the resulting anchorage length may exceed ℓ_{dt} . Extending the bar to the far side of the column core helps engage the entire joint in resisting the anchorage forces and thereby improves the performance of the joint.

If closely spaced headed bars are used, the potential for concrete breakout failure exists. For joints as shown in Fig. R25.4.4.2c and R25.4.4.2d, anchorage strengths will be generally higher if the anchorage length is equal to or greater than $d/1.5$ (Eligehausen 2006b), as shown in Fig. R25.4.4.2c, or by providing reinforcement in the form of hoops and ties to establish a load path in accordance with strut-and-tie modeling principles, as shown in Fig. R25.4.4.2d. Strut-and-tie models should be verified in accordance with Chapter 23. Note that the strut-and-tie models illustrated in Fig. R25.4.4.2c and R25.4.4.2d rely on a vertical strut from a column extending above the joint. Beam-column joints at roof-level and portal frames are vulnerable to joint failure and should be properly detailed to restrain diagonal cracking through the joint and breakout of the bars through the top surface.

For cases where development length cannot be designed in accordance with 25.4.4.2, use of the provisions of Chapter 17 should be considered.

25.4.4.3 For the calculation of ℓ_{dt} , modification factors ψ_e , ψ_p , and ψ_o , ~~and ψ_e~~ shall be in

accordance with Table 25.4.4.3.

Table 25.4.4.3—Modification factors for development of headed bars in tension

Modification factor	Condition	Value of factor
Epoxy ψ_e	Epoxy-coated or zinc and epoxy dual-coated reinforcement	1.2
	Uncoated or zinc-coated (galvanized) reinforcement	1.0
Parallel tie reinforcement ψ_p	For No. 11 and smaller bars with $A_{tr} \geq 0.3A_{hs}$ or $s^{[1]} \geq 6d_b^{[2,3]}$	1.0
	Other	1.6
Parallel tie reinforcement and headed bar spacing $\psi_p^{[3]}$	$s^{[1]} \geq 3d_b^{[2]}$ When calculating ψ_p , A_{tr}/A_{hs} shall not exceed 0.3 and s/d_b shall not exceed 8	$\frac{1}{4} \left(7 - 10 \frac{A_{tr}}{A_{hs}} - 0.5 \frac{s}{d_b} + \frac{A_{tr}}{A_{hs}} \frac{s}{d_b} \right)$
Location ψ_o	For headed bars: (1) Terminating inside column core with side cover to bar ≥ 2.5 in.; or (2) With side cover to bar $\geq 6d_b$	1.0
	Other	1.25
Concrete strength ψ_e	For $f'_e < 6000$ psi	$f'_e/15,000 + 0.6$
	For $f'_e \geq 6000$ psi	1.0

^[1]s is minimum center-to-center spacing of headed bars

^[2] d_b is nominal diameter of headed bar.

^[3]Refer to 25.4.4.5.

R25.4.4.3 The epoxy factor 1.2 is based conservatively on the value used for epoxy-coated standard hooks. The location factor ψ_o accounts for the confinement provided by the reinforcement within columns and large side cover for other members.

The factor ψ_p for headed reinforcement is similar to the confining reinforcement factor for

hooked bars (Shao et al. 2016). Like confining reinforcement for hooked bars, parallel ties are more effective for more closely-spaced headed bars, and the effects of increasing the area of parallel ties and increasing the spacing of headed bars are not directly additive. Unlike hooked bars, ~~however,~~ test results indicate that only tie or hoop reinforcement parallel to headed bars contributes to anchorage strength and reduces development length (Thompson et al. 2005, 2006a,b).

25.4.4.4 For beam column joints, the total cross-sectional area of parallel tie reinforcement A_{tt} shall consist of ties or stirrups oriented parallel to ℓ_{dt} and located within $8d_b$ of the centerline of the headed bar toward the middle of the joint, where d_b is the nominal diameter of the headed bar.

R25.4.4.4 Reinforcement oriented parallel to the development length of the headed bars, located within the region defined in 25.4.4.4 (Fig. R25.4.4.4) contributes to anchorage strength in proportion to its area (Shao et al. 2016). This reinforcement serves to tie concrete near the head to concrete on the other side of the failure surface, thus mobilizing additional anchorage strength. With the exception of vertical joint reinforcement in the form of stirrups that are well anchored to the far side of the joint, reinforcement oriented perpendicular to the development length has been shown in a number of cases to be ineffective in improving the anchorage of headed deformed bars (Thompson et al. 2005, 2006a,b). Both legs of individual stirrups and ties parallel to the headed bars contribute to A_{tt} .

25.4.4.5 For anchorages other than in beam-column joints, parallel tie reinforcement, A_{tt} , shall ~~not be considered, taken as the total parallel tie reinforcement located on all sides of the headed bars within an $8d_b$ radial distance from the centerline of the headed bars and ψ_p shall be taken as 1.0 provided the spacing is at least $6d_b$.~~

R25.4.4.5 ~~No evidence is available regarding the effect of parallel reinforcement on the development length of headed bars except in beam-column joints~~ For members other than beam-column joints, test results indicate that the total cross-section area of parallel tie reinforcement A_{tt}

located on all sides of headed bars within $8d_b$ of the centerline of headed bars, not limited to a single side as is the case in beam-column joints, contribute to anchorage strength.

CHAPTER 4: ANALYSIS OF BEAM-COLUMN JOINT SPECIMENS WITH BEAM BARS ANCHORED WITH HOOKS SUBJECTED TO REVERSED CYCLIC LOADING

4.1 INTRODUCTION

An analysis of exterior beam-column joint specimens containing hooked bars tested under reversed cyclic loading is presented in this chapter. The results of 146 specimens from 24 studies were analyzed using descriptive equations for anchorage strength and design provisions for the development length of hooked bars proposed by Ajaam et al. (2017), presented in detail in Section 1.3.2. The effects of test parameters, including embedment length, concrete compressive strength, center-to-center spacing between the hooked bars, bar size, and confining reinforcement within the joint region on the performance of the beam-column joints subjected to reversed cyclic loading are discussed.

This chapter includes the results of exterior beam-column joint specimens tested under reversed cyclic loading by Hanson and Connor (1967), Hanson (1971), Megget (1974), Uzumeri (1977), Lee et al. (1977), Scribner (1978), Paulay and Scarpas (1981), Ehsani and Wight (1982), Kanada et al. (1984), Zerbe and Durrani (1985), Ehsani et al. (1987), Ehsani and Alameddine (1991), Kaku and Asakusa (1991), Tsonos et al. (1992), Pantelides et al. (2002), Chutarat and Aboutaha (2003), Hwang et al. (2005), Lee and Ko (2007), Chun et al. (2007), Tsonos (2007), Kang et al. (2010), Chun and Shin (2014), Hwang et al. (2014), and Choi and Bae (2019). Complete details of these studies are presented in Appendix D.

4.2 ANALYSIS BASED ON PROPOSED DESCRIPTIVE AND DESIGN EQUATIONS

Test results of 146 exterior beam-column joint specimens subjected to reversed cyclic loading are analyzed using descriptive equations for anchorage strength and design provisions for the development length of hooked bars based on monotonic loading. The analysis is conducted to investigate the applicability of these equations to joints subjected to reversed cyclic loading.

4.2.1 Descriptive Equations and Design Provisions Proposed by Ajaam et al. (2017)

Ajaam et al. (2017) developed descriptive equations for anchorage strength and design provisions for the development length of hooked bars, as described in Section 1.3.2, based on test

results of 353 exterior beam-column joint specimens subjected to monotonic loading. Equations (4.1) and (4.2) are the descriptive equations for the anchorage strength of hooked bars without and with confining reinforcement, respectively.

$$T_h = \left(294 f_{cm}^{0.295} \ell_{eh}^{1.0845} d_b^{0.47} \right) \left(0.0974 \frac{c_{ch}}{d_b} + 0.3911 \right) \quad (4.1)$$

with $\left(0.0974 \frac{c_{ch}}{d_b} + 0.3911 \right) \leq 1.0$

$$T_h = \left(294 f_{cm}^{0.295} \ell_{eh}^{1.0845} d_b^{0.47} + 55050 \left(\frac{A_{th}}{n} \right)^{1.0175} d_b^{0.73} \right) \left(0.0516 \frac{c_{ch}}{d_b} + 0.6572 \right) \quad (4.2)$$

with $\left(0.0516 \frac{c_{ch}}{d_b} + 0.6572 \right) \leq 1.0$

where T_h is the anchorage strength of a hooked bar (lb) equal to the product of the area of a hooked bar, A_b , and the bar stress at anchorage failure, f_s ; f_{cm} is the measured concrete compressive strength (psi); ℓ_{eh} is the embedment length of the hooked bar (in.); d_b is the diameter of the hooked bar (in.); c_{ch} is the center-to-center spacing between hooked bars (in.); A_{th} is the total cross-sectional area of all parallel confining reinforcement located within $8d_b$ of the top of the hooked bars for No. 3 through No. 8 bars or within $10d_b$ for No. 9 through No. 11 bars (in.²), as shown in Figure (4.1); and n is the number of hooked bars being developed in tension.

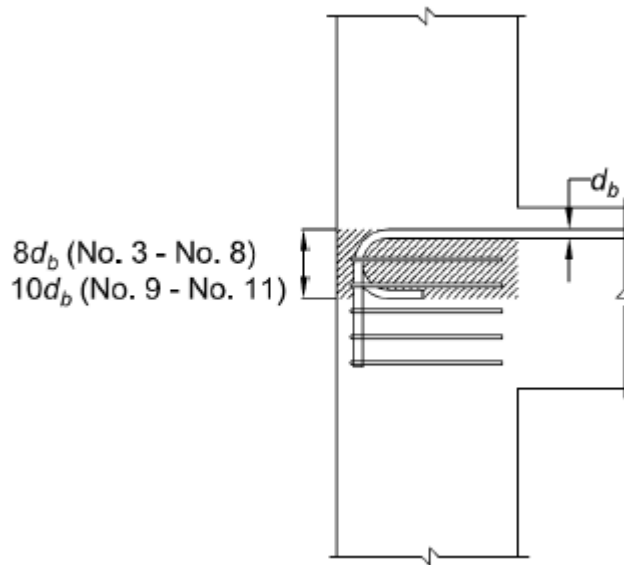


Figure 4.1 Effective confining reinforcement for hooked bars within the joint region of beam-column joints suggested by Ajaam et al. (2017)

Ajaam et al. (2017) developed design provisions [Eq. (4.3)] for the development length of hooked bars based on the descriptive equations [Eq. (4.1) and (4.2)]. The design provisions incorporate a strength reduction factor of 0.81 to ensure that no more than 5% of the specimens used to develop the equation have a ratio of test-to-calculated failure load less than 1.0.

$$\ell_{dh} = 0.003 \frac{f_y \psi_e \psi_{cs} \psi_o}{\lambda f_c^{1.25}} d_b^{1.5} \quad (4.3)$$

where ℓ_{dh} is the development length of a hooked bar in tension (in.) not less than the greater of $8d_b$ and 6 in.; f_y is the specified yield strength of the hooked bar (psi); ψ_e is a modification factor for epoxy coated or zinc and epoxy dual-coated reinforcement; ψ_{cs} is a modification factor for confining reinforcement and bar spacing; ψ_o is a modification factor for bar location; λ is a factor for lightweight concrete; f_c is the specified concrete compressive strength (psi); d_b is the diameter of the hooked bar (in.).

The proposed design provisions apply to hooked bars with yield strengths up to 120,000 psi and concrete compressive strengths up to 16,000 psi. The modification factor ψ_e is equal to 1.2 for epoxy-coated or zinc and epoxy dual-coated reinforcement and 1.0 for uncoated or zinc-coated (galvanized) reinforcement, and is retained from the current code provisions; the factor ψ_o is equal to 1.0 for hooked bars terminating inside a column core with clear side cover to the bar ≥ 2.5 in., or terminating in a supporting member with side cover to the bar $\geq 6d_b$; in other cases, ψ_o is taken as 1.25. Values for the confining reinforcement and bar spacing factor ψ_{cs} are calculated using Table 4.1. The factor λ is equal to 0.75 for lightweight concrete and 1.0 for normalweight concrete and is retained from the current code provisions.

Table 4.1 Modification factor ψ_{cs} for confining reinforcement, expressed as ratio of area of confining reinforcement, A_{th} , to area of hooked bars, A_{hs} , and center-to center bar spacing, c_{ch} ^[1]

Confinement level	f_y	c_{ch}	
		$2d_b$	$\geq 6d_b$
$\frac{A_{th}}{A_{hs}} \geq 0.2$ ^[2] or $\frac{A_{th}}{A_{hs}} \geq 0.4$ ^[3]	60,000	0.6	0.5
	120,000	0.66	0.55
No confining reinforcement	all	1.0	0.6

^[1] ψ_{cs} may be linearly interpolated for spacing or yield strengths not listed

^[2] Confining reinforcement parallel to straight portion of bar

^[3] Confining reinforcement perpendicular to straight portion of bar

4.2.2 Exterior Beam-Column Joints

The performance of 146 exterior beam-column joint specimens subjected to reversed cyclic loading is examined in this section using the descriptive equations for the anchorage strength and design provisions for the development length of hooked bars. Relevant details of the beam-column joint specimens are presented in Table 4.2, and complete details are presented in Appendix C. Table 4.2 includes the key parameters of the test specimens: f_y is the measured yield strength of the hooked bars; c_{so} is the clear concrete cover to the bar; ℓ_{eh} is the embedment length of the hooked bar; ℓ_{ehy} is the embedment length required to yield the hooked bar; d is the distance from the centroid of the tension bar to the extreme compression fiber of the beam; M_n is the nominal flexural strength of the test beam; M_{peak} is the peak moment applied to the test beam; V_p is the peak joint shear applied at the beam-column joint; V_n is the nominal joint shear strength; $\delta_{0.8 peak}$ is the drift ratio at drop to 80% of the peak load, where the drift is defined as the ratio of displacement at the loading point in the direction of the load to the distance between the loading point and center of the beam-column joints; T' is the estimated test failure load on the hooked bar calculated using Eq. (4.4).

The appropriate descriptive equation, Eq. (4.1) or (4.2), is used to calculate the embedment length required to yield a hooked bar based on the measured (not specified) yield strength, by

solving for ℓ_{eh} and replacing T_h with $A_b f_y$. The nominal flexural strength M_n of the test beam is also calculated based on the measured yield strength (Darwin and Dolan 2021). When calculating the nominal flexural strength, compression reinforcement is not considered unless the member is over-reinforced, as was the case for specimens I, I-A, and V tested by Hanson and Connor (1967); specimens 9 through 12 tested by Scribner (1978); all specimens tested by Pantelides et al. (2002); T3-600 tested by Hwang et al. (2014); and H0.7S, H1.0S, H0.7U, and H1.0U tested by Chun and Shin (2014), which were analyzed as doubly reinforced sections. The peak moment applied to the test beam M_{peak} is calculated at the beam-column joint interface, which is also the critical section for the hooked bars in tension.

Table 4.2 Detail of exterior beam-column joint specimens tested under reversed cyclic loading

Study ^[1]		Specimen	Bar Size ^[2]	f_y (ksi)	f_{cm} (psi)	c_{so} (in.)	$\frac{c_{ch}}{d_b}$	$\frac{A_{th}}{A_{hs}}$	ℓ_{eh} (in.)	ℓ_{ehy} (in.)
1	Hanson and Connor (1967)	I ^[3]	No. 9	51.6	3470	3.0	2.3	0.30	13.5	11.2
		I-A ^[3]	No. 9	47.8	3200	3.0	2.3	0.17	13.5	10.8
		II	No. 9	48.3	3650	3.0	2.3	0.30	13.5	10.3
		V ^{[3][4]}	No. 9	51.0	3300	3.0	2.3	0.00	13.5	16.6
		V-A ^[4]	No. 9	49.8	5420	3.0	2.3	0.00	13.5	16.4
2	Hanson (1971)	1 ^[5]	No. 8	63.1	5500	3.0	2.7	0.38	13.5	11.8
		3 ^[5]	No. 8	64.1	5200	3.0	2.7	0.21	13.5	12.1
		4	No. 8	63.4	5380	3.0	2.7	0.14	13.5	12.6
		5	No. 8	65.0	5230	3.0	2.7	0.21	13.5	12.2
3	Megget (1974)	Unit A	D25	54.7	3200	3.3	2.7	0.68	12.6	11.7
4	Uzumeri (1977)	1 ^{[4][5]}	No. 9	50.3	4460	3.5	3.0	0.00	13.0	15.6
		2 ^[4]	No. 9	50.6	4510	3.5	3.0	0.00	13.0	15.7
		3 ^[5]	No. 9	50.8	3920	3.5	3.0	0.29	13.0	11.5
		4 ^[5]	No. 9	50.6	4490	3.5	3.0	0.53	13.0	11.1
		5 ^{[4][5]}	No. 9	50.4	4630	2.0	4.4	0.00	13.0	16.2
		6	No. 9	51.1	5250	2.0	4.4	0.93	13.0	12.6
		7	No. 9	51.1	4460	2.0	4.4	0.53	13.0	13.1
		8	No. 9	51.1	3820	2.0	2.9	0.70	13.0	15.1
5	Lee et al. (1977)	1	No. 6	52.5	4200	2.4	3.3	1.00	9.4	8.6
		2	No. 6	48.6	4200	2.4	3.3	1.00	9.4	7.9
		3	No. 6	48.7	4100	2.4	3.3	0.23	9.4	8.0
		4	No. 6	48.9	4000	2.4	3.3	0.23	9.4	8.1
		5	No. 6	50.9	3600	2.4	3.3	1.00	9.4	8.7
		6	No. 6	51.6	3600	2.4	3.3	0.23	9.4	8.8
		7	No. 6	47.5	3700	2.4	3.3	0.23	9.4	8.0
		8	No. 6	48.2	4200	2.4	3.3	0.23	9.4	7.9

^[1] Values given in SI units are converted to in.-lb (1 in. = 25.4 mm; 1 psi = 1/145 MPa; and 1 kip = 4.4484 kN); notations used in these studies are described in Appendix A

^[2] Bar sizes are presented in SI and in.-lb as reported in the original studies

^[3] Analyzed as a doubly reinforced section to calculate the nominal flexural strength M_n ; all other specimens are analyzed as a single reinforced

^[4] Specimens did not contain confining reinforcement parallel to the hooked bars within the joint region

^[5] Specimens had transverse beams on one or both sides of the test beam. These transverse beams meet the dimensional requirements of Sections 18.8.4 and 15.2.8 of ACI 318-19 and Section 4.3 of ACI 352R-02 to be considered effective in increasing the joint shear strength

^[6] Specimens had $d/\ell_{eh} > 1.5$

Table 4.2 Cont. Detail of exterior beam-column joint specimens tested under reversed cyclic loading

Study ^[1]		Specimen	$\frac{\ell_{eh}}{\ell_{ehy}}$	$\frac{d}{\ell_{eh}}$	M_n (kip.in.)	M_{peak} (kip.in.)	$\frac{M_{peak}}{M_n}$	$\frac{V_p}{V_n}$	$\delta_{0.8 peak}$ ^[7]	$\frac{T'}{T_h}$
1	Hanson and Connor (1967)	I ^[3]	1.21	1.33	3018	3384	1.12	0.91	0.043	1.12
		I-A ^[3]	1.24	1.33	2796	2976	1.06	0.83	0.057	1.06
		II	1.32	1.33	2892	3036	1.05	0.80	0.035	1.04
		V ^{[3][4]}	0.81	1.33	2964	2640	0.89	0.73	0.051	1.11
		V-A ^[4]	0.82	1.33	3156	3372	1.07	0.95	0.021	1.32
2	Hanson (1971)	1 ^[5]	1.15	0.62	3229	3374	1.04	0.72	0.060	1.04
		3 ^[5]	1.11	0.62	3253	3662	1.13	0.80	0.035	1.12
		4	1.08	0.62	3234	3638	1.13	0.99	0.030	1.12
		5	1.10	0.62	3294	3614	1.10	0.98	0.045	1.09
3	Megget (1974)	Unit A	1.07	1.25	1923	1944	1.01	1.01	0.175	1.01
4	Uzumeri (1977)	1 ^{[4][5]}	0.83	1.35	2340	2475	1.06	0.63	0.033	1.29
		2 ^[4]	0.83	1.35	2352	2419	1.03	0.76	0.021	1.26
		3 ^[5]	1.13	1.35	2340	2588	1.11	0.69	0.055	1.10
		4 ^[5]	1.17	1.35	2352	2700	1.15	0.73	0.095	1.14
		5 ^{[4][5]}	0.80	1.35	2364	2531	1.07	0.60	0.016	1.36
		6	1.03	1.35	2412	2700	1.12	0.84	0.061	1.11
		7	0.99	1.35	2400	2813	1.17	0.87	0.063	1.18
		8	0.86	1.35	3132	3263	1.04	1.13	0.045	1.19
5	Lee et al. (1977)	1	1.09	0.85	332	372	1.12	0.80	0.042	1.11
		2	1.18	0.85	310	349	1.12	0.75	0.055	1.12
		3	1.17	0.85	310	314	1.01	0.69	0.042	1.01
		4	1.16	0.85	310	360	1.16	0.80	0.055	1.16
		5	1.08	0.85	317	382	1.20	0.89	0.059	1.20
		6	1.06	0.85	321	371	1.16	0.87	0.062	1.15
		7	1.17	0.85	300	361	1.20	0.83	0.060	1.20
		8	1.19	0.85	308	355	1.15	0.77	0.058	1.15

^[1] Values given in SI units are converted to in.-lb (1 in. = 25.4 mm; 1 psi = 1/145 MPa; and 1 kip = 4.4484 kN); notations used in these studies are described in Appendix A

^[3] Analyzed as a doubly reinforced section to calculate the nominal flexural strength M_n ; all other specimens are analyzed as a single reinforced

^[4] Specimens did not contain confining reinforcement parallel to the hooked bars within the joint region

^[5] Specimens had transverse beams on one or both sides of the test beam. These transverse beams meet the dimensional requirements of Sections 18.8.4 and 15.2.8 of ACI 318-19 and Section 4.3 of ACI 352R-02 to be considered effective in increasing the joint shear strength

^[6] Specimens had $d/\ell_{eh} > 1.5$

^[7] Drift ratio at drop to 80% of the peak load

Table 4.2 Cont. Detail of exterior beam-column joint specimens tested under reversed cyclic loading

Study ^[1]	Specimen	Bar Size ^[2]	f_y (ksi)	f_{cm} (psi)	c_{so} (in.)	$\frac{c_{ch}}{d_b}$	$\frac{A_{th}}{A_{hs}}$	ℓ_{eh} (in.)	ℓ_{ehy} (in.)	
6	Scribner (1978)	1	No. 6	48.9	4950	1.0	6.9	0.75	11.0	6.3
		2	No. 6	48.9	5050	1.0	6.9	0.75	11.0	6.2
		3	No. 6	48.9	4940	1.5	2.8	0.67	10.5	7.9
		4	No. 6	48.9	4950	1.5	2.8	0.67	10.5	7.9
		5	No. 6	52.7	3680	1.0	6.9	0.75	11.0	7.4
		6	No. 6	52.7	4080	1.0	6.9	0.75	11.0	7.2
		7	No. 6	52.7	3840	1.5	2.8	0.67	10.5	9.2
		8	No. 6	52.7	3920	1.5	2.8	0.67	10.5	9.1
		9 ^[3]	No. 8	60.2	5130	2.4	2.1	0.25	16.6	15.1
		10 ^[3]	No. 8	60.2	5210	2.4	2.1	0.25	16.6	15.0
		11 ^[3]	No. 8	60.2	4730	2.4	2.1	0.25	16.6	15.4
		12 ^[3]	No. 8	60.2	4760	2.4	2.1	0.25	16.6	15.4
7	Paulay and Scarpas (1981)	Unit 1	D20	42.9	3280	3.4	4.4	0.48	16.6	5.8
		Unit 2	D20	42.9	3260	3.4	4.4	0.25	16.6	5.8
		Unit 3	D20	42.9	3900	3.4	4.4	0.33	16.6	5.5
8	Ehsani and Wight (1982)	2 ^[6]	No. 7	48.0	5070	2.4	3.5	0.11	7.4	9.6
		4 ^[6]	No. 7	48.0	6470	2.4	3.5	0.22	7.4	8.4
9	Kanada et al. (1984)	U40L ^[4]	D19	56.2	3530	2.4	2.8	0.00	9.0	13.2
		U41L	D19	56.2	3870	2.4	2.8	0.22	9.0	9.8
		U42L	D19	56.2	4370	2.4	2.8	0.33	9.0	9.5
		U41S ^[6]	D19	56.2	3870	2.4	2.8	0.22	6.0	9.8
		U42S ^[6]	D19	56.2	4370	2.4	2.8	0.33	6.0	9.5
		U20L ^[4]	D19	56.2	3870	2.4	8.4	0.00	9.0	8.8
		U21L	D19	56.2	4370	2.4	8.4	0.45	9.0	7.5
		U21S ^[6]	D19	56.2	3870	2.4	8.4	0.45	6.0	7.8
		U22S ^[6]	D19	56.2	4370	2.4	8.4	0.67	6.0	7.5
		R41L	D19	56.2	3140	2.4	2.8	0.22	9.0	10.4
		R42S ^[6]	D19	56.2	3140	2.4	2.8	0.33	6.0	10.4

^[1] Values given in SI units are converted to in.-lb (1 in. = 25.4 mm; 1 psi = 1/145 MPa; and 1 kip = 4.4484 kN); notations used in these studies are described in Appendix A

^[2] Bar sizes are presented in SI and in.-lb as reported in the original studies

^[3] Analyzed as a doubly reinforced section to calculate the nominal flexural strength M_n ; all other specimens are analyzed as a single reinforced

^[4] Specimens did not contain confining reinforcement parallel to the hooked bars within the joint region

^[5] Specimens had transverse beams on one or both sides of the test beam. These transverse beams meet the dimensional requirements of Sections 18.8.4 and 15.2.8 of ACI 318-19 and Section 4.3 of ACI 352R-02 to be considered effective in increasing the joint shear strength

^[6] Specimens had $d/\ell_{eh} > 1.5$

Table 4.2 Cont. Detail of exterior beam-column joint specimens tested under reversed cyclic loading

Study ^[1]		Specimen	$\frac{\ell_{eh}}{\ell_{ehy}}$	$\frac{d}{\ell_{eh}}$	M_n (kip.in.)	M_{peak} (kip.in.)	$\frac{M_{peak}}{M_n}$	$\frac{V_p}{V_n}$	$\delta_{0.8 peak}$ ^[7]	$\frac{T'}{T_h}$
6	Scribner (1978)	1	1.75	0.78	343	481	1.41	0.70	0.060	1.40
		2	1.76	0.78	343	498	1.45	0.72	0.058	1.44
		3	1.32	0.96	590	706	1.20	0.88	0.047	1.19
		4	1.32	0.96	747	818	1.10	1.03	0.063	1.09
		5	1.49	0.78	356	453	1.27	0.76	0.066	1.26
		6	1.53	0.78	360	468	1.30	0.74	0.061	1.29
		7	1.14	0.96	710	751	1.06	1.07	0.060	1.05
		8	1.15	0.96	743	809	1.09	1.14	0.061	1.08
		9	1.10	0.73	2472	2508	1.01	1.15	0.076	1.01
		10	1.10	0.73	2520	2592	1.03	1.18	0.084	1.02
		11	1.08	0.73	2472	2501	1.01	1.19	0.052	1.01
		12	1.08	0.73	2520	2539	1.01	1.18	0.053	1.00
7	Paulay and Scarpas (1981)	Unit 1	2.86	1.30	2418	3118	1.29	0.61	0.032	1.28
		Unit 2	2.86	1.29	3481	4385	1.26	0.90	0.038	1.25
		Unit 3	3.00	1.30	2418	3340	1.38	0.61	0.035	1.37
8	Ehsani and Wight (1982)	2 ^[6]	0.77	1.93	1747	1860	1.06	1.18	0.038	1.27
		4 ^[6]	0.88	1.93	1776	2400	1.35	1.35	0.056	1.39
9	Kanada et al. (1984)	U40L ^[4]	0.68	1.45	1129	885	0.78	0.63	0.033	1.19
		U41L	0.91	1.45	1143	1172	1.02	0.79	0.038	1.11
		U42L	0.95	1.45	1160	1165	1.00	0.74	0.033	1.06
		U41S ^[6]	0.61	2.17	1143	631	0.55	0.43	0.014	0.88
		U42S ^[6]	0.63	2.17	1160	690	0.59	0.44	0.020	0.92
		U20L ^[4]	1.02	1.45	608	651	1.07	0.44	0.011	1.07
		U21L	1.19	1.45	613	684	1.12	0.43	0.020	1.11
		U21S ^[6]	0.77	2.17	608	495	0.81	0.33	0.022	1.03
		U22S ^[6]	0.79	2.17	613	573	0.94	0.36	0.030	1.15
		R41L	0.86	1.45	1110	1022	0.92	0.77	0.038	1.06
		R42S ^[6]	0.58	2.17	1110	664	0.60	0.50	0.018	1.00

^[1] Values given in SI units are converted to in.-lb (1 in. = 25.4 mm; 1 psi = 1/145 MPa; and 1 kip = 4.4484 kN); notations used in these studies are described in Appendix A

^[3] Analyzed as a doubly reinforced section to calculate the nominal flexural strength M_n ; all other specimens are analyzed as a single reinforced

^[4] Specimens did not contain confining reinforcement parallel to the hooked bars within the joint region

^[5] Specimens had transverse beams on one or both sides of the test beam. These transverse beams meet the dimensional requirements of Sections 18.8.4 and 15.2.8 of ACI 318-19 and Section 4.3 of ACI 352R-02 to be considered effective in increasing the joint shear strength

^[6] Specimens had $d/\ell_{eh} > 1.5$

^[7] Drift ratio at drop to 80% of the peak load

Table 4.2 Cont. Detail of exterior beam-column joint specimens tested under reversed cyclic loading

Study ^[1]		Specimen	Bar Size ^[2]	f_y (ksi)	f_{cm} (psi)	c_{so} (in.)	$\frac{c_{ch}}{d_b}$	$\frac{A_{th}}{A_{hs}}$	ℓ_{eh} (in.)	ℓ_{ehy} (in.)
9	Kanada et al. (1984)	R21L	D19	56.2	3140	2.4	8.4	0.45	9.0	8.3
		R21S ^[6]	D19	56.2	3140	2.4	8.4	0.45	6.0	8.3
10	Zerbe and Durrani (1985)	J1 ^[6]	No. 6	60.0	5710	3.0	2.3	0.45	7.8	7.7
		J2 ^{[5][6]}	No. 6	60.0	5650	3.0	2.3	0.45	7.8	7.7
		J3 ^[6]	No. 6	60.0	5780	3.0	2.3	0.45	7.8	7.7
		J4 ^{[5][6]}	No. 6	60.0	5940	3.0	2.3	0.45	7.8	7.6
		J5 ^{[5][6]}	No. 6	60.0	5610	3.0	2.3	0.45	7.8	7.7
		J6 ^{[5][6]}	No. 6	60.0	5690	3.0	2.3	0.45	7.8	7.7
11	Ehsani et al. (1987)	1	No. 6	70.0	9380	2.4	5.2	0.36	10.8	8.3
		2	No. 6	70.0	9760	2.4	5.2	0.36	10.8	8.2
		3 ^[6]	No. 6	70.0	9380	2.4	4.1	0.36	9.2	8.8
		4 ^[6]	No. 7	62.0	9760	2.4	3.5	0.27	9.3	9.8
		5 ^[6]	No. 7	48.0	6470	2.4	3.5	0.22	8.6	8.4
12	Kaku and Asakusa (1991)	1	D13	56.7	4510	1.6	3.3	0.22	7.7	5.3
		2	D13	56.7	6050	1.6	3.3	0.22	7.7	4.9
		3	D13	56.7	6050	1.6	3.3	0.22	7.7	4.9
		4	D13	56.7	6480	1.6	3.3	0.06	7.7	5.1
		5	D13	56.7	5320	1.6	3.3	0.06	7.7	5.4
		6	D13	56.7	5860	1.6	3.3	0.06	7.7	5.2
		7	D13	56.7	4670	1.6	3.3	0.22	7.7	5.3
		8	D13	56.7	5970	1.6	3.3	0.22	7.7	4.9
		9	D13	56.7	5890	1.6	3.3	0.22	7.7	5.0
		10	D13	56.7	6440	1.6	3.3	0.06	7.7	5.1
		11	D13	56.7	6080	1.6	3.3	0.06	7.7	5.2
		12	D13	56.7	5090	1.6	3.3	0.06	7.7	5.4
		13	D13	56.7	6730	1.6	3.3	0.22	7.7	4.8
		14	D13	56.7	5950	1.6	3.3	0.06	7.7	5.2

^[1] Values given in SI units are converted to in.-lb (1 in. = 25.4 mm; 1 psi = 1/145 MPa; and 1 kip = 4.4484 kN); notations used in these studies are described in Appendix A

^[2] Bar sizes are presented in SI and in.-lb as reported in the original studies

^[3] Analyzed as a doubly reinforced section to calculate the nominal flexural strength M_n ; all other specimens are analyzed as a single reinforced

^[4] Specimens did not contain confining reinforcement parallel to the hooked bars within the joint region

^[5] Specimens had transverse beams on one or both sides of the test beam. These transverse beams meet the dimensional requirements of Sections 18.8.4 and 15.2.8 of ACI 318-19 and Section 4.3 of ACI 352R-02 to be considered effective in increasing the joint shear strength

^[6] Specimens had $d/\ell_{eh} > 1.5$

Table 4.2 Cont. Detail of exterior beam-column joint specimens tested under reversed cyclic loading

Study ^[1]		Specimen	$\frac{\ell_{eh}}{\ell_{ehy}}$	$\frac{d}{\ell_{eh}}$	M_n (kip.in.)	M_{peak} (kip.in.)	$\frac{M_{peak}}{M_n}$	$\frac{V_p}{V_n}$	$\delta_{0.8 peak}$ ^[7]	$\frac{T'}{T_h}$
9	Kanada et al. (1984)	R21L	1.09	1.45	600	664	1.11	0.50	0.022	1.10
		R21S ^[6]	0.73	2.17	600	495	0.82	0.37	0.022	1.10
10	Zerbe and Durrani (1985)	J1 ^[6]	1.01	1.63	1216	1287	1.06	0.85	0.053	1.05
		J2 ^{[5][6]}	1.00	1.63	1214	1518	1.25	1.01	0.052	1.24
		J3 ^[6]	1.01	1.63	1216	1320	1.09	0.87	0.053	1.08
		J4 ^{[5][6]}	1.02	1.63	1900	2079	1.09	1.35	0.05	1.09
		J5 ^{[5][6]}	1.00	1.63	2221	2244	1.01	1.49	0.051	1.01
		J6 ^{[5][6]}	1.00	1.63	2546	2211	0.87	1.46	0.052	0.86
11	Ehsani et al. (1987)	1	1.30	1.47	1729	2170	1.26	0.61	0.062	1.25
		2	1.32	1.47	2041	2666	1.31	0.74	0.064	1.30
		3 ^[6]	1.04	1.57	1663	1984	1.19	0.82	0.060	1.19
		4 ^[6]	0.94	1.55	2290	2232	0.97	0.91	0.058	1.03
		5 ^[6]	1.02	1.67	2101	2280	1.09	1.05	0.065	1.08
12	Kaku and Asakusa (1991)	1	1.44	1.04	335	427	1.27	0.83	0.055	1.27
		2	1.56	1.04	341	430	1.26	0.73	0.065	1.26
		3	1.56	1.04	338	374	1.10	0.63	0.065	1.10
		4	1.51	1.04	334	412	1.23	0.67	0.060	1.23
		5	1.43	1.04	332	380	1.14	0.68	0.055	1.14
		6	1.47	1.04	340	360	1.06	0.62	0.052	1.06
		7	1.46	1.04	335	428	1.28	0.82	0.060	1.27
		8	1.56	1.04	335	419	1.25	0.71	0.063	1.25
		9	1.55	1.04	335	406	1.21	0.69	0.068	1.21
		10	1.51	1.04	334	418	1.25	0.68	0.059	1.25
		11	1.48	1.04	334	397	1.19	0.67	0.048	1.19
		12	1.41	1.04	336	357	1.06	0.66	0.053	1.06
		13	1.61	1.04	339	360	1.06	0.58	0.065	1.06
		14	1.48	1.04	334	389	1.16	0.66	0.045	1.16

^[1] Values given in SI units are converted to in.-lb (1 in. = 25.4 mm; 1 psi = 1/145 MPa; and 1 kip = 4.4484 kN); notations used in these studies are described in Appendix A

^[3] Analyzed as a doubly reinforced section to calculate the nominal flexural strength M_n ; all other specimens are analyzed as a single reinforced

^[4] Specimens did not contain confining reinforcement parallel to the hooked bars within the joint region

^[5] Specimens had transverse beams on one or both sides of the test beam. These transverse beams meet the dimensional requirements of Sections 18.8.4 and 15.2.8 of ACI 318-19 and Section 4.3 of ACI 352R-02 to be considered effective in increasing the joint shear strength

^[6] Specimens had $d/\ell_{eh} > 1.5$

^[7] Drift ratio at drop to 80% of the peak load

Table 4.2 Cont. Detail of exterior beam-column joint specimens tested under reversed cyclic loading

Study ^[1]		Specimen	Bar Size ^[2]	f_y (ksi)	f_{cm} (psi)	c_{so} (in.)	$\frac{c_{ch}}{d_b}$	$\frac{A_{th}}{A_{hs}}$	ℓ_{eh} (in.)	ℓ_{ehy} (in.)
12	Kaku and Asakusa (1991)	15	D13	56.7	5760	1.6	3.3	0.06	7.7	5.2
		16	D13	56.7	5420	1.6	3.3	0.22	7.7	5.1
13	Ehsani and Alameddine (1991)	LL8 ^[6]	No. 8	66.3	8600	3.0	2.2	0.57	10.5	11.4
		LH8 ^[6]	No. 8	66.3	8600	3.0	2.2	0.76	10.5	11.4
		HL8 ^[6]	No. 9	64.2	8600	3.0	1.9	0.45	10.5	13.1
		HH8 ^[6]	No. 9	64.2	8600	3.0	1.9	0.60	10.5	13.1
		LL11 ^[6]	No. 8	66.3	10700	3.0	2.2	0.57	10.5	10.8
		LH11 ^[6]	No. 8	66.3	10700	3.0	2.2	0.76	10.5	10.8
		HL11 ^[6]	No. 9	64.2	10700	3.0	1.9	0.45	10.5	12.3
		HH11 ^[6]	No. 9	64.2	10700	3.0	1.9	0.60	10.5	12.3
		LL14 ^[6]	No. 8	66.3	13700	3.0	2.2	0.57	10.5	10.1
		LH14 ^[6]	No. 8	66.3	13700	3.0	2.2	0.76	10.5	10.1
HH14 ^[6]	No. 9	64.2	13700	3.0	1.9	0.60	10.5	11.5		
14	Tsonos et al. (1992)	S1 ^[6]	D14	70.3	5360	0.7	10.7	0.33	6.5	5.9
		S2 ^[6]	D12	76.7	3770	0.7	6.3	0.30	6.5	5.9
		S6' ^[6]	D14	70.3	4200	0.7	3.6	0.16	6.5	7.6
15	Pantelides et al. (2002)	2 ^{[3][4]}	No. 9	65.9	6700	1.9	2.1	0.00	16.1	15.6
		4 ^{[3][4]}	No. 9	65.9	5940	1.9	2.1	0.00	16.1	16.1
		5 ^{[3][4]}	No. 9	65.9	5370	1.9	2.1	0.00	16.1	16.6
		6 ^{[3][4]}	No. 9	65.9	5820	1.9	2.1	0.00	16.1	16.2
16	Chutarat and Aboutaha (2003)	Specimen I	No. 8	70.0	4000	3.3	2.8	0.76	12.8	14.2
17	Hwang et al. (2005)	0T0 ^[4]	No. 8	62.4	9760	4.0	2.5	0.00	13.7	11.5
		3T44	No. 8	62.4	11140	4.0	2.5	0.76	13.7	9.8
		1B8	No. 8	63.1	8960	4.0	2.5	0.50	13.7	10.5
		3T3	No. 8	62.4	10010	4.0	2.5	0.21	13.7	10.0

^[1] Values given in SI units are converted to in.-lb (1 in. = 25.4 mm; 1 psi = 1/145 MPa; and 1 kip = 4.4484 kN); notations used in these studies are described in Appendix A

^[2] Bar sizes are presented in SI and in.-lb as reported in the original studies

^[3] Analyzed as a doubly reinforced section to calculate the nominal flexural strength M_n ; all other specimens are analyzed as a single reinforced

^[4] Specimens did not contain confining reinforcement parallel to the hooked bars within the joint region

^[5] Specimens had transverse beams on one or both sides of the test beam. These transverse beams meet the dimensional requirements of Sections 18.8.4 and 15.2.8 of ACI 318-19 and Section 4.3 of ACI 352R-02 to be considered effective in increasing the joint shear strength

^[6] Specimens had $d/\ell_{eh} > 1.5$

Table 4.2 Cont. Detail of exterior beam-column joint specimens tested under reversed cyclic loading

Study ^[1]		Specimen	$\frac{\ell_{eh}}{\ell_{ehy}}$	$\frac{d}{\ell_{eh}}$	M_n (kip.in.)	M_{peak} (kip.in.)	$\frac{M_{peak}}{M_n}$	$\frac{V_p}{V_n}$	$\delta_{0.8 peak}$ ^[7]	$\frac{T'}{T_h}$
12	Kaku and Asakusa (1991)	15	1.46	1.04	333	397	1.19	0.69	0.060	1.19
		16	1.52	1.04	334	432	1.29	0.77	0.055	1.29
13	Ehsani and Alameddine (1991)	LL8 ^[6]	0.92	1.62	3027	3517	1.16	0.89	0.055	1.25
		LH8 ^[6]	0.92	1.62	3027	3402	1.12	0.86	0.061	1.21
		HL8 ^[6]	0.80	1.62	3637	3708	1.02	1.02	0.043	1.24
		HH8 ^[6]	0.80	1.62	3637	3743	1.03	1.02	0.063	1.25
		LL11 ^[6]	0.98	1.62	3118	3020	0.97	0.71	0.056	0.99
		LH11 ^[6]	0.98	1.62	3081	4018	1.30	0.86	0.064	1.33
		HL11 ^[6]	0.85	1.62	3845	3731	0.97	0.89	0.041	1.12
		HH11 ^[6]	0.85	1.62	3872	4089	1.06	0.94	0.063	1.22
		LL14 ^[6]	1.04	1.62	3112	3701	1.19	0.72	0.060	1.18
		LH14 ^[6]	1.04	1.62	3112	3780	1.21	0.73	0.064	1.21
HH14 ^[6]	0.91	1.62	3830	4084	1.07	0.84	0.054	1.16		
14	Tsonos et al. (1992)	S1 ^[6]	1.09	1.67	348	452	1.30	0.66	0.065	1.29
		S2 ^[6]	1.10	1.67	404	465	1.15	0.82	0.030	1.15
		S6' ^[6]	0.85	1.67	646	666	1.03	1.11	0.035	1.21
15	Pantelides et al. (2002)	2 ^{[3][4]}	1.03	0.84	2932	3005	1.02	1.11	0.025	1.02
		4 ^{[3][4]}	1.00	0.84	2932	3100	1.06	1.21	0.018	1.06
		5 ^{[3][4]}	0.97	0.84	2932	3000	1.02	1.24	0.025	1.05
		6 ^{[3][4]}	0.99	0.84	2932	2950	1.01	1.17	0.028	1.01
16	Chutarat and Aboutaha (2003)	Specimen I	0.90	1.19	2848	3344	1.17	1.19	0.074	1.30
17	Hwang et al. (2005)	0T0 ^[4]	1.18	1.11	2794	3229	1.16	0.69	0.060	1.16
		3T44	1.40	1.11	2817	3447	1.22	0.69	0.087	1.22
		1B8	1.30	1.11	2807	4069	1.45	0.91	0.060	1.44
		3T3	1.36	1.11	2798	3666	1.31	0.78	0.100	1.30

^[1] Values given in SI units are converted to in.-lb (1 in. = 25.4 mm; 1 psi = 1/145 MPa; and 1 kip = 4.4484 kN); notations used in these studies are described in Appendix A

^[3] Analyzed as a doubly reinforced section to calculate the nominal flexural strength M_n ; all other specimens are analyzed as a single reinforced

^[4] Specimens did not contain confining reinforcement parallel to the hooked bars within the joint region

^[5] Specimens had transverse beams on one or both sides of the test beam. These transverse beams meet the dimensional requirements of Sections 18.8.4 and 15.2.8 of ACI 318-19 and Section 4.3 of ACI 352R-02 to be considered effective in increasing the joint shear strength

^[6] Specimens had $d/\ell_{eh} > 1.5$

^[7] Drift ratio at drop to 80% of the peak load

Table 4.2 Cont. Detail of exterior beam-column joint specimens tested under reversed cyclic loading

Study ^[1]		Specimen	Bar Size ^[2]	f_y (ksi)	f_{cm} (psi)	c_{so} (in.)	$\frac{c_{ch}}{d_b}$	$\frac{A_{th}}{A_{hs}}$	ℓ_{eh} (in.)	ℓ_{ehy} (in.)
17	Hwang et al. (2005)	2T4	No. 8	62.4	10300	4.0	2.5	0.13	13.7	10.5
		1T44	No. 8	62.4	10560	4.0	2.5	0.25	13.7	9.9
		3T4	No. 8	71.2	10910	4.0	2.5	0.38	15.5	11.3
		2T5	No. 8	71.2	11110	4.0	2.5	0.20	15.5	11.3
		1T55	No. 8	71.2	10110	4.0	2.5	0.39	15.5	11.5
18	Tsonos (2007)	A1 ^[6]	D10	73.0	5080	1.0	4.7	0.36	6.5	4.4
		E1 ^[6]	D14	72.0	3190	0.9	5.0	0.24	6.4	7.7
		E2 ^[6]	D14	72.0	5080	0.9	10.0	0.37	6.4	6.2
		G1 ^[6]	D14	72.0	3190	0.9	5.0	0.12	6.4	7.9
19	Chun et al. (2007)	JC-1	D22	58.4	8950	3.4	3.4	0.09	15.8	8.2
		JC-2	D22	58.4	8720	3.4	3.4	0.05	13.9	8.5
		WC ^[4]	D25	62.5	8180	2.1	6.6	0.00	15.7	12.0
		JC-No. 11-1	D36	66.4	4760	6.0	4.3	0.51	18.9	17.9
20	Lee and Ko (2007)	S0	D22	66.0	4730	4.6	2.3	0.28	21.0	11.0
		W0	D22	66.0	4190	8.6	2.3	0.46	13.1	11.4
21	Kang et al. (2010)	Jk ^[6]	D19	67.0	4200	2.6	5.2	0.25	11.3	7.8
22	Hwang et al. (2014)	T1-400	D22	75.4	4640	4.5	3.7	0.38	19.6	11.6
		T2-600	D22	103.0	4640	4.5	3.7	0.67	19.6	15.9
		T3-600 ^[3]	D25	92.1	4290	4.5	3.3	0.51	19.6	18.0
23	Chun and Shin (2014)	H0.7S ^[3]	D19	70.8	3710	3.0	2.3	0.29	9.0	9.4
		H1.0S ^[3]	D19	70.8	3710	3.0	2.3	0.58	9.0	9.4
		H1.5S ^[6]	D19	70.8	3710	3.0	2.3	0.58	9.0	9.4
		H2.0S ^[6]	D19	70.8	3830	3.0	2.3	0.58	9.0	8.6
		H2.5S ^[6]	D19	70.8	3830	3.0	2.3	0.58	9.0	8.6
		H0.7U ^[3]	D19	70.8	3710	3.0	2.3	0.19	9.0	9.5
		H1.0U ^[3]	D19	70.8	3710	3.0	2.3	0.38	9.0	9.4
24	Choi and Bae (2019)	JTR-0-BTR	D25	68.4	7950	3.1	4.6	1.01	8.3	10.3
		JNR-0-BTR ^[4]	D25	68.4	7950	3.1	4.6	0.00	8.3	12.6
		JTR-0-BNR	D25	68.4	7950	3.1	4.6	1.01	8.3	10.3

^[1] Values given in SI units are converted to in.-lb (1 in. = 25.4 mm; 1 psi = 1/145 MPa; and 1 kip = 4.4484 kN); notations used in these studies are described in Appendix A

^[2] Bar sizes are presented in SI and in.-lb as reported in the original studies

^[3] Analyzed as a doubly reinforced section to calculate the nominal flexural strength M_n ; all other specimens are analyzed as a single reinforced

^[4] Specimens did not contain confining reinforcement parallel to the hooked bars within the joint region

^[6] Specimens had $d/\ell_{eh} > 1.5$

Table 4.2 Cont. Detail of exterior beam-column joint specimens tested under reversed cyclic loading

Study ^[1]		Specimen	$\frac{\ell_{eh}}{\ell_{ehy}}$	$\frac{d}{\ell_{eh}}$	M_n (kip.in.)	M_{peak} (kip.in.)	$\frac{M_{peak}}{M_n}$	$\frac{V_p}{V_n}$	$\delta_{0.8 peak}$ ^[7]	$\frac{T'}{T_h}$
17	Hwang et al. (2005)	2T4	1.30	1.11	2803	3498	1.25	0.73	0.075	1.24
		1T44	1.38	1.11	2808	3363	1.20	0.69	0.080	1.19
		3T4	1.37	0.98	3185	3599	1.13	0.63	0.070	1.13
		2T5	1.38	0.98	3189	3767	1.18	0.66	0.070	1.18
		1T55	1.34	0.98	3168	3649	1.15	0.67	0.070	1.15
18	Tsonos (2007)	A1 ^[6]	1.47	1.64	359	454	1.26	0.73	0.045	1.26
		E1 ^[6]	0.84	1.66	486	558	1.15	1.14	0.060	1.37
		E2 ^[6]	1.04	1.66	348	438	1.26	0.71	0.065	1.26
		G1 ^[6]	0.82	1.66	486	494	1.02	1.01	0.040	1.25
19	Chun et al. (2007)	JC-1	1.93	1.10	2328	3195	1.37	0.49	0.045	1.37
		JC-2	1.64	1.24	4204	4983	1.19	0.80	0.070	1.18
		WC ^[4]	1.31	0.84	4726	5611	1.19	0.53	0.053	1.19
		JC-No. 11-1	1.05	0.90	4567	4912	1.08	0.61	0.054	1.07
20	Lee and Ko (2007)	S0	1.90	0.76	2275	3075	1.35	0.59	0.065	1.35
		W0	1.15	1.22	2241	2857	1.27	0.59	0.055	1.27
21	Kang et al. (2010)	Jk ^[6]	1.43	1.73	2177	2721	1.25	0.55	0.035	1.24
22	Hwang et al. (2014)	T1-400	1.69	0.87	3878	4658	1.20	0.78	0.032	1.20
		T2-600	1.23	0.90	3807	4844	1.27	0.75	0.038	1.27
		T3-600 ^[3]	1.09	0.90	4282	5403	1.26	0.83	0.048	1.26
23	Chun and Shin (2014)	H0.7S ^[3]	0.95	0.6	492	612	1.24	1.18	0.100	1.30
		H1.0S ^[3]	0.95	1.0	984	1080	1.10	1.03	0.070	1.15
		H1.5S ^[6]	0.95	1.7	1728	1752	1.01	0.91	0.050	1.06
		H2.0S ^[6]	1.04	2.4	2484	2760	1.11	0.82	0.070	1.11
		H2.5S ^[6]	1.04	3.0	3216	3252	1.01	0.71	0.050	1.01
		H0.7U ^[3]	0.95	0.6	492	576	1.17	1.12	0.100	1.23
		H1.0U ^[3]	0.95	1.0	984	1020	1.04	0.97	0.070	1.08
24	Choi and Bae (2019)	JTR-0-BTR	0.81	1.45	1221	1275	1.04	0.70	0.044	1.26
		JNR-0-BTR ^[4]	0.66	1.45	1221	1080	0.88	0.59	0.019	1.38
		JTR-0-BNR	0.81	1.45	1221	1221	1.00	0.67	0.047	1.21

^[1] Values given in SI units are converted to in.-lb (1 in. = 25.4 mm; 1 psi = 1/145 MPa; and 1 kip = 4.4484 kN); notations used in these studies are described in Appendix A

^[3] Analyzed as a doubly reinforced section to calculate the nominal flexural strength M_n ; all other specimens are analyzed as a single reinforced

^[4] Specimens did not contain confining reinforcement parallel to the hooked bars within the joint region

^[6] Specimens had $d/\ell_{eh} > 1.5$

^[7] Drift ratio at drop to 80% of the peak load

Because of the effect of joint shear on the performance of beam-column joints subjected to reversed cyclic loading, including potential effects on the anchorage performance of hooked bars, beam-column joint specimens with a ratio of peak joint shear to nominal joint shear strength $V_p/V_n \leq 1.0$ and those with $V_p/V_n > 1.0$ are initially examined separately. The nominal joint shear strength V_n is calculated as $12\sqrt{f'_c}A_j$ in accordance with Section 18.8.4.3 of ACI 318-19, where A_j is the effective cross-sectional area within the beam-column joint in a plane parallel to the hooked bars calculated in accordance with Section 15.4.2.4 of ACI 318-19 and f'_c is concrete compressive strength. The nominal joint shear strength V_n is also calculated in accordance with Section 4.3 of ACI 352R-02, with a 15,000 psi upper limit on f'_c . The peak and nominal joint shear strength values are given in Table C.4 of Appendix C. The effect of joint shear strength on the anchorage performance of the hooked bar is discussed in Sections 4.2.2.1 and 4.2.2.2.

Figure 4.2 shows the plot of the ratio of the peak moment M_{peak} to the nominal flexural strength M_n versus the ratio of the actual embedment length of the hooked bar ℓ_{eh} to the embedment length required to yield the bar ℓ_{ehy} . Linear trendlines for specimens with $\ell_{eh}/\ell_{ehy} \leq 1.0$ and $\ell_{eh}/\ell_{ehy} \geq 1.0$ are shown in the figure. Figure 4.2 only includes specimens with $V_p/V_n \leq 1.0$ (0.43 to 1.00). Beam-column joint specimens with a ratio of effective beam depth to embedment length $d/\ell_{eh} > 1.5$ were not included when Ajaam et al. (2017) developed the descriptive and design equations, Eq. (4.1) through (4.3). Therefore, beam-column joint specimens tested under reversed cyclic loading that had $d/\ell_{eh} > 1.5$ are not included in Figure 4.2 and are analyzed independently in Section 4.2.2.3. Beam-column joint specimens included in Figure 4.2 had a ratio of d/ℓ_{eh} ranging from 0.6 to 1.5. In Figure 4.3, the ratio of the peak moment M_{peak} to the nominal flexural strength M_n is plotted versus the ratio of the actual embedment length of the hooked bar ℓ_{eh} to the embedment length required to yield the bar ℓ_{ehy} for specimens with $V_p/V_n > 1.0$ (1.01 to 1.24).

The beam-column joint specimens were considered to have performed satisfactorily if they met two criteria: first, the ratio of measured peak moment to nominal flexural strength (M_{peak}/M_n) was greater than or equal to 1.0, and second, the reduction in peak moment was $\leq 20\%$ at the end of the first complete cycle at 3.5% drift, where the drift is defined as the ratio of displacement at the loading point in the direction of the load to the distance between the loading point and center of the beam-column joints. The values of the drift ratio at drop to 80% from the peak load ($\delta_{0.8peak}$)

are given in Table (4.2). ACI 374.1-05, Section 9.1.3 utilizes similar acceptance criteria for weak beam-strong column connections, with the exception that the peak moment reduction could be up to 25% at the end of the third complete cycle at 3.5% drift. The acceptance criteria used in this study were used by Kang et al. (2009) for beam-columns joints in which the beam bars were anchored using heads. The results presented in Figures 4.2 and 4.3 are discussed next.

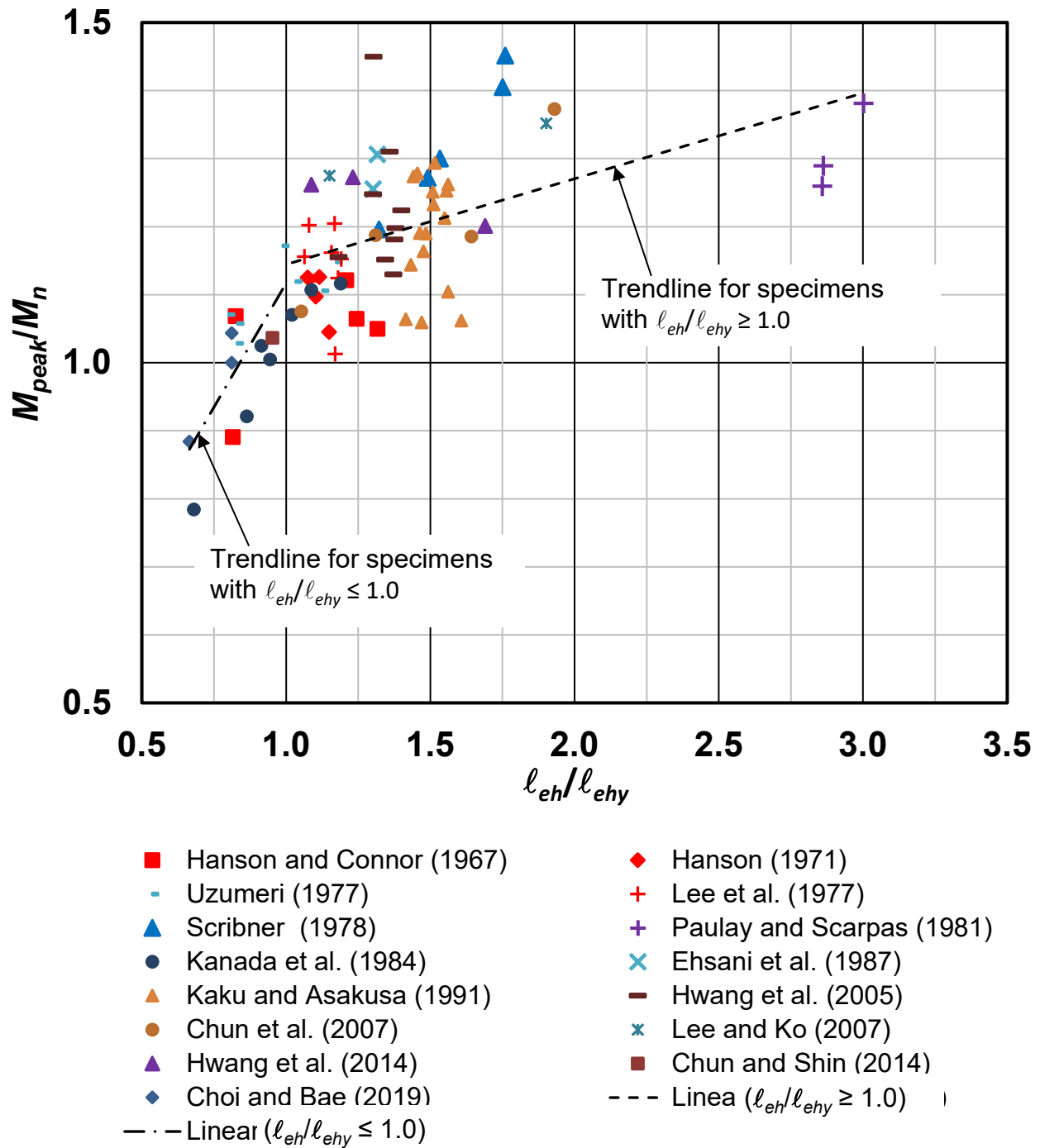


Figure 4.2 M_{peak}/M_n versus l_{eh}/l_{ehy} for specimens with $d/l_{eh} \leq 1.5$ and $V_p/V_n \leq 1.0$. M_{peak}/M_n is the ratio of peak moment to nominal flexural strength, and l_{eh}/l_{ehy} is the ratio of embedment length to the embedment length required to yield the hooked bar calculated using the descriptive equations developed by Ajaam et al. (2017), Eq. (4.1) and (4.2)

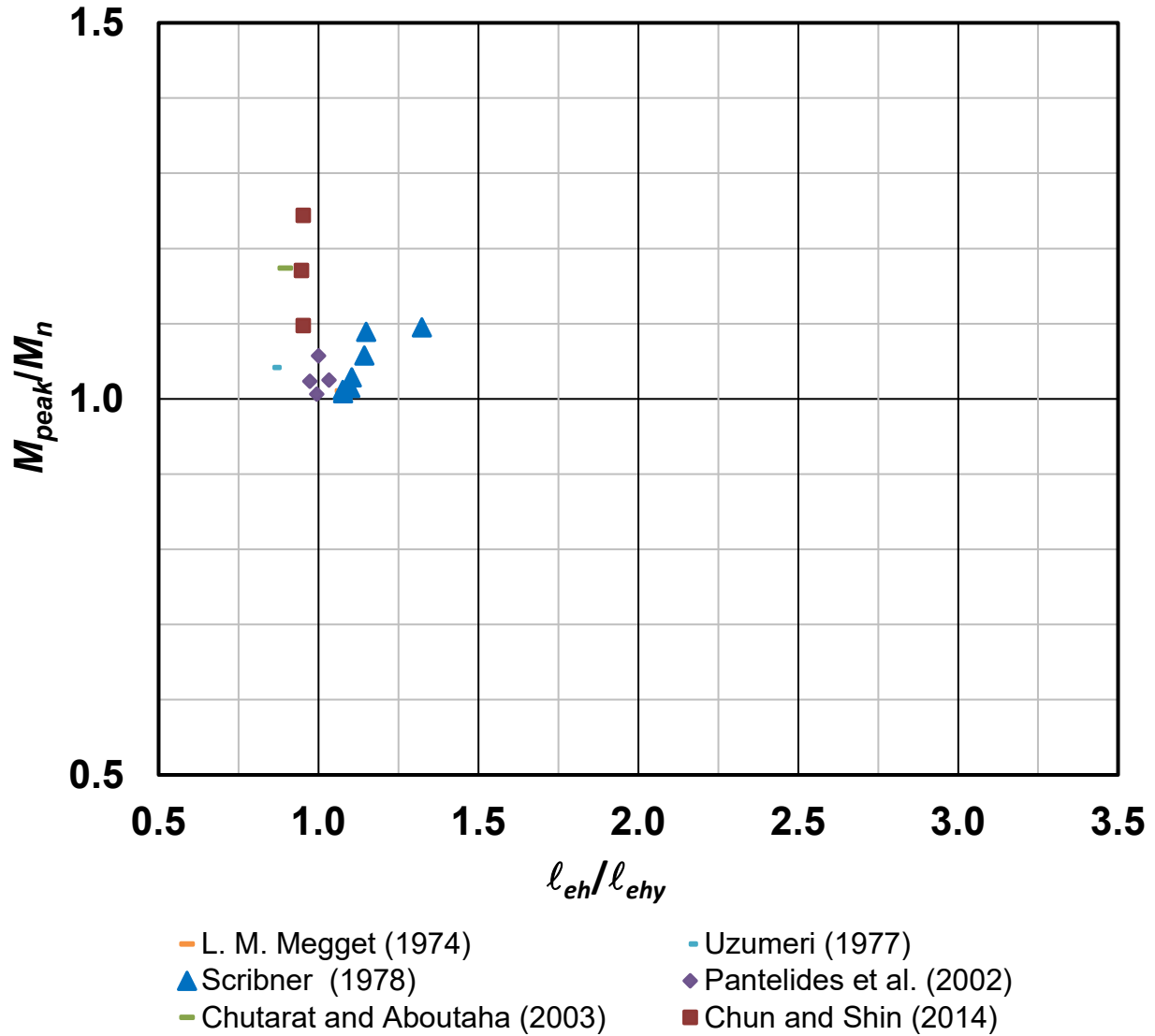


Figure 4.3 M_{peak}/M_n versus l_{eh}/l_{ehy} for specimens with $d/l_{eh} \leq 1.5$ and $V_p/V_n > 1.0$. M_{peak}/M_n is the ratio of peak moment to nominal flexural strength, and l_{eh}/l_{ehy} is the ratio of embedment length to the embedment length required to yield the hooked bar calculated using the descriptive equations developed by Ajaam et al. (2017), Eq. (4.1) and (4.2)

4.2.2.1 Specimens with $d/l_{eh} \leq 1.5$ and $l_{eh}/l_{ehy} < 1.0$

The descriptive equations, Eq. (4.1) and (4.2), were developed using exterior beam-column joint specimens with $d/l_{eh} \leq 1.5$ under monotonic loading (Ajaam et al. 2017). In this section, the applicability of those equations to beam-column joint specimens with $d/l_{eh} \leq 1.5$ and $l_{eh}/l_{ehy} < 1.0$ subjected to reversed cyclic loading is evaluated.

Twenty-one of the exterior beam-column joint specimens with $d/\ell_{eh} \leq 1.5$ subjected to reversed cyclic loading contained hooked bars with actual embedment lengths, ℓ_{eh} , less than that required to yield the hooked bar, ℓ_{ehy} , calculated using Eq. (4.1) or (4.2). Out of the 21 specimens, 14 had a ratio of peak joint shear to nominal joint shear strength $V_p/V_n \leq 1.0$ and seven had $V_p/V_n > 1.0$. Hooked bar sizes ranged from No. 6 (D19) to No. 9 (D29), with yield strengths ranging from 49,800 to 70,800 psi. Concrete compressive strengths ranged from 3,140 to 7,950 psi. The concrete side cover to the hooked bar ranged from 1.7 to $3.9d_b$ (2 to 3.5 in.), and center-to-center spacing between the hooked bars ranged from 2.1 to $4.6d_b$ (1.8 to 4.9 in.). Confining reinforcement within the joint region parallel to the straight portion of the hooked bars ranged from none to eight No. 4 hoops. Twelve specimens contained confining reinforcement parallel to the straight portion of the hooked bars within the joint region and nine contained none. Two specimens tested by Uzumeri (1977), Specimens 1 and 5 with $\ell_{eh}/\ell_{ehy} < 1.0$, contained transverse beams perpendicular to the test beam at the joint. The transverse beams in those specimens had widths greater than $\frac{3}{4}$ of the effective joint width, which is defined in accordance with Section 15.4.2.4 of ACI 318-19 as the minimum of column width, beam width plus joint depth, and twice the perpendicular distance from the longitudinal axis of the beam to the nearest side face of the column. Therefore, these transverse beams satisfy the minimum dimensional requirement to be considered effective in increasing the joint shear strength in accordance with Section 18.8.4.3 of ACI 318-19, and the nominal joint shear strength (V_n) of these specimens, as calculated in accordance with Section 18.8.4.3 of ACI 318-19, is $15\sqrt{f'_c}A_j$, where A_j is the effective cross-sectional area within the beam-column joint in a plane parallel to the hooked bars calculated in accordance with Section 15.4.2.4 of ACI 318-19.

As shown in Figure 4.2, the trendline for the 14 specimens with $\ell_{eh}/\ell_{ehy} < 1.0$ exhibits an increase in M_{peak}/M_n with an increase in ℓ_{eh}/ℓ_{ehy} , as would be expected. This agrees with the findings by Ajaam et al. (2017) that increasing the embedment length increased the anchorage strength of the hooked bars. Figure 4.3 shows the data for the seven specimens with $\ell_{eh}/\ell_{ehy} < 1.0$ and $V_p/V_n > 1.0$. In this case, no trend is observed for values of ℓ_{eh}/ℓ_{ehy} between 0.86 and 0.99 and values of M_{peak}/M_n between 1.01 and 1.24. Due to the small number of specimens with $\ell_{eh}/\ell_{ehy} < 1.0$ and $V_p/V_n > 1.0$, it is hard to draw any conclusions for this case.

Out of 21 specimens with $\ell_{eh}/\ell_{ehy} < 1.0$, shown in Figures 4.2 and 4.3, four had values of

M_{peak}/M_n less than 1.0. Two of these four specimens had M_{peak}/M_n equal to 0.78 and 0.88 and ℓ_{eh}/ℓ_{ehy} equal to 0.68 and 0.66, respectively, while the other two had M_{peak}/M_n equal to 0.89 and 0.92 and ℓ_{eh}/ℓ_{ehy} equal to 0.81 and 0.86, respectively. These specimens experienced joint deterioration and exhibited diagonal cracks within the joint region, similar to that observed by Ajaam et al. (2017) for simulated exterior beam-column joint specimens tested under monotonic loading. None of these four specimens displayed flexural hinging within the beam, most likely due to inadequate embedment lengths to yield the bars. Of the remaining 17 specimens where $M_{peak}/M_n \geq 1.0$ with ℓ_{eh}/ℓ_{ehy} ranging between 0.8 and 0.99, six specimens—specimen V-A tested by Hanson and Connor (1967), specimens 1, 2 and 5 tested by Uzumeri (1977), and specimens 5 and 6 tested by Pantelides et al. (2002)—showed a 20% reduction in the peak moment at less than 3.5% (1.6 to 3.3%) drift, and the remaining 11 specimens had a reduction in the peak moment of less than 20% at 3.5% drift. Twelve of the seventeen specimens exhibited flexural hinging within the beam, while the remaining five specimens, specimens 1, 2, and 5 tested by Uzumeri (1977), and specimens 5 and 6 tested by Pantelides et al. (2002), failed in the joint region due to the absence of confining reinforcement in the joint. Figures 4.2 and 4.3 show conclusively that the descriptive equations Eq. (4.1) and (4.2) are applicable for members subjected to reversed cyclic loading as well as monotonic loading.

4.2.2.2 Specimens with $d/\ell_{eh} \leq 1.5$ and $\ell_{eh}/\ell_{ehy} \geq 1.0$

Specimens with embedment lengths adequate to yield the hooked bars ($\ell_{eh}/\ell_{ehy} \geq 1.0$) are expected to show post-yield behavior, which is characterized by a slight increase in anchorage strength as embedment length increases due to strain hardening of the steel. The descriptive equations, Eq. (4.1) and (4.2), are used to examine beam-column joint specimens with $\ell_{eh}/\ell_{ehy} \geq 1.0$ subjected to reversed cyclic loading to see if such post-yield behavior is observed in these specimens.

The results for the beam-column joint specimens with d/ℓ_{eh} and $\ell_{eh}/\ell_{ehy} \geq 1.0$ are shown in Figures 4.2 and 4.3 (65 with $V_p/V_n \leq 1.0$ in Figure 4.2 and 10 with $V_p/V_n > 1.0$ in Figure 4.3). ℓ_{eh}/ℓ_{ehy} ranged from 1.02 to 3.0 for the joints with $V_p/V_n \leq 1.0$ and 1.0 to 1.32 for the joints with $V_p/V_n > 1.0$. Hooked bar sizes ranged from No. 4 (D13) to No. 11 (D36), with yield strengths

ranging from 42,900 to 103,000 psi. Concrete compressive strengths ranged from 3,140 to 11,140 psi. The concrete side cover on the hooked bars ranged from 1.4 to $9.8d_b$ (1.03 to 8.6 in.), and center-to-center spacing between the hooked bars ranged from 2.1 to $8.4d_b$ (1.7 to 6.6 in.). Confining reinforcement within the joint region parallel to the straight portion of the hooked bars ranged from none to 8 No. 3 or No. 4 hoops. Out of 75 specimens, 70 contained confining reinforcement parallel to the straight portion of the hooked bars within the joint region, and five specimens did not. Four specimens with $\ell_{eh}/\ell_{ehy} \geq 1.0$, two tested by Hanson (1971), Specimens 1 and 3, and two tested by Uzumeri (1977), Specimens 3 and 4, contained transverse beams perpendicular to the test beam at the joint. The transverse beams in these specimens had widths greater than $\frac{3}{4}$ of the effective joint width, which is defined in accordance with Section 15.4.2.4 of ACI 318-19 as the minimum of column width, beam width plus joint depth, and twice the perpendicular distance from the longitudinal axis of the beam to the nearest side face of the column. Because these transverse beams satisfy the minimum dimensional requirement to be considered effective in increasing the joint shear strength in accordance with Section 18.8.4.3 of ACI 318-19, the nominal joint shear strength (V_n) of these specimens is $15\sqrt{f'_c}A_j$, as described in Section 4.2.2.1. In all cases, joints with $\ell_{eh}/\ell_{ehy} \geq 1.0$ had values of $M_{peak}/M_n \geq 1.0$.

In Figure 4.2, the trendline for the 65 specimens with $\ell_{eh}/\ell_{ehy} \geq 1.0$ shows an increase in M_{peak}/M_n with an increase in embedment length, but at a significantly lower rate of change than the trendline for specimens with $\ell_{eh}/\ell_{ehy} < 1.0$. This is consistent with the hooked bars yielding and strain hardening for $\ell_{eh} \geq \ell_{ehy}$. Out of the 65 specimens, 59 exhibited less than a 20% reduction in the peak moment at about 3.5% drift, while the remaining specimens, Specimen 4 tested by Hanson (1971), Unit 1 tested by Paulay and Scarpas (1981), Specimens U20L, U21L, and R21L tested by Kanada et al. (1984), and Specimen T1-400 tested by Hwang et al. (2014), exhibited a 20% reduction in the peak moment at less than 3.5% (1.1 to 3.2%) drift.

Figures 4.4 and 4.5 provide an understanding of the relationship between M_{peak}/M_n and V_p/V_n for beam-column joint specimens subjected to reversed cyclic loading with $\ell_{eh}/\ell_{ehy} < 1.0$ and $\ell_{eh}/\ell_{ehy} \geq 1.0$. In Figure 4.4, the relationship between V_p/V_n and ℓ_{eh}/ℓ_{ehy} for specimens with $d/\ell_{eh} \leq 1.5$ is presented. Overall, as ℓ_{eh}/ℓ_{ehy} increases, V_p/V_n decreases. This is likely due to the fact that as the embedment length increases, the column depth increases, resulting in a higher nominal joint

shear strength V_n , which reduces V_p/V_n and improves the response of the specimen to reversed cyclic loading. For specimens with $d/\ell_{eh} \leq 1.5$ and $\ell_{eh}/\ell_{ehy} \geq 1.0$, M_{peak}/M_n is plotted versus V_p/V_n in Figure 4.5. The apparent downward trend in M_{peak}/M_n with increasing V_p/V_n in the figure suggests that the increase in M_{peak}/M_n with increasing ℓ_{eh}/ℓ_{ehy} may be related to V_p/V_n , at least to some extent. Reduced M_{peak}/M_n is obviously associated with joint deterioration during cyclic loading at higher V_p/V_n values.

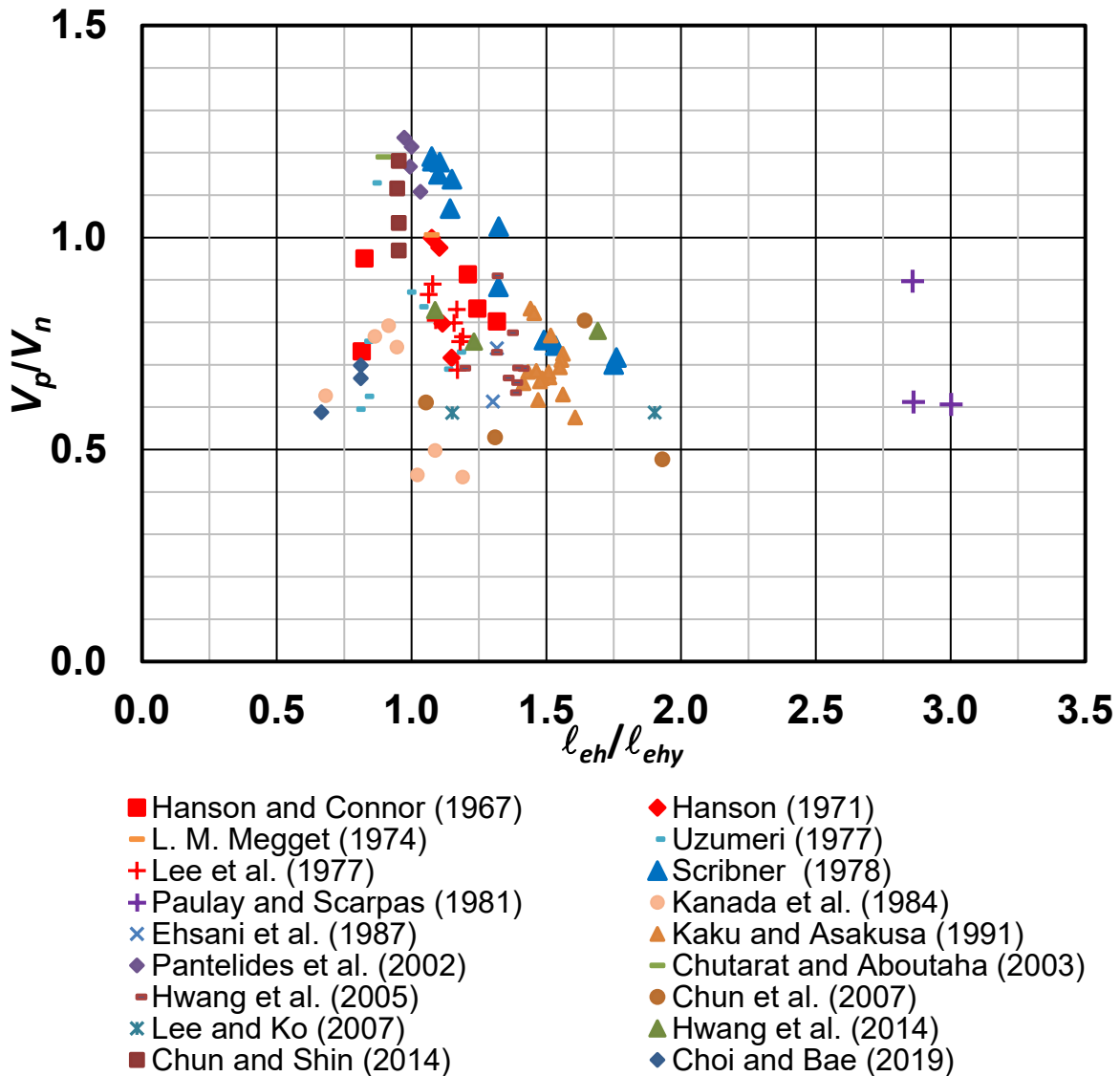


Figure 4.4 V_p/V_n versus ℓ_{eh}/ℓ_{ehy} for specimens with $d/\ell_{eh} \leq 1.5$. V_p/V_n is the ratio of peak joint shear to nominal joint shear strength, and ℓ_{eh}/ℓ_{ehy} is the ratio of embedment length to the embedment length required to yield the hooked bar calculated using the descriptive equations developed by Ajaam et al. (2017), Eq. (4.1) and (4.2)

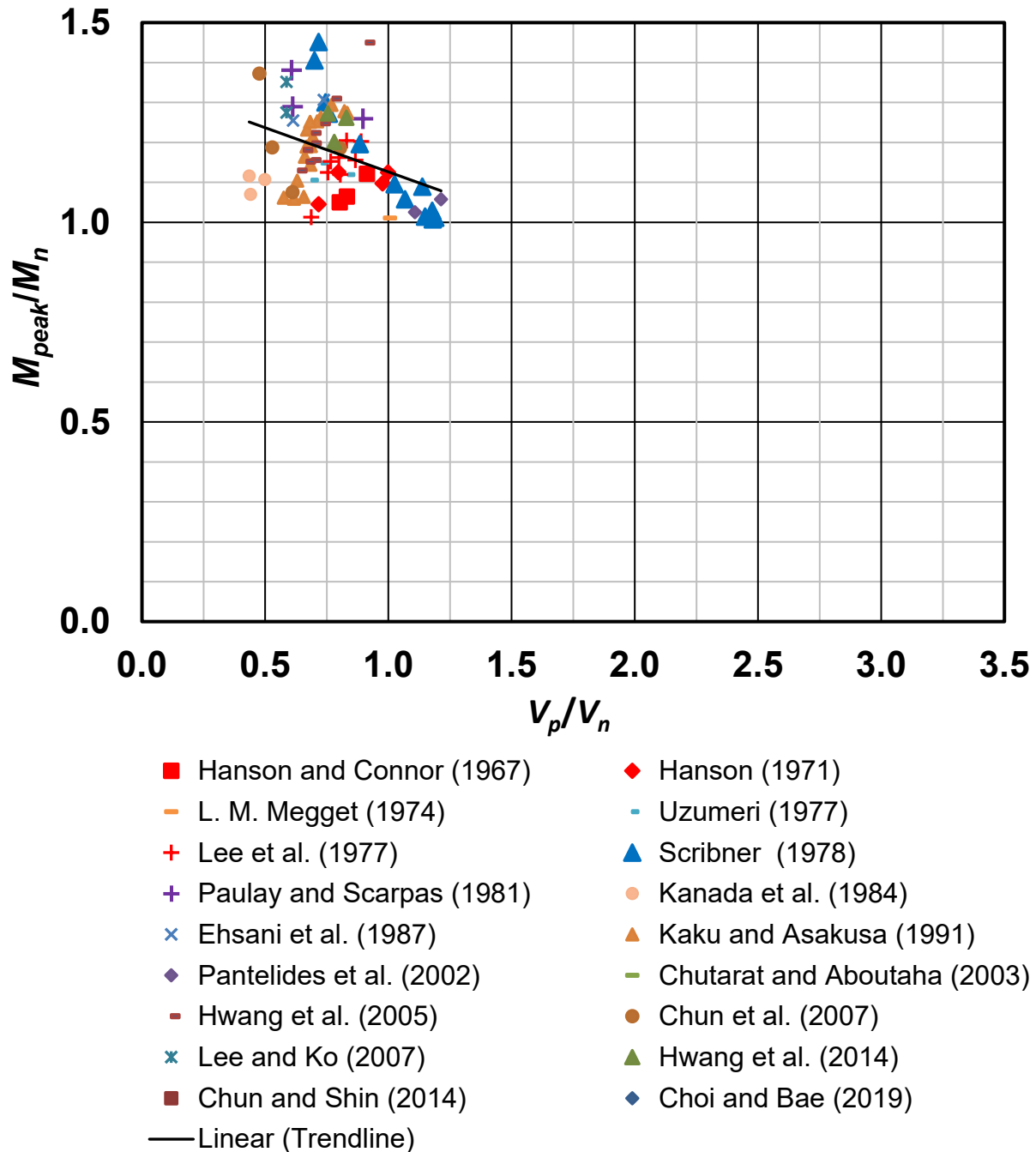


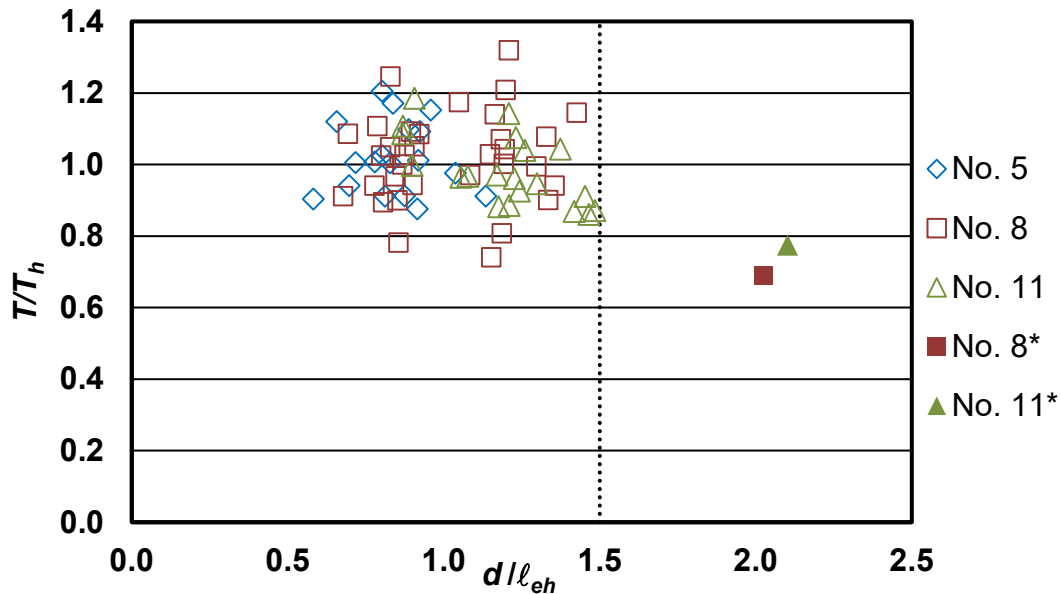
Figure 4.5 M_{peak}/M_n versus V_p/V_n for specimens with $d/l_{eh} \leq 1.5$ and $l_{eh}/l_{ey} \geq 1.0$. M_{peak}/M_n is the ratio of peak moment to nominal flexural strength, and V_p/V_n is the ratio of peak joint shear to nominal joint shear strength

4.2.2.3 Specimens with $d/l_{eh} > 1.5$

Ajaam et al. (2017) found that exterior beam-column joint specimens with a ratio of

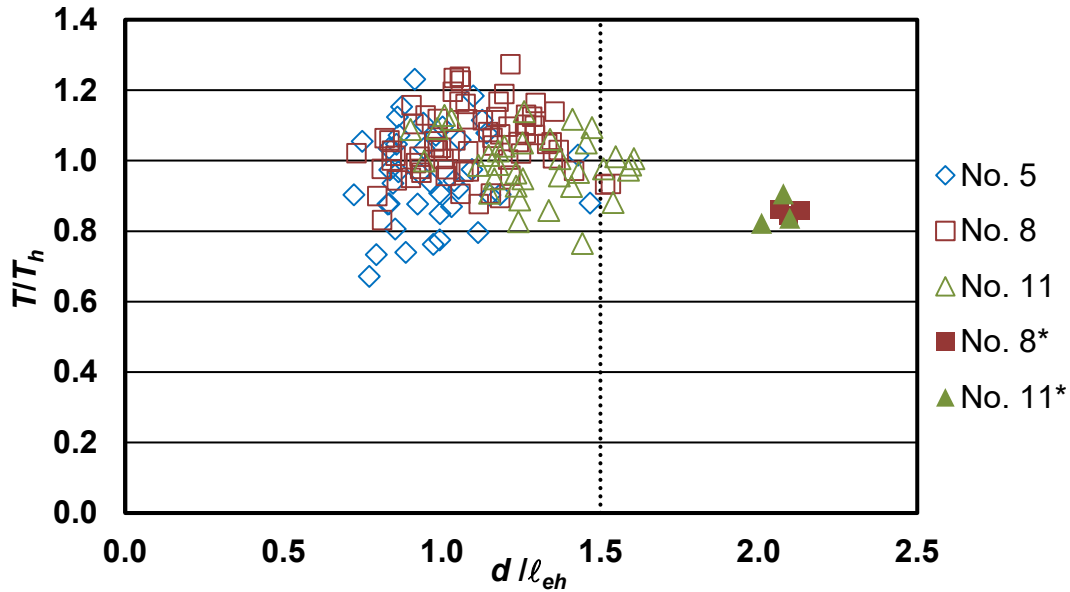
effective beam depth to embedment length $d/\ell_{eh} > 1.5$ exhibited lower anchorage strengths on average than specimens with $d/\ell_{eh} \leq 1.5$. This observation matches Commentary Section R25.4.4.2 of ACI 318-19 for headed bars, which states that “anchorage strengths will be generally higher if the anchorage length is equal to or greater than $d/1.5$.” Specimens with $d/\ell_{eh} > 1.5$ were not used in the development of the descriptive equations, Eq. (4.1) and (4.2). Beam-column joint specimens subjected to reversed cyclic loading with $d/\ell_{eh} > 1.5$ are examined in this section to investigate if the joint performance was affected.

Figures 4.6 and 4.7 show the test-to-calculated strength ratio T/T_h versus d/ℓ_{eh} for specimens tested by Ajaam et al. (2017) under monotonic loading without and with confining reinforcement, respectively. T is the average peak load (total peak load applied on the specimen divided by the number of hooked bars being developed), and T_h is the anchorage strength of a hooked bar calculated using the descriptive equations, Eq. (4.1) and (4.2).



* Specimens not used to develop the descriptive equations [Eq. (4.1) and (4.2)]

Figure 4.6 Ratio of test-to-calculated bar force at failure T/T_h versus ratio of effective beam depth to embedment length d/ℓ_{eh} for specimens without confining reinforcement [T_h is calculated using Eq. (4.1)] (Ajaam et al. 2017)



* Specimens not used to develop the descriptive equations [Eq. (4.1) and (4.2)]

Figure 4.7 Ratio of test-to-calculated bar force at failure T/T_h versus ratio of effective beam depth to embedment length d/l_{eh} for specimens with confining reinforcement [T_h is calculated using Eq. (4.2)] (Ajaam et al. 2017)

As shown in Figures 4.6 and 4.7, the anchorage strengths of monotonically-loaded specimens with $d/l_{eh} > 1.5$ average 32 and 19%, respectively, lower than the specimens with $d/l_{eh} \leq 1.5$. As was observed by Ajaam et al. (2017), the presence of confining reinforcement reduces the impact of having $d/l_{eh} > 1.5$ on anchorage strength.

The ratio of effective beam depth to embedment length d/l_{eh} for 39 of the 135 beam-column joint specimens that were subjected to reversed cyclic loading (see Table 4.2) was greater than 1.5, with values ranging from 1.55 to 3.01. These included two specimens tested by Ehsani and Wight (1982), six specimens tested by Kanada et al. (1984), six specimens tested by Zerbe and Durrani (1985), three specimens tested by Ehsani et al. (1987), 11 specimens tested by Ehsani and Alameddine (1991), three specimens tested by Tsonos et al. (1992), four specimens tested by Tsonos (2007), one specimen tested by Kang et al. (2010), and three specimens tested by Chun and Shin (2014). Of the 39 specimens, 17 had $\ell_{eh}/\ell_{ehy} \geq 1.0$, and the remaining 22 had $\ell_{eh}/\ell_{ehy} < 1.0$. Concrete compressive strengths ranged from 3,140 to 13,700 psi. The hooked bar sizes ranged from No. 3 (D10) to No. 9 (D29), with yield strengths ranging from 48,000 to 76,700 psi. Concrete side cover to the hooked bar and minimum center-to-center spacing between the hooked bars

ranged from 1.3 to $4.0d_b$ (0.7 to 3.0 in.) and 1.9 to $10.7d_b$ (1.8 to 6.3 in.), respectively. Out of the 39 specimens, six specimens tested by Kanada et al. (1984) contained hooked bars terminated at 50% of the column depth; nine specimens, six tested by Zerbe and Durrani (1985), two tested by Ehsani and Wight (1982), and one tested by Kang et al. (2010) contained hooked bars terminated at 64% of the column depth; 17 specimens, three tested by Ehsani et al. (1987), 11 tested by Ehsani and Alameddine (1991), and three tested by Chun and Shin (2014) contained hooked bars terminated at 75% of the column depth; and the remaining seven specimens, three tested by Tsonos et al. (1992) and four tested by Tsonos (2007) contained hooked bars terminated at 83% of the column depth.

The values of the joint confining reinforcement ratio A_{th}/A_{hs} are presented in Table 4.2 and repeated here in Table 4.3. Out of the 39 specimens, the 17 with $\ell_{eh}/\ell_{ehy} \geq 1.0$ had A_{th}/A_{hs} ranging from 0.22 to 0.76, and the 22 specimens with $\ell_{eh}/\ell_{ehy} < 1.0$ had A_{th}/A_{hs} ranging from 0.11 to 0.76. Again, as a reminder, A_{th} for Eq. (4.2) is defined as the area of confining reinforcement within $8d_b$ of the top of the hooked bars for No. 3 through No. 8 bars or within $10d_b$ for No. 9 through No. 11 bars, not $15d_b$ as defined in ACI 318-19, where d_b is the diameter of the hooked bar. As shown in Table 4.3, 36 specimens had values of A_{th}/A_{hs} greater than the upper limit of 0.2 on A_{th}/A_{hs} allowed in Eq. (4.2), and three specimens had values of A_{th}/A_{hs} less than or equal to 0.2. The effect of d/ℓ_{eh} and confining reinforcement within the joint region on the performance of the 39 specimens is discussed next.

Table 4.3 Detail of exterior beam-column joint specimens tested under reversed cyclic loading with $d/\ell_{eh} > 1.5$

Study ^[1]	Specimen	Bar Size ^[2]	f_y (ksi)	f_{cm} (psi)	$\frac{A_{th}}{A_{hs}}$	ℓ_{eh} (in.)	ℓ_{ehy} (in.)	$\frac{\ell_{eh}}{\ell_{ehy}}$	$\frac{d}{\ell_{eh}}$
Ehsani and Wight (1982)	2 ^[6]	No. 7	48.0	5070	0.11	7.4	9.6	0.77	1.93
	4 ^[6]	No. 7	48.0	6470	0.22	7.4	8.4	0.88	1.93
Kanada et al. (1984)	U41S ^[6]	D19	56.2	3870	0.22	6.0	9.8	0.61	2.17
	U42S ^[6]	D19	56.2	4370	0.33	6.0	9.5	0.63	2.17
	U21S ^[6]	D19	56.2	3870	0.45	6.0	7.8	0.77	2.17
	U22S ^[6]	D19	56.2	4370	0.67	6.0	7.5	0.79	2.17
	R42S ^[6]	D19	56.2	3140	0.33	6.0	10.4	0.58	2.17
	R21S ^[6]	D19	56.2	3140	0.45	6.0	8.3	0.73	2.17
Zerbe and Durrani (1985)	J1 ^[6]	No. 6	60.0	5710	0.45	7.8	7.7	1.01	1.63
	J2 ^{[5][6]}	No. 6	60.0	5650	0.45	7.8	7.7	1.00	1.63
	J3 ^[6]	No. 6	60.0	5780	0.45	7.8	7.7	1.01	1.63
	J4 ^{[5][6]}	No. 6	60.0	5940	0.45	7.8	7.6	1.02	1.63
	J5 ^{[5][6]}	No. 6	60.0	5610	0.45	7.8	7.7	1.00	1.63
	J6 ^{[5][6]}	No. 6	60.0	5690	0.45	7.8	7.7	1.00	1.63
Ehsani et al. (1987)	3 ^[6]	No. 6	70.0	9380	0.36	9.2	8.8	1.04	1.57
	4 ^[6]	No. 7	62.0	9760	0.27	9.3	9.8	0.94	1.55
	5 ^[6]	No. 7	48.0	6470	0.22	8.6	8.4	1.02	1.67
Ehsani and Alameddine (1991)	LL8 ^[6]	No. 8	66.3	8600	0.57	10.5	11.4	0.92	1.62
	LH8 ^[6]	No. 8	66.3	8600	0.76	10.5	11.4	0.92	1.62
	HL8 ^[6]	No. 9	64.2	8600	0.45	10.5	13.1	0.80	1.62
	HH8 ^[6]	No. 9	64.2	8600	0.60	10.5	13.1	0.80	1.62
	LL11 ^[6]	No. 8	66.3	10700	0.57	10.5	10.8	0.98	1.62
	LH11 ^[6]	No. 8	66.3	10700	0.76	10.5	10.8	0.98	1.62
	HL11 ^[6]	No. 9	64.2	10700	0.45	10.5	12.3	0.85	1.62
	HH11 ^[6]	No. 9	64.2	10700	0.60	10.5	12.3	0.85	1.62
	LL14 ^[6]	No. 8	66.3	13700	0.57	10.5	10.1	1.04	1.62
	LH14 ^[6]	No. 8	66.3	13700	0.76	10.5	10.1	1.04	1.62
HH14 ^[6]	No. 9	64.2	13700	0.60	10.5	11.5	0.91	1.62	

^[1] Values given in SI units are converted to in.-lb (1 in. = 25.4 mm; 1 psi = 1/145 MPa; and 1 kip = 4.4484 kN); notations used in these studies are described in Appendix A

^[2] Bar sizes are presented in SI and in.-lb as reported in the original studies

^[5] Specimens had transverse beams on one or both sides of the test beam. These transverse beams meet the dimensional requirements of Sections 18.8.4 and 15.2.8 of ACI 318-19 and Section 4.3 of ACI 352R-02 to be considered effective in increasing the joint shear strength

^[6] Specimens had $d/\ell_{eh} > 1.5$

Table 4.3 Cont. Detail of exterior beam-column joint specimens tested under reversed cyclic loading with $d/\ell_{eh} > 1.5$

Study ^[1]	Specimen	Bar Size ^[2]	f_y (ksi)	f_{cm} (psi)	$\frac{A_{th}}{A_{hs}}$	ℓ_{eh} (in.)	ℓ_{ehy} (in.)	$\frac{\ell_{eh}}{\ell_{ehy}}$	$\frac{d}{\ell_{eh}}$
Tsonos et al. (1992)	S1 ^[6]	D14	70.3	5360	0.33	6.5	5.9	1.09	1.67
	S2 ^[6]	D12	76.7	3770	0.30	6.5	5.9	1.10	1.67
	S6' ^[6]	D14	70.3	4200	0.16	6.5	7.6	0.85	1.67
Tsonos (2007)	A1 ^[6]	D10	73.0	5080	0.36	6.5	4.4	1.47	1.64
	E1 ^[6]	D14	72.0	3190	0.24	6.4	7.7	0.84	1.66
	E2 ^[6]	D14	72.0	5080	0.37	6.4	6.2	1.04	1.66
	G1 ^[6]	D14	72.0	3190	0.12	6.4	7.9	0.82	1.66
Kang et al. (2010)	Jk ^[6]	D19	67.0	4200	0.25	11.3	7.8	1.43	1.73
Chun and Shin (2014)	H1.5S ^[6]	D19	70.8	3710	0.58	9.0	9.4	0.95	1.7
	H2.0S ^[6]	D19	70.8	3830	0.58	9.0	8.6	1.04	2.4
	H2.5S ^[6]	D19	70.8	3830	0.58	9.0	8.6	1.04	3.0

^[1] Values given in SI units are converted to in.-lb (1 in. = 25.4 mm; 1 psi = 1/145 MPa; and 1 kip = 4.4484 kN); notations used in these studies are described in Appendix A

^[2] Bar sizes are presented in SI and in.-lb as reported in the original studies

^[6] Specimens had $d/\ell_{eh} > 1.5$

An approach for beam-column joints with $d/\ell_{eh} > 1.5$ is recommended by Section R25.4.4.2 of the Commentary of ACI 318R-19, which, in addressing a similar case for headed bars, recommends “providing reinforcement in the form of hoops and ties to establish a load path in accordance with strut-and-tie modeling principles.” To evaluate specimens subjected to reversed cyclic loading with $d/\ell_{eh} > 1.5$ and check if there was sufficient confining reinforcement within the joint region, anchorage strengths of hooked bars with d/ℓ_{eh} greater than 1.5 are calculated using the strut-and-tie modeling approach. In this approach, all confining reinforcement within the joint region (not the effective confining reinforcement A_{th} , as presented in Section 4.2.1) is assumed, for simplicity, to serve as a single tie with a total force of $f_{ytr}A_v$, as shown in Figure 4.8, where f_{ytr} is the yield strength of the confining reinforcement (ksi) and A_v is the total area of confining reinforcement parallel to the hooked bar (in.²). This tie is used to transfer the force in the hooked bars nT' to the compression region of the beam, where n is the number of hooked bars in tension, and T' is the estimated peak force (kips) in each hooked bar. The force in the hooked bar in beam-column joint specimens subjected to reversed cyclic loading was not directly measured during the tests. Therefore, Eq. (4.4) is used to approximate the peak force in each hooked bar T' .

$$T' = \frac{M_{peak}}{M_n} A_b f_y \quad (4.4)$$

where M_{peak} is the peak moment calculated at the beam-column joint interface (kip-in.); M_n is the nominal flexural strength of the main beam (kip-in.); A_b is the area of a hooked bar (in.²); and f_y is the yield strength of the hooked bar (ksi).

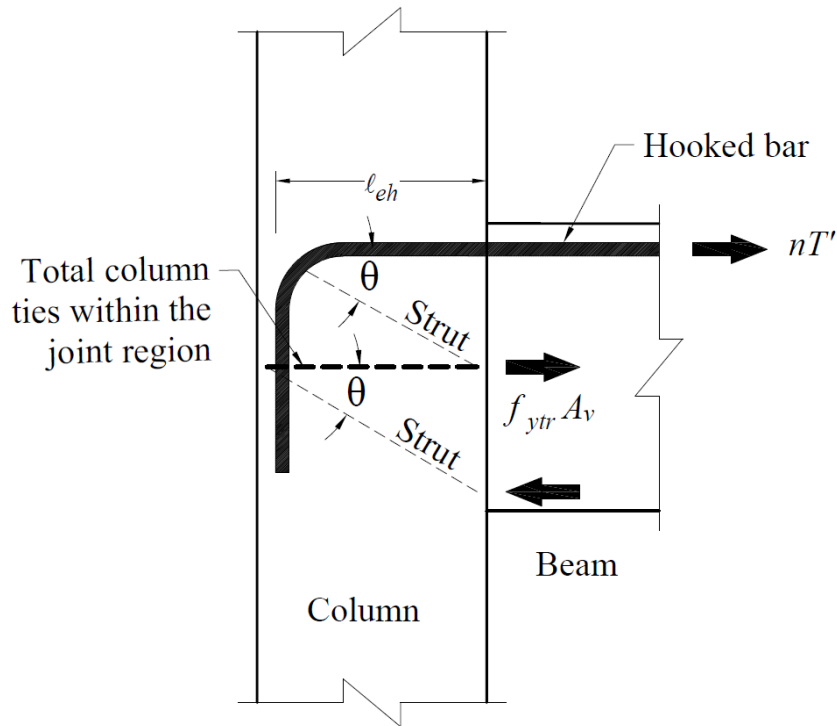


Figure 4.8 Load transfer within the beam-column joint based on the strut-and-tie mechanism (column longitudinal reinforcement and beam compression reinforcement are not shown for clarity)

In this analysis, specimens with $f_{ytr} A_v$ greater than or equal to nT' are considered to have adequate confining reinforcement within the joint region to transfer load using the strut-and-tie mechanism. The summary results of the evaluation of the 39 specimens with $d/l_{eh} > 1.5$ are presented in Table 4.4, and details of the specimens are provided in Table C.4 of Appendix C. Only four of the 39 specimens had $f_{ytr} A_v$ values greater than or equal to nT' as required by a strut-and-tie model, one tested by Ehsani and Alameddine (1991) [LH8] and three tested by Chun and Shin (2014) [H1.5S, H2.0S, and H2.5S]. These four specimens, with values of d/l_{eh} ranging from 1.62 to 3.0, had values of l_{eh}/l_{ehy} between 0.88 and 0.90 and M_{peak}/M_n values between 1.01 and

1.12, with a peak moment reduction of less than 20% at 3.5% drift. This observation indicates that beam-column joint specimens with d/ℓ_{eh} greater than 1.5 (up to 3.0) containing a sufficient amount of confining reinforcement within the joint region, as determined by the strut-and-tie modeling approach, performed satisfactorily under reversed cyclic loading. The performance of other specimens with $f_{ytr}A_v < nT'$ is discussed next.

Figure 4.9 shows M_{peak}/M_n plotted versus ℓ_{eh}/ℓ_{ehy} for specimens with $d/\ell_{eh} > 1.5$. For comparison, trendlines for specimens with $d/\ell_{eh} \leq 1.5$ are shown in the figure, along with trendlines for specimens with $d/\ell_{eh} > 1.5$. As shown in the figure, for specimens with $\ell_{eh}/\ell_{ehy} < 1.0$, the trendline for the 22 specimens with $d/\ell_{eh} > 1.5$ crosses and goes above the trendline for specimens with $d/\ell_{eh} \leq 1.5$ as ℓ_{eh}/ℓ_{ehy} approaches 1.0, whereas for specimens with $\ell_{eh}/\ell_{ehy} \geq 1.0$, the trendline for the 17 specimens with $d/\ell_{eh} > 1.5$ is above and parallel to the trendline for specimens with $d/\ell_{eh} \leq 1.5$. All specimens with $\ell_{eh}/\ell_{ehy} \geq 1.0$, including those that did not have enough confining reinforcement to transfer bar force to the compression region of the beam based on the strut-and-tie model approach ($f_{ytr}A_v < nT'$), had values of $M_{peak}/M_n \geq 1.0$ and showed no more than a 20% reduction in the peak moment at 3.5% drift. These observations indicate that given $\ell_{eh} > \ell_{ehy}$, the performance of specimens, including those with $f_{ytr}A_v < nT'$, under reversed cyclic loading was not substantially affected in cases where d/ℓ_{eh} was greater than 1.5 (up to the maximum value of 3.0).

Table 4.4 Test parameters for exterior beam-column joint specimens containing hooked bars with $d/\ell_{eh} > 1.5$ and tested under reversed cyclic loading

Study ^[1]	Specimen	Bar Size ^[2]	f_y (ksi)	f_{cm} (psi)	$\frac{d}{\ell_{eh}}$	f_{ytr} (ksi)	A_v (in. ²)	nT' (kips)	$\frac{f_{ytr} A_v}{nT'}$
Ehsani and Wight (1982)	2	No. 7	48.0	5070	1.93	63.4	0.80	170.8	0.30
	4	No. 7	48.0	6470	1.93	63.4	1.20	214.0	0.36
Kanada et al. (1984)	U41S	D19	56.2	3870	2.17	43.0	0.39	54.8	0.31
	U42S	D19	56.2	4370	2.17	43.0	0.59	59.0	0.43
	U21S	D19	56.2	3870	2.17	43.0	0.39	40.4	0.42
	U22S	D19	56.2	4370	2.17	43.0	0.59	46.4	0.54
	R42S	D19	56.2	3140	2.17	43.0	0.59	59.4	0.42
	R21S	D19	56.2	3140	2.17	43.0	0.39	40.9	0.41
Zerbe and Durrani (1985)	J1	No. 6	60.0	5710	1.63	77.0	1.20	111.8	0.83
	J2 ^[3]	No. 6	60.0	5650	1.63	77.0	1.20	132.0	0.70
	J3	No. 6	60.0	5780	1.63	77.0	1.20	114.6	0.81
	J4 ^[3]	No. 6	60.0	5940	1.63	77.0	1.20	115.5	0.80
	J5 ^[3]	No. 6	60.0	5610	1.63	77.0	1.20	106.7	0.87
	J6 ^[3]	No. 6	60.0	5690	1.63	77.0	1.20	191.7	0.48
Ehsani et al. (1987)	3	No. 6	70.0	9380	1.57	63.4	1.20	183.7	0.41
	4	No. 7	62.0	9760	1.55	63.4	1.20	181.3	0.42
	5	No. 7	48.0	6470	1.67	63.4	1.20	187.5	0.41
Ehsani and Alameddine (1991)	LL8	No. 8	66.3	8600	1.62	64.8	2.40	243.4	0.64
	LH8	No. 8	66.3	8600	1.62	64.8	3.60	235.5	1.00
	HL8	No. 9	64.2	8600	1.62	64.8	2.40	261.8	0.59
	HH8	No. 9	64.2	8600	1.62	64.8	3.60	264.3	0.88
	LL11	No. 8	66.3	10700	1.62	64.8	2.40	202.9	0.77
	LH11	No. 8	66.3	10700	1.62	64.8	3.60	273.2	0.85
	HL11	No. 9	64.2	10700	1.62	64.8	2.40	249.2	0.62
	HH11	No. 9	64.2	10700	1.62	64.8	3.60	271.2	0.86
	LL14	No. 8	66.3	13700	1.62	64.8	2.40	249.2	0.62
	LH14	No. 8	66.3	13700	1.62	64.8	3.60	254.5	0.92
HH14	No. 9	64.2	13700	1.62	64.8	3.60	273.8	0.85	
Tsonos et al. (1992)	S1	D14	70.3	5360	1.67	71.7	0.47	43.6	0.77
	S2	D12	76.7	3770	1.67	71.7	0.47	46.4	0.72
	S6'	D14	70.3	4200	1.67	71.7	0.47	69.1	0.49

^[1] Values given in SI units are converted to in.-lb (1 in. = 25.4 mm; 1 psi = 1/145 MPa; and 1 kip = 4.4484 kN); notations used in these studies are described in Appendix A

^[2] Bar sizes are presented in SI and in.-lb as reported in the original studies

^[3] Specimens had transverse beams on one or both sides of the test beam. These transverse beams meet the dimensional requirements of Section 18.8.4 of ACI 318-19 and Section 4.3 of ACI 352R-02 to be considered effective in increasing the joint shear strength

Table 4.4 Cont. Test parameters for exterior beam-column joint specimens containing hooked bars with $d/\ell_{eh} > 1.5$ and tested under reversed cyclic loading

Study ^[1]	Specimen	Bar Size ^[2]	f_y (ksi)	f_{cm} (psi)	$\frac{d}{\ell_{eh}}$	f_{ytr} (ksi)	A_v (in. ²)	nT' (kips)	$\frac{f_{ytr} A_v}{nT'}$
Tsonos (2007)	A1	D10	73.0	5080	1.64	78.0	0.44	45.0	0.76
	E1	D14	72.0	3190	1.66	78.0	0.44	59.2	0.58
	E2	D14	72.0	5080	1.66	78.0	0.44	43.3	0.79
	G1	D14	72.0	3190	1.66	78.0	0.18	52.5	0.26
Kang et al. (2010)	JK	D19	67.0	4200	1.73	83.0	0.88	147.4	0.50
Chun and Shin (2014)	H1.5S	D19	70.8	3710	1.70	66.7	3.00	126.3	1.58
	H2.0S	D19	70.8	3830	2.40	66.7	4.20	138.5	2.02
	H2.5S	D19	70.8	3830	3.00	66.7	5.40	126.0	2.86

^[1] Values given in SI units are converted to in.-lb (1 in. = 25.4 mm; 1 psi = 1/145 MPa; and 1 kip = 4.4484 kN); notations used in these studies are described in Appendix A

^[2] Bar sizes are presented in SI and in.-lb as reported in the original studies

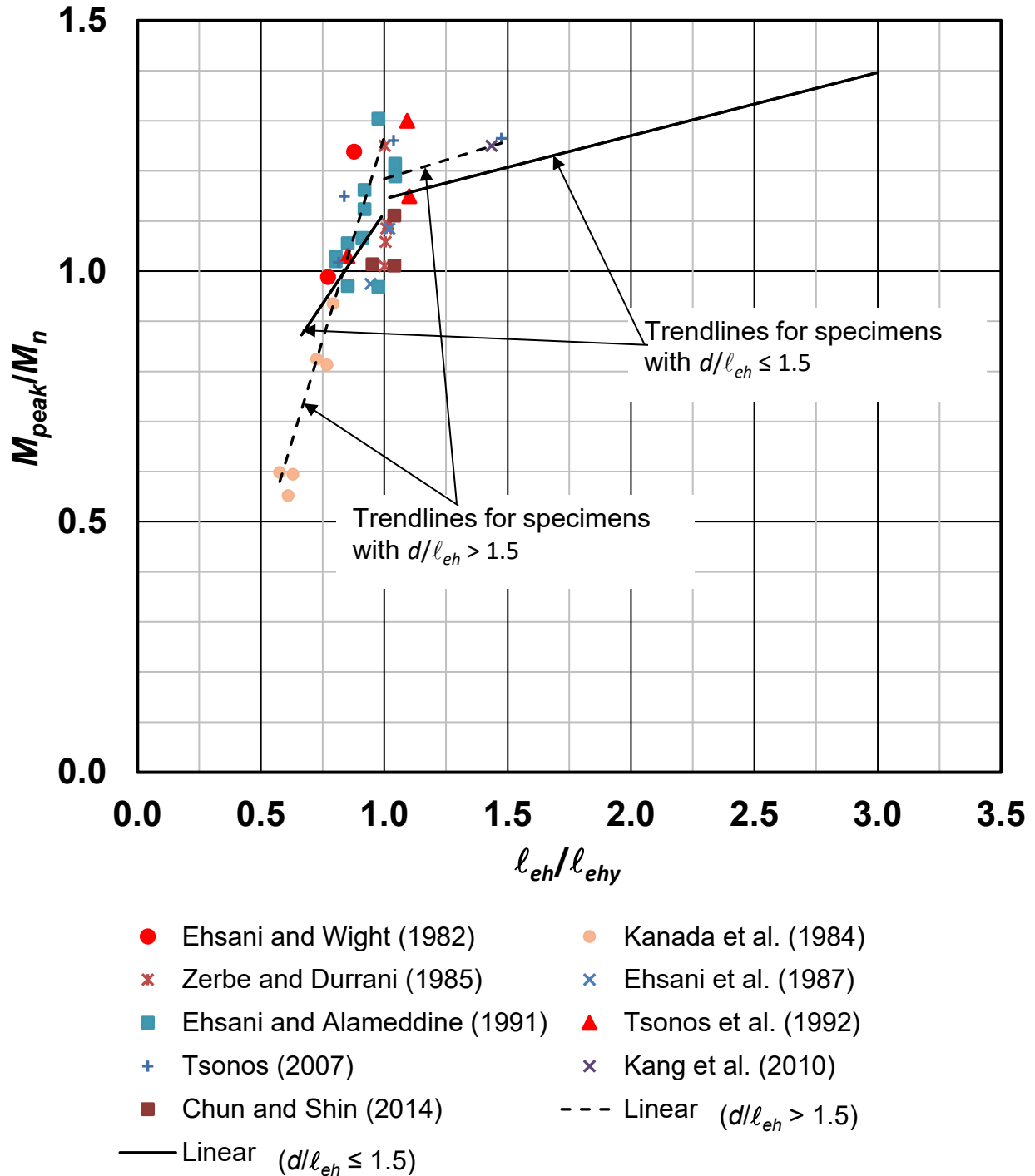


Figure 4.9 M_{peak}/M_n versus ℓ_{eh}/ℓ_{ehy} for specimens with $d/\ell_{eh} > 1.5$. M_{peak}/M_n is the ratio of peak moment to nominal flexural strength, and ℓ_{eh}/ℓ_{ehy} is the ratio of embedment length to the embedment length required to yield the hooked bar calculated using the descriptive equations developed by Ajaam et al. (2017), Eq. (4.1) and (4.2)

4.2.2.4 Applicability of Descriptive Equations to Predict Anchorage Strength of Hooked Bars Anchored in Members Subjected to Reversed Cyclic Loading

The applicability of the descriptive equations developed by Ajaam et al. (2017) for the anchorage strength of hooked bars in beam-column joints tested under monotonic loading to predict the anchorage strength of hooked bars anchored in members subjected to reversed cyclic loading is investigated in this section. The descriptive equations, Eq. (4.1) and (4.2), are presented in detail in Section 4.2.1. In this investigation, the bar forces at failure in beam-column joint specimens subjected to reversed cyclic loading evaluated in this chapter and shown in Table 4.5 are compared with the bar forces predicted by the descriptive equations. The force in the hooked bars at failure T' is estimated using Eq. (4.4), and the anchorage strength T_h is calculated using the descriptive equations, Eq. (4.1) and (4.2). The descriptive equations give an average ratio of test-to-calculated failure load for beam-column joint specimens tested under monotonic loading equal to 1.0. Therefore, the descriptive equations can be considered to have accurately predicted the anchorage strength of hooked bars subjected to reversed cyclic loading if the average ratio of test to calculated bar force at failure is greater than or equal to 1.0. As mentioned earlier in Section 4.2.2, beam-column joint specimens with a ratio of effective beam depth to embedment length $d/\ell_{eh} > 1.5$ were not included when Ajaam et al. (2017) developed the descriptive equations, Eq. (4.1) and (4.2). Therefore, only beam-column joint specimens with $d/\ell_{eh} \leq 1.5$ (ranging from 0.6 to 1.5) were included in this investigation. As found earlier in Sections 4.2.2.1 and 4.2.2.2, the anchorage performance of the hooked bars in beam-column joints subjected to reversed cyclic loading was affected by high joint shear. Therefore, only beam-column joint specimens with the ratio of peak joint shear (V_p) to nominal joint shear strength (V_n) less than or equal to 1.0 (V_p/V_n ranging from 0.43 to 1.00) were included in this investigation. To this end, the test results of 79 exterior beam-column joint specimens (shown in Table 4.5) tested under reversed cyclic loading with $d/\ell_{eh} \leq 1.5$ and $V_p/V_n \leq 1.0$ are used in this evaluation.

Table 4.5 Detail of exterior beam-column joint specimens tested under reversed cyclic loading with $d/\ell_{eh} \leq 1.5$ and $V_p/V_n \leq 1.0$ used in this evaluation and comparisons with descriptive equations, Eq. (4.1) and (4.2)

Study ^[1]		Specimen	Bar Size ^[2]	f_y (ksi)	f_{cm} (psi)	$\frac{\ell_{eh}}{\ell_{ehy}}$	T' (kips)	T_h (kips)	$\frac{T'}{T_h}$
1	Hanson and Connor (1967)	I ^[3]	No. 9	51.6	3470	1.21	57.9	51.9	1.12
		I-A ^[3]	No. 9	47.8	3200	1.24	50.9	48.0	1.06
		II	No. 9	48.3	3650	1.32	50.7	48.6	1.04
		V ^{[3][4]}	No. 9	51.0	3300	0.81	45.4	40.8	1.11
		V-A ^[4]	No. 9	49.8	5420	0.82	53.2	40.4	1.32
2	Hanson (1971)	1 ^[5]	No. 8	63.1	5500	1.15	52.1	50.1	1.04
		3 ^[5]	No. 8	64.1	5200	1.11	57.0	50.9	1.12
		4	No. 8	63.4	5380	1.08	56.3	50.3	1.12
		5	No. 8	65.0	5230	1.10	56.3	51.6	1.09
4	Uzumeri (1977)	1 ^{[4][5]}	No. 9	50.3	4460	0.83	53.2	41.2	1.29
		2 ^[4]	No. 9	50.6	4510	0.83	52.0	41.3	1.26
		3 ^[5]	No. 9	50.8	3920	1.13	56.2	51.1	1.10
		4 ^[5]	No. 9	50.6	4490	1.17	58.1	50.9	1.14
		5 ^{[4][5]}	No. 9	50.4	4630	0.80	54.0	39.6	1.36
		6	No. 9	51.1	5250	1.03	57.2	51.3	1.11
		7	No. 9	51.1	4460	0.99	59.9	50.8	1.18
5	Lee et al. (1977)	1	No. 6	52.5	4200	1.09	25.9	23.2	1.11
		2	No. 6	48.6	4200	1.18	24.0	21.5	1.12
		3	No. 6	48.7	4100	1.17	21.7	21.5	1.01
		4	No. 6	48.9	4000	1.16	25.0	21.6	1.16
		5	No. 6	50.9	3600	1.08	26.9	22.5	1.20
		6	No. 6	51.6	3600	1.06	26.2	22.8	1.15
		7	No. 6	47.5	3700	1.17	25.2	21.0	1.20
		8	No. 6	48.2	4200	1.19	24.4	21.3	1.15

^[1] Values given in SI units are converted to in.-lb (1 in. = 25.4 mm; 1 psi = 1/145 MPa; and 1 kip = 4.4484 kN); notations used in these studies are described in Appendix A

^[2] Bar sizes are presented in SI and in.-lb as reported in the original studies

^[3] Analyzed as a doubly reinforced section to calculate the nominal flexural strength M_n ; all other specimens are analyzed as a single reinforced

^[4] Specimens did not contain confining reinforcement parallel to the hooked bars within the joint region

^[5] Specimens had transverse beams on one or both sides of the test beam. These transverse beams meet the dimensional requirements of Section 18.8.4 of ACI 318-19 and Section 4.3 of ACI 352R-02 to be considered effective in increasing the joint shear strength

Table 4.5 Cont. Detail of exterior beam-column joint specimens tested under reversed cyclic loading with $d/\ell_{eh} \leq 1.5$ and $V_p/V_n \leq 1.0$ used in this evaluation and comparisons with descriptive equations, Eq. (4.1) and (4.2)

Study ^[1]		Specimen	Bar Size ^[2]	f_y (ksi)	f_{cm} (psi)	$\frac{\ell_{eh}}{\ell_{ehy}}$	T' (kips)	T_h (kips)	$\frac{T'}{T_h}$
6	Scribner (1978)	1	No. 6	48.9	4950	1.75	30.2	21.6	1.40
		2	No. 6	48.9	5050	1.76	31.2	21.6	1.44
		3	No. 6	48.9	4940	1.32	25.7	21.6	1.19
		5	No. 6	52.7	3680	1.49	29.5	23.3	1.26
		6	No. 6	52.7	4080	1.53	30.1	23.3	1.29
7	Paulay and Scarpas (1981)	Unit 1	D20	42.9	3280	2.86	27.0	21.1	1.28
		Unit 2	D20	42.9	3260	2.86	26.3	21.1	1.25
		Unit 3	D20	42.9	3900	3.00	28.9	21.1	1.37
9	Kanada et al. (1984)	U40L ^[4]	D19	56.2	3530	0.68	19.5	16.4	1.19
		U41L	D19	56.2	3870	0.91	25.4	22.9	1.11
		U42L	D19	56.2	4370	0.95	24.9	23.6	1.06
		U20L ^[4]	D19	56.2	3870	1.02	26.6	24.8	1.07
		U21L	D19	56.2	4370	1.19	27.7	25.0	1.11
		R41L	D19	56.2	3140	0.86	22.9	21.7	1.06
		R21L	D19	56.2	3140	1.09	27.5	25.0	1.10
11	Ehsani et al. (1987)	1	No. 6	70.0	9380	1.30	38.7	30.9	1.25
		2	No. 6	70.0	9760	1.32	40.2	30.9	1.30
12	Kaku and Asakusa (1991)	1	D13	56.7	4510	1.44	14.2	11.2	1.27
		2	D13	56.7	6050	1.56	14.1	11.2	1.26
		3	D13	56.7	6050	1.56	12.3	11.2	1.10
		4	D13	56.7	6480	1.51	13.7	11.2	1.23
		5	D13	56.7	5320	1.43	12.7	11.2	1.14
		6	D13	56.7	5860	1.47	11.8	11.2	1.06
		7	D13	56.7	4670	1.46	14.2	11.2	1.27
		8	D13	56.7	5970	1.56	13.9	11.2	1.25
		9	D13	56.7	5890	1.55	13.5	11.2	1.21
		10	D13	56.7	6440	1.51	13.9	11.2	1.25
		11	D13	56.7	6080	1.48	13.2	11.2	1.19

^[1] Values given in SI units are converted to in.-lb (1 in. = 25.4 mm; 1 psi = 1/145 MPa; and 1 kip = 4.4484 kN); notations used in these studies are described in Appendix A

^[2] Bar sizes are presented in SI and in.-lb as reported in the original studies

^[4] Specimens did not contain confining reinforcement parallel to the hooked bars within the joint region

Table 4.5 Cont. Detail of exterior beam-column joint specimens tested under reversed cyclic loading with $d/\ell_{eh} \leq 1.5$ and $V_p/V_n \leq 1.0$ used in this evaluation and comparisons with descriptive equations, Eq. (4.1) and (4.2)

Study ^[1]		Specimen	Bar Size ^[2]	f_y (ksi)	f_{cm} (psi)	$\frac{\ell_{eh}}{\ell_{ehy}}$	T' (kips)	T_h (kips)	$\frac{T'}{T_h}$
12	Kaku and Asakusa (1991)	12	D13	56.7	5090	1.41	11.8	11.2	1.06
		13	D13	56.7	6730	1.61	11.8	11.2	1.06
		14	D13	56.7	5950	1.48	13.0	11.2	1.16
		15	D13	56.7	5760	1.46	13.3	11.2	1.19
		16	D13	56.7	5420	1.52	14.4	11.2	1.29
17	Hwang et al. (2005)	0T0 ^[4]	No. 8	62.4	9760	1.18	56.9	49.3	1.16
		3T44	No. 8	62.4	11140	1.40	60.3	49.5	1.22
		1B8	No. 8	63.1	8960	1.30	72.3	50.1	1.44
		3T3	No. 8	62.4	10010	1.36	64.5	49.5	1.30
		2T4	No. 8	62.4	10300	1.30	61.5	49.4	1.24
		1T44	No. 8	62.4	10560	1.38	59.0	49.5	1.19
		3T4	No. 8	71.2	10910	1.37	63.6	56.5	1.13
		2T5	No. 8	71.2	11110	1.38	66.4	56.5	1.18
		1T55	No. 8	71.2	10110	1.34	64.8	56.5	1.15
19	Chun et al. (2007)	JC-1	D22	58.4	8950	1.93	48.1	35.2	1.37
		JC-2	D22	58.4	8720	1.64	41.6	35.1	1.18
		WC ^[4]	D25	62.5	8180	1.31	58.6	49.4	1.19
		JC-No. 11-1	D36	66.4	4760	1.05	111.4	104.0	1.07
20	Lee and Ko (2007)	S0	D22	66.0	4730	1.90	53.5	39.8	1.35
		W0	D22	66.0	4190	1.15	50.5	39.8	1.27
22	Hwang et al. (2014)	T1-400	D22	75.4	4640	1.69	54.3	45.5	1.20
		T2-600	D22	103.0	4640	1.23	78.6	62.0	1.27
		T3-600 ^[3]	D25	92.1	4290	1.09	91.8	73.0	1.26
23	Chun and Shin (2014)	H1.0U	D19	70.8	3710	0.95	32.3	29.8	1.08
24	Choi and Bae (2019)	JTR-0-BTR	D25	68.4	7950	0.81	56.4	44.8	1.26
		JNR-0-BTR ^[4]	D25	68.4	7950	0.66	47.8	34.7	1.38
		JTR-0-BNR	D25	68.4	7950	0.81	54.0	44.8	1.21

^[1] Values given in SI units are converted to in.-lb (1 in. = 25.4 mm; 1 psi = 1/145 MPa; and 1 kip = 4.4484 kN); notations used in these studies are described in Appendix A

^[2] Bar sizes are presented in SI and in.-lb as reported in the original studies

^[3] Analyzed as a doubly reinforced section to calculate the nominal flexural strength M_n ; all other specimens are analyzed as a single reinforced

^[4] Specimens did not contain confining reinforcement parallel to the hooked bars within the joint region

Fourteen beam-column joint specimens tested under reversed cyclic loading with $d/\ell_{eh} \leq 1.5$ and $V_p/V_n \leq 1.0$ used in this evaluation had $\ell_{eh}/\ell_{ehy} < 1.0$. Concrete compressive strengths

ranged from 3,140 to 7,950 psi. Hooked bar sizes ranged from No. 6 (D19) to No. 9 (D29), with yield strengths ranging from 49,800 to 70,800 psi. The concrete side cover to the hooked bar ranged from 1.8 to $3.9d_b$ (2 to 3.5 in.), and center-to-center spacing between the hooked bars ranged from 2.3 to $4.6d_b$ (1.8 to 4.9 in.). The embedment length of the hooked bars ranged from 8.3 to $12d_b$ (8.3 to 13.5 in.). Statistical parameters, including maximum, minimum, mean, standard deviation (STD), and coefficient of variation (COV), of T'/T_h for the specimens with $\ell_{eh}/\ell_{ehy} < 1.0$ are presented in Table 4.6. For comparison, the statistical parameters of T'/T_h for the beam-column joint specimens tested under monotonic loading and used by Ajaam et al. (2017) to develop the descriptive equations, Eq. (4.1) and (4.2), are also presented in Table 4.6, where T is the measured average bar force at failure (total peak load carried by the specimen divided by the number of hooked bars being developed). The values of T'/T_h for the 14 specimens with $\ell_{eh}/\ell_{ehy} < 1.0$ ranged between 1.06 and 1.38 with a mean, standard deviation (STD), and coefficient of variation (COV) of 1.20, 0.110, and 0.091, respectively, as shown in Table 4.6. The ratio of test to calculated failure load of hooked bars T'/T_h in the specimens tested and used by Ajaam et al. (2017) to develop descriptive equations, Eq. (4.1) and (4.2), ranged from 0.74 to 1.32 with a mean, STD, and COV of 1.00, 0.115, and 0.115, and from 0.67 to 1.27 with a mean, STD, and COV of 1.00, 0.112, and 0.112, respectively. These findings indicate that the descriptive equations successfully capture the anchorage behavior of the hooked bars with $\ell_{eh}/\ell_{ehy} < 1.0$ subjected to reversed cyclic loading.

Table 4.6 Statistical parameters for test-to-calculated ratio in beam-column joint specimens with $\ell_{eh}/\ell_{ehy} < 1.0$ tested under reversed cyclic loading and in beam-column joint specimens tested under monotonic loading and used by Ajaam et al. (2017) to develop the descriptive equations, Eq. (4.1) and (4.2)

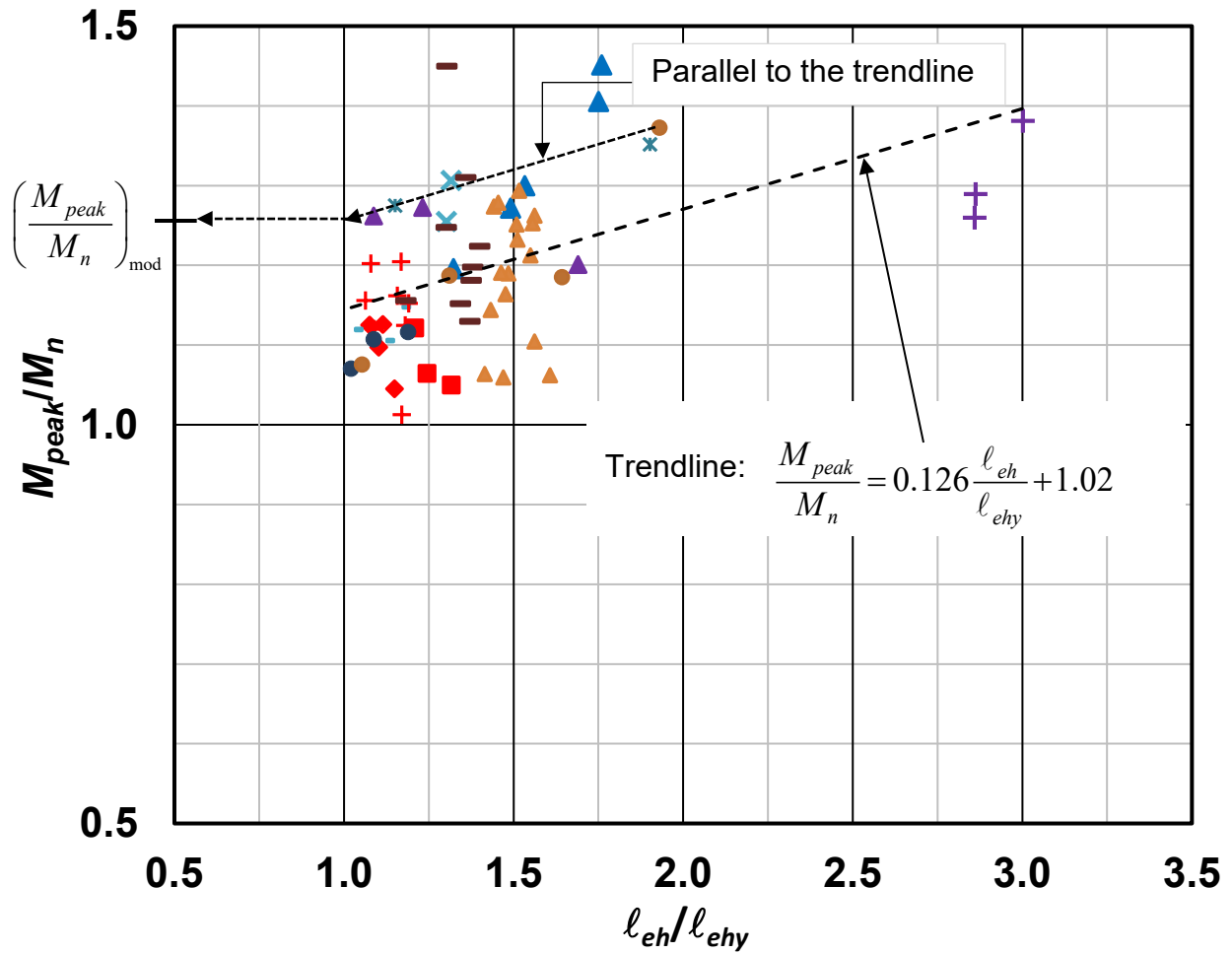
Test/Calculated	T'/T_h	T/T_h	
Statistical Parameters	Specimens tested under reversed cyclic loading with $\ell_{eh}/\ell_{ehy} < 1.0$	Specimens tested and used by Ajaam et al. (2017) to develop Eq. (4.1)	Specimens tested and used by Ajaam et al. (2017) to develop Eq. (4.2)
Max	1.38	1.32	1.27
Min	1.06	0.74	0.67
Mean	1.20	1.00	1.00
STD	0.110	0.115	0.112
COV	0.091	0.115	0.112
Number of specimens	14	88	149

A similar analysis was carried out on specimens with $\ell_{eh}/\ell_{ehy} \geq 1.0$ that were subjected to reversed cyclic loading. Sixty-five beam-column joint specimens tested under reversed cyclic loading with $d/\ell_{eh} \leq 1.5$ and $V_p/V_n \leq 1.0$ used in this evaluation had $\ell_{eh}/\ell_{ehy} \geq 1.0$. Concrete compressive strengths ranged from 3,140 to 11,140 psi. Hooked bar sizes ranged from No. 4 (D13) to No. 11 (D36), with yield strengths ranging from 42,900 to 103,000 psi. The concrete side cover to the hooked bar ranged from 1.4 to $9.8d_b$ (1.03 to 8.6 in.), and center-to-center spacing between the hooked bars ranged from 2.3 to $8.4d_b$ (1.7 to 6.6 in.). The embedment length of the hooked bars ranged from 11.5 to $24d_b$ (7.7 to 21.0 in.). All the sixty-five specimens with $\ell_{eh}/\ell_{ehy} \geq 1.0$ had $M_{peak}/M_n \geq 1.0$. The statistical parameters, including maximum, minimum, mean, standard deviation (STD), and coefficient of variation (COV), of T'_{mod}/T_h for the specimens with $\ell_{eh}/\ell_{ehy} \geq 1.0$ are presented in Table 4.7. T'_{mod} is the modified bar force at failure T' corresponding to the value of M_{peak}/M_n projected on the line $\ell_{eh}/\ell_{ehy} = 1.0$ line by extending a line parallel to the trend line for specimens with $\ell_{eh}/\ell_{ehy} \geq 1.0$, as shown in Figure 4.10 for one specimen, and calculated using Eq. (4.5). The anchorage strength of the hooked bar T_h is calculated using the descriptive equations, Eq. (4.1) and (4.2), corresponding to $\ell_{eh} = \ell_{ehy}$ as for T'_{mod} .

$$T'_{\text{mod}} = \left(\frac{M_{\text{peak}}}{M_n} \right)_{\text{mod}} A_b f_y \quad (4.5)$$

$$\text{with } \left(\frac{M_{\text{peak}}}{M_n} \right)_{\text{mod}} = \frac{M_{\text{peak}}}{M_n} - 0.126 \left(\frac{\ell_{eh}}{\ell_{ehy}} - 1 \right)$$

where the coefficient of 0.126 is the slope of the trendline for specimens with $\ell_{eh}/\ell_{ehy} \geq 1.0$ in Figure 4.10. An example of calculating $(M_{\text{peak}}/M_n)_{\text{mod}}$ is shown graphically in Figure 4.10.



- | | |
|----------------------------|--|
| ■ Hanson and Connor (1967) | ◆ Hanson (1971) |
| - Uzumeri (1977) | + Lee et al. (1977) |
| ▲ Scribner (1978) | + Paulay and Scarpas (1981) |
| ● Kanada et al. (1984) | × Ehsani et al. (1987) |
| ▲ Kaku and Asakusa (1991) | - Hwang et al. (2005) |
| ● Chun et al. (2007) | × Lee and Ko (2007) |
| ▲ Hwang et al. (2014) | ■ Chun and Shin (2014) |
| ◆ Choi and Bae (2019) | - - - Linear ($l_{eh}/l_{ehy} \geq 1.0$) |

Figure 4.10 M_{peak}/M_n versus l_{eh}/l_{ehy} for beam-column joint specimens with $l_{eh}/l_{ehy} \geq 1.0$. The value of M_{peak}/M_n for one specimen is projected on the line $l_{eh}/l_{ehy} = 1.0$ line by extending a line parallel to the trend line for specimens with $l_{eh}/l_{ehy} \geq 1.0$

The values of T'_{mod}/T_h for the 65 beam-column joint specimens with $l_{eh}/l_{ehy} \geq 1.0$ (presented in Table 4.8) ranged between 0.98 and 1.41 with a mean, STD, and COV of 1.14, 0.087,

and 0.076, respectively, as shown in Table 4.7. As mentioned earlier that the ratio of test to calculated failure load of hooked bars T/T_h in the specimens tested and used by Ajaam et al. (2017) to develop the descriptive equations, Eq. (4.1) and (4.2), ranged from 0.74 to 1.32 with a mean, STD, and COV of 1.00, 0.115, and 0.115, and from 0.67 to 1.27 with a mean, STD, and COV of 1.00, 0.112, and 0.112, respectively, as shown in Table 4.6. These results indicate that the descriptive equations conservatively capture the anchorage behavior of the hooked bars with $l_{eh}/l_{ehy} \geq 1.0$ subjected to reversed cyclic loading.

Table 4.7 Statistical parameters for T'_{mod}/T_h in beam-column joint specimens with $l_{eh}/l_{ehy} \geq 1.0$ tested under reversed cyclic loading

Test/Calculated	T'_{mod}/T_h
Statistical Parameters	Specimens tested under reversed cyclic loading with $l_{eh}/l_{ehy} \geq 1.0$
Max	1.41
Min	0.98
Mean	1.14
STD	0.087
COV	0.076
Number of specimens	65

Table 4.8 Detail of exterior beam-column joint specimens tested under reversed cyclic loading with $d/\ell_{eh} \leq 1.5$, $V_p/V_n \leq 1.0$, and $\ell_{eh}/\ell_{ehy} \geq 1.0$ used in this evaluation and comparisons with descriptive equations, Eq. (4.1) and (4.2)

Study ^[1]		Specimen	Bar Size ^[2]	f_y (ksi)	f_{cm} (psi)	$\frac{\ell_{eh}}{\ell_{ehy}}$	T'_{mod} (kips)	T_h (kips)	$\frac{T'_{mod}}{T_h}$
1	Hanson and Connor (1967)	I ^[3]	No. 9	51.6	3470	1.21	56.5	51.9	1.09
		I-A ^[3]	No. 9	47.8	3200	1.24	49.4	48.0	1.03
		II	No. 9	48.3	3650	1.32	48.8	48.6	1.00
2	Hanson (1971)	1 ^[5]	No. 8	63.1	5500	1.15	51.2	50.1	1.02
		3 ^[5]	No. 8	64.1	5200	1.11	56.3	50.9	1.11
		4	No. 8	63.4	5380	1.08	55.9	50.3	1.11
		5	No. 8	65.0	5230	1.10	55.7	51.6	1.08
4	Uzumeri (1977)	3 ^[5]	No. 9	50.8	3920	1.13	55.4	51.1	1.08
		4 ^[5]	No. 9	50.6	4490	1.17	57.0	50.9	1.12
		6	No. 9	51.1	5250	1.03	57.0	51.3	1.11
5	Lee et al. (1977)	1	No. 6	52.5	4200	1.09	25.6	23.2	1.1
		2	No. 6	48.6	4200	1.18	23.6	21.5	1.1
		3	No. 6	48.7	4100	1.17	21.2	21.5	1.0
		4	No. 6	48.9	4000	1.16	24.6	21.6	1.1
		5	No. 6	50.9	3600	1.08	26.7	22.5	1.2
		6	No. 6	51.6	3600	1.06	26.1	22.8	1.1
		7	No. 6	47.5	3700	1.17	24.7	21.0	1.2
		8	No. 6	48.2	4200	1.19	23.9	21.3	1.1
6	Scribner (1978)	1	No. 6	48.9	4950	1.75	28.2	21.6	1.3
		2	No. 6	48.9	5050	1.76	29.2	21.6	1.3
		3	No. 6	48.9	4940	1.32	24.9	21.6	1.1
		5	No. 6	52.7	3680	1.49	28.1	23.3	1.2
		6	No. 6	52.7	4080	1.53	28.6	23.3	1.2
7	Paulay and Scarpas (1981)	Unit 1	D20	42.9	3280	2.86	22.0	21.1	1.05
		Unit 2	D20	42.9	3260	2.86	21.4	21.1	1.02
		Unit 3	D20	42.9	3900	3.00	23.6	21.1	1.12

^[1] Values given in SI units are converted to in.-lb (1 in. = 25.4 mm; 1 psi = 1/145 MPa; and 1 kip = 4.4484 kN); notations used in these studies are described in Appendix A

^[2] Bar sizes are presented in SI and in.-lb as reported in the original studies

^[3] Analyzed as a doubly reinforced section to calculate the nominal flexural strength M_n ; all other specimens are analyzed as a single reinforced

^[4] Specimens did not contain confining reinforcement parallel to the hooked bars within the joint region

^[5] Specimens had transverse beams on one or both sides of the test beam. These transverse beams meet the dimensional requirements of Section 18.8.4 of ACI 318-19 and Section 4.3 of ACI 352R-02 to be considered effective in increasing the joint shear strength

Table 4.8 Cont. Detail of exterior beam-column joint specimens tested under reversed cyclic loading with $d/\ell_{eh} \leq 1.5$, $V_p/V_n \leq 1.0$, and $\ell_{eh}/\ell_{ehy} \geq 1.0$ used in this evaluation and comparisons with descriptive equations, Eq. (4.1) and (4.2)

Study ^[1]		Specimen	Bar Size ^[2]	f_y (ksi)	f_{cm} (psi)	$\frac{\ell_{eh}}{\ell_{ehy}}$	T'_{mod} (kips)	T_h (kips)	$\frac{T'_{mod}}{T_h}$
9	Kanada et al. (1984)	U20L ^[4]	D19	56.2	3870	1.02	26.5	24.8	1.07
		U21L	D19	56.2	4370	1.19	27.1	25.0	1.09
		R21L	D19	56.2	3140	1.09	27.2	25.0	1.09
11	Ehsani et al. (1987)	1	No. 6	70.0	9380	1.30	37.5	30.9	1.21
		2	No. 6	70.0	9760	1.32	39.0	30.9	1.26
12	Kaku and Asakusa (1991)	1	D13	56.7	4510	1.44	13.6	11.2	1.21
		2	D13	56.7	6050	1.56	13.3	11.2	1.19
		3	D13	56.7	6050	1.56	11.5	11.2	1.03
		4	D13	56.7	6480	1.51	13.0	11.2	1.17
		5	D13	56.7	5320	1.43	12.1	11.2	1.09
		6	D13	56.7	5860	1.47	11.1	11.2	1.00
		7	D13	56.7	4670	1.46	13.6	11.2	1.22
		8	D13	56.7	5970	1.56	13.2	11.2	1.18
		9	D13	56.7	5890	1.55	12.7	11.2	1.14
		10	D13	56.7	6440	1.51	13.2	11.2	1.19
		11	D13	56.7	6080	1.48	12.6	11.2	1.13
		12	D13	56.7	5090	1.41	11.3	11.2	1.01
		13	D13	56.7	6730	1.61	11.0	11.2	0.98
		14	D13	56.7	5950	1.48	12.3	11.2	1.10
		15	D13	56.7	5760	1.46	12.6	11.2	1.13
		16	D13	56.7	5420	1.52	13.7	11.2	1.22
17	Hwang et al. (2005)	0T0 ^[4]	No. 8	62.4	9760	1.18	55.8	49.3	1.13
		3T44	No. 8	62.4	11140	1.40	57.8	49.5	1.17
		1B8	No. 8	63.1	8960	1.30	70.4	50.1	1.41
		3T3	No. 8	62.4	10010	1.36	62.3	49.5	1.26
		2T4	No. 8	62.4	10300	1.30	59.6	49.4	1.21
		1T44	No. 8	62.4	10560	1.38	56.7	49.5	1.14

^[1] Values given in SI units are converted to in.-lb (1 in. = 25.4 mm; 1 psi = 1/145 MPa; and 1 kip = 4.4484 kN); notations used in these studies are described in Appendix A

^[2] Bar sizes are presented in SI and in.-lb as reported in the original studies

^[3] Analyzed as a doubly reinforced section to calculate the nominal flexural strength M_n ; all other specimens are analyzed as a single reinforced

^[4] Specimens did not contain confining reinforcement parallel to the hooked bars within the joint region

Table 4.8 Cont. Detail of exterior beam-column joint specimens tested under reversed cyclic loading with $d/\ell_{eh} \leq 1.5$, $V_p/V_n \leq 1.0$, and $\ell_{eh}/\ell_{ehy} \geq 1.0$ used in this evaluation and comparisons with descriptive equations, Eq. (4.1) and (4.2)

Study ^[1]		Specimen	Bar Size ^[2]	f_y (ksi)	f_{cm} (psi)	$\frac{\ell_{eh}}{\ell_{ehy}}$	T'_{mod} (kips)	T_h (kips)	$\frac{T'_{mod}}{T_h}$
17	Hwang et al. (2005)	3T4	No. 8	71.2	10910	1.37	60.9	56.5	1.08
		2T5	No. 8	71.2	11110	1.38	63.8	56.5	1.13
		1T55	No. 8	71.2	10110	1.34	62.4	56.5	1.10
19	Chun et al. (2007)	JC-1	D22	58.4	8950	1.93	44.0	35.2	1.25
		JC-2	D22	58.4	8720	1.64	38.7	35.1	1.10
		WC ^[4]	D25	62.5	8180	1.31	56.7	49.4	1.15
		JC-No. 11-1	D36	66.4	4760	1.05	110.7	104.0	1.06
20	Lee and Ko (2007)	S0	D22	66.0	4730	1.90	49.0	39.8	1.23
		W0	D22	66.0	4190	1.15	49.7	39.8	1.25
22	Hwang et al. (2014)	T1-400	D22	75.4	4640	1.69	50.4	45.5	1.11
		T2-600	D22	103.0	4640	1.23	76.8	62.0	1.24
		T3-600 ^[3]	D25	92.1	4290	1.09	91.0	73.0	1.25

^[1] Values given in SI units are converted to in.-lb (1 in. = 25.4 mm; 1 psi = 1/145 MPa; and 1 kip = 4.4484 kN); notations used in these studies are described in Appendix A

^[2] Bar sizes are presented in SI and in.-lb as reported in the original studies

^[3] Analyzed as a doubly reinforced section to calculate the nominal flexural strength M_n ; all other specimens are analyzed as a single reinforced

^[4] Specimens did not contain confining reinforcement parallel to the hooked bars within the joint region

The estimated hooked bar forces at failure T'_{mod} for the 65 exterior beam-column joint specimens tested under reversed cyclic loading with $d/\ell_{eh} \leq 1.5$, $V_p/V_n \leq 1.0$, and $\ell_{eh}/\ell_{ehy} \geq 1.0$ are plotted versus the calculated failure loads T_h [based on the descriptive equations, Eq. (4.1) and (4.2)] in Figure 4.11. The broken line represents equality, where the calculated and the estimated hooked bar forces at failure are equal. The solid line is the trend line for the data. As shown in the figure, the trend line is above and close to the broken line, indicating that the descriptive equations, Eq. (4.1) and (4.2), provide a somewhat conservative estimate of the anchorage strength of hooked bars with and without confining reinforcement in beam-column joint specimens subjected to reversed cyclic loading.

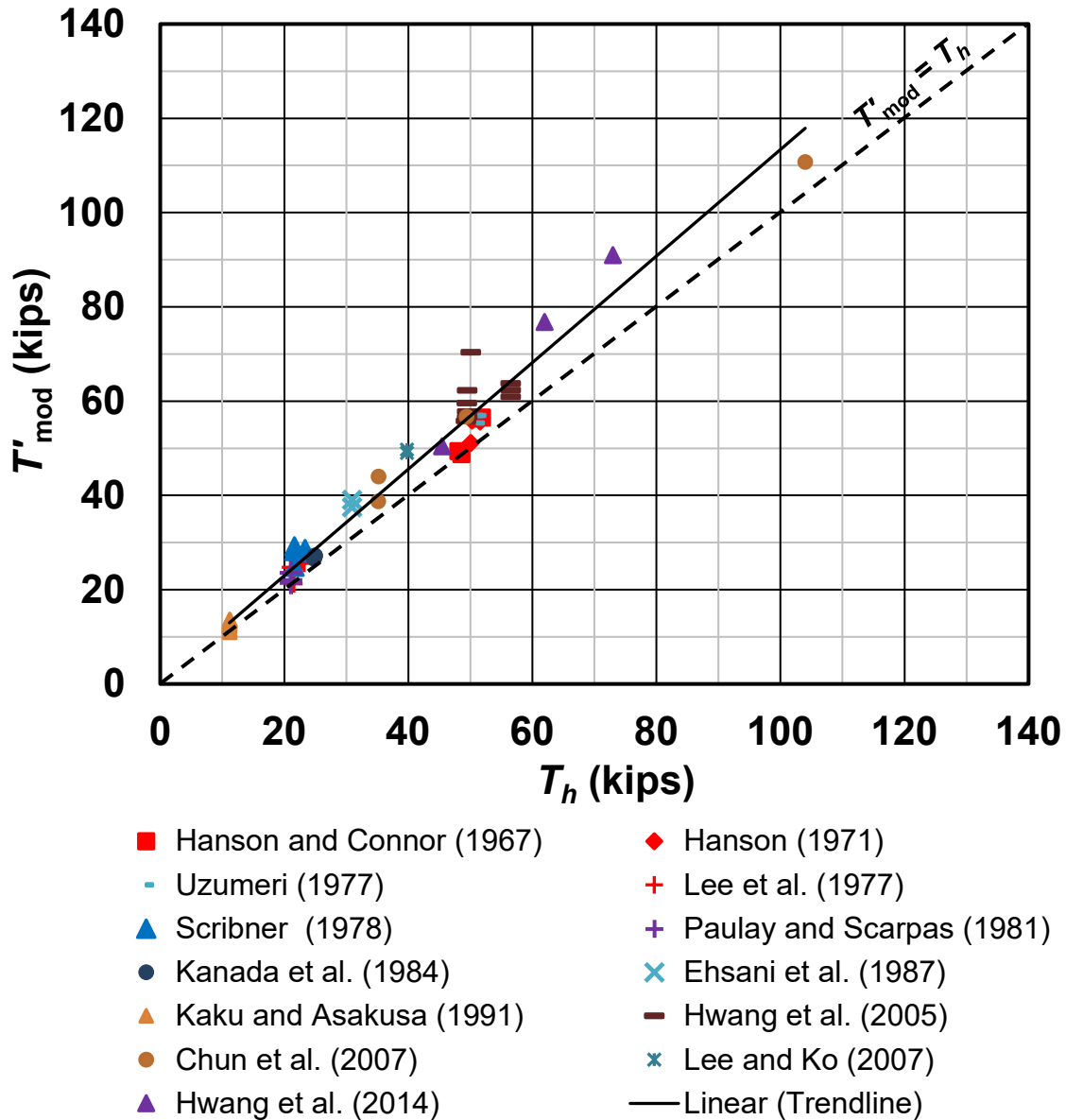


Figure 4.11 Estimated hooked bar force at failure T'_{mod} versus hooked bar force T_h [based on the descriptive equations, Eq. (4.1) and (4.2)] for specimens with $d/\ell_{eh} \leq 1.5$, $V_p/V_n \leq 1.0$, and $\ell_{eh}/\ell_{ehy} \geq 1.0$.

In summary, of the 146 beam-column joint specimens tested under reversed cyclic loading in the database, 65 satisfied the criteria of having $d/\ell_{eh} \leq 1.5$, $V_p/V_n \leq 1.0$, and $\ell_{eh}/\ell_{ehy} \geq 1.0$. These specimens, on average, satisfied the requirements for minimum strength and deformation capacity, with $M_{peak}/M_n \geq 1.0$ and $\delta_{0.8peak} \geq 3.5\%$. According to the results of the analyses presented in this chapter, it is concluded that the descriptive equations developed for beam-column joint specimens

tested under monotonic loading, which serve as the basis for the development length provisions for hooked bars in ACI 318-19, are sufficient for determining the required embedment length of hooked bars in beam-column joints subjected to reversed cyclic loading.

4.3 GUIDELINES AND RECOMMENDATIONS FOR CHAPTER 18 OF ACI 318-19

As mentioned in Sections 1.1 and 1.6.3, the development length provisions for hooked bars in tension under reversed cyclic loading in Section 18.8.5.1 of ACI 318-19 were derived directly from the development length provisions for non-seismic (monotonic) loading (Section 25.4.3.1) that existed in ACI 318 Building Codes prior to 2019. Even though the development length provisions (Section 25.4.3.1) were updated in ACI 318-19 based on the comprehensive study conducted at KU using specimens tested under monotonic loading (Sperry et al. 2015a,b, 2017a,b, 2018, Ajaam et al. 2017, 2018, Yasso et al. 2017), the Code design provisions for the development length of hooked bars in tension subjected to reversed cyclic loading remained unchanged. This has resulted in provisions allowing development lengths for hooked bars designed in accordance with Chapter 18 to be *shorter* than those needed for gravity load by Chapter 25, as shown in Section 4.3.1, which is an odd situation. The analyses in this chapter were performed to examine the suitability of applying the development length requirements of 25.4.3 to the design of hooked bars subjected to reversed cyclic stress. Those analyses show that the descriptive equations developed by Ajaam et al. (2017), Eq. (4.1) and (4.2), for the anchorage strength of hooked bars in beam-column joints tested under monotonic loading are suitable for predicting the anchorage strength of hooked bars anchored in members subjected to reversed cyclic loading. These findings strongly suggest that a single approach be used in ACI 318 for calculating the development length of hooked bars anchored in members subjected to gravity and seismic loading using Section 25.4.3.1 of ACI 318-19. Section 4.3.2 addresses the proposed changes in Chapter 18 of ACI 318-19.

4.3.1 Comparison Between the Development Lengths of Hooked Bars Required for Seismic and Non-Seismic (Gravity) Loading (Chapter 18 vs. 25 of ACI 318-19)

The development length provisions for hooked bars in tension under *non-seismic (gravity) loading* (Section 25.4.3.1 of ACI 318-19) and under reversed cyclic loading (Section 18.8.5.1 of

ACI 318-19) are described in Sections 1.6.2 and 1.6.3, respectively. In accordance with Section 25.4.3.1 of ACI 318-19, the development length of a standard hooked bar in tension, ℓ_{dh} , for non-seismic (gravity) loading is given in Eq. (4.6), with ℓ_{dh} not less than the greater of $8d_b$ and 6 in., while, in accordance with Section 18.8.5.1 of ACI 318-19, the development length of a standard hooked bar in tension, ℓ_{dh} , for No. 11 and smaller bars embedded in beam-column joints in special moment frames with capability of sustaining reversed cyclic loading is given in Eq. (4.7), with ℓ_{dh} not less than the maximum of $8d_b$ and 6 in. for normalweight concrete and $10d_b$ and 7.5 in. for lightweight concrete.

$$\ell_{dh} = \left(\frac{f_y \psi_e \psi_r \psi_o \psi_c}{55 \lambda \sqrt{f'_c}} \right) d_b^{1.5} \quad (4.6)$$

$$\ell_{dh} = \frac{f_y d_b}{65 \lambda \sqrt{f'_c}} \quad (4.7)$$

where ℓ_{dh} is the development length of a hooked bar in tension (in.); f_y is the specified yield strength of the hooked bar (psi); d_b is the hooked bar diameter (in.); f'_c is the specified concrete compressive strength (psi); ψ_e is a factor based on the presence or absence of a coating on the bars, equal to 1.2 for epoxy-coated or zinc and epoxy dual-coated reinforcement and 1.0 for uncoated or zinc-coated (galvanized) reinforcement; ψ_r is a confining reinforcement factor equal to 1.0 for No. 11 and smaller hooked bars spaced at a center-to-center distance not less than $6d_b$ and for hooked bars with A_{th}/A_{hs} not less than 0.4, where A_{th} is the total cross-sectional area of ties or stirrups confining hooked bars (in.²) and A_{hs} is the total cross-sectional area of hooked bars being developed at a critical section (in.²); otherwise, ψ_r is equal to 1.6; ψ_o is the bar location factor equal to 1.0 for No. 11 and smaller hooked or headed bars anchored within a column core with side cover not less than 2.5 in. or in other members with side cover not less than $6d_b$; otherwise, ψ_o is equal to 1.25; ψ_c is the concrete strength factor equal to $f'_c/15,000 + 0.6$ if f'_c is less than 6000 psi and equal to 1.0 if f'_c is greater than or equal to 6000 psi; λ is a lightweight concrete factor equal to 0.75 for lightweight concrete and 1.0 for normalweight concrete. The modification factors in Eq. (4.6) are defined in Table 25.4.3.2 of ACI 318-19.

By way of an example, the development lengths of hooked bars ℓ_{dh} designed in accordance with the provisions in Chapter 25 are compared with those designed in accordance with Chapter 18 of ACI 318-19 for No. 8 and No. 11 bars with a yield strength of 60,000 psi cast in concrete with a compressive strength of 6000 psi: The modification factors in Eq. (4.6) are taken as 1.0. Comparing the values of ℓ_{dh} calculated using Eq. (4.6) and (4.7), it is found that the development lengths of No 8 and No. 11 hooked bars required for seismic loading according to Eq. (4.7) are 85% and 71%, respectively, of those required for *gravity loading* alone according to Eq. (4.6). Because the development lengths of hooked bars designed in accordance with Chapter 18 are shorter than those needed for gravity load by Chapter 25, the Code change presented in Section 4.3.2 is clearly warranted.

4.3.2 Proposed Changes in Chapter 18 of ACI 318-19

Based on the analysis presented in this chapter and the summary conclusions given in Section 4.3, proposed changes to Chapter 18 of ACI 318-19 are provided in this section. The original text of the Code is presented in black, while proposed code and commentary changes are shown in **red underlined** or **strikeout**.

18.8.5 *Development length of bars in tension*

18.8.5.1 For bar sizes No. 3 through No. 11 terminating in a standard hook, ℓ_{dh} shall be calculated by Eq. (18.8.5.1), but ℓ_{dh} shall be at least the greater of **$8d_b$** and 6 in. for normalweight concrete and at least the greater of **$10d_b$** and 7-1/2 in. for lightweight concrete, **but ℓ_{dh} shall not be less than the development length requirements of Section 25.4.3.**

$$\ell_{dh} = f_y d_b / (65\lambda\sqrt{f'_c}) \quad (18.8.5.1)$$

The value of λ shall be 0.75 for concrete containing lightweight aggregate and 1.0 otherwise.

The hook shall be located within the confined core of a column or of a boundary element, with the hook bent into the joint.

R18.8.5 *Development length of bars in tension*

R18.8.5.1 **The design provisions for the development of standard hooked bars for beam-**

column joints under reversed cyclic loading Eq. (18.8.5.1) first appeared in Appendix A of ACI 318-83 Building Code, with no changes in the current ACI 318-19 provisions. Eq. (18.8.5.1), however, by itself does not provide an adequate development length in all cases, especially for larger bars.

Minimum embedment length in tension for deformed bars with standard hooks is determined using Eq. (18.8.5.1), ~~which is based on the requirements of 25.4.3~~ but not less than the requirements of 25.4.3. The embedment length of a bar with a standard hook is the distance, parallel to the bar, from the critical section (where the bar is to be developed) to a tangent drawn to the outside edge of the hook. The tangent is to be drawn perpendicular to the axis of the bar (refer to Table 25.3.1).

The requirement for the hook to project into the joint is to improve development of a diagonal compression strut across the joint. The requirement applies to beam and column bars terminated at a joint with a standard hook.

18.8.5.3 For bar sizes No. 3 through No. 11, ℓ_d , the development length in tension for a straight bar, shall be at least the greater of (a) and (b):

(a) 2.5 times the length in accordance with 18.8.5.1, without the requirements of Section 25.4.3, if the depth of the concrete cast in one lift beneath the bar does not exceed 12 in.

(b) 3.25 times the length in accordance with 18.8.5.1, without the requirements of Section 25.4.3, if the depth of the concrete cast in one lift beneath the bar exceeds 12 in.

R18.8.5.3 Minimum development length in tension for straight bars is a multiple of the length indicated by 18.8.5.1, without the requirements of 25.4.3. Section 18.8.5.3(b) refers to top bars. Lack of reference to No. 14 and No. 18 bars in 18.8.5 is due to the paucity of information on anchorage of such bars subjected to load reversals simulating earthquake effects.

CHAPTER 5: SUMMARY AND CONCLUSIONS

5.1 SUMMARY

Hooked and headed reinforcing bars are commonly used as a means of shortening development length of reinforcing bars, but a limited amount of previous research has resulted in restrictions on their use in practice. This study included two phases: In the first phase, 31 tests of simulated column-foundation joints were conducted to investigate the anchorage strength and behavior of large and high-strength headed bars. The work involved 15 specimens, each with one to three simulated column-foundation joints. The main variables were distance between the anchored headed bar and the compression reaction, number of headed bars tested simultaneously (1 or 2), size of the headed bars (No. 11 or No. 14), center-to-center spacing between headed bars loaded simultaneously (3.2 or $8.2d_b$), amount of parallel tie reinforcement within the joint region (zero to six No. 4 closed stirrups), and concrete compressive strength (5,060 to 14,470 psi). The embedment length of the headed bars ranged from $12\frac{5}{8}$ to 14 in. The stresses in the headed bars at failure ranged from 41,800 to 144,400 psi. The net bearing area of the headed bars ranged from 4.2 to $9.2A_b$. This phase also included an evaluation of tests on headed bars tested in simulated column-foundation joints by DeVries et al. (1999), Choi et al. (2002), and Ghimire et al. (2018), and on anchor bolts tested in steel column-concrete foundation joints by Worsfold et al. (2022). The test results of the current and previous studies were compared with anchorage strengths based on the descriptive equations for headed bars developed at the University of Kansas by Shao et al. (2016), the anchorage provisions in Section 17.6.2 of ACI 318-19 with a strength reduction factor equal to 1.0, the design provisions in Section 25.4.4 of ACI 318-19, and proposed code provisions. Recommended changes to Chapters 17 and 25 of ACI 318-19 were presented.

The second phase of the study involved the analysis of test results from 24 studies that included 146 exterior beam-column joint specimens subjected to reversed cyclic loading. Key variables included embedment lengths of the hooked bars (6 to 21 in.), concrete compressive strength (3,140 to 13,700 psi), center-to-center spacing between the hooked bars (1.75 to 6.5 in.), bar size (No. 3 to No. 9), and confining reinforcement within the joint region parallel to the straight portion of the hooked bars (none to nine hoops spaced at 1.25 to 6.0 in.). The yield strength of the hooked bars ranged from 42,900 to 103,000 psi. Concrete side cover ranged from 0.7 to 8.6 in.

Column axial compressive load applied during the test ranged from zero to $0.25A_gf'_c$, where A_g is the column cross-sectional area (in.²) and f'_c is the nominal concrete compressive strength (psi). The data from these tests are analyzed using the equations developed by Ajaam et al. (2017) at the University of Kansas for beam-column joints tested under monotonic loading to investigate the applicability of the equations to predict the anchorage strength of hooked bars anchored in members subjected to reversed cyclic loading. This analysis is used, in turn, to propose a change in Section 18.8.5.1 of ACI 318 to require the use of Section 25.4.3 of ACI 318 to establish the minimum development length ℓ_{dh} for hooked bars anchored in joints for frames subjected to seismic loading. Proposed changes to Chapter 18 of ACI 318-19 were presented.

5.2 CONCLUSION

Based on the test results and analysis presented in this report, the following conclusions can be drawn:

1. Anchorage strength of headed bars anchored in column-foundation joints is improved by parallel tie reinforcement located on all sides of the headed bars, a contribution that is not included in the provisions of ACI 318-19.
2. Test results of simulated column-foundation joint specimens tested under monotonic loading show that the distance between the headed bar and the compression reaction (nearest support reaction), with a test range of up to 2.79 times the embedment length, has no effect on the anchorage strength. The anchorage strength of headed bars decreased, however, for the two specimens in which the distance between the headed bar and compression reaction equaled 5.3 and 5.6 times the embedment length.
3. Similar to observations for beam-column joints, the anchorage strength of headed bars anchored in simulated column-foundation joints decreases as the center-to-center spacing decreases below $8d_b$.
4. The descriptive equations developed based on tests of beam-column joints are suitable for predicting the anchorage strength of headed bars anchored in column-foundation joints.
5. The anchorage strength of headed bars with net bearing areas of 2.6 to $3.2A_b$ tested under monotonic loading is lower than that of the headed bars with a minimum net bearing area

of $4A_b$. Results from a single specimen tested under reversed cyclic loading with anchor bolts having a net head bearing area of $1.5A_b$, however, gave a similar strength to headed bars with bearing areas above $4A_b$.

6. The anchorage provisions in Chapter 17 of ACI 318-19 do not accurately predict the anchorage strength of headed bars tested when parallel tie/anchor reinforcement is used because the anchorage provisions account for the contribution of concrete and parallel tie reinforcement (anchor reinforcement) separately, with only the stronger of the two controlling the strength. Therefore, the ACI 318 Code should consider including provisions that combine the contributions of concrete strength and parallel tie reinforcement.
7. The descriptive equations developed by Shao et al. (2016) accurately capture the effect of parallel tie reinforcement and the contribution of concrete strength to the anchorage strength of headed bars in column-foundation joints. Therefore, a version of the descriptive equations could be used within the anchorage provisions in Chapter 17 of the ACI 318 Code.
8. The design provisions in Chapter 25 of ACI 318-19 should be further modified to accurately represent the effect of parallel tie reinforcement in connections other than beam-column joints.
9. The proposed Code provisions accurately capture the effect of parallel tie reinforcement on the anchorage strength of headed bars. Therefore, ACI 318-19 Code should consider including the proposed Code provisions in the next version.
10. The descriptive equations developed by Ajaam et al. (2017) for the anchorage strength of hooked bars in beam-column joints tested under monotonic loading, which serve as the basis for the development length provisions for hooked bars in ACI 318-19, are suitable for predicting the anchorage strength of hooked bars anchored in members subjected to reversed cyclic loading.
11. The current code provisions for the development length of hooked bars in tension under reversed cyclic loading in earthquake resistant structures (Section 18.8.5.1 of ACI 318-19) were derived directly from the development length provisions for non-seismic loading (Section 25.4.3.1) that existed in ACI 318 Building Codes before 2019. Even though the

development length provisions for monotonic loading (Section 25.4.3.1) were modified in the 2019 Code, the code design provisions for the development length of hooked bars in tension under cyclic loading did not change. This has resulted in provisions allowing development lengths for hooked bars designed in accordance with Chapter 18 to be *shorter* than those needed for gravity load by Chapter 25. Changes in Chapter 18 of ACI 318-19 are proposed that require the use of Section 25.4.3 of ACI 318 to establish the minimum development length ℓ_{dh} for hooked bars anchored in members subjected to seismic loading.

12. The test results of exterior beam-column joint specimens tested under reversed cyclic loading show that the distance between the hooked bars and compression reaction (compression region of the beam), with a test range of up to 3.0 times the embedment length, had no effect on the anchorage strength.

5.3 FUTURE WORK

In the current investigation, a maximum of two headed bars were tested simultaneously in simulated column-foundation joints. It is suggested that additional tests be conducted on groups of three or four headed bars loaded simultaneously.

The maximum bar size of headed bars evaluated in the current study is No. 14. There is interest, however, in using larger No. 18 headed bars. Therefore, it is recommended that tests be performed to investigate the anchorage strength of No. 18 headed bars in simulated column-foundation joints without and with parallel tie reinforcement.

In the current and previous studies, headed bars were investigated in normalweight concrete; there is no information regarding headed bars tested in lightweight concrete. As a result, the development length provisions of ACI 318-19 are only permitted for use with headed bars in normalweight concrete. To understand headed bar anchorage behavior and permit their use in lightweight concrete, tests are recommended.

REFERENCES

ACI Committee 318, 1983, *Building Code Requirements for Structural Concrete (ACI 318-83) and Commentary (ACI 318R-83)*, American Concrete Institute, Farmington Hills, Michigan, 111 pp.

ACI Committee 318, 1999, *Building Code Requirements for Structural Concrete (ACI 318-99) and Commentary (ACI 318R-99)*, American Concrete Institute, Farmington Hills, Michigan, 369 pp.

ACI Committee 318, 2002, *Building Code Requirements for Structural Concrete (ACI 318-02) and Commentary (ACI 318R-02)*, American Concrete Institute, Farmington Hills, Michigan, 443 pp.

ACI Committee 318, 2005, *Building Code Requirements for Structural Concrete (ACI 318-05) and Commentary (ACI 318R-05)*, American Concrete Institute, Farmington Hills, Michigan, 430 pp.

ACI Committee 318, 2008, *Building Code Requirements for Structural Concrete (ACI 318-08) and Commentary (ACI 318R-08)*, American Concrete Institute, Farmington Hills, Michigan, 465 pp.

ACI Committee 318, 2011, *Building Code Requirements for Structural Concrete (ACI 318-11) and Commentary (ACI 318R-11)*, American Concrete Institute, Farmington Hills, Michigan, 503 pp.

ACI Committee 318, 2014, *Building Code Requirements for Structural Concrete (ACI 318-14) and Commentary (ACI 318R-14)*, American Concrete Institute, Farmington Hills, Michigan, 520 pp.

ACI Committee 318, 2019, *Building Code Requirements for Structural Concrete (ACI 318-19) and Commentary (ACI 318R-19)*, American Concrete Institute, Farmington Hills, Michigan, 624 pp.

ACI Committee 352, 2002, *Recommendation for Design of Beam-Column Connections in Monolithic Reinforced Concrete Structures (ACI 352R-02, reapproved 2010)*, American Concrete Institute, Farmington Hills, Michigan, 38 pp.

ACI Committee 349, 2006, *Code Requirements for Nuclear Safety Related Concrete Structures (ACI 349-06)*, American Concrete Institute, Farmington Hills, Michigan, 157 pp.

ACI Committee 408, 2003, *Bond and Development of Straight Reinforcement in Tension (ACI 408R-03)*, American Concrete Institute, Farmington Hills, Michigan, 49 pp.

Ajaam, A., Darwin, D., and O'Reilly, M., 2017, "Anchorage Strength Reinforcing Bars with Standard Hooks," *SM Report No. 125*, University of Kansas Center for Research, Inc., Lawrence, Kansas, Apr., 346 pp.

Ajaam, A., Yasso, S., Darwin, D., O'Reilly, M., and Sperry, J., 2018, "Anchorage Strength of Closely Spaced Hooked Bars," *ACI Structural Journal*, Vol. 115, No. 4, July, pp. 1143-1152

ASTM A615, 2016, *Standard Specification for Deformed and Plain Carbon-Steel Bars for Concrete Reinforcement (ASTM A615/A615M-16)*, ASTM International, West Conshohocken, PA, 8 pp.

ASTM A615, 2020, *Standard Specification for Deformed and Plain Carbon-Steel Bars for Concrete Reinforcement (ASTM A615/A615M-20)*, ASTM International, West Conshohocken, PA, 8 pp.

ASTM A706, 2016, *Standard Specification for Deformed and Plain Low-Alloy Steel Bars for Concrete Reinforcement (ASTM A706/A706M-16)*, ASTM International, West Conshohocken, PA, 7 pp.

ASTM A970, 2016, *Standard Specification for Headed Steel Bars for Concrete Reinforcement (ASTM A970/A970M-16)*, ASTM International, West Conshohocken, PA, 9 pp.

ASTM A970, 2017, *Standard Specification for Headed Steel Bars for Concrete Reinforcement (ASTM A970/A970M-17)*, ASTM International, West Conshohocken, PA, 9 pp.

ASTM A1035, 2015, *Standard Specification for Deformed and Plain, Low-Carbon, Chromium, Steel Bars for Concrete Reinforcement (ASTM A1035/A1035M-15)*, ASTM International, West Conshohocken, PA, 7 pp.

Bashandy, T. R., 1996, "Application of Headed Bars in Concrete Members," *Ph.D. dissertation*, University of Texas at Austin, Austin, TX, Dec., 303 pp.

Choi, D.-U., Hong, S.-G., and Lee, C.-Y., 2002, "Test of Headed Reinforcement in Pullout," *KCI Concrete Journal*, Vol. 14, No. 3, Sep., pp. 102-110.

Choi, D.-U., 2006, "Test of Headed Reinforcement in Pullout II: Deep Embedment," *International Journal of Concrete Structures and Materials*, Vol. 18, No. 3E, Aug., pp. 151-159.

Choi, C., and Bae, B., 2019, "Effectiveness of Steel Fiber as Hoops in Exterior Beam-to-Column Joints under Cyclic Loading," *ACI Structural Journal*, Vol. 116, No. 2, Mar., pp. 205-220.

Chutarat, N., and Aboutaha, R., 2003, "Cyclic Response of Exterior Reinforced Concrete Beam-Column Joints Reinforced with Headed Bars Experimental Investigation," *ACI Structural Journal*, Vol. 100, No. 2, Mar.-Apr., pp. 259-264.

Chun, S., Lee, S., Kang, T., Oh, B., and Wallace, J., 2007, "Mechanical Anchorage in Exterior Beam-Column Joints Subjected to Cyclic Loading," *ACI Structural Journal*, Vol. 104, No. 1, Jan.-Feb., pp. 102-112.

Chun, S. C., Oh, B., Lee, S. H., and Naito, C. J., 2009, "Anchorage Strength and Behavior of Headed Bars in Exterior Beam-Column Joints," *ACI Structural Journal*, Vol. 106, No. 5, Sep.-Oct., pp. 579-590.

Chun, S., and Shin, Y., 2014, "Cyclic Testing of Exterior Beam-Column Joints with Varying Joint Aspect Ratio," *ACI Structural Journal*, Vol. 111, No. 3, May-June, pp. 693-704.

Craig, R., Mahadev, S., Patel, C., Viteri, M., and Kertesz, C., 1984, "Behavior of Joints Using Reinforced Fibrous Concrete," Fiber Reinforced Concrete, SP 81, *American Concrete Institute*, Detroit, MI, pp. 125-167.

Darwin, D., and Dolan, C. W., 2021, *Design of Concrete Structures*, 16th ed., McGraw-Hill, New York, 880 pp.

DeVries, R. A., 1996, "Anchorage of Headed Reinforcement in Concrete," *PhD Dissertation*, The University of Texas at Austin, Austin, Texas, Dec., 314 pp.

DeVries, R. A., Jirsa, J. O., and Bashandy, T., 1999, "Anchorage Capacity in Concrete of Headed Reinforcement with Shallow Embedments," *ACI Structural Journal*, Vol. 96, No. 5, Sep.-Oct., pp. 728-736.

Ehsani, M., and Alameddine, F., 1991, "Design Recommendations for Type 2 High-Strength Reinforced Concrete Connections," *ACI Structural Journal*, Vol. 88, No. 3, May-June, pp. 227-291.

Ehsani, M., and Wight, J., 1982, "Behavior of External Reinforced Concrete Beam to Column Connections Subjected to Earthquake Type Loading," *Report No. NSF/CEE-82099*, University of Michigan, Department of Civil Engineering, Ann Arbor, MI, July, 270 pp.

Ehsani, M., Moussa, A., and Vallenilla, C., 1987, "Comparison of Inelastic Behavior of Reinforced Ordinary- and High-Strength Concrete Frames," *ACI Structural Journal*, Vol. 84, No. 2, Mar.-Apr., pp. 161-169.

Eligehausen, R., Mällée, R., and Silva, J., 2006b, "*Anchorage in Concrete Construction*," Ernst & Sohn (J. T. Wiley), Berlin, Germany, May, 380 pp.

Fishburn, C. D., 1947, (iley), Berlid Slip Under Load of Bent-Bar Anchorages and Straight Embedments in Haydite Concrete, *ACI Journal*, Proceedings Vol. 44, Dec., pp. 289-305.

Fuchs, W., Eligehausen, R., and Breen, J. E., 1995, "Concrete Capacity Design (CCD) Approach for Fastening to Concrete," *ACI Structural Journal*, Vol. 92, No. 1, Jan.-Feb., pp. 73-94.

Fujii, S., and Morita, S., 1991, "Comparison Between Interior and Exterior RC Beam-Column Joint Behavior," Design of Beam-Column Joints for Seismic Resistance, SP 123-6, *American Concrete Institute*, Detroit, MI, pp. 145-165.

- Ghimire, K., Darwin, D., and O'Reilly, M., 2018, "Anchorage of Headed Reinforcing Bars in Concrete," *SM Report No. 127*, University of Kansas Center for Research, Inc., Lawrence, KS, Jan., 278 pp.
- Ghimire, K., Shao, Y., Darwin, D., and O'Reilly, M., 2019a, "Conventional and High-Strength Headed Bars—Part 1: Anchorage Tests," *ACI Structural Journal*, Vol. 116, No. 3, May, pp. 255-264.
- Ghimire, K., Shao, Y., Darwin, D., and O'Reilly, M., 2019b, "Conventional and High-Strength Headed Bars—Part 2: Data Analysis," *ACI Structural Journal*, Vol. 116, No. 3, May, pp. 265-272.
- Ghimire, K. P., Darwin, D., and Lepage, A., 2021, "Headed Bars in Beam-Column Joints Subjected to Reversed Cyclic Loading," *ACI Structural Journal*, Vol. 118, No. 3, May, pp. 27-33.
- Hamad, B., Jirsa, J., and D'Abreu de Paulo, N., 1993, "Anchorage Strength of Epoxy-Coated Hooked Bars," *ACI Structural Journal*, Vol. 90, No. 2, Mar.-Apr., pp. 210-217.
- Hanson, N., and Connor, H., 1967, "Seismic Resistance of Reinforced Concrete Beam-Column Joints," *Journal of the Structural Division*, Vol. 93, ST 5, Oct., pp. 535-560.
- Hanson, N., 1971, "Seismic Resistance of Concrete frames with grade 60 reinforcement," *Journal of the Structural Division*, ASCE, Vol. 97, ST6, June, pp. 1685-1700.
- Hribar, J. A. and Vasko, R. C., 1969, "End Anchorage of High Strength Steel Reinforcing Bars," *ACI Journal*, Proceedings Vol. 66, Nov., pp. 875-883.
- Hwang, H., Park, H., Choi, W., Chung, L., and Kim, J., 2014, "Cyclic Loading Test for Beam-Column Connections with 600 MPa (87 ksi) Beam Flexural Reinforcing Bars," *ACI Structural Journal*, Vol. 111, No. 4, July-Aug., pp. 913-924.
- Hwang, S., Lee, H., Liao, T., Wang, K., and Tsai, H., 2005, "Role of Hoops on Shear Strength of Reinforced Concrete Beam-Column Joints," *ACI Structural Journal*, Vol. 102, No. 3, May-June, pp. 445-453.
- Kanada, K., Kondo, G., Fujii, S., and Morita, S., 1984, "Relation Between Beam Bar Anchorage and Shear Resistance at Exterior Beam-Column Joints," *Transactions of the Japan Concrete Institute*, V. 6, pp. 433-440.
- Kaku, T., and Asakusa, H., 1991, "Ductility Estimation of Exterior Beam-Column Subassemblies in Reinforced Concrete Frames," *Design of Beam-Column Joints for Seismic Resistance*, SP 123-7, *American Concrete Institute*, Detroit, MI, pp. 167-185.
- Kang, T., Ha, S., and Choi, D., 2010, "Bar Pullout Tests and Seismic Tests of Small-Headed Bars in Beam-Column Joints," *ACI Structural Journal*, Vol. 107, No. 1, Jan.-Feb., pp. 32-42.

Lee, H., and Ko, J., 2007 “Eccentric Reinforced Concrete Beam-Column Connections Subjected to Cyclic Loading in Principal Directions,” *ACI Structural Journal*, Vol. 104, No. 4, July-Aug., pp. 459-467.

Lee, D. N., Wight, J. K., and Hanson, R. D., 1976, “Original and Repaired Reinforced Concrete Beam-Column Subassemblages Subjected to Earthquake Type Loading,” *Report No. UMEE 76S4*, University of Michigan, Department of Civil Engineering, Ann Arbor, MI, Apr., 206 pp.

Lee, D. N., Wight, J. K., and Hanson, R. D., 1976, “RC Beam-Column Joints Under Large Load Reversals,” *Journal of the Structural Division*, Vol. 103, ST12, Oct., pp. 2337-2350.

Marques, J. L., and Jirsa, J. O., 1975, “A Study of Hooked Bar Anchorages in Beam-Column Joints,” *ACI Journal*, Proceedings Vol. 72, No. 5, May-Jun., pp. 198-209.

Megget, L., 1974, “Cyclic Behavior of Exterior Reinforced Concrete Beam-Column Joints,” *Bulletin of the New Zealand National Society for Earthquake Engineering*, Vol. 7, No. 1, Mar., pp. 27-47.

McMackin, P. J., Slutter, R. G., and Fisher, J. W., 1973, “Headed Steel Anchor under Combined Loading,” *AISC Engineering Journal*, Vol. 10, No. 2, Apr.-Jun., pp. 43-52.

Minor, J. and Jirsa, J., 1975, “Behavior of Bent Bar Anchorages,” *ACI Journal*, Proceedings Vol. 72, No. 4, Apr., pp. 141-149.

Nilforoush, R., Nilsson, M., and Elfgren, L., 2017, “Experimental Evaluation of Tensile Behaviour of Single Cast-in-Place Anchor Bolts in Plain and Steel Fibre-Reinforced Normal- and High-Strength Concrete,” *Engineering Structures*, Vol. 147, pp. 195-206.

Pantelides, C., Clyde, C., and Reaveley, L., 2002, “Performance-Based Evaluation of Reinforced Concrete Building Exterior Joints for Seismic Excitation,” *Earthquake Engineering Research Institute, Earthquake Spectra*, Vol. 18, No. 3, Aug., pp. 449–480.

Paulay, T., and Scarpas, A., 1981, “The Behavior of Exterior Beam-Column Joints,” *Bulletin of the New Zealand National Society for Earthquake Engineering*, Vol. 14, No. 3, Sep., pp. 131-144.

Ramirez, J. and Russell, B., 2008, “Transfer, Development, and Splice Length for Strand/reinforcement in High-strength Concrete,” *Transportation Research Board, National Research Council*, Washington, D.C., 99-120 pp.

Soroushian, P., Obaseki, K., Nagi, M., and Rojas, M., 1988, “Seismic Exc in Exterior Beam-Column Connections,” *ACI Structural Journal*, Vol. 85, No. 3, May-Jun., pp. 269-276.

Shao, Y., Darwin, D., O’Reilly, M., Lequesne, R. D., Ghimire, K., and Hano, M., 2016, “Anchorage of Conventional and High-Strength Headed Reinforcing Bars,” *SM Report No. 117*, University of Kansas Center for Research, Inc., Lawrence, KS, Aug., 334 pp.

Sperry, J., Al-Yasso, S., Searle, N., DeRubeis, M., Darwin, D., O'Reilly, M., Matamoros, A., Feldman, L., Lepage, A., Lequesne, R., and Ajaam, A., 2015a, "Anchorage of High-Strength Reinforcing Bars with Standard Hooks," *SM Report* No. 111, University of Kansas Center for Research, Inc., Lawrence, Kansas, June, 243 pp.

Sperry, J., Darwin, D., O'Reilly, M., and Lequesne, R., 2015b, "Anchorage Strength of Conventional and High-Strength Hooked Bars in Concrete," *SM Report* No. 115, University of Kansas Center for Research, Inc., Lawrence, Kansas, Dec., 266 pp.

Sperry, J., Yasso, S., Searle, N., DeRubeis, M., Darwin, D., O'Reilly, M., Matamoros, A., Feldman, L., Lepage, A., Lequesne, R., and Ajaam, A., 2017a, "Conventional and High-Strength Hooked Bars—Part 1: Anchorage Tests," *ACI Structural Journal*, Vol. 114, No. 1, Jan.-Feb., pp. 255-265.

Sperry, J., Darwin, D., O'Reilly, M., Lequesne, R., Yasso, S., Matamoros, A., Feldman, L., and Lepage, A., 2017b, "Conventional and High-Strength Hooked Bars—Part 2: Data Analysis," *ACI Structural Journal*, Vol. 114, No. 1, Jan.-Feb., pp. 267-276.

Sperry, J., Darwin, D., O'Reilly, M., Lepage, A., Lequesne, R., Matamoros, A., Feldman, L., Yasso, S., Searle, N., DeRubeis, M., and Ajaam, A., 2018, "Conventional and High-Strength Steel Hooked Bars: Detailing Effects," *ACI Structural Journal*, Vol. 115, No. 1, Jan., pp. 247-257.

Stoker, J. R., Boulware, R. L., Crozier, W. F., and Swirsky, R. A., 1974, "Anchorage Devices for Large Diameter Reinforcing Bars," *Report* No. CA-DOT-TL-6626-1-73-30, Transportation Laboratory, California Division of Highways, Sacramento, California, Sep., 63 pp.

Scribner, C. F., 1978, "Delaying Shear Strength Decay in Reinforced Concrete Flexural Members under Large Load Reversals," *Report* No. UMEE 78R2, University of Michigan, Department of Civil Engineering, Ann Arbor, MI, May, 221 pp.

Tsonos, A., Tegos, I., and Penelis, G., 1992, "Seismic Resistance of Type 2 Exterior Beam-Column Joints Reinforced with Inclined Bars," *ACI Structural Journal*, Vol. 89, No. 1, Jan.-Feb., pp. 3-12.

Tsonos, A., 2007, "Cyclic Load Behavior of Reinforced Concrete Beam-Column Subassemblages of Modern Structures," *ACI Structural Journal*, Vol. 104, No. 4, July-Aug., pp. 468-478.

Uzumeri, S., 1977, "Strength and Ductility of Cast-In-Place Beam-Column Joints," *Reinforced Concrete Structures in Seismic Zones*, SP 53-12, American Concrete Institute, Farmington Hills, MI, pp. 293-350.

Viest, I. M., 1956, "Investigation of Stud Shear Connectors for Composite Concrete and Steel T-Beams," *Journal of American Concrete Institute*, Vol. 27, No. 8, Apr., pp. 875-892.

Yasso, S., Darwin, D., and O'Reilly, M., 2017, "Anchorage Strength of Standard Hooked Bars in Simulated Exterior Beam-Column Joints," *SM Report* No. 124, University of Kansas Center for Research, Inc., Lawrence, Kansas, Apr., 307 pp.

Yasso, S., Darwin, D., and O'Reilly, M. O., 2021, "Effects of Concrete Tail Cover and Tail Kickout on Anchorage Strength of 90-Degree Hooks," *ACI Structural Journal*, Vol. 118, No. 6, Nov. 2021, pp. 227-236 .

Zerbe, H., and Durrani, A., 1985, "Effect of a Slab on The Behavior of Exterior Beam to Column Connections," *Report* No. 30, Department of Civil Engineering, Rice University, Houston, Texas, Mar., 159 pp.

Zuo, J., and Darwin, D., 1998, "Bond Strength of High Relative Rib Area Reinforcing Bars," *SM Report* No. 46, University of Kansas Center for Research, Inc., Lawrence, Kansas, Jan., 350 pp.

APPENDIX A: NOTATION

A_b	Cross-sectional area of an individual headed or hooked deformed bar
A_{brg}	Net bearing area of the head of headed deformed bar calculated as the gross head area minus the bar area if there is no obstruction. However, the net bearing area of the head is calculated as the gross head area minus the maximum area of the obstruction adjacent to the head if there is an obstruction
A_g	Gross cross-sectional area of column in exterior beam-column joint
A_{hs}	Total cross-sectional area of headed or hooked deformed bars being developed (nA_b)
A_j	Effective cross-sectional area within the beam-column joint in a plane parallel to the hooked bars (Section 4.2.2)
A_{Nc}	Projected concrete failure area of group of headed bars
A_{Nco}	Projected concrete failure area of a single headed bar ($9\ell_{eh}^2$)
A_{st}	Total cross-sectional area of reinforcement perpendicular to the headed bar within a $1.5\ell_{eh}$ radial distance from the center of the bar
A_{tr}	Cross-sectional area of a single leg of confining reinforcement (or anchor reinforcement) parallel to the headed or hooked bar within the joint region
A_{tt}	Total cross-sectional area of all confining reinforcement parallel to headed bars being developed and located within $8d_b$ of the top or bottom of the test bars for No. 3 through No. 8 hooked bars or within $10d_b$ for No. 9 through No. 11 hooked bars
A_{th}	Total cross-sectional area of all confining reinforcement parallel to hooked bars being developed and located within $8d_b$ of the top or bottom of the test bars for No. 3 through No. 8 hooked bars or within $10d_b$ for No. 9 through No. 11 hooked bars
A_v	Total cross-sectional area of confining reinforcement parallel to the hooked bar ($N_{total} A_{tr,i}$) assumed to serve as a single tie (Section 4.2.2.3)
b_b	Width of beam in exterior beam-column joints
b_c	Width of column in exterior beam-column joints
b_j	Effective width of beam-column joint perpendicular to the hooked bars in tension calculated based on Section 15.4.2.4 of ACI 318-14
$b_{j,ACI 352}$	Effective width of beam-column joint perpendicular to the hooked bars in tension calculated based on Section 4.3.1 of ACI 352R-02
c_{a1}	Minimum distance from the center of the headed bar to the edge of concrete
c_{a2}	Minimum distance from the center of the headed bar to the edge of concrete in the direction perpendicular to c_{a1}
c_{bc}	Clear cover measured from the back of the head to the back of the member
c_{ch}	Center-to-center spacing between adjacent headed or hooked bars
c_{so}	Clear cover measured from the headed or hooked bar to the nearest free concrete face of the member within the anchorage region

d	Distance from the centroid of the tension bar to the extreme compression fiber of the beam in exterior joints; diameter of the head (Table 2.3)
d'	Distance from the centroid of the compression bar to the extreme compression fiber of the beam in exterior joints
d_b	Nominal diameter of the headed or hooked bar
f'_c	Specified compressive strength of concrete
f_{cm}	Measured compressive strength of concrete
f_{su}	Stress in the headed bar at failure
f_y	Measured yield strength of the headed or hooked bar
$f_{ytr,1}$	Measured yield strength of confining reinforcement (hoops) parallel to the headed or hooked bar within the joint region
h_b	Depth of beam in exterior beam-column joints
h_c	Depth of column in exterior beam-column joints
h_{cl}	Distance between the center of headed bar to the inner face of the nearest support plate (Figures 1.34 and 3.8)
h_{ef}	Embedment length of the anchor (Sections 1.4 and 1.7.1)
k_c	Coefficient for concrete breakout strength in tension
ℓ_{dh}	Development length in tension of deformed bar or deformed wire with a standard hook, measured from outside end of hook, point of tangency, toward critical section
ℓ_{dt}	Development length in tension of headed deformed bar, measured from the critical section to the bearing face of the head
ℓ_{eh}	Embedment length measured from the critical section to the bearing face of the head; Embedment length measured from the critical section to the back of the hook
ℓ_{ehy}	Embedment length required to yield the hooked bars calculated using the descriptive equations, Eq. (4.1) and (4.2)
M_{peak}	Peak moment at critical section of hooked bars in beam-column joints subjected to reversed cyclic loading
M_n	Nominal flexural strength of beam in exterior beam-column joints
n	Number of headed bars loaded simultaneously in tension; number of hooked bars at the tension face of the beam in exterior beam-column joints
N	Number of legs of effective confining reinforcement A_{tr} or A_{th} in the joint region
N_{ar}	Nominal anchorage strength of a single headed bar based on anchor reinforcement
N_{arg}	Nominal anchorage strength of a group of headed bars based on anchor reinforcement
N_b	Basic concrete breakout strength of a single headed bar in tension
N_{cb}	Nominal concrete breakout strength of a single headed bar in tension
N_{cbg}	Nominal concrete breakout strength of a group of headed bars in tension
N_{sb}	Nominal side-face blowout strength of a single headed bar in tension
N_{sbg}	Nominal side-face blowout strength of a group of headed bars in tension

N_{total}	Total number of legs of confining reinforcement within a beam-column joint
N_{tr}	Total number of legs of anchor reinforcement parallel to the headed bars within $0.5\ell_{eh}$ radial distance from the center of the bar
p	Probability value from student t-test
s	Center-to-center spacing between adjacent headed bars
s_{tr}	Center-to-center spacing of confining reinforcement (hoops) within the joint region
T	Test failure load on a headed bar
T'	Estimated test failure load on a hooked bar in beam-column joints subjected to reversed cyclic loading calculated using Eq. (4.4)
T'_{mod}	Modified bar force T' in beam-column joint specimens with $\ell_{eh} \geq \ell_{ehy}$ calculated using Eq. (4.5)
T_{anc}	Nominal anchorage strength of each headed bar in tension governed by concrete breakout, or anchor reinforcement, calculated using Eq. (3.9) based on anchorage design provisions in Chapter 17 of ACI 318-19
T_{ACI318}	Anchorage strength of a headed bar calculated using Eq. (3.11) based on design provisions in Chapter 25 of ACI 318-19
T_{calc}	Anchorage strength of a headed bar calculated using Eq. (3.14) based on proposed Code provisions
T_c	Anchorage strength of a headed or hooked bar without confining reinforcement in Eq. (1.2), (1.4) and (1.7); contribution of concrete to anchorage strength of a headed or hooked bar
T_h	Anchorage strength of a headed or hooked bar with confining reinforcement in Eq. (1.3), (1.5) and (1.8); anchorage strength of a headed or hooked bar calculated using descriptive equations in Sections 3.2 and 4.2.1
T_N	Normalized load on a headed bar at failure calculated using Eq. (3.1) and (3.2)
t	Thickness of the head (Tables 2.3)
V_n	Nominal joint shear strength calculated in accordance with the joint shear strength requirements of Section 18.8.4 of ACI 318-19
$V_{n,ACI352}$	Nominal joint shear strength calculated in accordance with Section 4.3 of ACI 352R-02
V_p	Peak joint shear applied at the beam-column joint
w/c	Water-to-cement ratio by weight
$\delta_{0.8peak}$	Drift ratio at drop to 80% from the peak load
ψ_{cs}	Factor used to modify development length based on confining reinforcement and bar spacing
ψ_e	Factor used to modify development length based on reinforcement coating
$\psi_{ec,N}$	Factor used to modify tensile strength of anchors based on eccentricity of applied loads
$\psi_{ed,N}$	Factor used to modify tensile strength of anchors based on proximity to edges of concrete member

$\Psi_{c,N}$	Factor used to modify tensile strength of anchors based on presence or absence of cracks in concrete
$\Psi_{cp,N}$	factor used to modify tensile strength of postinstalled anchors intended for use in uncracked concrete without supplementary reinforcement to account for the splitting tensile stresses due to installation
Ψ_o	Factor used to modify development length based on bar location within member
Ψ_p	Factor used to modify development length for headed bars based on parallel tie reinforcement
Ψ_r	Factor used to modify development length for hooked bars based on confining reinforcement
θ	Strut angle in beam-column joints (Figure 4.8)
λ, λ_a	Modification factor to reflect the reduced mechanical properties of lightweight concrete relative to normalweight concrete of the same compressive strength

Acronym list

ACI	American Concrete Institute
ASTM	American Society of Testing and Materials - International
COV	Coefficient of Variation
MAX	Maximum
MIN	Minimum
SG	Specific Gravity
SN	Specimen Number
SSD	Saturated Surface Dry
STD	Standard Deviation

APPENDIX B: DETAILS OF SLAB SPECIMENS TESTED IN THE CURRENT STUDY

B.1 STRESS-STRAIN CURVES FOR HEADED BARS

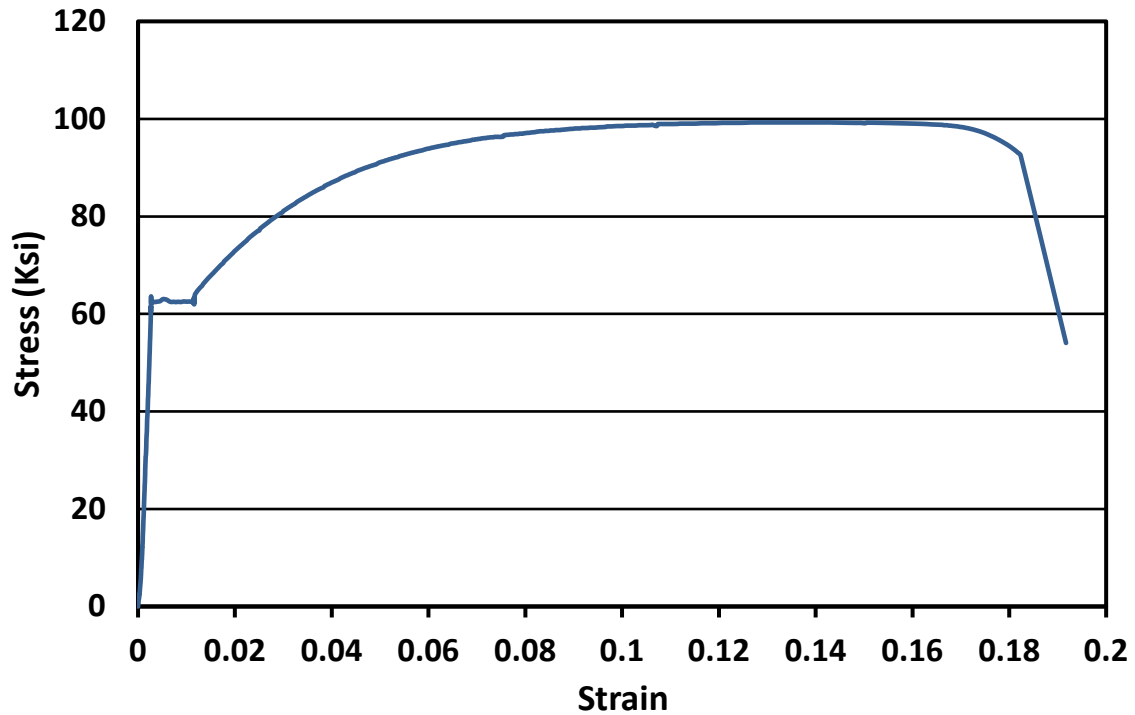


Figure B.1 Stress-strain curve for No. 4 bar (A615 steel)

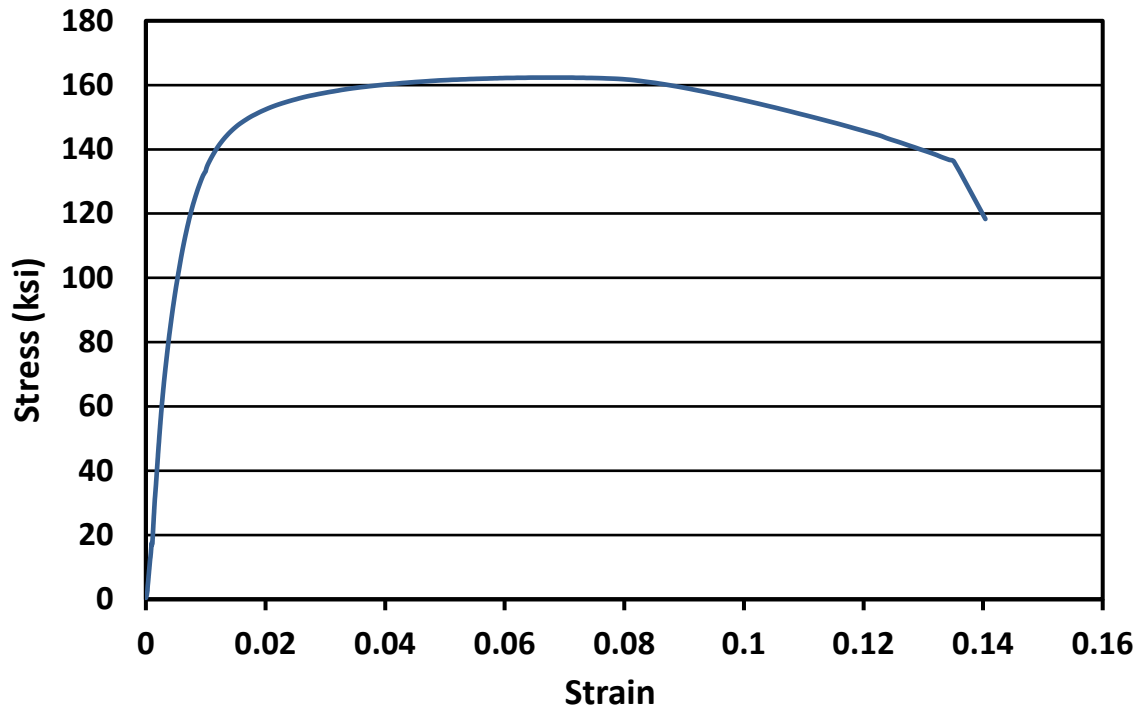


Figure B.2 Stress-strain curve for No. 11 headed bar (A1035 steel)

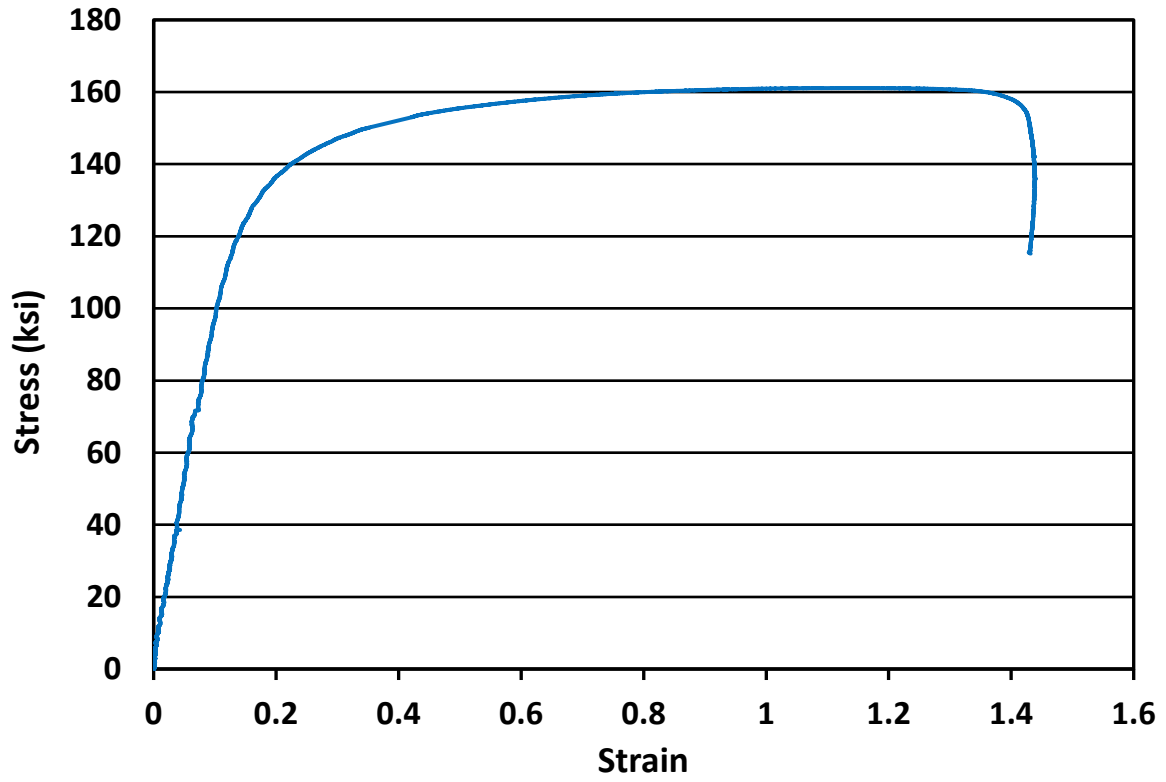


Figure B.3 Stress-strain curve for No. 14 headed bar (A1035 steel)

B.2 SCHEMATICS OF SLAB SPECIMENS

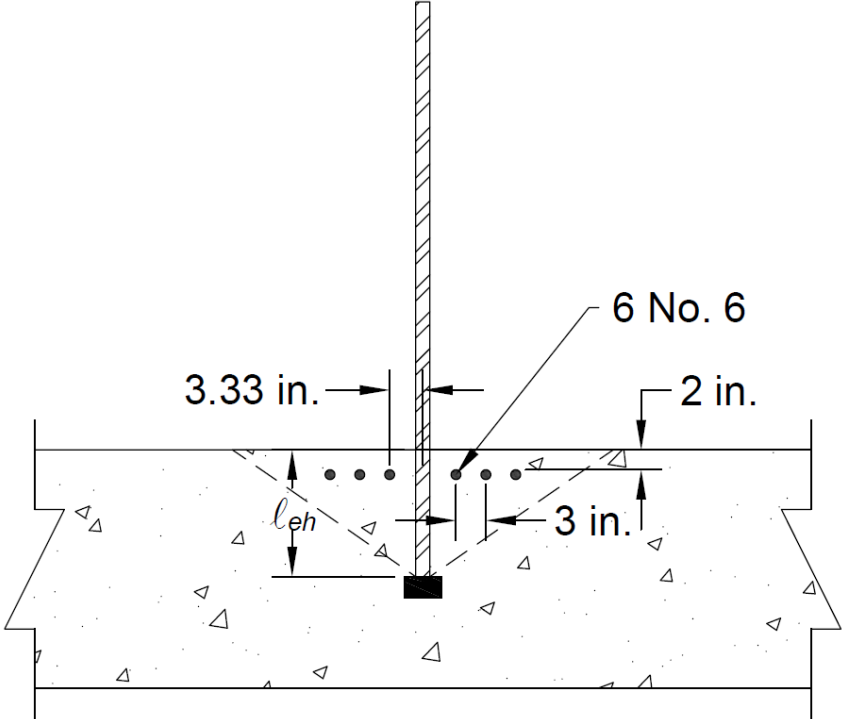


Figure B.4 Cross-section view of slab specimen 11-5-S5.5-6#6-0-12.75 with no parallel ties

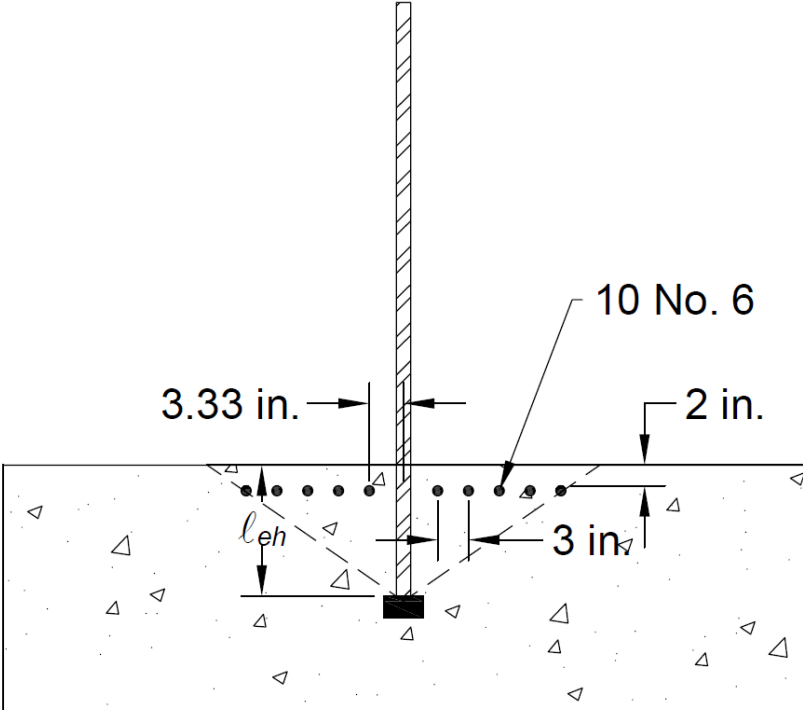


Figure B.5 Cross-section view of slab specimen 11-5-S5.5-10#6-0-12.75 with no parallel ties

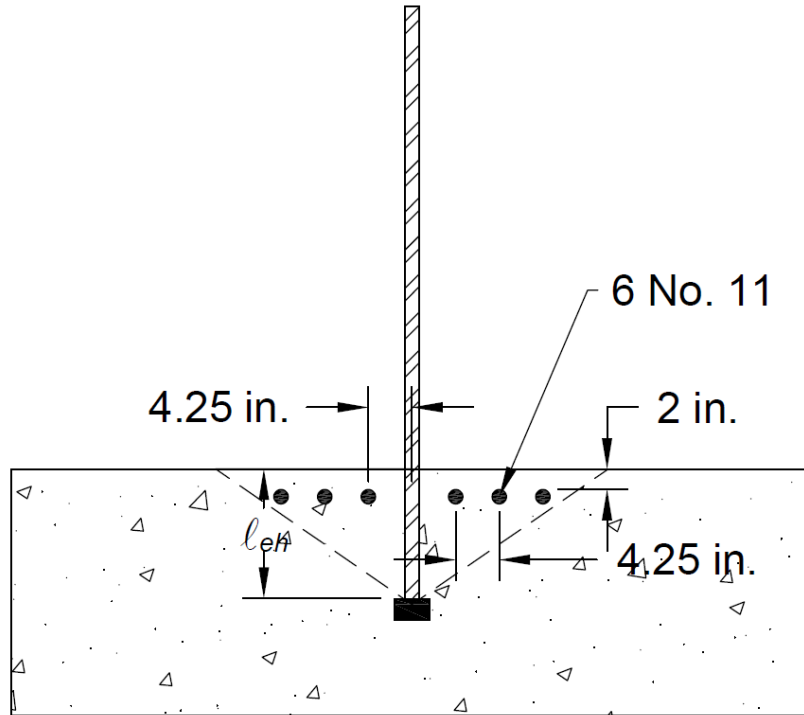


Figure B.6 Cross-section view of slab specimen 11-5-S5.5-6#11-0-12.75 with no parallel ties

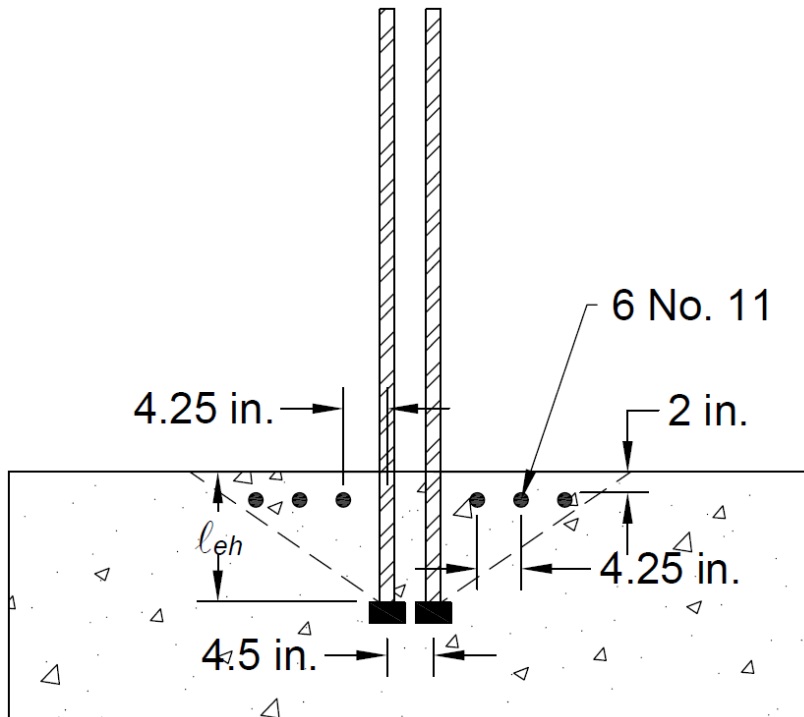


Figure B.7 Cross-section view of slab specimen (2@3.2)11-5-S5.5-6#11-0-12.75 with no parallel ties

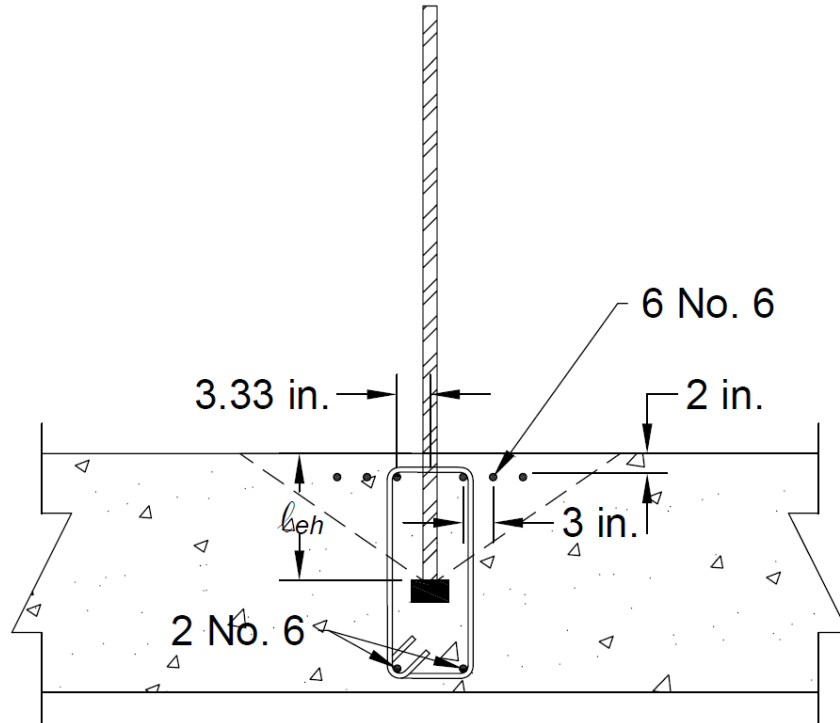


Figure B.8 Cross-section view of slab specimen 11-5-S5.5-6#6-2#4-12.75 with parallel ties

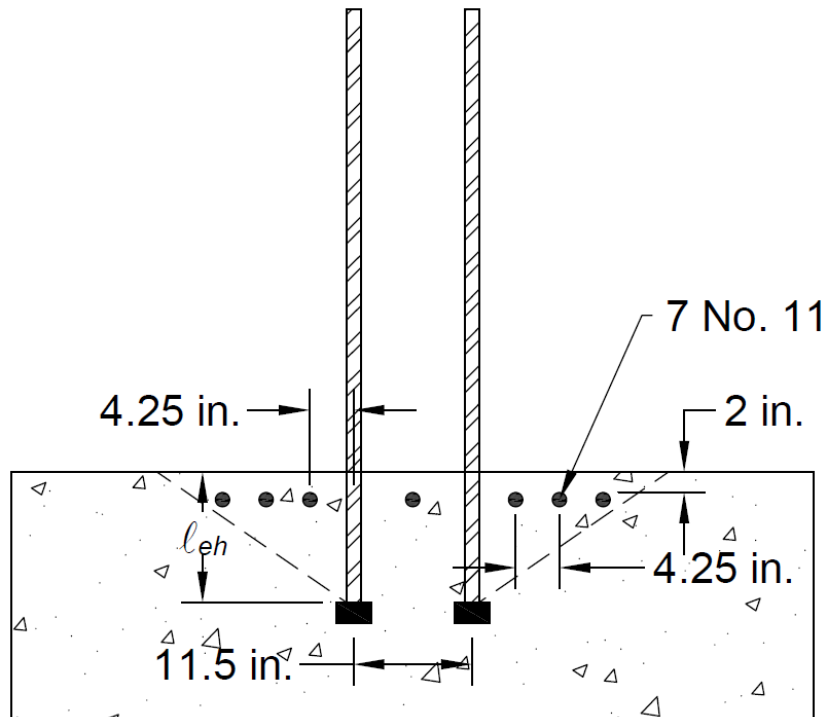


Figure B.9 Cross-section view of slab specimens (2@8.2)11-5-S5.5-7#11-0-12.75, (2@8.2)11-15-S9.2-7#11-0-12.75, (2@6.8)14-5-B4.2-7#11-0-12.75, and (2@6.8)14-15-B4.2-7#11-0-12.75 with no parallel ties

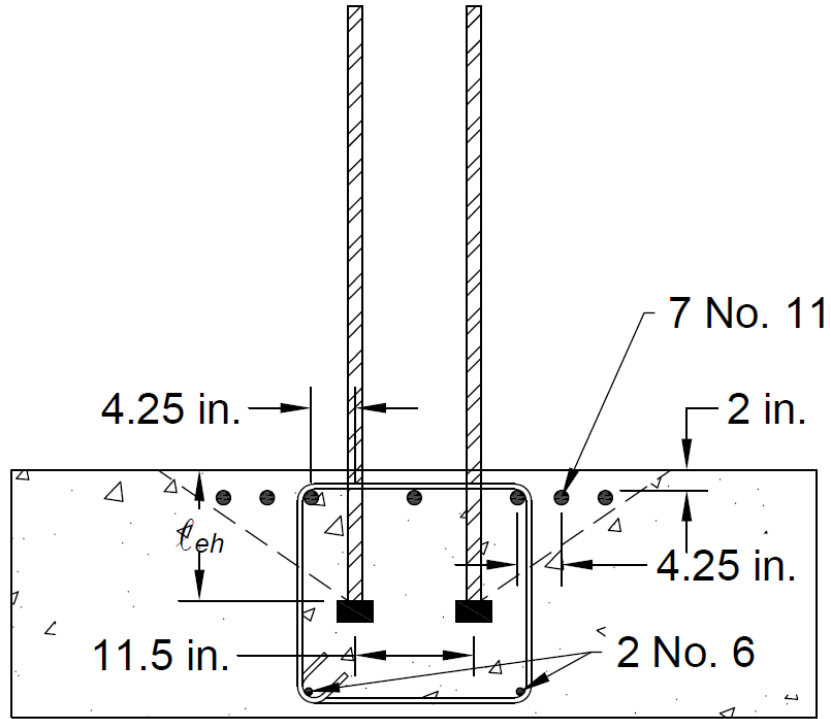


Figure B.10 Cross-section view of slab specimens (2@8.2)11-5-S9.2-7#11-3#4-12.75, (2@8.2)11-5-S9.2-7#11-6#4-12.75, (2@8.2)11-15-S9.2-7#11-3#4-12.75, (2@8.2)11-15-S9.2-7#11-6#4-12.75, (2@6.8)14-5-B4.2-7#11-3#4-12.75, (2@6.8)14-5-B4.2-7#11-6#4-12.75, (2@6.8)14-15-B4.2-7#11-3#4-12.75, and (2@6.8)14-15-B4.2-7#11-6#4-12.75 with parallel ties

B.3 TEST RESULTS AND SPECIMENS CONSTRUCTED AND TESTED IN THE CURRENT STUDY

Table B.1 Detail of slab specimens^[1]

Specimens ^[2]			Head Type ^[3]	$\frac{A_{brg}}{A_b}$	A_{st} (in. ²)	$\frac{A_{st}}{A_b}$	c_{bc} (in.)	c_{ch} ^[4] (in.)	c_{so} (in.)	ℓ_{eh} (in.)
SN	Description	Head								
1	11-5-S5.5-6#6-0-12.75	A	S5.5	5.5	2.64	1.69	7.9	38.0	18.3	13.38
	11-5-S5.5-6#6-0-12.75	B	S5.5	5.5	2.64	1.69	7.9	38.0	18.3	13.13
	11-5-S5.5-6#6-0-12.75	C	S5.5	5.5	2.64	1.69	8.1	78.0	38.3	13.38
2	11-5-S5.5-10#6-0-12.75	A	S5.5	5.5	4.40	2.82	7.9	64.5	31.5	13.38
	11-5-S5.5-10#6-0-12.75	B	S5.5	5.5	4.40	2.82	8.5	64.5	31.5	12.75
3	11-5-S5.5-6#11-0-12.75 ^[5]	A	S5.5	5.5	9.36	6.00	7.6	78.0	38.3	13.63
4	(2@3.2)11-5-S5.5-6#11-0-12.75	A1	S5.5	5.5	9.36	6.00	7.8	4.5	31.5	13.50
		A2	S5.5	5.5	9.36	6.00	7.8	4.5	31.5	13.50
	(2@3.2)11-5-S5.5-6#11-0-12.75	B1	S5.5	5.5	9.36	6.00	7.9	4.5	31.5	13.38
		B2	S5.5	5.5	9.36	6.00	7.9	4.5	31.5	13.38
5	11-5-S5.5-6#6-2#4-12.75	A	S5.5	5.5	2.64	1.69	8.3	38.0	18.3	13.00
	11-5-S5.5-6#6-2#4-12.75	B	S5.5	5.5	2.64	1.69	8.1	38.0	18.3	12.88
	11-5-S5.5-6#6-2#4-12.75	C	S5.5	5.5	2.64	1.69	8.4	78.0	38.3	13.13
6	(2@8.2)11-5-S5.5-7#11-0-12.75	A1	S5.5	5.5	10.92	7.00	7.8	11.5	32.5	13.50
		A2	S5.5	5.5	10.92	7.00	7.8	11.5	32.5	13.50
	(2@8.2)11-5-S5.5-7#11-0-12.75	B1	S5.5	5.5	10.92	7.00	7.2	11.5	32.5	14.06
		B2	S5.5	5.5	10.92	7.00	7.2	11.5	32.5	14.06
7	(2@8.2)11-5-S5.5-7#11-0-12.75	A1	S5.5	5.5	10.92	7.00	8.0	11.5	32.5	13.25
		A2	S5.5	5.5	10.92	7.00	8.0	11.5	32.5	13.25
	(2@8.2)11-5-S5.5-7#11-0-12.75	B1	S5.5	5.5	10.92	7.00	7.9	11.5	32.5	13.31
		B2	S5.5	5.5	10.92	7.00	7.9	11.5	32.5	13.31
8	(2@8.2)11-5-S9.2-7#11-3#4-12.75	A1	S9.2	9.2	10.92	7.00	7.1	11.5	32.5	13.13
		A2	S9.2	9.2	10.92	7.00	7.1	11.5	32.5	13.13
	(2@8.2)11-5-S9.2-7#11-6#4-12.75	B1	S9.2	9.2	10.92	7.00	7.3	11.5	32.5	13.00
		B2	S9.2	9.2	10.92	7.00	7.3	11.5	32.5	13.00
9	(2@8.2)11-5-S9.2-7#11-3#4-12.75	A1	S9.2	9.2	10.92	7.00	7.0	11.5	32.5	13.25
		A2	S9.2	9.2	10.92	7.00	7.0	11.5	32.5	13.25
	(2@8.2)11-5-S9.2-7#11-6#4-12.75	B1	S9.2	9.2	10.92	7.00	6.9	11.5	32.5	13.38
		B2	S9.2	9.2	10.92	7.00	6.9	11.5	32.5	13.38

^[1] Notation described in Appendix A

^[2] Multiple headed bars in a single specimen loaded individually are denoted by letters A, B, and C, and grouped headed bars loaded simultaneously are denoted with a number after a common letter (A1, A2); specimen dimensions shown in Figures 2.2 through 2.10

^[3] Details of heads provided in Section 2.1.2

^[4] c_{ch} for tests with individual headed bars is taken as twice of the minimum concrete cover to the center of the bar [that is, $c_{ch} = 2 \times (c_{so} + d_b/2)$]

^[5] Specimen contained a single centrally placed headed bar

Table B.1 Cont. Detail of slab specimens^[1]

Specimens ^[2]			f_{cm}	f_{su}	h_{cl}	$\frac{h_{cl}}{\ell_{eh}}$	A_{tt}	$\frac{A_{tt}}{A_{hs}}$	T_{peak}	T_{total}	T	
SN	Description	Head	(psi)	(psi)	(in.)		(in. ²)		(kips)	(kips)	(kips)	
1	11-5-S5.5-6#6-0-12.75	A	5060	94.3	24.7	1.85	0.0	0.0	147.1	-	147.1	
	11-5-S5.5-6#6-0-12.75	B		88.3	24.7	1.88	0.0	0.0	137.8	-	137.8	
	11-5-S5.5-6#6-0-12.75	C		87.3	24.7	1.85	0.0	0.0	136.3	-	136.3	
2	11-5-S5.5-10#6-0-12.75	A	5490	103.2	19.7	1.47	0.0	0.0	161.0	-	161.0	
	11-5-S5.5-10#6-0-12.75	B		92.1	19.7	1.55	0.0	0.0	143.7	-	143.7	
3	11-5-S5.5-6#11-0-12.75 ^[5]	A	5740	76.4	71.4	5.24	0.0	0.0	119.2	-	119.2	
4	(2@3.2)11-5-S5.5-6#11-0-12.75	A1	5550	54.2	19.7	1.46	0.0	0.0	84.6	180.5	90.3	
		A2		61.5	19.7	1.46	0.0	0.0	95.9			
	(2@3.2)11-5-S5.5-6#11-0-12.75	B1	6190	41.9	19.7	1.47	0.0	0.0	65.3	154.3	77.2	
		B2		57.1	19.7	1.47	0.0	0.0	89.0			
5	11-5-S5.5-6#6-2#4-12.75	A	5810	130.6	24.7	1.90	0.8	0.51	203.7	-	203.7	
	11-5-S5.5-6#6-2#4-12.75	B		141.6	24.7	1.92	0.8	0.51	220.9	-	220.9	
	11-5-S5.5-6#6-2#4-12.75	C		144.4	24.7	1.88	0.8	0.51	225.2	-	225.2	
6	(2@8.2)11-5-S5.5-7#11-0-12.75	A1	5370	58.5	19.7	1.46	0.0	0.0	91.3	199.0	99.5	
		A2		69.0	19.7	1.46	0.0	0.0	107.7			
	(2@8.2)11-5-S5.5-7#11-0-12.75	B1		6190	57.6	19.7	1.40	0.0	0.0	89.8	213.0	106.5
		B2			79.0	19.7	1.40	0.0	0.0	123.2		
7	(2@8.2)11-5-S5.5-7#11-0-12.75	A1	5110	54.3	19.7	1.49	0.0	0.0	84.7	176.2	88.1	
		A2		58.7	19.7	1.49	0.0	0.0	91.5			
	(2@8.2)11-5-S5.5-7#11-0-12.75	B1		6190	60.1	19.7	1.48	0.0	0.0	93.7	175.3	87.7
		B2			52.3	19.7	1.48	0.0	0.0	81.6		
8	(2@8.2)11-5-S9.2-7#11-3#4-12.75	A1	7950	83.6	19.7	1.50	0.8	0.26	130.4	267.0	133.5	
		A2		87.5	19.7	1.50	0.8	0.26	136.5			
	(2@8.2)11-5-S9.2-7#11-6#4-12.75	B1		6190	122.1	19.7	1.52	1.6	0.51	190.4	370.0	185.0
		B2			115.1	19.7	1.52	1.6	0.51	179.6		
9	(2@8.2)11-5-S9.2-7#11-3#4-12.75	A1	7680	88.8	19.7	1.49	0.8	0.26	138.6	281.3	140.7	
		A2		91.5	19.7	1.49	0.8	0.26	142.7			
	(2@8.2)11-5-S9.2-7#11-6#4-12.75	B1		6190	114.9	19.7	1.47	1.6	0.51	179.3	354.2	177.1
		B2			112.1	19.7	1.47	1.6	0.51	174.9		

^[1] Notation described in Appendix A

^[2] Multiple headed bars in a single specimen loaded individually are denoted by letters A, B, and C, and grouped headed bars loaded simultaneously are denoted with a number after a common letter (A1, A2); specimen dimensions shown in Figures 2.2 through 2.10

^[3] Details of heads provided in Section 2.1.2

^[4] c_{ch} for tests with individual headed bars is taken as twice of the minimum concrete cover to the center of the bar [that is, $c_{ch} = 2 \times (c_{so} + d_b/2)$]

^[5] Specimen contained a single centrally placed headed bar

Table B.1 Cont. Detail of slab specimens^[1]

Specimens ^[2]			T_{anc}	T_h	$T_{ACI\ 318}$	T_{calc}	$\frac{T}{T_{anc}}$	$\frac{T}{T_h}$	$\frac{T}{T_{ACI\ 318}}$	$\frac{T}{T_{calc}}$	Ψ_o
SN	Description	Head	(kips)	(kips)	(kips)	(kips)					
1	11-5-S5.5-6#6-0-12.75	A	142.3	98.6	70.9	84.1	1.03	1.49	2.07	1.75	1.0
	11-5-S5.5-6#6-0-12.75	B	137.9	96.7	69.6	82.5	1.00	1.42	1.98	1.67	1.0
	11-5-S5.5-6#6-0-12.75	C	142.3	98.6	70.9	84.1	0.96	1.38	1.92	1.62	1.0
2	11-5-S5.5-10#6-0-12.75	A	148.3	100.6	71.7	85.8	1.09	1.60	2.25	1.88	1.0
	11-5-S5.5-10#6-0-12.75	B	136.9	95.7	68.3	81.8	1.05	1.50	2.10	1.76	1.0
3	11-5-S5.5-6#11-0-12.75 ^[5]	A	156.4	103.6	73.4	88.4	0.76	1.15	1.62	1.35	1.0
4	(2@3.2)11-5-S5.5-6#11-0-12.75	A1	84.1	62.2	45.3	48.3	1.07	1.45	1.99	1.87	1.0
		A2									
	(2@3.2)11-5-S5.5-6#11-0-12.75	B1	87.5	63.3	46.0	49.1	0.88	1.22	1.68	1.57	1.0
		B2									
5	11-5-S5.5-6#6-2#4-12.75	A	145.5	129.9	70.1	105.8	1.40	1.57	2.90	1.93	1.0
	11-5-S5.5-6#6-2#4-12.75	B	143.1	128.9	69.5	104.7	1.54	1.71	3.18	2.11	1.0
	11-5-S5.5-6#6-2#4-12.75	C	147.8	130.9	70.8	106.8	1.52	1.72	3.18	2.11	1.0
6	(2@8.2)11-5-S5.5-6#11-0-12.75	A1	95.6	101.0	72.2	86.1	1.04	0.99	1.38	1.16	1.0
		A2									
	(2@8.2)11-5-S5.5-6#11-0-12.75	B1	101.4	105.2	75.1	89.7	1.05	1.01	1.42	1.19	1.0
		B2									
7	(2@8.2)11-5-S5.5-6#11-0-12.75	A1	90.8	97.9	70.4	83.5	0.97	0.90	1.25	1.06	1.0
		A2									
	(2@8.2)11-5-S5.5-6#11-0-12.75	B1	91.4	98.4	70.7	83.9	0.96	0.89	1.24	1.04	1.0
		B2									
8	(2@8.2)11-5-S9.2-7#11-3#4-12.75	A1	111.7	134.2	81.8	111.4	1.19	0.99	1.63	1.20	1.0
		A2									
	(2@8.2)11-5-S9.2-7#11-6#4-12.75	B1	110.2	137.6	81.0	114.4	1.68	1.34	2.28	1.62	1.0
		B2									
9	(2@8.2)11-5-S9.2-7#11-3#4-12.75	A1	111.3	134.4	81.1	111.5	1.26	1.05	1.73	1.26	1.0
		A2									
	(2@8.2)11-5-S9.2-7#11-6#4-12.75	B1	112.8	139.9	81.9	116.7	1.57	1.27	2.16	1.52	1.0
		B2									

^[1] Notation described in Appendix A

^[2] Multiple headed bars in a single specimen loaded individually are denoted by letters A, B, and C, and grouped headed bars loaded simultaneously are denoted with a number after a common letter (A1, A2); specimen dimensions shown in Figures 2.2 through 2.10

^[3] Details of heads provided in Section 2.1.2

^[4] c_{ch} for tests with individual headed bars is taken as twice of the minimum concrete cover to the center of the bar [that is, $c_{ch} = 2 \times (c_{so} + d_b/2)$]

^[5] Specimen contained a single centrally placed headed bar

Table B.1 Cont. Detail of slab specimens^[1]

Specimens ^[2]			Head Type ^[3]	$\frac{A_{brg}}{A_b}$	A_{st} (in. ²)	$\frac{A_{st}}{A_b}$	c_{bc} (in.)	c_{ch} ^[4] (in.)	c_{so} (in.)	ℓ_{eh} (in.)
SN	Description	Head								
10	(2@8.2)11-15-S9.2-7#11-0-12.75	A1	S9.2	9.2	10.92	7.00	7.6	11.5	32.5	12.69
		A2	S9.2	9.2	10.92	7.00	7.6	11.5	32.5	12.69
	(2@8.2)11-15-S9.2-7#11-0-12.75	B1	S9.2	9.2	10.92	7.00	7.5	11.5	32.5	12.75
		B2	S9.2	9.2	10.92	7.00	7.5	11.5	32.5	12.75
11	(2@8.2)11-15-S9.2-7#11-3#4-12.75	A1	S9.2	9.2	10.92	7.00	7.5	11.5	32.5	12.75
		A2	S9.2	9.2	10.92	7.00	7.5	11.5	32.5	12.75
	(2@8.2)11-15-S9.2-7#11-6#4-12.75	B1	S9.2	9.2	10.92	7.00	7.6	11.5	32.5	12.63
		B2	S9.2	9.2	10.92	7.00	7.6	11.5	32.5	12.63
12	(2@6.8)14-5-B4.2-7#11-0-12.75	A1	B4.2	4.2	10.92	4.85	6.6	11.5	32.4	13.00
		A2	B4.2	4.2	10.92	4.85	6.6	11.5	32.4	13.00
	(2@6.8)14-5-B4.2-7#11-0-12.75	B1	B4.2	4.2	10.92	4.85	6.5	11.5	32.4	13.13
		B2	B4.2	4.2	10.92	4.85	6.5	11.5	32.4	13.13
13	(2@6.8)14-5-B4.2-7#11-3#4-12.75	A1	B4.2	4.2	10.92	4.85	6.6	11.5	32.4	13.00
		A2	B4.2	4.2	10.92	4.85	6.6	11.5	32.4	13.00
	(2@6.8)14-5-B4.2-7#11-6#4-12.75	B1	B4.2	4.2	10.92	4.85	6.9	11.5	32.4	12.75
		B2	B4.2	4.2	10.92	4.85	6.9	11.5	32.4	12.75
14	(2@6.8)14-15-B4.2-7#11-0-12.75	A1	B4.2	4.2	10.92	4.85	6.5	11.5	32.4	13.13
		A2	B4.2	4.2	10.92	4.85	6.5	11.5	32.4	13.13
	(2@6.8)14-15-B4.2-7#11-0-12.75	B1	B4.2	4.2	10.92	4.85	6.5	11.5	32.4	13.13
		B2	B4.2	4.2	10.92	4.85	6.5	11.5	32.4	13.13
15	(2@6.8)14-15-B4.2-7#11-3#4-12.75	A1	B4.2	4.2	10.92	4.85	6.3	11.5	32.4	13.38
		A2	B4.2	4.2	10.92	4.85	6.3	11.5	32.4	13.38
	(2@6.8)14-15-B4.2-7#11-6#4-12.75	B1	B4.2	4.2	10.92	4.85	6.8	11.5	32.4	12.88
		B2	B4.2	4.2	10.92	4.85	6.8	11.5	32.4	12.88

^[1] Notation described in Appendix A

^[2] Multiple headed bars in a single specimen loaded individually are denoted by letters A, B, and C, and grouped headed bars loaded simultaneously are denoted with a number after a common letter (A1, A2); specimen dimensions shown in Figures 2.2 through 2.10

^[3] Details of heads provided in Section 2.1.2

^[4] c_{ch} for tests with individual headed bars is taken as twice of the minimum concrete cover to the center of the bar [that is, $c_{ch} = 2 \times (c_{so} + d_b/2)$]

^[5] Specimen contained a single centrally placed headed bar

Table B.1 Cont. Detail of slab specimens ^[1]

Specimens ^[2]			f_{cm}	f_{su}	h_{cl}	$\frac{h_{cl}}{\ell_{eh}}$	A_{tt}	$\frac{A_{tt}}{A_{hs}}$	T_{peak}	T_{total}	T
SN	Description	Head	(psi)	(psi)	(in.)		(in. ²)		(kips)	(kips)	(kips)
10	(2@8.2)11-15-S9.2-7#11-0-12.75	A1	14470	79.7	19.7	1.55	0.0	0.00	124.3	249.6	124.8
		A2		80.3	19.7	1.55	0.0	0.00	125.3		
	(2@8.2)11-15-S9.2-7#11-0-12.75	B1		86.2	19.7	1.55	0.0	0.00	134.5	261.9	131.0
		B2		81.7	19.7	1.55	0.0	0.00	127.4		
11	(2@8.2)11-15-S9.2-7#11-3#4-12.75	A1	14140	100.4	19.7	1.55	0.8	0.26	156.6	314.5	157.3
		A2		101.2	19.7	1.55	0.8	0.26	157.9		
	(2@8.2)11-15-S9.2-7#11-6#4-12.75	B1	14080	107.9	19.7	1.56	1.6	0.51	168.4	335.5	167.8
		B2		107.1	19.7	1.56	1.6	0.51	167.1		
12	(2@6.8)14-5-B4.2-7#11-0-12.75	A1	6040	54.0	19.9	1.53	0.0	0.00	121.5	239.0	119.5
		A2		52.2	19.9	1.53	0.0	0.00	117.5		
	(2@6.8)14-5-B4.2-7#11-0-12.75	B1	6180	57.4	19.9	1.51	0.0	0.00	129.1	259.0	129.5
		B2		57.7	19.9	1.51	0.0	0.00	129.9		
13	(2@6.8)14-5-B4.2-7#11-3#4-12.75	A1	5440	61.8	19.9	1.53	1.2	0.27	139.0	274.6	137.3
		A2		60.3	19.9	1.53	1.2	0.27	135.6		
	(2@6.8)14-5-B4.2-7#11-6#4-12.75	B1	5480	72.9	19.9	1.56	2.4	0.53	164.0	319.8	159.9
		B2		69.2	19.9	1.56	2.4	0.53	155.8		
14	(2@6.8)14-15-B4.2-7#11-0-12.75	A1	14030	76.1	19.9	1.51	0.0	0.00	171.2	346.0	173.0
		A2		77.7	19.9	1.51	0.0	0.00	174.8		
	(2@6.8)14-15-B4.2-7#11-0-12.75	B1	14050	71.3	19.9	1.51	0.0	0.00	160.5	323.8	161.9
		B2		72.6	19.9	1.51	0.0	0.00	163.3		
15	(2@6.8)14-15-B4.2-7#11-3#4-12.75	A1	13190	81.2	19.9	1.48	1.2	0.27	182.6	370.1	185.1
		A2		83.3	19.9	1.48	1.2	0.27	187.5		
	(2@6.8)14-15-B4.2-7#11-6#4-12.75	B1	13020	86.7	19.9	1.54	2.4	0.53	195.0	388.8	194.4
		B2		86.1	19.9	1.54	2.4	0.53	193.8		

^[1] Notation described in Appendix A

^[2] Multiple headed bars in a single specimen loaded individually are denoted by letters A, B, and C, and grouped headed bars loaded simultaneously are denoted with a number after a common letter (A1, A2); specimen dimensions shown in Figures 2.2 through 2.10

^[3] Details of heads provided in Section 2.1.2

^[4] c_{ch} for tests with individual headed bars is taken as twice of the minimum concrete cover to the center of the bar [that is, $c_{ch} = 2 \times (c_{so} + d_b/2)$]

^[5] Specimen contained a single centrally placed headed bar

Table B.1 Cont. Detail of slab specimens^[1]

Specimens ^[2]			T_{anc}	T_h	$T_{ACI 318}$	T_{calc}	$\frac{T}{T_{anc}}$	$\frac{T}{T_h}$	$\frac{T}{T_{ACI 318}}$	$\frac{T}{T_{calc}}$	Ψ_o
SN	Description	Head	(kips)	(kips)	(kips)	(kips)					
10	(2@8.2)11-15-S9.2-7#11-0-12.75	A1	143.5	120.2	106.7	103.7	0.87	1.04	1.17	1.20	1.0
		A2									1.0
	(2@8.2)11-15-S9.2-7#11-0-12.75	B1	144.5	120.8	107.2	104.2	0.91	1.08	1.22	1.26	1.0
		B2									1.0
11	(2@8.2)11-15-S9.2-7#11-3#4-12.75	A1	142.9	146.5	105.9	125.0	1.10	1.07	1.48	1.26	1.0
		A2									1.0
	(2@8.2)11-15-S9.2-7#11-6#4-12.75	B1	140.6	149.7	104.7	128.1	1.19	1.12	1.60	1.31	1.0
		B2									1.0
12	(2@6.8)14-5-B4.2-7#11-0-12.75	A1	96.0	97.2	77.4	77.9	1.24	1.23	1.54	1.53	1.0
		A2									1.0
	(2@6.8)14-5-B4.2-7#11-0-12.75	B1	98.5	98.7	79.0	79.1	1.32	1.31	1.64	1.64	1.0
		B2									1.0
13	(2@6.8)14-5-B4.2-7#11-3#4-12.75	A1	91.1	145.2	76.3	99.6	1.51	0.95	1.80	1.38	1.0
		A2									1.0
	(2@6.8)14-5-B4.2-7#11-6#4-12.75	B1	88.9	149.0	74.9	101.8	1.80	1.07	2.13	1.57	1.0
		B2									1.0
14	(2@6.8)14-15-B4.2-7#11-0-12.75	A1	148.4	120.1	119.1	97.1	1.17	1.44	1.45	1.78	1.0
		A2									1.0
	(2@6.8)14-15-B4.2-7#11-0-12.75	B1	148.5	120.2	119.2	97.2	1.09	1.35	1.36	1.67	1.0
		B2									1.0
15	(2@6.8)14-15-B4.2-7#11-3#4-12.75	A1	147.8	172.6	117.7	127.8	1.25	1.07	1.57	1.45	1.0
		A2									1.0
	(2@6.8)14-15-B4.2-7#11-6#4-12.75	B1	139.0	172.9	112.5	127.6	1.40	1.12	1.73	1.52	1.0
		B2									1.0

^[1] Notation described in Appendix A

^[2] Multiple headed bars in a single specimen loaded individually are denoted by letters A, B, and C, and grouped headed bars loaded simultaneously are denoted with a number after a common letter (A1, A2); specimen dimensions shown in Figures 2.2 through 2.10

^[3] Details of heads provided in Section 2.1.2

^[4] c_{ch} for tests with individual headed bars is taken as twice of the minimum concrete cover to the center of the bar [that is, $c_{ch} = 2 \times (c_{so} + d_b/2)$]

^[5] Specimen contained a single centrally placed headed bar

**APPENDIX C: TEST RESULTS AND SPECIMENS FROM OTHER STUDIES
INCLUDED IN THE CURRENT STUDY**

C.1 SLAB SPECIMENS TESTED BY DEVRIES ET AL. (1999) AND CHOI ET AL. (2002)

Table C.1 Data for specimens tested by DeVries et al. (1999) and Choi et al. (2002) ^[1]

Study	Specimen	Bar size ^[2]	A_b (in. ²)	$\frac{A_{brg}}{A_b}$	A_{hs} (in. ²)	A_{Nc} (in. ²)	A_{tr} (in. ²)	A_{tt} (in. ²)	$\frac{A_{st}}{nA_b}$
DeVries et al. (1999)	T2B2	D20	0.49	6.9	0.49	420	0	0	0.0
	T2B4	D20	0.49	6.9	0.49	420	0	0	0.4
	T2B6	D20	0.49	6.9	0.49	241	0	0	0.0
	T2B8	D20	0.49	6.9	0.49	241	0	0	0.4
Choi et al. (2002)	S16-7db.1	D16	0.31	3.2	0.31	175	0	0	0
	S16-7db.2	D16	0.31	3.2	0.31	175	0	0	0
	S25-7db.1	D25	0.79	3.0	0.79	427	0	0	0
	S25-7db.2	D25	0.79	3.0	0.79	427	0	0	0
	E16-7db.1	D16	0.31	3.2	0.31	112	0	0	0
	E16-7db.2	D16	0.31	3.2	0.31	112	0	0	0
	E19-7db.1	D19	0.44	2.6	0.44	165	0	0	0
	E19-7db.2	D19	0.44	2.6	0.44	165	0	0	0
	E19-7db.3	D19	0.44	2.6	0.44	206	0	0	0
	E19-7db.4	D19	0.44	2.6	0.44	206	0	0	0
	E25-7db.1	D25	0.79	3.0	0.79	275	0	0	0
	E25-7db.2	D25	0.79	3.0	0.79	275	0	0	0

^[1] Columns arranged in alphabetical order of notation; notation described in Appendix A

^[2] Bar sizes are presented in SI as reported in the original studies

Table C.1 Cont. Data for specimens tested by DeVries et al. (1999) and Choi et al. (2002) ^[1]

Study	Specimen	$\frac{A_u}{A_{hs}}$	$\frac{c_{ch}^{[3]}}{d_b}$	$\frac{c_{so}}{d_b}$	$d_b^{[4]}$ (in.)	$f_{cm}^{[4]}$ (ksi)	f_{su} (ksi)	$f_y^{[4]}$ (ksi)	$\ell_{eh}^{[4]}$ (in.)
DeVries et al. (1999)	T2B2	0	5.1	2.0	0.79	4790	67.9	80.3	9.0
	T2B4	0	5.1	2.0	0.79	4790	78.9	80.3	9.0
	T2B6	0	5.1	2.0	0.79	4790	56.0	80.3	9.0
	T2B8	0	5.1	2.0	0.79	4790	57.3	80.3	9.0
Choi et al. (2002)	S16-7db.1	0	114.4	56.7	0.625	5270	52.9	60.9	4.4
	S16-7db.2	0	113.4	56.2	0.625	5270	58.0	60.9	4.4
	S25-7db.1	0	71.1	35.1	1	5270	45.5	60.9	6.9
	S25-7db.2	0	70.9	34.9	1	5270	43.0	60.9	6.9
	E16-7db.1	0	6.0	2.5	0.625	5270	34.1	60.9	4.4
	E16-7db.2	0	6.0	2.5	0.625	5270	34.1	60.9	4.4
	E19-7db.1	0	7.0	3.0	0.75	3930	26.6	52.2	5.2
	E19-7db.2	0	7.0	3.0	0.75	3930	24.5	52.2	5.2
	E19-7db.3	0	14.0	6.5	0.75	3930	39.9	52.2	5.2
	E19-7db.4	0	14.0	6.5	0.75	3930	38.3	52.2	5.2
	E25-7db.1	0	5.9	2.5	1	5270	24.8	60.9	6.9
	E25-7db.2	0	5.9	2.5	1	5270	26.2	60.9	6.9

^[1] Columns arranged in alphabetical order of notation; notation described in Appendix A

^[3] c_{ch} for tests with individual headed bars is taken as twice of the minimum concrete cover to the center of the bar [that is, $c_{ch} = 2 \times (c_{so} + d_b/2)$]

^[4] Values are converted from the SI unit (1 in. = 25.4 mm; 1 psi = 1/145 MPa; and 1 kip = 4.4484 kN)

Table C.1 Cont. Data for specimens tested by DeVries et al. (1999) and Choi et al. (2002) ^[1]

Study	Specimen	N	N_{ar} (kips)	N_{cb} (kips)	N_{sb} (kips)	N_{tr}	n	S_{tr} ^[4] (in.)	T ^[4] (kips)	T_{anc} (kips)
DeVries et al. (1999)	T2B2	0	0.0	24.0	40.9	0	1	-	33.3	31.9
	T2B4	0	0.0	24.0	40.9	0	1	-	38.7	31.9
	T2B6	0	0.0	13.8	40.9	0	1	-	27.4	18.3
	T2B8	0	0.0	13.8	40.9	0	1	-	28.1	18.3
Choi et al. (2002)	S16-7db.1	0	0.0	20.2	-	0	1	-	16.4	26.8
	S16-7db.2	0	0.0	20.2	-	0	1	-	18.0	26.8
	S25-7db.1	0	0.0	39.4	-	0	1	-	36.0	52.3
	S25-7db.2	0	0.0	39.4	-	0	1	-	33.9	52.3
	E16-7db.1	0	0.0	10.2	-	0	1	-	10.6	13.5
	E16-7db.2	0	0.0	10.2	-	0	1	-	10.6	13.5
	E19-7db.1	0	0.0	12.1	-	0	1	-	11.7	16.0
	E19-7db.2	0	0.0	12.1	-	0	1	-	10.8	16.0
	E19-7db.3	0	0.0	16.9	-	0	1	-	17.5	22.4
	E19-7db.4	0	0.0	16.9	-	0	1	-	16.9	22.4
	E25-7db.1	0	0.0	19.9	-	0	1	-	19.6	26.4
	E25-7db.2	0	0.0	19.9	-	0	1	-	20.7	26.4

^[1] Columns arranged in alphabetical order of notation; notation described in Appendix A

^[4] Values are converted from the SI unit (1 in. = 25.4 mm; 1 psi = 1/145 MPa; and 1 kip = 4.4484 kN)

Table C.1 Cont. Data for specimens tested by DeVries et al. (1999) and Choi et al. (2002) ^[1]

Study	Specimen	T_h (kips)	$T_{ACI\ 318}$ (kips)	T_{calc} (kips)	$\frac{T}{T_{anc}}$	$\frac{T}{T_h}$	$\frac{T}{T_{ACI\ 318}}$	$\frac{T}{T_{calc}}$	ψ_o	Remarks
DeVries et al. (1999)	T2B2	32.6	17.7	22.6	1.04	1.02	1.88	1.48	1.25	Edge bars in slab specimens
	T2B4	32.6	17.7	22.6	1.21	1.19	2.18	1.71	1.25	
	T2B6	32.6	17.7	22.6	1.50	0.84	1.55	1.22	1.25	Corner bars in slab specimens
	T2B8	32.6	17.7	22.6	1.53	0.86	1.58	1.25	1.25	
Choi et al. (2002)	S16-7db.1	23.9	15.8	18.9	0.61	0.69	1.04	0.87	1.0	Center bars in slab specimens
	S16-7db.2	23.9	15.8	18.9	0.67	0.75	1.14	0.95	1.0	
	S25-7db.1	44.6	31.2	37.1	0.69	0.81	1.15	0.97	1.0	
	S25-7db.2	44.6	31.2	37.1	0.65	0.76	1.09	0.91	1.0	
	E16-7db.1	16.2	12.7	11.4	0.78	0.65	0.83	0.93	1.25	Edge bars in slab specimens
	E16-7db.2	16.2	12.7	11.4	0.78	0.65	0.83	0.93	1.25	
	E19-7db.1	21.1	15.5	15.5	0.73	0.55	0.76	0.76	1.25	
	E19-7db.2	21.1	15.5	15.5	0.67	0.51	0.70	0.70	1.25	
	E19-7db.3	22.7	15.5	17.9	0.78	0.77	1.13	0.98	1.25	
	E19-7db.4	22.7	15.5	17.9	0.75	0.74	1.09	0.94	1.25	
	E25-7db.1	29.9	15.6	22.0	0.74	0.65	1.26	0.89	1.25	
	E25-7db.2	29.9	15.6	22.0	0.78	0.69	1.33	0.94	1.25	

^[1] Columns arranged in alphabetical order of notation; notation described in Appendix A

C.2 SLAB SPECIMENS TESTED AT THE UNIVERSITY OF KANSAS

Table C.2 Data for slab specimens tested by Ghimire et al. (2018) ^[1]

SN	Specimens		$\frac{A_{brg}}{A_b}$	A_{st} (in. ²)	$\frac{A_{st}}{A_b}$	c_{bc} (in.)	c_{ch} ^[3] (in.)	c_{so} (in.)	$\frac{d}{\ell_{eh}}$
	Description	Headed bar ^[2]							
1	8-5-T9.5-8#5-6 ^[4]	A	9.5	1.02	1.29	7.0	48	23.5	1.48
	8-5-T9.5-8#5-6 ^[4]	B	9.5	1.02	1.29	6.8	48	23.5	1.44
2	8-5-T4.0-8#5-6	A	4.0	0	0	6.5	48	23.5	1.38
	8-5-T4.0-8#5-6	B	4.0	0	0	7.5	48	23.5	1.55
3	8-5-F4.1-8#5-6 ^[4]	A	4.1	1.02	1.29	7.6	48	23.5	1.63
	8-5-F4.1-8#5-6 ^[4]	B	4.1	1.02	1.29	7.6	48	23.5	1.63
4	8-5-F9.1-8#5-6 ^[4]	A	9.1	1.02	1.29	7.9	48	23.5	1.71
	8-5-F9.1-8#5-6 ^[4]	B	9.1	1.02	1.29	8.0	48	23.5	1.69
5	8-5-F4.1-2#8-6	A	4.1	0	0	9.0	48	23.5	1.96
	8-5-F9.1-2#8-6	B	9.1	0	0	9.0	48	23.5	1.96
6	8-5-T4.0-2#8-6	A	4.0	0	0	8.9	48	23.5	1.93
	8-5-T9.5-2#8-6	B	9.5	0	0	8.9	48	23.5	1.90
7	8-8-O12.9-6#5-6	A	13.0	0	0	8.8	48	23.5	1.79
	8-8-O9.1-6#5-6	B	9.1	0	0	8.8	48	23.5	1.89
8	8-8-S6.5-6#5-6	A	6.5	0	0	8.6	48	23.5	1.78
	8-8-O4.5-6#5-6	B	4.5	0	0	8.5	48	23.5	1.86
9	8-5-S14.9-6#5-6	A	15.0	0	0	8.5	48	23.5	1.84
	8-5-S6.5-6#5-6	B	6.5	0	0	8.5	48	23.5	1.75
10	8-5-O12.9-6#5-6	A	13.0	0	0	8.4	48	23.5	1.73
	8-5-O4.5-6#5-6	B	4.5	0	0	8.5	48	23.5	1.77
11	8-5-S9.5-6#5-6	A	9.5	0	0	8.5	48	23.5	1.79
	8-5-S9.5-6#5-6	B	9.5	0	0	8.6	48	23.5	1.83
12	8-5-F4.1-6#5-6 ^[5]	-	4.1	0	0	6.6	48	23.5	5.73
13	8-5-F4.1-0-6	A	4.1	0	0	12.0	32	15.5	2.49
	8-5-F4.1-0-6	B	4.1	0	0	12.0	32	15.5	2.91
	8-5-F4.1-2#5-6	C	4.1	0.62	0.78	12.0	32	15.5	2.74
14	8-5-F4.1-4#5-6	A	4.1	1.24	1.57	12.0	32	15.5	3.00
	8-5-F4.1-4#5-6	B	4.1	1.24	1.57	12.0	32	15.5	2.98
	8-5-F4.1-4#5-6	C	4.1	1.24	1.57	12.0	32	15.5	2.70
15	8-5-F4.1-6#5-6	A	4.1	1.86	2.35	12.0	32	15.5	2.89
	8-5-F4.1-6#5-6	B	4.1	1.86	2.35	12.0	32	15.5	2.72
	8-5-F4.1-6#5-6	C	4.1	1.86	2.35	12.0	32	15.5	2.65

^[1] Notation described in Appendix A; all specimens contained No. 8 headed bars

^[2] Multiple headed bars in a single specimen loaded individually are denoted by letters A, B, and C

^[3] c_{ch} for tests with individual headed bars is taken as twice of the minimum concrete cover to the center of the bar [that is, $c_{ch} = 2 \times (c_{so} + d_b/2)$]

^[4] In addition to 8 No. 5 bars as reinforcement perpendicular to the headed bar, specimens contained No. 4 bars spaced at 12 in. in a direction perpendicular to the No. 5 bars

^[5] Specimen contained a single centrally placed headed bar

Table C.2 Cont. Data for slab specimens tested by Ghimire et al. (2018) ^[1]

Specimens			f_{cm} (psi)	f_{su} (psi)	h_{cl} (in.)	ℓ_{eh} (in.)	$\frac{h_{cl}}{\ell_{eh}}$	T (kips)	T_{anc} (kips)
SN	Description	Headed bar ^[2]							
1	8-5-T9.5-8#5-6 ^[4]	A	7040	83.0	10.5	8.00	1.31	65.6	75.6
	8-5-T9.5-8#5-6 ^[4]	B	7040	85.8	10.5	8.25	1.27	67.8	79.2
2	8-5-T4.0-8#5-6	A	7040	78.2	10.5	8.50	1.24	61.8	82.8
	8-5-T4.0-8#5-6	B	7040	71.3	10.5	7.50	1.40	56.3	68.6
3	8-5-F4.1-8#5-6 ^[4]	A	5220	87.2	10.5	7.44	1.41	68.9	58.4
	8-5-F4.1-8#5-6 ^[4]	B	5220	81.5	10.5	7.38	1.42	64.4	57.7
4	8-5-F9.1-8#5-6 ^[4]	A	5220	88.5	10.5	7.13	1.47	69.9	54.8
	8-5-F9.1-8#5-6 ^[4]	B	5220	69.5	10.5	7.00	1.50	54.9	53.3
5	8-5-F4.1-2#8-6	A	7390	81.5	10.5	6.00	1.75	64.4	50.3
	8-5-F9.1-2#8-6	B	7390	82.3	10.5	6.00	1.75	65.0	50.3
6	8-5-T4.0-2#8-6	A	7390	76.6	10.5	6.06	1.73	60.5	51.1
	8-5-T9.5-2#8-6	B	7390	73.0	10.5	6.13	1.71	57.7	52.0
7	8-8-O12.9-6#5-6	A	8620	100.0	9.8	6.25	1.56	79.0	57.8
	8-8-O9.1-6#5-6	B	8620	89.7	10.5	6.25	1.68	70.9	57.8
8	8-8-S6.5-6#5-6	A	8620	92.4	10.0	6.38	1.57	73.0	59.6
	8-8-O4.5-6#5-6	B	8620	93.7	10.8	6.50	1.65	74.0	61.3
9	8-5-S14.9-6#5-6	A	4200	78.2	10.3	6.50	1.58	61.8	42.8
	8-5-S6.5-6#5-6	B	4200	62.3	10.0	6.50	1.54	49.2	42.8
10	8-5-O12.9-6#5-6	A	4200	66.3	10.0	6.63	1.51	52.4	44.1
	8-5-O4.5-6#5-6	B	4200	63.4	10.1	6.50	1.56	50.1	42.8
11	8-5-S9.5-6#5-6	A	4200	61.9	10.3	6.50	1.58	48.9	42.8
	8-5-S9.5-6#5-6	B	4200	69.0	10.1	6.38	1.59	54.5	41.6
12	8-5-F4.1-6#5-6 ^[5]	-	4200	49.5	47.3	8.44	5.60	39.1	63.3
13	8-5-F4.1-0-6	A	5180	63.9	15.0	6.50	2.31	50.5	47.5
	8-5-F4.1-0-6	B	5180	61.9	17.0	6.25	2.72	48.9	44.8
	8-5-F4.1-2#5-6	C	5180	77.8	17.0	6.75	2.52	61.5	50.3
14	8-5-F4.1-4#5-6	A	5180	67.6	16.8	6.00	2.79	53.4	42.1
	8-5-F4.1-4#5-6	B	5180	66.3	17.0	6.13	2.78	52.4	43.5
	8-5-F4.1-4#5-6	C	5460	67.7	17.0	6.75	2.52	53.5	51.6
15	8-5-F4.1-6#5-6	A	5460	59.8	17.0	6.25	2.72	47.3	46.0
	8-5-F4.1-6#5-6	B	5460	70.8	16.8	6.63	2.53	55.9	50.2
	8-5-F4.1-6#5-6	C	5460	66.6	17.0	6.88	2.47	52.6	53.1

^[1] Notation described in Appendix A; all specimens contained No. 8 headed bars

^[2] Multiple headed bars in a single specimen loaded individually are denoted by letters A, B, and C

^[4] In addition to 8 No. 5 bars as reinforcement perpendicular to the headed bar, specimens contained No. 4 bars spaced at 12 in. in a direction perpendicular to the No. 5 bars

^[5] Specimen contained a single centrally placed headed bar

Table C.2 Cont. Data for slab specimens tested by Ghimire et al. (2018) ^[1]

Specimens			T_h (kips)	T_{ACI318} (kips)	T_{calc} (kips)	$\frac{T}{T_{anc}}$	$\frac{T}{T_h}$	$\frac{T}{T_{ACI318}}$	$\frac{T}{T_{calc}}$	Ψ_o
SN	Description	Headed bar ^[2]								
1	8-5-T9.5-8#5-6 ^[4]	A	55.8	39.8	46.3	0.87	1.18	1.65	1.42	1.0
	8-5-T9.5-8#5-6 ^[4]	B	57.5	41.0	47.8	0.86	1.18	1.65	1.42	1.0
2	8-5-T4.0-8#5-6	A	59.3	42.3	49.2	0.75	1.04	1.46	1.26	1.0
	8-5-T4.0-8#5-6	B	52.2	37.3	43.4	0.82	1.08	1.51	1.30	1.0
3	8-5-F4.1-8#5-6 ^[4]	A	48.2	33.6	40.0	1.18	1.43	2.05	1.72	1.0
	8-5-F4.1-8#5-6 ^[4]	B	47.8	33.3	39.6	1.12	1.35	1.93	1.62	1.0
4	8-5-F9.1-8#5-6 ^[4]	A	46.1	32.2	38.3	1.28	1.52	2.17	1.82	1.0
	8-5-F9.1-8#5-6 ^[4]	B	45.2	31.6	37.6	1.03	1.21	1.74	1.46	1.0
5	8-5-F4.1-2#8-6	A	41.9	30.6	35.2	1.28	1.54	2.11	1.83	1.0
	8-5-F9.1-2#8-6	B	41.9	30.6	35.2	1.29	1.55	2.13	1.85	1.0
6	8-5-T4.0-2#8-6	A	42.4	30.9	35.5	1.18	1.43	1.96	1.70	1.0
	8-5-T9.5-2#8-6	B	42.9	31.2	35.9	1.11	1.35	1.85	1.61	1.0
7	8-8-O12.9-6#5-6	A	45.4	34.4	38.1	1.37	1.74	2.30	2.08	1.0
	8-8-O9.1-6#5-6	B	45.4	34.4	38.1	1.23	1.56	2.06	1.86	1.0
8	8-8-S6.5-6#5-6	A	46.4	35.1	38.9	1.23	1.57	2.08	1.88	1.0
	8-8-O4.5-6#5-6	B	47.3	35.8	39.6	1.21	1.57	2.07	1.87	1.0
9	8-5-S14.9-6#5-6	A	39.8	28.4	33.1	1.44	1.55	2.18	1.87	1.0
	8-5-S6.5-6#5-6	B	39.8	28.4	33.1	1.15	1.24	1.73	1.49	1.0
10	8-5-O12.9-6#5-6	A	40.6	28.9	33.7	1.19	1.29	1.81	1.55	1.0
	8-5-O4.5-6#5-6	B	39.8	28.4	33.1	1.17	1.26	1.77	1.51	1.0
11	8-5-S9.5-6#5-6	A	39.8	28.4	33.1	1.14	1.23	1.72	1.48	1.0
	8-5-S9.5-6#5-6	B	39.0	27.8	32.5	1.31	1.40	1.96	1.68	1.0
12	8-5-F4.1-6#5-6 ^[5]	-	52.0	36.8	42.9	0.62	0.75	1.06	0.91	1.0
13	8-5-F4.1-0-6	A	41.8	29.3	34.9	1.06	1.21	1.72	1.45	1.0
	8-5-F4.1-0-6	B	40.2	28.2	33.5	1.09	1.22	1.73	1.46	1.0
	8-5-F4.1-2#5-6	C	43.5	30.4	36.2	1.22	1.41	2.02	1.70	1.0
14	8-5-F4.1-4#5-6	A	38.5	27.1	32.2	1.27	1.39	1.97	1.66	1.0
	8-5-F4.1-4#5-6	B	39.4	27.7	32.9	1.20	1.33	1.89	1.59	1.0
	8-5-F4.1-4#5-6	C	44.0	30.7	36.7	1.04	1.22	1.75	1.46	1.0
15	8-5-F4.1-6#5-6	A	40.7	28.4	34.0	1.03	1.16	1.67	1.39	1.0
	8-5-F4.1-6#5-6	B	43.2	30.1	36.0	1.11	1.29	1.86	1.55	1.0
	8-5-F4.1-6#5-6	C	44.9	31.2	37.4	0.99	1.17	1.68	1.41	1.0

^[1] Notation described in Appendix A; all specimens contained No. 8 headed bars

^[2] Multiple headed bars in a single specimen loaded individually are denoted by letters A, B, and C

^[4] In addition to 8 No. 5 bars as reinforcement perpendicular to the headed bar, specimens contained No. 4 bars spaced at 12 in. in a direction perpendicular to the No. 5 bars

^[5] Specimen contained a single centrally placed headed bar

C.3 SLAB SPECIMENS TESTED AT THE UNIVERSITY OF CALIFORNIA, BERKELEY

Table C.3 Data for slab specimens tested by Worsfold et al. (2022) ^[1]

Specimens		A_b	$\frac{A_{brg}}{A_b}$	A_{tt}	$\frac{A_{tt}}{A_{hs}}$	c_{ch}	c_{so}	d_b	f_{cm}
SN	Description	(in. ²)		(in. ²)		(in.)	(in.)	(in.)	(psi)
1	M01	1.77	1.5	0.0	0.00	5.0	33.75	1.5	3700
2	M02	1.77	5.5	3.2	0.45	5.0	33.75	1.5	3930

^[1] Columns arranged in alphabetical order of notation; notation described in Appendix A

Table C.3 Cont. Data for slab specimens tested by Worsfold et al. (2022) ^[1]

Specimens		f_{su}	h_{cl}	ℓ_{eh}	$\frac{h_{cl}}{\ell_{eh}}$	T	T_{anc}	T_h
SN	Description	(psi)	(in.)	(in.)		(kips)	(kips)	(kips)
1	M01	37.6	21.3	14.3	1.49	66.5	45.9	62.4
2	M02	63.9	21.3	14.3	1.49	113.0	47.3	103.9

^[1] Columns arranged in alphabetical order of notation; notation described in Appendix A

Table C.3 Cont. Data for slab specimens tested by Worsfold et al. (2022) ^[1]

Specimens		$T_{ACI 318}$	T_{calc}	$\frac{T}{T_{anc}}$	$\frac{T}{T_h}$	$\frac{T}{T_{ACI 318}}$	$\frac{T}{T_{calc}}$	Ψ_o
SN	Description	(kips)	(kips)					
1	M01	46.3	48.3	1.45	1.07	1.44	1.38	1.00
2	M02	46.9	78.4	2.39	1.09	2.41	1.44	1.00

^[1] Columns arranged in alphabetical order of notation; notation described in Appendix A

C.4 EXTERIOR BEAM-COLUMN JOINT SPECIMENS

Table C.4 Data for exterior beam-column joint specimens tested under reversed cyclic loading ^[1]

Study	Specimen	Bar Size ^[2]	A_b (in. ²)	A_{hs} (in. ²)	A_{tr} (in. ²)	A_{th} (in. ²)	$\frac{A_{th}}{A_{hs}}$	A_v (in. ²)	b_b (in.)	
1	Hanson and Connor (1967)	I ^[3]	No. 9	1.00	4.00	0.20	1.20	0.30	2.00	12.0
		I-A ^[3]	No. 9	1.00	4.00	0.11	0.66	0.17	1.10	12.0
		II	No. 9	1.00	4.00	0.20	1.20	0.30	2.00	12.0
		III ^[7]	No. 9	1.00	4.00	0.20	1.20	0.30	2.00	12.0
		IV ^[7]	No. 9	1.00	4.00	0.20	1.20	0.30	2.00	12.0
		V ^{[3][4]}	No. 9	1.00	4.00	0.00	0.00	0.00	0.00	12.0
		V-A ^[4]	No. 9	1.00	4.00	0.00	0.00	0.00	0.00	12.0
2	Hanson (1971)	1 ^[5]	No. 8	0.79	3.16	0.20	1.20	0.38	2.40	12.0
		3 ^[5]	No. 8	0.79	3.16	0.11	0.66	0.21	1.10	12.0
		4	No. 8	0.79	3.16	0.11	0.44	0.14	0.88	12.0
		5	No. 8	0.79	3.16	0.11	0.66	0.21	1.32	12.0
3	Megget (1974)	Unit A	D25	0.79	2.37	0.20	1.60	0.68	2.40	10.0
4	Uzumeri (1977)	1 ^{[4][5]}	No. 9	1.00	3.00	0.00	0.00	0.00	0.00	12.0
		2 ^[4]	No. 9	1.00	3.00	0.00	0.00	0.00	0.00	12.0
		3 ^[5]	No. 9	1.00	3.00	0.11	0.88	0.29	0.88	12.0
		4 ^[5]	No. 9	1.00	3.00	0.20	1.60	0.53	1.60	12.0
		5 ^{[4][5]}	No. 9	1.00	3.00	0.00	0.00	0.00	0.00	15.0
		6	No. 9	1.00	3.00	0.20	2.80	0.93	3.20	15.0
		7	No. 9	1.00	3.00	0.20	1.60	0.53	1.60	15.0
		8	No. 9	1.00	4.00	0.20	2.80	0.70	3.20	15.0
5	Lee et al. (1977)	1	No. 6	0.44	0.88	0.11	0.88	1.00	0.88	8.0
		2	No. 6	0.44	0.88	0.11	0.88	1.00	0.88	8.0
		3	No. 6	0.44	0.88	0.05	0.20	0.23	0.20	8.0
		4	No. 6	0.44	0.88	0.05	0.20	0.23	0.20	8.0
		5	No. 6	0.44	0.88	0.11	0.88	1.00	0.88	8.0
		6	No. 6	0.44	0.88	0.05	0.20	0.23	0.20	8.0
		7	No. 6	0.44	0.88	0.05	0.20	0.23	0.20	8.0
		8	No. 6	0.44	0.88	0.05	0.20	0.23	0.20	8.0

^[1] Columns arranged in alphabetical order of notation; notation described in Appendix A; values given in SI units are converted to in.-lb (1 in. = 25.4 mm; 1 psi = 1/145 Mpa; and 1 kip = 4.4484 kN)

^[2] Bar sizes are presented in SI and in.-lb as reported in the original studies

^[3] Analyzed as a doubly reinforced section to calculate the nominal flexural strength M_n ; all other specimens are analyzed as a single reinforced

^[4] Specimens did not contain confining reinforcement parallel to the hooked bars within the joint region

^[5] Specimens had transverse beams on one or both sides of the test beam. These transverse beams meet the dimensional requirements of Sections 18.8.4 and 15.2.8 of ACI 318-19 and Section 4.3 of ACI 352R-02 to be considered effective in increasing the joint shear strength

^[6] Specimens had $d/\ell_{eh} > 1.5$

^[7] Specimens had column to beam flexural strength ratio, M_R , less than 1.2

Table C.4 Cont. Data for exterior beam-column joint specimens tested under reversed cyclic loading^[1]

Study		Specimen	b_c (in.)	b_j (in.)	$b_{j,ACI 352}$ (in.)	c_{ch} (in.)	$\frac{c_{ch}}{d_b}$	c_{so} (in.)	$\frac{c_{so}}{d_b}$	d
1	Hanson and Connor (1967)	I ^[3]	15.0	15.0	13.5	2.6	2.3	3.0	2.7	17.9
		I-A ^[3]	15.0	15.0	13.5	2.6	2.3	3.0	2.7	17.9
		II	15.0	15.0	13.5	2.6	2.3	3.0	2.7	17.9
		III ^[7]	12.0	12.0	12.0	2.6	2.3	1.5	1.3	17.9
		IV ^[7]	12.0	12.0	12.0	2.6	2.3	1.5	1.3	17.9
		V ^{[3][4]}	15.0	15.0	13.5	2.6	2.3	3.0	2.7	17.9
		V-A ^[4]	15.0	15.0	13.5	2.6	2.3	3.0	2.7	17.9
2	Hanson (1971)	1 ^[5]	15.0	15.0	13.5	2.7	2.7	3.0	3.0	18.0
		3 ^[5]	15.0	15.0	13.5	2.7	2.7	3.0	3.0	18.0
		4	15.0	15.0	13.5	2.7	2.7	3.0	3.0	18.0
		5	15.0	15.0	13.5	2.7	2.7	3.0	3.0	18.0
3	Megget (1974)	Unit A	13.0	13.0	11.5	2.7	2.7	3.3	3.3	15.7
4	Uzumeri (1977)	1 ^{[4][5]}	15.0	15.0	13.5	3.4	3.0	3.5	3.1	17.6
		2 ^[4]	15.0	15.0	13.5	3.4	3.0	3.5	3.1	17.6
		3 ^[5]	15.0	15.0	13.5	3.4	3.0	3.5	3.1	17.6
		4 ^[5]	15.0	15.0	13.5	3.4	3.0	3.5	3.1	17.6
		5 ^{[4][5]}	15.0	15.0	15.0	4.9	4.4	2.0	1.8	17.6
		6	15.0	15.0	15.0	4.9	4.4	2.0	1.8	17.6
		7	15.0	15.0	15.0	4.9	4.4	2.0	1.8	17.6
		8	15.0	15.0	15.0	3.3	2.9	2.0	1.8	17.6
5	Lee et al. (1977)	1	8.0	8.0	8.0	2.5	3.3	2.4	3.2	8.0
		2	8.0	8.0	8.0	2.5	3.3	2.4	3.2	8.0
		3	8.0	8.0	8.0	2.5	3.3	2.4	3.2	8.0
		4	8.0	8.0	8.0	2.5	3.3	2.4	3.2	8.0
		5	8.0	8.0	8.0	2.5	3.3	2.4	3.2	8.0
		6	8.0	8.0	8.0	2.5	3.3	2.4	3.2	8.0
		7	8.0	8.0	8.0	2.5	3.3	2.4	3.2	8.0
		8	8.0	8.0	8.0	2.5	3.3	2.4	3.2	8.0

[1] Columns arranged in alphabetical order of notation; notation described in Appendix A; values given in SI units are converted to in.-lb (1 in. = 25.4 mm; 1 psi = 1/145 Mpa; and 1 kip = 4.4484 kN)

[2] Bar sizes are presented in SI and in.-lb as reported in the original studies

[3] Analyzed as a doubly reinforced section to calculate the nominal flexural strength M_n ; all other specimens are analyzed as a single reinforced

[4] Specimens did not contain confining reinforcement parallel to the hooked bars within the joint region

[5] Specimens had transverse beams on one or both sides of the test beam. These transverse beams meet the dimensional requirements of Sections 18.8.4 and 15.2.8 of ACI 318-19 and Section 4.3 of ACI 352R-02 to be considered effective in increasing the joint shear strength

[6] Specimens had $d/\ell_{ch} > 1.5$

[7] Specimens had column to beam flexural strength ratio, M_R , less than 1.2

Table C.4 Cont. Data for exterior beam-column joint specimens tested under reversed cyclic loading^[1]

Study		Specimen	$\frac{d}{\ell_{eh}}$	d' (in.)	d_b (in.)	f_{cm} ^[8] (psi)	f_{cm} ^[9] (psi)	f_y (ksi)	$f_{ytr,l}$ (ksi)	$f_{ytr,l} A_v$ (kips)
1	Hanson and Connor (1967)	I ^[3]	1.33	2.1	1.128	5720	3470	51.6	46.6	93.2
		I-A ^[3]	1.33	2.1	1.128	5330	3200	47.8	52.8	58.1
		II	1.33	2.1	1.128	5960	3650	48.3	54.8	109.6
		III ^[7]	1.33	2.1	1.128	4940	3200	48.2	49.2	98.4
		IV ^[7]	1.33	2.1	1.128	3490	3480	49.9	50.5	101.0
		V ^{[3][4]}	1.33	2.1	1.128	5420	3300	51.0	0.0	0.0
		V-A ^[4]	1.33	2.1	1.128	5240	5420	49.8	0.0	0.0
2	Hanson (1971)	1 ^[5]	0.62	2.0	1	5610	5500	63.1	66.8	160.3
		3 ^[5]	0.62	2.0	1	5340	5200	64.1	73.5	80.9
		4	0.62	2.0	1	5240	5380	63.4	73.5	64.7
		5	0.62	2.0	1	5420	5230	65.0	73.5	97.0
3	Megget (1974)	Unit A	1.25	2.4	1	3200	3200	54.7	46.0	110.4
4	Uzumeri (1977)	1 ^{[4][5]}	1.35	2.4	1.128	4460	4460	50.3	0.0	0.0
		2 ^[4]	1.35	2.4	1.128	4510	4510	50.6	0.0	0.0
		3 ^[5]	1.35	2.4	1.128	3920	3920	50.8	62.0	54.6
		4 ^[5]	1.35	2.4	1.128	4490	4490	50.6	55.0	88.0
		5 ^{[4][5]}	1.35	2.4	1.128	4630	4630	50.4	0.0	0.0
		6	1.35	2.4	1.128	5250	5250	51.1	51.8	165.8
		7	1.35	2.4	1.128	4460	4460	51.1	53.0	84.8
		8	1.35	2.4	1.128	3820	3820	51.1	53.0	169.6
5	Lee et al. (1977)	1	0.85	2.0	0.75	4200	4200	52.5	56.4	49.6
		2	0.85	2.0	0.75	4200	4200	48.6	56.4	49.6
		3	0.85	2.0	0.75	4100	4100	48.7	39.6	7.9
		4	0.85	2.0	0.75	4000	4000	48.9	39.6	7.9
		5	0.85	2.0	0.75	3600	3600	50.9	56.4	49.6
		6	0.85	2.0	0.75	3600	3600	51.6	39.6	7.9
		7	0.85	2.0	0.75	3700	3700	47.5	39.6	7.9
		8	0.85	2.0	0.75	4200	4200	48.2	39.6	7.9

^[1] Columns arranged in alphabetical order of notation; notation described in Appendix A; values given in SI units are converted to in.-lb (1 in. = 25.4 mm; 1 psi = 1/145 Mpa; and 1 kip = 4.4484 kN)

^[3] Analyzed as a doubly reinforced section to calculate the nominal flexural strength M_n ; all other specimens are analyzed as a single reinforced

^[4] Specimens did not contain confining reinforcement parallel to the hooked bars within the joint region

^[5] Specimens had transverse beams on one or both sides of the test beam. These transverse beams meet the dimensional requirements of Sections 18.8.4 and 15.2.8 of ACI 318-19 and Section 4.3 of ACI 352R-02 to be considered effective in increasing the joint shear strength

^[7] Specimens had column to beam flexural strength ratio, M_R , less than 1.2

^[8] Column concrete compressive strength

^[9] Beam concrete compressive strength

Table C.4 Cont. Data for exterior beam-column joint specimens tested under reversed cyclic loading^[1]

Study		Specimen	h_b (in.)	h_c (in.)	ℓ_{dh} (in.)	$\frac{\ell_{dh}}{d_b}$	ℓ_{eh} (in.)	$\frac{\ell_{eh}}{d_b}$	ℓ_{ehy} (in.)	$\frac{\ell_{ehy}}{d_b}$
1	Hanson and Connor (1967)	I ^[3]	20.0	15.0	12.6	11.2	13.5	12.0	11.2	9.9
		I-A ^[3]	20.0	15.0	13.2	11.7	13.5	12.0	10.8	9.6
		II	20.0	15.0	11.7	10.4	13.5	12.0	10.3	9.1
		III ^[7]	20.0	15.0	15.3	13.6	13.5	12.0	13.8	12.2
		IV ^[7]	20.0	15.0	17.3	15.3	13.5	12.0	15.7	14.0
		V ^{[3][4]}	20.0	15.0	20.7	18.3	13.5	12.0	16.6	14.7
		V-A ^[4]	20.0	15.0	20.4	18.0	13.5	12.0	16.4	14.5
2	Hanson (1971)	1 ^[5]	20.0	15.0	12.8	12.8	13.5	13.5	11.8	11.8
		3 ^[5]	20.0	15.0	13.1	13.1	13.5	13.5	12.1	12.1
		4	20.0	15.0	15.4	15.4	13.5	13.5	12.6	12.6
		5	20.0	15.0	13.3	13.3	13.5	13.5	12.2	12.2
3	Megget (1974)	Unit A	18.1	15.0	12.7	12.7	12.6	12.6	11.7	11.7
4	Uzumeri (1977)	1 ^{[4][5]}	20.0	15.0	19.8	17.6	13.0	11.5	15.6	13.8
		2 ^[4]	20.0	15.0	19.9	17.6	13.0	11.5	15.7	13.9
		3 ^[5]	20.0	15.0	13.2	11.7	13.0	11.5	11.5	10.2
		4 ^[5]	20.0	15.0	12.7	11.3	13.0	11.5	11.1	9.8
		5 ^{[4][5]}	20.0	15.0	20.9	18.6	13.0	11.5	16.2	14.4
		6	20.0	15.0	14.6	12.9	13.0	11.5	12.6	11.1
		7	20.0	15.0	15.2	13.5	13.0	11.5	13.1	11.7
		8	20.0	15.0	16.9	14.9	13.0	11.5	15.1	13.4
5	Lee et al. (1977)	1	10.0	11.0	9.0	12.0	9.4	12.5	8.6	11.5
		2	10.0	11.0	8.3	11.1	9.4	12.5	7.9	10.6
		3	10.0	11.0	8.4	11.2	9.4	12.5	8.0	10.7
		4	10.0	11.0	8.5	11.3	9.4	12.5	8.1	10.8
		5	10.0	11.0	9.1	12.1	9.4	12.5	8.7	11.6
		6	10.0	11.0	9.2	12.3	9.4	12.5	8.8	11.8
		7	10.0	11.0	8.4	11.2	9.4	12.5	8.0	10.7
		8	10.0	11.0	8.3	11.0	9.4	12.5	7.9	10.5

^[1] Columns arranged in alphabetical order of notation; notation described in Appendix A; values given in SI units are converted to in.-lb (1 in. = 25.4 mm; 1 psi = 1/145 Mpa; and 1 kip = 4.4484 kN)

^[2] Bar sizes are presented in SI and in.-lb as reported in the original studies

^[3] Analyzed as a doubly reinforced section to calculate the nominal flexural strength M_n ; all other specimens are analyzed as a single reinforced

^[4] Specimens did not contain confining reinforcement parallel to the hooked bars within the joint region

^[5] Specimens had transverse beams on one or both sides of the test beam. These transverse beams meet the dimensional requirements of Sections 18.8.4 and 15.2.8 of ACI 318-19 and Section 4.3 of ACI 352R-02 to be considered effective in increasing the joint shear strength

^[6] Specimens had $d/\ell_{eh} > 1.5$

^[7] Specimens had column to beam flexural strength ratio, M_R , less than 1.2

Table C.4 Cont. Data for exterior beam-column joint specimens tested under reversed cyclic loading^[1]

Study		Specimen	$\frac{\ell_{eh}}{h_c}$	$\frac{\ell_{eh}}{\ell_{dh}}$	$\frac{\ell_{eh}}{\ell_{ehy}}$	M_n (kip.in.)	M_{peak} (kip.in.)	$\frac{M_{peak}}{M_n}$	N	N_{total}
1	Hanson and Connor (1967)	I ^[3]	0.9	1.07	1.21	3018	3384	1.12	3	5
		I-A ^[3]	0.9	1.02	1.24	2796	2976	1.06	3	5
		II	0.9	1.15	1.32	2892	3036	1.05	3	5
		III ^[7]	0.9	0.88	0.98	2820	2616	0.93	3	5
		IV ^[7]	0.9	0.78	0.86	2952	2892	0.98	3	5
		V ^{[3][4]}	0.9	0.65	0.81	2964	2640	0.89	0	0
		V-A ^[4]	0.9	0.66	0.82	3156	3372	1.07	0	0
2	Hanson (1971)	1 ^[5]	0.9	1.06	1.15	3229	3374	1.04	3	6
		3 ^[5]	0.9	1.03	1.11	3253	3662	1.13	3	5
		4	0.9	0.88	1.08	3234	3638	1.13	2	4
		5	0.9	1.02	1.10	3294	3614	1.10	3	6
3	Megget (1974)	Unit A	0.8	0.99	1.07	1923	1944	1.01	4	6
4	Uzumeri (1977)	1 ^{[4][5]}	0.9	0.66	0.83	2340	2475	1.06	0	0
		2 ^[4]	0.9	0.65	0.83	2352	2419	1.03	0	0
		3 ^[5]	0.9	0.98	1.13	2340	2588	1.11	4	4
		4 ^[5]	0.9	1.02	1.17	2352	2700	1.15	4	4
		5 ^{[4][5]}	0.9	0.62	0.80	2364	2531	1.07	0	0
		6	0.9	0.89	1.03	2412	2700	1.12	7	8
		7	0.9	0.86	0.99	2400	2813	1.17	4	4
		8	0.9	0.77	0.86	3132	3263	1.04	7	8
5	Lee et al. (1977)	1	0.9	1.04	1.09	332	372	1.12	4	4
		2	0.9	1.13	1.18	310	349	1.12	4	4
		3	0.9	1.12	1.17	310	314	1.01	2	2
		4	0.9	1.10	1.16	310	360	1.16	2	2
		5	0.9	1.03	1.08	317	382	1.20	4	4
		6	0.9	1.02	1.06	321	371	1.16	2	2
		7	0.9	1.12	1.17	300	361	1.20	2	2
		8	0.9	1.13	1.19	308	355	1.15	2	2

[1] Columns arranged in alphabetical order of notation; notation described in Appendix A; values given in SI units are converted to in.-lb (1 in. = 25.4 mm; 1 psi = 1/145 Mpa; and 1 kip = 4.4484 kN)

[2] Bar sizes are presented in SI and in.-lb as reported in the original studies

[3] Analyzed as a doubly reinforced section to calculate the nominal flexural strength M_n ; all other specimens are analyzed as a single reinforced

[4] Specimens did not contain confining reinforcement parallel to the hooked bars within the joint region

[5] Specimens had transverse beams on one or both sides of the test beam. These transverse beams meet the dimensional requirements of Sections 18.8.4 and 15.2.8 of ACI 318-19 and Section 4.3 of ACI 352R-02 to be considered effective in increasing the joint shear strength

[6] Specimens had $d/\ell_{eh} > 1.5$

[7] Specimens had column to beam flexural strength ratio, M_R , less than 1.2

Table C.4 Cont. Data for exterior beam-column joint specimens tested under reversed cyclic loading^[1]

Study	Specimen	<i>n</i>	<i>nT'</i> (kips)	<i>s_{tr}</i> (in.)	<i>T_h</i> (kips)	<i>T'</i> (kips)	<i>T'</i> _{mod} (kips)	$\frac{T'}{T_h}$	$\frac{T'_{mod}}{T_h}$	
1	Hanson and Connor (1967)	I ^[3]	4	231.4	4.5	51.9	57.9	56.5	1.12	1.09
		I-A ^[3]	4	203.5	4.5	48.0	50.9	49.4	1.06	1.03
		II	4	202.8	4.5	48.6	50.7	48.8	1.04	1.00
		III ^[7]	4	178.9	4.5	47.5	44.7	-	0.94	-
		IV ^[7]	4	195.5	4.5	43.6	48.9	-	1.12	-
		V ^{[3][4]}	4	181.7	0.0	40.8	45.4	-	1.11	-
		V-A ^[4]	4	212.8	0.0	40.4	53.2	-	1.32	-
2	Hanson (1971)	1 ^[5]	4	208.4	3.2	50.1	52.1	51.2	1.04	1.02
		3 ^[5]	4	228.0	4.0	50.9	57.0	56.3	1.12	1.11
		4	4	225.4	5.3	50.3	56.3	55.9	1.12	1.11
		5	4	225.4	3.2	51.6	56.3	55.7	1.09	1.08
3	Megget (1974)	Unit A	3	131.0	2.0	43.4	43.7	43.4	1.01	1.00
4	Uzumeri (1977)	1 ^{[4][5]}	3	159.6	0.0	41.2	53.2	-	1.29	-
		2 ^[4]	3	156.1	0.0	41.3	52.0	-	1.26	-
		3 ^[5]	3	168.5	3.0	51.1	56.2	55.5	1.10	1.08
		4 ^[5]	3	174.3	3.0	50.9	58.1	57.2	1.14	1.12
		5 ^{[4][5]}	3	161.9	0.0	39.6	54.0	-	1.36	-
		6	3	171.6	1.8	51.3	57.2	57.0	1.11	1.11
		7	3	179.6	3.0	50.8	59.9	-	1.18	-
		8	4	212.9	1.8	44.8	53.2	-	1.19	-
5	Lee et al. (1977)	1	2	51.7	1.25	23.2	25.9	25.6	1.11	1.10
		2	2	48.1	1.25	21.5	24.0	23.6	1.12	1.10
		3	2	43.4	3.00	21.5	21.7	21.2	1.01	0.99
		4	2	50.0	3.00	21.6	25.0	24.6	1.16	1.14
		5	2	53.9	1.25	22.5	26.9	26.7	1.20	1.19
		6	2	52.5	3.00	22.8	26.2	26.1	1.15	1.14
		7	2	50.3	3.00	21.0	25.2	24.7	1.20	1.18
		8	2	48.9	3.00	21.3	24.4	23.9	1.15	1.12

^[1] Columns arranged in alphabetical order of notation; notation described in Appendix A; values given in SI units are converted to in.-lb (1 in. = 25.4 mm; 1 psi = 1/145 Mpa; and 1 kip = 4.4484 kN)

^[2] Bar sizes are presented in SI and in.-lb as reported in the original studies

^[3] Analyzed as a doubly reinforced section to calculate the nominal flexural strength M_n ; all other specimens are analyzed as a single reinforced

^[4] Specimens did not contain confining reinforcement parallel to the hooked bars within the joint region

^[5] Specimens had transverse beams on one or both sides of the test beam. These transverse beams meet the dimensional requirements of Sections 18.8.4 and 15.2.8 of ACI 318-19 and Section 4.3 of ACI 352R-02 to be considered effective in increasing the joint shear strength

^[6] Specimens had $d/\ell_{eh} > 1.5$

^[7] Specimens had column to beam flexural strength ratio, M_R , less than 1.2

Table C.4 Cont. Data for exterior beam-column joint specimens tested under reversed cyclic loading^[1]

Study		Specimen	V_n (kips)	$V_{n,ACI 352}$ (kips)	V_p (kips)	$\frac{V_p}{V_n}$	$\delta_{0.8 peak}$	Ψ_o
1	Hanson and Connor (1967)	I ^[3]	204.2	183.8	186.4	0.91	0.043	1.00
		I-A ^[3]	197.0	177.3	163.9	0.83	0.057	1.00
		II	208.4	187.6	167.2	0.80	0.035	1.00
		III ^[7]	151.7	151.7	144.1	0.95	0.029	1.25
		IV ^[7]	127.6	127.6	159.3	1.25	0.082	1.25
		V ^{[3][4]}	198.8	178.9	145.4	0.73	0.051	1.00
		V-A ^[4]	195.4	175.8	185.8	0.95	0.021	1.00
2	Hanson (1971)	1 ^[5]	252.8	227.5	181.1	0.72	0.060	1.00
		3 ^[5]	246.6	222.0	196.6	0.80	0.035	1.00
		4	195.4	175.9	195.3	1.00	0.030	1.00
		5	198.8	178.9	194.0	0.98	0.045	1.00
3	Megget (1974)	Unit A	131.9	117.0	132.8	1.01	0.175	1.00
4	Uzumeri (1977)	1 ^{[4][5]}	225.4	202.9	140.9	0.63	0.033	1.00
		2 ^[4]	181.3	163.2	136.9	0.76	0.021	1.00
		3 ^[5]	211.3	190.2	145.7	0.69	0.055	1.00
		4 ^[5]	226.2	203.5	165.1	0.73	0.095	1.00
		5 ^{[4][5]}	229.6	229.6	136.7	0.60	0.016	1.25
		6	195.6	195.6	163.7	0.84	0.061	1.25
		7	180.3	180.3	157.1	0.87	0.063	1.25
		8	166.9	166.9	188.4	1.13	0.045	1.25
5	Lee et al. (1977)	1	68.4	68.4	55.1	0.80	0.042	1.25
		2	68.4	68.4	51.6	0.75	0.055	1.25
		3	67.6	67.6	46.5	0.69	0.042	1.25
		4	66.8	66.8	53.3	0.80	0.055	1.25
		5	63.4	63.4	56.4	0.89	0.059	1.25
		6	63.4	63.4	54.9	0.87	0.062	1.25
		7	64.2	64.2	53.3	0.83	0.060	1.25
		8	68.4	68.4	52.4	0.77	0.058	1.25

^[1] Columns arranged in alphabetical order of notation; notation described in Appendix A; values given in SI units are converted to in.-lb (1 in. = 25.4 mm; 1 psi = 1/145 Mpa; and 1 kip = 4.4484 kN)

^[2] Bar sizes are presented in SI and in.-lb as reported in the original studies

^[3] Analyzed as a doubly reinforced section to calculate the nominal flexural strength M_n ; all other specimens are analyzed as a single reinforced

^[4] Specimens did not contain confining reinforcement parallel to the hooked bars within the joint region

^[5] Specimens had transverse beams on one or both sides of the test beam. These transverse beams meet the dimensional requirements of Sections 18.8.4 and 15.2.8 of ACI 318-19 and Section 4.3 of ACI 352R-02 to be considered effective in increasing the joint shear strength

^[6] Specimens had $d/\ell_{eh} > 1.5$

^[7] Specimens had column to beam flexural strength ratio, M_R , less than 1.2

Table C.4 Cont. Data for exterior beam-column joint specimens tested under reversed cyclic loading ^[1]

Study	Specimen	Bar Size ^[2]	A_b (in. ²)	A_{hs} (in. ²)	A_{tr} (in. ²)	A_{th} (in. ²)	$\frac{A_{th}}{A_{hs}}$	A_v (in. ²)	b_b (in.)	
6	Scribner (1978)	1	No. 6	0.44	0.88	0.11	0.66	0.75	0.66	8.0
		2	No. 6	0.44	0.88	0.11	0.66	0.75	0.66	8.0
		3	No. 6	0.44	1.32	0.11	0.88	0.67	1.10	8.0
		4	No. 6	0.44	1.32	0.11	0.88	0.67	1.10	8.0
		5	No. 6	0.44	0.88	0.11	0.66	0.75	0.66	8.0
		6	No. 6	0.44	0.88	0.11	0.66	0.75	0.66	8.0
		7	No. 6	0.44	1.32	0.11	0.88	0.67	1.10	8.0
		8	No. 6	0.44	1.32	0.11	0.88	0.67	1.10	8.0
		9	No. 8	0.79	3.16	0.20	0.80	0.25	1.60	10.0
		10	No. 8	0.79	3.16	0.20	0.80	0.25	1.60	10.0
		11	No. 8	0.79	3.16	0.20	0.80	0.25	1.60	10.0
		12	No. 8	0.79	3.16	0.20	0.80	0.25	1.60	10.0
7	Paulay and Scarpas (1981)	Unit 1	D20	0.49	2.92	0.18	1.40	0.48	2.80	14.0
		Unit 2	D20	0.49	3.90	0.12	0.97	0.25	1.46	14.0
		Unit 3	D20	0.49	2.92	0.12	0.97	0.33	1.95	14.0
8	Ehsani and Wight (1982)	1 ^[7]	No. 7	0.60	3.60	0.20	0.40	0.11	0.80	10.2
		2 ^[6]	No. 7	0.60	3.60	0.20	0.40	0.11	0.80	10.2
		3 ^[7]	No. 7	0.60	3.60	0.20	0.80	0.22	1.20	10.2
		4 ^[6]	No. 7	0.60	3.60	0.20	0.80	0.22	1.20	10.2
9	Kanada et al. (1984)	U40L ^[4]	D19	0.44	1.77	0.00	0.00	0.00	0.00	10.2
		U41L	D19	0.44	1.77	0.10	0.39	0.22	0.39	10.2
		U42L	D19	0.44	1.77	0.10	0.59	0.33	0.59	10.2
		U41S ^[6]	D19	0.44	1.77	0.10	0.39	0.22	0.39	10.2
		U40L ^[4]	D19	0.44	1.77	0.10	0.59	0.33	0.59	10.2
		U20L ^[4]	D19	0.44	0.88	0.00	0.00	0.00	0.00	10.2
		U21L	D19	0.44	0.88	0.10	0.39	0.45	0.39	10.2
		U21S ^[6]	D19	0.44	0.88	0.10	0.39	0.45	0.39	10.2

^[1] Columns arranged in alphabetical order of notation; notation described in Appendix A; values given in SI units are converted to in.-lb (1 in. = 25.4 mm; 1 psi = 1/145 Mpa; and 1 kip = 4.4484 kN)

^[2] Bar sizes are presented in SI and in.-lb as reported in the original studies

^[3] Analyzed as a doubly reinforced section to calculate the nominal flexural strength M_n ; all other specimens are analyzed as a single reinforced

^[4] Specimens did not contain confining reinforcement parallel to the hooked bars within the joint region

^[5] Specimens had transverse beams on one or both sides of the test beam. These transverse beams meet the dimensional requirements of Sections 18.8.4 and 15.2.8 of ACI 318-19 and Section 4.3 of ACI 352R-02 to be considered effective in increasing the joint shear strength

^[6] Specimens had $d/\ell_{eh} > 1.5$

^[7] Specimens had column to beam flexural strength ratio, M_R , less than 1.2

Table C.4 Cont. Data for exterior beam-column joint specimens tested under reversed cyclic loading^[1]

Study	Specimen	b_c (in.)	b_j (in.)	$b_{j,ACI 352}$ (in.)	c_{ch} (in.)	$\frac{c_{ch}}{d_b}$	c_{so} (in.)	$\frac{c_{so}}{d_b}$	d	
6	Scribner (1978)	1	8.0	8.0	8.0	5.2	6.9	1.0	1.4	8.6
		2	8.0	8.0	8.0	5.2	6.9	1.0	1.4	8.6
		3	8.0	8.0	8.0	2.1	2.8	1.5	2.0	10.1
		4	8.0	8.0	8.0	2.1	2.8	1.5	2.0	10.1
		5	8.0	8.0	8.0	5.2	6.9	1.0	1.4	8.6
		6	8.0	8.0	8.0	5.2	6.9	1.0	1.4	8.6
		7	8.0	8.0	8.0	2.1	2.8	1.5	2.0	10.1
		8	8.0	8.0	8.0	2.1	2.8	1.5	2.0	10.1
		9	12.0	12.0	11.0	2.1	2.1	2.4	2.4	12.1
		10	12.0	12.0	11.0	2.1	2.1	2.4	2.4	12.1
		11	12.0	12.0	11.0	2.1	2.1	2.4	2.4	12.1
		12	12.0	12.0	11.0	2.1	2.1	2.4	2.4	12.1
7	Paulay and Scarpas (1981)	Unit 1	18.0	18.0	16.0	3.5	4.4	3.4	4.3	21.7
		Unit 2	18.0	18.0	16.0	3.5	4.4	3.4	4.3	21.5
		Unit 3	18.0	18.0	16.0	3.5	4.4	3.4	4.3	21.7
8	Ehsani and Wight (1982)	1 ^[7]	11.8	11.8	11.0	3.1	3.5	2.4	2.7	15.9
		2 ^[6]	11.8	11.8	11.0	3.1	3.5	2.4	2.7	14.3
		3 ^[7]	11.8	11.8	11.0	3.1	3.5	2.4	2.7	15.9
		4 ^[6]	11.8	11.8	11.0	3.1	3.5	2.4	2.7	14.3
9	Kanada et al. (1984)	U40L ^[4]	11.8	11.8	11.0	2.1	2.8	2.4	3.2	13.0
		U41L	11.8	11.8	11.0	2.1	2.8	2.4	3.2	13.0
		U42L	11.8	11.8	11.0	2.1	2.8	2.4	3.2	13.0
		U41S ^[6]	11.8	11.8	11.0	2.1	2.8	2.4	3.2	13.0
		U42S ^[6]	11.8	11.8	11.0	2.1	2.8	2.4	3.2	13.0
		U20L ^[4]	11.8	11.8	11.0	6.3	8.4	2.4	3.2	13.0
		U21L	11.8	11.8	11.0	6.3	8.4	2.4	3.2	13.0
		U21S ^[6]	11.8	11.8	11.0	6.3	8.4	2.4	3.2	13.0

^[1] Columns arranged in alphabetical order of notation; notation described in Appendix A; values given in SI units are converted to in.-lb (1 in. = 25.4 mm; 1 psi = 1/145 Mpa; and 1 kip = 4.4484 kN)

^[2] Bar sizes are presented in SI and in.-lb as reported in the original studies

^[3] Analyzed as a doubly reinforced section to calculate the nominal flexural strength M_n ; all other specimens are analyzed as a single reinforced

^[4] Specimens did not contain confining reinforcement parallel to the hooked bars within the joint region

^[5] Specimens had transverse beams on one or both sides of the test beam. These transverse beams meet the dimensional requirements of Sections 18.8.4 and 15.2.8 of ACI 318-19 and Section 4.3 of ACI 352R-02 to be considered effective in increasing the joint shear strength

^[6] Specimens had $d/\ell_{ch} > 1.5$

^[7] Specimens had column to beam flexural strength ratio, M_R , less than 1.2

Table C.4 Cont. Data for exterior beam-column joint specimens tested under reversed cyclic loading^[1]

Study		Specimen	$\frac{d}{\ell_{eh}}$	d' (in.)	d_b (in.)	f_{cm} ^[8] (psi)	f_{cm} ^[9] (psi)	f_y (ksi)	$f_{ytr,t}$ (ksi)	$f_{ytr,t} A_v$ (kips)
6	Scribner (1978)	1	0.78	1.3	0.75	4950	4950	48.9	75.5	49.8
		2	0.78	1.3	0.75	5050	5050	48.9	75.5	49.8
		3	0.96	1.8	0.75	4940	4940	48.9	75.5	83.1
		4	0.96	1.8	0.75	4950	4950	48.9	75.5	83.1
		5	0.78	1.3	0.75	3680	3680	52.7	75.5	49.8
		6	0.78	1.3	0.75	4080	4080	52.7	75.5	49.8
		7	0.96	1.8	0.75	3840	3840	52.7	75.5	83.1
		8	0.96	1.8	0.75	3920	3920	52.7	75.5	83.1
		9	0.73	1.8	1	5130	5130	60.2	75.5	120.8
		10	0.73	1.8	1	5210	5210	60.2	75.5	120.8
		11	0.73	1.8	1	4730	4730	60.2	75.5	120.8
		12	0.73	1.8	1	4760	4760	60.2	75.5	120.8
7	Paulay and Scarpas (1981)	Unit 1	1.30	2.4	0.79	3280	3280	42.9	47.3	132.6
		Unit 2	1.29	2.6	0.79	3260	3260	42.9	46.0	66.9
		Unit 3	1.30	2.4	0.79	3900	3900	42.9	46.0	89.2
8	Ehsani and Wight (1982)	1 ^[7]	2.15	3.0	0.875	4870	4870	48.0	63.4	50.7
		2 ^[6]	1.93	3.0	0.875	5070	5070	48.0	63.4	50.7
		3 ^[7]	2.15	3.0	0.875	5930	5930	48.0	63.4	76.1
		4 ^[6]	1.93	3.0	0.875	6470	6470	48.0	63.4	76.1
9	Kanada et al. (1984)	U40L ^[4]	1.45	2.0	0.75	3530	3530	56.2	0.0	0.0
		U41L	1.45	2.0	0.75	3870	3870	56.2	42.7	16.8
		U42L	1.45	2.0	0.75	4370	4370	56.2	42.7	25.2
		U41S ^[6]	2.17	2.0	0.75	3870	3870	56.2	42.7	16.8
		U42S ^[6]	2.17	2.0	0.75	4370	4370	56.2	42.7	25.2
		U20L ^[4]	1.45	2.0	0.75	3870	3870	56.2	0.0	0.0
		U21L	1.45	2.0	0.75	4370	4370	56.2	42.7	16.8
		U21S ^[6]	2.17	2.0	0.75	3870	3870	56.2	42.7	16.8

^[1] Columns arranged in alphabetical order of notation; notation described in Appendix A; values given in SI units are converted to in.-lb (1 in. = 25.4 mm; 1 psi = 1/145 Mpa; and 1 kip = 4.4484 kN)

^[4] Specimens did not contain confining reinforcement parallel to the hooked bars within the joint region

^[5] Specimens had transverse beams on one or both sides of the test beam. These transverse beams meet the dimensional requirements of Sections 18.8.4 and 15.2.8 of ACI 318-19 and Section 4.3 of ACI 352R-02 to be considered effective in increasing the joint shear strength

^[6] Specimens had $d/\ell_{eh} > 1.5$

^[7] Specimens had column to beam flexural strength ratio, M_R , less than 1.2

^[8] Column concrete compressive strength

^[9] Beam concrete compressive strength

Table C.4 Cont. Data for exterior beam-column joint specimens tested under reversed cyclic loading^[1]

Study		Specimen	h_b (in.)	h_c (in.)	ℓ_{dh} (in.)	$\frac{\ell_{dh}}{d_b}$	ℓ_{eh} (in.)	$\frac{\ell_{eh}}{d_b}$	ℓ_{ehy} (in.)	$\frac{\ell_{ehy}}{d_b}$
6	Scribner (1978)	1	10.0	12.0	7.1	9.5	11.0	14.6	6.3	8.4
		2	10.0	12.0	7.1	9.4	11.0	14.6	6.2	8.3
		3	12.0	12.0	8.2	11.0	10.5	14.0	7.9	10.6
		4	12.0	12.0	8.2	11.0	10.5	14.0	7.9	10.6
		5	10.0	12.0	8.2	11.0	11.0	14.6	7.4	9.8
		6	10.0	12.0	8.0	10.7	11.0	14.6	7.2	9.5
		7	12.0	12.0	9.5	12.6	10.5	14.0	9.2	12.2
		8	12.0	12.0	9.4	12.5	10.5	14.0	9.1	12.2
		9	14.0	18.0	16.0	16.0	16.6	16.6	15.1	15.1
		10	14.0	18.0	15.9	15.9	16.6	16.6	15.0	15.0
		11	14.0	18.0	16.3	16.3	16.6	16.6	15.4	15.4
		12	14.0	18.0	16.3	16.3	16.6	16.6	15.4	15.4
7	Paulay and Scarpas (1981)	Unit 1	24.0	18.0	6.4	8.1	16.6	21.1	5.8	7.4
		Unit 2	24.0	18.0	6.4	8.2	16.6	21.1	5.8	7.4
		Unit 3	24.0	18.0	6.1	7.8	16.6	21.1	5.5	7.0
8	Ehsani and Wight (1982)	1 ^[7]	18.9	11.8	12.1	13.9	7.4	8.5	10.1	11.5
		2 ^[6]	17.3	11.8	12.0	13.7	7.4	8.5	9.6	11.0
		3 ^[7]	18.9	11.8	9.4	10.8	7.4	8.5	9.2	10.5
		4 ^[6]	17.3	11.8	9.2	10.5	7.4	8.5	8.4	9.6
9	Kanada et al. (1984)	U40L ^[4]	15.0	11.8	16.4	21.8	9.0	12.0	13.2	17.6
		U41L	15.0	11.8	10.1	13.4	9.0	12.0	9.8	13.1
		U42L	15.0	11.8	9.8	13.0	9.0	12.0	9.5	12.7
		U41S ^[6]	15.0	11.8	10.1	13.4	6.0	8.0	9.8	13.1
		U42S ^[6]	15.0	11.8	9.8	13.0	6.0	8.0	9.5	12.7
		U20L ^[4]	15.0	11.8	10.4	13.9	9.0	12.0	8.8	11.7
		U21L	15.0	11.8	8.4	11.2	9.0	12.0	7.5	10.1
		U21S ^[6]	15.0	11.8	8.7	11.6	6.0	8.0	7.8	10.4

^[1] Columns arranged in alphabetical order of notation; notation described in Appendix A; values given in SI units are converted to in.-lb (1 in. = 25.4 mm; 1 psi = 1/145 Mpa; and 1 kip = 4.4484 kN)

^[2] Bar sizes are presented in SI and in.-lb as reported in the original studies

^[3] Analyzed as a doubly reinforced section to calculate the nominal flexural strength M_n ; all other specimens are analyzed as a single reinforced

^[4] Specimens did not contain confining reinforcement parallel to the hooked bars within the joint region

^[5] Specimens had transverse beams on one or both sides of the test beam. These transverse beams meet the dimensional requirements of Sections 18.8.4 and 15.2.8 of ACI 318-19 and Section 4.3 of ACI 352R-02 to be considered effective in increasing the joint shear strength

^[6] Specimens had $d/\ell_{eh} > 1.5$

^[7] Specimens had column to beam flexural strength ratio, M_R , less than 1.2

Table C.4 Cont. Data for exterior beam-column joint specimens tested under reversed cyclic loading^[1]

Study	Specimen	$\frac{\ell_{eh}}{h_c}$	$\frac{\ell_{eh}}{\ell_{dh}}$	$\frac{\ell_{eh}}{\ell_{ehy}}$	M_n (kip.in.)	M_{peak} (kip.in.)	$\frac{M_{peak}}{M_n}$	N	N_{total}	
6	Scribner (1978)	1	0.9	1.55	1.75	343	481	1.41	3	3
		2	0.9	1.55	1.76	343	498	1.45	3	3
		3	0.9	1.27	1.32	590	706	1.20	4	5
		4	0.9	1.27	1.32	747	818	1.10	4	5
		5	0.9	1.33	1.49	356	453	1.27	3	3
		6	0.9	1.37	1.53	360	468	1.30	3	3
		7	0.9	1.11	1.14	710	751	1.06	4	5
		8	0.9	1.11	1.15	743	809	1.09	4	5
		9	0.9	1.04	1.10	2472	2508	1.01	2	4
		10	0.9	1.04	1.10	2520	2592	1.03	2	4
		11	0.9	1.02	1.08	2472	2501	1.01	2	4
		12	0.9	1.02	1.08	2520	2539	1.01	2	4
7	Paulay and Scarpas (1981)	Unit 1	0.9	2.59	2.86	2418	3118	1.29	2	4
		Unit 2	0.9	2.59	2.86	3481	4385	1.26	2	3
		Unit 3	0.9	2.71	3.00	2418	3340	1.38	2	4
8	Ehsani and Wight (1982)	1 ^[7]	0.6	0.61	0.74	2394	2040	0.85	1	2
		2 ^[6]	0.6	0.62	0.77	1882	1860	0.99	1	2
		3 ^[7]	0.6	0.79	0.81	2457	2520	1.03	2	3
		4 ^[6]	0.6	0.80	0.88	1938	2400	1.24	2	3
9	Kanada et al. (1984)	U40L ^[4]	0.8	0.55	0.68	1129	885	0.78	0	0
		U41L	0.8	0.89	0.91	1143	1172	1.02	2	2
		U42L	0.8	0.92	0.95	1160	1165	1.00	3	3
		U41S ^[6]	0.5	0.59	0.61	1143	631	0.55	2	2
		U42S ^[6]	0.5	0.61	0.63	1160	690	0.59	3	3
		U20L ^[4]	0.8	0.86	1.02	608	651	1.07	0	0
		U21L	0.8	1.07	1.19	613	684	1.12	2	2
		U21S ^[6]	0.5	0.69	0.77	608	495	0.81	2	2

^[1] Columns arranged in alphabetical order of notation; notation described in Appendix A; values given in SI units are converted to in.-lb (1 in. = 25.4 mm; 1 psi = 1/145 Mpa; and 1 kip = 4.4484 kN)

^[2] Bar sizes are presented in SI and in.-lb as reported in the original studies

^[3] Analyzed as a doubly reinforced section to calculate the nominal flexural strength M_n ; all other specimens are analyzed as a single reinforced

^[4] Specimens did not contain confining reinforcement parallel to the hooked bars within the joint region

^[5] Specimens had transverse beams on one or both sides of the test beam. These transverse beams meet the dimensional requirements of Sections 18.8.4 and 15.2.8 of ACI 318-19 and Section 4.3 of ACI 352R-02 to be considered effective in increasing the joint shear strength

^[6] Specimens had $d/\ell_{eh} > 1.5$

^[7] Specimens had column to beam flexural strength ratio, M_R , less than 1.2

Table C.4 Cont. Data for exterior beam-column joint specimens tested under reversed cyclic loading^[1]

Study		Specimen	n	nT' (kips)	s_{tr} (in.)	T_h (kips)	T' (kips)	T'_{mod} (kips)	$\frac{T'}{T_h}$	$\frac{T'_{mod}}{T_h}$
6	Scribner (1978)	1	2	60.5	1.75	21.6	30.2	28.2	1.40	1.30
		2	2	62.5	1.75	21.6	31.2	29.2	1.44	1.35
		3	3	77.2	1.50	21.6	25.7	24.9	1.19	1.15
		4	3	70.7	1.50	21.6	23.6	22.7	1.09	1.05
		5	2	59.0	1.75	23.3	29.5	28.1	1.26	1.20
		6	2	60.3	1.75	23.3	30.1	28.6	1.29	1.23
		7	3	73.6	1.50	23.3	24.5	24.1	1.05	1.04
		8	3	75.8	1.50	23.3	25.3	24.8	1.08	1.07
		9	4	193.0	2.00	47.7	48.3	47.7	1.01	1.00
		10	4	195.7	2.00	47.7	48.9	48.3	1.02	1.01
		11	4	192.5	2.00	47.7	48.1	47.7	1.01	1.00
		12	4	191.7	2.00	47.7	47.9	47.5	1.00	0.99
7	Paulay and Scarpas (1981)	Unit 1	6	161.7	4.3	21.1	27.0	22.0	1.28	1.05
		Unit 2	8	210.6	5.9	21.1	26.3	21.4	1.25	1.02
		Unit 3	6	173.2	4.3	21.1	28.9	23.6	1.37	1.12
8	Ehsani and Wight (1982)	1 ^[7]	6	179.6	4.4	22.1	29.9	-	1.35	-
		2 ^[6]	6	170.8	3.9	22.4	28.5	-	1.27	-
		3 ^[7]	6	218.9	3.3	25.1	36.5	-	1.45	-
		4 ^[6]	6	214.0	3.0	25.7	35.7	-	1.39	-
9	Kanada et al. (1984)	U40L ^[4]	4	77.8	0.0	16.4	19.5	-	1.19	-
		U41L	4	101.7	3.9	22.9	25.4	-	1.11	-
		U42L	4	99.7	2.0	23.6	24.9	-	1.06	-
		U41S ^[6]	4	54.8	3.9	15.6	13.7	-	0.88	-
		U42S ^[6]	4	59.0	2.0	16.1	14.8	-	0.92	-
		U20L ^[4]	2	53.1	0.0	24.8	26.6	26.5	1.07	1.07
		U21L	2	55.4	3.9	25.0	27.7	27.1	1.11	1.09
U21S ^[6]	2	40.4	3.9	19.5	20.2	-	1.03	-		

^[1] Columns arranged in alphabetical order of notation; notation described in Appendix A; values given in SI units are converted to in.-lb (1 in. = 25.4 mm; 1 psi = 1/145 Mpa; and 1 kip = 4.4484 kN)

^[2] Bar sizes are presented in SI and in.-lb as reported in the original studies

^[3] Analyzed as a doubly reinforced section to calculate the nominal flexural strength M_n ; all other specimens are analyzed as a single reinforced

^[4] Specimens did not contain confining reinforcement parallel to the hooked bars within the joint region

^[5] Specimens had transverse beams on one or both sides of the test beam. These transverse beams meet the dimensional requirements of Sections 18.8.4 and 15.2.8 of ACI 318-19 and Section 4.3 of ACI 352R-02 to be considered effective in increasing the joint shear strength

^[6] Specimens had $d/\ell_{eh} > 1.5$

^[7] Specimens had column to beam flexural strength ratio, M_R , less than 1.2

Table C.4 Cont. Data for exterior beam-column joint specimens tested under reversed cyclic loading^[1]

Study		Specimen	V_n (kips)	$V_{n,ACI 352}$ (kips)	V_p (kips)	$\frac{V_p}{V_n}$	$\delta_{0.8 peak}$	Ψ_o
6	Scribner (1978)	1	81.1	81.1	56.8	0.70	0.060	1.25
		2	81.9	81.9	58.7	0.72	0.058	1.25
		3	81.0	81.0	71.5	0.88	0.047	1.25
		4	81.1	81.1	83.1	1.03	0.063	1.25
		5	69.9	69.9	53.0	0.76	0.066	1.25
		6	73.6	73.6	54.8	0.74	0.061	1.25
		7	71.4	71.4	76.2	1.07	0.060	1.25
		8	72.1	72.1	82.1	1.14	0.061	1.25
		9	185.6	170.2	213.3	1.15	0.076	1.25
		10	187.1	171.5	220.4	1.18	0.084	1.25
		11	178.3	163.4	212.2	1.19	0.052	1.25
		12	178.8	163.9	211.1	1.18	0.053	1.25
7	Paulay and Scarpas (1981)	Unit 1	222.4	197.8	136.1	0.61	0.032	1.00
		Unit 2	221.9	197.4	199.1	0.90	0.038	1.00
		Unit 3	242.6	215.8	147.2	0.61	0.035	1.00
8	Ehsani and Wight (1982)	1 ^[7]	116.6	108.7	131.5	1.13	0.038	1.25
		2 ^[6]	119.0	110.9	140.3	1.18	0.038	1.25
		3 ^[7]	128.7	119.9	162.4	1.26	0.053	1.25
		4 ^[6]	134.4	125.3	181.0	1.35	0.056	1.25
9	Kanada et al. (1984)	U40L ^[4]	99.4	92.8	62.3	0.63	0.033	1.25
		U41L	104.1	97.2	82.5	0.79	0.038	1.25
		U42L	110.6	103.2	82.0	0.74	0.033	1.25
		U41S ^[6]	104.1	97.2	44.4	0.43	0.014	1.25
		U42S ^[6]	110.6	103.2	48.6	0.44	0.020	1.25
		U20L ^[4]	104.1	97.2	45.8	0.44	0.011	1.25
		U21L	110.6	103.2	48.1	0.43	0.020	1.25
		U21S ^[6]	104.1	97.2	34.8	0.33	0.022	1.25

^[1] Columns arranged in alphabetical order of notation; notation described in Appendix A; values given in SI units are converted to in.-lb (1 in. = 25.4 mm; 1 psi = 1/145 Mpa; and 1 kip = 4.4484 kN)

^[2] Bar sizes are presented in SI and in.-lb as reported in the original studies

^[3] Analyzed as a doubly reinforced section to calculate the nominal flexural strength M_n ; all other specimens are analyzed as a single reinforced

^[4] Specimens did not contain confining reinforcement parallel to the hooked bars within the joint region

^[5] Specimens had transverse beams on one or both sides of the test beam. These transverse beams meet the dimensional requirements of Sections 18.8.4 and 15.2.8 of ACI 318-19 and Section 4.3 of ACI 352R-02 to be considered effective in increasing the joint shear strength

^[6] Specimens had $d/\ell_{eh} > 1.5$

^[7] Specimens had column to beam flexural strength ratio, M_R , less than 1.2

Table C.4 Cont. Data for exterior beam-column joint specimens tested under reversed cyclic loading ^[1]

Study		Specimen	Bar Size ^[2]	A_b (in. ²)	A_{hs} (in. ²)	A_{tr} (in. ²)	A_{th} (in. ²)	$\frac{A_{th}}{A_{hs}}$	A_v (in. ²)	b_b (in.)
9	Kanada et al. (1984)	U22S ^[6]	D19	0.44	0.88	0.10	0.59	0.67	0.59	10.2
		R41L	D19	0.44	1.77	0.10	0.39	0.22	0.39	10.2
		R42S ^[6]	D19	0.44	1.77	0.10	0.59	0.33	0.59	10.2
		R21L	D19	0.44	0.88	0.10	0.39	0.45	0.39	10.2
		R21S ^[6]	D19	0.44	0.88	0.10	0.39	0.45	0.39	10.2
10	Zerbe and Durrani (1985)	J1 ^[6]	No. 6	0.44	1.76	0.20	0.80	0.45	1.20	10.0
		J2 ^{[5][6]}	No. 6	0.44	1.76	0.20	0.80	0.45	1.20	10.0
		J3 ^[6]	No. 6	0.44	1.76	0.20	0.80	0.45	1.20	10.0
		J4 ^{[5][6]}	No. 6	0.44	1.76	0.20	0.80	0.45	1.20	10.0
		J5 ^{[5][6]}	No. 6	0.44	1.76	0.20	0.80	0.45	1.20	10.0
		J6 ^{[5][6]}	No. 6	0.44	1.76	0.20	0.80	0.45	1.20	10.0
		J7 ^[7]	No. 6	0.44	1.76	0.20	0.80	0.45	1.20	12.0
11	Ehsani et al. (1987)	1	No. 6	0.44	2.20	0.20	0.80	0.36	1.20	11.8
		2	No. 6	0.44	2.20	0.20	0.80	0.36	1.20	11.8
		3 ^[6]	No. 6	0.44	2.20	0.20	0.80	0.36	1.20	10.2
		4 ^[6]	No. 7	0.60	3.00	0.20	0.80	0.27	1.20	10.2
		5 ^[6]	No. 7	0.60	3.60	0.20	0.80	0.22	1.20	10.2
12	Kaku and Asakusa (1991)	1	D13	0.20	0.79	0.04	0.18	0.22	0.35	6.3
		2	D13	0.20	0.79	0.04	0.18	0.22	0.35	6.3
		3	D13	0.20	0.79	0.04	0.18	0.22	0.35	6.3
		4	D13	0.20	0.79	0.01	0.04	0.06	0.09	6.3
		5	D13	0.20	0.79	0.01	0.04	0.06	0.09	6.3
		6	D13	0.20	0.79	0.01	0.04	0.06	0.09	6.3
		7	D13	0.20	0.79	0.04	0.18	0.22	0.35	6.3
		8	D13	0.20	0.79	0.04	0.18	0.22	0.35	6.3
		9	D13	0.20	0.79	0.04	0.18	0.22	0.35	6.3

^[1] Columns arranged in alphabetical order of notation; notation described in Appendix A; values given in SI units are converted to in.-lb (1 in. = 25.4 mm; 1 psi = 1/145 Mpa; and 1 kip = 4.4484 kN)

^[2] Bar sizes are presented in SI and in.-lb as reported in the original studies

^[3] Analyzed as a doubly reinforced section to calculate the nominal flexural strength M_n ; all other specimens are analyzed as a single reinforced

^[4] Specimens did not contain confining reinforcement parallel to the hooked bars within the joint region

^[5] Specimens had transverse beams on one or both sides of the test beam. These transverse beams meet the dimensional requirements of Sections 18.8.4 and 15.2.8 of ACI 318-19 and Section 4.3 of ACI 352R-02 to be considered effective in increasing the joint shear strength

^[6] Specimens had $d/\ell_{eh} > 1.5$

^[7] Specimens had column to beam flexural strength ratio, M_R , less than 1.2

Table C.4 Cont. Data for exterior beam-column joint specimens tested under reversed cyclic loading^[1]

Study		Specimen	b_c (in.)	b_j (in.)	b_j , ACI 352 (in.)	c_{ch} (in.)	$\frac{c_{ch}}{d_b}$	c_{so} (in.)	$\frac{c_{so}}{d_b}$	d
9	Kanada et al. (1984)	U22S ^[6]	11.8	11.8	11.0	6.3	8.4	2.4	3.2	13.0
		R41L	11.8	11.8	11.0	2.1	2.8	2.4	3.2	13.0
		R42S ^[6]	11.8	11.8	11.0	2.1	2.8	2.4	3.2	13.0
		R21L	11.8	11.8	11.0	6.3	8.4	2.4	3.2	13.0
		R21S ^[6]	11.8	11.8	11.0	6.3	8.4	2.4	3.2	13.0
10	Zerbe and Durrani (1985)	J1 ^[6]	12.0	12.0	11.0	1.8	2.3	3.0	4.0	12.6
		J2 ^{[5][6]}	12.0	12.0	11.0	1.8	2.3	3.0	4.0	12.6
		J3 ^[6]	12.0	12.0	11.0	1.8	2.3	3.0	4.0	12.6
		J4 ^{[5][6]}	12.0	12.0	11.0	1.8	2.3	3.0	4.0	12.6
		J5 ^{[5][6]}	12.0	12.0	11.0	1.8	2.3	3.0	4.0	12.6
		J6 ^{[5][6]}	12.0	12.0	11.0	1.8	2.3	3.0	4.0	12.6
		J7 ^[7]	12.0	12.0	12.0	1.8	2.3	3.0	4.0	12.6
11	Ehsani et al. (1987)	1	13.4	13.4	12.6	3.9	5.2	2.4	3.2	15.9
		2	13.4	13.4	12.6	3.9	5.2	2.4	3.2	15.9
		3 ^[6]	11.8	11.8	11.0	3.1	4.1	2.4	3.2	14.4
		4 ^[6]	11.8	11.8	11.0	3.1	3.5	2.4	2.7	14.4
		5 ^[6]	11.8	11.8	11.0	3.1	3.5	2.4	2.7	14.4
12	Kaku and Asakusa (1991)	1	8.7	8.7	7.5	1.7	3.3	1.6	3.2	8.0
		2	8.7	8.7	7.5	1.7	3.3	1.6	3.2	8.0
		3	8.7	8.7	7.5	1.7	3.3	1.6	3.2	8.0
		4	8.7	8.7	7.5	1.7	3.3	1.6	3.2	8.0
		5	8.7	8.7	7.5	1.7	3.3	1.6	3.2	8.0
		6	8.7	8.7	7.5	1.7	3.3	1.6	3.2	8.0
		7	8.7	8.7	7.5	1.7	3.3	1.6	3.2	8.0
		8	8.7	8.7	7.5	1.7	3.3	1.6	3.2	8.0
		9	8.7	8.7	7.5	1.7	3.3	1.6	3.2	8.0

[1] Columns arranged in alphabetical order of notation; notation described in Appendix A; values given in SI units are converted to in.-lb (1 in. = 25.4 mm; 1 psi = 1/145 Mpa; and 1 kip = 4.4484 kN)

[2] Bar sizes are presented in SI and in.-lb as reported in the original studies

[3] Analyzed as a doubly reinforced section to calculate the nominal flexural strength M_n ; all other specimens are analyzed as a single reinforced

[4] Specimens did not contain confining reinforcement parallel to the hooked bars within the joint region

[5] Specimens had transverse beams on one or both sides of the test beam. These transverse beams meet the dimensional requirements of Sections 18.8.4 and 15.2.8 of ACI 318-19 and Section 4.3 of ACI 352R-02 to be considered effective in increasing the joint shear strength

[6] Specimens had $d/\ell_{ch} > 1.5$

[7] Specimens had column to beam flexural strength ratio, M_R , less than 1.2

Table C.4 Cont. Data for exterior beam-column joint specimens tested under reversed cyclic loading^[1]

Study		Specimen	$\frac{d}{\ell_{eh}}$	d' (in.)	d_b (in.)	f_{cm} ^[8] (psi)	f_{cm} ^[9] (psi)	f_y (ksi)	$f_{ytr,l}$ (ksi)	$f_{ytr,l} A_v$ (kips)
9	Kanada et al. (1984)	U22S ^[6]	2.17	2.0	0.75	4370	4370	56.2	42.7	25.2
		R41L	1.45	2.0	0.75	3140	3140	56.2	42.7	16.8
		R42S ^[6]	2.17	2.0	0.75	3140	3140	56.2	42.7	25.2
		R21L	1.45	2.0	0.75	3140	3140	56.2	42.7	16.8
		R21S ^[6]	2.17	2.0	0.75	3140	3140	56.2	42.7	16.8
10	Zerbe and Durrani (1985)	J1 ^[6]	1.63	2.4	0.75	5710	5710	60.0	77.0	92.4
		J2 ^{[5][6]}	1.63	2.4	0.75	5650	5650	60.0	77.0	92.4
		J3 ^[6]	1.63	2.4	0.75	5780	5780	60.0	77.0	92.4
		J4 ^{[5][6]}	1.63	2.4	0.75	5940	5940	60.0	77.0	92.4
		J5 ^{[5][6]}	1.63	2.4	0.75	5610	5610	60.0	77.0	92.4
		J6 ^{[5][6]}	1.63	2.4	0.75	5690	5690	60.0	77.0	92.4
		J7 ^[7]	1.63	2.4	0.75	5900	5900	60.0	77.0	92.4
11	Ehsani et al. (1987)	1	1.47	3.0	0.75	9380	9380	70.0	63.4	76.1
		2	1.47	3.0	0.75	9760	9760	70.0	63.4	76.1
		3 ^[6]	1.57	2.9	0.75	9380	9380	70.0	63.4	76.1
		4 ^[6]	1.55	2.9	0.875	9760	9760	62.0	63.4	76.1
		5 ^[6]	1.67	2.9	0.875	6470	6470	48.0	63.4	76.1
12	Kaku and Asakusa (1991)	1	1.04	0.7	0.5	4510	4510	56.7	36.3	12.7
		2	1.04	0.7	0.5	6050	6050	56.7	36.3	12.7
		3	1.04	0.7	0.5	6050	6050	56.7	36.3	12.7
		4	1.04	0.7	0.5	6480	6480	56.7	40.7	3.6
		5	1.04	0.7	0.5	5320	5320	56.7	40.7	3.6
		6	1.04	0.7	0.5	5860	5860	56.7	40.7	3.6
		7	1.04	0.7	0.5	4670	4670	56.7	36.3	12.7
		8	1.04	0.7	0.5	5970	5970	56.7	36.3	12.7
		9	1.04	0.7	0.5	5890	5890	56.7	36.3	12.7

[1] Columns arranged in alphabetical order of notation; notation described in Appendix A; values given in SI units are converted to in.-lb (1 in. = 25.4 mm; 1 psi = 1/145 Mpa; and 1 kip = 4.4484 kN)

[4] Specimens did not contain confining reinforcement parallel to the hooked bars within the joint region

[5] Specimens had transverse beams on one or both sides of the test beam. These transverse beams meet the dimensional requirements of Sections 18.8.4 and 15.2.8 of ACI 318-19 and Section 4.3 of ACI 352R-02 to be considered effective in increasing the joint shear strength

[6] Specimens had $d/\ell_{eh} > 1.5$

[7] Specimens had column to beam flexural strength ratio, M_R , less than 1.2

[8] Column concrete compressive strength

[9] Beam concrete compressive strength

Table C.4 Cont. Data for exterior beam-column joint specimens tested under reversed cyclic loading ^[1]

Study		Specimen	h_b (in.)	h_c (in.)	ℓ_{dh} (in.)	$\frac{\ell_{dh}}{d_b}$	ℓ_{eh} (in.)	$\frac{\ell_{eh}}{d_b}$	ℓ_{ehy} (in.)	$\frac{\ell_{ehy}}{d_b}$
9	Kanada et al. (1984)	U22S ^[6]	15.0	11.8	8.4	11.2	6.0	8.0	7.5	10.1
		R41L	15.0	11.8	10.6	14.1	9.0	12.0	10.4	13.8
		R42S ^[6]	15.0	11.8	10.6	14.1	6.0	8.0	10.4	13.8
		R21L	15.0	11.8	9.1	12.2	9.0	12.0	8.3	11.0
		R21S ^[6]	15.0	11.8	9.1	12.2	6.0	8.0	8.3	11.0
10	Zerbe and Durrani (1985)	J1 ^[6]	15.0	12.0	8.0	10.6	7.8	10.3	7.7	10.3
		J2 ^{[5][6]}	15.0	12.0	8.0	10.6	7.8	10.3	7.7	10.3
		J3 ^[6]	15.0	12.0	7.9	10.6	7.8	10.3	7.7	10.2
		J4 ^{[5][6]}	15.0	12.0	7.9	10.5	7.8	10.3	7.6	10.2
		J5 ^{[5][6]}	15.0	12.0	8.0	10.7	7.8	10.3	7.7	10.3
		J6 ^{[5][6]}	15.0	12.0	8.0	10.6	7.8	10.3	7.7	10.3
		J7 ^[7]	15.0	12.0	7.9	10.5	7.8	10.3	7.6	10.2
11	Ehsani et al. (1987)	1	18.9	13.4	9.0	12.0	10.8	14.4	8.3	11.1
		2	18.9	13.4	8.9	11.9	10.8	14.4	8.2	10.9
		3 ^[6]	17.3	11.8	9.5	12.6	9.2	12.3	8.8	11.8
		4 ^[6]	17.3	11.8	10.7	12.3	9.3	10.6	9.8	11.3
		5 ^[6]	17.3	11.8	9.2	10.5	8.6	9.8	8.4	9.6
12	Kaku and Asakusa (1991)	1	8.7	8.7	5.2	10.4	7.7	15.4	5.3	10.7
		2	8.7	8.7	4.8	9.7	7.7	15.4	4.9	9.8
		3	8.7	8.7	4.8	9.7	7.7	15.4	4.9	9.8
		4	8.7	8.7	6.6	13.2	7.7	15.4	5.1	10.2
		5	8.7	8.7	6.9	13.8	7.7	15.4	5.4	10.7
		6	8.7	8.7	6.7	13.5	7.7	15.4	5.2	10.4
		7	8.7	8.7	5.2	10.3	7.7	15.4	5.3	10.6
		8	8.7	8.7	4.9	9.7	7.7	15.4	4.9	9.9
		9	8.7	8.7	4.9	9.7	7.7	15.4	5.0	9.9

^[1] Columns arranged in alphabetical order of notation; notation described in Appendix A; values given in SI units are converted to in.-lb (1 in. = 25.4 mm; 1 psi = 1/145 Mpa; and 1 kip = 4.4484 kN)

^[2] Bar sizes are presented in SI and in.-lb as reported in the original studies

^[3] Analyzed as a doubly reinforced section to calculate the nominal flexural strength M_n ; all other specimens are analyzed as a single reinforced

^[4] Specimens did not contain confining reinforcement parallel to the hooked bars within the joint region

^[5] Specimens had transverse beams on one or both sides of the test beam. These transverse beams meet the dimensional requirements of Sections 18.8.4 and 15.2.8 of ACI 318-19 and Section 4.3 of ACI 352R-02 to be considered effective in increasing the joint shear strength

^[6] Specimens had $d/\ell_{eh} > 1.5$

^[7] Specimens had column to beam flexural strength ratio, M_R , less than 1.2

Table C.4 Cont. Data for exterior beam-column joint specimens tested under reversed cyclic loading^[1]

Study		Specimen	$\frac{\ell_{eh}}{h_c}$	$\frac{\ell_{eh}}{\ell_{dh}}$	$\frac{\ell_{eh}}{\ell_{ehy}}$	M_n (kip.in.)	M_{peak} (kip.in.)	$\frac{M_{peak}}{M_n}$	N	N_{total}
9	Kanada et al. (1984)	U22S ^[6]	0.5	0.71	0.79	613	573	0.94	3	3
		R41L	0.8	0.85	0.86	1110	1022	0.92	2	2
		R42S ^[6]	0.5	0.56	0.58	1110	664	0.60	3	3
		R21L	0.8	0.98	1.09	600	664	1.11	2	2
		R21S ^[6]	0.5	0.65	0.73	600	495	0.82	2	2
10	Zerbe and Durrani (1985)	J1 ^[6]	0.6	0.97	1.01	1216	1287	1.06	2	3
		J2 ^{[5][6]}	0.6	0.97	1.00	1214	1518	1.25	2	3
		J3 ^[6]	0.6	0.98	1.01	1216	1320	1.09	2	3
		J4 ^{[5][6]}	0.6	0.98	1.02	1900	2079	1.09	2	3
		J5 ^{[5][6]}	0.6	0.97	1.00	2221	2244	1.01	2	3
		J6 ^{[5][6]}	0.6	0.97	1.00	1218	2211	1.82	2	3
		J7 ^[7]	0.6	0.98	1.01	2869	2211	0.77	2	3
11	Ehsani et al. (1987)	1	0.8	1.20	1.30	1729	2170	1.26	2	3
		2	0.8	1.21	1.32	2041	2666	1.31	2	3
		3 ^[6]	0.8	0.97	1.04	1663	1984	1.19	2	3
		4 ^[6]	0.8	0.87	0.94	2290	2232	0.97	2	3
		5 ^[6]	0.7	0.93	1.02	2101	2280	1.09	2	3
12	Kaku and Asakusa (1991)	1	0.9	1.48	1.44	335	427	1.27	2	4
		2	0.9	1.59	1.56	341	430	1.26	2	4
		3	0.9	1.59	1.56	338	374	1.10	2	4
		4	0.9	1.17	1.51	334	412	1.23	2	4
		5	0.9	1.11	1.43	332	380	1.14	2	4
		6	0.9	1.14	1.47	340	360	1.06	2	4
		7	0.9	1.49	1.46	335	428	1.28	2	4
		8	0.9	1.58	1.56	335	419	1.25	2	4
		9	0.9	1.58	1.55	335	406	1.21	2	4

[1] Columns arranged in alphabetical order of notation; notation described in Appendix A; values given in SI units are converted to in.-lb (1 in. = 25.4 mm; 1 psi = 1/145 Mpa; and 1 kip = 4.4484 kN)

[2] Bar sizes are presented in SI and in.-lb as reported in the original studies

[3] Analyzed as a doubly reinforced section to calculate the nominal flexural strength M_n ; all other specimens are analyzed as a single reinforced

[4] Specimens did not contain confining reinforcement parallel to the hooked bars within the joint region

[5] Specimens had transverse beams on one or both sides of the test beam. These transverse beams meet the dimensional requirements of Sections 18.8.4 and 15.2.8 of ACI 318-19 and Section 4.3 of ACI 352R-02 to be considered effective in increasing the joint shear strength

[6] Specimens had $d/\ell_{eh} > 1.5$

[7] Specimens had column to beam flexural strength ratio, M_R , less than 1.2

Table C.4 Cont. Data for exterior beam-column joint specimens tested under reversed cyclic loading^[1]

Study		Specimen	n	nT' (kips)	s_{tr} (in.)	T_h (kips)	T' (kips)	T'_{mod} (kips)	$\frac{T'}{T_h}$	$\frac{T'_{mod}}{T_h}$
9	Kanada et al. (1984)	U22S ^[6]	2	46.4	2.0	20.1	23.2	-	1.15	-
		R41L	4	91.4	3.9	21.7	22.9	-	1.06	-
		R42S ^[6]	4	59.4	2.0	14.8	14.9	-	1.00	-
		R21L	2	54.9	3.9	25.0	27.5	27.2	1.10	1.09
		R21S ^[6]	2	40.9	3.9	18.5	20.5	-	1.10	-
10	Zerbe and Durrani (1985)	J1 ^[6]	4	111.8	3.0	26.5	27.9	27.9	1.05	1.05
		J2 ^{[5][6]}	4	132.0	3.0	26.5	33.0	33.0	1.24	1.24
		J3 ^[6]	4	114.6	3.0	26.5	28.7	28.6	1.08	1.08
		J4 ^{[5][6]}	4	115.5	3.0	26.5	28.9	28.8	1.09	1.09
		J5 ^{[5][6]}	4	106.7	3.0	26.5	26.7	26.7	1.01	1.01
		J6 ^{[5][6]}	4	91.7	3.0	26.5	22.9	22.9	0.86	0.86
		J7 ^[7]	4	81.4	3.0	26.5	20.3	20.3	0.77	0.8
11	Ehsani et al. (1987)	1	5	193.3	3.5	30.9	38.7	37.5	1.25	1.21
		2	5	201.2	3.5	30.9	40.2	39.0	1.30	1.26
		3 ^[6]	5	183.7	2.2	30.9	36.7	36.6	1.19	1.18
		4 ^[6]	5	181.3	2.5	35.3	36.3	-	1.03	-
		5 ^[6]	6	187.5	2.5	28.9	31.3	31.2	1.08	1.08
12	Kaku and Asakusa (1991)	1	4	56.7	2.0	11.2	14.2	13.6	1.27	1.21
		2	4	56.2	2.0	11.2	14.1	13.3	1.26	1.19
		3	4	49.2	2.0	11.2	12.3	11.5	1.10	1.03
		4	4	54.9	2.0	11.2	13.7	13.0	1.23	1.17
		5	4	50.9	2.0	11.2	12.7	12.1	1.14	1.09
		6	4	47.2	2.0	11.2	11.8	11.1	1.06	1.00
		7	4	56.9	2.0	11.2	14.2	13.6	1.27	1.22
		8	4	55.8	2.0	11.2	13.9	13.2	1.25	1.18
		9	4	54.0	2.0	11.2	13.5	12.7	1.21	1.14

[1] Columns arranged in alphabetical order of notation; notation described in Appendix A; values given in SI units are converted to in.-lb (1 in. = 25.4 mm; 1 psi = 1/145 Mpa; and 1 kip = 4.4484 kN)

[2] Bar sizes are presented in SI and in.-lb as reported in the original studies

[3] Analyzed as a doubly reinforced section to calculate the nominal flexural strength M_n ; all other specimens are analyzed as a single reinforced

[4] Specimens did not contain confining reinforcement parallel to the hooked bars within the joint region

[5] Specimens had transverse beams on one or both sides of the test beam. These transverse beams meet the dimensional requirements of Sections 18.8.4 and 15.2.8 of ACI 318-19 and Section 4.3 of ACI 352R-02 to be considered effective in increasing the joint shear strength

[6] Specimens had $d/\ell_{eh} > 1.5$

[7] Specimens had column to beam flexural strength ratio, M_R , less than 1.2

Table C.4 Cont. Data for exterior beam-column joint specimens tested under reversed cyclic loading^[1]

Study		Specimen	V_n (kips)	V_n , ACI 352 (kips)	V_p (kips)	$\frac{V_p}{V_n}$	$\delta_{0.8 peak}$	Ψ_o
9	Kanada et al. (1984)	U22S ^[6]	110.6	103.2	40.3	0.36	0.030	1.25
		R41L	93.9	87.6	71.9	0.77	0.038	1.25
		R42S ^[6]	93.9	87.6	46.7	0.50	0.018	1.25
		R21L	93.9	87.6	46.7	0.50	0.022	1.25
		R21S ^[6]	93.9	87.6	34.8	0.37	0.022	1.25
10	Zerbe and Durrani (1985)	J1 ^[6]	130.6	119.7	110.9	0.85	0.053	1.00
		J2 ^{[5][6]}	162.4	148.8	130.8	0.81	0.052	1.00
		J3 ^[6]	131.4	120.4	113.8	0.87	0.053	1.00
		J4 ^{[5][6]}	133.2	122.1	179.2	1.35	0.050	1.00
		J5 ^{[5][6]}	161.8	148.3	193.4	1.20	0.051	1.00
		J6 ^{[5][6]}	162.9	149.4	190.6	1.17	0.052	1.00
		J7 ^[7]	132.7	132.7	190.6	1.44	0.050	1.00
11	Ehsani et al. (1987)	1	208.7	196.2	128.0	0.61	0.062	1.25
		2	212.9	200.2	157.2	0.74	0.064	1.25
		3 ^[6]	161.8	150.9	133.2	0.82	0.060	1.25
		4 ^[6]	165.1	153.9	149.8	0.91	0.058	1.25
		5 ^[6]	134.4	125.3	141.6	1.05	0.065	1.25
12	Kaku and Asakusa (1991)	1	60.5	52.2	50.3	0.83	0.055	1.25
		2	70.0	60.5	50.8	0.73	0.065	1.25
		3	70.0	60.5	44.1	0.63	0.065	1.25
		4	72.5	62.6	48.6	0.67	0.060	1.25
		5	65.7	56.7	44.8	0.68	0.055	1.25
		6	68.9	59.5	42.5	0.62	0.052	1.25
		7	61.5	53.1	50.5	0.82	0.060	1.25
		8	69.6	60.1	49.5	0.71	0.063	1.25
		9	69.1	59.7	47.9	0.69	0.068	1.25

^[1] Columns arranged in alphabetical order of notation; notation described in Appendix A; values given in SI units are converted to in.-lb (1 in. = 25.4 mm; 1 psi = 1/145 Mpa; and 1 kip = 4.4484 kN)

^[2] Bar sizes are presented in SI and in.-lb as reported in the original studies

^[3] Analyzed as a doubly reinforced section to calculate the nominal flexural strength M_n ; all other specimens are analyzed as a single reinforced

^[4] Specimens did not contain confining reinforcement parallel to the hooked bars within the joint region

^[5] Specimens had transverse beams on one or both sides of the test beam. These transverse beams meet the dimensional requirements of Sections 18.8.4 and 15.2.8 of ACI 318-19 and Section 4.3 of ACI 352R-02 to be considered effective in increasing the joint shear strength

^[6] Specimens had $d/\ell_{eh} > 1.5$

^[7] Specimens had column to beam flexural strength ratio, M_R , less than 1.2

Table C.4 Cont. Data for exterior beam-column joint specimens tested under reversed cyclic loading^[1]

Study		Specimen	Bar Size ^[2]	A_b (in. ²)	A_{hs} (in. ²)	A_{tr} (in. ²)	A_{th} (in. ²)	$\frac{A_{th}}{A_{hs}}$	A_v (in. ²)	b_b (in.)
12	Kaku and Asakusa (1991)	10	D13	0.20	0.79	0.01	0.04	0.06	0.09	6.3
		11	D13	0.20	0.79	0.01	0.04	0.06	0.09	6.3
		12	D13	0.20	0.79	0.01	0.04	0.06	0.09	6.3
		13	D13	0.20	0.79	0.04	0.18	0.22	0.35	6.3
		14	D13	0.20	0.79	0.01	0.04	0.06	0.09	6.3
		15	D13	0.20	0.79	0.01	0.04	0.06	0.09	6.3
		16	D13	0.20	0.79	0.04	0.18	0.22	0.35	6.3
		17 ^[7]	D13	0.20	0.79	0.04	0.18	0.22	0.35	6.3
		18 ^[7]	D13	0.20	0.79	0.04	0.18	0.22	0.35	6.3
13	Ehsani and Alameddine (1991)	LL8 ^[6]	No. 8	0.79	3.16	0.20	1.80	0.57	2.40	12.5
		LH8 ^[6]	No. 8	0.79	3.16	0.20	2.40	0.76	3.60	12.5
		HL8 ^[6]	No. 9	1.00	4.00	0.20	1.80	0.45	2.40	12.5
		HH8 ^[6]	No. 9	1.00	4.00	0.20	2.40	0.60	3.60	12.5
		LL11 ^[6]	No. 8	0.79	3.16	0.20	1.80	0.57	2.40	12.5
		LH11 ^[6]	No. 8	0.79	3.16	0.20	2.40	0.76	3.60	12.5
		HL11 ^[6]	No. 9	1.00	4.00	0.20	1.80	0.45	2.40	12.5
		HH11 ^[6]	No. 9	1.00	4.00	0.20	2.40	0.60	3.60	12.5
		LL14 ^[6]	No. 8	0.79	3.16	0.20	1.80	0.57	2.40	12.5
		LH14 ^[6]	No. 8	0.79	3.16	0.20	2.40	0.76	3.60	12.5
HH14 ^[6]	No. 9	1.00	4.00	0.20	2.40	0.60	3.60	12.5		
14	Tsonos et al. (1992)	S1 ^[6]	D14	0.24	0.48	0.08	0.16	0.33	0.47	7.9
		S2 ^[6]	D12	0.18	0.53	0.08	0.16	0.30	0.47	7.9
		S3 ^[7]	D12	0.18	0.70	0.08	0.16	0.22	0.47	7.9
		S4 ^[7]	D14	0.24	0.95	0.08	0.16	0.16	0.47	7.9
		S5 ^[7]	D14	0.24	0.95	0.08	0.16	0.16	0.47	7.9

^[1] Columns arranged in alphabetical order of notation; notation described in Appendix A; values given in SI units are converted to in.-lb (1 in. = 25.4 mm; 1 psi = 1/145 Mpa; and 1 kip = 4.4484 kN)

^[2] Bar sizes are presented in SI and in.-lb as reported in the original studies

^[3] Analyzed as a doubly reinforced section to calculate the nominal flexural strength M_n ; all other specimens are analyzed as a single reinforced

^[4] Specimens did not contain confining reinforcement parallel to the hooked bars within the joint region

^[5] Specimens had transverse beams on one or both sides of the test beam. These transverse beams meet the dimensional requirements of Sections 18.8.4 and 15.2.8 of ACI 318-19 and Section 4.3 of ACI 352R-02 to be considered effective in increasing the joint shear strength

^[6] Specimens had $d/\ell_{eh} > 1.5$

^[7] Specimens had column to beam flexural strength ratio, M_R , less than 1.2

Table C.4 Cont. Data for exterior beam-column joint specimens tested under reversed cyclic loading^[1]

Study		Specimen	b_c (in.)	b_j (in.)	b_j , ACI 352 (in.)	c_{ch} (in.)	$\frac{c_{ch}}{d_b}$	c_{so} (in.)	$\frac{c_{so}}{d_b}$	d
12	Kaku and Asakusa (1991)	10	8.7	8.7	7.5	1.7	3.3	1.6	3.2	8.0
		11	8.7	8.7	7.5	1.7	3.3	1.6	3.2	8.0
		12	8.7	8.7	7.5	1.7	3.3	1.6	3.2	8.0
		13	8.7	8.7	7.5	1.7	3.3	1.6	3.2	8.0
		14	8.7	8.7	7.5	1.7	3.3	1.6	3.2	8.0
		15	8.7	8.7	7.5	1.7	3.3	1.6	3.2	8.0
		16	8.7	8.7	7.5	1.7	3.3	1.6	3.2	8.0
		17 ^[7]	8.7	8.7	7.5	1.7	3.3	1.6	3.2	8.0
		18 ^[7]	8.7	8.7	7.5	1.7	3.3	1.6	3.2	8.0
13	Ehsani and Alameddine (1991)	LL8 ^[6]	14.0	14.0	13.3	2.2	2.2	3.0	3.0	17.0
		LH8 ^[6]	14.0	14.0	13.3	2.2	2.2	3.0	3.0	17.0
		HL8 ^[6]	14.0	14.0	13.3	2.2	1.9	3.0	2.7	17.0
		HH8 ^[6]	14.0	14.0	13.3	2.2	1.9	3.0	2.7	17.0
		LL11 ^[6]	14.0	14.0	13.3	2.2	2.2	3.0	3.0	17.0
		LH11 ^[6]	14.0	14.0	13.3	2.2	2.2	3.0	3.0	17.0
		HL11 ^[6]	14.0	14.0	13.3	2.2	1.9	3.0	2.7	17.0
		HH11 ^[6]	14.0	14.0	13.3	2.2	1.9	3.0	2.7	17.0
		LL14 ^[6]	14.0	14.0	13.3	2.2	2.2	3.0	3.0	17.0
		LH14 ^[6]	14.0	14.0	13.3	2.2	2.2	3.0	3.0	17.0
HH14 ^[6]	14.0	14.0	13.3	2.2	1.9	3.0	2.7	17.0		
14	Tsonos et al. (1992)	S1 ^[6]	7.9	7.9	7.9	5.9	10.7	0.7	1.3	10.8
		S2 ^[6]	7.9	7.9	7.9	3.0	6.3	0.7	1.5	10.8
		S3 ^[7]	7.9	7.9	7.9	2.0	4.2	0.7	1.5	10.8
		S4 ^[7]	7.9	7.9	7.9	2.0	3.6	0.7	1.3	10.8
		S5 ^[7]	7.9	7.9	7.9	2.0	3.6	0.7	1.3	10.8

[1] Columns arranged in alphabetical order of notation; notation described in Appendix A; values given in SI units are converted to in.-lb (1 in. = 25.4 mm; 1 psi = 1/145 Mpa; and 1 kip = 4.4484 kN)

[2] Bar sizes are presented in SI and in.-lb as reported in the original studies

[3] Analyzed as a doubly reinforced section to calculate the nominal flexural strength M_n ; all other specimens are analyzed as a single reinforced

[4] Specimens did not contain confining reinforcement parallel to the hooked bars within the joint region

[5] Specimens had transverse beams on one or both sides of the test beam. These transverse beams meet the dimensional requirements of Sections 18.8.4 and 15.2.8 of ACI 318-19 and Section 4.3 of ACI 352R-02 to be considered effective in increasing the joint shear strength

[6] Specimens had $d/\ell_{ch} > 1.5$

[7] Specimens had column to beam flexural strength ratio, M_R , less than 1.2

Table C.4 Cont. Data for exterior beam-column joint specimens tested under reversed cyclic loading^[1]

Study		Specimen	$\frac{d}{\ell_{eh}}$	d' (in.)	d_b (in.)	f_{cm} ^[8] (psi)	f_{cm} ^[9] (psi)	f_y (ksi)	$f_{ytr,l}$ (ksi)	$f_{ytr,l} A_v$ (kips)
12	Kaku and Asakusa (1991)	10	1.04	0.7	0.5	6440	6440	56.7	40.7	3.6
		11	1.04	0.7	0.5	6080	6080	56.7	40.7	3.6
		12	1.04	0.7	0.5	5090	5090	56.7	40.7	3.6
		13	1.04	0.7	0.5	6730	6730	56.7	36.3	12.7
		14	1.04	0.7	0.5	5950	5950	56.7	40.7	3.6
		15	1.04	0.7	0.5	5760	5760	56.7	40.7	3.6
		16	1.04	0.7	0.5	5420	5420	56.7	36.3	12.7
		17 ^[7]	1.04	0.7	0.5	5760	5760	56.7	36.3	12.7
		18 ^[7]	1.04	0.7	0.5	5900	5900	56.7	36.3	12.7
13	Ehsani and Alameddine (1991)	LL8 ^[6]	1.62	3.0	1	8600	8600	66.3	64.8	155.4
		LH8 ^[6]	1.62	3.0	1	8600	8600	66.3	64.8	233.1
		HL8 ^[6]	1.62	3.0	1.128	8600	8600	64.2	64.8	155.4
		HH8 ^[6]	1.62	3.0	1.128	8600	8600	64.2	64.8	233.1
		LL11 ^[6]	1.62	3.0	1	10700	10700	66.3	64.8	155.4
		LH11 ^[6]	1.62	3.0	1	10700	10700	66.3	64.8	233.1
		HL11 ^[6]	1.62	3.0	1.128	10700	10700	64.2	64.8	155.4
		HH11 ^[6]	1.62	3.0	1.128	10700	10700	64.2	64.8	233.1
		LL14 ^[6]	1.62	3.0	1	13700	13700	66.3	64.8	155.4
		LH14 ^[6]	1.62	3.0	1	13700	13700	66.3	64.8	233.1
HH14 ^[6]	1.62	3.0	1.128	13700	13700	64.2	64.8	233.1		
14	Tsonos et al. (1992)	S1 ^[6]	1.67	1.0	0.55	5360	5360	70.3	71.7	33.5
		S2 ^[6]	1.67	1.0	0.47	3770	3770	76.7	71.7	33.5
		S3 ^[7]	1.67	1.0	0.47	2750	2750	76.67	71.7	33.5
		S4 ^[7]	1.67	1.0	0.55	3040	3040	70.3	71.7	33.5
		S5 ^[7]	1.67	1.0	0.55	3620	3620	70.3	71.7	33.5

[1] Columns arranged in alphabetical order of notation; notation described in Appendix A; values given in SI units are converted to in.-lb (1 in. = 25.4 mm; 1 psi = 1/145 Mpa; and 1 kip = 4.4484 kN)

[4] Specimens did not contain confining reinforcement parallel to the hooked bars within the joint region

[5] Specimens had transverse beams on one or both sides of the test beam. These transverse beams meet the dimensional requirements of Sections 18.8.4 and 15.2.8 of ACI 318-19 and Section 4.3 of ACI 352R-02 to be considered effective in increasing the joint shear strength

[6] Specimens had $d/\ell_{eh} > 1.5$

[7] Specimens had column to beam flexural strength ratio, M_R , less than 1.2

[8] Column concrete compressive strength

[9] Beam concrete compressive strength

Table C.4 Cont. Data for exterior beam-column joint specimens tested under reversed cyclic loading^[1]

Study		Specimen	h_b (in.)	h_c (in.)	ℓ_{dh} (in.)	$\frac{\ell_{dh}}{d_b}$	ℓ_{eh} (in.)	$\frac{\ell_{eh}}{d_b}$	ℓ_{ehy} (in.)	$\frac{\ell_{ehy}}{d_b}$
12	Kaku and Asakusa (1991)	10	8.7	8.7	6.6	13.2	7.7	15.4	5.1	10.2
		11	8.7	8.7	6.7	13.4	7.7	15.4	5.2	10.3
		12	8.7	8.7	7.0	14.0	7.7	15.4	5.4	10.9
		13	8.7	8.7	4.7	9.4	7.7	15.4	4.8	9.6
		14	8.7	8.7	6.7	13.4	7.7	15.4	5.2	10.4
		15	8.7	8.7	6.8	13.5	7.7	15.4	5.2	10.5
		16	8.7	8.7	5.0	9.9	7.7	15.4	5.1	10.1
		17 ^[7]	8.7	8.7	4.9	9.8	7.7	15.4	5.1	10.3
		18 ^[7]	8.7	8.7	4.9	9.7	7.7	15.4	5.1	10.2
13	Ehsani and Alameddine (1991)	LL8 ^[6]	20.0	14.0	12.3	12.3	10.5	10.5	11.4	11.4
		LH8 ^[6]	20.0	14.0	12.3	12.3	10.5	10.5	11.4	11.4
		HL8 ^[6]	20.0	14.0	14.4	12.7	10.5	9.3	13.1	11.6
		HH8 ^[6]	20.0	14.0	14.4	12.7	10.5	9.3	13.1	11.6
		LL11 ^[6]	20.0	14.0	11.7	11.7	10.5	10.5	10.8	10.8
		LH11 ^[6]	20.0	14.0	11.7	11.7	10.5	10.5	10.8	10.8
		HL11 ^[6]	20.0	14.0	13.6	12.1	10.5	9.3	12.3	10.9
		HH11 ^[6]	20.0	14.0	13.6	12.1	10.5	9.3	12.3	10.9
		LL14 ^[6]	20.0	14.0	11.0	11.0	10.5	10.5	10.1	10.1
		LH14 ^[6]	20.0	14.0	11.0	11.0	10.5	10.5	10.1	10.1
HH14 ^[6]	20.0	14.0	12.8	11.3	10.5	9.3	11.5	10.2		
14	Tsonos et al. (1992)	S1 ^[6]	11.8	7.9	6.3	11.4	6.5	11.8	5.9	10.8
		S2 ^[6]	11.8	7.9	6.0	12.6	6.5	13.8	5.9	12.5
		S3 ^[7]	11.8	7.9	7.0	14.9	6.5	13.8	7.4	15.6
		S4 ^[7]	11.8	7.9	8.9	16.1	6.5	11.8	8.6	15.5
		S5 ^[7]	11.8	7.9	8.5	15.5	6.5	11.8	8.2	14.8

^[1] Columns arranged in alphabetical order of notation; notation described in Appendix A; values given in SI units are converted to in.-lb (1 in. = 25.4 mm; 1 psi = 1/145 Mpa; and 1 kip = 4.4484 kN)

^[2] Bar sizes are presented in SI and in.-lb as reported in the original studies

^[3] Analyzed as a doubly reinforced section to calculate the nominal flexural strength M_n ; all other specimens are analyzed as a single reinforced

^[4] Specimens did not contain confining reinforcement parallel to the hooked bars within the joint region

^[5] Specimens had transverse beams on one or both sides of the test beam. These transverse beams meet the dimensional requirements of Sections 18.8.4 and 15.2.8 of ACI 318-19 and Section 4.3 of ACI 352R-02 to be considered effective in increasing the joint shear strength

^[6] Specimens had $d/\ell_{eh} > 1.5$

^[7] Specimens had column to beam flexural strength ratio, M_R , less than 1.2

Table C.4 Cont. Data for exterior beam-column joint specimens tested under reversed cyclic loading^[1]

Study		Specimen	$\frac{\ell_{eh}}{h_c}$	$\frac{\ell_{eh}}{\ell_{dh}}$	$\frac{\ell_{eh}}{\ell_{ehy}}$	M_n (kip.in.)	M_{peak} (kip.in.)	$\frac{M_{peak}}{M_n}$	N	N_{total}
12	Kaku and Asakusa (1991)	10	0.9	1.17	1.51	334	418	1.25	2	4
		11	0.9	1.15	1.48	334	397	1.19	2	4
		12	0.9	1.10	1.41	336	357	1.06	2	4
		13	0.9	1.63	1.61	339	360	1.06	2	4
		14	0.9	1.14	1.48	334	389	1.16	2	4
		15	0.9	1.13	1.46	333	397	1.19	2	4
		16	0.9	1.54	1.52	334	432	1.29	2	4
		17 ^[7]	0.9	1.57	1.49	338	304	0.90	2	4
		18 ^[7]	0.9	1.58	1.50	330	205	0.62	2	4
13	Ehsani and Alameddine (1991)	LL8 ^[6]	0.8	0.85	0.92	3027	3517	1.16	3	4
		LH8 ^[6]	0.8	0.85	0.92	3027	3402	1.12	4	6
		HL8 ^[6]	0.8	0.73	0.80	3637	3708	1.02	3	4
		HH8 ^[6]	0.8	0.73	0.80	3637	3743	1.03	4	6
		LL11 ^[6]	0.8	0.90	0.98	3118	3020	0.97	3	4
		LH11 ^[6]	0.8	0.90	0.98	3081	4018	1.30	4	6
		HL11 ^[6]	0.8	0.77	0.85	3845	3731	0.97	3	4
		HH11 ^[6]	0.8	0.77	0.85	3872	4089	1.06	4	6
		LL14 ^[6]	0.8	0.96	1.04	3112	3701	1.19	3	4
		LH14 ^[6]	0.8	0.96	1.04	3112	3780	1.21	4	6
HH14 ^[6]	0.8	0.82	0.91	3830	4084	1.07	4	6		
14	Tsonos et al. (1992)	S1 ^[6]	0.8	1.03	1.09	348	452	1.30	1	3
		S2 ^[6]	0.8	1.09	1.10	404	465	1.15	1	3
		S3 ^[7]	0.8	0.92	0.88	504	524	1.04	1	3
		S4 ^[7]	0.8	0.73	0.76	616	480	0.78	1	3
		S5 ^[7]	0.8	0.76	0.80	634	532	0.84	1	3

^[1] Columns arranged in alphabetical order of notation; notation described in Appendix A; values given in SI units are converted to in.-lb (1 in. = 25.4 mm; 1 psi = 1/145 Mpa; and 1 kip = 4.4484 kN)

^[2] Bar sizes are presented in SI and in.-lb as reported in the original studies

^[3] Analyzed as a doubly reinforced section to calculate the nominal flexural strength M_n ; all other specimens are analyzed as a single reinforced

^[4] Specimens did not contain confining reinforcement parallel to the hooked bars within the joint region

^[5] Specimens had transverse beams on one or both sides of the test beam. These transverse beams meet the dimensional requirements of Sections 18.8.4 and 15.2.8 of ACI 318-19 and Section 4.3 of ACI 352R-02 to be considered effective in increasing the joint shear strength

^[6] Specimens had $d/\ell_{eh} > 1.5$

^[7] Specimens had column to beam flexural strength ratio, M_R , less than 1.2

Table C.4 Cont. Data for exterior beam-column joint specimens tested under reversed cyclic loading^[1]

Study		Specimen	<i>n</i>	<i>nT'</i> (kips)	<i>s_{tr}</i> (in.)	<i>T_h</i> (kips)	<i>T'</i> (kips)	<i>T'</i> _{mod} (kips)	$\frac{T'}{T_h}$	$\frac{T'_{mod}}{T_h}$
12	Kaku and Asakusa (1991)	10	4	55.7	2.0	11.2	13.9	13.2	1.25	1.19
		11	4	53.0	2.0	11.2	13.2	12.6	1.19	1.13
		12	4	47.4	2.0	11.2	11.8	11.3	1.06	1.01
		13	4	47.3	2.0	11.2	11.8	11.0	1.06	0.98
		14	4	51.8	2.0	11.2	13.0	12.3	1.16	1.10
		15	4	53.0	2.0	11.2	13.3	12.6	1.19	1.13
		16	4	57.6	2.0	11.2	14.4	13.7	1.29	1.22
		17 ^[7]	4	39.9	2.0	11.2	10.0	9.2	0.89	0.8
		18 ^[7]	4	27.7	2.0	11.2	6.9	6.2	0.62	0.6
13	Ehsani and Alameddine (1991)	LL8 ^[6]	4	243.4	3.5	48.6	60.9	-	1.25	-
		LH8 ^[6]	4	235.5	2.3	48.6	58.9	-	1.21	-
		HL8 ^[6]	4	261.8	3.5	52.7	65.5	-	1.24	-
		HH8 ^[6]	4	264.3	2.3	52.7	66.1	-	1.25	-
		LL11 ^[6]	4	202.9	3.5	51.4	50.7	-	0.99	-
		LH11 ^[6]	4	273.2	2.3	51.4	68.3	-	1.33	-
		HL11 ^[6]	4	249.2	3.5	55.6	62.3	-	1.12	-
		HH11 ^[6]	4	271.2	2.3	55.6	67.8	-	1.22	-
		LL14 ^[6]	4	249.2	3.5	52.6	62.3	62.0	1.18	1.18
		LH14 ^[6]	4	254.5	2.3	52.6	63.6	63.3	1.21	1.20
HH14 ^[6]	4	273.8	2.3	59.1	68.5	-	1.16	-		
14	Tsonos et al. (1992)	S1 ^[6]	2	43.6	2.5	16.8	21.8	21.6	1.29	1.28
		S2 ^[6]	3	46.4	2.5	13.5	15.5	15.3	1.15	1.13
		S3 ^[7]	4	55.9	2.5	12.1	14.0	-	1.15	-
		S4 ^[7]	4	52.3	2.5	13.1	13.1	-	1.00	-
		S5 ^[7]	4	56.4	2.5	13.7	14.1	-	1.03	-

^[1] Columns arranged in alphabetical order of notation; notation described in Appendix A; values given in SI units are converted to in.-lb (1 in. = 25.4 mm; 1 psi = 1/145 Mpa; and 1 kip = 4.4484 kN)

^[2] Bar sizes are presented in SI and in.-lb as reported in the original studies

^[3] Analyzed as a doubly reinforced section to calculate the nominal flexural strength M_n ; all other specimens are analyzed as a single reinforced

^[4] Specimens did not contain confining reinforcement parallel to the hooked bars within the joint region

^[5] Specimens had transverse beams on one or both sides of the test beam. These transverse beams meet the dimensional requirements of Sections 18.8.4 and 15.2.8 of ACI 318-19 and Section 4.3 of ACI 352R-02 to be considered effective in increasing the joint shear strength

^[6] Specimens had $d/\ell_{eh} > 1.5$

^[7] Specimens had column to beam flexural strength ratio, M_R , less than 1.2

Table C.4 Cont. Data for exterior beam-column joint specimens tested under reversed cyclic loading^[1]

Study		Specimen	V_n (kips)	$V_{n,ACI 352}$ (kips)	V_p (kips)	$\frac{V_p}{V_n}$	$\delta_{0.8 peak}$	Ψ_o
12	Kaku and Asakusa (1991)	10	72.2	62.4	49.3	0.68	0.059	1.25
		11	70.2	60.6	46.9	0.67	0.048	1.25
		12	64.2	55.5	42.1	0.66	0.053	1.25
		13	73.8	63.8	42.5	0.58	0.065	1.25
		14	69.4	59.9	45.9	0.66	0.045	1.25
		15	68.3	59.0	46.8	0.69	0.060	1.25
		16	66.3	57.3	51.0	0.77	0.055	1.25
		17 ^[7]	68.3	59.0	35.8	0.52	0.070	1.25
		18 ^[7]	69.2	59.7	24.2	0.35	0.040	1.25
13	Ehsani and Alameddine (1991)	LL8 ^[6]	218.1	206.4	193.4	0.89	0.055	1.00
		LH8 ^[6]	218.1	206.4	188.4	0.86	0.061	1.00
		HL8 ^[6]	218.1	206.4	221.8	1.02	0.043	1.00
		HH8 ^[6]	218.1	206.4	221.6	1.02	0.063	1.00
		LL11 ^[6]	243.3	230.3	172.9	0.71	0.056	1.00
		LH11 ^[6]	243.3	230.3	210.0	0.86	0.064	1.00
		HL11 ^[6]	243.3	230.3	217.5	0.89	0.041	1.00
		HH11 ^[6]	243.3	230.3	229.5	0.94	0.063	1.00
		LL14 ^[6]	275.3	260.5	197.3	0.72	0.060	1.00
		LH14 ^[6]	275.3	260.5	200.2	0.73	0.064	1.00
HH14 ^[6]	275.3	260.5	232.1	0.84	0.054	1.00		
14	Tsonos et al. (1992)	S1 ^[6]	54.5	54.5	36.2	0.66	0.065	1.25
		S2 ^[6]	45.7	45.7	37.3	0.82	0.030	1.25
		S3 ^[7]	39.0	39.0	42.0	1.08	-	1.25
		S4 ^[7]	41.0	41.0	38.5	0.94	-	1.25
		S5 ^[7]	44.8	44.8	42.7	0.95	-	1.25

^[1] Columns arranged in alphabetical order of notation; notation described in Appendix A; values given in SI units are converted to in.-lb (1 in. = 25.4 mm; 1 psi = 1/145 Mpa; and 1 kip = 4.4484 kN)

^[2] Bar sizes are presented in SI and in.-lb as reported in the original studies

^[3] Analyzed as a doubly reinforced section to calculate the nominal flexural strength M_n ; all other specimens are analyzed as a single reinforced

^[4] Specimens did not contain confining reinforcement parallel to the hooked bars within the joint region

^[5] Specimens had transverse beams on one or both sides of the test beam. These transverse beams meet the dimensional requirements of Sections 18.8.4 and 15.2.8 of ACI 318-19 and Section 4.3 of ACI 352R-02 to be considered effective in increasing the joint shear strength

^[6] Specimens had $d/\ell_{eh} > 1.5$

^[7] Specimens had column to beam flexural strength ratio, M_R , less than 1.2

Table C.4 Cont. Data for exterior beam-column joint specimens tested under reversed cyclic loading^[1]

Study	Specimen	Bar Size ^[2]	A_b (in. ²)	A_{hs} (in. ²)	A_{tr} (in. ²)	A_{th} (in. ²)	$\frac{A_{th}}{A_{hs}}$	A_v (in. ²)	b_b (in.)	
14	Tsonos et al. (1992)	S6 ^[7]	D14	0.24	0.95	0.08	0.16	0.16	0.47	7.9
		S6' ^[6]	D14	0.24	0.95	0.08	0.16	0.16	0.47	7.9
15	Pantelides et al. (2002)	2 ^{[3][4]}	No. 9	1.00	4.00	0.00	0.00	0.00	0.00	12.0
		4 ^{[3][4]}	No. 9	1.00	4.00	0.00	0.00	0.00	0.00	12.0
		5 ^{[3][4]}	No. 9	1.00	4.00	0.00	0.00	0.00	0.00	12.0
		6 ^{[3][4]}	No. 9	1.00	4.00	0.00	0.00	0.00	0.00	12.0
16	Chutarat and Aboutaha (2003)	Specimen I	No. 8	0.79	3.16	0.20	2.40	0.76	3.20	14.0
17	Hwang et al. (2005)	0T0 ^[4]	No. 8	0.79	3.16	0.00	0.00	0.00	0.00	12.6
		3T44	No. 8	0.79	3.16	0.20	2.40	0.76	3.60	12.6
		1B8	No. 8	0.79	3.16	0.79	1.58	0.50	1.58	12.6
		3T3	No. 8	0.79	3.16	0.11	0.66	0.21	0.99	12.6
		2T4	No. 8	0.79	3.16	0.20	0.40	0.13	0.80	12.6
		1T44	No. 8	0.79	3.16	0.20	0.80	0.25	0.80	12.6
		3T4	No. 8	0.79	3.16	0.20	1.20	0.38	1.80	12.6
		2T5	No. 8	0.79	3.16	0.31	0.62	0.20	1.24	12.6
1T55	No. 8	0.79	3.16	0.31	1.24	0.39	1.24	12.6		
18	Tsonos (2007)	A1 ^[6]	D10	0.12	0.49	0.04	0.18	0.36	0.44	7.9
		E1 ^[6]	D14	0.24	0.72	0.04	0.18	0.24	0.44	7.9
		E2 ^[6]	D14	0.24	0.48	0.04	0.18	0.37	0.44	7.9
		G1 ^[6]	D14	0.24	0.72	0.04	0.09	0.12	0.18	7.9
19	Chun et al. (2007)	JC-1	D22	0.60	2.40	0.11	0.22	0.09	0.44	13.8
		JC-2	D22	0.60	4.80	0.11	0.22	0.05	0.44	13.8
		WC ^[4]	D25	0.79	3.95	0.00	0.00	0.00	0.00	31.5
		JC-No. 11-1	D36	1.56	4.68	0.20	2.40	0.51	2.40	17.7
20	Lee and Ko (2007)	S0	D22	0.60	2.40	0.11	0.66	0.28	0.99	12.0
		W0	D22	0.60	2.40	0.11	1.10	0.46	1.65	12.0

^[1] Columns arranged in alphabetical order of notation; notation described in Appendix A; values given in SI units are converted to in.-lb (1 in. = 25.4 mm; 1 psi = 1/145 Mpa; and 1 kip = 4.4484 kN)

^[2] Bar sizes are presented in SI and in.-lb as reported in the original studies

^[3] Analyzed as a doubly reinforced section to calculate the nominal flexural strength M_n ; all other specimens are analyzed as a single reinforced

^[4] Specimens did not contain confining reinforcement parallel to the hooked bars within the joint region

^[5] Specimens had transverse beams on one or both sides of the test beam. These transverse beams meet the dimensional requirements of Sections 18.8.4 and 15.2.8 of ACI 318-19 and Section 4.3 of ACI 352R-02 to be considered effective in increasing the joint shear strength

^[6] Specimens had $d/\ell_{eh} > 1.5$

^[7] Specimens had column to beam flexural strength ratio, M_R , less than 1.2

Table C.4 Cont. Data for exterior beam-column joint specimens tested under reversed cyclic loading^[1]

Study		Specimen	b_c (in.)	b_j (in.)	$b_{j,ACI352}$ (in.)	c_{ch} (in.)	$\frac{c_{ch}}{d_b}$	c_{so} (in.)	$\frac{c_{so}}{d_b}$	d
14	Tsonos et al. (1992)	S6 ^[7]	7.9	7.9	7.9	2.0	3.6	0.7	1.3	10.8
		S6' ^[6]	7.9	7.9	7.9	2.0	3.6	0.7	1.3	10.8
15	Pantelides et al. (2002)	2 ^{[3][4]}	12.0	12.0	12.0	2.4	2.1	1.9	1.7	13.6
		4 ^{[3][4]}	12.0	12.0	12.0	2.4	2.1	1.9	1.7	13.6
		5 ^{[3][4]}	12.0	12.0	12.0	2.4	2.1	1.9	1.7	13.6
		6 ^{[3][4]}	12.0	12.0	12.0	2.4	2.1	1.9	1.7	13.6
16	Chutarat and Aboutaha (2003)	Specimen I	16.0	16.0	15.0	2.8	2.8	3.3	3.3	15.2
17	Hwang et al. (2005)	0T0 ^[4]	16.5	16.5	14.6	2.5	2.5	4.0	4.0	15.1
		3T44	16.5	16.5	14.6	2.5	2.5	4.0	4.0	15.1
		1B8	16.5	16.5	14.6	2.5	2.5	4.0	4.0	15.1
		3T3	16.5	16.5	14.6	2.5	2.5	4.0	4.0	15.1
		2T4	16.5	16.5	14.6	2.5	2.5	4.0	4.0	15.1
		1T44	16.5	16.5	14.6	2.5	2.5	4.0	4.0	15.1
		3T4	17.7	17.7	15.2	2.5	2.5	4.0	4.0	15.1
		2T5	17.7	17.7	15.2	2.5	2.5	4.0	4.0	15.1
18	Tsonos (2007)	A1 ^[6]	7.9	7.9	7.9	1.8	4.7	1.0	2.5	10.6
		E1 ^[6]	7.9	7.9	7.9	2.8	5.0	0.9	1.6	10.6
		E2 ^[6]	7.9	7.9	7.9	5.5	10.0	0.9	1.6	10.6
		G1 ^[6]	7.9	7.9	7.9	2.8	5.0	0.9	1.6	10.6
19	Chun et al. (2007)	JC-1	16.7	16.7	15.3	3.0	3.4	3.4	3.9	17.3
		JC-2	16.7	16.7	15.3	3.0	3.4	3.4	3.9	17.3
		WC ^[4]	31.5	31.5	31.5	6.6	6.6	2.1	2.1	13.1
		JC-No. 11-1	25.6	25.6	21.7	6.1	4.3	6.0	4.3	17.1
20	Lee and Ko (2007)	S0	16.0	16.0	14.0	2.0	2.3	4.6	5.2	16.0
		W0	24.0	24.0	16.0	2.0	2.3	8.6	9.8	16.0

^[1] Columns arranged in alphabetical order of notation; notation described in Appendix A; values given in SI units are converted to in.-lb (1 in. = 25.4 mm; 1 psi = 1/145 Mpa; and 1 kip = 4.4484 kN)

^[2] Bar sizes are presented in SI and in.-lb as reported in the original studies

^[3] Analyzed as a doubly reinforced section to calculate the nominal flexural strength M_n ; all other specimens are analyzed as a single reinforced

^[4] Specimens did not contain confining reinforcement parallel to the hooked bars within the joint region

^[5] Specimens had transverse beams on one or both sides of the test beam. These transverse beams meet the dimensional requirements of Sections 18.8.4 and 15.2.8 of ACI 318-19 and Section 4.3 of ACI 352R-02 to be considered effective in increasing the joint shear strength

^[6] Specimens had $d/\ell_{ch} > 1.5$

^[7] Specimens had column to beam flexural strength ratio, M_R , less than 1.2

Table C.4 Cont. Data for exterior beam-column joint specimens tested under reversed cyclic loading^[1]

Study		Specimen	$\frac{d}{\ell_{eh}}$	d' (in.)	d_b (in.)	f_{cm} ^[8] (psi)	f_{cm} ^[9] (psi)	f_y (ksi)	$f_{ytr,t}$ (ksi)	$f_{ytr,t} A_v$ (kips)
14	Tsonos et al. (1992)	S6 ^[7]	1.67	1.0	0.55	4780	4780	70.3	71.7	33.5
		S6' ^[6]	1.67	1.0	0.55	4200	4200	70.3	71.7	33.5
15	Pantelides et al. (2002)	2 ^{[3][4]}	0.84	2.4	1.128	6700	6700	65.9	0.0	0.0
		4 ^{[3][4]}	0.84	2.4	1.128	5940	5940	65.9	0.0	0.0
		5 ^{[3][4]}	0.84	2.4	1.128	5370	5370	65.9	0.0	0.0
		6 ^{[3][4]}	0.84	2.4	1.128	5820	5820	65.9	0.0	0.0
16	Chutarat and Aboutaha (2003)	Specimen I	1.19	2.8	1	4000	4000	70.0	53.0	169.6
17	Hwang et al. (2005)	0T0 ^[4]	1.11	2.6	1	9760	9760	62.4	0.0	0.0
		3T44	1.11	2.6	1	11140	11140	62.4	72.2	260.0
		1B8	1.11	2.6	1	8960	8960	63.1	63.1	99.7
		3T3	1.11	2.6	1	10010	10010	62.4	68.3	67.6
		2T4	1.11	2.6	1	10300	10300	62.4	72.2	57.8
		1T44	1.11	2.6	1	10560	10560	62.4	72.2	57.8
		3T4	0.98	2.6	1	10910	10910	71.2	63.2	113.8
		2T5	0.98	2.6	1	11110	11110	71.2	68.0	84.3
18	Tsonos (2007)	A1 ^[6]	1.64	1.2	0.39	5080	5080	73.0	78.0	34.2
		E1 ^[6]	1.66	1.2	0.55	3190	3190	72.0	78.0	34.2
		E2 ^[6]	1.66	1.2	0.55	5080	5080	72.0	78.0	34.2
		G1 ^[6]	1.66	1.2	0.55	3190	3190	72.0	78.0	13.7
19	Chun et al. (2007)	JC-1	1.10	2.4	0.875	8950	8950	58.4	55.7	24.5
		JC-2	1.24	2.4	0.875	8720	8720	58.4	55.7	24.5
		WC ^[4]	0.84	2.6	1	8180	8180	62.5	0.0	0.0
		JC-No. 11-1	0.90	2.8	1.41	4760	4760	66.4	72.5	174.0
20	Lee and Ko (2007)	S0	0.76	2.0	0.875	4730	4730	66.0	68.0	67.3
		W0	1.22	2.0	0.875	4190	4190	66.0	68.0	112.2

^[1] Columns arranged in alphabetical order of notation; notation described in Appendix A; values given in SI units are converted to in.-lb (1 in. = 25.4 mm; 1 psi = 1/145 Mpa; and 1 kip = 4.4484 kN)

^[3] Analyzed as a doubly reinforced section to calculate the nominal flexural strength M_n ; all other specimens are analyzed as a single reinforced

^[4] Specimens did not contain confining reinforcement parallel to the hooked bars within the joint region

^[6] Specimens had $d/\ell_{eh} > 1.5$

^[7] Specimens had column to beam flexural strength ratio, M_R , less than 1.2

^[8] Column concrete compressive strength

^[9] Beam concrete compressive strength

Table C.4 Cont. Data for exterior beam-column joint specimens tested under reversed cyclic loading ^[1]

Study		Specimen	h_b (in.)	h_c (in.)	ℓ_{dh} (in.)	$\frac{\ell_{dh}}{d_b}$	ℓ_{eh} (in.)	$\frac{\ell_{eh}}{d_b}$	ℓ_{ehy} (in.)	$\frac{\ell_{ehy}}{d_b}$
14	Tsonos et al. (1992)	S6 ^[7]	11.8	7.9	7.9	14.4	6.5	11.8	7.6	13.7
		S6' ^[6]	11.8	7.9	8.2	14.9	6.5	11.8	7.6	13.9
15	Pantelides et al. (2002)	2 ^{[3][4]}	16.0	18.0	32.4	28.7	16.1	14.3	15.6	13.8
		4 ^{[3][4]}	16.0	18.0	33.4	29.6	16.1	14.3	16.1	14.3
		5 ^{[3][4]}	16.0	18.0	34.2	30.3	16.1	14.3	16.6	14.7
		6 ^{[3][4]}	16.0	18.0	33.5	29.7	16.1	14.3	16.2	14.4
16	Chutarat and Aboutaha (2003)	Specimen I	18.0	16.0	15.3	15.3	12.8	12.8	14.2	14.2
17	Hwang et al. (2005)	0T0 ^[4]	17.7	16.5	17.9	17.9	13.7	13.7	11.5	11.5
		3T44	17.7	16.5	10.7	10.7	13.7	13.7	9.8	9.8
		1B8	17.7	16.5	11.4	11.4	13.7	13.7	10.5	10.5
		3T3	17.7	16.5	11.0	11.0	13.7	13.7	10.0	10.0
		2T4	17.7	16.5	13.4	13.4	13.7	13.7	10.5	10.5
		1T44	17.7	16.5	10.9	10.9	13.7	13.7	9.9	9.9
		3T4	17.7	17.7	12.3	12.3	15.5	15.5	11.3	11.3
		2T5	17.7	17.7	12.4	12.4	15.5	15.5	11.3	11.3
1T55	17.7	17.7	12.5	12.5	15.5	15.5	11.5	11.5		
18	Tsonos (2007)	A1 ^[6]	11.8	7.9	4.3	10.9	6.5	16.5	4.4	11.2
		E1 ^[6]	11.8	7.9	7.7	14.0	6.4	11.6	7.7	13.9
		E2 ^[6]	11.8	7.9	6.5	11.9	6.4	11.6	6.2	11.2
		G1 ^[6]	11.8	7.9	8.7	15.8	6.4	11.6	7.9	14.3
19	Chun et al. (2007)	JC-1	19.7	19.7	10.7	12.2	15.8	18.0	8.2	9.3
		JC-2	19.7	19.7	11.7	13.4	13.9	15.9	8.5	9.7
		WC ^[4]	15.7	23.6	14.8	14.8	15.7	15.7	12.0	12.0
		JC-No. 11-1	19.9	20.5	21.8	15.5	18.9	13.4	17.9	12.7
20	Lee and Ko (2007)	S0	18.0	24.0	11.6	13.2	21.0	24.0	11.0	12.6
		W0	18.0	16.0	11.9	13.6	13.1	15.0	11.4	13.0

^[1] Columns arranged in alphabetical order of notation; notation described in Appendix A; values given in SI units are converted to in.-lb (1 in. = 25.4 mm; 1 psi = 1/145 Mpa; and 1 kip = 4.4484 kN)

^[2] Bar sizes are presented in SI and in.-lb as reported in the original studies

^[3] Analyzed as a doubly reinforced section to calculate the nominal flexural strength M_n ; all other specimens are analyzed as a single reinforced

^[4] Specimens did not contain confining reinforcement parallel to the hooked bars within the joint region

^[5] Specimens had transverse beams on one or both sides of the test beam. These transverse beams meet the dimensional requirements of Sections 18.8.4 and 15.2.8 of ACI 318-19 and Section 4.3 of ACI 352R-02 to be considered effective in increasing the joint shear strength

^[6] Specimens had $d/\ell_{eh} > 1.5$

^[7] Specimens had column to beam flexural strength ratio, M_R , less than 1.2

Table C.4 Cont. Data for exterior beam-column joint specimens tested under reversed cyclic loading^[1]

Study	Specimen	$\frac{\ell_{eh}}{h_c}$	$\frac{\ell_{eh}}{\ell_{dh}}$	$\frac{\ell_{eh}}{\ell_{ehy}}$	M_n (kip.in.)	M_{peak} (kip.in.)	$\frac{M_{peak}}{M_n}$	N	N_{total}	
14	Tsonos et al. (1992)	S6 ^[7]	0.8	0.82	0.86	656	518	0.79	1	3
		S6' ^[6]	0.8	0.79	0.85	646	666	1.03	1	3
15	Pantelides et al. (2002)	2 ^{[3][4]}	0.9	0.50	1.03	2932	3005	1.02	0	0
		4 ^{[3][4]}	0.9	0.48	1.00	2932	3100	1.06	0	0
		5 ^{[3][4]}	0.9	0.47	0.97	2932	3000	1.02	0	0
		6 ^{[3][4]}	0.9	0.48	0.99	2932	2950	1.01	0	0
16	Chutarat and Aboutaha (2003)	Specimen I	0.8	0.83	0.90	2848	3344	1.17	3	4
17	Hwang et al. (2005)	0T0 ^[4]	0.8	0.76	1.18	2794	3229	1.16	0	0
		3T44	0.8	1.27	1.40	2817	3447	1.22	4	6
		1B8	0.8	1.19	1.30	2807	4069	1.45	1	1
		3T3	0.8	1.24	1.36	2798	3666	1.31	2	3
		2T4	0.8	1.02	1.30	2803	3498	1.25	1	2
		1T44	0.8	1.26	1.38	2808	3363	1.20	2	2
		3T4	0.9	1.26	1.37	3185	3599	1.13	2	3
		2T5	0.9	1.25	1.38	3189	3767	1.18	1	2
18	Tsonos (2007)	A1 ^[6]	0.8	1.52	1.47	359	454	1.26	2	5
		E1 ^[6]	0.8	0.83	0.84	486	558	1.15	2	5
		E2 ^[6]	0.8	0.98	1.04	348	438	1.26	2	5
		G1 ^[6]	0.8	0.74	0.82	486	494	1.02	1	2
19	Chun et al. (2007)	JC-1	0.8	1.48	1.93	2328	3195	1.37	1	2
		JC-2	0.7	1.19	1.64	4204	4983	1.19	1	2
		WC ^[4]	0.7	1.06	1.31	4726	5611	1.19	0	0
		JC-No. 11-1	0.9	0.87	1.05	4567	4912	1.08	3	3
20	Lee and Ko (2007)	S0	0.9	1.81	1.90	2275	3075	1.35	2	3
		W0	0.8	1.10	1.15	2241	2857	1.27	2	3

^[1] Columns arranged in alphabetical order of notation; notation described in Appendix A; values given in SI units are converted to in.-lb (1 in. = 25.4 mm; 1 psi = 1/145 Mpa; and 1 kip = 4.4484 kN)

^[2] Bar sizes are presented in SI and in.-lb as reported in the original studies

^[3] Analyzed as a doubly reinforced section to calculate the nominal flexural strength M_n ; all other specimens are analyzed as a single reinforced

^[4] Specimens did not contain confining reinforcement parallel to the hooked bars within the joint region

^[5] Specimens had transverse beams on one or both sides of the test beam. These transverse beams meet the dimensional requirements of Sections 18.8.4 and 15.2.8 of ACI 318-19 and Section 4.3 of ACI 352R-02 to be considered effective in increasing the joint shear strength

^[6] Specimens had $d/\ell_{eh} > 1.5$

^[7] Specimens had column to beam flexural strength ratio, M_R , less than 1.2

Table C.4 Cont. Data for exterior beam-column joint specimens tested under reversed cyclic loading^[1]

Study		Specimen	<i>n</i>	<i>nT'</i> (kips)	<i>Str</i> (in.)	<i>T_h</i> (kips)	<i>T'</i> (kips)	<i>T'</i> _{mod} (kips)	$\frac{T'}{T_h}$	$\frac{T'_{mod}}{T_h}$
14	Tsonos et al. (1992)	S6 ^[7]	4	53.0	2.5	14.8	13.3	-	0.90	-
		S6' ^[6]	4	69.1	2.5	14.3	17.3	-	1.21	-
15	Pantelides et al. (2002)	2 ^{[3][4]}	4	270.2	0.0	65.9	67.5	67.3	1.02	1.02
		4 ^{[3][4]}	4	278.7	0.0	65.9	69.7	-	1.06	-
		5 ^{[3][4]}	4	269.7	0.0	64.0	67.4	-	1.05	-
		6 ^{[3][4]}	4	265.2	0.0	65.5	66.3	-	1.01	-
16	Chutarat and Aboutaha (2003)	Specimen I	4	259.7	3.1	50.1	64.9	-	1.30	-
17	Hwang et al. (2005)	0T0 ^[4]	4	227.8	0.0	49.3	56.9	55.8	1.16	1.13
		3T44	4	241.2	3.8	49.5	60.3	57.8	1.22	1.17
		1B8	4	289.0	6.3	50.1	72.3	70.4	1.44	1.41
		3T3	4	258.2	3.8	49.5	64.5	62.3	1.30	1.26
		2T4	4	245.9	5.7	49.4	61.5	59.6	1.24	1.21
		1T44	4	236.1	6.3	49.5	59.0	56.7	1.19	1.14
		3T4	4	254.2	3.8	56.5	63.6	60.9	1.13	1.08
		2T5	4	265.8	5.7	56.5	66.4	63.8	1.18	1.13
18	Tsonos (2007)	A1 ^[6]	4	45.0	2.0	8.9	11.2	10.7	1.26	1.20
		E1 ^[6]	3	59.2	2.0	14.4	19.7	-	1.37	-
		E2 ^[6]	2	43.3	1.9	17.2	21.7	21.6	1.26	1.25
		G1 ^[6]	3	52.5	3.9	14.0	17.5	-	1.25	-
19	Chun et al. (2007)	JC-1	4	192.5	5.9	35.2	48.1	44.0	1.37	1.25
		JC-2	8	332.5	5.9	35.1	41.6	38.7	1.18	1.10
		WC ^[4]	5	293.1	0.0	49.4	58.6	56.7	1.19	1.15
		JC-No. 11-1	3	334.3	4.7	104.0	111.4	110.7	1.07	1.06
20	Lee and Ko (2007)	S0	4	214.1	3.9	39.8	53.5	49.0	1.35	1.23
		W0	4	202.0	3.9	39.8	50.5	49.7	1.27	1.25

^[1] Columns arranged in alphabetical order of notation; notation described in Appendix A; values given in SI units are converted to in.-lb (1 in. = 25.4 mm; 1 psi = 1/145 Mpa; and 1 kip = 4.4484 kN)

^[2] Bar sizes are presented in SI and in.-lb as reported in the original studies

^[3] Analyzed as a doubly reinforced section to calculate the nominal flexural strength M_n ; all other specimens are analyzed as a single reinforced

^[4] Specimens did not contain confining reinforcement parallel to the hooked bars within the joint region

^[5] Specimens had transverse beams on one or both sides of the test beam. These transverse beams meet the dimensional requirements of Sections 18.8.4 and 15.2.8 of ACI 318-19 and Section 4.3 of ACI 352R-02 to be considered effective in increasing the joint shear strength

^[6] Specimens had $d/\ell_{eh} > 1.5$

^[7] Specimens had column to beam flexural strength ratio, M_R , less than 1.2

Table C.4 Cont. Data for exterior beam-column joint specimens tested under reversed cyclic loading^[1]

Study		Specimen	V_n (kips)	$V_{n,ACI 352}$ (kips)	V_p (kips)	$\frac{V_p}{V_n}$	$\delta_{0.8 peak}$	Ψ_o
14	Tsonos et al. (1992)	S6 ^[7]	51.4	51.4	41.5	0.81	-	1.25
		S6' ^[6]	48.2	48.2	53.4	1.11	0.035	1.25
15	Pantelides et al. (2002)	2 ^{[3][4]}	212.2	212.2	235.1	1.11	0.025	1.25
		4 ^{[3][4]}	199.8	199.8	242.5	1.21	0.018	1.25
		5 ^{[3][4]}	189.9	189.9	234.7	1.24	0.025	1.25
		6 ^{[3][4]}	197.7	197.7	230.8	1.17	0.028	1.25
16	Chutarat and Aboutaha (2003)	Specimen I	194.3	182.1	231.2	1.19	0.074	1.00
17	Hwang et al. (2005)	0T0 ^[4]	324.2	285.6	224.1	0.69	0.060	1.00
		3T44	346.3	305.1	239.4	0.69	0.087	1.00
		1B8	310.6	273.7	282.6	0.91	0.060	1.00
		3T3	328.2	289.2	254.5	0.78	0.100	1.00
		2T4	333.0	293.3	242.8	0.73	0.075	1.00
		1T44	337.1	297.0	233.6	0.69	0.080	1.00
		3T4	393.4	336.5	249.5	0.63	0.070	1.00
		2T5	397.0	339.7	261.2	0.66	0.070	1.00
18	Tsonos (2007)	A1 ^[6]	53.0	53.0	38.9	0.73	0.045	1.25
		E1 ^[6]	42.0	42.0	47.8	1.14	0.060	1.25
		E2 ^[6]	53.0	53.0	37.6	0.71	0.065	1.25
		G1 ^[6]	42.0	42.0	42.3	1.01	0.040	1.25
19	Chun et al. (2007)	JC-1	373.9	340.9	178.3	0.48	0.045	1.00
		JC-2	369.0	336.4	296.7	0.80	0.070	1.00
		WC ^[4]	807.4	807.4	426.7	0.53	0.053	1.25
		JC-No. 11-1	433.6	366.9	265.0	0.61	0.054	1.00
20	Lee and Ko (2007)	S0	316.8	277.2	186.0	0.59	0.065	1.00
		W0	298.3	198.9	175.0	0.59	0.055	1.00

^[1] Columns arranged in alphabetical order of notation; notation described in Appendix A; values given in SI units are converted to in.-lb (1 in. = 25.4 mm; 1 psi = 1/145 Mpa; and 1 kip = 4.4484 kN)

^[2] Bar sizes are presented in SI and in.-lb as reported in the original studies

^[3] Analyzed as a doubly reinforced section to calculate the nominal flexural strength M_n ; all other specimens are analyzed as a single reinforced

^[4] Specimens did not contain confining reinforcement parallel to the hooked bars within the joint region

^[5] Specimens had transverse beams on one or both sides of the test beam. These transverse beams meet the dimensional requirements of Sections 18.8.4 and 15.2.8 of ACI 318-19 and Section 4.3 of ACI 352R-02 to be considered effective in increasing the joint shear strength

^[6] Specimens had $d/\ell_{eh} > 1.5$

^[7] Specimens had column to beam flexural strength ratio, M_R , less than 1.2

Table C.4 Cont. Data for exterior beam-column joint specimens tested under reversed cyclic loading^[1]

Study		Specimen	Bar Size ^[2]	A_b (in. ²)	A_{hs} (in. ²)	A_{tr} (in. ²)	A_{th} (in. ²)	$\frac{A_{th}}{A_{hs}}$	A_v (in. ²)	b_b (in.)
21	Kang et al. (2010)	Jk ^[6]	D19	0.44	1.76	0.11	0.44	0.25	0.88	17.7
22	Hwang et al. (2014)	T1-400	D22	0.60	4.20	0.20	1.60	0.38	2.40	13.8
		T2-600	D22	0.60	2.40	0.20	1.60	0.67	2.40	13.8
		T3-600 ^[3]	D25	0.79	3.16	0.20	1.60	0.51	2.40	13.8
23	Chun and Shin (2014)	H0.7S ^[3]	D19	0.44	1.76	0.20	0.51	0.29	0.60	9.8
		H1.0S ^[3]	D19	0.44	1.76	0.20	1.02	0.58	1.80	9.8
		H1.5S ^[6]	D19	0.44	1.76	0.20	1.02	0.58	3.00	9.8
		H2.0S ^[6]	D19	0.44	1.76	0.20	1.02	0.58	4.20	9.8
		H2.5S ^[6]	D19	0.44	1.76	0.20	1.02	0.58	5.40	9.8
		H0.7U ^[3]	D19	0.44	1.76	0.11	0.33	0.19	0.33	9.8
		H1.0U ^[3]	D19	0.44	1.76	0.11	0.66	0.38	0.99	9.8
24	Choi and Bae (2019)	JTR-0-BTR	D25	0.79	1.58	0.20	1.60	1.01	1.60	9.8
		JNR-0-BTR ^[4]	D25	0.79	1.58	0.00	0.00	0.00	0.00	9.8
		JTR-0-BNR	D25	0.79	1.58	0.20	1.60	1.01	1.60	9.8

^[1] Columns arranged in alphabetical order of notation; notation described in Appendix A; values given in SI units are converted to in.-lb (1 in. = 25.4 mm; 1 psi = 1/145 Mpa; and 1 kip = 4.4484 kN)

^[2] Bar sizes are presented in SI and in.-lb as reported in the original studies

^[3] Analyzed as a doubly reinforced section to calculate the nominal flexural strength M_n ; all other specimens are analyzed as a single reinforced

^[4] Specimens did not contain confining reinforcement parallel to the hooked bars within the joint region

^[5] Specimens had transverse beams on one or both sides of the test beam. These transverse beams meet the dimensional requirements of Sections 18.8.4 and 15.2.8 of ACI 318-19 and Section 4.3 of ACI 352R-02 to be considered effective in increasing the joint shear strength

^[6] Specimens had $d/\ell_{eh} > 1.5$

^[7] Specimens had column to beam flexural strength ratio, M_R , less than 1.2

Table C.4 Cont. Data for exterior beam-column joint specimens tested under reversed cyclic loading^[1]

Study		Specimen	b_c (in.)	b_j (in.)	$b_{j,ACI 352}$ (in.)	c_{ch} (in.)	$\frac{c_{ch}}{d_b}$	c_{so} (in.)	$\frac{c_{so}}{d_b}$	d
21	Kang et al. (2010)	Jk ^[6]	17.7	17.7	17.7	3.9	5.2	2.6	3.5	19.4
22	Hwang et al. (2014)	T1-400	19.7	19.7	16.7	3.3	3.7	4.5	5.1	17.1
		T2-600	19.7	19.7	16.7	3.3	3.7	4.5	5.1	17.7
		T3-600 ^[3]	19.7	19.7	16.7	3.3	3.3	4.5	4.5	17.6
23	Chun and Shin (2014)	H0.7S ^[3]	12.0	12.0	10.9	1.8	2.3	3.0	3.9	5.4
		H1.0S ^[3]	12.0	12.0	10.9	1.8	2.3	3.0	3.9	9.4
		H1.5S ^[6]	12.0	12.0	10.9	1.8	2.3	3.0	3.9	15.3
		H2.0S ^[6]	12.0	12.0	10.9	1.8	2.3	3.0	3.9	21.2
		H2.5S ^[6]	12.0	12.0	10.9	1.8	2.3	3.0	3.9	27.1
		H0.7U ^[3]	12.0	12.0	10.9	1.8	2.3	3.0	3.9	5.4
		H1.0U ^[3]	12.0	12.0	10.9	1.8	2.3	3.0	3.9	9.4
24	Choi and Bae (2019)	JTR-0-BTR	11.8	11.8	10.8	4.6	4.6	3.1	3.1	12.1
		JNR-0-BTR ^[4]	11.8	11.8	10.8	4.6	4.6	3.1	3.1	12.1
		JTR-0-BNR	11.8	11.8	10.8	4.6	4.6	3.1	3.1	12.1

^[1] Columns arranged in alphabetical order of notation; notation described in Appendix A; values given in SI units are converted to in.-lb (1 in. = 25.4 mm; 1 psi = 1/145 Mpa; and 1 kip = 4.4484 kN)

^[2] Bar sizes are presented in SI and in.-lb as reported in the original studies

^[3] Analyzed as a doubly reinforced section to calculate the nominal flexural strength M_n ; all other specimens are analyzed as a single reinforced

^[4] Specimens did not contain confining reinforcement parallel to the hooked bars within the joint region

^[5] Specimens had transverse beams on one or both sides of the test beam. These transverse beams meet the dimensional requirements of Sections 18.8.4 and 15.2.8 of ACI 318-19 and Section 4.3 of ACI 352R-02 to be considered effective in increasing the joint shear strength

^[6] Specimens had $d/\ell_{ch} > 1.5$

^[7] Specimens had column to beam flexural strength ratio, M_R , less than 1.2

Table C.4 Cont. Data for exterior beam-column joint specimens tested under reversed cyclic loading^[1]

Study	Specimen	$\frac{d}{\ell_{eh}}$	d' (in.)	d_b (in.)	f_{cm} ^[8] (psi)	f_{cm} ^[9] (psi)	f_y (ksi)	$f_{ytr,l}$ (ksi)	$f_{ytr,l} A_v$ (kips)	
21	Kang et al. (2010)	Jk ^[6]	1.73	1.8	0.75	4200	4200	67.0	83.0	73.0
22	Hwang et al. (2014)	T1-400	0.87	2.6	0.875	4640	4640	75.4	64.7	155.2
		T2-600	0.90	2.0	0.875	4640	4640	103.0	64.7	155.2
		T3-600 ^[3]	0.90	2.1	1	4290	4290	92.1	64.7	155.2
23	Chun and Shin (2014)	H0.7S ^[3]	0.60	2.5	0.75	5050	3710	70.8	66.7	40.0
		H1.0S ^[3]	1.04	2.4	0.75	5050	3710	70.8	66.7	120.1
		H1.5S ^[6]	1.70	2.4	0.75	5050	3710	70.8	66.7	200.1
		H2.0S ^[6]	2.35	2.4	0.75	6990	3830	70.8	66.7	280.1
		H2.5S ^[6]	3.01	2.4	0.75	6990	3830	70.8	66.7	360.2
		H0.7U ^[3]	0.60	2.5	0.75	5050	3710	70.8	62.4	20.6
		H1.0U ^[3]	1.04	2.4	0.75	5050	3710	70.8	62.4	61.8
24	Choi and Bae (2019)	JTR-0-BTR	1.45	2.6	1	7950	7950	68.4	58.0	92.8
		JNR-0-BTR ^[4]	1.45	2.6	1	7950	7950	68.4	0.0	0.0
		JTR-0-BNR	1.45	2.6	1	7950	7950	68.4	58.0	92.8

^[1] Columns arranged in alphabetical order of notation; notation described in Appendix A; values given in SI units are converted to in.-lb (1 in. = 25.4 mm; 1 psi = 1/145 Mpa; and 1 kip = 4.4484 kN)

^[3] Analyzed as a doubly reinforced section to calculate the nominal flexural strength M_n ; all other specimens are analyzed as a single reinforced

^[4] Specimens did not contain confining reinforcement parallel to the hooked bars within the joint region

^[6] Specimens had $d/\ell_{eh} > 1.5$

^[7] Specimens had column to beam flexural strength ratio, M_R , less than 1.2

^[8] Column concrete compressive strength

^[9] Beam concrete compressive strength

Table C.4 Cont. Data for exterior beam-column joint specimens tested under reversed cyclic loading^[1]

Study		Specimen	h_b (in.)	h_c (in.)	ℓ_{dh} (in.)	$\frac{\ell_{dh}}{d_b}$	ℓ_{eh} (in.)	$\frac{\ell_{eh}}{d_b}$	ℓ_{ehy} (in.)	$\frac{\ell_{ehy}}{d_b}$
21	Kang et al. (2010)	Jk ^[6]	21.3	17.7	8.4	11.2	11.3	15.0	7.8	10.5
22	Hwang et al. (2014)	T1-400	19.7	21.7	12.5	14.3	19.6	22.4	11.6	13.3
		T2-600	19.7	21.7	17.1	19.5	19.6	22.4	15.9	18.2
		T3-600 ^[3]	19.7	21.7	19.4	19.4	19.6	19.6	18.0	18.0
23	Chun and Shin (2014)	H0.7S ^[3]	7.9	12.0	9.7	12.9	9.0	12.0	9.4	12.6
		H1.0S ^[3]	11.8	12.0	9.7	12.9	9.0	12.0	9.4	12.6
		H1.5S ^[6]	17.7	12.0	9.7	12.9	9.0	12.0	9.4	12.6
		H2.0S ^[6]	23.6	12.0	8.9	11.9	9.0	12.0	8.6	11.5
		H2.5S ^[6]	29.5	12.0	8.9	11.9	9.0	12.0	8.6	11.5
		H0.7U ^[3]	7.9	12.0	10.1	13.4	9.0	12.0	9.5	12.7
		H1.0U ^[3]	11.8	12.0	9.7	12.9	9.0	12.0	9.4	12.6
24	Choi and Bae (2019)	JTR-0-BTR	14.8	11.8	11.6	11.6	8.3	8.3	10.3	10.3
		JNR-0-BTR ^[4]	14.8	11.8	16.2	16.2	8.3	8.3	12.6	12.6
		JTR-0-BNR	14.8	11.8	11.6	11.6	8.3	8.3	10.3	10.3

^[1] Columns arranged in alphabetical order of notation; notation described in Appendix A; values given in SI units are converted to in.-lb (1 in. = 25.4 mm; 1 psi = 1/145 Mpa; and 1 kip = 4.4484 kN)

^[2] Bar sizes are presented in SI and in.-lb as reported in the original studies

^[3] Analyzed as a doubly reinforced section to calculate the nominal flexural strength M_n ; all other specimens are analyzed as a single reinforced

^[4] Specimens did not contain confining reinforcement parallel to the hooked bars within the joint region

^[5] Specimens had transverse beams on one or both sides of the test beam. These transverse beams meet the dimensional requirements of Sections 18.8.4 and 15.2.8 of ACI 318-19 and Section 4.3 of ACI 352R-02 to be considered effective in increasing the joint shear strength

^[6] Specimens had $d/\ell_{eh} > 1.5$

^[7] Specimens had column to beam flexural strength ratio, M_R , less than 1.2

Table C.4 Cont. Data for exterior beam-column joint specimens tested under reversed cyclic loading^[1]

Study		Specimen	$\frac{\ell_{eh}}{h_c}$	$\frac{\ell_{eh}}{\ell_{dh}}$	$\frac{\ell_{eh}}{\ell_{ehy}}$	M_n (kip.in.)	M_{peak} (kip.in.)	$\frac{M_{peak}}{M_n}$	N	N_{total}
21	Kang et al. (2010)	Jk ^[6]	0.6	1.33	1.43	2177	2721	1.25	2	4
22	Hwang et al. (2014)	T1-400	0.9	1.57	1.69	3878	4658	1.20	2	3
		T2-600	0.9	1.15	1.23	3807	4844	1.27	2	3
		T3-600 ^[3]	0.9	1.01	1.09	4282	5403	1.26	2	3
23	Chun and Shin (2014)	H0.7S ^[3]	0.8	0.93	0.95	492	612	1.24	1	1
		H1.0S ^[3]	0.8	0.93	0.95	984	1080	1.10	2	3
		H1.5S ^[6]	0.8	0.93	0.95	1728	1752	1.01	2	5
		H2.0S ^[6]	0.8	1.01	1.04	2484	2760	1.11	2	7
		H2.5S ^[6]	0.8	1.01	1.04	3216	3252	1.01	2	9
		H0.7U ^[3]	0.8	0.89	0.95	492	576	1.17	1	1
		H1.0U ^[3]	0.8	0.93	0.95	984	1020	1.04	2	3
24	Choi and Bae (2019)	JTR-0-BTR	0.7	0.72	0.81	1221	1275	1.04	4	4
		JNR-0-BTR ^[4]	0.7	0.52	0.66	1221	1080	0.88	0	0
		JTR-0-BNR	0.7	0.72	0.81	1221	1221	1.00	4	4

^[1] Columns arranged in alphabetical order of notation; notation described in Appendix A; values given in SI units are converted to in.-lb (1 in. = 25.4 mm; 1 psi = 1/145 Mpa; and 1 kip = 4.4484 kN)

^[2] Bar sizes are presented in SI and in.-lb as reported in the original studies

^[3] Analyzed as a doubly reinforced section to calculate the nominal flexural strength M_n ; all other specimens are analyzed as a single reinforced

^[4] Specimens did not contain confining reinforcement parallel to the hooked bars within the joint region

^[5] Specimens had transverse beams on one or both sides of the test beam. These transverse beams meet the dimensional requirements of Sections 18.8.4 and 15.2.8 of ACI 318-19 and Section 4.3 of ACI 352R-02 to be considered effective in increasing the joint shear strength

^[6] Specimens had $d/\ell_{eh} > 1.5$

^[7] Specimens had column to beam flexural strength ratio, M_R , less than 1.2

Table C.4 Cont. Data for exterior beam-column joint specimens tested under reversed cyclic loading^[1]

Study		Specimen	<i>n</i>	<i>nT'</i> (kips)	<i>s_{tr}</i> (in.)	<i>T_h</i> (kips)	<i>T'</i> (kips)	<i>T'</i> _{mod} (kips)	$\frac{T'}{T_h}$	$\frac{T'_{mod}}{T_h}$
21	Kang et al. (2010)	Jk ^[6]	4	147.4	4.7	29.6	36.9	35.2	1.24	1.19
22	Hwang et al. (2014)	T1-400	7	380.4	3.9	45.4	54.3	50.4	1.20	1.11
		T2-600	4	314.4	3.9	62.0	78.6	76.8	1.27	1.24
		T3-600 ^[3]	4	367.1	3.9	73.0	91.8	91.0	1.26	1.25
23	Chun and Shin (2014)	H0.7S ^[3]	4	155.0	3.0	29.8	38.8	-	1.30	-
		H1.0S ^[3]	4	136.8	3.0	29.8	34.2	-	1.15	-
		H1.5S ^[6]	4	126.3	3.0	29.8	31.6	-	1.06	-
		H2.0S ^[6]	4	138.5	3.0	31.3	34.6	34.5	1.11	1.10
		H2.5S ^[6]	4	126.0	3.0	31.3	31.5	31.3	1.01	1.00
		H0.7U ^[3]	4	145.9	3.0	29.6	36.5	-	1.23	-
		H1.0U ^[3]	4	129.2	3.0	29.8	32.3	-	1.08	-
24	Choi and Bae (2019)	JTR-0-BTR	2	112.8	2.4	44.8	56.4	-	1.26	-
		JNR-0-BTR ^[4]	2	95.5	0.0	34.7	47.8	-	1.38	-
		JTR-0-BNR	2	108.1	2.4	44.8	54.0	-	1.21	-

^[1] Columns arranged in alphabetical order of notation; notation described in Appendix A; values given in SI units are converted to in.-lb (1 in. = 25.4 mm; 1 psi = 1/145 Mpa; and 1 kip = 4.4484 kN)

^[2] Bar sizes are presented in SI and in.-lb as reported in the original studies

^[3] Analyzed as a doubly reinforced section to calculate the nominal flexural strength M_n ; all other specimens are analyzed as a single reinforced

^[4] Specimens did not contain confining reinforcement parallel to the hooked bars within the joint region

^[5] Specimens had transverse beams on one or both sides of the test beam. These transverse beams meet the dimensional requirements of Sections 18.8.4 and 15.2.8 of ACI 318-19 and Section 4.3 of ACI 352R-02 to be considered effective in increasing the joint shear strength

^[6] Specimens had $d/\ell_{eh} > 1.5$

^[7] Specimens had column to beam flexural strength ratio, M_R , less than 1.2

Table C.4 Cont. Data for exterior beam-column joint specimens tested under reversed cyclic loading^[1]

Study		Specimen	V_n (kips)	$V_{n,ACI 352}$ (kips)	V_p (kips)	$\frac{V_p}{V_n}$	$\delta_{0.8 peak}$	Ψ_o
21	Kang et al. (2010)	Jk ^[6]	244.1	244.1	134.0	0.55	0.035	1.00
22	Hwang et al. (2014)	T1-400	348.4	296.2	271.8	0.78	0.032	1.00
		T2-600	348.4	296.2	262.9	0.75	0.038	1.00
		T3-600 ^[3]	335.1	284.8	277.8	0.83	0.048	1.00
23	Chun and Shin (2014)	H0.7S ^[3]	122.8	111.5	145.0	1.18	0.100	1.00
		H1.0S ^[3]	122.8	111.5	127.0	1.03	0.070	1.00
		H1.5S ^[6]	122.8	111.5	112.0	0.91	0.050	1.00
		H2.0S ^[6]	144.5	131.2	118.0	0.82	0.070	1.00
		H2.5S ^[6]	144.5	131.2	102.0	0.71	0.050	1.00
		H0.7U ^[3]	122.8	111.5	137.0	1.12	0.100	1.00
		H1.0U ^[3]	122.8	111.5	119.0	0.97	0.070	1.00
24	Choi and Bae (2019)	JTR-0-BTR	149.2	136.8	104.2	0.70	0.044	1.00
		JNR-0-BTR ^[4]	149.2	136.8	87.8	0.59	0.019	1.00
		JTR-0-BNR	149.2	136.8	99.7	0.67	0.047	1.00

^[1] Columns arranged in alphabetical order of notation; notation described in Appendix A; values given in SI units are converted to in.-lb (1 in. = 25.4 mm; 1 psi = 1/145 Mpa; and 1 kip = 4.4484 kN)

^[2] Bar sizes are presented in SI and in.-lb as reported in the original studies

^[3] Analyzed as a doubly reinforced section to calculate the nominal flexural strength M_n ; all other specimens are analyzed as a single reinforced

^[4] Specimens did not contain confining reinforcement parallel to the hooked bars within the joint region

^[5] Specimens had transverse beams on one or both sides of the test beam. These transverse beams meet the dimensional requirements of Sections 18.8.4 and 15.2.8 of ACI 318-19 and Section 4.3 of ACI 352R-02 to be considered effective in increasing the joint shear strength

^[6] Specimens had $d/\ell_{ch} > 1.5$

^[7] Specimens had column to beam flexural strength ratio, M_R , less than 1.2

APPENDIX D: SUMMARY OF STUDIES ON BEAM-COLUMN JOINT SPECIMENS TESTED UNDER REVERSED CYCLIC LOADING

This study includes an analysis of the results of 146 exterior beam-column joint specimens containing hooked bars tested under reversed cyclic loading by Hanson and Connor (1967), Hanson (1971), Megget (1974), Uzumeri (1977), Lee et al. (1977), Scribner (1978), Paulay and Scarpas (1981), Ehsani and Wight (1982), Kanada et al. (1984), Zerbe and Durrani (1985), Ehsani et al. (1987), Ehsani and Alameddine (1991), Kaku and Asakusa (1991), Tsonos et al. (1992), Pantelides et al. (2002), Chutarat and Aboutaha (2003), Hwang et al. (2005), Lee and Ko (2007), Chun et al. (2007), Tsonos (2007), Kang et al. (2010), Chun and Shin (2014), Hwang et al. (2014), and Choi and Bae (2019). The specimens contained hooked bars ranging in size from No. 3 to No. 9, with peak bar stresses ranging from 42,900 to 103,000 psi, and concretes with compressive strengths ranging from 3,140 to 13,700 psi. A detailed summary of these studies is presented in this appendix.

Hanson and Connor (1967)

Hanson and Connor (1967) tested seven exterior beam-column joint specimens to determine the required joint reinforcement to maintain ultimate capacity for cast-in-place beams and columns subjected to reversed cyclic loading. The principle variables were column size, column load, and the amount of confining reinforcement in the joint. Four and two No. 9 hooked bars were used as top and bottom beam longitudinal reinforcement, respectively, anchored in the column. Concrete compressive strength and the yield strength of hooked bars ranged from 3,200 to 5,420 psi and from 47,800 to 51,600 psi, respectively. The center-to-center spacing between the hooked bars was $2.3d_b$ (2.6 in.), and the clear side concrete cover to the bar was $2.7d_b$ (3.0 in.). The embedment length of the hooked bars was $12d_b$ (13.5 in.). Hanson and Connor found that confining reinforcement (hoops) is required for exterior beam-column joints. In addition, they concluded that hoops are not required for exterior joints that are confined on at least three sides by beams or spandrels of approximately equal depth and meet the ACI 318 requirements for the concrete strength required to transfer the column load through the joint. Hanson and Connor found that properly designed and detailed exterior beam-column joints can resist moderate earthquakes without losing strength.

Hanson (1971)

Hanson (1971) tested five beam-column joint specimens to investigate the behavior of Grade 60 No. 8 hooked reinforcement anchored in beam-column joint specimens subjected to reversed cyclic loading. The five beam-column joints represented assemblies from different locations in a frame made up of 12 in. \times 20 in. beams and 15 in. \times 15 in. columns. Concrete compressive strengths ranged from 5200 to 5500 psi, and the yield strength of the hooked bars ranged from 63,100 to 65,000 psi. The center-to-center spacing between the hooked bars was $2.7d_b$ (2.7 in.), and the clear side concrete cover to the bar was $3.0d_b$ (3.0 in.). The embedment length of the hooked bars was $13.5d_b$ (13.5 in.). A constant axial load of 640 kips, $\frac{1}{3}$ of the column capacity, was applied on all specimens except specimen 5; a constant load of 320 kips, $\frac{1}{6}$ the column capacity, was used on specimen 5. Hanson found that the presence of confining reinforcement in the joint region improves the anchorage strength of hooked bars and controls the joint shear distortion and cracking. Hanson concluded that Grade 60 hooked reinforcing bars are suitable for use in structures designed to develop ductile behavior.

Megget (1974)

Megget (1974) tested two exterior beam-column joint specimens to investigate the effect of the presence of transverse beam stubs on the behavior of the external beam-column joints. The two specimens were identical, except one had transverse beam stubs on both sides of the main test beam, and the other did not. Concrete compressive strength and the yield strength of hooked bars were 3,200 psi and 54,700 psi, respectively. The center-to-center spacing between the No. 8 hooked bars was $2.7d_b$ (2.7 in.), and the clear side concrete cover to the hooked bar was $3.3d_b$ (3.3 in.). The embedment length of the hooked bars was $12.6d_b$ (12.6 in.). Six No. 4 hoops were used as confining reinforcement within the joint region. A constant axial load of 44 kips was applied to the specimens throughout the test. Megget found that the presence of transverse beam stubs significantly contributes to the confinement of the joint core concrete and causes a plastic hinge to form in the main beam rather than in the beam-column joint region.

Uzumeri (1977)

Uzumeri (1977) tested eight exterior beam-column joint specimens to investigate the effects of the amount of confining reinforcement and the presence of transverse beam stub on the

behavior of beam-column joints subjected to reversed cyclic loading. The transverse beam stub was located only on one side of the column in four specimens, whereas the other four had no transverse beam stub. Three of the eight specimens had no confining reinforcement, and the remaining five included confining reinforcement ranging from four to eight No. 3 or No. 4 hoops in the joint region. A constant axial load of 520 kips was applied to the column throughout the test. Concrete compressive strength and the yield strength of the No. 9 hooked bars ranged from 3,820 to 5,250 psi and 50,300 to 51,100 psi, respectively. The center-to-center spacing between the hooked bars ranged from 2.9 to $4.4d_b$ (3.3 to 4.9 in.), and the clear side concrete cover to the hooked bar ranged from 1.8 to $3.1d_b$ (2.0 to 3.5 in.). The embedment length of the hooked bars was $11.5d_b$ (13.0 in.). Uzumeri found that the presence of confining reinforcement in beam-column joints increased the anchorage strength and ductility of the beam-column joints subjected to reversed cyclic loading. Uzumeri observed that, within the limitations of the tests, the presence of the transverse beam stub on one side of the beam-column joints showed no significant effect on the behavior of beam-column joint specimens tested under reversed cyclic loading.

Lee et al. (1977)

Lee et al. (1977) tested eight exterior beam-column joint specimens with two design procedures and loading conditions to investigate the behavior of exterior beam-column joints subjected to reversed cyclic loading. The beam-column joints were designed using two criteria: the first is referred to as Type 1 design using the ACI 318-71 for non-seismic conditions, and the second design is referred to as Type 2 design using the ACI 318-71 and the ACI 352 Recommendations for Seismic Conditions. The amount of transverse reinforcement in the specimens was the main difference between the two designs. Three of the eight specimens were designed in accordance with the Type 1 design procedure and the remaining five were designed following the Type 2 design procedure. The main parameters were the amount of confining reinforcement within the joint region, the magnitude of axial load on the column, and the severity of loading. Two displacement patterns (9 and 12 cycles) were used to obtain different degrees of damage during testing. The displacement patterns were meant to simulate the type of displacements the beam-column joints may be subjected to during moderate and severe earthquakes. Of the eight specimens, two were subjected to the displacement pattern representing

a moderate earthquake loading, and the remaining six were subjected to the displacement pattern representing a severe earthquake loading. Four specimens had a constant axial load of 40 kips applied to the column throughout the test, while the others had zero axial loads. Specimens contained No. 2 or No. 3 bars (hoops) spaced at 3 or 1.25 in., respectively, as confining reinforcement within the joint region. Beam and column cross-section dimensions for all specimens were 8×10 in. and 8×11 in., respectively. Concrete compressive strengths ranged from 3,600 to 4,200 psi. The No. 6 hooked bars with a yield strength ranging from 47,500 to 52,500 psi were used as longitudinal beam reinforcing bars. The center-to-center spacing between the hooked bars was $3.3d_b$ (2.5 in.), and the clear side concrete cover to the hooked bar was $3.2d_b$ (2.4 in.). The embedment length of the hooked bars was $12.5d_b$ (9.4 in.). Lee et al. found that the joints for specimens with axial loads of 40 kips were stiffer than those without axial loads. They observed that Type 2 design specimens performed better during testing and had less load degradation than Type 1 design specimens. Lee et al. concluded that the additional transverse reinforcement in Type 2 designed specimens provided better confinement for the beam core, resulting in less strength degradation and more energy dissipation during the test.

Scribner (1978)

Scribner (1978) tested 12 exterior beam-column joint specimens to evaluate the effect of intermediate longitudinal reinforcement in preventing shear strength and stiffness deterioration in beam-column joints subjected to reversed cyclic loading. The main variables were the presence of intermediate longitudinal bars in half of the specimens and the amount of confining reinforcement within the joint region. Intermediate longitudinal bars consisted of four No. 2, No. 3, or No. 4 bars placed in two layers at approximately the third points between tension and compression reinforcement of the beam. The 12 specimens were divided into two groups. Group 1 consisted of eight specimens tested using No. 6 hooked bars as beam longitudinal reinforcement. The column cross-section dimensions for all specimens in group 1 were 8×12 in., whereas the beam cross-section dimensions were a width of 8 in. and a height of 10 or 12 in. Group 2 consisted of four specimens tested with No. 8 hooked bars as beam longitudinal reinforcement. The dimensions of the beam and the column cross-section for all specimens in group 2 were 10×14 in. and 12×18 in., respectively. Constant axial loads of 40 and 100 kips were applied to the columns in groups 1

and 2, respectively, throughout the test. Confining reinforcement of No. 3 and No. 4 bars were used in the joint region in groups 1 and 2, respectively. Concrete compressive strengths ranged from 3,680 to 5,210 psi, and the yield strength of hooked bars ranged from 48,900 to 60,200 psi. The center-to-center spacing between the hooked bars ranged from 2.1 to $6.9d_b$ (2.1 to 5.2 in.), and the clear side concrete cover to the hooked bar ranged from 1.4 to $2.4d_b$ (1.0 to 2.4 in.). The embedment length of the hooked bars ranged from 14.0 to $16.6d_b$ (10.5 to 16.6 in.). Scribner found that the presence of the intermediate longitudinal reinforcement increased the energy dissipation capacity of the exterior beam-column joints and prevented significant strength and stiffness decay during reversed cyclic loading. Scribner also observed that the presence of the intermediate longitudinal reinforcement and confining reinforcement limited shear strength decay.

Paulay and Scarpas (1981)

Paulay and Scarpas (1981) tested three exterior beam-column joint specimens to study the effect of confining reinforcement in the joint region and the presence of intermediate column bars on the anchorage strength and behavior of the exterior beam-column joints subjected to reversed cyclic loading. The intermediate column bars were placed on the sides of the beam longitudinal hooked bars used as vertical joint shear reinforcement. A constant axial load of $0.05 f'_c A_g$ was applied to specimens 1 and 3 throughout the test, while specimen 2 was subjected to a load of $0.15 f'_c A_g$, where f'_c is the design concrete compressive strength and A_g is the cross-section area of the column. Specimen 1 had confining reinforcement in accordance with the New Zealand code requirements, whereas specimens 2 and 3 had 50% of the amount of confining reinforcement recommended in New Zealand. Measured concrete compressive strengths ranged from 3,260 to 3,900 psi, and the yield strength of the No. 6 (D20) hooked bars was 42,900 psi. The center-to-center spacing between the hooked bars was $4.4d_b$ (3.5 in.), and the clear side concrete cover to the hooked bar was $4.3d_b$ (3.4 in.). The embedment length of the hooked bars was $21.1d_b$ (16.7 in.). Paulay and Scarpas found that specimens with approximately 50% of the recommended confining reinforcement performed satisfactorily. As a result, they concluded that the confining reinforcement required to carry the joint design shear force in exterior beam-column joints could be considerably decreased.

Ehsani and Wight (1982)

Ehsani and Wight (1982) tested 12 exterior beam-column joint specimens to study the effect of confining reinforcement within the joint region and the presence of transverse beams and slab on the anchorage strength and behavior of exterior beam-column joints subjected to reversed cyclic loading. The main parameters were the flexural strength ratio (the flexural capacity of the columns to that of the beams), ranging from 1.1 to 2.0, percentage of the confining reinforcement within the joint region, ranging from 0.86% to 1.86%, and joint shear stress, either $10\sqrt{f'_c}$ or $14\sqrt{f'_c}$, where f'_c is the design concrete compressive strength (4000 psi). Six of the 12 specimens had transverse beams and a slab, while the others did not. Measured concrete compressive strengths ranged from 3,470 to 6,470 psi, and the yield strength of the No. 7 hooked bars was 48,000 psi. A constant axial load of 80 kips was applied to the specimens throughout the test. Ehsani and Wight concluded that the flexural strength ratio for exterior beam-column joints without and with transverse beams and a slab should be greater than 1.4 and 1.2, respectively, to ensure that plastic flexural hinges form in beams rather than columns. They discovered that to delay the rapid deterioration of joint concrete, the joint shear stress should be less than or equal $12\sqrt{f'_c}$. Ehsani and Wight observed that the larger percentage of confining reinforcement within the joint region improved the behavior of the exterior beam-column joints.

Kanada et al. (1984)

Kanada et al. (1984) tested 16 exterior beam-column joint specimens under reversed cyclic loading to investigate the relationship between the anchorage capacity and the joint shear strength. Of the 16 specimens, 13 had No. 6 bars with 90° standard hooks, and three had No. 6 bars with heads as beam longitudinal reinforcement. The primary variables examined were the anchorage of beam bars to the column, amount of confining reinforcement within the joint region, and percentage of beam bars. No axial load was applied to the specimens. Concrete compressive strengths ranged from 3,140 to 4,370 psi, and the yield strength of hooked bars was 56,200 psi. The center-to-center spacing between the hooked bars ranged from $2.8d_b$ (2.1 to 6.3 in.), and the clear side concrete cover to the hooked bar was $3.2d_b$ (2.4 in.). The embedment length of the hooked bars ranged from 8 to $12d_b$ (6 to 9 in.). Kanada et al. observed that it was more accurate to take the effective joint depth equal to the projected development length of hooked beam bars to

calculate the joint shear. Kanada et al. concluded that the main function of the confining reinforcement in the joint region is to delay the deterioration of the joint core concrete and to strengthen the inclined compression strut under large reversed cyclic loading.

Zerbe and Durrani (1985)

Zerbe and Durrani (1985) tested seven exterior beam-column joint specimens to investigate the effect of transverse beams, with and without a slab, on the performance of exterior beam-column joints subjected to reversed cyclic loading. Three of the seven specimens did not have a slab and acted as reference specimens, and the remaining four contained slabs with different widths. Concrete compressive strengths ranged from 5,610 to 5,940 psi, and the yield strength of the No. 6 hooked bars was 60,000 psi. The center-to-center spacing between the hooked bars was $2.3d_b$ (1.75 in.), and the clear side concrete cover to the hooked bar was $4d_b$ (3 in.). The embedment length of the hooked bars was $10.3d_b$ (7.8 in.). Zerbe and Durrani concluded that the contribution of a slab must be considered in the flexural strength of beams to avoid the possible formation of plastic hinges in columns instead of in beams in exterior beam-column joints. They suggested that the lateral confinement, which is primarily provided by the transverse beams, is responsible for the increased strength and stiffness of joints with transverse beams. They recommended that the beam longitudinal reinforcement be terminated in a stub outside the joint core to avoid steel congestion in the exterior joint.

Ehsani et al. (1987)

Ehsani et al. (1987) examined five exterior beam-column joint specimens to investigate the effect of different shear stress levels on beam-column joints constructed with high-strength concrete and compared the results with a similar specimen constructed with normal-strength concrete. The main variable was joint shear stress, which ranged between $7.52\sqrt{f'_c}$ and $12.84\sqrt{f'_c}$, where f'_c is the measured concrete compressive strength (psi). A constant axial load ranging from 30 to 86 kips was applied to the columns. Concrete compressive strengths ranged from 6,470 to 9,760 psi, and the yield strength of the No. 6 and No. 7 hooked bars ranged from 48,000 to 70,000 psi. The center-to-center spacing between the hooked bars ranged from 3.5 to $5.2d_b$ (3.1 to 3.9 in.), and the clear side concrete cover to the hooked bar ranged from 2.7 to $3.2d_b$ (2.3 to 2.4 in.). The embedment length of the hooked bars ranged from 9.8 to $14.4d_b$ (8.6 to 10.8 in.). Ehsani

et al. suggested that the maximum permitted joint shear stress should be a function of the concrete compressive strength but provided no specifics. They also indicated that the shear stress factors provided by ACI 352R-85 should be modified before they can be safely applied to beam-column joints designed with high-strength concrete, but again provided no specifics. Ehsani et al. found that even in the presence of high flexural strength ratios, high joint shear stresses significantly reduce the energy-absorption capability of beam-column joints. Ehsani et al. also observed that specimens with lower joint shear stresses could withstand more cycles of loading, which ultimately resulted in more severe damage to the concrete, exposing the bars that then buckled.

Ehsani and Alameddine (1991)

Ehsani and Alameddine (1991) tested 12 exterior beam-column joint specimens to investigate the effects of joint shear stress and confining reinforcement within the joint region on the behavior of high-strength reinforced concrete beam-column joints subjected to reversed cyclic loading. The main variables were concrete compressive strength, ranging from 8,600 to 13,700 psi, joint shear stress, 1100 or 1400 psi, and the amount of confining reinforcement within the joint region, 4 or 6 No. 4 hoops. A constant axial load was applied to the columns ranging from 50 to 136 kips. The yield strength of the No. 8 and No. 9 hooked bars ranged from 64,200 to 66,300 psi. The center-to-center spacing between the hooked bars ranged from 1.92 to $2.17d_b$ (2.17 in.), and the clear side concrete cover to the hooked bar was 3 in., and the embedment length of the hooked bars was 10.5 in. Ehsani and Alameddine concluded that the joint shear stress and the confining reinforcement within the joint region are the key factors in achieving adequate strength and ductility of the joint. In addition, they observed that a column to beam flexural strength ratio of at least 1.4 is essential in helping formation of a plastic hinge in the beam rather than the column. Ehsani and Alameddine found that the deterioration of the joint concrete was delayed significantly and the cyclic load carrying capacity of the specimens was more stable throughout the test in beam-column joint specimens subjected low joint shear stress, on the order of $12\sqrt{8000}$ (≈ 1100 psi). They observed that increasing the confining reinforcement in the joint region provides additional confinement for the joint concrete and delays joint deterioration. Ehsani and Alameddine observed that by increasing the confining reinforcement and decreasing the joint shear stress, slippage or pullout of the hooked bars was reduced or delayed.

Kaku and Asakusa (1991)

Kaku and Asakusa (1991) tested 18 reinforced concrete exterior beam-column joint specimens under reversed cyclic loading. The specimens were designed so that either the beam or the column bars yielded prior to joint shear failure. The main variables were column axial load, amount of confining reinforcement within the joint region, and the presence of intermediate column bars. Concrete compressive strengths ranged from 4,510 to 6,730 psi, and the yield strength of the No. 4 hooked bars was 56,700 psi. The center-to-center spacing between the hooked bars was $3.3d_b$ (1.7 in.), and the clear side concrete cover to the hooked bar was $3.2d_b$ (1.6 in.). The embedment length of the hooked bars was $15.4d_b$ (7.7 in.). A constant axial load was applied to the columns ranging from 0 to 81 kips. Kaku and Asakusa found that the ductility of the exterior beam-column joints increased as the column axial load and the amount of confining reinforcement within the joint region increased. They also observed that the presence of intermediate column bars increased the ductility of the specimens.

Tsonos et al. (1992)

Tsonos et al. (1992) tested 20 exterior beam-column joint specimens to investigate the behavior of external beam-column joints constructed with inclined column longitudinal reinforcing bars within the joint and tested under reversed cyclic loading. Figure D.1 shows schematic drawings of exterior beam-column joints with conventional and nonconventional column longitudinal reinforcing bars. The main variables were the number of inclined reinforcing bars, the ratio of the column-to-beam flexural strength, and the joint shear stress. The 20 specimens tested in eight series. In six series, the first specimen in each series was constructed with conventional column longitudinal reinforcement, while the second specimen was constructed with four crossed, inclined bars bent diagonally across the joint core, as shown in Figure D.1. Another series had two specimens constructed with conventional column longitudinal reinforcement and one specimen constructed with four crossed, inclined bars bent diagonally across the joint core. The last series had five specimens constructed with conventional column longitudinal reinforcement, two of which were cast with fiber-reinforced concrete containing 1.0 percent by volume of steel fibers. Concrete compressive strengths ranged from 3,770 to 5,360 psi, and the yield strength of the No. 4 (D14) hooked bars ranged from 70,300 to 76,700 psi. The center-to-

center spacing between the hooked bars ranged from 3.6 to $10.7d_b$ (1.97 to 5.91 in.), and the clear side concrete cover to the hooked bar ranged from 1.3 to $1.5d_b$ (0.71 in.). The embedment length of the hooked bars ranged from 11.8 to $13.8d_b$ (6.5 in.). Tsonos et al. found that the use of crossed inclined reinforcing bars (nonconventional column longitudinal reinforcing bars) in the joint region is one of the most efficient methods to improve the seismic resistance of exterior beam-column joints. They reported that external beam-column joints with crossed inclined reinforcing bars exhibited high strength and no significant degradation after reaching their maximum capacity and that the presence of crossed inclined reinforcing bars introduces an additional new mechanism of shear transfer. Tsonos et al. found that both exterior beam-column joints, conventionally reinforced and with crossed inclined reinforcing bars, performed satisfactorily with low joint shear stress and high column-beam flexural strength ratios.

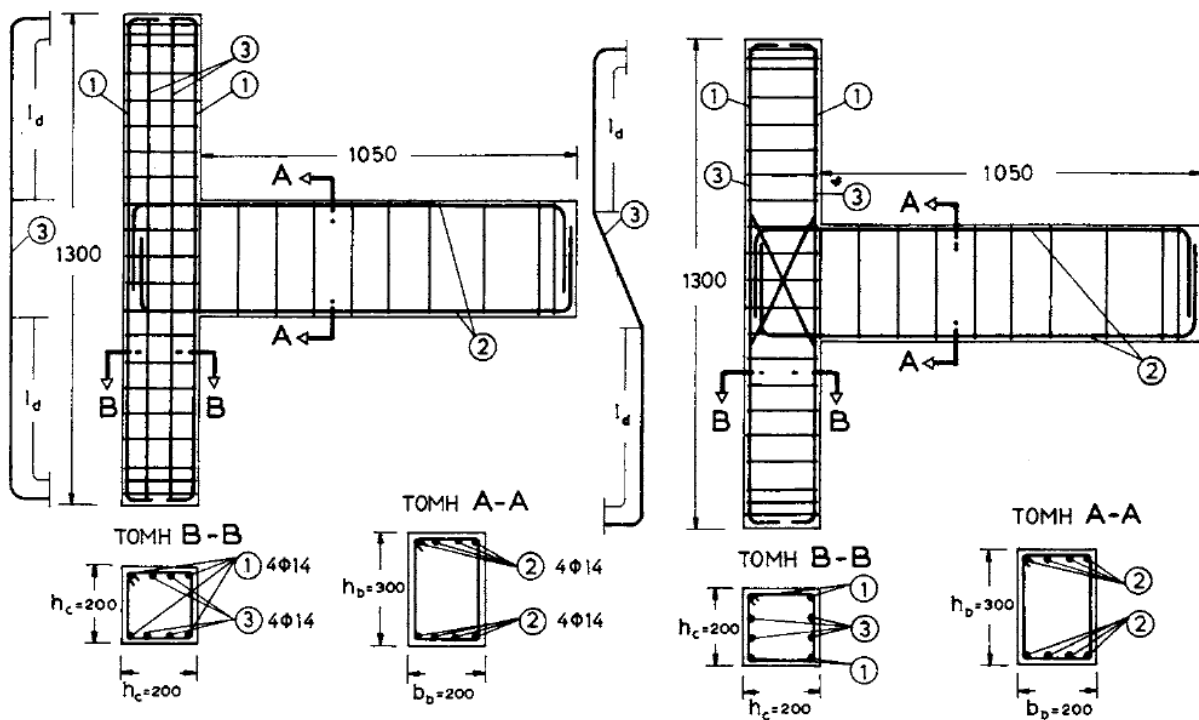


Figure D.1 Schematic drawings of exterior beam-column joints with conventional and nonconventional column longitudinal reinforcing bars (Tsonos et al. 1992)

Pantelides et al. (2002)

Pantelides et al. (2002) tested four exterior beam-column joint specimens under reversed cyclic loading. They examined the performance of the specimens in terms of lateral load capacity,

drift ratio (ratio of displacement at the loading point in the direction of the load to the distance between the loading point and the beam-column joint's center), axial load, joint shear stress, ductility, and residual strength. Two column axial load levels ($0.1f'_cA_g$ and $0.25f'_cA_g$) were used to investigate their effect on the performance of the joints subjected to reversed cyclic loading, where f'_c is the design concrete compressive strength (psi) and A_g is the cross-section area of the column. There was no confining reinforcement within the joint region. All specimens had the same dimensions and detailing. The width and depth of the beams were 12 and 16 in., respectively. Four No. 9 hooked reinforcing bars were used as beam top and bottom longitudinal reinforcement. The column width was 12 in., and the depth was 18 in. The column was reinforced with eight No. 7 bars evenly distributed around the perimeter. Concrete compressive strengths ranged from 5,370 to 6,700 psi, and the yield strength of the No. 9 hooked bars was 65,900 psi. The center-to-center spacing between the hooked bars was $2.1d_b$ (2.4 in.), and the clear side concrete cover to the hooked bar was $1.7d_b$ (1.9 in.). The embedment length of the hooked bars was $14.3d_b$ (16.1 in.). Pantelides et al. found that specimens with lower axial loads were 1.7 times more ductile than those with higher column axial loads. The specimens subjected to the higher axial load dissipated 20% less energy than those subjected to the smaller level of axial load. In addition, Pantelides et al. discovered that yielding of the beam longitudinal bars began at drift ratios of 0.5 to 0.6% for specimens with the $0.1f'_cA_g$ axial column load, while for specimens with the $0.25f'_cA_g$ axial load, yielding did not begin until drift ratios of 0.7 to 1%.

Chutarat and Aboutaha (2003)

Chutarat and Aboutaha (2003) tested four exterior beam-column joint specimens with hooked bars as the main beam longitudinal reinforcement under reversed cyclic loading to investigate a practical solution for relocating potential beam plastic hinge regions by the use of straight-headed bars, as shown in Figure D.2. Two of the four specimens were tested with additional straight-headed bars and two without the additional bars. The straight-headed bars extended 20 in. into the beam for specimens with a relocated beam plastic hinge region, as shown in Figure D.2. The concrete compressive strength ranged from 4,000 to 4,800 psi, and the yield strength of the No. 8 hooked bars was 70,000 psi. The center-to-center spacing between the hooked bars was $2.8d_b$ (2.8 in.), and the clear side concrete cover to the hooked bar was $3.3d_b$ (3.3 in.).

The embedment length of the hooked bars was $12.8d_b$ (12.8 in.). Chutarat and Aboutaha concluded that the beam plastic hinge region can be successfully moved from the column face to an exact predetermined location using straight-headed bars. They found that specimens with straight-headed bars developed a beam plastic hinge away from the face of the column near the head of the straight-headed bars, and the specimens developed their ultimate strength by fracture of the beam longitudinal bars.

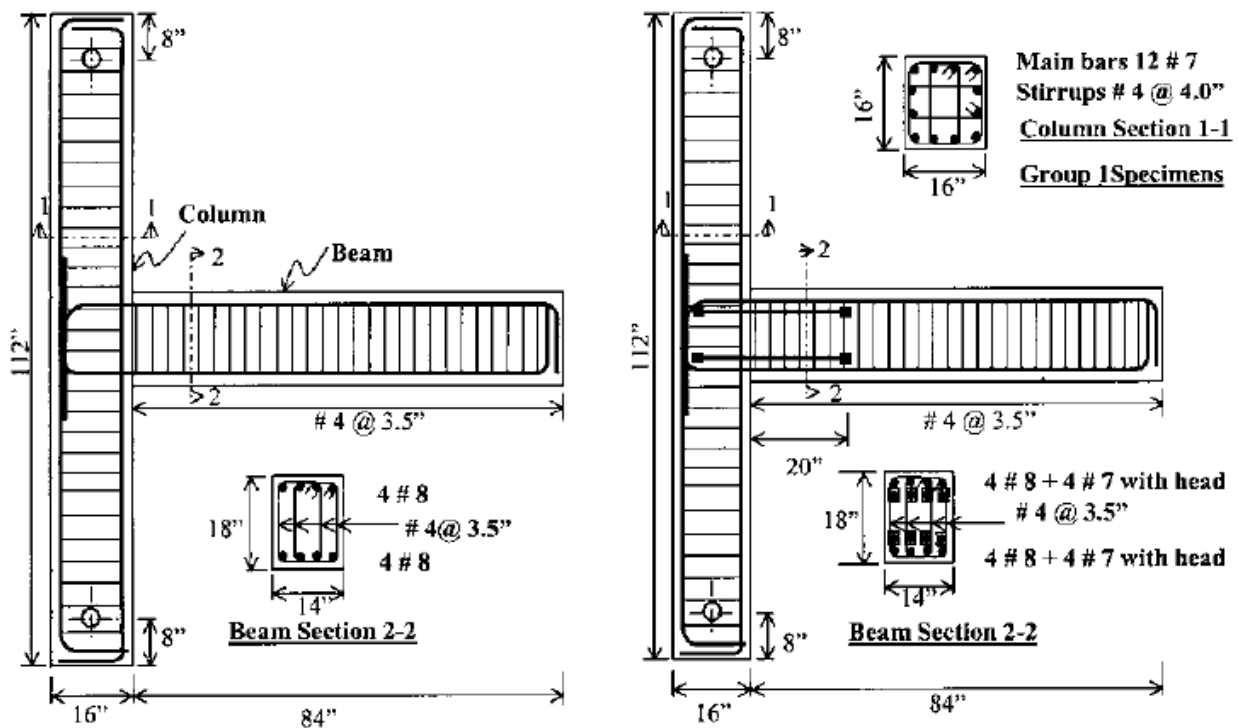


Figure D.2 Schematic drawings of exterior beam-column joints with and without straight-headed bars (Chutarat and Aboutaha 2003)

Hwang et al. (2005)

Hwang et al. (2005) tested nine exterior beam-column joint specimens to investigate the effect of confining reinforcement within the joint region on the shear strength and behavior of exterior beam-column joints subjected to reversed cyclic loading. The main parameters were the quantity and detailing of the confining reinforcement within the joint region. In all specimens, shear reinforcement in the beam and columns was sufficient to prevent shear failure outside the joint. Concrete compressive strengths ranged from 8,960 to 11,140 psi, and the yield strength of the No. 8 hooked bars ranged from 62,400 to 71,200 psi. The center-to-center spacing between the

hooked bars was $2.5d_b$ (2.5 in.), and the clear side concrete cover to the hooked bar was $4d_b$ (4 in.). The embedment length of the hooked bars ranged from 13.7 to $15.5d_b$ (13.7 to 15.5 in.). Hwang et al. concluded that the primary role of the confining reinforcement within the joint region is to carry shear as a tension tie and to constrain the width of the crack. They also found that less confining reinforcement within the joint region with wider spacing could be used without significantly affecting the performance of the beam-column joints. Hwang et al. observed that confining reinforcement within the joint region effectively restrained the deterioration of exterior beam-column joints subjected to reversed cyclic loading.

Lee and Ko (2007)

Lee and Ko (2007) tested five exterior beam-column joint specimens to investigate the effect of the eccentricity between the beam and column centerline on the performance of exterior beam-column joints subjected to reversed cyclic loading. The exterior beam-column joints were constructed with one concentric or eccentric beam framing into a rectangular column in the strong or weak direction, as shown in Figure D.3. The main variables were the lateral loading directions and the eccentricity between the beam and column centerlines. As shown in Figure D.3, the five specimens are designated as S0, S50 (Series S), W0, W75, and W150 (Series W). The first character of the designation (S or W) represents one south or west beam framing into the rectangular column in either the strong or weak direction. Two concentric (S0 and W0) and three eccentric (S50, W75, and W150) joints were tested. The column had dimensions of 16×24 in. and was reinforced with 12 No. 7 longitudinal bars distributed evenly around the cross-section. The beam was 12×18 in. and reinforced with four No. 7 longitudinal bars at both the top and bottom. Concrete compressive strengths ranged from 4,190 to 4,730 psi, and the yield strength of hooked bars was 66,000 psi. The center-to-center spacing between the hooked bars was $2.3d_b$ (2.0 in.), and the clear side concrete cover to the hooked bar ranged from 5.2 to $9.8d_b$ (4.6 to 8.6 in.). The embedment length of the hooked bars ranged from 15 to $24d_b$ (13.1 to 21.0 in.). A constant axial load $0.1f'_cA_g$ was applied to the columns, where f'_c is the design concrete compressive strength and A_g is the area of column cross-section. Lee and Ko found that the joint shear capacity of a rectangular joint is greater in the strong direction than in the weak direction. They observed that specimens subjected to lateral loading in the strong direction were capable of supporting the

complete formation of a beam plastic hinge, whereas specimens with the joint shear acting along the weak direction of the column exhibited significant damage at the joints. Lee and Ko concluded that the joint eccentricity between the centerlines of the beam and the column had a detrimental effect on the performance of the beam-column joints subjected to reversed cyclic loading. They found that little effect on the performance of beam-column joints for a joint eccentricity of $b_c/8$, where b_c is the width of the column, but observed significant reductions in the strength, ductility, and energy dissipation capacity when the eccentricity increased to $b_c/4$.

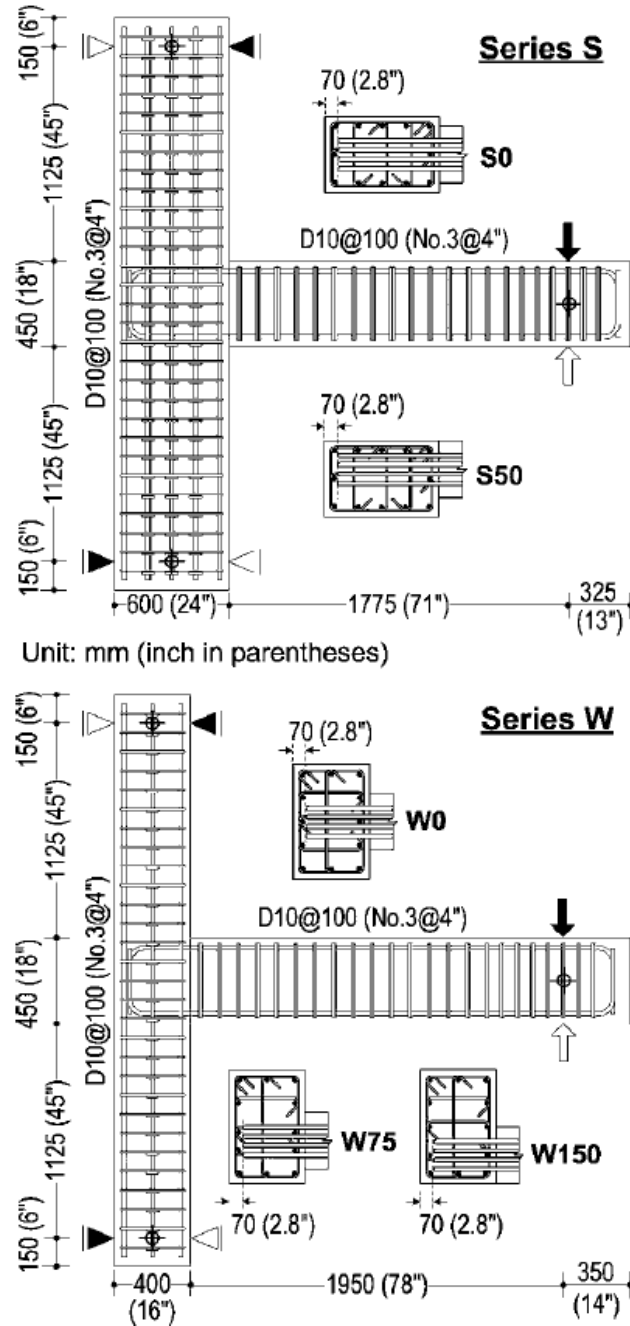


Figure D.3 Schematic drawings of exterior beam-column joints with one concentric or eccentric beam (Lee and Ko 2007)

Chun et al. (2007)

Chun et al. (2007) investigated the effect of the anchorage type (hooked or headed bars) and the bar size on the anchorage strength of exterior joint specimens subjected to reversed cyclic loading. Seven exterior and five knee beam-column joints and two wide-beam-to-wall joint specimens were tested. Concrete compressive strengths ranged from 4,760 to 8,950 psi. Beam

reinforcement consisted of D22 (No. 7), D25 (No. 8), or D36 (No. 11) hooked and headed bars with actual yield strengths ranging between 58,450 and 67,880 psi. The center-to-center spacing between the longitudinal reinforcing bars of the beam ranged from 3 to $6.6d_b$ (3.4 to 6.6 in.), and the clear side concrete cover to the bar ranged from 2.1 to $4.3d_b$ (1.9 to 6 in.). The embedment lengths of the anchored bars ranged from 12.3 to $18d_b$ (13.9 to 18.9 in.). The joints were designed and constructed in accordance with the ACI 352R-02 requirements for Type 1 and Type 2 joints. Type 1 joints are designed for non-seismic requirements and do not take into account significant inelastic deformation, whereas Type 2 joints are designed for seismic loading and take into account deformation due to load reversals into the inelastic range. A constant column axial load of 110 kips ($0.05A_gf'_c$) was applied to the specimens containing No. 7 and No. 8 bars, where f'_c is the design concrete compressive strength and A_g is the gross cross-sectional area of the column. The test specimens were designed based on a strong column-weak beam to ensure yielding of the anchored bars. The specimens were loaded to five drift levels corresponding to 1, 2, 4, 8, and 12 times the displacement at first yield, with three cycles per drift level, except for the specimens containing No. 11 bars, which were loaded monotonically while increasing the drift level from 0.5 to 10%. The first drift level was selected to be within an elastic range in all cases. Chun et al. found that exterior beam-column joint specimens constructed with headed and hooked bars and tested under reversed cyclic loading showed similar hysteretic behavior. Specimens with both hooked and headed bars maintained the peak load at approximately 4% drift and 80% of the peak load at 3.5% drift.

Tsonos (2007)

Tsonos (2007) tested four exterior beam-column joint specimens to study the performance of the joints subjected to reversed cyclic loading. The main parameters were the column-beam flexural strength ratio, amount of confining reinforcement within the joint region, and joint shear stress. The cross-sectional dimensions of the four specimens were identical, but the reinforcement ratios varied. The beam dimensions were 8×12 in., and the column dimensions were 8×8 in. Three specimens (E_1 , E_2 , and G_1) had the same longitudinal column reinforcement, eight No. 4 bars, whereas the fourth specimen (A_1) consisted of eight No. 3 bars distributed evenly around the column cross-section. Specimens E_1 and G_1 had three No. 4 hooked bars each as top and bottom

beam reinforcement, while specimens A₁ and E₂ had four No. 3 hooked bars and two No. 4 hooked bars as top and bottom beam reinforcement, respectively. The longitudinal beam reinforcement was chosen to produce low joint shear stresses in specimens A₁ and E₂, and high joint shear stresses in specimens E₁ and G₁. Confining reinforcement within the region ranged from 2 to 5 No. 2 hoops. The specimens were subjected to a constant axial load of 45 kips throughout the test. Concrete compressive strengths ranged from 3,190 to 5,080 psi, and the yield strength of hooked bars ranged from 72,000 to 73,000 psi. The center-to-center spacing between the hooked bars ranged from 4.7 to 10.0d_b (1.8 to 5.5 in.), and the clear side concrete cover to the hooked bars ranged from 1.6 to 2.5d_b (0.9 to 1.0 in.). The embedment length of the hooked bars ranged from 11.6 to 16.5d_b (6.4 to 6.5 in.). Tsonos found that specimens with low joint shear stresses showed satisfactory performance, and failed in beam flexural, while specimens with high joint shear stress performed poorly and exhibited joint shear failure.

Kang et al. (2010)

Kang et al. (2010) tested two exterior beam-column joint specimens to investigate the seismic behavior of the anchored bars in exterior beam-column joints subjected to reversed cyclic loading. One specimen contained No. 6 bars with a 90-degree hook and the other contained bars of the same size with a head as beam longitudinal reinforcing bars, as shown in Figure D.4. Both beam-column joint specimens contained four No. 6 (D19) anchored bars as top and bottom beam reinforcement anchored in the column with an embedment length of 15d_b. The joint region contained 4 No. 3 (D10) hoops as confining reinforcement. Concrete compressive strengths were 4200 psi and 4220 psi for specimens with hooked and headed bars, respectively, and the yield strengths of the hooked and headed bars were 66,700 psi and 69,750 psi, respectively. No axial load was placed on the columns. The specimens were loaded to drift levels of 0.4 to 3.5%, with three cycles at each drift level. Kang et al. discovered that both specimens behaved in a relatively ductile manner failed by beam flexural yielding. The specimens reached the peak loads at drifts of 2 to 2.5% and maintained that maximum load until about 3.58% drift for specimens with headed bars, whereas for specimens with hooked bars, after reaching the peak load, subsequently dropped to 80% of the peak load at 3.46% drift.

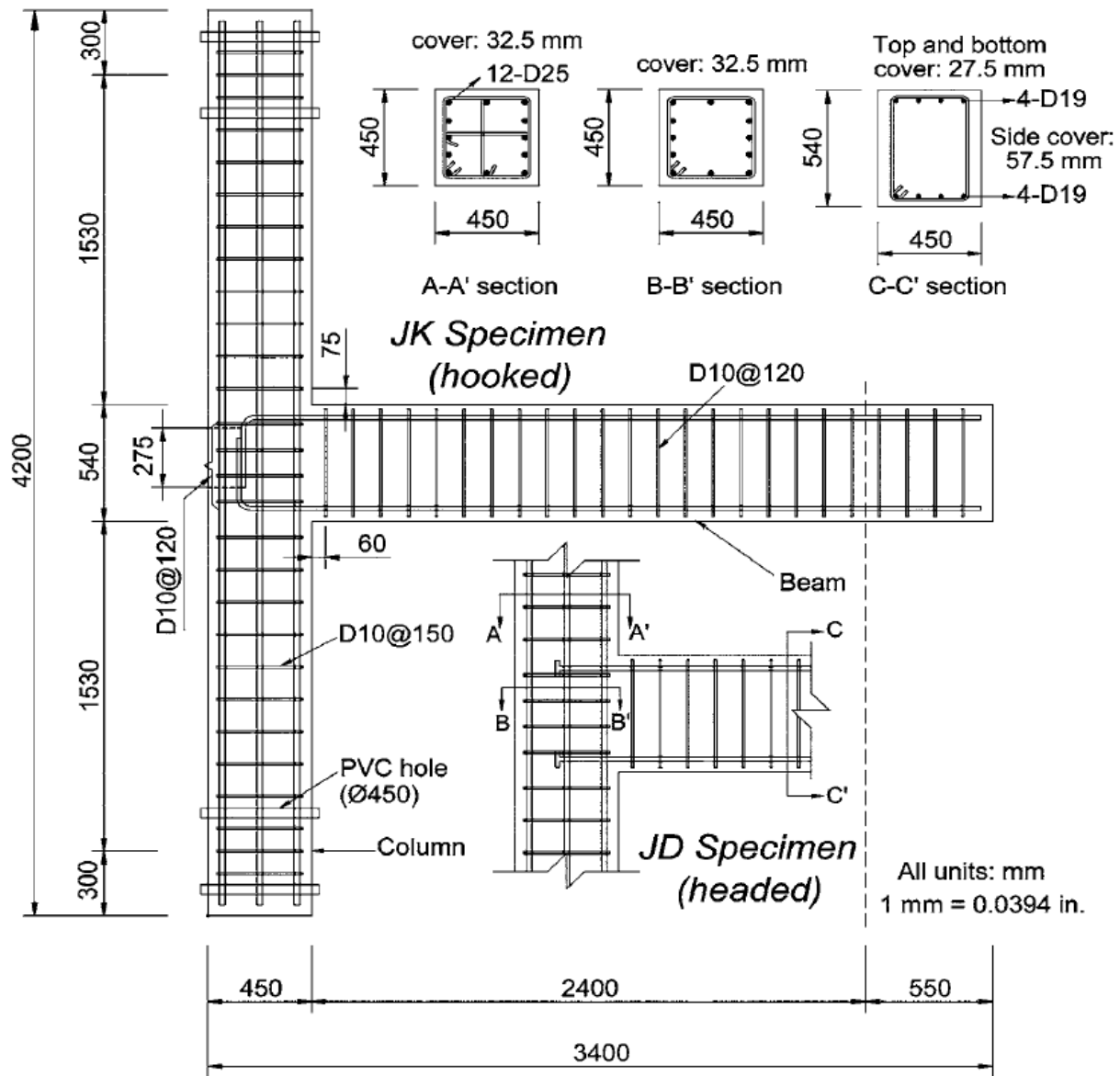


Figure D.4 Detail of exterior beam-column joint specimens containing hooked and headed bars (Kang et al. 2010)

Chun and Shin (2014)

Chun and Shin (2014) tested 14 exterior beam-column joint specimens to examine the effect of joint aspect ratio (beam depth to column depth) and confining reinforcement on the anchorage strength of hooked and headed bars in exterior beam-column joints subjected to reversed cyclic loading. The main variables were the joint aspect ratio (0.67 to 2.5), the amount of confining reinforcement within the joint region (four specimens with joint aspect ratios of 0.67 and 1.0 had two-thirds of the confining reinforcement required by ACI 352 and the remaining 10,

with joint aspect ratios of 1.5, 2.0 and 2.5, had the full amount of the confining reinforcement required by ACI 352), and anchorage type for the beam bars (hooks or heads). Seven of the 14 exterior beam-column joints contained standard 90° hooked bars, and seven had headed bars as the longitudinal reinforcement of the beam. The specimens had a 12 × 12 in. column and a 9.8 in. wide beam; total beam depths ranged from 7.9 to 29.5 in. depending on the joint aspect ratio. Ten of the specimens contained confining reinforcement consisting of three legs - two D13 (No. 4) legs in the form of a hoop and one D10 (No. 3) leg in the form of a cross tie – spaced at 3 in. within the joint region, in accordance with the joint confining reinforcement requirements of Section 4.2.2.2 of ACI 352R-02. In the other four specimens also had three legs spaced at 3 in., but the hoop was reduced to a D10 (No. 3), resulting in two-thirds of the confining reinforcement required in Section 4.2.2.2 of ACI 352R-02. The top and bottom bars for the beam reinforcing bars consisted of four and three D19 (No. 6) bars, respectively. The center-to-center spacing between the longitudinal reinforcing bars of the beam was $2.3d_b$ (1.75 in.), and the clear side concrete cover to the bar was $3.9d_b$ (3.0 in.). The embedment length of the bars in all specimens was $12d_b$ (9 in.). Concrete compressive strengths were between 3,710 and 3,830 psi. No column axial load was applied during the test.

The peak moments were 1.1% to 24% greater than the nominal moment capacity based on the yield strengths of the beam reinforcement. All specimens maintained their peak load at a 3.5% drift ratio. Specimens with joint aspect ratios less than or equal to 1.0 failed by flexural hinging at the beam away from the joint with limited joint damage. Specimens with joint aspect ratios equal to or greater than or equal to 1.5 failed by hinging at the column, with extensive joint deterioration characterized by substantial spalling of the joint cover concrete. As the joint aspect ratio increased, the joint damage increased while beam damage decreased. Chun and Shin found that for joint aspect ratios less than or equal to 1.0, joints with less confining reinforcement (two-thirds of the confining reinforcement required by ACI 352) exhibited similar behavior to the joints designed in accordance with ACI 352R-02. Chun and Shin discovered that there was no significant difference in failure modes, moment-drift relation, joint distortion, and energy dissipation between specimens with hooked bars or headed bars.

Hwang et al. (2014)

Hwang et al. (2014) tested three exterior beam-column joint specimens to evaluate the performance of exterior beam-column joints constructed with high-strength (87,000 psi) beam flexural reinforcement under reversed cyclic loading. The main parameters were the diameter and the yield strength of the beam longitudinal reinforcing bars. The specimens had beam and column cross-sectional dimensions of 350×500 mm (14×20 in.) and 500×550 mm (20×22 in.), respectively. Four legs (two hoops) of D13 (No. 4) spaced at 100 mm (4 in.) were used as confining reinforcement within the joint region in all three specimens. Concrete compressive strengths ranged from 4,290 to 4,640 psi, and the yield strength of hooked bars ranged from 75,400 to 103,000 psi. The diameter of the hooked bars ranged from D19 to D25 (No. 6 to No. 8), as shown in Figure D.5. The center-to-center spacing between the hooked bars ranged from 3.25 to $3.71d_b$ (3.25 in.), and the clear side concrete cover to the hooked bars ranged from 4.5 to $5.1d_b$ (4.5 in.). The embedment length of the hooked bars ranged from 19.6 to $22.4d_b$ (19.6 in.). No axial load was applied to the column. Hwang et al. found that due to insufficient hooked bar development length in compression, concrete cover spalling and punching occurred at the location of the beam bottom bars in the exterior face of the column, in addition to the concrete crushing at the beam bottom. Hwang et al. concluded that the load-carrying capacities of exterior beam-column joints subjected to reversed cyclic loading with high-strength (87,000 psi) beam flexural reinforcement agreed with the predicted nominal strengths.

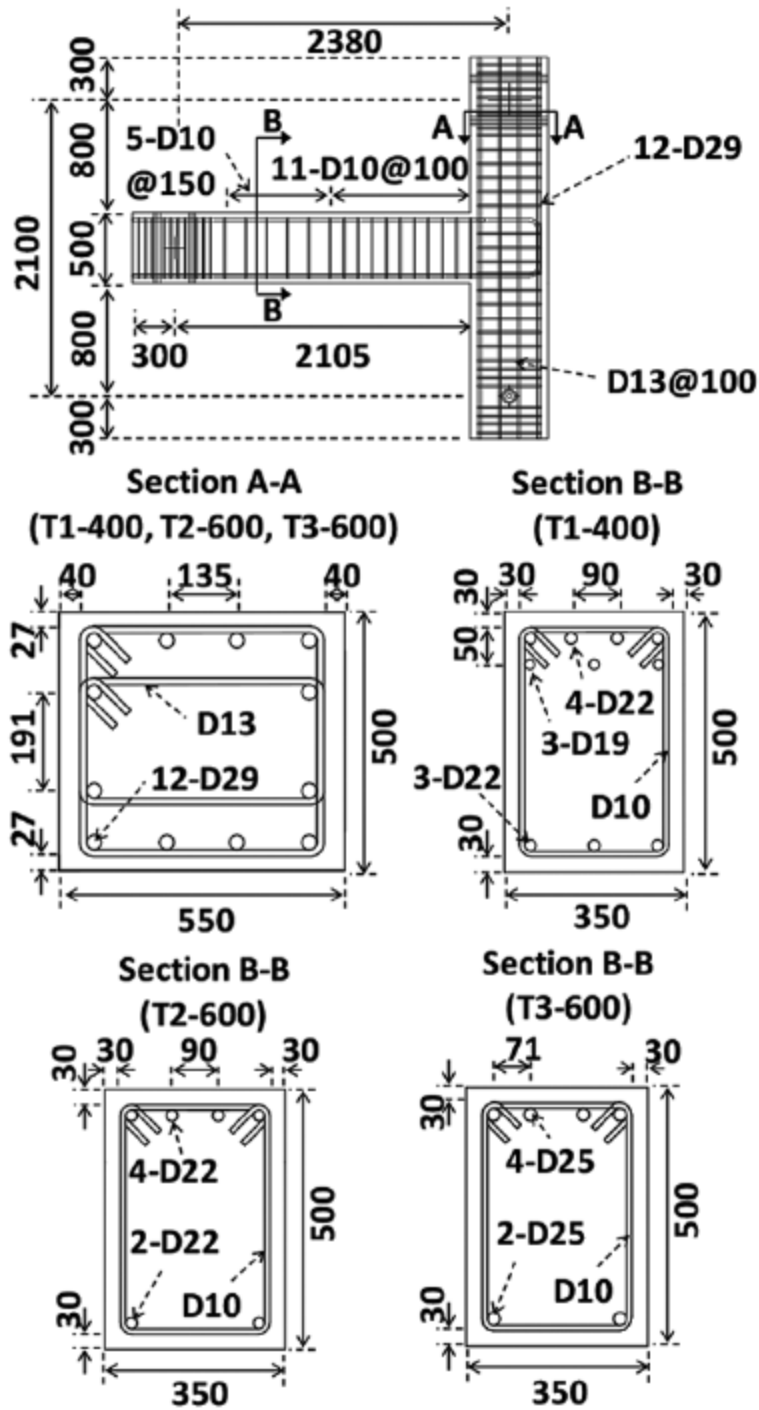


Figure D.5 Detail of exterior beam-column joint specimens (Hwang et al. 2014)

Choi and Bae (2019)

Choi and Bae (2019) tested seven exterior beam-column joint specimens to investigate the effect of steel fibers on the anchorage strength and behavior of exterior beam-column joints

subjected to reversed cyclic loading. The main parameters were the presence of steel fibers, the amount of confining reinforcement within the joint region, and the spacing between the confining reinforcement in the beam. Of the seven specimens, four had steel fibers with and without the presence of confining reinforcement within the joint region, and three did not; of the three specimens without steel fibers, two had confining reinforcement within the joint region and one had none. A constant axial load of $0.1f'_cA_g$ was applied to the column throughout the test, where f'_c is the design concrete compressive strength and A_g is the area of column cross-section. The beam and column cross-sectional were, respectively, 250×375 mm (10×15 in.) and 300×300 mm (12×12 in.). Confining reinforcement within the joint region consisted of two legs (a hoop) of D13 (No. 4) spaced at 60 mm (2.4 in.). The concrete compressive strength was 7,950 psi, and the yield strength of the hooked bars was 68,400 psi. Two D25 (No. 8) hooked bars were used as longitudinal beam reinforcing bars at the top and bottom of the beam. The center-to-center spacing between the hooked bars was $4.6d_b$ (4.6 in.), and the clear side concrete cover to the hooked bar was $3.1d_b$ (3.1 in.). The embedment length of the hooked bars was $8.3d_b$ (8.3 in.). Choi and Bae found that steel fibers increase joint strength even when no hoops are present. They also observed that the bond strength between reinforcement and concrete in the joint region increased as the steel fiber content increased, but the rate of increase in strength decreased with increasing steel fiber content. Choi and Bae discovered that using an adequate quantity of steel fibers in exterior beam-column joints can change the mode of failure from joint shear failure to beam flexural failure.

